



## Durham E-Theses

---

### *X-ray double crystal characterisation of epitaxial layers*

Hill, Martin John

#### How to cite:

---

Hill, Martin John (1985) *X-ray double crystal characterisation of epitaxial layers*, Durham theses, Durham University. Available at Durham E-Theses Online: <http://etheses.dur.ac.uk/7232/>

#### Use policy

---

The full-text may be used and/or reproduced, and given to third parties in any format or medium, without prior permission or charge, for personal research or study, educational, or not-for-profit purposes provided that:

- a full bibliographic reference is made to the original source
- a [link](#) is made to the metadata record in Durham E-Theses
- the full-text is not changed in any way

The full-text must not be sold in any format or medium without the formal permission of the copyright holders.

Please consult the [full Durham E-Theses policy](#) for further details.

X-RAY DOUBLE CRYSTAL CHARACTERISATION  
OF  
EPITAXIAL LAYERS

---

MARTIN JOHN HILL, B.Sc.

The copyright of this thesis rests with the author.  
No quotation from it should be published without  
his prior written consent and information derived  
from it should be acknowledged.

Thesis submitted to the University of  
Durham in Candidature for the Degree of  
Doctor of Philosophy (November, 1985).



Theris  
1985/H12

## A B S T R A C T

Double crystal x-ray diffractometry is a well established method for the measurement of the lattice parameter difference between epitaxial layers and substrates. The diffracted intensity profile versus angle, rocking curves, are highly sensitive to such variations giving rise to complex peak shapes. Consequently, computer simulation is required to enable complete interpretation of the measured data.

A detailed description of a computer simulation technique suitable for calculating rocking curves from arbitrary III-V structures, based on the Takagi-Taupin equations for dynamical diffraction from a non uniform crystal, is presented.

Radiation from synchrotron and laboratory sources has been used to measure rocking curves from single uniform and single graded layers of (Ga,In)(As,P) on (001) InP substrates and artificial superlattices of both (Ga,Al)As on (001) GaAs and (Ga,In)As on (001) InP. Excellent agreement has been obtained between computed and experimental curves for all types of structure, enabling the layer thicknesses and compositions to be determined to within 0.1 $\mu$ m and 10 ppm respectively. For single layers less than 0.5  $\mu$ m thick highly asymmetric reflections are shown to give greatly increased diffracted intensities from the layer, enabling more accurate interpretation. There will always be doubt as to the validity of the lattice parameter profile deduced for a graded layer from a single curve. Rocking curves at various wavelengths, using synchrotron radiation, have been used to confirm the profile determined previously using a single measurement from a laboratory source. For superlattices, the dynamical theory approach permits

satellite peaks, allowing the individual layer thicknesses and compositions to be determined in addition to the repeat period. Further, this dynamical approach is particularly suitable for calculating the complete rocking curve where thick confining layers are present and is also directly applicable to multiple layers with varying layer thicknesses.

## A C K N O W L E D G E M E N T S

Financial support from the Science and Engineering Research Council and British Telecommunications plc through a CASE award is gratefully acknowledged. I would also like to thank the SERC for making available the facilities of the S.R.S., Daresbury Laboratory.

It is my pleasure to acknowledge the help and assistance from the following people during the course of this work.

Firstly, I would like to thank Professor A.W. Wolfendale and Professor B.H. Bransden for making available the facilities of the Department of Physics at the University of Durham.

I am grateful to Dr. B.K. Tanner for his supervision of this project and his continued enthusiasm. Thanks are also due to Mrs. M.A.G. Halliwell of British Telecom Research Laboratories for initiating this project. I am also grateful to her colleagues; Dr. M.H. Lyons for his thoughtful suggestions, Dr. M.R. Taylor and Dr. M. Hockly for the transmission electron microscopy results; Mr. D.A. Andrews for the samples provided.

I also thank the technical staff of the Department of Physics, especially Mr. D. Josling, Mr. T. Jackson, Mr. P. Armstrong and Mr. G. Teasdale for their help and advice.

I am particularly grateful to Mr. S.J. Barnett for his help in performing many of the experiments at the S.R.S., to Dr. D.Y. Parpia and Dr. M. Surowiec for their useful discussions.

Finally, I would like to thank my parents for their assistance, encouragement and support.

## LIST OF PUBLICATIONS

- HALLIWELL, M.A.G., LYONS, M.H. and HILL, M.J. (1984) J. Cryst. Growth, **68**, 523-531.
- HILL, M.J., TANNER, B.K. and HALLIWELL, M.A.G. (1984) Proc. Mater. Res. Soc. November Meet. Boston, USA. Layered Structures, Epitaxy and Interfaces II, Vol 37, 53-58.
- HILL, M.J., TANNER, B.K., HALLIWELL, M.A.G. and LYONS, M.H. (1985) J. Appl. Cryst. **18** (in press).
- TANNER, B.K., BARNETT, S.J. and HILL, M.J. (1985) Microscopy of Semiconductor Materials, Oxford 1985 (in press).
- TANNER, B.K. and HILL, M.J. (1985) Proc. Denver Conf. Applications of X-ray Analysis, Denver, USA. To be published in: Advances in X-ray Analysis Vol. 29 (1986).

## C O N T E N T S

	<u>PAGE</u>
TITLE PAGE	i
ABSTRACT	ii
ACKNOWLEDGEMENTS	iv
LIST OF PUBLICATIONS	v
<u>CHAPTER 1: INTRODUCTION</u>	
1.1 III-V OPTOELECTRONIC DEVICES AND SUPERLATTICES	1
1.1.1 Optoelectronic Devices	1
1.1.2 Superlattices	3
1.2 GROWTH TECHNIQUES FOR III-V EPITAXY	7
1.2.1 Liquid Phase Epitaxy (LPE)	7
1.2.2 Vapour Phase Epitaxy (VPE)	8
1.2.3 Metallo Organic Chemical Vapour Deposition (MOCVD)	9
1.2.4 Molecular Beam Epitaxy (MBE)	10
1.3 LATTIC MISMATCH AND TETRAGONAL DISTORTION OF THE EPITAXIAL LAYER	
1.3.1 Misfit stress in a single epitaxial layer - substrate composite	13
1.3.2 Stress distribution	15
1.3.3 Parallel mismatch and interfacial dislocation density	18
1.3.4 Tetragonal distortion	19
1.4 VEGARD'S LAW AND BANDGAPS	21
1.5 CHARACTERISATION OF EPITAXIAL LAYERS	23



	<u>PAGE</u>
<u>CHAPTER 2:</u> DOUBLE CRYSTAL DIFFRACTOMETRY	26
2.1 GENERAL THEORY OF THE DOUBLE CRYSTAL CAMERA	26
2.2 THE EFFECT OF VERTICAL DIVERGENCE ON THE ROCKING CURVE	32
2.3 DOUBLE CRYSTAL X-RAY DIFFRACTION CHARACTERISATION OF EPITAXIAL AND ION IMPLANTED LAYERS AND SUPERLATTICES	37
2.3.1 Diffusion and ion implanted layers	39
2.3.2 Heteroepitaxial layers	44
2.3.3 Superlattices	49
 <u>CHAPTER 3:</u> CALCULATING ROCKING CURVES	 53
3.1 DYNAMICAL DIFFRACTION THEORY	53
3.2 THE TAKAGI-TAUPIN EQUATIONS	57
3.3 SOLUTION OF THE TAKAGI-TAUPIN EQUATIONS AND CALCULATIONS OF THE ROCKING CURVE	65
3.4 THE EFFECT OF SAMPLE CURVATURE ON THE ROCKING CURVE	69
3.5 COMPUTATION OF ROCKING CURVES	71
3.5.1 The Pascal Programme	72
3.5.2 The Fortran Programme	74
 <u>CHAPTER 4:</u> EXPERIMENTAL TECHNIQUES AND INSTRUMENTATION	 78
4.1 THE SIX INCH CAMERA AT DURHAM	78
4.1.1 Computer Control	79
4.1.2 Design of the ICC R5232 Serial Interface	82
4.2 THE TWELVE INCH CAMERA AT DARESBURY	84
4.2.1 Computer Control and Instrumentation	86
4.3 ALIGNING THE CAMERAS AND RECORDING ROCKING CURVES	87
4.3.1 The six inch camera	88
4.3.2 The twelve inch camera	89
 <u>CHAPTER 5:</u> SINGLE UNIFORM LAYERS	 92
5.1 SURFACE SYMMETRIC REFLECTIONS	93
5.2 THE USE OF ASYMMETRIC REFLECTIONS TO STUDY THIN LAYERS	100
 <u>CHAPTER 6:</u> SINGLE LAYERS WITH A DEPTH DEPENDENT COMPOSITION	 110

	<u>PAGE</u>
<u>CHAPTER 7: MULTIPLE AND MULTILAYER STRUCTURES</u>	124
7.1 EXPERIMENTAL RESULTS	129
7.2 THE EFFECT OF ADDING A CAPPING LAYER TO THE SUPERLATTICE	137
7.3 THE EFFECT OF DISPERSION IN THE SUPERLATTICE PERIOD AND OF INTER DIFFUSION BETWEEN THE LAYERS	138
<u>DISCUSSION AND SUGGESTION FOR FURTHER WORK</u>	142
<u>APPENDIX A: COMPUTER PROGRAMMES FOR THE CALCULATION             OF ROCKING CURVES</u>	147
<u>APPENDIX B: MINICAM ICC SOFTWARE FOR CONTROL OF THE             SERIAL PARTS WITH ASCII DATA TRANSMISSION</u>	182
<u>APPENDIX C: LISTINGS OF THE DOUBLE CRYSTAL CONTROL             PROGRAMMES FOR THE BBC MICROCOMPUTER</u>	241
<u>REFERENCES</u>	284

## CHAPTER 1

### INTRODUCTION

#### 1.1 III-V Optoelectronic Devices and Superlattices

##### 1.1.1 Optoelectronic Devices

Currently the majority of fibre optic based telecommunications systems being installed are based on graded index fibre, operating with gallium arsenide lasers or light emitting diodes (l.e.d.s) as the light sources. Operation is at the near infra red, between 0.8 and 0.9  $\mu\text{m}$ , with silicon based detectors. Speeds between 8 and 140 Mbit/s are possible over lengths up to about 8 km without repeaters. Recently improved manufacture has lead to fibres with superior attenuation characteristics further into the infra red, in the 1.2 to 1.6  $\mu\text{m}$  region. Therefore, new materials are required to produce the optoelectronic devices operating at these wavelengths, with the most promising being based on gallium indium arsenide (GaInAs) and gallium indium arsenide phosphide (GaInAsP), epitaxially grown on indium phosphide (InP) substrates. Utilising graded index fibre, systems operating at 1.3  $\mu\text{m}$  are capable of speeds between 8 and 140 Mbit/s with lengths of 10 to 20 km between repeaters.

More recently, attention has been focussed on monomode fibres, in which the central core is so small (5 - 10  $\mu\text{m}$ ) that only one mode of propagation is possible. This eliminates the modal spread that limits the length between repeaters of graded index, multimode fibre. Close to 1.3  $\mu\text{m}$



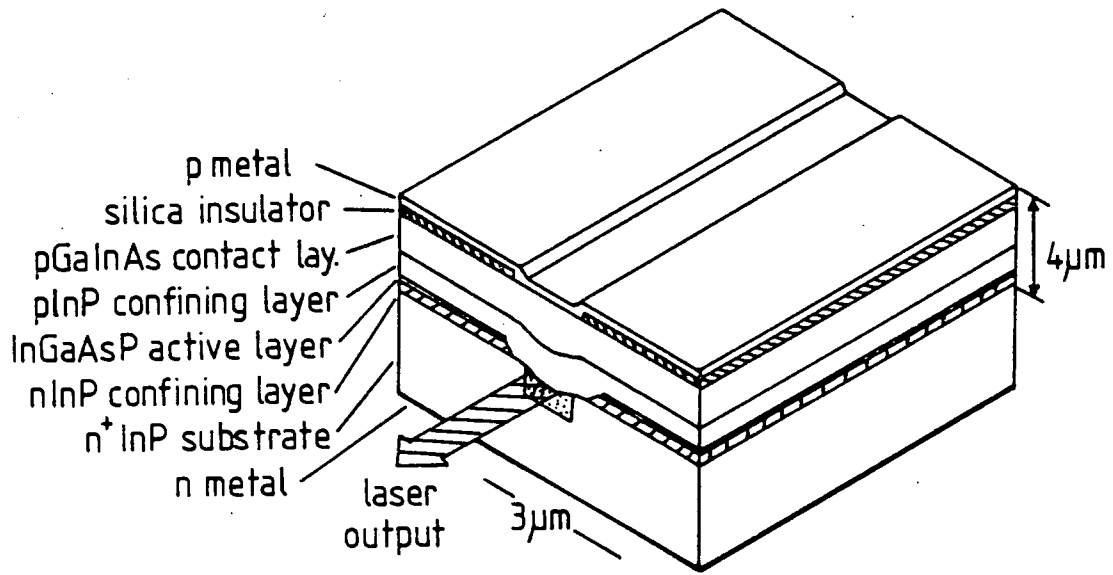


Fig. 1.1 Schematic diagram of a (Ga,In)(As,P) channel substrate buried heterostructure laser (c.s.b.h.)

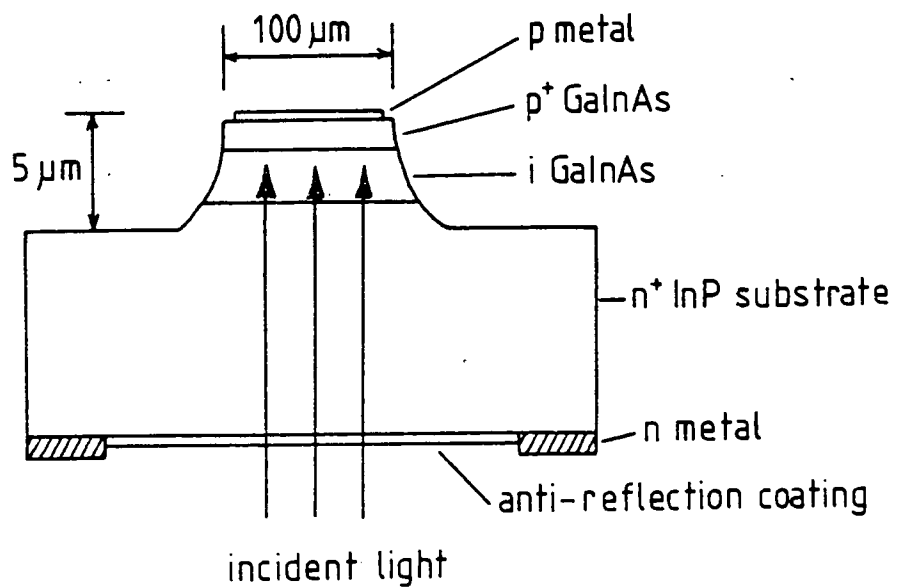


Fig. 1.3 Schematic diagram of a GaInAs p.i.n. detector as used in fibre optic systems operating in the range 1.3-1.55 μm.

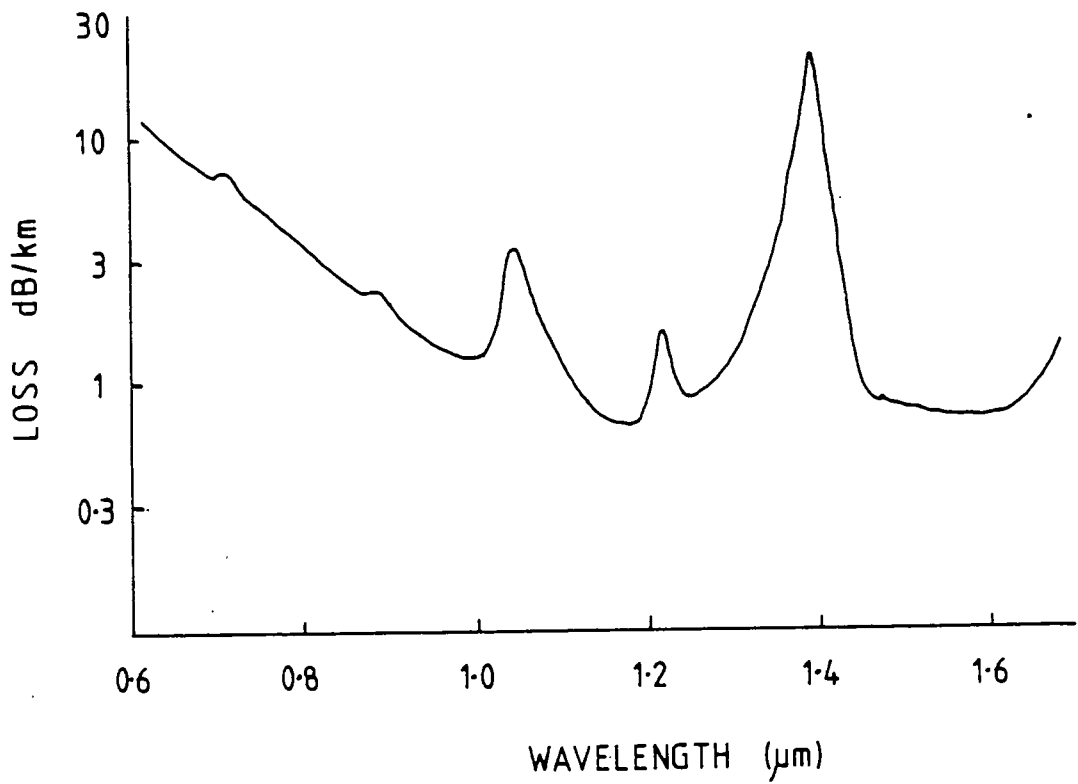


Fig. 1.2 Attenuation of silica based optical fibre as a function of wavelength in the infra red region.

the fibre chromatic dispersion is a minimum, so that even with a source of non zero spectral width there is no first order limitation on bandwidth. Systems have been demonstrated at 140 Mbit/s over lengths of 64 km and at 650 Mbit/s over 32 km without repeaters. Launching the light into such a small region of fibre is a considerable problem, hence the need for laser light sources as opposed to l.e.d.s. The double heterostructure laser, and its close derivatives, have been developed to provide such sources. The schematic diagram of a channel substrate buried heterostructure laser (c.s.b.h.) is shown in fig. 1.1.

The attenuation of silica based optical fibres reaches an absolute minimum of about 0.15 dB/km at 1.55  $\mu\text{m}$ , but chromatic dispersion is present at this wavelength (Ainslie et al, 1979). Fig. 1.2 shows this loss as a function of wavelength. Therefore, in order to develop longer lengths of fibre between repeaters the chromatic dispersion must be reduced. This can be achieved by both moving the zero dispersion point in the fibre towards 1.55  $\mu\text{m}$  and limiting the spectral width of the laser sources.

Clearly, to make full use of the low attenuation of the fibre the highest possible sensitivity is required at the detector. Silicon avalanche photodiodes (a.p.d.s) are the standard at 0.85  $\mu\text{m}$ , but they are insensitive in the 1.2 - 1.6  $\mu\text{m}$  range. Germanium a.p.d.s have been developed but have signal to noise ratios inferior to the silicon a.p.d.s. At present the major effort is in developing GaInAs type non

avalanching detectors (p.i.n. type) and GaInAsP based avalanching detectors. The schematic diagram of a GaInAs p.i.n. detector is shown in fig. 1.3. Light is incident through the transparent InP substrate and is almost all absorbed in the i-GaInAs layer, with nearly 100% quantum efficiency.

### 1.1.2 Superlattices

Artificial semiconductor superlattices are composed of a periodic sequence of thin (50 - 200 Å) layers of alternating composition (eg AlAs/GaAs, GaAlAs/GaAs, GaInAs/InP etc). Interest in such structures originates from the work of Esaki and Tsu (1970) to produce a one dimensional periodic potential by a periodic variation of either impurities or alloy composition in semiconductors, with the period shorter than the electron mean free path. They first considered the compositional superlattice and predicted that they should exhibit unusual transport phenomena. These peculiarities originate from the splitting of the conduction and valence bands into narrow mini or sub bands. This splitting is a consequence of the reduction of the original Brillouin zone due to the strongly increased (superlattice) periodicity. Also in the early 1970's Dohler (1972a,b) analysed in great detail the electronic properties of doping superlattices. In addition to the phenomena characteristic of compositional superlattices, a number of new peculiarities which are specific to doping superlattices were predicted. These unique features arise from the unusual

indirect energy gap in real space of the layered material.

The first artificial superlattices were reported by Esaki, Chang and Tsu (1971), where they were obtained by periodic variation of the phosphorous content in layers of  $\text{GaAs}_{1-x}\text{P}_x$  grown by vapour phase epitaxy. The first superlattices grown by molecular beam epitaxy were reported by Chang et al (1973). This prototype structure consisted of several hundred alternating layers of GaAs and  $\text{Ga}_{1-x}\text{Al}_x\text{As}$ , grown on a GaAs substrate. Periods ranging from 50 to 200 Å were grown with various compositions of GaAlAs. Early experiments on these structures were used to investigate transport anomalies (Esaki and Chang, 1974) and to demonstrate the quantum mechanical particle in a box behaviour of electrons (Dingle, 1975). The introduction of modulation doping in GaAlAs/GaAs superlattices (Dingle et al, 1978) subsequently modified the established square well concept, and it extended the underlying physics to totally new fundamental phenomena including the quantised Hall effect (von Klitzing et al, 1981), near zero resistance state (Tsui et al, 1982a) and electron localization in a two dimensional electron gas in strong magnetic fields (Tsui et al, 1982b; Ebert et al, 1982).

The so called type II compositional superlattice was conceived by Sai-Halasz et al (1977) and exemplified by the material combination of  $\text{Ga}_{1-x}\text{In}_x\text{As}$  and  $\text{GaAs}_y\text{Sb}_{1-y}$  (Sakaki et al, 1977). The type II superlattice differs from its type I counterpart by the sign of the band edge discontinuity



between the two components of the superlattice. While in the type I superlattice the conduction and valence band edge discontinuities have opposite signs, the type II system is characterised by a band edge modulation which has the same sign for the conduction and valence bands. In the case of small  $x$  and  $y$  values (and in the pure binary system), the bottom of the conduction band of GaInAs becomes even lower in energy than the top of the valence band of GaAsSb. This coexistence of conduction and valence band states in the respective constituent layers can lead to an electron transfer from the GaAsSb to the GaInAs layers, if the layers are sufficiently thin, resulting in a semiconductor-semimetal transition (Sai-Halasz et al 1978).

Significant improvements in the spatial control of dopant incorporation during molecular beam epitaxial growth was required before the first doping superlattices could be realised (Ploog et al, 1981a). Many of the electronic peculiarities of GaAs superlattices predicted by Dohler (1972a,b) have since been demonstrated by detailed experiments on the tunability of photoluminescence (Dohler et al, 1981; Jung et al, 1982), tunability of electroluminescence (Kunzel et al, 1982) and on two dimensional carrier confinement and tunability of subband spacing (Dohler et al, 1981; Zeller et al, 1982; Maan et al, 1983). These measurements provided the experimental evidence that GaAs doping superlattices indeed formed a new class of semiconductor materials. The electronic properties

of a doping superlattice are no longer fixed material parameters but tunable quantities.

Recently, improvements in growth techniques have also enabled the growth of superlattices from constituent materials with large differences in lattice parameter (Matthews and Blakeslee, 1977). Such 'strained layer' superlattices (SLS's) were theoretically predicted to have electrical properties that depended on the state of strain of the individual layers as well as on the composition modulation (Osbourn, 1982). These superlattices are grown by alternately depositing lattice mismatched materials so that strain is necessary to form a coherent interface, but where the layers are below the critical thickness for dislocation generation. A buffer layer of graded composition is also grown between the substrate and the first layer which tends to force any grown-in dislocations towards the edge of the sample, thus enabling relatively low quality substrates to be used. The metallo organic chemical vapour deposition (MOCVD) growth technique is often used to grow such structures. The intentionally built-in strain and freedom to combine lattice mismatched semiconductors has spurred interest in these structures. GaAsP/GaAs SLS's have recently been shown to possess an independently variable band gap and lattice constant (Osbourn et al, 1982; Biefield et al, 1983), and have also exhibited stimulated emission (Ludowise et al, 1983). Quantum size effects observed as optical transitions in both photoluminescence and excitation

spectroscopy have also been observed (Gourley and Biefield, 1984).

## 1.2 Growth Techniques for III-V Epitaxy

At present there are four widely used epitaxial growth techniques, namely liquid techniques (liquid phase epitaxy), vapour transport techniques (vapour phase epitaxy, metallo organic chemical vapour deposition) and molecular transport techniques (molecular beam epitaxy). These four techniques vary considerably in operation and complexity, as well as being suited to growing layers for different applications.

### 1.2.1 Liquid phase epitaxy (LPE)

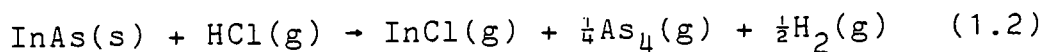
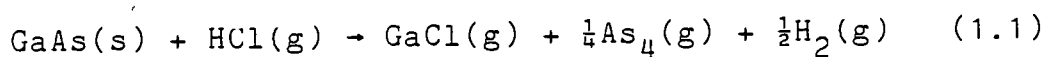
LPE is particularly suited to growing relatively thick layers (2 - 10  $\mu\text{m}$ ) of high crystalline quality. A two piece graphite sliding boat is used to hold the substrate while the liquified material for the layer is held in the top, sliding, part. This is heated in a furnace to the required temperature (about 660  $^{\circ}\text{C}$  for GaInAs layers) and the molten material slowly slid across the surface of the substrate. A step or ramp cooling technique is used to promote crystal growth, while the furnace is filled with  $\text{PH}_3$  and  $\text{H}_2$ , the  $\text{PH}_3$  preventing substrate degradation through loss of phosphorous.

It has been reported (Stringfellow, 1972) that lattice matched layers of GaInP were grown preferentially to lattice mismatched layers, due to the higher free energy associated with a lattice mismatched layer. However, Hsieh et al (1977)

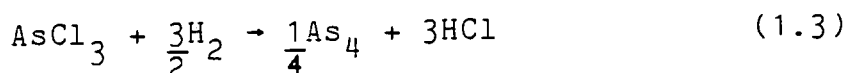
were unable to find any evidence of this effect for the growth of GaInAs on InP substrates. In particular, the lattice parameter of the layer was found to be a sensitive function of the growth solution composition, the supercooling time and the time of contact between the solution and substrate.

### 1.2.2 Vapour phase epitaxy (VPE)

Vapour phase epitaxy has been used extensively to grow ternary layers of (Ga,In)As, although it is also suited to the growth of quaternary and higher alloys. Binary compounds of Ga and In are transported in the vapour phase over the heated substrate along with As gas, leading to growth at the substrate surface according to the equilibrium conditions. Ga and In are transported as metal chlorides by passing hydrogen over the heated metal source, according to



The Ga and In are usually combined in a mixed metal alloy source. The ternary composition is then a function of the ratio of halide pressures and the ratio of equilibrium constants, which is a function of temperature only. Arsenic is introduced into the system by the decomposition of arsenic trichloride,



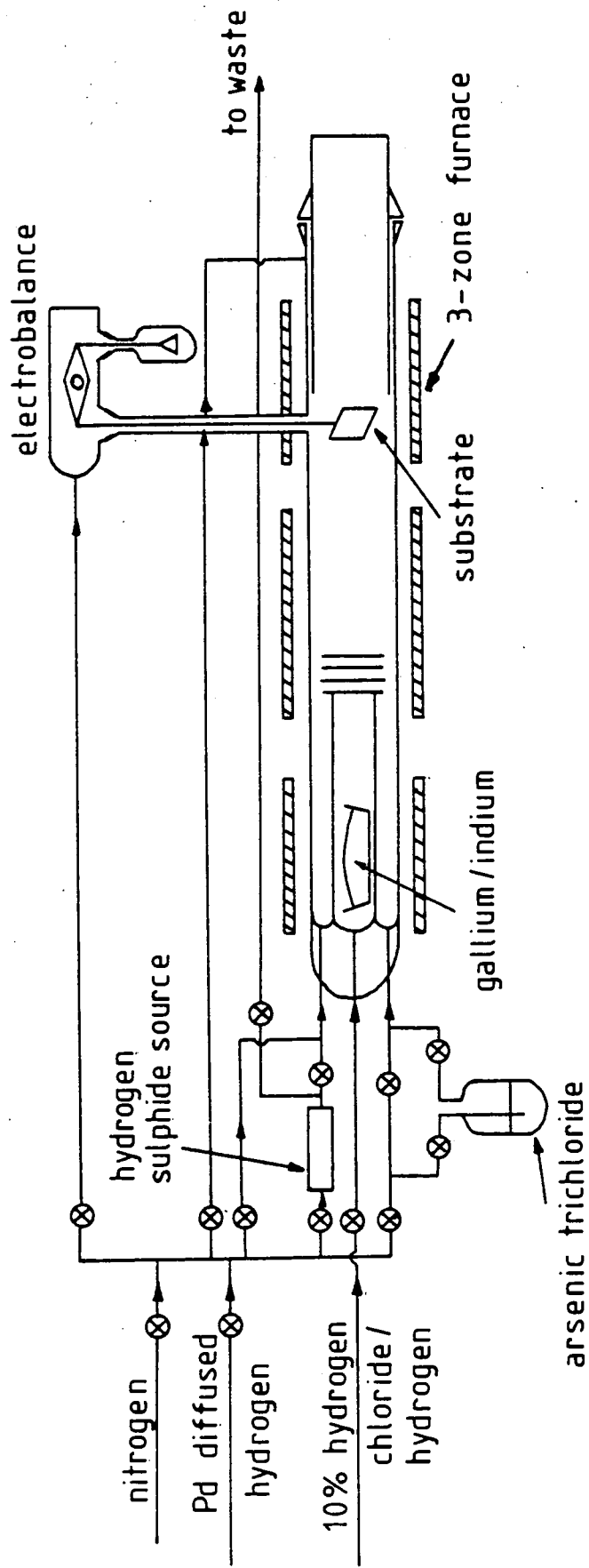


Fig. 1.4 A typical vapour phase epitaxial growth apparatus as used for the growth of GaInAs layers on InP substrates.

Since the equilibrium constants for the interaction of In and Ga with HCl are different Ga is transported preferentially. As the required ratio of Ga to In in the metal source is only about 6% the Ga concentration is reduced as a function of growth time, leading to an increasingly In rich layer (Chatterjee et al, 1982). This effect can be minimised by using an overlarge melt. Hydrogen sulphide is used as a dopant and a diagram of a typical growth apparatus is shown in fig. 1.4. Growth temperatures are typically 630 - 660 °C giving growth rates in the range 1.5 to 2.0 µm/hour, the amount of material grown can be continuously monitored with an electrobalance.

### 1.2.3 Metallo organic chemical vapour deposition (MOCVD)

MOCVD is a similar technique to VPE but the gases used are of different composition. Growth of GaInAs takes place by introducing metered amounts of TEIn (triethylindium), TEGa (triethylgallium) and AsH<sub>3</sub> into a quartz reaction chamber containing the RF heated substrate, placed on a susceptor surface. The hot susceptor has a catalytic effect on the decomposition of the gaseous products, and growth primarily occurs at this surface. The growth rate is proportional to the flow rate of the group III species, but is independent of temperature and also of the partial pressure of AsH<sub>3</sub>. Growth occurs according to the following scheme

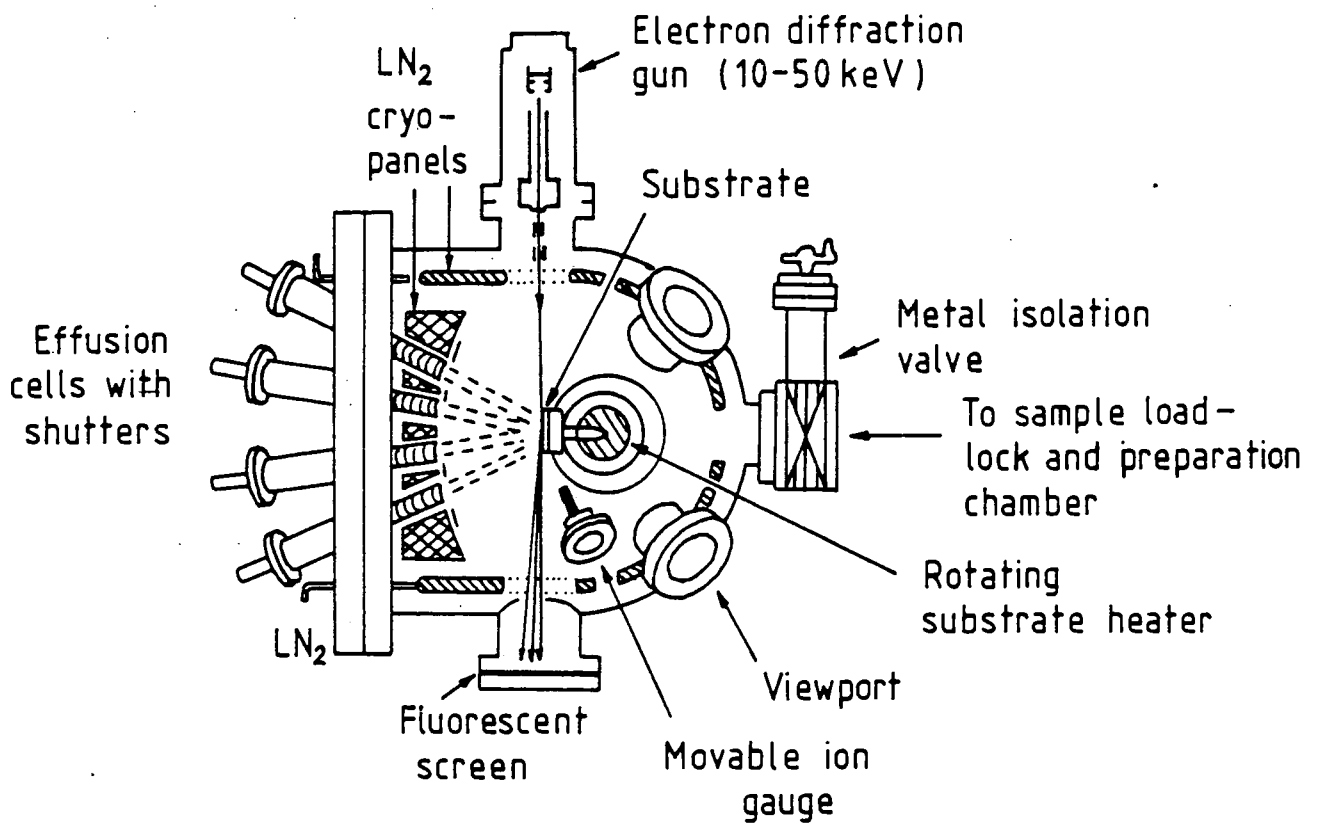
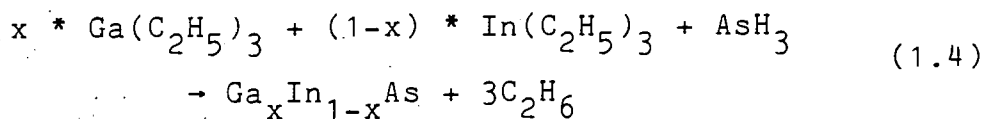


Fig. 1.5 A typical MBE growth apparatus as used for the growth of (Ga,Al)As layers on GaAs substrates.



Typically growth temperatures are  $\sim 550$  °C and with the usual gas flow rates produces growth at the order of 300 Å/min. The growth temperature is less than that used in VPE systems which leads to an improvement in the sharpness of the interfaces due to reduced interdiffusion.

Many of the recently developed systems have computer controlled mass flow valves to control the growth rate, thus enabling the growth of superlattices, as an alternative to the MBE technique. In particular MOCVD is better suited to the growth of the (Ga,In)As alloys than is MBE.

#### 1.2.4 Molecular beam epitaxy (MBE)

Molecular beam epitaxy is the most flexible technique available for the growth of artificial superlattices, particularly those based on (Ga,Al)As. This method is based on the reaction of thermal beams of atoms or molecules directed onto a heated substrate under ultra high vacuum conditions. This technique enables control of composition, thickness and doping level down to the atomic scale. Detailed reviews have been presented by Cho and Arthur (1975), Ploog (1980,1981,1982), Chang (1980a) and Foxon and Joyce (1981). Since the growth is a kinetic and not an equilibrium process abrupt changes in composition can be achieved by stopping the beam of the species required. A typical growth apparatus is shown in fig. 1.5. The effusion



cells are individually shuttered, operated by vacuum feedthroughs, and may additionally be computer controlled for the accurate growth of repeat layer sequences. Low growth rates of about  $1 \mu\text{m}/\text{hour}$  are usual with growth temperatures of  $530 - 630 \text{ }^\circ\text{C}$  for GaAs and  $630 - 670 \text{ }^\circ\text{C}$  for GaAlAs. The use of  $\text{LN}_2$  cooled cryopanel for pumping of the condensable residual gas species is required for the growth of high quality GaAlAs (Jung et al, 1983 ).

Since the growth takes place inside a UHV system it is ideal for in situ surface studies such as Auger electron spectroscopy, reflection high energy electron diffraction (RHEED) and secondary ion mass spectroscopy (SIMS), although the addition of these techniques adds significantly to the cost of the system.

### 1.3 Lattice Mismatch and Tetragonal Distortion of the Epitaxial Layer

Since ternary alloys of III-V elements are only lattice matched to binary III-V substrates at one composition any deviation from this matched value will lead to misfit stress occurring during growth. Clearly, any lattice parameter measurements performed will be on this final structure and it is, therefore, important to be able to relate these values to the initial compositions. This can only be performed if we understand how the lattice is deformed during growth. Since the stresses associated with the interface and the epilayer are directly related to the

generation and propagation of dislocations we must include the effect of misfit dislocations in any prediction of the misfit stress. Ternary alloys are clearly restricted in their compositional range if large values of misfit stress are not to occur, thus making the alteration of the band gap rather difficult. For this reason the extra degree of freedom provided by quaternary alloys has greatly increased their popularity. The original composition of the quaternary cannot be determined from a lattice parameter measurement alone, the measurement of the band gap is usually used to provide the additional parameters required.

Misfit stress has been quantitatively described without the inclusion of the effects of misfit dislocations by a large number of workers (Jesser and Kuhlman-Wilsdorf, 1978; Hornstra and Bartels, 1978; Bartels and Nijman, 1978; Matsui et al, 1979). Their predictions have been compared with experimental observations for dislocation free samples and found to be in good agreement.

The stress distribution inside the heteroepitaxial layer has been used to determine the radius of curvature of the crystal by a number of authors. A simple beam bending theory for single layers has been developed by Timoshenko (1925) based on the theory of a bimetallic strip. However, inconsistencies in the theory have been reported for it is not internally consistent when the two phase composite strip is reduced to a single phase strip. The bending moment for such a two phase composite strip has been derived properly

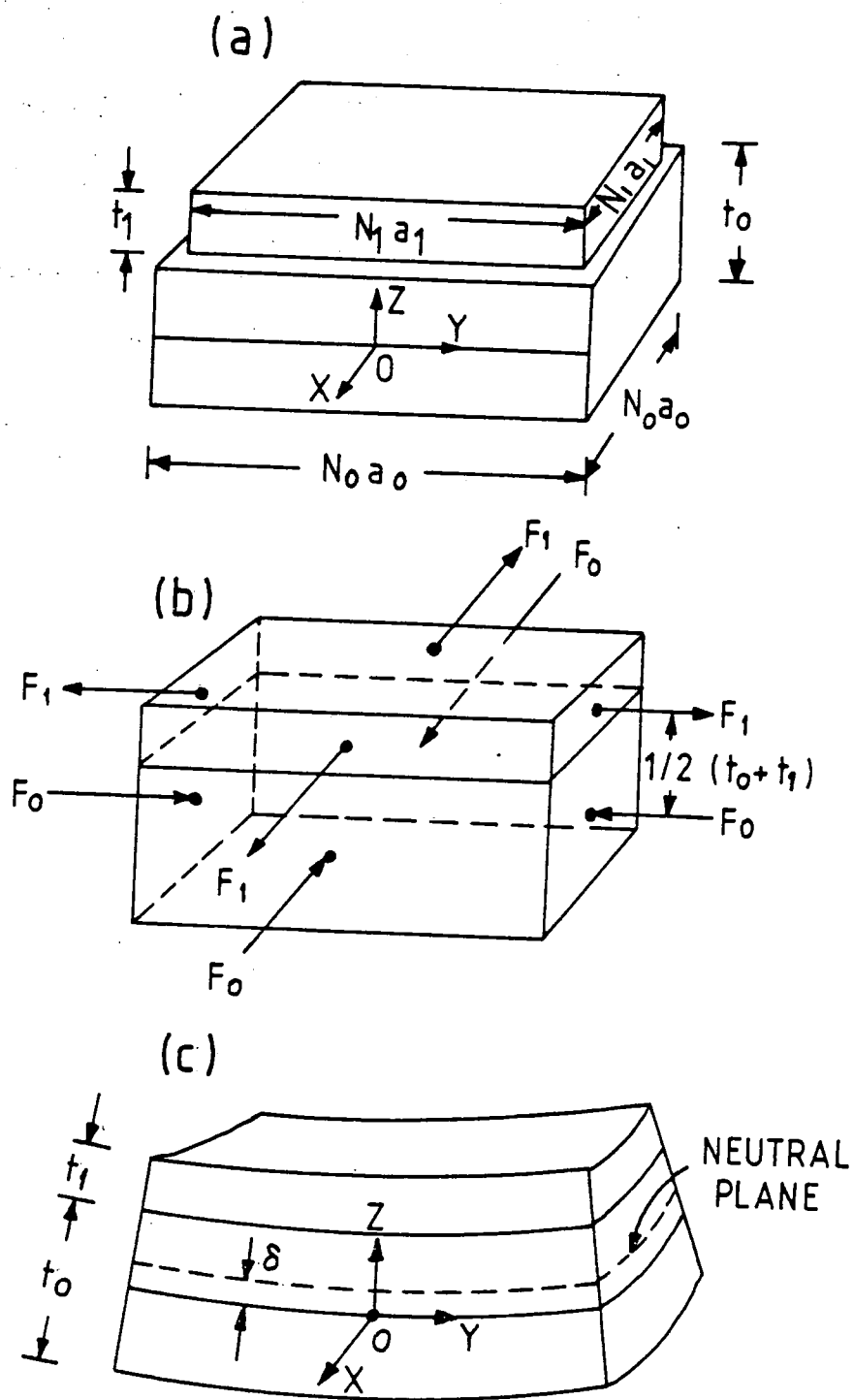


Fig. 1.6 Formation of a two layer composite (a) two single crystal plates with lattice constants  $a_1$  and  $a_0$ , number of atoms along the edge  $N_1$  and  $N_0$ , and thicknesses  $t_1$  and  $t_0$ , respectively; (b) Plate 1 is stretched and plate 0 is compressed to match the macroscopic dimensions, the two plates are then bonded to form a composite; (c) the composite bends towards the side with shorter lattice constant after the removal of the external stresses.

by Davidenkov (1961). Chu et al (1985) have since used this approach to analyse in detail this situation with the inclusion of the effect of interfacial misfit dislocations. The misfit stress in arbitrary multiple layer systems without the effect of misfit dislocations has been determined by Vilms and Kerps (1982) and Olsen and Ettenberg (1977), while Chu et al (1985) have extended their approach to cover these structures.

### 1.3.1 Misfit stress in a single epitaxial layer-substrate composite

Following Chu et al (1985) we consider the effect of bonding a thin plate of isotropic single crystal of size  $N_1 a_1 \times N_1 a_1 \times t_1$  onto a substrate of size  $N_0 a_0 \times N_0 a_0 \times t_0$  ( $N_i$  is the number of unit cells along an edge,  $a_i$  the lattice parameter and  $t_i$  the thickness of the plate), as shown in fig. 1.6. For a coherent interface, with no misfit dislocations,  $N_1$  must become equal to  $N_0$  during epitaxy. We can initially assume that  $a_1$  is less than  $a_0$ , without any loss of generality, which gives  $l_1 = N_0 a_1$  less than  $l_0 = N_0 a_0$ . The bonding process is then achieved by applying equal and opposite forces,  $F$ , to stretch plate 1 and compress plate 0, uniformly in the lateral direction, to the final dimension  $l_f \times l_f$ . The two plates can then be bonded together with perfect alignment of the atomic planes. At the moment the two plates are bonded the composite experiences an applied bending moment  $F(t_0 + t_1)/2$ , which is counterbalanced by the moment resulting from the internal elastic stress. Finally

the applied forces are removed and the moments from the elastic stress bend the composite in the direction shown in fig. 1.6. This bending relaxes some of the stress with the final radius of curvature being determined by the final state of the internal stress.

In order to include the effect of a partially coherent interface (ie one containing misfit dislocations) we introduce an effective lattice constant. If we consider the bonding of two plates where  $a_1$  is less than  $a_0$ ,  $N_1$  greater than  $N_0$  and  $l_1 = N_1 a_1$  smaller than  $l_0 = N_0 a_0$  when the macroscopic dimensions are matched an extra number of atomic planes  $N_1 - N_0$  exist in plate 1 and are terminated at the interface. These then become the interfacial misfit dislocations. If the Burgers vector along the interface is  $b_I$  the total amount of mismatch taken up by the misfit dislocations in plate 1 is  $(N_1 - N_0)b_I$ . This corresponds to  $(N_1 - N_0)b_I / N_0$  per bonded atom. An effective lattice parameter  $a_1'$  can then be defined as

$$a_1' = a_1 + \frac{N_1 - N_0}{N_0} b_I \quad (1.5)$$

If we let  $\rho$  be the linear density of misfit dislocations given by  $\rho = (N_1 - N_0) / N_0 a_0$  the effective lattice becomes

$$a_1' = a_1 + a_0 \rho b_I \quad (1.6)$$

### 1.3.2 Stress distribution

The balance of forces acting on the sample gives

$$F_1 + F_0 = 0 \quad (1.7)$$

while balancing the moments acting on the sample gives

$$F_1 \frac{t_0 + t_1}{2} + F_0 \frac{t_0}{2} = M_0 + M_1 \quad (1.8)$$

where the forces are taken to act at the centre plane of each layer.

$M_0$  and  $M_1$  are given by

$$M_0 = \frac{E_0}{1-\nu} \frac{1}{R} \int_{-t_0/2}^{t_0/2} (z-\delta)^2 l_f dz \quad (1.9)$$

$$M_1 = \frac{E_1}{1-\nu} \frac{1}{R} \int_{t_0/2}^{t_0/2 + t_1} (z-\delta)^2 l_f dz \quad (1.10)$$

where  $R$  is the radius of curvature,  $\nu$  is Poisson's ratio (which is assumed equal for the two plates), and  $\delta$  is the shift of the neutral axis from  $t_0/2$ , as in fig. 1.6. As given by Davidenkov (1961)

$$\delta = \frac{E_0}{E_1} \frac{t_1}{t_0} \frac{(1 + t_1/t_0)}{(1 + E_0 t_1/E_1 t_0)} \quad (1.11)$$

Thus, 
$$M_0 = \frac{E_0 l_f}{(1-\nu)R} \left( \frac{t_0^3}{12} + t_0 \delta^2 \right) = \frac{E_0 I_0}{(1-\nu)R} \quad (1.12)$$

$$M_1 = \frac{E_1 l_f}{(1-\nu)R} \left[ \frac{t_1^3}{12} + t_1 \left( \delta - \frac{t_1 + t_0}{2} \right)^2 \right] = \frac{E_1 I_1}{(1-\nu)R} \quad (1.13)$$

where  $I_i$ ,  $i=0$  and  $1$ , is defined as the moment of inertia

associated with each plate of the composite. We note that for the case  $E_1/E_0 \approx 1$  and  $t_1/t_0 \ll 1$ , and keeping only the lowest order terms in  $t_1/t_0$  these become

$$\delta = \frac{t_1}{2} \quad (1.14)$$

$$I_0 = \frac{l_f t_0^3}{12} \quad (1.15)$$

$$I_1 = l_f \left( \frac{t_1^3}{12} + \frac{t_1 t_0^2}{4} \right) \approx l_f \frac{t_1 t_0^2}{4} \quad (1.16)$$

Now the strain in any layer is given by the sum of the strain due to the force  $F_i$  and the strain due to the bending,  $(z - \frac{1}{2}t_i)/R$ , where  $z$  is the distance in the  $i$ th layer from the bottom of the  $i$ th layer.

Clearly the atomic separation in each layer must match at the interface for coherency, thus

$$a_1 \left[ 1 + \frac{F_1}{l_f t_1} \frac{(1-\nu)}{E_1} - \frac{t_1}{2R} \right] + \rho b_I a_0 = a_0 \left[ 1 + \frac{F_0}{l_f t_0} \frac{(1-\nu)}{E_0} + \frac{t_0}{2R} \right] \quad (1.17)$$

Now, since from force equilibrium we have  $F_1 = -F_0$  this becomes

$$a_1 - \frac{a_1 F_0 (1-\nu)}{l_f t_1 E_1} - \frac{a_1 t_1}{2R} + \rho b_I a_0 = a_0 + \frac{a_0 F_0 (1-\nu)}{l_f t_0 E_0} + \frac{a_0 t_0}{2R} \quad (1.18)$$

$$\text{ie } \frac{-F_0(1-\nu)}{l_f t_1 E_1} \frac{a_1}{a_0} \left[ 1 + \frac{a_0 E_1 t_1}{a_1 E_0 t_0} \right] = \frac{a_0 - a_1}{a_0} - \rho b_I + \frac{t_0}{2R} \left( 1 + \frac{a_1 t_1}{a_0 t_0} \right) \quad (1.19)$$

$$\text{ie } F_0 = - \frac{a_0}{a_1} \frac{l_f E_1 t_1}{1-\nu} \frac{1}{1 + a_0/a_1 E_1/E_0 t_1/t_0} \times \left[ \frac{a_0 - a_1}{a_0} - \rho b_I + \frac{t_0}{2R} \left( 1 + \frac{a_1 t_1}{a_0 t_0} \right) \right] \quad (1.20)$$

The stress at any point in each layer is given by

$$\sigma_{xx}^i = \frac{F_i}{l_f t_i} + \frac{E_i}{(1-\nu)} \frac{(z_i - t_i/2)}{R} \quad (1.21)$$

where  $z_i$ ,  $i=0$  and  $1$ , is measured from the bottom of the  $i$ th layer.

We then obtain

$$\sigma_{xx}^0 = - \frac{E_1}{(1-\nu)} \left[ \frac{a_0}{a_1} \frac{t_1}{t_0} \frac{1}{1 + a_0/a_1 E_1/E_0 t_1/t_0} \times \left\{ \frac{a_0 - a_1}{a_0} + \frac{t_0}{2R} \left( 1 + \frac{a_1 t_1}{a_0 t_0} \right) - \rho b_I \right\} + \frac{E_0}{E_1} \frac{(z_0 - t_0/2)}{R} \right] \quad (1.22)$$



and

$$\begin{aligned} \sigma'_{xx} = & - \frac{E_1}{(1-\nu)} \left[ \frac{a_0}{a_1} \frac{1}{1 + a_0/a_1 E_1/E_0 t_1/t_0} \right. \\ & \times \left\{ \frac{a_0 - a_1}{a_0} + \frac{t_0}{2R} \left( 1 + \frac{a_1 t_1}{a_0 t_0} \right) - \rho b_I \right\} \\ & \left. + \frac{(z_0 - t_0/2)}{R} \right] \end{aligned} \quad (1.23)$$

We note that the above equations differ slightly from those given by Chu et al (1985) which are dimensionally incorrect.

Clearly the other stress components will be

$$\sigma_{yy}^i = \sigma_{xx}^i \quad (1.24)$$

$$\sigma_{zz}^i = \sigma_{xy}^i = \sigma_{xz}^i = \sigma_{yz}^i = 0 \quad (1.25)$$

for  $i=0$  and  $1$ .

The radius of curvature is given by

$$\frac{1}{R} = \frac{2E_1 t_1 t_0 (1 + t_1/t_0) a_0/a_1}{A} \left\{ \frac{a_0 - a_1}{a_0} - \rho b_I \right\} \quad (1.26)$$

where

$$A = 4 \left( 1 + \frac{a_0}{a_1} \frac{E_1}{E_0} \frac{t_1}{t_0} \right) \left( \frac{E_0 I_0}{l_f} + \frac{E_1 I_1}{l_f} \right) \quad (1.27)$$

$$- \frac{a_0}{a_1} E_1 t_1 t_0 (t_1 + t_0) \left( 1 + \frac{a_1}{a_0} \frac{t_1}{t_0} \right)$$

### 1.3.3 Parallel mismatch and interfacial dislocation density

Since the parallel mismatch,  $(\Delta a/a)_{11}$ , is defined as the lattice mismatch in the plane parallel to the (001)

interface, a coherent interface will have  $(\Delta a/a)_{11}=0$ . The parallel mismatch can only be non zero in the presence of misfit dislocations. Now  $a_1 = a_1 + a_0 \rho b_I$ , so if we stress the lattice such that  $a_1$  and  $a_0$  match the final value  $a_f$  the lattice constant  $a_1$  is changed to  $a_{1f}$  and we have

$$a_f = a_{1f} + a_f \rho b_I \quad (1.28)$$

Therefore, 
$$\left( \frac{\Delta a}{a} \right)_{11} = \frac{a_f - a_{1f}}{a_f} = \rho b_I \quad (1.29)$$

We note that with no misfit dislocations  $a_1$  and  $a_0$  must be strained to the same final value.

#### 1.3.4 Tetragonal distortion

Tetragonal distortion occurs because the lattice is free to expand in the z direction, ie perpendicular to the interface. Since  $\sigma_{xx}^{\circ}$  and  $\sigma_{xx}^{\prime}$  are opposite in sign the cubic lattices will distort in the opposite sense.

The lattice constants perpendicular to the interface are given by

$$a_1^{\perp} = a_1 \left( 1 - 2\nu \frac{\sigma_{xx}^{\prime}}{E_1} \right) \quad (1.30)$$

and

$$a_0^{\perp} = a_0 \left( 1 - 2\nu \frac{\sigma_{xx}^{\circ}}{E_0} \right) \quad (1.31)$$

where the second terms are  $e_{zz}$  due to the Poisson

effect. Therefore,

$$\left(\frac{\Delta a}{a}\right)_{\perp} = \frac{a_0^{\perp} - a_1^{\perp}}{a_0} \quad (1.32)$$

and substituting the value for  $\sigma_{xx}$  and  $\sigma_{yy}$  we obtain

$$\left(\frac{\Delta a}{a}\right)_{\perp} = \left(\frac{\Delta a}{a}\right)_{\parallel} \frac{1 + \nu}{1 - \nu} - \frac{2\nu}{1 - \nu} \rho b_{\perp} \quad (1.33)$$

Replacing  $\rho b_{\perp}$  by the parallel mismatch we obtain

$$\left(\frac{\Delta a}{a}\right)_{\perp} = \frac{1 - \nu}{1 + \nu} \left(\frac{\Delta a}{a}\right)_{\parallel} + \frac{2\nu}{1 + \nu} \left(\frac{\Delta a}{a}\right)_{\parallel} \quad (1.34)$$

We note that from equation (1.27) that  $1/R = 0$  if the parallel mismatch is equal to the perpendicular mismatch, ie for a completely incoherent interface. Therefore, coherently matched layers must produce a structure that has a non infinite radius of curvature unless the relaxed lattice mismatch is zero.

This procedure can be extended to multiple layer structures giving, after some work,

$$\left(\frac{\Delta a}{a}\right)_{\perp} = \frac{1 + \nu}{1 - \nu} \left(\frac{\Delta a}{a}\right)_{\parallel} - \frac{2\nu}{1 - \nu} \rho_i b_{\perp i} \quad (1.35)$$

for  $i=1, N$  where  $N$  is the number of layers.

We note that we have assumed isotropic elasticity in deriving the above equations and also that the layer/substrate interface is of the type (001). The reader is referred to the paper of Honstra and Bartels (1978) for results when epitaxy is not on a (001) plane, although

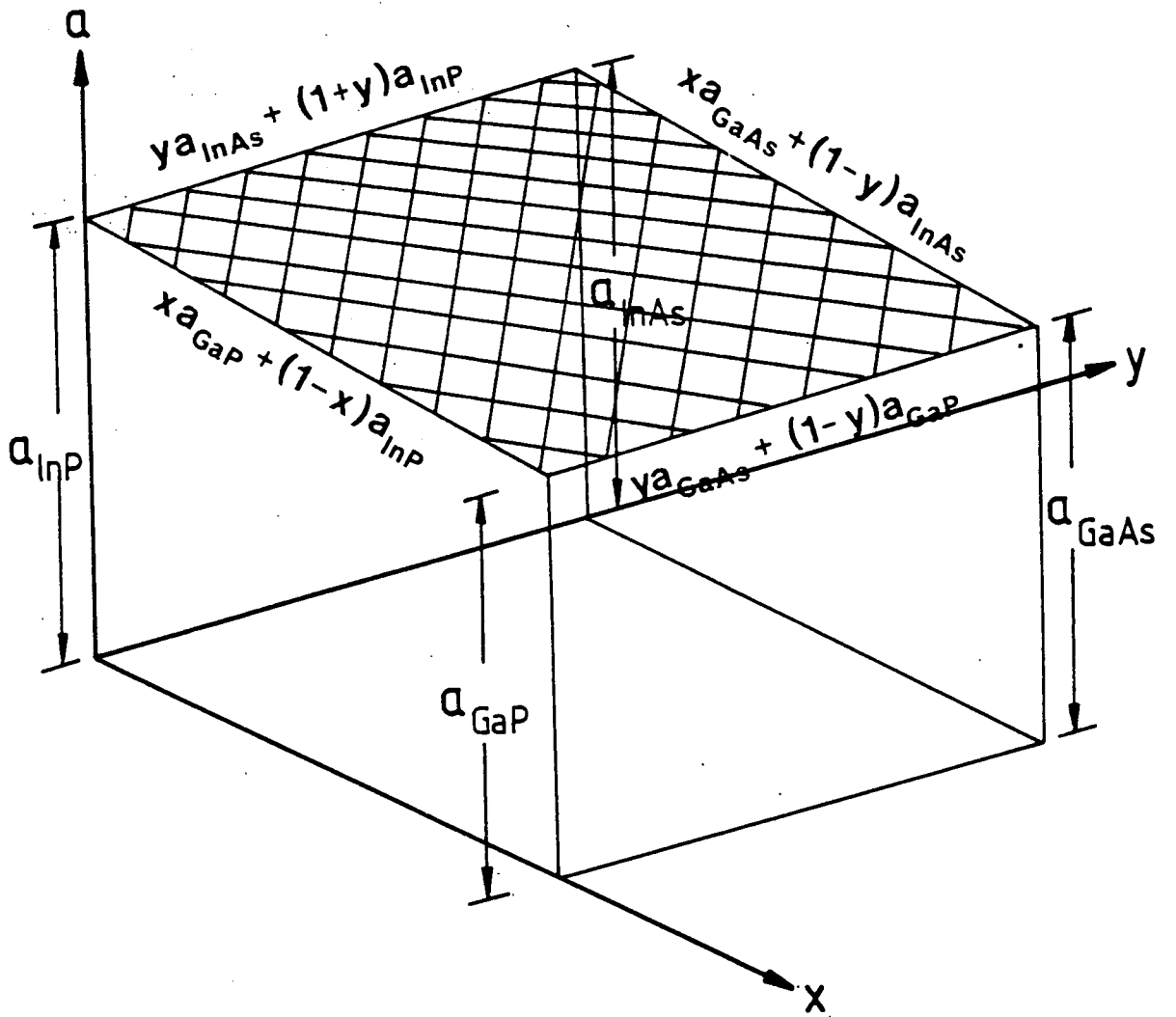


Fig. 1.7 Surface representing the lattice parameter of  $\text{Ga}_x\text{In}_{1-x}\text{As}_y\text{P}_{1-y}$  as a function of  $x$  and  $y$ .

partial coherency of the interface is not included.

As already mentioned, the relaxed lattice mismatch  $(\Delta a/a)_r$  can be directly related to the composition for ternary alloys, using Vegard's law, but not for quaternary or higher alloys. For quaternaries another, independent, measurement relating  $x$  and  $y$  is required.

#### 1.4 Vegard's Law and Band Gaps

Once the relaxed lattice parameter of the layer has been determined the composition of the layer can be found. For ternary alloys the composition is given by Vegard's law, since the lattice parameter is a linear function of the composition. For example for  $\text{Ga}_x\text{In}_{1-x}\text{As}$  we have

$$a(\text{Ga}_x\text{In}_{1-x}\text{As}) = (1-x)a(\text{InAs}) + xa(\text{GaAs}) \quad (1.36)$$

where  $a(\text{alloy})$  is the relaxed lattice parameter of the alloy. Clearly, similar equations exist for other ternaries. Thus  $x$  can easily be determined.

For quaternaries the variation in lattice parameter is slightly more complicated. Taking  $\text{Ga}_x\text{In}_{1-x}\text{As}_y\text{P}_{1-y}$  as an example, the lattice parameter is given by the surface shown in fig. 1.7. Considering the change in lattice parameter parallel to the  $x$  and  $y$  axes we obtain

$$\frac{\partial a}{\partial x} = ya(\text{GaAs}) + (1-y)a(\text{GaP}) - ya(\text{InAs}) - (1-y)a(\text{InP}) \quad (1.37)$$

and

$$\frac{\partial a}{\partial y} = xa(\text{GaAs}) + (1-x)a(\text{InAs}) - xa(\text{GaP}) - (1-x)a(\text{InP}) \quad (1.38)$$

With the limit that at  $x=0, y=0$   $a=a(\text{InP})$  we obtain

$$\begin{aligned} a(\text{Ga}_x\text{In}_{1-x}\text{As}_y\text{P}_{1-y}) &= xya(\text{GaAs}) + x(1-y)a(\text{GaP}) \quad (1.39) \\ &+ (1-x)ya(\text{InAs}) \\ &+ (1-x)(1-y)a(\text{InP}) \end{aligned}$$

Clearly, we cannot determine  $x$  and  $y$  from this single equation. Empirical relationships between the composition and band gap have been determined by Nahory et al (1978). The variations found to best fit the experimental data are shown in Table 1.1 and the values of the lattice parameters for some of the common III-V binary alloys are shown in Table 1.2.

We note that the equation for the quaternary could be found in a similar manner to the lattice parameter by integrating the partial derivatives found from the ternary variations, with the required equation being that of a surface similar to that in fig. 1.7. This relation would then be

$$\begin{aligned} E_g(x,y) &= 1.35 + 0.668x - 1.17y + 0.758x^2 - 0.18y^2 \\ &- 0.069xy - 0.322x^2y + 0.03xy^2 \text{ eV} \quad (1.40) \end{aligned}$$

However, Nahory et al (1978) found that the relation given in Table 1.1 gave a better fit to the experimental data.

TABLE 1.1

Band gaps of some of the common III-V ternary and quaternary compounds.

Alloy	Band gap (eV)
$\text{In}_{1-x}\text{Ga}_x\text{As}$	$E_g(x) = 0.36 + 0.629x + 0.436x^2$
$\text{InAs}_y\text{P}_{1-y}$	$E_g(y) = 1.35 - 1.17y + 0.18y^2$
$\text{In}_{1-x}\text{Ga}_x\text{P}$	$E_g(x) = 1.35 + 0.668x + 0.758x^2$
$\text{GaAs}_{1-y}\text{P}_y$	$E_g(y) = 2.77 - 1.56y + 0.21y^2$
$\text{In}_{1-x}\text{Ga}_x\text{As}_y\text{P}_{1-y}$	$E_g(x,y) = 1.35 - 0.72y + 0.12y^2$

TABLE 1.2

Lattice parameters of some of the more common binary III-V alloys.

Alloy	Lattice Parameter (Å)
GaAs	5.6535
InP	5.8688
InAs	6.0590
GaP	5.4512

### 1.5 Characterisation of Epitaxial Layers

The main requirements of any characterisation technique are the determination of the layer composition and the layer thickness. If more than one layer is present the individual thicknesses and compositions should also be determined. Also, if a continuous variation in composition is present in a layer this needs to be determined. The crystalline quality (surface morphology and dislocation density) of the layer is also important. A number of techniques are available including transmission electron microscopy (TEM), Auger

electron spectroscopy (AES), Rutherford backscattering (RBS), secondary ion mass spectrometry (SIMS), reflection high energy electron diffraction (RHEED) plus many varied X-ray and electrical methods. In particular, the first few techniques require extensive sample preparation and extremely expensive apparatus.

Of these techniques TEM is the most widely used, but since electrons are absorbed by very small amounts of material the samples need to be considerably thinned. For layered structures these thin sections need to be taken perpendicular to the layer interfaces. Since only a small region of the sample can be studied some doubt exists as to it being representative of the bulk sample. Also since some of the strain present in the bulk sample may be relieved during the thinning process errors may be present in any lattice parameter determination. TEM is particularly useful for studying the repeat periodicity and layer thicknesses of superlattices, see for example Petroff et al (1984).

Clearly, since the lattice parameter of a mismatched layer is different from that of the substrate X-ray diffraction should be able to detect this difference through the change in Bragg angle for a given reflection. Advantages of X-ray techniques are that little or no sample preparation is required and that it is non destructive. However, due to the magnitude of the mismatch usually found in III-V materials being of the order of parts in  $10^3$  (often less) difficulties arise with single crystal techniques which are



limited by the angular width of the reflection, which is determined by the collimation and hence beam divergence being used. Nevertheless, single crystal techniques have been used, but are limited to detecting mismatches down to the order of  $5 \times 10^{-4}$  (see for example Isherwood, Brown and Halliwell, 1981; Chang et al, 1979; Chang, 1980b). It has been well known since the 1920's that the double crystal spectrometer can overcome these problems and that the sensitivity to lattice mismatch will then be limited by the dynamical width of the reflections themselves (the order of 10 seconds of arc for the majority of reflections from III-V materials).

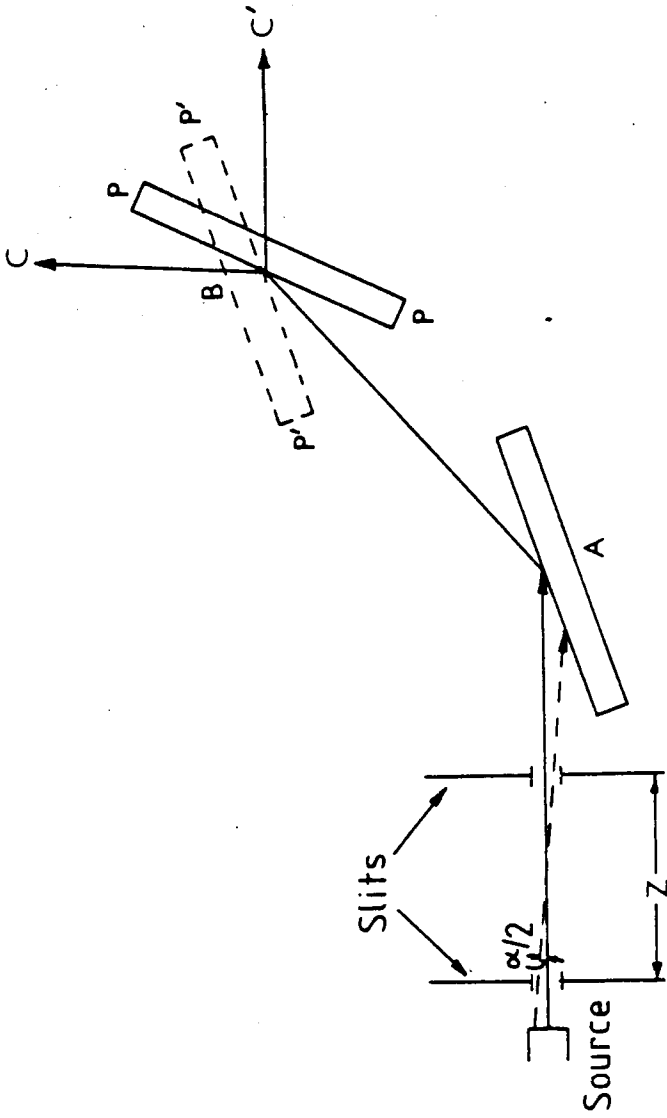


Fig. 2.1 The two possible settings of a double crystal spectrometer. The beam incident on crystal A is characterised by two angles of divergence:  $\alpha$  - horizontal and  $\phi$  - vertical.

## CHAPTER 2

## DOUBLE CRYSTAL DIFFRACTOMETRY

## 2.1 General Theory of the Double Crystal Camera

The double crystal spectrometer (or diffractometer) has the property of removing the effect of the X-ray linewidth and beam divergence on the reflection profile of a crystal. This effect has been well known since the 1920's, and the reader is referred to the papers of Allison and Williams (1930), Allison (1932) Compton and Allison (1935) and du Mond (1937). Double crystal diffractometers have been in existence since the early 1930's (Compton, 1931; du Mond and Marlow, 1937), but only recently has their use become more widespread with the development of highly perfect semiconductor crystals.

The designs of the double crystal spectrometer, for which the theory was developed, are based on combining two crystals with successive Bragg reflection as shown in fig. 2.1. The X-ray beam passes through two parallel horizontal and vertical slits before being incident on the monochromator crystal A. As a result it is characterised by two values of divergence:  $\alpha$  - horizontal divergence and  $\varphi$  - vertical divergence. The maximum values of these angles are then given by

$$\alpha_m = c/z, \quad \varphi_m = h/z \quad (2.1)$$

where  $c$  is the width and  $h$  the height of the slits, with  $z$

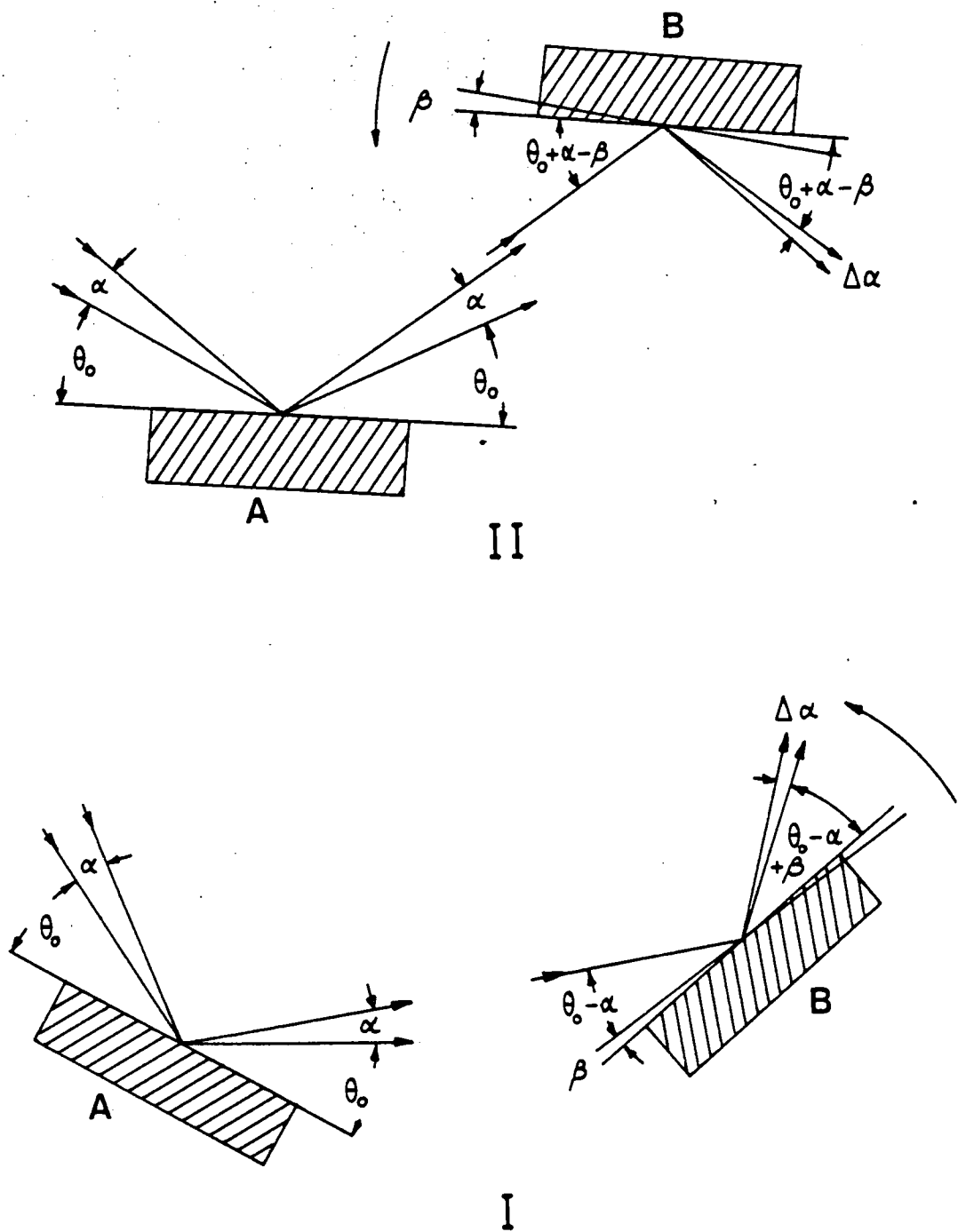


Fig. 2.2 The x-ray paths and angles for the two possible settings of the double crystal spectrometer.

the distance between them. Clearly there are two fundamentally possible settings of the spectrometer as shown in fig. 2.2, with the second crystal B in either the PP or P'P' positions.

The first crystal A is aligned so that a central ray in the incident beam makes an angle  $\theta_0 = \theta + \eta_0$  with the reflecting planes, corresponding to the centre of the total reflection region. We note that the value of  $\eta_0$  is dependent on the refractive index of the crystal and its value is given in the next chapter. Consequently the maximum of the reflection profile does not correspond exactly with the kinematic Bragg angle  $\theta$ . Crystal B is then set up in an arbitrary initial position, close to the position of reflection. Rotating crystal B about the vertical axis and recording the reflected intensity as a function of angle gives the rocking curve. Therefore, we need to obtain the relationship between this curve and the true dynamical diffraction curve from crystal B alone. We first consider the values of the angles formed by the various rays in the incident beam with crystals A and B at various wavelengths.

Following Compton and Allison (1935) and Pinsker (1978) the deviation of an arbitrary ray in the incident beam from the central ray is ( $\theta$  is the glancing angle and  $n_A$  the order of the reflection)

$$\alpha = \frac{1}{2} \phi^2 \tan \theta(\lambda_0, n_A) - (\lambda - \lambda_0) \left( \frac{d\theta}{d\lambda} \right)'_0 \quad (2.2)$$

where the central ray is characterised by the parameters  $\theta_0$ ,

$\lambda_0$ ,  $\alpha=0$  and  $\varphi=0$ . The second term corresponds to the deviation due to vertical divergence and the third due to non monochromaticity. The last term takes this form after assuming that within the spectral width of the incident beam the reflection angles change only slightly.

For the second crystal the deviation from the central ray is given by

$$\pm \beta \mp \alpha - \frac{1}{2} \varphi^2 \tan \theta (\lambda_0, n_B) - (\lambda - \lambda_0) \left( \frac{d\theta}{d\lambda} \right)_0^2 \quad (2.3)$$

The upper signs correspond to position I and the lower to position II.

We must now account for the intensity distribution within the original beam in relation to the divergence and wavelength. We assign functions  $G(\alpha, \varphi)$ ,  $J(\lambda - \lambda_0)$  to represent these distributions. The functions are normalised so that the intensity within an interval  $(d\alpha, d\varphi, d\lambda)$  is determined by multiplying by the interval.

The total power reflected by the second crystal is then

$$P(\beta) = \int_{-\varphi_m}^{\varphi_m} \int_{\lambda_{min}}^{\lambda_{max}} \int_{-\alpha_m}^{\alpha_m} G(\alpha, \varphi) J(\lambda - \lambda_0) \quad (2.4)$$

$$\times C_A \left[ \alpha - \frac{1}{2} \varphi^2 \tan \theta_1 - (\lambda - \lambda_0) \left( \frac{d\theta}{d\lambda} \right)_0 \right]$$

$$\times C_B \left[ \pm \beta \mp \alpha - \frac{1}{2} \varphi^2 \tan \theta_2 - (\lambda - \lambda_0) \left( \frac{d\theta}{d\lambda} \right)_0^2 \right] d\alpha d\varphi d\lambda$$

where  $C_A$  and  $C_B$  are expressions corresponding to the reflection curves of crystals A and B. The rocking curve is then given by  $P(\beta)$  over the range of angles  $\beta$  required.

We can study the general properties of this equation by considering  $C_A$  and  $C_B$  to be non zero only when their arguments are zero (although this is unphysical it is a reasonable approximation). Therefore,

$$\alpha - \frac{1}{2}\phi^2 \tan\theta(\lambda_0, n_A) - (\lambda - \lambda_0) \left( \frac{d\theta}{d\lambda} \right)'_0 = 0 \quad (2.5)$$

and

$$\pm\beta \mp \alpha - \frac{1}{2}\phi^2 \tan\theta(\lambda_0, n_B) - (\lambda - \lambda_0) \left( \frac{d\theta}{d\lambda} \right)'_0 = 0 \quad (2.6)$$

Eliminating  $\alpha$  gives

$$\begin{aligned} \beta - \frac{\phi^2}{2} [\tan\theta(\lambda_0, n_A) \pm \tan\theta(\lambda_0, n_B)] \\ - (\lambda - \lambda_0) \left[ \left( \frac{d\theta}{d\lambda} \right)'_0 \pm \left( \frac{d\theta}{d\lambda} \right)'_0 \right] = 0 \end{aligned} \quad (2.7)$$

Now defining  $D$  as

$$D = \left( \frac{d\theta}{d\lambda} \right)'_0 \pm \left( \frac{d\theta}{d\lambda} \right)'_0 \quad (2.8)$$

which with the Bragg equation gives

$$D = \frac{n_A}{2d \cos\theta(\lambda_0, n_A)} \pm \frac{n_B}{2d \cos\theta(\lambda_0, n_B)} \quad (2.9)$$

ie

$$\beta = \frac{1}{2} D \lambda_0 \phi^2 + D(\lambda - \lambda_0) \quad (2.10)$$

Now the dispersion in the double crystal arrangement is defined as  $\frac{d\beta}{d\lambda}$ , which gives

$$\text{dispersion} = \frac{d\beta}{d\lambda} = D \quad (2.11)$$

Hence, for the type II arrangement where two identical reflections are used the dispersion is zero.

We will now consider the (+-) type II arrangement. For two identical crystals we have  $C_A = C_B = C$  and  $\theta(\lambda_0, n_A) = \theta(\lambda_0, n_B) = \theta$ , giving

$$P(\beta) = \int_{-\phi_m}^{\phi_m} \int_{\lambda_{min}}^{\lambda_{max}} \int_{-\alpha_m}^{\alpha_m} G(\alpha, \varphi) J(\lambda - \lambda_0) \quad (2.12)$$

$$\times C \left[ \alpha - \frac{1}{2} \varphi^2 \tan \theta - (\lambda - \lambda_0) \left( \frac{d\theta}{d\lambda} \right)_0 \right]$$

$$\times C \left[ -\beta + \alpha - \frac{1}{2} \varphi^2 \tan \theta - (\lambda - \lambda_0) \left( \frac{d\theta}{d\lambda} \right)_0 \right]^2 d\alpha d\varphi d\lambda$$

For nearly perfect crystals  $C$  is only <sup>non-</sup>zero over a range of a few seconds of arc ( $10^{-5}$  radians), when we are within the dynamical diffraction width. The function  $G(\alpha, \varphi)$  can be written as

$$G(\alpha, \varphi) = G_1(\alpha) G_2(\varphi) \quad (2.13)$$

Although  $G_i$  are different from zero over the range of a few minutes of arc, when the term  $\frac{1}{2} \varphi^2 \tan \theta$  is considered the effective region of variation of  $G_2$  is about the same as function  $C$ . It can, however, be shown that the shape of the resultant reflection curve is independent of the vertical divergence of the beam incident on the first crystal in the parallel arrangement (see the next section). For each of the



monochromatic components of the incident beam the effective range of the argument is very small as, approximately,

$$\alpha_e \approx (\lambda - \lambda_0) \left( \frac{d\theta}{d\lambda} \right)_0 \quad (2.14)$$

This estimate corresponds to the crystal A transforming the incident beam into a set of parallel beams for the monochromatic components.

The effective range of the wavelengths taking part in the formation of the maximum inside the reflection curve is estimated at

$$\lambda_0 \pm \left( \frac{d\lambda}{d\theta} \right)_0 \alpha_m \quad (2.15)$$

Typically this amounts to a range that considerably exceeds the half width of the spectral lines.

The function  $P(\beta)$  is different from zero over a very small range of the arguments. Thus in the scheme  $(+n, -n)$  the half width of the reflection curve is comparable to the half width of the dynamical diffraction peak from one crystal. This value is typically exceeded by a factor of 1.3.

Comparing the narrow range of the functions  $C$ , which are taken into account during integration, and the wide ranges of the variables  $\alpha$ ,  $\varphi$  and  $\lambda$  (the functions  $G_1$ ,  $G_2$  and  $J$  change gradually over seconds of arc) we have the expression for the reflection curve as

$$P(\beta) = k \int_{-\infty}^{\infty} C(\alpha) C(\alpha - \beta) d\alpha \quad (2.16)$$

where  $k$  represents the functions  $G_1$ ,  $G_2$  and  $J$ . Conversion between this curve and the dynamical curve of the crystal has been shown to be not possible by Laue (1931).

We also note that, from inspection of this equation, that the  $(+n, -n)$  rocking curve is symmetric about  $\alpha=0$  even if the curves  $C$  are not symmetrical.

For non polarised radiation, as produced in the characteristic lines of conventional X-ray sources, we must add the contribution from  $\sigma$  and  $\pi$  polarisations. Thus

$$P(\beta) = k \int_{-\infty}^{\infty} [ C_{\sigma}(\alpha)C_{\sigma}(\alpha-\beta) + C_{\pi}(\alpha)C_{\pi}(\alpha-\beta) ] d\alpha \quad (2.17)$$

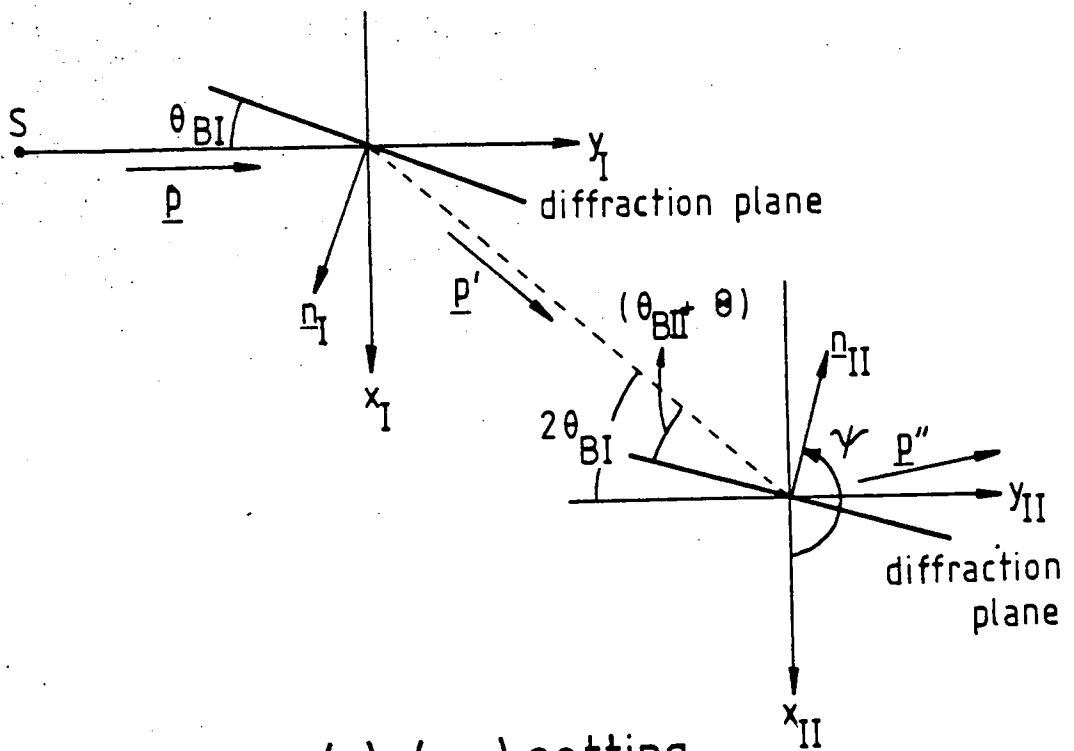
gives the rocking curve for unpolarised radiation.

Often the reflecting power is required and this is defined as

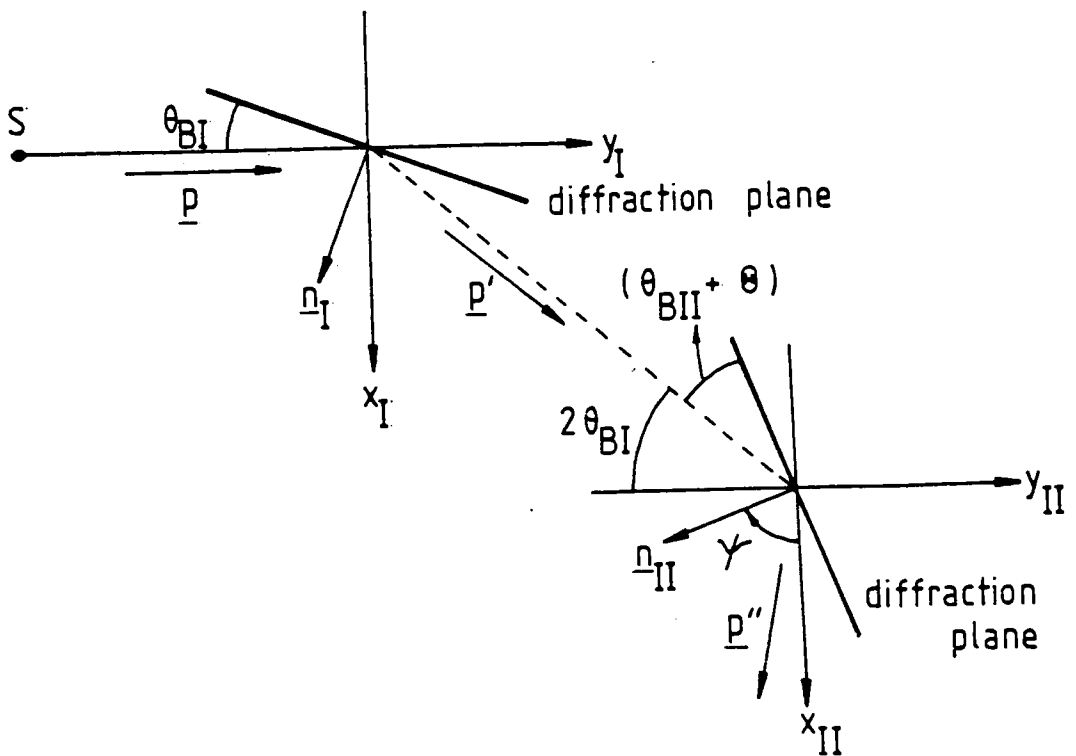
$$R(\beta) = \frac{\int_{-\infty}^{\infty} [C_{\sigma}(\alpha)C_{\sigma}(\alpha-\beta) + C_{\pi}(\alpha)C_{\pi}(\alpha-\beta)] d\alpha}{\int_{-\infty}^{\infty} C_{\sigma}(\alpha) d\alpha + \int_{-\infty}^{\infty} C_{\pi}(\alpha) d\alpha} \quad (2.18)$$

## 2.2 The effect of vertical divergence on the rocking curve

The effect of vertical divergence needs to be considered where there is a non zero angle between the plane of the normal of the second crystal and that of the first crystal, ie the second crystal is tilted with respect to the first crystal. This effect has been studied in detail by Schwarzschild (1928), Jager (1965, 1966) and more recently by



(a) (+ -) setting



(b) (++) setting

Fig. 2.3 The direction vectors and angles of the x-ray beams as required for the effect of vertical divergence.

Yoshimura (1984). The reader is referred to these papers for a complete description, while a summary of the results are presented here.

Following Yoshimura (1984), we can write the diffraction conditions as

$$\underline{p} \cdot \underline{n}_I = -\sin\theta_I; \quad \underline{p}' \cdot \underline{n}_I = \sin\theta'_I; \quad (2.19)$$

$$[\underline{p} \times \underline{n}_I] / \cos\theta_I = [\underline{p}' \times \underline{n}_I] / \cos\theta'_I \quad (2.20)$$

for the first crystal, and

$$\underline{p}' \cdot \underline{n}_{II} = -\sin\theta_{II}; \quad \underline{p}'' \cdot \underline{n}_{II} = \sin\theta'_{II}; \quad (2.21)$$

$$[\underline{p}' \times \underline{n}_{II}] / \cos\theta_{II} = [\underline{p}'' \times \underline{n}_{II}] / \cos\theta'_{II} \quad (2.22)$$

for the second crystal. The angles  $\theta_i$  are given by

$$\theta_I = \theta_{BI} + \eta_I; \quad \theta'_I = \theta_{BI} + \eta'_I \quad (2.23)$$

$$\theta_{II} = \theta_{BII} + \eta_{II}; \quad \theta'_{II} = \theta_{BII} + \eta'_{II} \quad (2.24)$$

where

$$\eta_I = (\Delta\lambda/\lambda)\tan\theta_{BI} + (1-1/b_I)u_I + |1/b_I|^{\frac{1}{2}}v_I W_I \quad (2.25)$$

$$\eta'_I = (\Delta\lambda/\lambda)\tan\theta_{BI} + (1-b_I)u_I + |b_I|^{\frac{1}{2}}v_I W_I \quad (2.26)$$

$$\eta_{II} = (\Delta\lambda/\lambda)\tan\theta_{BII} + (1-1/b_{II})u_{II} + |1/b_{II}|^{\frac{1}{2}}v_{II} W_{II} \quad (2.27)$$

$$\eta'_{II} = (\Delta\lambda/\lambda)\tan\theta_{BII} + (1-b_{II})u_{II} + |b_{II}|^{\frac{1}{2}}v_{II} W_{II} \quad (2.28)$$

The direction of the vectors and crystals are as shown in fig. 2.3.  $\underline{p}$ ,  $\underline{p}'$  and  $\underline{p}''$  represent the directions of the X-

ray beams,  $\underline{n}_I$  and  $\underline{n}_{II}$  unit normals to the diffracting planes and  $\theta_I$ ,  $\theta'_I$ ,  $\theta_{II}$ ,  $\theta'_{II}$  are the angles the X-ray beams form with the diffraction planes for the two crystals.  $b_I$  and  $b_{II}$  are, as usual, the asymmetry factors,  $\gamma_0/\gamma_h$ .  $\theta_{BI}$  and  $\theta_{BII}$  are the kinematical Bragg angles,  $u_I$  and  $u_{II}$  the deviation due to the refraction effect and  $v_I$ ,  $v_{II}$  the half widths of the diffraction peaks.  $W_I$  and  $W_{II}$  represent the deviation from the exact Bragg angle, i.e.  $-1 < W_i < 1$  corresponds to the total reflection range. The second crystal is tilted by an angle  $\rho$  with respect to the first crystal.

Yoshimura (1984) has shown that the relationship between the angular position of the second crystal  $\theta$ , such that a beam from the first crystal with parameter  $W_I$  is diffracted by the second crystal with parameter  $W_{II}$  in the parallel (+-) setting, is

$$\begin{aligned}
 z_I/f = & \sin(\theta_B - \alpha_I) \cos \theta_B \{ \rho [ (\theta + \Delta\theta_u) \cos \theta_B \sin \alpha_I \\
 & - (\eta + \Delta\theta_u) \sin \theta_B \cos \alpha_I ] \pm [ (\theta + \Delta\theta_u) \sin \theta_B \cos \alpha_I \\
 & - (\eta + \Delta\theta_B) \cos \theta_B \sin \alpha_I ] \\
 & \times [ (\theta + \Delta\theta_u)^2 + \rho^2 - (\eta + \Delta\theta_u)^2 ]^{\frac{1}{2}} \} \\
 & \times \{ [ (\theta + \Delta\theta_u) \sin \theta_B \cos \alpha_I - (\eta + \Delta\theta_u) \cos \theta_B \sin \alpha_I ]^2 \\
 & + \rho^2 \sin(\theta_B + \alpha_I) \sin(\theta_B - \alpha_I) \}^{-1} \quad (2.29)
 \end{aligned}$$

Where the vertical coordinate of the incident beam on the first crystal is  $z_I$  and the distance to the X-ray source is

f.  $\alpha_I$  is the angle between the diffraction plane and the surface of the first crystal. The  $\pm$  sign is taken according to  $\alpha_I + \theta_B > 0$  or  $\alpha_I + \theta_B < 0$ .  $\theta_B$  is taken as  $\theta_B = \theta_{BI} = \theta_{BII}$  while  $\eta$  is defined as

$$\begin{aligned} \eta &= \eta_{II} - \eta_I + \frac{1}{2}\rho^2 \tan\theta_B \\ &= [(1-1/b_{II})u_{II} - (1-b_I)u_I] \\ &\quad + (|1/b_{II}|^{\frac{1}{2}}v_{II}W_{II} - |b_I|^{\frac{1}{2}}v_IW_I) \\ &\quad + \Delta\lambda/\lambda_0 \Delta\theta_u / \cos^2\theta_B + \frac{1}{2}\rho^2 \tan\theta_B \end{aligned} \quad (2.30)$$

where  $\Delta\theta_u = \theta_{BII} - \theta_{BI}$  accounts for lattice deformation in the second crystal. For the non parallel (+-) setting and the (++) setting the above equation can be replaced by

$$\begin{aligned} z_I/f &= \{ -\rho \cos\theta_{BI} \pm (\cos\theta_{BI} \cos\theta_{BII})^{\frac{1}{2}} \\ &\quad \times [2\sin(\theta_{BII} \mp \theta_{BI})(\theta - \eta) + \rho^2 (\cos\theta_{BI} / \cos\theta_{BII})]^{\frac{1}{2}} \} \\ &\quad \times [\sin(\theta_{BII} \mp \theta_{BI})]^{-1} \end{aligned} \quad (2.31)$$

The upper sign is for the (+-) setting and the lower for the (++) setting.  $\eta$  given by

$$\begin{aligned} \eta &= [(1-1/b_{II})u_{II} \mp (1-b_I)u_I] \\ &\quad + (|1/b_{II}|^{\frac{1}{2}}v_{II}W_{II} \mp |b_I|^{\frac{1}{2}}v_IW_I) \\ &\quad + \Delta\lambda/\lambda_0 (\tan\theta_{BII} \mp \tan\theta_{BI}) + \frac{1}{2}\rho^2 \tan\theta_{BII} \end{aligned} \quad (2.32)$$

(signs as before).

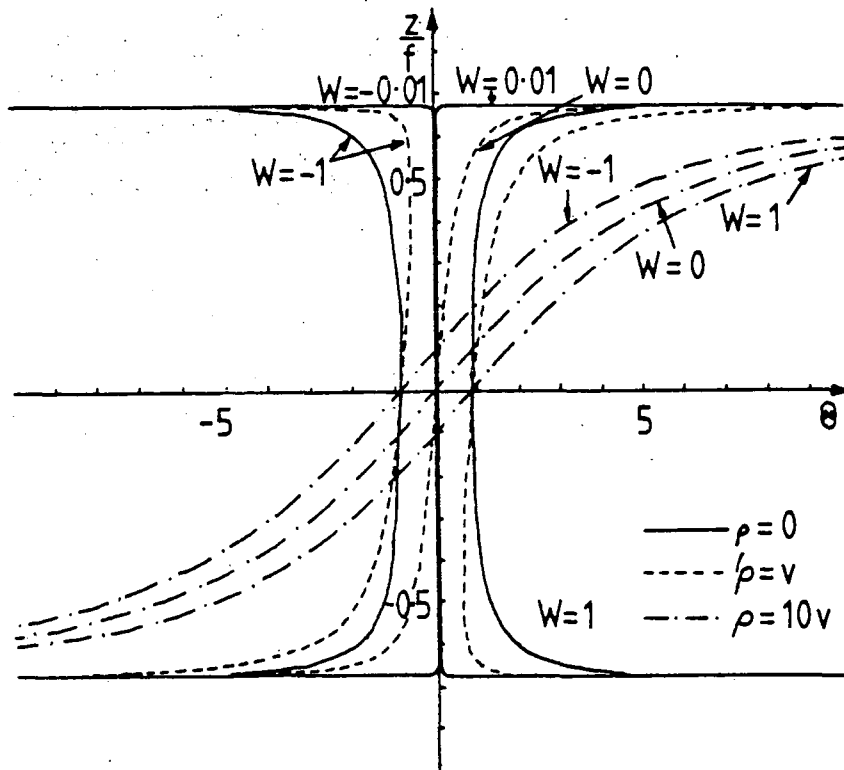


Fig. 2.4 The change in crystal angle ( $\theta$ ) required to diffract a beam with value  $W$  as a function of  $z/f$ , the position of the incident beam on the first crystal, for a parallel (+-) setting with two silicon (333) reflections and  $\text{CuK}\alpha_1$  radiation, for varying values of  $\rho$  the tilt angle.  $v = 1.55^\circ$ .

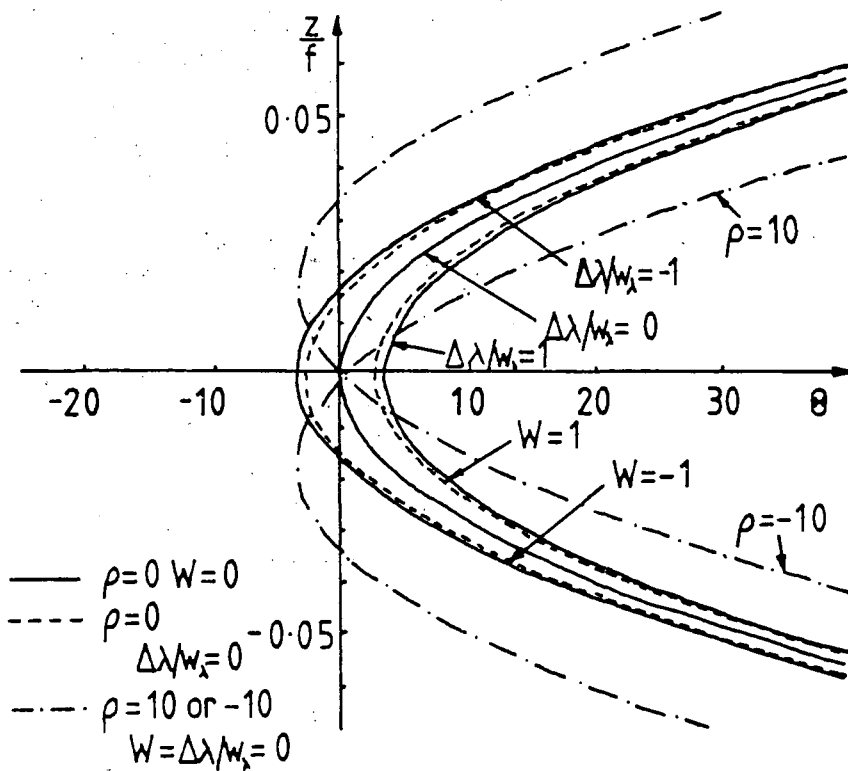


Fig. 2.5. Curve of  $z/f$  vs  $(\theta)$  for a non parallel (+-) setting with si (111) and si ( $\overline{220}$ ) reflections.  $\text{CuK}\alpha_1$  radiation with the abscissa scaled in units of 1.55 arc secs.



The curve of  $z/f$  vs  $\theta$  is shown in fig. 2.4 for a parallel (+-) setting with two Si (333) reflections. The rocking curve at a particular height  $z/f$  is given by traversing the curve along a line with  $y=z/f$  parallel to the  $\theta$  axis. We note that for no tilt, ie  $\rho=0$ , the situation corresponds to the condition where the vertically divergent beam can be diffracted over its entire length with the same intensity. The curve for a non parallel (+-) arrangement, with Si (111) and Si (220) reflections, is shown in fig. 2.5. As can be seen the wavelength and parameter  $W$  vary rapidly with  $z/f$  along the line  $\theta=0$ , while the distribution of high diffracted intensity is concentrated over a narrow vertical range.

From equation (2.29), substituting  $z/f=0$ , we can find the value of  $\theta$  at which the  $z/f$  curve crosses the  $z/f=0$  line as a function of  $\rho$ , the tilt angle. We obtain

$$\begin{aligned} \theta_0 &= \eta_0 & (2.33) \\ &= [(1-1/b_{II})u_{II} - (1-b_I)u_I] + wW \\ &\quad + \Delta\lambda/\lambda_0 \Delta\theta_u/\cos^2\theta_B + \frac{1}{2}\rho^2 \tan\theta_B, \end{aligned}$$

where  $w$  is the half width of the integrated reflection curve obtained by integrating the reflection curves over the height of the X-ray beam incident on the first crystal.  $W$  is analogous to  $W_I$  and  $W_{II}$  for this integrated curve. Equation (2.33) is plotted in fig. 2.6. This curve has been used to aid the rapid alignment of the double crystal arrangement to

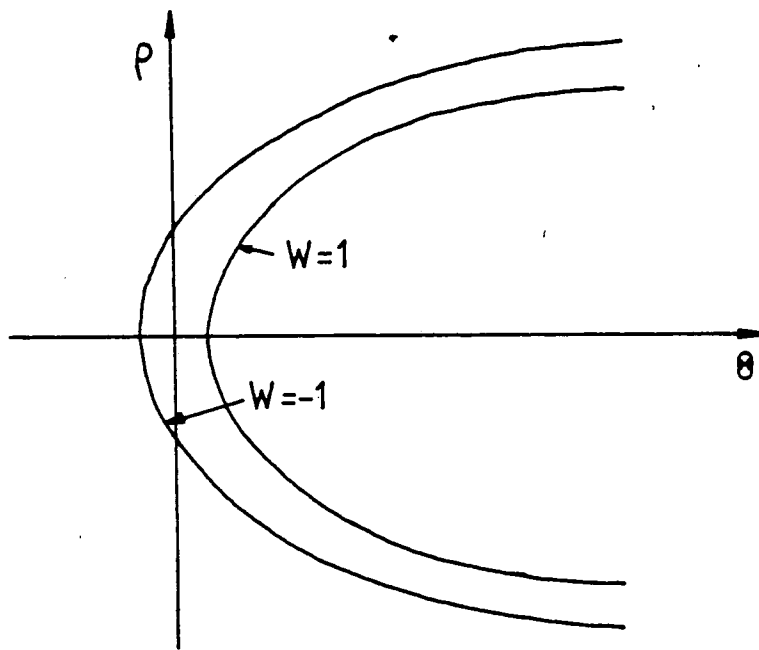


Fig. 2.6 Change in angle  $\theta$  required to give the centre of Bragg reflection tilt angle  $p$ .

the position  $\rho=0$  (see for example Fewster, 1985).

The half width of the rocking curve measured by rotating the second crystal is clearly the half width of this integrated curve, ie  $w$ . Yoshimura (1985) has shown that this can be related to the half width at  $\rho=0$  by

$$w = \frac{w(z/f=0)}{[1 - (z/f)^2 / \cos^2 \theta_B]}^{1/2} \quad (2.34)$$

if we assume Gaussian forms for the two reflection curves and that  $z/f \ll 1$ .

Ignoring the refraction and dynamical effects Schwarzschild (1928) showed that the half width of this curve due to purely geometrical effects could be related to the tilt angle,  $\rho$ , by

$$w = 2\rho z/f \quad \text{for } \rho > z/f[\tan\theta_{BI} \pm \tan\theta_{BII}] \quad (2.35)$$

and

$$w = Mz^2/f^2 + \rho z/f + \rho^2/4M \quad \text{for } \rho < 2Mz/f \quad (2.36)$$

where  $M = \frac{1}{2}(\tan\theta_{BII} \pm \tan\theta_{BI})$  with the upper sign for the (++) setting and the lower for the (+-) setting. We note that for the parallel (+-) setting  $M=0$  so that the geometrical half width varies linearly with tilt angle.

### 2.3 Double Crystal X-ray Diffraction Characterisation of Epitaxial and Ion Implanted Layers and Superlattices

Both epitaxial layers and ion implanted layers are well suited for the application of double crystal X-ray diffractometry. In both systems a highly perfect substrate

material is present with an added distortion due to either the growth of an epitaxial layer with a slightly different lattice parameter ( $\Delta d/d < 10^{-4}$ ) or ion implantation into the substrate distorting the substrate lattice (again  $\Delta d/d < 10^{-4}$ ). Generally single crystal X-ray diffraction techniques do not have the required resolution to detect such small lattice parameter variations, although several techniques have been used for the measurement of mismatch in heteroepitaxial layers (Chang, Patel, Nannichi and de Prince, 1979; Chang, 1980b, Isherwood, Brown and Halliwell, 1981). The depth penetration of X-rays into typical semiconductor materials and for the usual reflections is the order of 10  $\mu\text{m}$ , which is highly suitable as the majority of epitaxial layers are less than 10  $\mu\text{m}$ .

To date there has been a considerable difference in the interpretation of rocking curves recorded from ion implanted systems and heteroepitaxial layered systems. The interpretation of rocking curves from epitaxial layered systems has been limited to measuring the perpendicular and parallel mismatch from the angular separation of the diffraction peaks, using both surface symmetric and asymmetric reflections. Little use has been made of theoretical simulations to aid the interpretation and to determine more parameters such as layer thicknesses and composition variations with depth. This is not the case, however, for diffusion and ion implanted layers where extensive use of theoretical simulations has enabled the

strain distribution as a function of depth to be accurately determined. Clearly, much can be gained by applying these simulations to the interpretation of rocking curves from heteroepitaxial systems.

Much use has been made of X-ray diffraction techniques to analyse the structure of both naturally occurring and artificial superlattices. Naturally occurring superlattices have long been known to produce additional satellite reflections in the region of the main diffraction peaks (Dehlinger, 1927), and similar observations have been made for artificial superlattices. Utilising single crystal techniques the position of these satellites can be measured and used to determine the superlattice period. However, the zeroth order satellite peak cannot be resolved from the main substrate diffraction peak from such measurements, and these peaks are essential in the determination of the composition of the superlattice. Consequently double crystal diffraction has also been used to study these structures and the use of both the kinematical and dynamical diffraction theories for simulation of the rocking curves enables complete characterisation of the superlattice.

### **2.3.1 Diffusion and ion implanted layers**

A wide variety of ion and diffusion implanted layers have been studied using double crystal diffractometry. Rocking curves from such structures exhibit highly asymmetrical peaks with additional fine structure and

oscillations up to 500-1000 arc seconds away from the main diffraction peak. The strain distribution and hence doping as a function of depth can be obtained from the rocking curve by comparison with theoretically calculated rocking curves for varying distributions. The distribution that gives a theoretical curve that best fits the experimental curve can be taken as the actual distribution.

Alpha irradiated (111) silicon was studied by Burgeat and Colella (1969). 333 rocking curves using  $\text{MoK}\alpha_1$  radiation were shown to exhibit a secondary peak on the low angle side of the main peak, displaced by 5-10 arc seconds and between 20% and 50% of the intensity of the main peak. Theoretical curves were calculated using the Takagi-Taupin equations for diffraction from a distorted crystal. The irradiated region of the crystal was divided into a number of laminae of constant lattice parameter, in which the Takagi-Taupin equations could be solved analytically to give the complex amplitude ratio of the diffracted and incident beams at the top of the laminae in relation to that at the bottom of the laminae. By matching this amplitude ratio at the interface of each laminae, the reflectivity at the surface of the crystal can be calculated, using the reflectivity for an infinitely thick crystal at the bottom of the first laminae. Using a computed profile for the number of displaced Si atoms as a function of depth the theoretical rocking curves were found to agree fairly well with the experimental ones. However, no attempt was made to calculate curves with a

slightly different strain distribution.

Fukuhara and Takano (1977a, 1977b) have similarly applied the dynamical theory approach to the simulation of rocking curves from boron, phosphorous and germanium diffusion doped silicon. Rocking curves from the boron and phosphorous doped silicon showed a broad tail on the high angle side of the peak, suggesting a decrease in the lattice parameter, while the germanium doped samples exhibited considerable detail on the low angle side. By calculating rocking curves for varying strain profiles, profiles were obtained that gave rocking curves that fitted the experimental curves extremely well. Far better agreement was obtained than that obtained by Burgeat and Colella. The deduced strain profiles monotonically decreased from the surface down to 10-15  $\mu\text{m}$  and were found to agree well with those obtained from resistivity measurements.

Ion implantation into silicon gives a much higher strain than that obtained by diffusion and over a much smaller region of the crystal. Consequently rocking curves exhibit non zero diffracted intensity up to the order of 1000 seconds from the main peak. Larson and Barhorst (1980) studied laser annealed boron implanted silicon. Oscillations in the tail of the rocking curves, on the low angle side of the substrate peak, were observed with intensities about 1% of that of the main peak. A similar approach to that of Burgeat and Colella and Fukuhara and Takano was used to calculate rocking curves for various

strain distributions. However, the inclusion of strain was slightly different in that a continuous distribution was used and the Takagi-Taupin equations solved numerically. The formalism of Klar and Rustichelli (1973) was used in these calculations. Excellent agreement between the rocking curves was found with the theoretical curve being highly sensitive to the strain profile. Although the magnitude of the strain differed to that obtained by SIMS measurements the shape agreed extremely well.

The effect of increasing Si implantation doses on rocking curves from GaAs, Si and Ge crystals has been studied by Speriosu et al (1982). For small doses Bragg case Pendellosung fringes were observed but the amplitude of these oscillations decreased rapidly as the dose was increased. This was expected as the Pendellosung fringes only occur in thin, perfect crystals and the increased dosage introduces large amounts of damage in the crystal. The kinematical theory of X-ray diffraction was used to calculate rocking curves, using an approach based on the previous work of Speriosu (1981). In a similar manner to the dynamical calculations of Fukuhara and Takano, the strained region was divided into a number of laminae of constant strain. Dynamical interactions among the beams from each laminae were ignored. The total diffracted amplitude is then given by the sum of the coherently interfering amplitudes from each laminae, adjusted for phase lags and normal absorption. The theoretical curves were found to agree



extremely well with the experimental ones, corresponding to Gaussian strain distributions with widths of typically 5000 Å and maxima of up to 0.7%. Clearly, with strains as large as these the kinematical approach is perfectly valid.

Various types of ion implantation into magnetic bubble garnets have also been studied using double crystal diffractometry. Ion implantation into magnetic films is particularly useful for the suppression of 'hard' bubbles and the control of bubble wall states. Additionally many of the techniques for achieving high packing densities require ion implantation (Voegli et al, 1974). Komenou et al (1978) have utilised the period of the Bragg case Pendellosung oscillations to determine the thickness of the strained region. Similar results to those obtained by Speriosu et al (1982) for silicon were obtained. By removing the implanted region using a step etching technique and measuring the rocking curve at each stage the thickness predicted by the period of the oscillations was found to be directly proportional to the amount of material removed. This confirmed the applicability of the technique even when the layer is not highly perfect.

More recently Speriosu and Wilts (1983) have made a detailed analysis of  $\text{He}^+$ ,  $\text{Ne}^+$  and  $\text{H}_2^+$  implantation into magnetic bubble garnets using both rocking curves and ferromagnetic resonance spectra (FMR). A wide range of doses were studied for all three species of ions with rocking

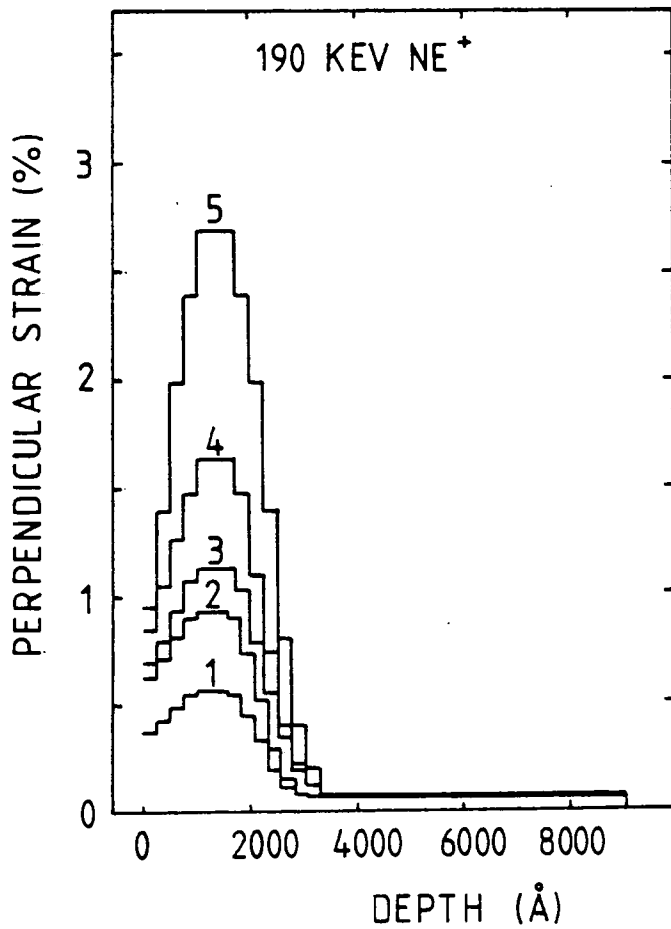
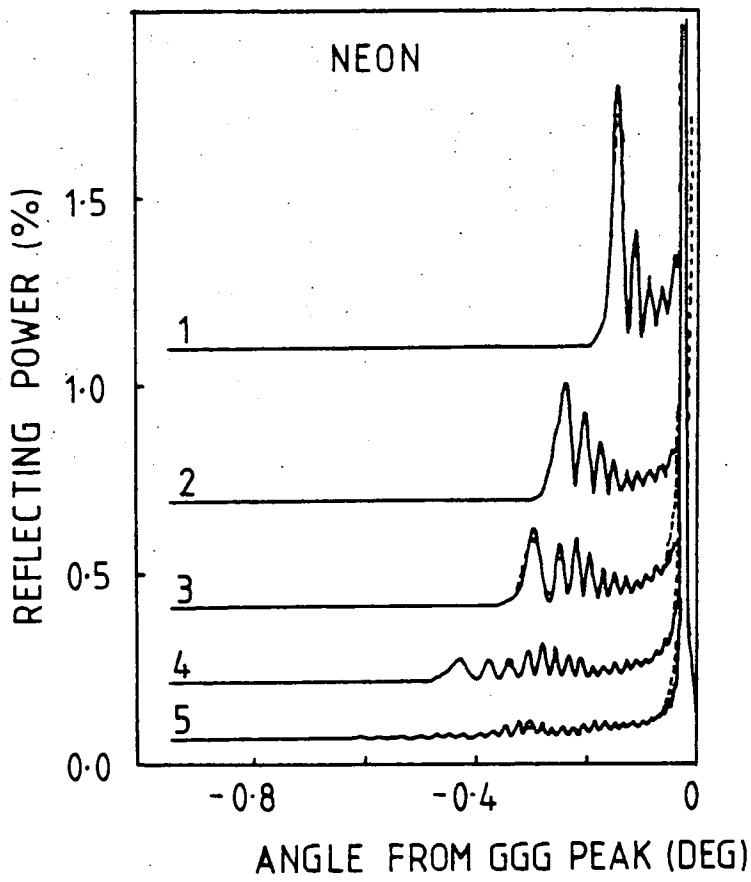


Fig. 2.7 Typical theoretical and experimental rocking curves for a Ne<sup>+</sup> implanted magnetic bubble garnet sample and the strain distributions determined.

curves similar in appearance to those obtained by Komenou et al (1978) found. The complete rocking curve was calculated using the kinematical theory in order to determine the strain distribution. Gaussian like strain distributions were again found with widths of the order of 5000 Å and maximum strains up to 3%. A typical theoretical and experimental curve are shown in fig. 2.7, along with the strain distribution determined. Agreement with the strain distribution from FMR was fairly good at low doses but considerable differences were found at higher doses.

Takeuchi et al (1983) have also studied ion implantation into bubble garnets but have used the dynamical diffraction theory to calculate the rocking curves. The approach used was that of Fukuhara and Takano. Comparison was made between the kinematical approach of Speriosu et al (1979), and considerable differences in the calculated curves were found. It appeared that some care needed to be taken in the choice of the depth included in the kinematical calculations before the dynamical intensity for the substrate is used. Comparison between the calculated and theoretical curves was again excellent.

### 2.3.2 Heteroepitaxial layers

Double crystal rocking curves from mismatched single layers of uniform composition are often rather more easy to interpret than those from ion or diffusion implanted layers since the epitaxial layers are usually more perfect than the implanted regions, giving rise to narrow, well resolved

peaks. The strains encountered are at least an order of magnitude smaller than those encountered in ion implanted crystals. For these types of layers measurement of the perpendicular and parallel mismatches and hence the composition is straightforward. However, this is not the case with multiple and graded composition layers.

Since GaAlAs is well matched to GaAs over a wide composition range and it is not particularly well suited for the manufacture of optoelectronic devices for fibre optic systems little work has been published on characterisation by double crystal diffractometry. Bartels and Nijman (1978) have studied the strain of  $\text{Ga}_{1-x}\text{Al}_x\text{As}$  layers grown on (001), (110), (111) and (113) oriented GaAs substrates. Double heterostructures consisting of  $3.2 \mu\text{m}$  n- $\text{Ga}_{0.71}\text{Al}_{0.29}\text{As}$  /  $0.3 \mu\text{m}$  p-GaAs /  $2.5 \mu\text{m}$  p- $\text{Ga}_{0.68}\text{Al}_{0.32}\text{As}$  /  $1.5 \mu\text{m}$  p-GaAs were studied with the perpendicular and parallel mismatches measured by using the (115) reflection. Bragg case Pendellosung fringes were also observed between the substrate and layer peaks.

Ternary compounds of (Ga,In)As grown on (001) InP substrates are rather more important than GaAlAs compounds due to their use in fibre optic systems. Since GaInAs is only well matched to InP over a small range of compositions, and good quality layers can only be grown when the lattice mismatch is  $\leq 800\text{ppm}$ , the growth of high quality layers is not straightforward. Of the growth techniques currently available Goetz et al (1983) have compared layers grown by

LPE, VPE and MOCVD. Some 30 samples were studied using double crystal diffractometry to compare the mismatches and layer qualities. Lattice mismatch was measured perpendicular to the interface using the 115 reflection and the layer quality estimated from the half width of the layer peak. In all cases the parallel mismatch was found to be at least an order of magnitude smaller than the perpendicular mismatch suggesting good coherency at the interface. LPE grown layers were found to be better matched to the substrate than those grown by both VPE and MOCVD and also had the narrowest peaks. Both the VPE and MOCVD grown layers gave peaks considerably broader than the theoretical width, suggesting a change in composition with depth. However, no attempt was made to measure this variation.

Similar results have been reported by Kawamura and Okamoto (1979) and by Macrander et al (1984) for MBE grown layers. Again the parallel mismatches were found to be at least an order of magnitude smaller than the perpendicular ones.

Using an automated scanning double crystal camera, with which rocking curves can be recorded automatically at a number of points over the sample, Halliwell et al (1983) have shown that variations in layer perfection occur for MBE grown ternary layers, with a noticeable decrease in layer perfection towards the edge of the sample. This was related to a fall in growth temperature at the edges of the sample, due to a variable thermal contact afforded by the indium

solder used to attach the sample to the holder.

Quaternary compounds of (Ga,In)(As,P) offer perhaps the best possibilities for producing high quality, variable band gap layers. LPE has been the favoured growth technique with many X-ray rocking curve studies of single layers being reported. Matsui et al (1979) and Burgeat et al (1981) have both shown that the composition of the layer varies as a function of the layer thickness. Matsui et al were able to show a continuous variation while Burgeat et al ascertained a stepwise variation. Both used a similar technique of step etching the sample and measuring the rocking curve at each stage. Some doubt exists as to both of these interpretations as no theoretical calculations were used for comparison. Matsui et al took only the angular separation of the maximum of the layer peak as a measure of the composition while Burgeat et al used large etch steps and associated each peak removed from the curve with the layer removed. Matsui et al showed that Auger electron spectroscopy also revealed a continuous linear variation in composition with depth.

Such variations were also reported by Tashima et al (1981) using the 006 reflection in conjunction with a modified powder goniometer. However, no effect could be observed from the thin region near to the interface expected to have a rapidly varying composition (Rezek et al, 1980).

Double heterostructure layers of GaInAsP/InP, grown by LPE, have been similarly studied by Oe et al (1978). Since the layers studied were only approximately 0.4  $\mu\text{m}$  thick no

composition variations were observed. Similar results were also obtained for 1.5  $\mu\text{m}$  GaInAsP / 8  $\mu\text{m}$  GaInP / InP layers by Bartels (1983) using a multiple crystal spectrometer with a four reflection Ge monochromator. Using the dynamical theory to calculate the peak heights expected from such a structure the layer thicknesses were found to agree well with those expected from the growth conditions.

Halliwell et al (1983) were also able to show an increase in the layer thickness perpendicular to the push direction for LPE grown quaternary layers. Layer quality remained good over the majority of the sample and the layer thicknesses were calculated to increase by about 50% towards the edges.

In none of the above work has the complete rocking curve been calculated and compared with the experimental curves. Clearly if the rocking curve from a layer with an arbitrary composition profile was calculated, comparison with experimental curves could be used to aid interpretation in a similar manner to that used for ion and diffusion implanted layers.

Using a similar approach to that of Burgeat and Colella (1969), Halliwell, Juler and Norman (1983) were able to obtain a fairly good agreement between theoretical and experimental curves from linearly graded single layers of GaInAs. The composition profile was also measured with electron probe X-ray microanalysis on a bevelled section, and agreement between the two methods was fairly good.

Discrepancies between the theoretical and experimental curves was thought to be due to a region of different composition near to the interface, a region that the microprobe cannot accurately measure due to the proximity of the substrate. This is in agreement with the observations of Rezek et al (1980).

Very thin heteroepitaxial layers have not been extensively studied by double crystal diffractometry, primarily because the diffracted intensity from such layers is very low for the normally used reflections. Instead other X-ray techniques such as low angle interference (Segmuller, 1973) have been used. However, the use of highly asymmetric reflections, in which either the diffracted or incident beams forms a low angle with the surface can overcome this problem (Tanner, Barnett and Hill, 1985).

### 2.3.3 Superlattices

X-ray diffraction studies of artificial superlattices were first reported by Segmuller and Blakeslee (1973) where alternating layers of  $\text{GaAs}_{0.5}\text{P}_{0.5}$  and GaAs formed the superlattice. Vapour phase transport was used as the growth technique. Measurements were recorded with a modified single crystal camera with radiation monochromated by a double reflecting channel cut Ge crystal. Satellite peaks were observed near to the 004 GaAs reflection. A model based on a Fourier decomposition of the composition variation was used to calculate the satellite intensities in conjunction with



the kinematical diffraction theory. This model was very similar to that of Dehlinger (1927) for the study of diffraction from cold worked metals, although a second harmonic term was included by Segmuller and Blakeslee. Similar theories have been presented by Kochendorfer (1939) and Daniel and Lipson (1943, 1944), where a sinusoidal variation in lattice parameter and structure factor was considered. Hargreaves (1951) studied the case for a square wave model of the superlattice, but his results were the same as those obtained by the sinusoidal models due to the approximations used. A sinusoidal model was also used by De Fontaine (1966) for such one dimensional variations.

Using this approach Segmuller and Blakeslee were able to calculate satellite intensity ratios for different strain and composition distributions. Reasonable agreement with the first order satellite peaks was found, although not for the second order satellites which were only observed for one sample. It was also found that this model gave better agreement than a step model, suggesting that some degree of interdiffusion had occurred at the interfaces.

This approach was repeated by Segmuller, Krishna and Esaki (1977) for GaAs/AlAs superlattices grown by MBE, where a greater number of high order satellites were observable. Low angle X-ray scattering interference has also been used to determine the ratio of thicknesses of the layers forming the repeat period (Chang et al, 1976). Calculated superlattice structure factors were found to agree fairly

well with those calculated from the satellite intensities assuming a perfect stepwise composition variation. The effect of interdiffusion between the layers and compositional non uniformity along the layers was also discussed. Both of these factors have the same effect of reducing the satellite intensities. Since the zeroth order peak, corresponding to the reflection from a layer with the average composition of the superlattice, could not be resolved from the substrate reflection their separation could not be used to determine the composition.

This kinematical approach to calculating satellite intensities has also been used by Fleming et al (1980) and Kevarec et al (1984). By calculating the change in the Fourier components of the strain modulation Fleming et al were able to measure the effect of interdiffusion as a function of annealing time for GaAs/AlAs superlattices, again grown by MBE. Up to eight harmonics were included in the Fourier series, although after long annealing times only the first two could be determined. The diffusion coefficients obtained were found to be in good agreement with those obtained from optical measurements (Dingle, 1977) and electron microscopy (Petroff, 1977), but were smaller than those obtained by Auger electron spectroscopy (Chang and Koma, 1976).

$\text{Ga}_{1-x}\text{Al}_x\text{As}/\text{GaAs}$  superlattices were studied by Kevarec et al using both a double crystal technique and a modified powder goniometer to observe the high order, weak

satellites. Clearly, for these superlattices the value  $x$  must also be determined and the separation of the zeroth order and substrate peaks can be used for this. Finally a step wise calculation of the structure factor was used to calculate the satellite intensities.

More recently Speriosu and Vreeland (1984) have applied their model of X-ray diffraction from ion implanted layers to the calculation of diffracted intensities from MBE grown GaAlAs/GaAs and MOCVD grown AlSb/GaSb superlattices. A step wise model was used with the inclusion of both perpendicular and parallel mismatches. Double crystal rocking curves of various reflections were recorded with  $\text{FeK}\alpha_1$  radiation. Good agreement was found with the calculated curves, particularly for the GaAlAs/GaAs samples.

The dynamical diffraction theory has not been extensively used in the calculation of diffracted intensities from superlattices, due to the individual layer thicknesses being very much less than the extinction distances. However, recently Vardanyan, Manoukyan and Petrosyan (1985) have pointed out that, as the total thickness of the superlattice is the order of an extinction distance, dynamical interactions between the beams from the layers should not be ignored. They have used the well known matrix method to calculate the overall diffracted intensities from a perfect superlattice.

## CHAPTER 3

### CALCULATING ROCKING CURVES

As we have seen, it is necessary to calculate rocking curves in order to extract as much information as possible as to the composition and thickness of any epitaxial layers. An approach based on dynamical diffraction theory will be used to calculate the single crystal reflection profiles for the crystals, the rocking curve is then the convolution of the reflection curves of the first and second crystals, as already seen.

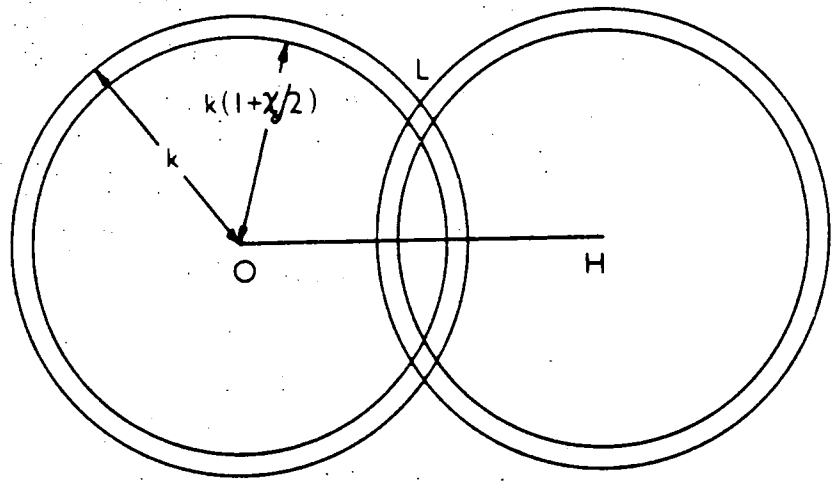
#### 3.1 Dynamical Diffraction Theory

There are many excellent reviews of dynamical diffraction theory available in the literature, the reader is referred to these for a complete description (Zachariasen, 1945; James, 1948; von Laue, 1960; Batterman and Cole, 1964; Pinsker, 1978).

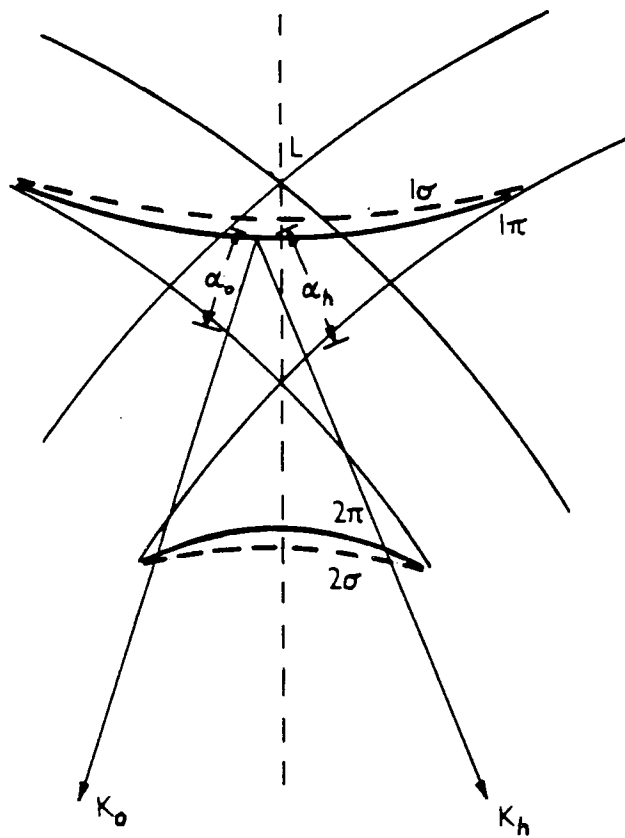
A solution is required to Maxwell's equations for a medium with a periodic, complex dielectric constant. The fundamental equation linking the incident and diffracted waves within the crystal is obtained,

$$\alpha_0 \alpha_h = \frac{k^2}{4} C^2 \chi_h \chi_{\bar{h}} \quad (3.1)$$

where 
$$\alpha_0 = \frac{k}{2} (\underline{K}_0 \cdot \underline{K}_0 - k^2 (1 + \chi_0)) \quad (3.2)$$



(a)



(b)

Fig. 3.1 (a) Laue construction for the diffraction of an incident beam of wavevector  $K$ .

(b) The dispersion surface construction showing the four possible branches. Arcs AA' and BB' are part of circles of radii  $K$  and  $k(1+\chi_0/2)$ .

and 
$$\alpha_h = \frac{k}{2} (\underline{K}_h \cdot \underline{K}_h - k^2 (1 + \chi_0)). \quad (3.3)$$

C is the polarisation factor (=1 for  $\sigma$  and  $=\cos 2\theta_B$  for  $\pi$  polarisations). As usual  $\underline{K}_0$ ,  $\underline{K}_h$  are the incident and diffracted wavevectors in the crystal and  $\chi_0$ ,  $\chi_h$ ,  $\chi_{\bar{h}}$  the complex susceptibilities. This equation can be usefully represented geometrically by the dispersion surface construction. Considering the Laue construction shown in fig. 3.1, surfaces on which the tails of the possible wavevectors  $\underline{K}_0$  and  $\underline{K}_h$  lie can be drawn asymptotic to spheres of radius  $k(1+\chi_0/2)$  and  $k$  drawn about the reciprocal lattice points 0 and H.  $\alpha_0$  and  $\alpha_h$  are then the perpendicular distances between the dispersion surface branches and these spheres. As this region is very small compared to the radius of the spheres the spheres can be approximated by planes, in which case the equation of the dispersion surface (3.1) becomes a hyperboloid of revolution. Generally there are four dispersion surface branches, two each for the two polarisation states.

Since any wave propagating within the crystal must have wavevectors lying on the dispersion surface we can determine both the amplitude and wavevector from the tie points excited on the surface. Hence this construction is extremely useful in visualising the physical processes occurring within the crystal.

The tie points excited on the dispersion surface are determined by the boundary conditions. Clearly these

conditions are extremely important as we must be able to determine the wave amplitudes outside the crystal, since it is only these that we can measure. The required condition is that the tangential components of the plane waves across the boundary must be equal. Hence the wavevectors inside the crystal can only differ from those outside by a vector perpendicular to the boundary. This condition can be used to determine the tie points excited on the dispersion surface.

For Bragg reflection no tie points can be excited in the central region of the reflection profile, thus no propagated wave can exist inside the crystal. Instead a highly damped, evanescent wave exists and the incident beam is totally externally reflected. The Bragg reflection profile, with zero absorption, will then have a flat topped central region. The actual position of the centre of this profile does not correspond to the kinematical Bragg angle due to the refractive effect. The corrected Bragg angle is given by

$$\theta_B = \theta_0 + x_0(1 - \gamma_h/\gamma_0)/2\sin 2\theta_0 \quad (3.4)$$

where  $\theta_0$  is the kinematical Bragg angle and  $\gamma_h, \gamma_0$  the usual asymmetry factors. We note that only for symmetric Laue case diffraction does  $\theta_B = \theta_0$ . The full width at half maximum of the reflection peak is given by

$$\Delta\theta_{\frac{1}{2}} = \frac{2C(x_h x_h^-)^{\frac{1}{2}}}{\sin 2\theta_B} \sqrt{\frac{|\gamma_h|}{\gamma_0}} \quad (3.5)$$

For Bragg geometry, with no crystal absorption, the reflected intensity ratio is given by (Pinsker, 1978)

$$R = \frac{1 - \cos 2A(y^2 - 1)^{\frac{1}{2}}}{\cosh 2v - \cos 2A(y^2 - 1)^{\frac{1}{2}}} \quad (3.6)$$

where

$$y = \frac{\beta}{2C(\chi_h \chi_{\bar{h}})^{\frac{1}{2}}(\gamma_h/\gamma_0)^{\frac{1}{2}}} \quad (3.7)$$

and

$$\beta = 2\Delta\theta \sin 2\theta - \chi_0(1 + |\gamma_h|/\gamma_0). \quad (3.8)$$

A is given by

$$A = \frac{\pi Ckt(\chi_h \chi_{\bar{h}})^{\frac{1}{2}}}{(\gamma_0 |\gamma_h|)^{\frac{1}{2}}} \quad (3.9)$$

and  $v$  by  $y = \sinh v$ .

We note that equation (3.6) describes subsidiary maxima of Bragg case Pendellosung in the lateral regions of the reflection peak. The expression vanishes to zero provided that

$$2A(y^2 - 1)^{\frac{1}{2}} = 2\pi m, \quad m \text{ an integer,} \quad (3.10)$$

giving an angular interval of

$$\Delta y \approx \frac{\pi}{A} = \frac{\lambda(\gamma_0 |\gamma_h|)^{\frac{1}{2}}}{Ct(\chi_h \chi_{\bar{h}})^{\frac{1}{2}}} \quad (3.11)$$

This interval corresponds to that for Laue case Pendellosung, and has been used in the determination of crystal thickness as previously described. We note that the length  $\lambda(\gamma_0 |\gamma_h|)^{\frac{1}{2}}/C(\chi_h \chi_{\bar{h}})^{\frac{1}{2}}$  is known as the extinction distance, and corresponds to the separation of the maxima of



the wavefield excited within the crystal due to the interference of the two waves propagating in the crystal. This length also gives an indication of the thickness of the crystal sampled by the X-ray beam during Bragg reflection, and is the order of 10  $\mu\text{m}$  for the majority of reflections for III-V materials. If absorption is included the Bragg case Pendellosung oscillations become rapidly damped as the thickness of the crystal is increased, hence these oscillations are only observable for thin crystals.

Clearly we could use this dynamical approach to calculate the rocking curve from a layered crystal, matching the wavevectors out of one layer into the next at each interface. For multiple layers, or graded layers divided into a number of laminae, this approach would be extremely laborious. A much simpler approach, which is well suited to computation, is to use the differential equations of Takagi and Taupin (Takagi, 1962, 1969; Taupin, 1964). However, it is rather difficult to visualise the physical processes occurring within the crystal with this approach, hence it is useful to keep the dispersion surface approach in mind.

### 3.2 The Takagi-Taupin Equations

The derivation of Taupin (1964), which has also been presented by Pinsker (1978), is followed here. The reader is referred to these works for complete details.

The electric displacement vector in a vacuum can be described by the expression

$$\underline{D} = \underline{D}_0(\underline{r}) \exp[i(\omega_0 t - 2\pi\phi_0(\underline{r}))] \quad (3.12)$$

where  $\omega_0$  is the cyclical frequency ( $\omega_0 = 2\pi\nu_0$ ). This expression describes an arbitrary wave. For a plane wave  $\phi_0(\underline{r}) = \underline{K}_0 \underline{r}$ ,  $|\underline{K}_0| = 1/\lambda$ . In the general case  $\underline{D}$  satisfies the wave equation in a vacuum

$$\nabla^2 \underline{D} + \frac{\omega^2}{c^2} \underline{D} = 0 \quad (3.13)$$

Substituting (3.12) into (3.13) gives

$$\begin{aligned} \nabla^2 \underline{D}_0 - i4\pi \sum_i \frac{\partial \phi_0}{\partial x_i} \frac{\partial \underline{D}_0}{\partial x_i} - i2\pi \underline{D}_0 \nabla^2 \phi_0 - 4\pi^2 \sum_j \frac{\partial \phi_0}{\partial x_j}{}^2 \underline{D}_0 \\ + \frac{4\pi^2}{\lambda^2} \underline{D}_0 = 0 \end{aligned} \quad (3.14)$$

Since  $\underline{D}_0$  and  $\phi_0$  are real functions of the coordinates separation into real and imaginary parts is straightforward.

Considering waves for which the radii of curvature of the equiphase surfaces are much larger than the wavelength  $\lambda$ ; for example,  $\lambda/R \ll 1$  can be assumed for a spherical wave thus

$$|\text{grad } \phi_0| \approx \lambda^{-1} [ 1 + O(\lambda^2/R^2) ] \quad (3.15)$$

where  $O(\lambda^2/R^2)$  represents negligibly small terms of higher orders of  $\lambda/R$ . For a nearly plane incident wave we have

$$\text{grad } \phi_0 = \underline{K}_0 + \Delta \underline{K}_0 \quad (3.16)$$

and  $\underline{k}_0 \Delta \underline{k}_0 = 0$ ,  $|\Delta \underline{k}_0| \ll |\underline{k}_0|$ . From (3.15) we then have

$$|\underline{k}_0| = \lambda^{-1}, \quad |\Delta \underline{k}_0| = R^{-1} \quad (3.17)$$

corresponding to an incident wave packet with an angular width of the order of  $1/R$ .

The function  $\underline{D}_0$  is retained for the phase when describing the wave inside the crystal. The amplitude  $\underline{D}_0$  becomes a complex function of the coordinates, which is dependent on the difference in the paths of propagation in the crystal and the vacuum. In the case of a perfect crystal we have a single pseudo periodic wave corresponding to the right hand side of

$$\begin{aligned} & \sum_i D_0^{(i)} \exp 2\pi i [\nu t - (\underline{k}_0^{(i)} \cdot \underline{r})] \\ & = \exp 2\pi i [\nu t - (\underline{k}_0 \cdot \underline{r})] \sum_i D_0^{(i)} \exp(\pm \pi i \Delta K z) \end{aligned} \quad (3.18)$$

and

$$\begin{aligned} & \sum_i D_h^{(i)} \exp 2\pi i [\nu t - (\underline{k}_h^{(i)} \cdot \underline{r})] \\ & = \exp 2\pi i [\nu t - (\underline{k}_h \cdot \underline{r})] \sum_i D_h^{(i)} \exp(\pm \pi i \Delta K z) \end{aligned}$$

for each state of polarisation. Hence the boundary condition

$$D_0^{(1)} + D_0^{(2)} = D_0^{(a)} \quad (3.19)$$

amounts to regarding  $\underline{D}_0$  as a function of the coordinates on transition from the vacuum to the crystal.

The wavefield in the crystal can be described through the use of a variable amplitude Bloch function,

$$\underline{D} = \sum_m \underline{D}_m \exp \{i[\omega t - 2\pi(\underline{k}_m \cdot \underline{r})]\}. \quad (3.20)$$

For a perfect crystal and plane waves the following values

remain constant

$$\underline{K}_m = \underline{K}_0 + \underline{h}_m, \quad \underline{K}_0 = \text{grad } \Phi_0. \quad (3.21)$$

However, generally  $\underline{K}_0$  and  $\underline{h}_m$  are functions of the coordinates. For each point in the crystal the vector  $\underline{h}_m$  can be determined. Additionally,

$$|\underline{h}_m(\underline{r})| = d_m^{-1}(\underline{r}). \quad (3.22)$$

Hence, moving from the plane  $n_m$  to the plane  $n_{m+1}$  of the same system, we have  $\Delta n_m = 1 = \underline{h}_m \underline{dr}$ , where  $\underline{dr}$  is the change in the radius  $\underline{r}$  in moving from the point  $\underline{r}$  on the  $n_m$ -th plane to the point  $\underline{r} + \underline{dr}$  on the  $n_{m+1}$ -th plane.

If  $n_m$  is regarded as a continuous function of the coordinates, which takes integral values on each plane  $m$ , we find

$$\underline{h}_m = \text{grad } n_m \quad (3.23)$$

$$\underline{D} = \sum_m \underline{D}_m [i(\omega_0 t - 2\pi\varphi_m)] \quad (3.24)$$

where 
$$\varphi_m(\underline{r}) = \varphi_0(\underline{r}) + n_m(\underline{r}). \quad (3.25)$$

The continuity of  $n_m$  breaks down in crystals containing dislocations. However, it can be shown that the results of the theory outlined can be used in the general case of an arbitrary distribution of  $n_m$  if the distortion,  $\partial u / \partial x$ , is small (ie  $\partial u / \partial x \ll 1$ ).

The dielectric constant remains a periodic function of the coordinates, but  $\epsilon(\underline{r})$  can be approximately assumed to be

an exponential function of  $n_m$  in each system of reflecting planes since  $\partial u / \partial x \ll 1$ .

$$\chi(\underline{r}) = \sum_m \chi_m \exp[-2\pi i n_m(\underline{r})] \quad (3.26)$$

$$\chi_m \equiv \chi_{hm} = -\frac{e^2}{mc^2} \frac{\lambda^2}{\pi V} F_{hm} \quad (3.27)$$

and for the general case of an absorbing crystal

$$\chi_0 = \chi_{0r} + i\chi_{0i}; \quad \chi^h = \chi_{hr} + i\chi_{hi}. \quad (3.28)$$

The variable representing the angular departure from the Bragg condition is taken as

$$\alpha_m = 2\Delta\theta_m \sin 2\theta_m \quad (3.29)$$

which is derived from the approximate value of the expressions

$$\alpha_m = K_0^{-2} [h_m^2 + 2(\underline{K}_0 \cdot \underline{h}_m)] = \lambda^2 (1/d_m^2 - 2\sin\theta_m/\lambda d_m) \quad (3.30)$$

where both  $d_m$  and  $\sin\theta_m$  are coordinate dependent.

The wave equation inside the crystal is derived from Maxwell's equations, which are

$$\text{curl } \underline{E} = c^{-1} \partial \underline{H} / \partial t, \quad \text{curl } \underline{H} = c^{-1} (\partial \underline{E} / \partial t + 4\pi \underline{J}) \quad (3.31)$$

$$\text{div } \underline{E} = 4\pi \rho; \quad \text{div } \underline{H} = 0.$$

Taking the curl of both sides we obtain

$$\text{curl curl } \underline{E} = c^{-1} \text{curl } \partial \underline{H} / \partial t = c^{-1} \partial / \partial t \text{curl } \underline{H} \quad (3.32)$$

$$\text{but} \quad \text{curl } \underline{H} = c^{-1} \partial \underline{D} / \partial t \quad (3.33)$$

and from  $\underline{D} = \epsilon \underline{E} = (1 + \chi) \underline{E}$ ,  $\underline{E} \approx (1 - \chi) \underline{D}$  we obtain

$$\text{curl curl } (1 - \chi) \underline{D} = 4\pi^2 / \lambda^2 \underline{D}. \quad (3.34)$$

In order to calculate the left hand side of equation (3.34) the value of  $(1 - \chi) \underline{D}$  is rewritten using the solution of the wave equation and the Fourier expansion of the polarisability. We can write  $n_K + n_L = n_{K+L}$  by analogy with the reciprocal vectors in the perfect crystal ie  $h_K + h_L = h_{K+L}$ . Thus

$$\begin{aligned} \underline{E} = (1 - \chi) \underline{D} &= \exp(i\omega t) \left[ \sum_m \underline{D}_m \exp(-i2\pi\phi_m) \right. \\ &\quad \left. - \sum_m \sum_h \chi_{m-h} \underline{D}_h \exp[-i2\pi(n_m + \phi_h)] \right] \\ &= \exp(i\omega_0 t) \sum_m \underline{Q}_m \exp(-i2\pi\phi_m) \end{aligned} \quad (3.35)$$

$$\underline{Q}_m = \underline{D}_m - \sum_h \chi_{m-h} \underline{D}_h \quad (3.36)$$

Omitting the factor  $\exp(i\omega_0 t)$  and using the following relations

$$\underline{K}_0 = \text{grad } \phi_0, \quad \underline{h}_m = \text{grad } n_m, \quad \underline{K}_m = \text{grad } \phi_m. \quad (3.37)$$

$$\text{and} \quad (\text{curl curl } \underline{E})_i = - \frac{\partial^2 E_i}{\partial x_k^2} + \frac{\partial^2 E_k}{\partial x_i \partial x_k} \quad (3.38)$$

where  $i$  and  $k$  take the value 1, 2 and 3, we obtain

$$\frac{\partial}{\partial x_k} (1 - \chi) D_{mi} = \exp(-i2\pi\phi_m) \frac{\partial Q_{mi}}{\partial x_k} - i2\pi K_{mk} Q_{mi} \quad (3.39)$$

Taking a second differential gives, after using

$$\frac{\partial K_{mk}}{\partial x_i} = \frac{\partial^2 \varphi_m}{\partial x_i \partial x_k} = \frac{\partial K_{mi}}{\partial x_k} \quad (3.40)$$

$$\begin{aligned} \text{curl curl } (1-\chi)\underline{D} = \sum_m \exp(-i2\pi\varphi_m) \{ & 4\pi^2 [K_m^2 Q_m - (\underline{K}_m \underline{Q}_m) \underline{K}_m] \\ & + i4\pi \underline{K}_m \frac{\partial Q_m}{\partial r} - i2\pi \text{grad } (\underline{K}_m \underline{Q}_m) \\ & - i2\pi \underline{K}_m \text{div } \underline{Q}_m + i2\pi Q_m \nabla^2 \varphi_m \\ & + \text{grad div } \underline{Q}_m \} = A \end{aligned} \quad (3.41)$$

With the Bloch solution we obtain

$$4\pi^2 / \lambda^2 \sum_m \underline{D}_m \exp(-i2\pi\varphi_m) = A. \quad (3.42)$$

This equation has an infinite number of unknowns. If it is assumed that the preexponential factors with number  $m$  only change over effective distances that are much larger than the wavelength each of the waves referring to different waves  $m$  can be equated. Thus

$$\begin{aligned} 4\pi^2 [K_m^2 Q_m^2 - K_0^2 (\underline{D}_m \underline{Q}_m) - (\underline{Q}_m \underline{K}_m)^2] + i2\pi \underline{K}_m \text{grad } Q_m^2 \\ + i2\pi [Q_m^2 \nabla^2 \varphi_m - \underline{Q}_m \text{grad} (\underline{K}_m \underline{Q}_m) - (\underline{K}_m \underline{Q}_m) \text{div } \underline{Q}_m] \\ + \underline{Q}_m \text{grad div } \underline{Q}_m - \underline{Q}_m \nabla^2 \underline{Q}_m = 0 \end{aligned} \quad (3.43)$$

replacing  $K_m^2$  by  $\alpha_m$  in (3.43) we obtain

$$\begin{aligned} 4\pi^2 [K_0^2 \alpha_m Q_m^2 - K_0^2 \sum x_{m-h} \underline{D}_h \underline{Q}_m - (\underline{Q}_m \underline{K}_m)^2] \\ + i2\pi [\underline{K}_m \text{grad } Q_m^2 + Q_m^2 \nabla^2 \varphi_m - \underline{Q}_m \text{grad} (\underline{K}_m \underline{Q}_m)] \\ - (\underline{K}_m \underline{Q}_m) \text{div } \underline{Q}_m + \underline{Q}_m \text{grad div } \underline{Q}_m - \underline{Q}_m \nabla^2 \underline{Q}_m = 0 \end{aligned} \quad (3.44)$$

This system contains terms which differ considerably in their order of magnitude. Terms small compared to  $Q_m^2 / \lambda^2 =$

1 are now eliminated. We then obtain (see Pinsker (1978) for a discussion of the magnitude of each term)

$$\alpha_m D_m - \sum_h \chi_{m-h} D_h \cos X_{mh} + i\lambda^2 / \pi (K_m \text{grad}) D_m = 0 \quad (3.45)$$

where  $\cos X_{mh}$  is the polarisation factor. The calculation of the solution for X-ray propagation in the perfect crystal is then the solution of this system in first order partial derivatives. The variable  $\alpha_m$  is calculated to allow for local deformations at any point in the crystal.

For the two beam case we need only consider  $m=0$  and  $m=h$ . Let  $\underline{s}_0$  and  $\underline{s}_h$  be unit vectors in the direction of the incident and diffracted beams respectively, thus

$$\underline{s}_0 = \lambda \underline{K}_0, \quad \underline{s}_h = \lambda \underline{K}_h \quad (3.46)$$

and for any point on the reflection plane

$$\underline{r} = s_0 \underline{s}_0 + s_h \underline{s}_h \quad (3.47)$$

and the system (3.35) reduces to

$$\frac{i\lambda}{\pi} \frac{\partial D_0}{\partial s_0} = \chi_0 D_0 + C \chi_h D_h \quad (3.48)$$

$$\frac{i\lambda}{\pi} \frac{\partial D_h}{\partial s_h} = (\chi_0 - \alpha_h) D_h + C \chi_h D_0.$$

$$C = \cos X_{0h}$$

Clearly, we can include the polarisation factor C in the



values  $x_h$  and  $x_{\bar{h}}$  by adding the symbols  $\sigma$  and  $\pi$ , ie

$$x_h^\sigma = x_h^\pi (|\cos 2\theta|)^{-1} \quad (3.49)$$

and

$$x_{\bar{h}}^\sigma = x_{\bar{h}}^\pi (|\cos 2\theta|)^{-1}.$$

### 3.3 Solution of the Takagi-Taupin Equations and Calculation of the Rocking Curve

The Takagi-Taupin equations (3.48) can now be used to calculate the reflectivity of a given crystal in the Bragg case. The amplitude ratio of the incident and diffracted beams is required. We will assume an incident plane wave, and that variations in diffracted intensity will be a function of depth only.

If  $\gamma_0$  and  $\gamma_h$  are the direction cosines of the incident and diffracted beams with respect to the surface, ie

$$z = s_0 \gamma_0 + s_h \gamma_h, \quad (3.50)$$

then (3.48) becomes

$$\begin{aligned} \frac{i\lambda}{\pi} \gamma_0 \frac{\partial D_0}{\partial z} &= x_0 D_0 + C x_{\bar{h}} D_h \\ \frac{i\lambda}{\pi} \gamma_h \frac{\partial D_h}{\partial z} &= (x_0 - \alpha_h) D_h + C x_h D_0 \end{aligned} \quad (3.51)$$

Now the complex reflection coefficient,  $X$ , is defined as

$$X = \sqrt{\frac{|\gamma_h|}{\gamma_0}} \frac{D_h}{D_0} \quad (3.52)$$

where the  $\gamma_h$ ,  $\gamma_0$  terms account for any beam expansion or compression. Differentiating (3.52) we obtain

$$\frac{dX}{dz} = \sqrt{\frac{|\gamma_h|}{\gamma_0}} \left\{ \frac{1}{D_0} \frac{\partial D_h}{\partial z} - \frac{D_h}{D_0^2} \frac{\partial D_0}{\partial z} \right\} \quad (3.53)$$

hence, substituting into (3.48) we arrive at

$$\frac{dX}{dz} = \sqrt{\frac{|\gamma_h|}{\gamma_0}} \left\{ C \frac{x_h}{\gamma_0} X^2 + \left( \frac{x_0}{\gamma_0} + \frac{x_0}{|\gamma_h|} - \frac{\alpha_h}{|\gamma_h|} \right) X + \frac{C x_h}{|\gamma_h|} \right\} \frac{i\pi}{\lambda} \quad (3.54)$$

where  $|\gamma_h| = -\gamma_h$  has been assumed for Bragg reflection. The expression is similar to that given by Burgeat and Collela (1967), but includes the factors  $\gamma_h$  and  $\gamma_0$  as required for non surface symmetric reflections. The susceptibilities  $x_h$  and  $x_{\bar{h}}$  are also included and are not assumed to be equal.

Clearly, in a crystal/layer structure containing compositional variations  $\alpha_h$  will be a function of the depth,  $z$ , below the surface. Solution of equation (3.54) would then need to be performed numerically. However, if we divide the

crystal into a number of laminae of constant composition (these laminae will correspond to individual layers if the layers are of uniform composition), in which  $\alpha_h(z)$  is taken to be constant, equation (3.54) can be solved analytically for each laminae. The complex amplitude ratios are then matched at each boundary in order to obtain the reflectivity at the surface.

Let us rewrite equation (3.54) as

$$\frac{dX}{dz} = iD(AX^2 + 2BX + E) \quad (3.55)$$

$$\text{where } D = \frac{\pi}{\lambda} \sqrt{\frac{|\gamma_h|}{\gamma_0}}, \quad A = C \frac{x_h}{\gamma_0}, \quad B = \frac{1}{2} \left( \frac{x_0}{\gamma_0} + \frac{x_0}{|\gamma_h|} - \frac{\alpha_h}{|\gamma_h|} \right), \quad E = C \frac{x_h}{|\gamma_h|}$$

Then

$$\frac{dX}{dz} = iDA \left[ \left( \frac{X+B}{A} \right)^2 - \frac{B^2}{A^2} + \frac{E}{A} \right] \quad (3.56)$$

With the substitution  $X = -\frac{B}{A} + \frac{\sqrt{EA - B^2}}{A} \tan Y$ ,

the RHS of (3.56) becomes

$$i DA \frac{(EA - B^2)}{A^2} (1 + \tan^2 Y)$$

and the LHS becomes  $\frac{\sqrt{EA - B^2}}{A} (1 + \tan^2 Y) \frac{dY}{dz}$

$$\text{ie } \frac{dY}{dz} = iD \sqrt{EA - B^2} \quad (3.57)$$

We can assume that the reflectivity is known at a depth  $W$ , ie  $X(W)=K$ , hence we obtain

$$\int_{Y(W)}^{Y(z)} dY = \int_W^Z iD \sqrt{EA - B^2} dz$$

$$\text{ie } Y(z) = iD \sqrt{EA - B^2} (z-W) + \tan^{-1} \left( \frac{AK + B}{\sqrt{EA - B^2}} \right)$$

$$\text{ie } X = \frac{1}{A} \left[ -B \sqrt{EA - B^2} + B(AK + B) \tan(iD \sqrt{EA - B^2} (z-W)) \right. \\ \left. + (EA - B^2) \tan(iD \sqrt{EA - B^2} (z-W)) \right. \\ \left. + (AK + B) \sqrt{EA - B^2} \right] \\ \times \left[ \sqrt{EA - B^2} - (AK + B) \tan(iD \sqrt{EA - B^2} (z-W)) \right]^{-1}$$

$$\text{ie } X = \frac{K \sqrt{EA - B^2} + (E + BK) \tan(iD \sqrt{EA - B^2} (z-W))}{\sqrt{EA - B^2} - (AK + B) \tan(iD \sqrt{EA - B^2} (z-W))} \quad (3.58)$$

Now for an infinitely thick crystal  $K \rightarrow 0$  as  $z-W \rightarrow \infty$ . Since  $\tan(a+ib) \rightarrow i$  as  $b \rightarrow \infty$  and  $\tan(a+ib) \rightarrow -i$  as  $b \rightarrow -\infty$  we can write (3.58) as

$$X = - \frac{B + \sqrt{B^2 - EA} \times \text{sign}(\text{Imaginary } \sqrt{B^2 - EA})}{A} \quad (3.59)$$

provided that  $B^2 - EA$  is not wholly real.

Now for a centrosymmetric crystal  $E=A$ , and writing  $B/A = \eta$  we obtain

$$X = \eta \pm \sqrt{\eta^2 - 1} \quad (3.60)$$

which is equivalent to the result derived for an infinitely thick crystal by Darwin (see for example Batterman and Cole, 1964).

The reflectivity which represents the Bragg reflection profile is then the modulus squared of this complex reflectivity, ie  $C = |X|^2$ .

In order to calculate the diffracted intensity from a layered crystal we use the equation for the reflectivity from an infinitely thick crystal for the reflectivity at the top of the substrate. This then provides the necessary boundary condition at the bottom of the first layer. Using equation (3.58) we can then obtain the reflectivity at the top of this layer. This process is then repeated until the reflectivity is obtained at the surface of the crystal, over the range of angles  $\alpha$  required.

Once the reflectivity is obtained we can calculate the rocking curve using the convolution equation (2.17), which gives the total power reflected by the second crystal at an angle  $\beta$ . The rocking curve is calculated by performing this integration for the range of angles  $\beta$  required.  $C_{A,B}$  are the single crystal reflectivities for the first and second crystals respectively. For the first crystal the reflectivity for an infinite crystal is used.

### 3.4 The Effect of Sample Curvature on the Rocking Curve

As already seen, the growth of a mismatched epitaxial layer on a substrate produces overall sample curvature. This curvature will, clearly, affect the shape of the rocking curve if the misorientation introduced is of similar order to the width of the rocking curve. There are two ways in which the misorientation can be introduced.

If we consider the incident beam passing through a

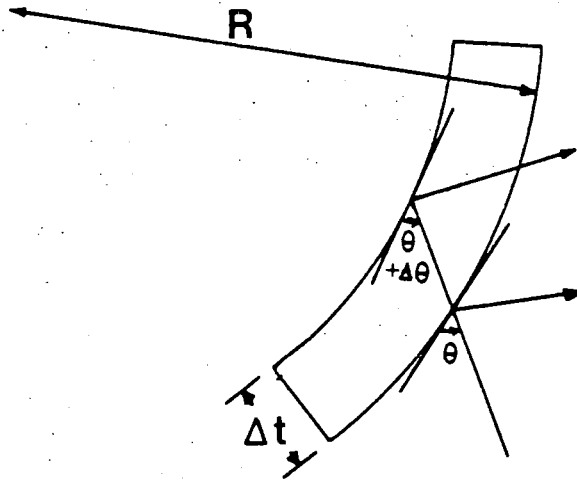


Fig. 3.2 Change in glancing angle  $\theta$  for an incident x-ray beam and a curved crystal of thickness  $\Delta t$ .  $R$  is the radius of curvature of the crystal.

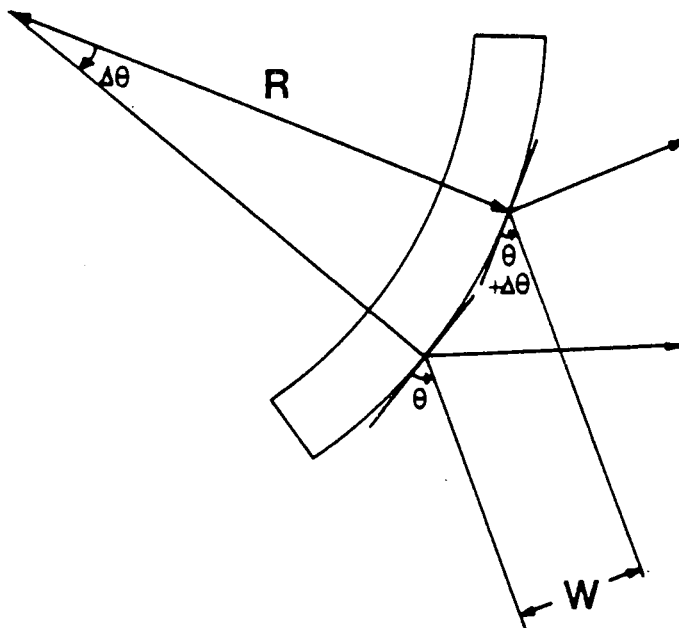


Fig. 3.4 Change in Bragg angle along an incident beam of width  $W$  for a crystal of radius of curvature  $R$ .

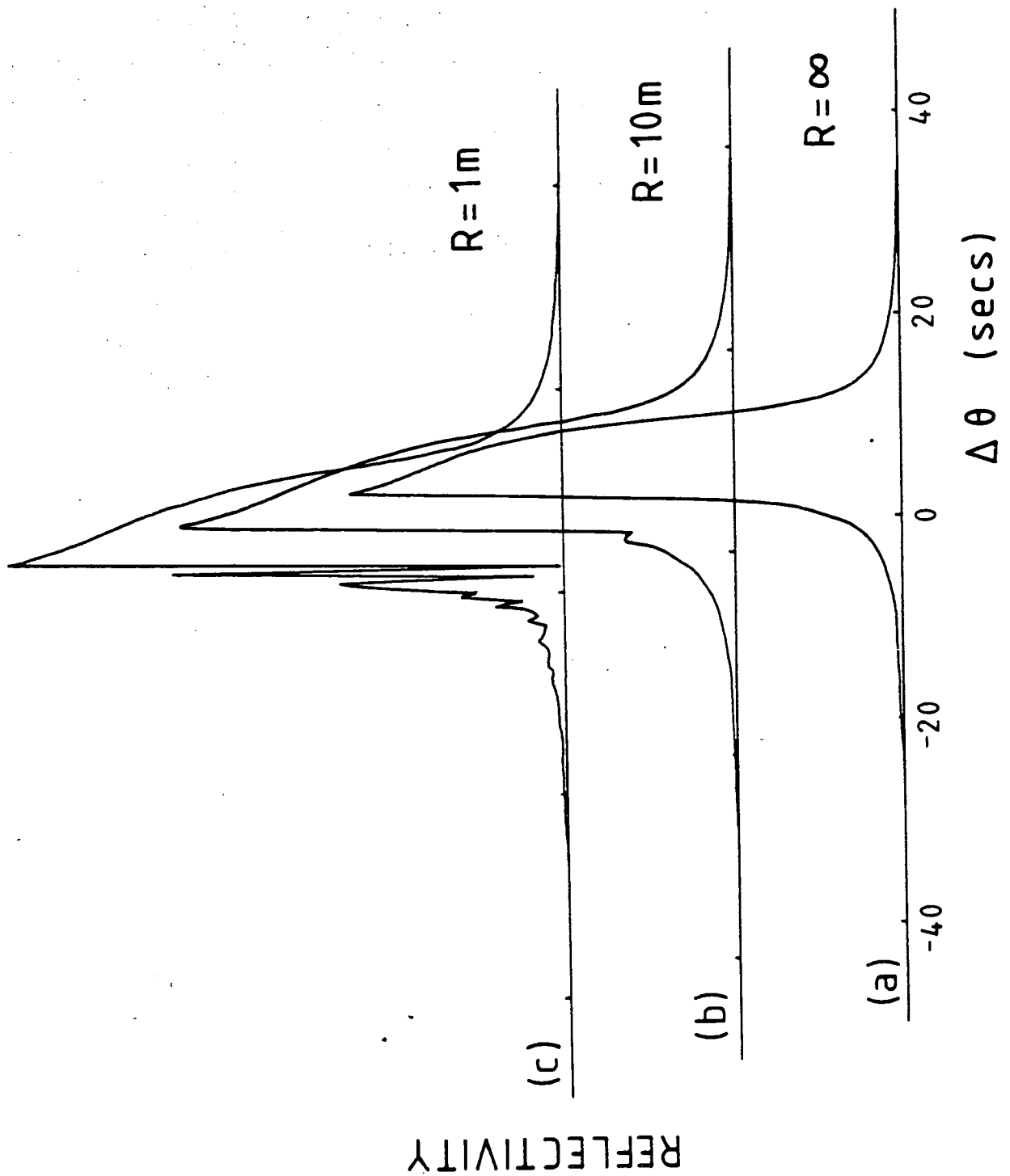


Fig. 3.3  $004 \text{ CuK}\alpha_1$  single crystal reflection curves for an InP crystal with (a) a flat crystal (b) a curved crystal with radius of curvature 10m and (c) a 1m radius of curvature. The effect assumed is that of the change in angle as a function of depth.

curved sample, the angle between the beam and the reflection planes will alter as a function of depth, as shown in fig.

3.2. This misorientation is given by

$$\Delta\theta = \Delta t \cot\theta / R \quad (3.61)$$

where  $R$  is the radius of curvature of the sample. We can calculate the reflection profile from such a crystal by dividing it into a number of laminae in which the Bragg angle is taken to be constant. Dividing a 1mm thick crystal into laminae of 1  $\mu\text{m}$  thickness 004  $\text{CuK}\alpha_1$  reflection curves for a flat crystal, a 10m curved crystal and a 1m curved crystal are shown in fig. 3.3. We note that the reflection profile is both broadened and, for the highly curved crystal, Bragg case Pendellosung fringes are visible. However, since the majority of crystals have curvatures greater than 1m this effect is not too important. Generally this effect is not so important as that reported for neutron diffraction (Klar and Rustichelli, 1973), due to the stronger absorption of X-rays by the crystal.

For X-ray diffraction the most important effect is due to the change in Bragg angle along the width of incident beam, as shown in fig. 3.4. For a particular angle at one extreme of the beam there will be an intensity contribution to the overall curve from all angles up to that subtended at the other extreme of the beam. Approximately, we find

$$\Delta\theta = W / (R \sin\theta) \quad (3.62)$$



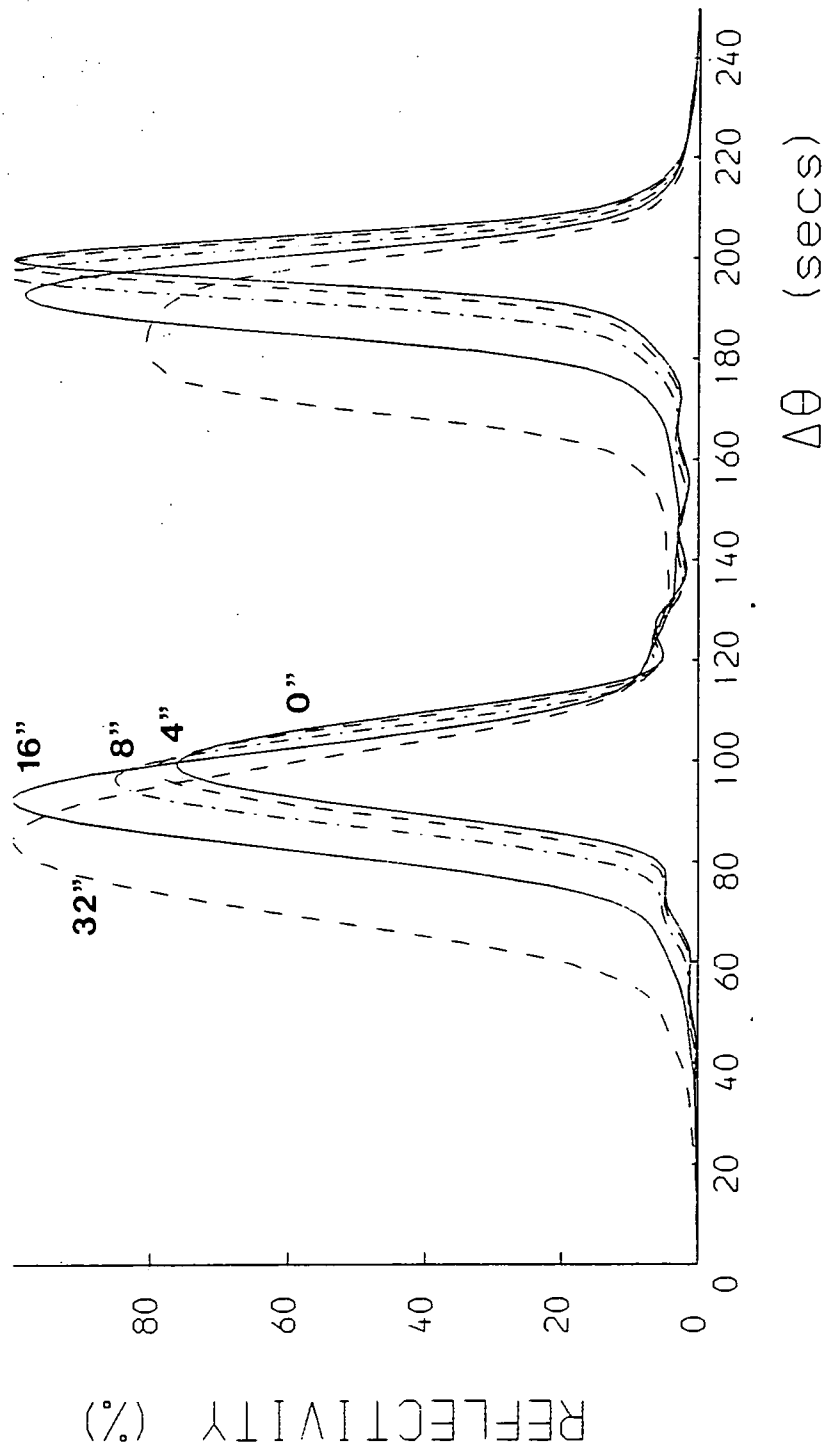


Fig. 3.5 The effect of sample curvature, assuming the effect due to beam width, on the 004 CuK $\alpha_1$  rocking curve from a sample with a 400 ppm mismatched 1 $\mu$ m thick GaInAs layer.

where  $W$  is the width of the incident beam. For a 004 reflection with  $\text{CuK}\alpha_1$  radiation from a 10m radius of curvature InP crystal this change in angle is approximately 20 arc secs for a 0.5mm wide beam, clearly a large angle compared to the 9 second theoretical half width of the reflection. Fig. 3.5 shows the effect of decreasing the radius of curvature on the rocking curve for such a crystal plus a 400 ppm mismatched 1  $\mu\text{m}$  thick GaInAs layer. Not only are the peaks broadened but the ratio of peak heights alters due to the difference in half widths of the peaks. The values of peak half widths and the ratio of peak heights are also given in Table 3.1.

TABLE 3.1

Values of the substrate and layer peak half widths and ratio of peak heights for an increasing sample curvature on a sample with a 1  $\mu\text{m}$ , 400 ppm mismatch GaInAs layer. The 004 reflection is used with  $\text{CuK}\alpha_1$  radiation.

$\Delta\theta$ due to sample curvature (secs)	$\Delta\theta_{\frac{1}{2}}$ of the substrate peak (secs) ( $\pm 0.4$ )	$\Delta\theta_{\frac{1}{2}}$ of the layer peak (secs) ( $\pm 0.4$ )	Ratio heights of substrate:layer peaks ( $\pm 0.01$ )
0	11.0	17.6	0.76
4	12.2	21.1	0.79
8	13.0	22.2	0.85
16	18.4	23.7	1.01
32	33.0	35.2	1.24

### 3.5 Computation of Rocking Curves

Since the susceptibilities  $\chi_0$ ,  $\chi_h$  and  $\chi_{\bar{h}}$  and the reflectivity  $X$  are complex, Fortran was chosen as the

programming language due to the ease of handling complex arithmetic. Unfortunately, Fortran is not well structured so Pascal was chosen to programme the interactive sections. Since Pascal also provides enumerated variables the accessing of the analytical approximation and dispersion correction data, required to calculate the structure factors for each material, was also simplified. The Fortran programme was written to calculate the reflectivities and convolution using the structure factors, Bragg angles, lattice parameters and layer thicknesses generated by the Pascal programme. This data was passed between the programmes in a data file. This technique is particularly useful as the Fortran programme requires the largest amount of CPU time and can be left to run in 'Batch' mode where large numbers of layers are present.

### 3.5.1 The Pascal Programme

This programme handles all the interactive sections of the overall calculation, enabling the layer parameters to be entered and easily edited. Once all the reflection and layer parameters have been entered the structure factors are calculated using the analytical approximation to provide the scattering factors (International Tables, 1974). The dispersion corrections are calculated at the required wavelength using a polynomial approximation to the tabulated values (International Tables).

Operation of the programme is outlined by the flow

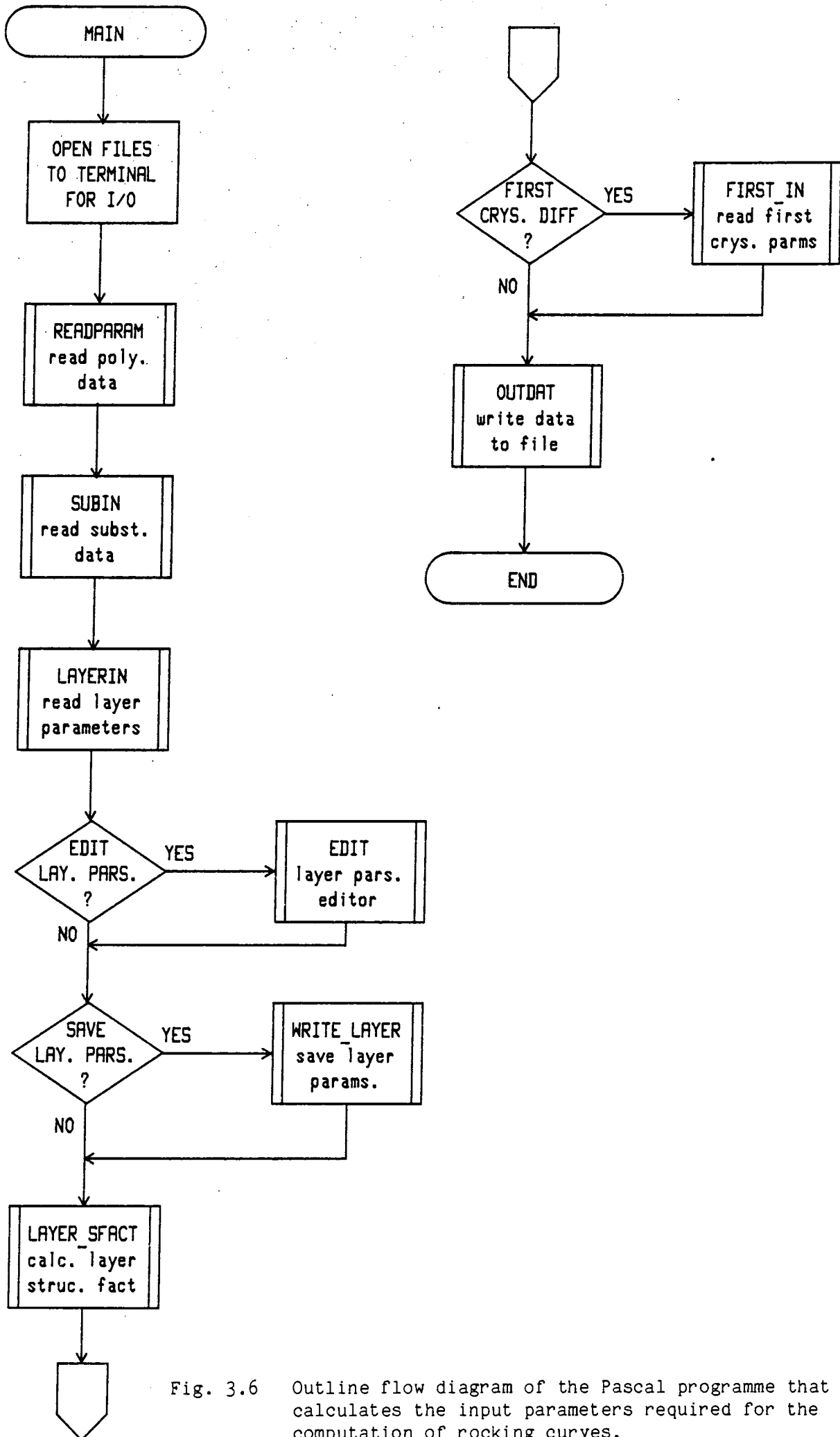


Fig. 3.6 Outline flow diagram of the Pascal programme that calculates the input parameters required for the computation of rocking curves.

diagram, fig. 3.6. Appendix A contains a complete listing of the programme. The analytical and dispersion approximation data is contained within a data file to allow additions for extra elements to be easily made. The material names entered by the user are converted into sets of elements by comparing the names with those expected for the various III-V combinations. If the material name is not recognised it is asked for again. Detection of an element within the set is then easily made. Thus code numbers do not need to be used for each material, hence making altering the programme straightforward.

In order to avoid entering the individual laminae/layers for graded and multiquantum wells, routines are provided to calculate these parameters. Once this data has been generated it can still be edited to allow for any additional variations. The layer parameters can also be saved in a disc file to be reused in a future calculation.

The layer editing routine allows any of the layer parameters to be altered and additionally for layers to be deleted or extra layers inserted.

For graded composition layers with a non linear variation with depth the layer parameters are assumed to lie on a variable radius curve. The variation from non linearity is entered as a percentage value with 100% corresponding to a curve with radius equal to the layer thickness and 0% corresponding to a linear variation.

Fig. 3.7 shows complete detailed flow diagrams of the

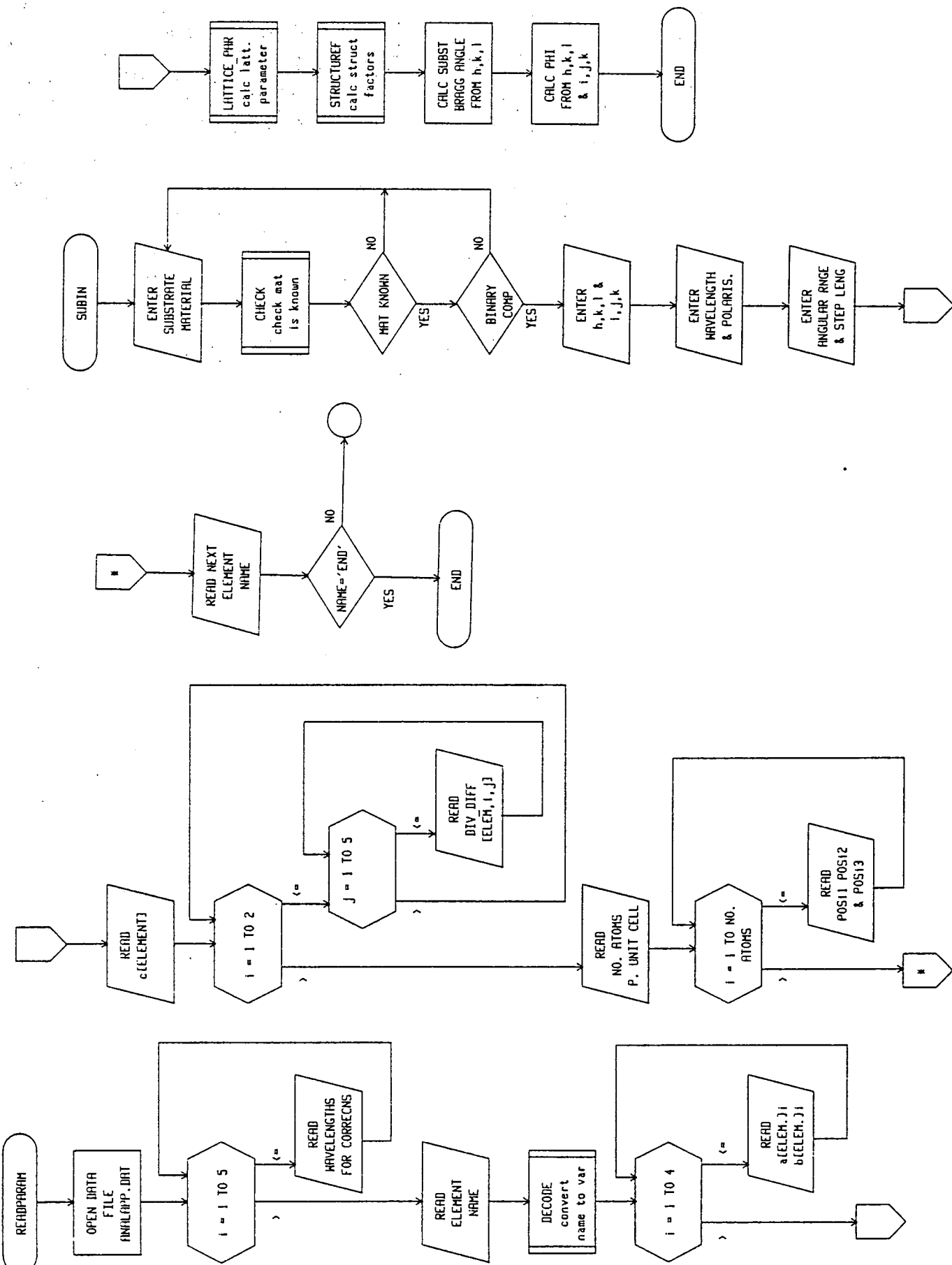
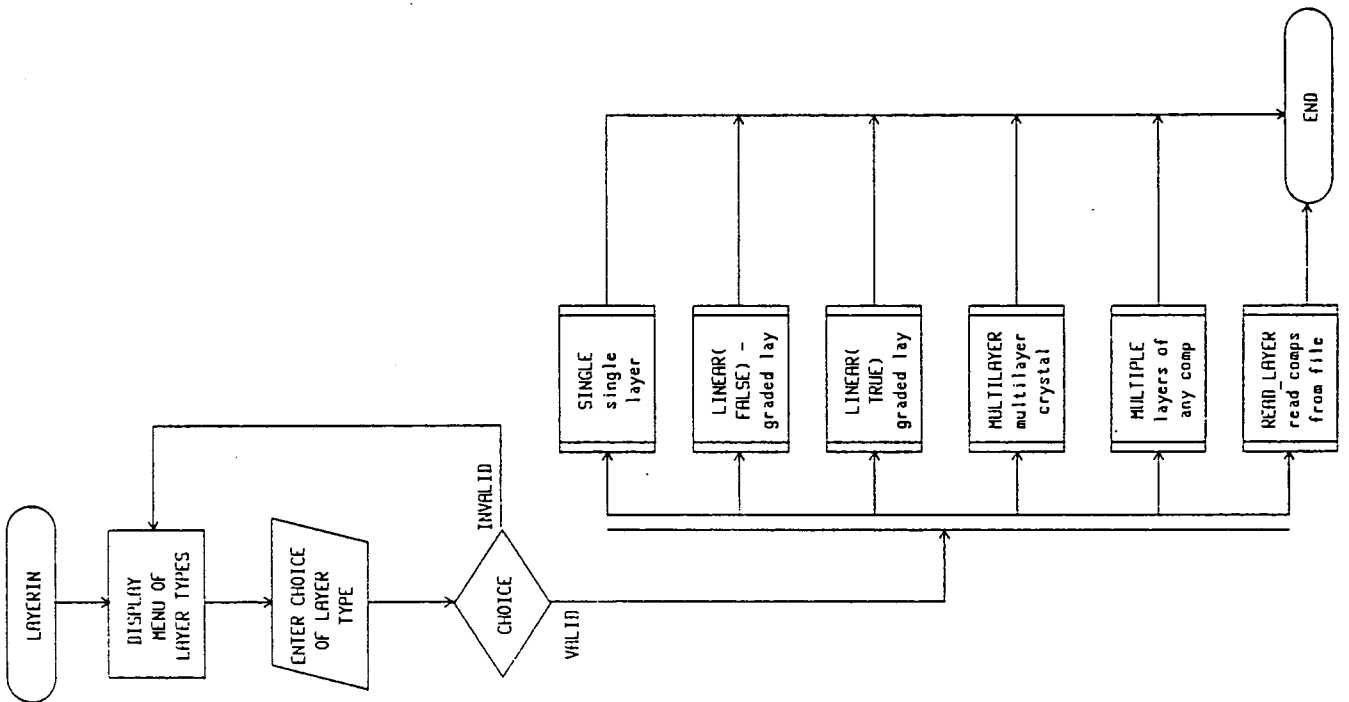
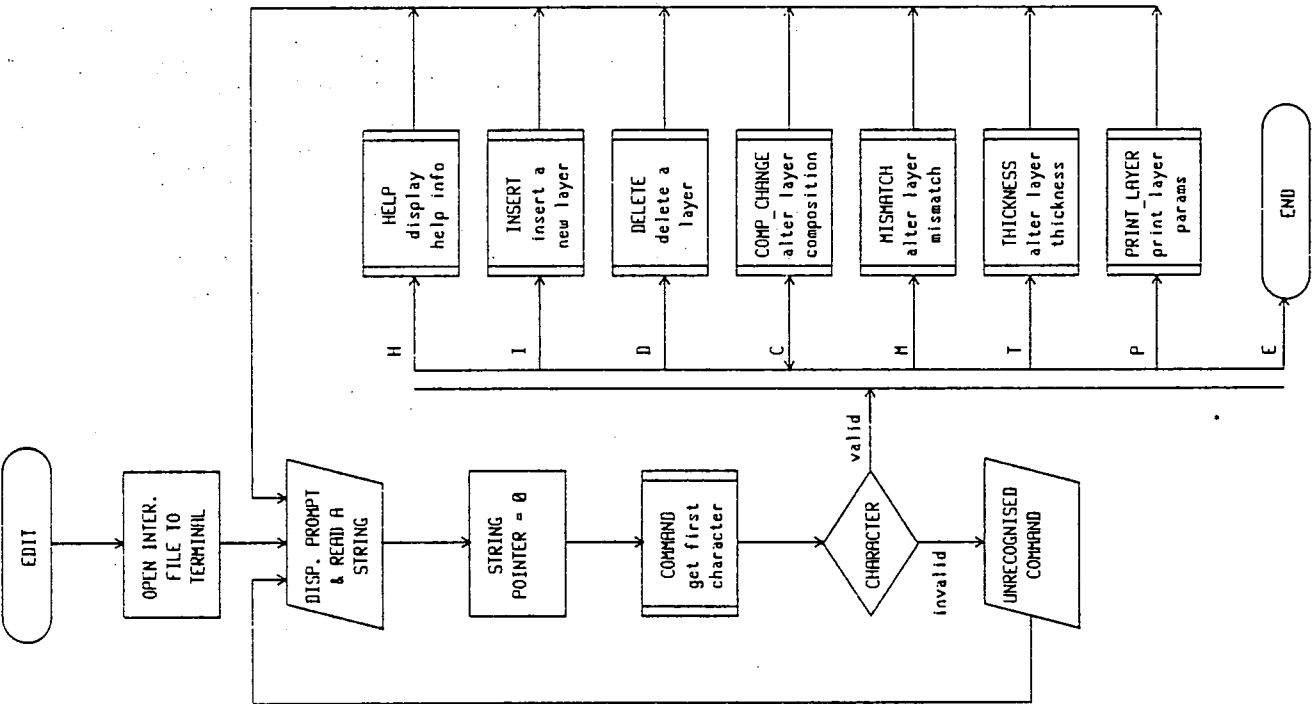
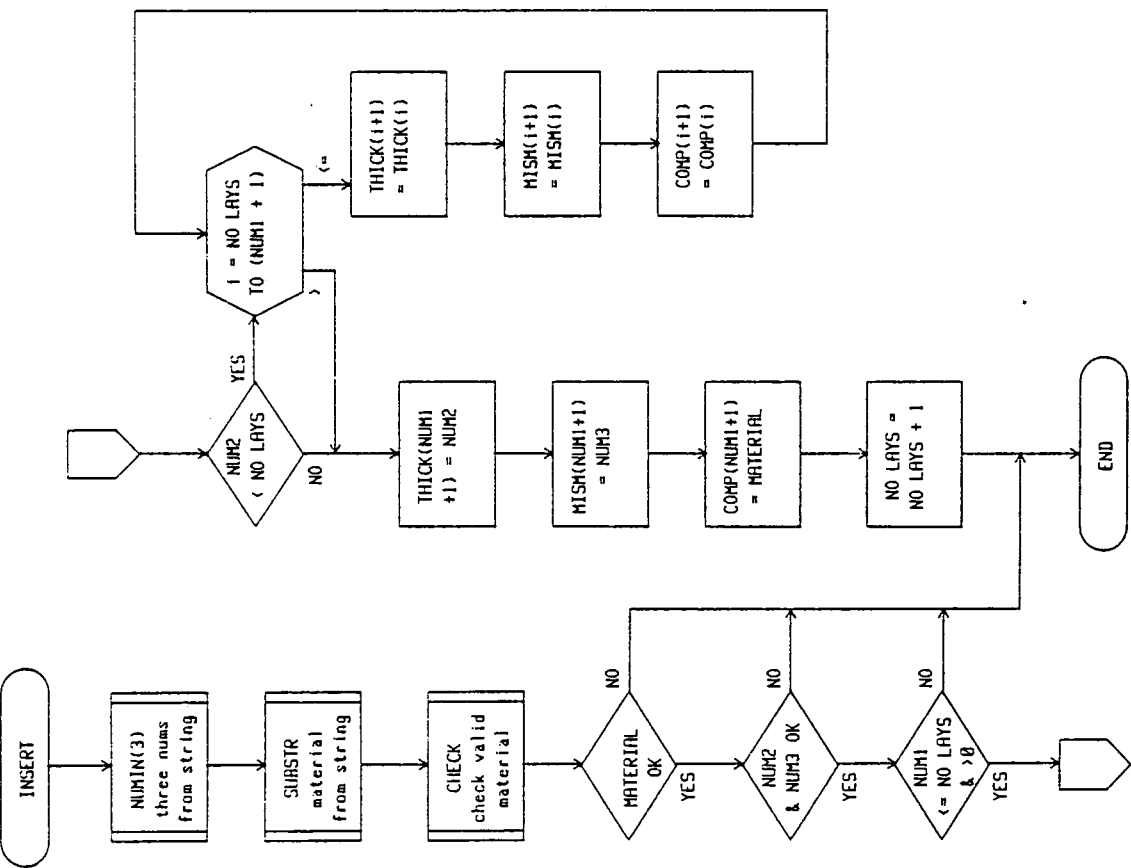
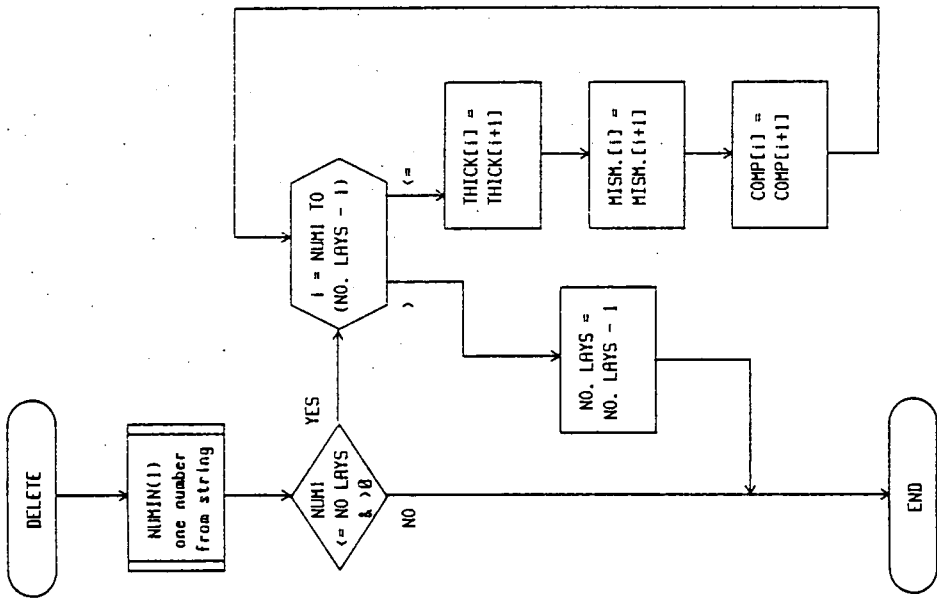
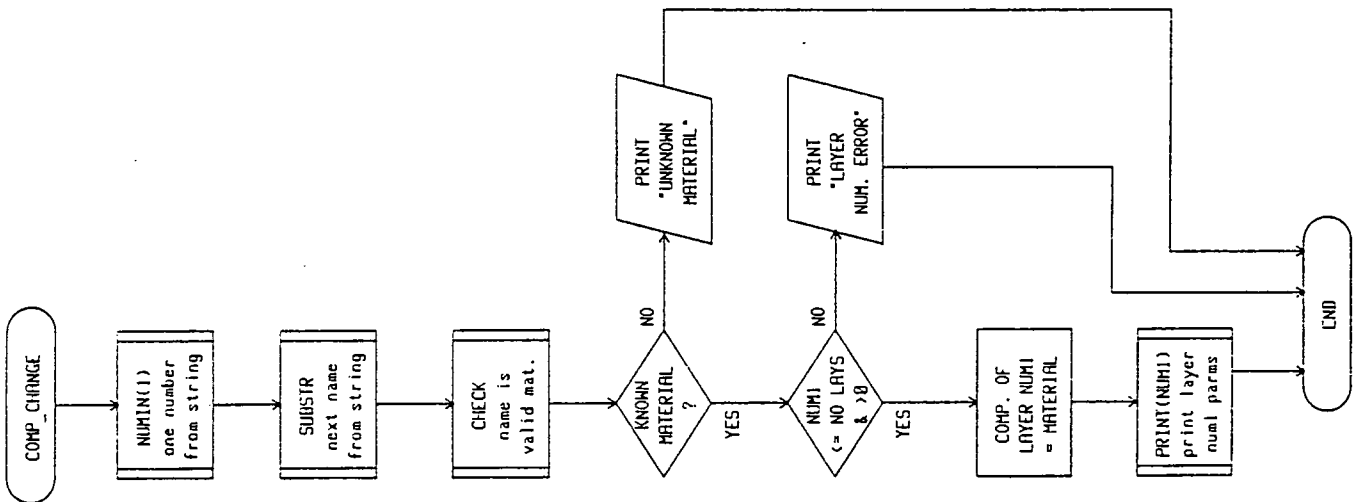
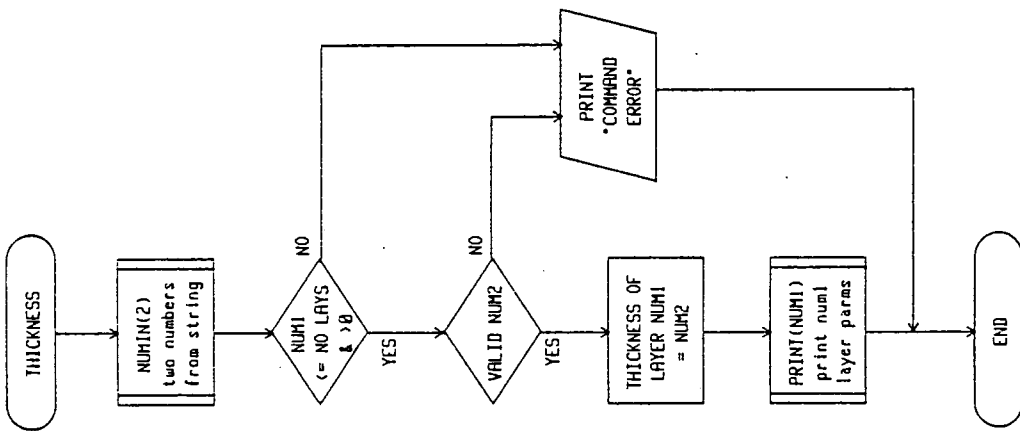
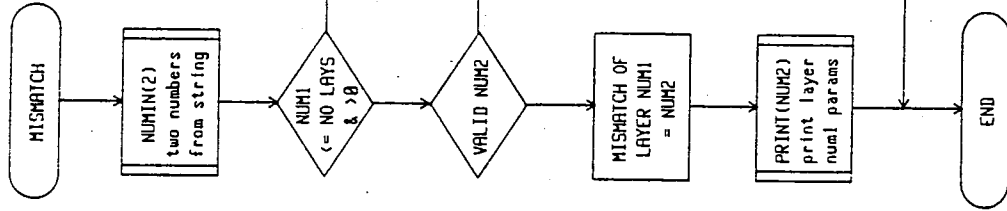


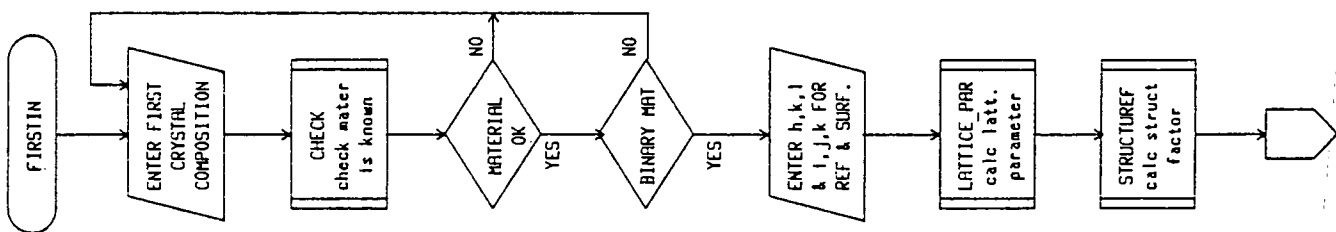
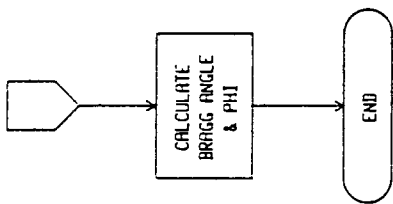
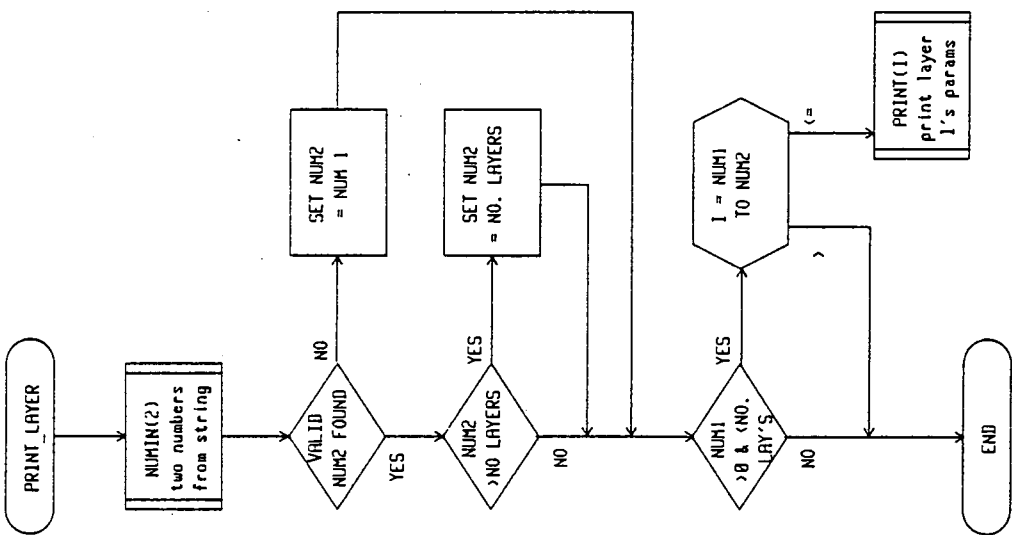
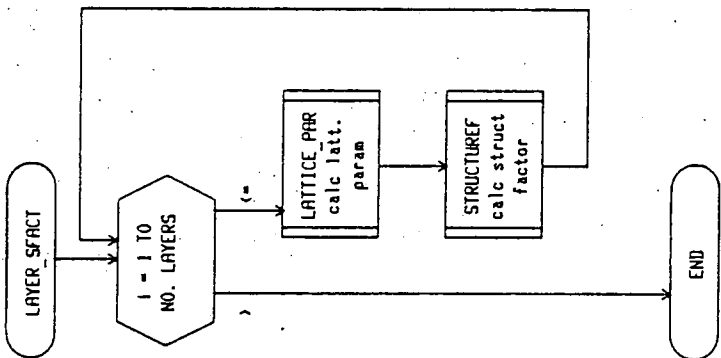
Fig. 3.7 Detailed flow diagram of the Pascal programme.

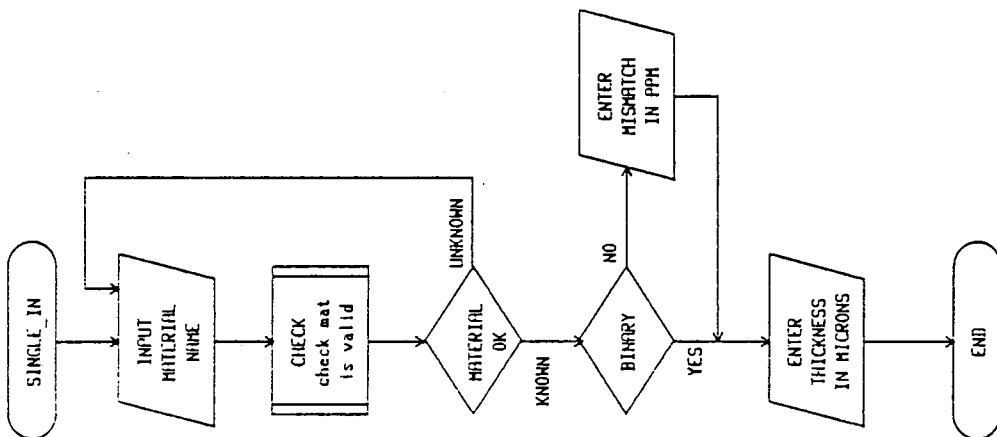
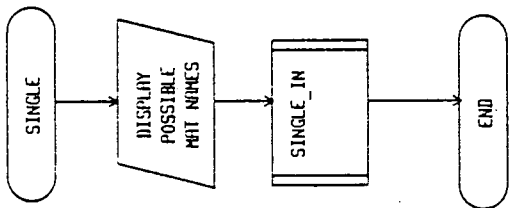
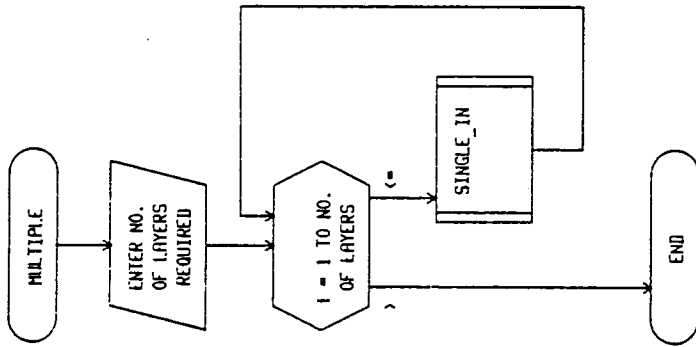
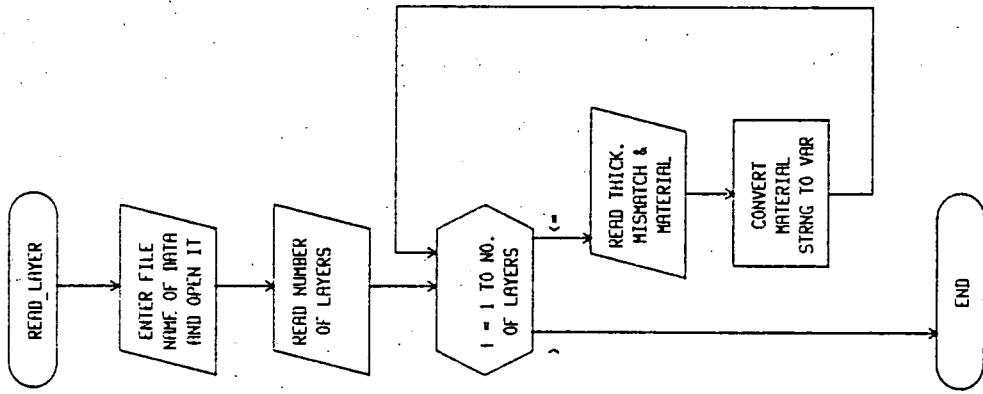


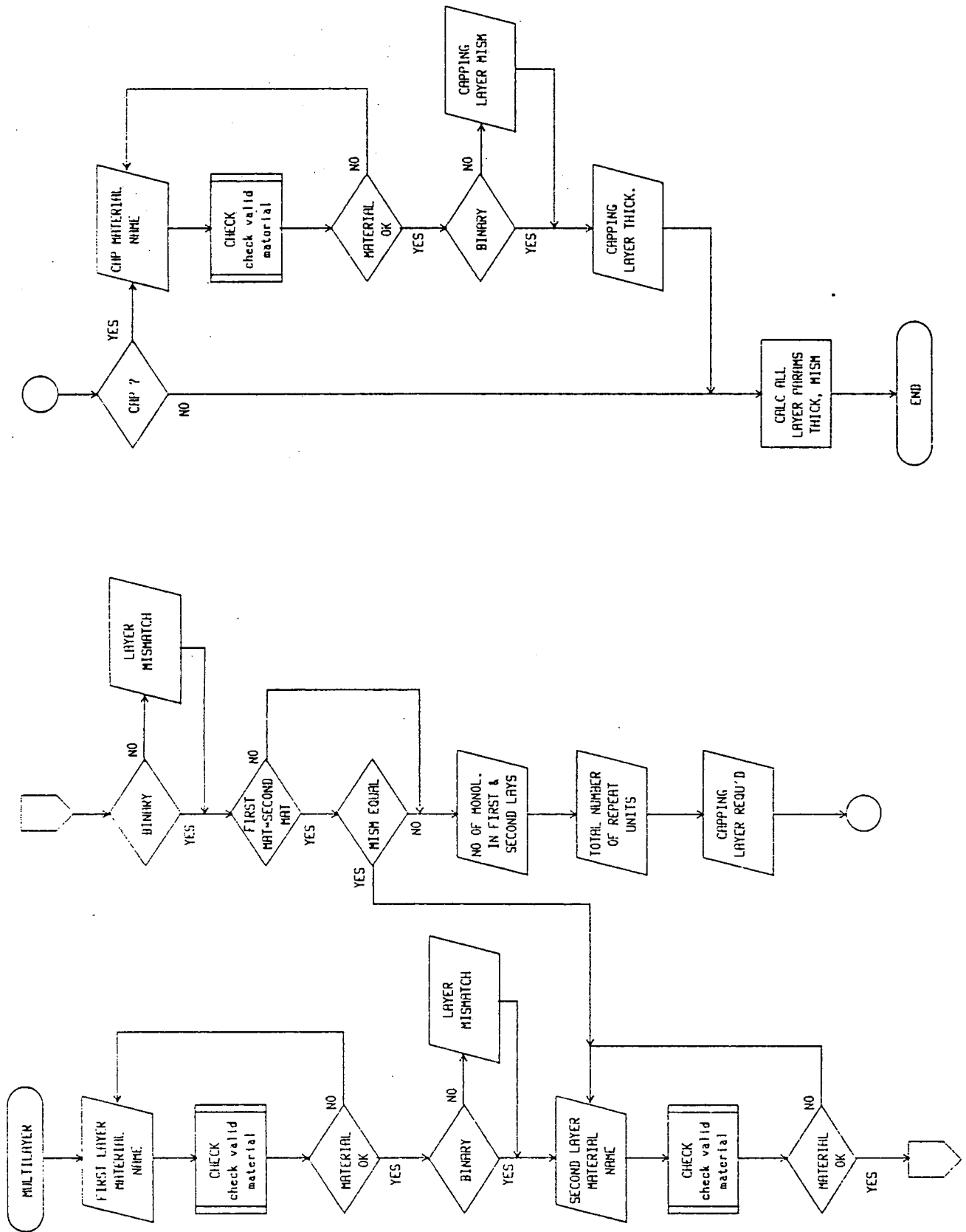


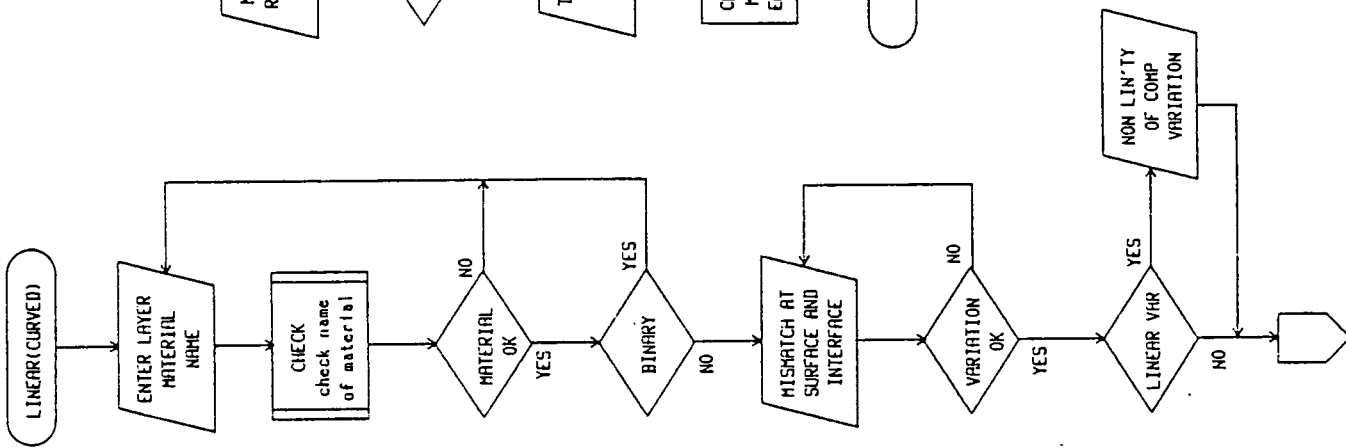
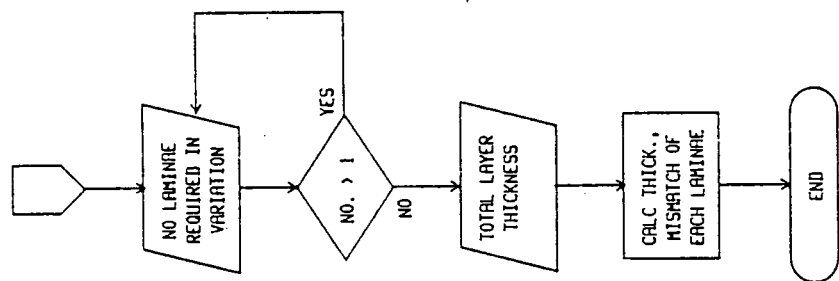
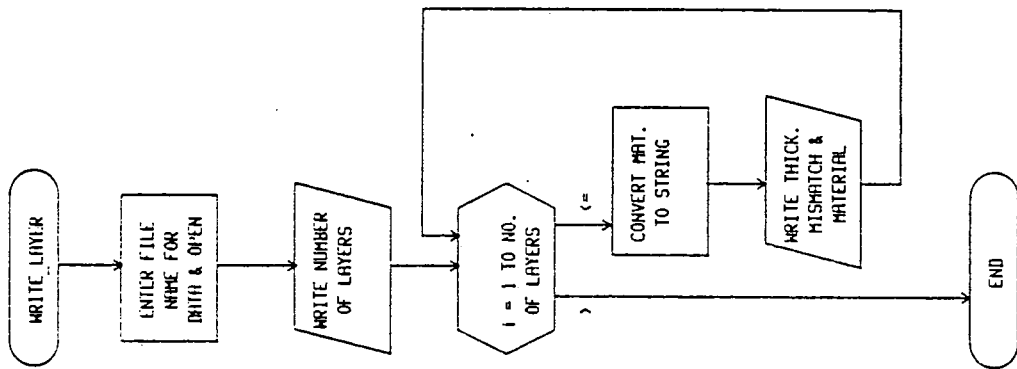
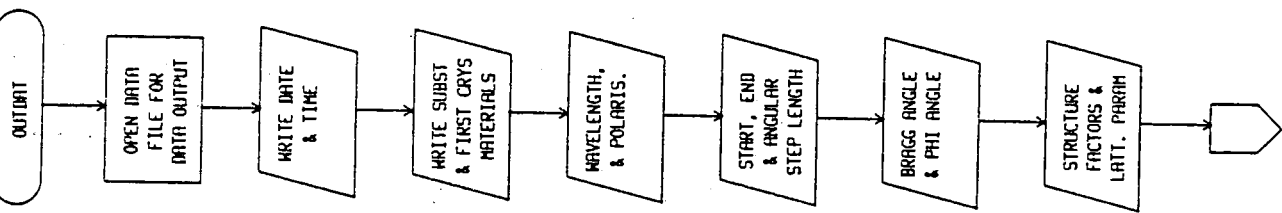
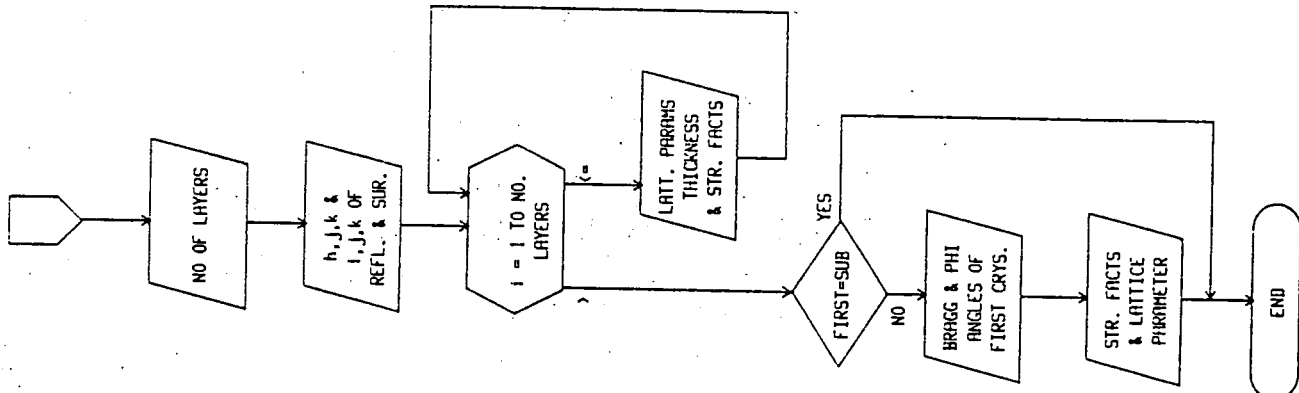












individual routines, and their operation is fairly straightforward. In particular the editing routine operates by inputting one command string, from which the individual functions remove their required number of variables, delimited by spaces. This method allows a variable number of parameters to be entered in the command string while still retaining a single line entry system.

At all stages of the programme unrecognised materials are detected and the user prompted for a new material. Additionally, ternary and higher alloys cannot be selected as substrates and composition variations will not be allowed for binary alloys. The percentage composition of each element in a chosen material is determined from the mismatch, according to the equations given in chapter 1. For quaternary alloys the band gap is also used. The material structure factors are calculated by multiplying the structure factor for the elements by their percentage in the material. This will be valid only if the various elements in the material are completely randomly distributed. Finally, the parameters required by the Fortran programme are output for every layer.

### 3.5.2 The Fortran Programme

Operation of this programme is outlined by the flow diagrams shown in fig 3.8. Appendix A contains a complete listing of the programme.

Once the data has been read from the data file the

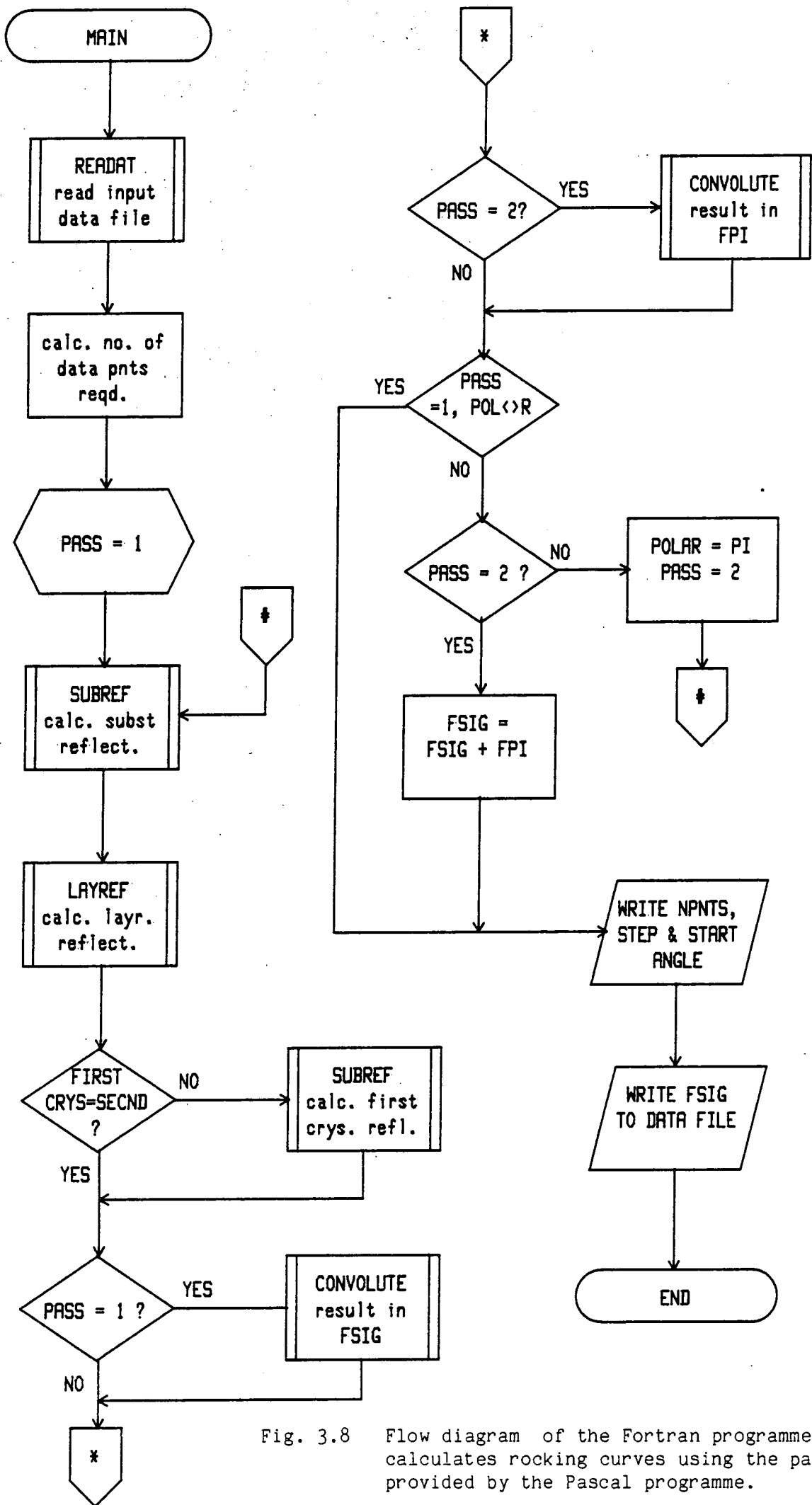


Fig. 3.8

Flow diagram of the Fortran programme that calculates rocking curves using the parameters provided by the Pascal programme.

reflectivities for the first and second crystals are calculated, over the range of angles required. If the first crystal is the same as the substrate of the second crystal the substrate reflectivity is used for the first crystal reflectivity. If the first crystal reflection is different from that of the second crystal, giving a non parallel arrangement, dispersion should be taken into account. However, the programme does not account for this effect making it only valid for the synchrotron source where the beam divergence is so small that dispersion can be neglected. The reflectivities are calculated using equations (3.58) and (3.59). This programme requires no knowledge of the materials being used and can therefore be used to calculate rocking curves from any material, provided that it is supplied with the appropriate structure factors and lattice parameters.

For each layer in the second crystal the deviation parameter  $\alpha_n$  is calculated, taking into account the difference in Bragg and phi angles for the layer and substrate. This is necessary since the range of angles specified are taken relative to the substrate Bragg angle. Thus, if we take  $\Delta\theta_{S,L}$  to be the angular deviation from the exact Bragg angle for the substrate and layer respectively, we have

for low angles of incidence

$$\Delta\theta_L = \Delta\theta_S + \theta_{BS} - \theta_{BL} - \varphi_S + \varphi_L \quad (3.62)$$



and for high angles of incidence

$$\Delta\theta_L = \Delta\theta_S + \theta_{BS} - \theta_{BL} + \varphi_S - \varphi_L. \quad (3.63)$$

For ease of calculation the convolution is calculated over the same range and interval as the single crystal reflectivities, although the routines can handle both a different range and interval. The convolution is calculated according to equation (2.17). For each value of  $\beta$  a multiplied curve is calculated and the area under it determined to give the reflectivity at the angle  $\beta$ . To calculate the multiplied curve the first crystal reflectivity at the angle  $\alpha$  is multiplied by the second crystal reflectivity at the angle  $(\alpha-\beta)$ . If the angle  $(\alpha-\beta)$  does not correspond to a data point on the other reflectivity curve linear interpolation between the nearest points is used. The curve is then generated by repeating this operation over the range of angles  $\alpha$ . Outside this range the reflectivities are taken to be zero.

If random polarisation is selected the entire calculation is repeated and the two convoluted curves added.

Finally, the rocking curve data is written to the output file, to be plotted by another programme. This approach allows the curve to be plotted on different scales without recalculating the curve. Additionally, the effect of sample curvature is added by the plotting programme, allowing the effect of different sample curvatures to be observed without recalculating the curve.

The plotting programme is straightforward and hence

will not be described in detail. A complete listing is contained in Appendix A. Rocking curve data is read from a file and plotted using GHOST routines. The plotfile produced by these routines can be plotted either on a graphics terminal or on a hardcopy plotter.



Fig. 4.1 Photograph of the six inch double crystal camera and the GX-6 x-ray generator at Durham. The camera is rigidly mounted on a separate table while the 1m collimator is equipped with an optical light source and adjustable slits.

## CHAPTER 4

### EXPERIMENTAL TECHNIQUES AND INSTRUMENTATION

Two types of double crystal camera have been used to measure the rocking curves presented here. A six inch axial separation camera, similar to that described by Hart (1980) and by Meriam Abdul Gani (1982), was used at Durham in conjunction with a Marconi-Elliott GX-6 rotating anode generator and with a Philips 1010 sealed tube generator. At the SRS, Daresbury Laboratory, a twelve inch axial separation camera, as described by Bowen and Davies (1983), was used on the Port 7 station. Both of these cameras have similar axial drive mechanisms, driving the axis via a stepper motor/gearbox/micrometer combination pushing a tangential arm attached to the axis. On the larger camera several other axes are motor driven including the detector arm and the camera itself. Computer control of the cameras was implemented at Durham with a BBC microcomputer and Minicam system, and at Daresbury with a PDP11/04 minicomputer and a CAMAC system.

#### 4.1 The Six Inch Camera at Durham

A photograph of the double axis camera, positioned to receive X-rays from the GX-6 generator, is shown in fig. 4.1. With 200 steps per revolution motors the drive system gives 0.177 and 0.121 arc seconds per motor step for the first and second axes respectively. The camera is rigidly



Fig. 4.2 Photograph showing the construction of the collimator and removable optical light source. The projector lamp and steel tube are mounted on a sliding mechanism allowing either the lamp or the steel tube to be positioned in line with the collimator tube.

mounted on a separate table to remove any vibration present in the generator. A collimator approximately 1m long is used, fixed at the optimum take-off angle with respect to the anode. In this arrangement the X-ray beam is horizontal so that an angled baseplate is not required for the camera, as it is with a vertically mounted sealed tube source.

In order to ease camera alignment a removable optical light source, consisting of a projector lamp mounted on a sliding arm, was fitted to the collimator. By placing the lamp in the centre of the collimator the light follows the same path as the X-rays, thus facilitating easy camera alignment. Additionally, where the crystals used are highly polished they can also be set close to the correct Bragg angle, for surface symmetric reflections, using this system. The construction of the light source is clear from the photograph shown in fig. 4.2. The cover has been removed, while the sliding part is slightly displaced from its 'home' position, where the steel tube mounted on the slide fits tightly between the two sections of collimator tube. This arrangement helps to reduce the amount of scattered radiation in the box.

#### **4.1.1 Computer control**

Previously this double axis camera had been controlled by a PET microcomputer and a memory mapped Minicam system (Meriam Abdul Gani, 1982). In this configuration the Minicam system appears as part of the microprocessor's

memory, being controlled by code within the microcomputer. Meriam Abdul Gani (1982) has described many of the boards available. Recently the Minicam system was improved by the addition of an intelligent controller card (ICC) based on a 6502 microprocessor. This board replaces the memory mapped interface with all the control software contained on the board. Communication to a computer is provided by an IEEE488 interface. The boards are then controlled by passing binary data along this bus, an 8 bit number selecting the operation required and additional variables being passed as two 16 bit numbers.

Unfortunately, the majority of inexpensive microcomputers are not equipped with an IEEE488 interface, notably the BBC microcomputer. Thus, even though this computer offers far greater performance, including high resolution graphics, than the PET computer communication with a Minicam system is not possible. Consequently, since the BBC computer, and many other inexpensive computers, is equipped with a serial RS232 port it was appropriate to add such a serial interface to the Minicam system. A full description of the design is given below. Since the RS232 standard is designed to transmit Ascii encoded data only 7 bits are required (although 8 bits are often available), thus making the transmission of binary data not straightforward. In order to avoid this problem the Minicam firmware was rewritten to allow Ascii transmission. Full details of the new software can be found in Appendix B.

Once the BBC microcomputer and the Minicam system can communicate with each other the actual control of the double crystal camera is easily implemented. Routines similar in outline to those described by Meriam Abdul Gani (1982) were implemented, with the addition of graphics routines to display the data collection in real time. Rocking curve data can be saved on floppy disc to be redisplayed later or plotted on a digital plotter such as the HP7470A or the PIXY3. The BBC microcomputer is also connected to the laboratory's local area network thus allowing this data to be transferred onto the University's mainframe computer for analysis and comparison with simulated rocking curves. With the addition of the Workstation Rom (available from the Computer Centre, University of Sussex) the BBC microcomputer can also act as a graphics terminal to the mainframe. A full description of the control software is given in Appendix C.

X-ray intensities were measured with a standard scintillator/photomultiplier system with a Harwell rack mounted H.T. supply and amplifier. Two of the 16 bit Minicam counters were cascaded to provide one 32 bit counter which was required when long counting times were used for the measurement of weak satellite peaks from superlattices. Since good counting statistics are required to observe such satellites long counting times are needed and the counter can overflow if a main diffraction peak is encountered.



#### 4.1.2 Design of the ICC RS232 Serial Interface

The fundamental requirements of the serial interface were that it should conform to the RS232 standard, operate at a variable baud rate, have a variable word format and utilise hardware handshaking (CTS/DTR type). High transmission speeds were also required to provide fast communication. Since many computers are equipped with only one serial interface once this is connected to the Minicom system it is no longer possible to use a serial printer or plotter without needing a data switch. Therefore, any plotter being used to plot rocking curves cannot be used under programme control without user intervention. Consequently, a second serial port was included in the ICC interface to enable data to be passed from one serial port to the other. Baud rates and word formats need to be individually controlled especially if a slow speed peripheral device is being used.

Since the Minicom bus is not a true microprocessor bus, being controlled by two interface adaptors, it is limited in speed and has several vital signals missing (particularly the processor clock required for synchronisation and the  $R/\bar{W}$ ,  $\overline{IRQ}$  and  $\overline{NMI}$  signals). Therefore, standard 6500/6800 peripheral IC's cannot be directly attached to this bus, hence it was decided to attach the serial interface directly to the ICC board and the microprocessor bus using the expansion connector located in the centre of the board. Since the Minicom manual does not give the pin-out of this

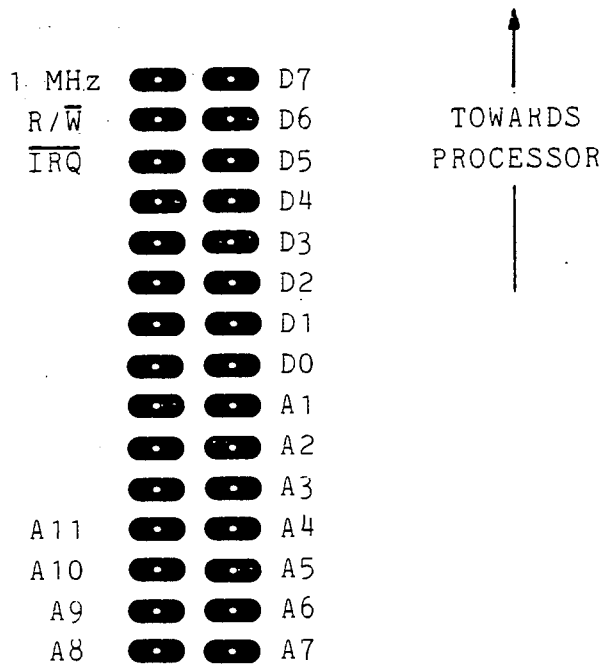


Fig. 4.3 Pin out of the connector in the centre of the Minicam ICC board. This connector allows access to the unbuffered microprocessor signals unlike the minicam bus.

connector it is shown in fig. 4.3 for reference.

The serial interface was designed around the 6850 ACIA which provides all the features required, including hardware handshaking, and is directly compatible with the 6502 processor. The receive and transmit clock inputs were tied together and the clock signal provided by a 2.4576 MHz crystal oscillator and a 4702B programmable divider. The 4702B is specifically designed for this use and provides a rate 16 times the majority of widely used baud rates. Therefore, the 6850 should be programmed, after reset, to divide the receive and transmit clocks by 16. Two of these combinations are included in the design to provide the two independent rates for the two 6850s. In order to provide a variable word format an 8-way dual-in-line switch, buffered by a 74LS244, is provided which can be read as a memory location. This value can then be used to programme the word selection bits of the 6850s.

The main ICC board decodes addresses within the range \$8000-\$803F to provide the chip enable signals for the two 6522 VIAs and the 68488 GPIA. However, only the \$8000, \$8010 and \$8020 lines are used leaving the \$8030 line free. A wire patch on the main board is used to link this signal with a spare pin on the expansion connector. This line plus the address lines A2 and A3 are connected to half of a 74LS139 dual 2 to 4 line decoder to provide the three enable lines for the two 6850s and the 74LS244. Thus the addresses of these chips are \$8030, \$8034 and \$8038.

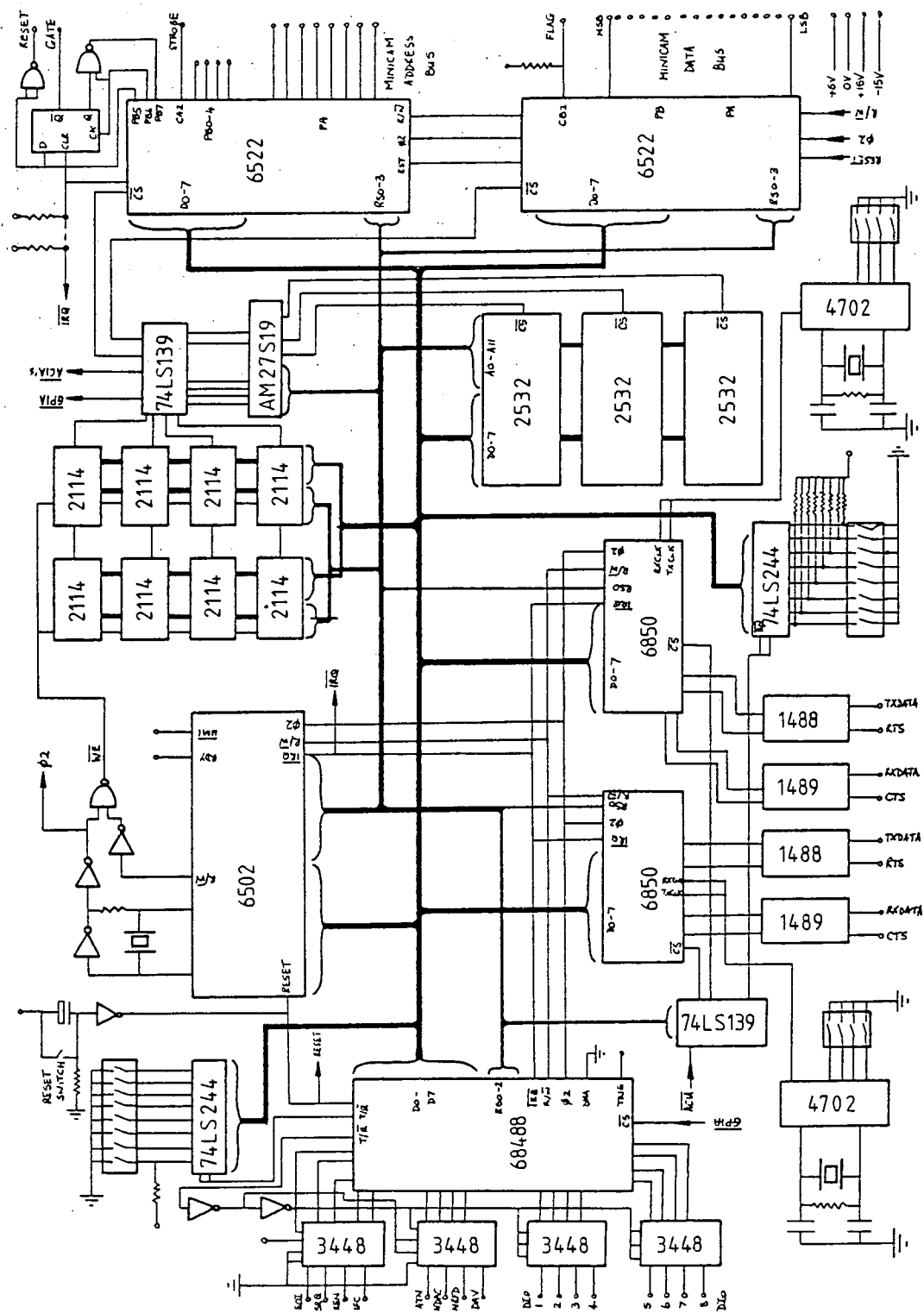


Fig. 4.4 Circuit diagram of the Minicam ICC board complete with the twin channel RS232 serial interface.

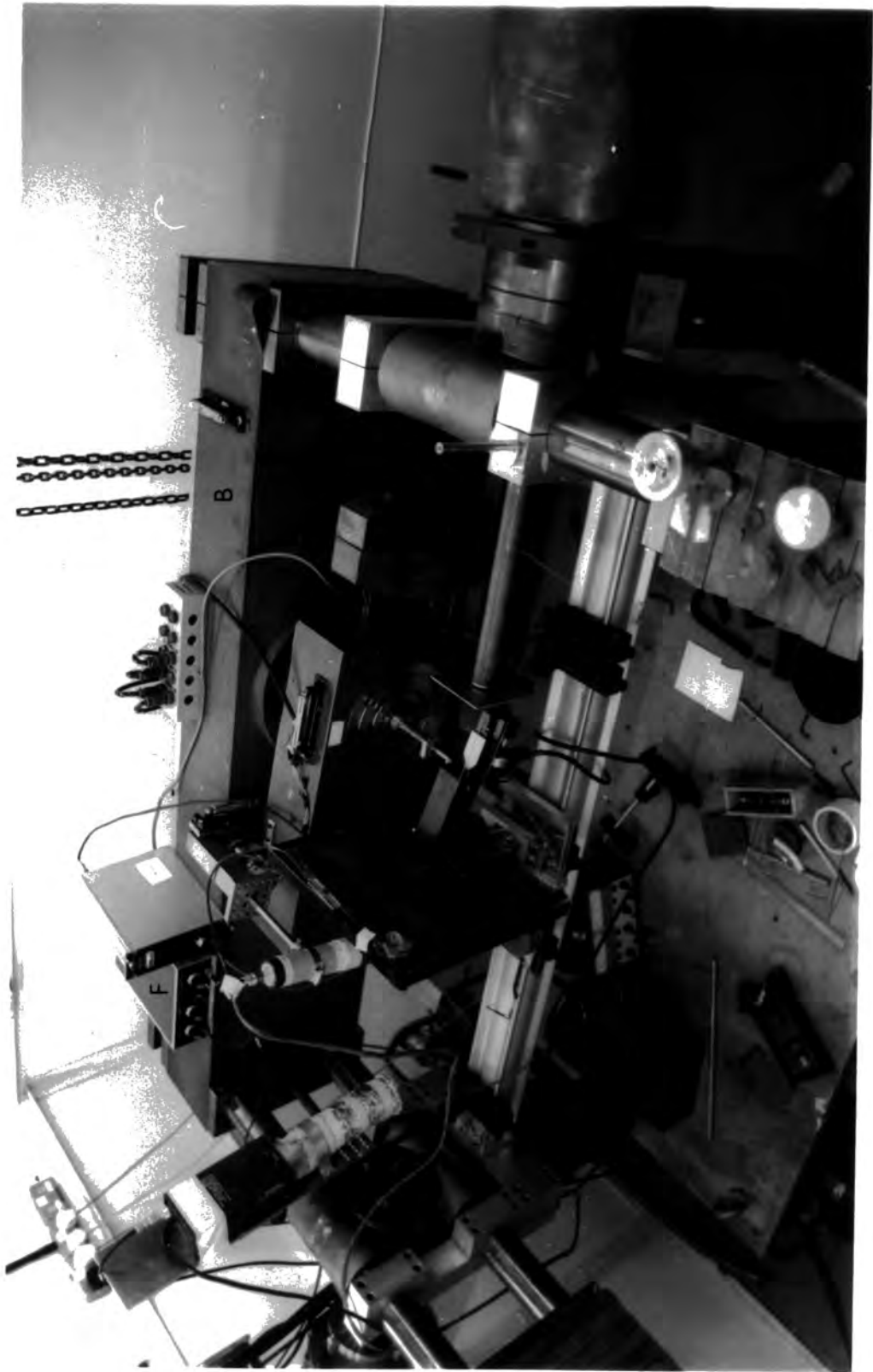


Fig. 4.5 Photograph of the 12 inch double crystal camera on the TOP2 station at the SRS, Daresbury Laboratory. The camera A, is mounted on a rotary table attached to a massive aluminium casting, B, which can be rotated about the x-ray beam. The black box monochromator, C, is shown as are the TV detector, D, and the scintillation detector, E. The H.T. supply and current amplifier, F, are used for the ionisation detector which is positioned behind the slits, G.

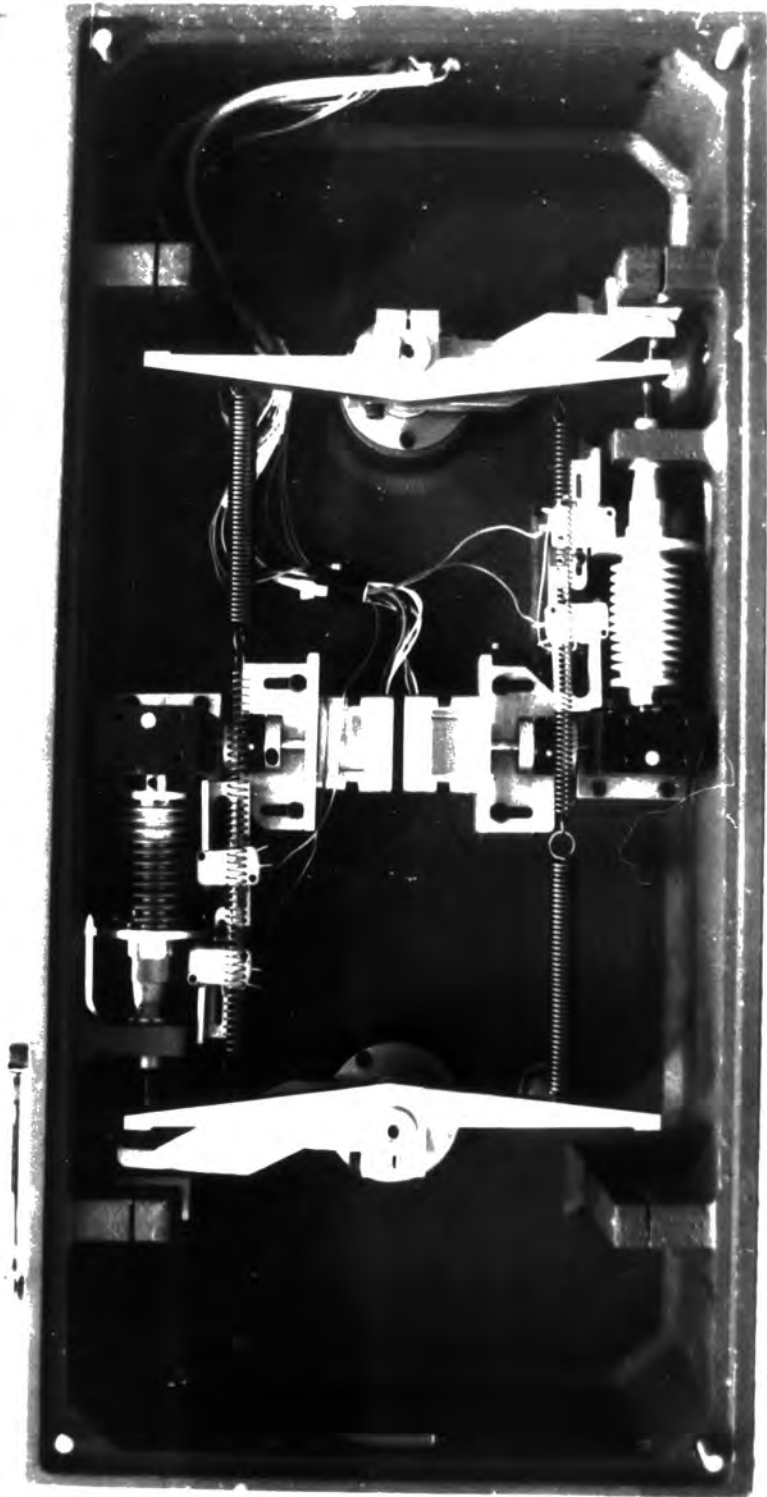


Fig. 4.6 Photograph of the 12 inch camera axial drives. The stepper motors, A, drive the tangent arm, B, via the gearbox and micrometer, C. A constant length micrometer is used.

The receive and transmit data lines plus the two hardware handshake lines CTS and RTS are converted to RS232 levels by 1488 and 1489 line drivers and receivers. Spare drivers on the 1488 are used to provide permanently asserted RTS, DCD and DSR signals.

The final circuit design, including the original ICC circuit, is shown in fig. 4.4.

#### 4.2 The Twelve Inch Camera at Daresbury

A photograph of the twelve inch camera, as installed in station 7.4 on the SRS, is shown in fig. 4.5. The micrometer/tangent arm drive system can be seen in fig. 4.6, which with 48 steps per revolution gives 0.20 arc seconds per motor step on both axes. The camera is mounted on a stepper motor driven rotary table, attached to a massive aluminium casting. This casting can be rotated around the horizontal X-ray beam to alter the polarisation state used for diffraction. With the camera vertical, ie the axes horizontal,  $\sigma$  polarisation is selected. As can be seen from fig. 4.5 the optical bench mounted between the casting pivots can be used to hold slits, shielding and TV detectors in position. The scintillation detector is mounted on the detector arm which is also stepper motor driven. Spirit levels are attached to the majority of the movable arms to enable easy alignment. The beam available is approximately 2 cm high and 12 cm wide and the source is about 60 m away. The photon flux as a function of energy as produced by the

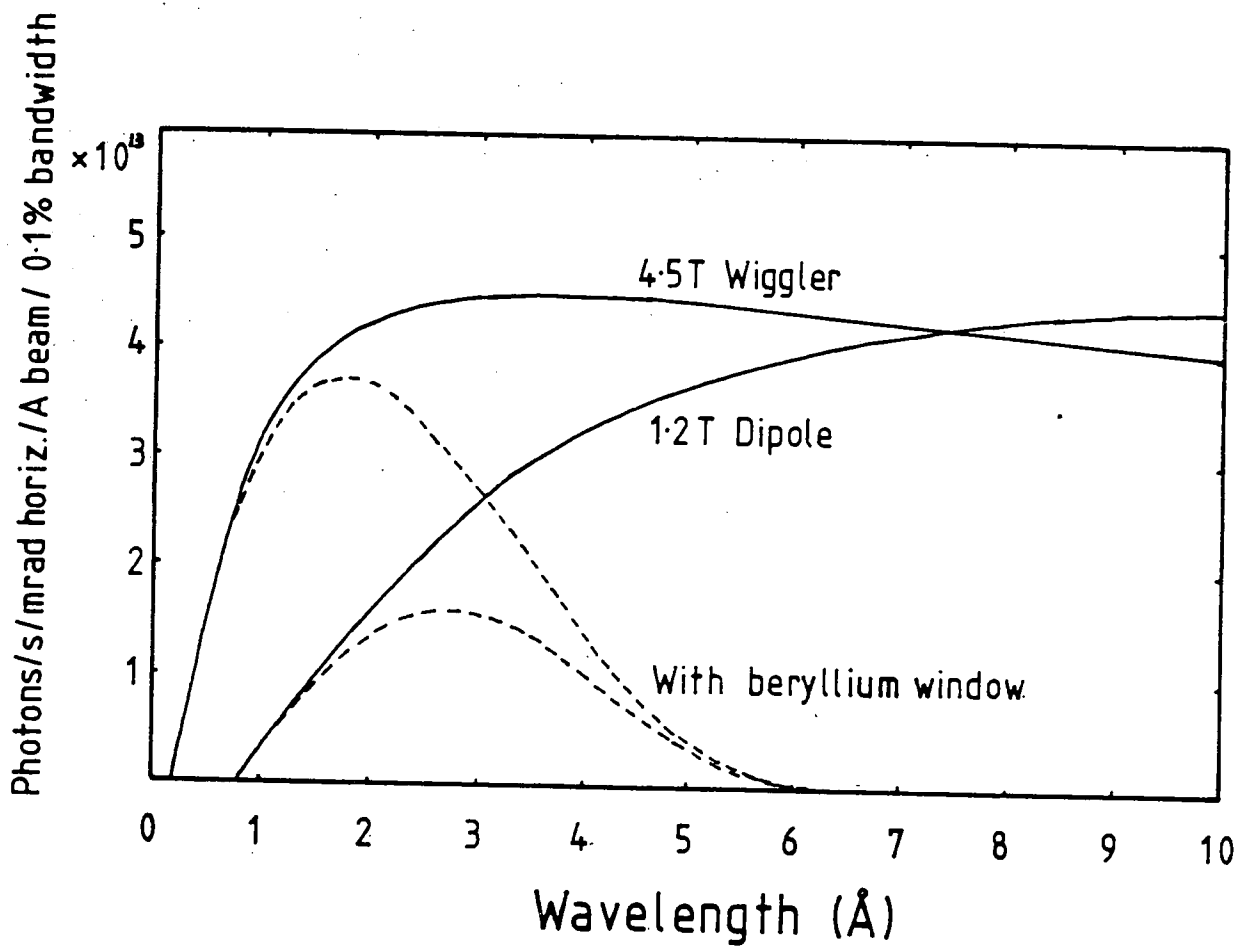


Fig. 4.7 The photon flux available at the SRS as a function of wavelength. The TOP2 station is on beam line 7 which is from a dipole magnet while the new TOP3 station is on the wiggler line. The dashed curves show the flux after passing through a beryllium window as on the TOP2 station.



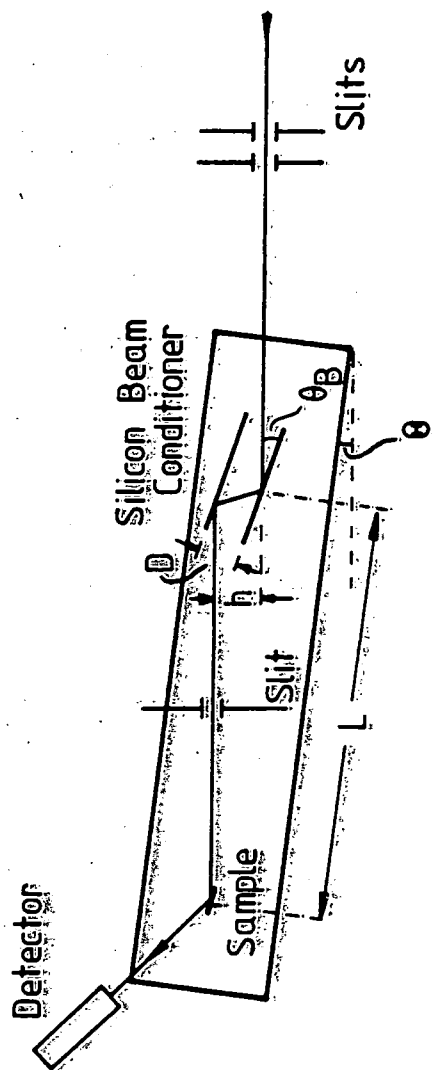


Fig. 4.8 The beam displacement which occurs when using the black box monochromator, giving an overall (+m,-m,+n) setting.

SRS is shown in fig. 4.7. This gives a minimum wavelength of about 0.6 Å while, since the station is an air station, the maximum useable at the camera is about 2.5 Å. Even if helium beam tubes were to be used the maximum wavelength is limited by the absorption of the beryllium window to approximately 5 Å.

A double reflecting 'black box' monochromator, consisting of two parallel Si (111) crystals mounted in an aluminium housing, is also available for use on this double crystal camera. The X-ray beam is doubly diffracted by two Si (111) reflections before being incident on the sample crystal. A diagram of the X-ray beam path is shown in fig. 4.8. The X-ray beam emerging from the monochromator is parallel to the incident beam, ie horizontal, but vertically displaced. Thus the camera has to be rotated in order to displace the second axis such that the beam passes through it. Since the Bragg angle of the silicon reflections is fairly small, of the order of 10 degrees for the wavelengths used, it does not change much with wavelength. The vertical displacement of the X-ray beam,  $h$ , is given by

$$h = 2 D \cos\theta_B, \quad (4.1)$$

where  $D$  is the crystal separation and  $\theta_B$  the Bragg angle. Hence, over the range of 0.5 Å to 2.0 Å this separation only changes by about 1 mm. Additionally, by rotating one of the silicon crystals with respect to the other suppression of harmonics is possible (Hart, 1980). A recent paper by Bonse

et al (1983) also outlines the design of some similar harmonic rejecting multi-reflection monochromators. Due to the low divergence of the X-ray beam on the SRS, approximately  $5 \times 10^{-6}$  radians for a 0.1mm entrance slit, the beam emerging from the monochromator is very nearly a plane wave. Consequently, a overall dispersive arrangement, ie (+n, -n, +m) as with a different sample reflection, can be successfully used without introducing any noticeable broadening of the rocking curve. Therefore, variable wavelength experiments can easily be performed since only the angle of the monochromator needs to be altered, any small change in the displacement of the X-ray beam being accounted for by adjusting the height of the entrance slits in front of the monochromator.

#### 4.2.1 Computer Control and Instrumentation

This camera is controlled by a PDP11/04 minicomputer and a CAMAC system, as are the majority of cameras at Daresbury. The CAMAC system is attached directly to the PDP11 UNIBUS and provides a wide variety of plug-in interface cards. A VT100 is used as the terminal. CAMAC cards control the stepper motors and floppy disc drives as well as providing the pulse counter and TV display driver. Initially, software to control the camera was written in Catex, a language similar to Basic but with additional commands to control the CAMAC system. A comprehensive manual control system was implemented, using a pocket

terminal as a keypad to select motors and speeds. Rocking curve collection routines, similar to those used on the six inch camera, were also added. Recently these programmes have been rewritten in Fortran by Daresbury Laboratory staff.

Rocking curves can be plotted on a HP7470A plotter and the data saved on a high capacity Winchester disc. An 8 inch floppy drive can also be used to save the data and transfer it to other computers. A standard PET 5¼ inch floppy drive was also interfaced to the PDP11 via a CAMAC IEEE488 interface card, allowing data to be saved on these discs and read into a Cifer 2684, with a similarly interfaced PET disc drive, for replotting in Durham. The Cifer also allowed this data to be transferred onto the University's mainframe computer.

X-ray intensity was measured with a Nuclear Enterprises scintillation detector with NIM based power supply, amplifier and discriminator. The pulses were counted with a CAMAC pulse counter with a pulse generator providing the necessary timing pulses.

#### 4.3 Aligning the Cameras and Recording Rocking Curves

The techniques for aligning both cameras are fairly similar, although at the SRS it is rather more straightforward due to the smooth, continuous wavelength spectrum.

#### 4.3.1 The Six Inch Camera

This camera is set in the zero position by adjusting it so that the X-ray beam passes through the centre of both axes. This is easily accomplished using the optical light source, but can be checked with X-rays using either a fluorescent screen or dental film. The camera is then rigidly secured to the table. For a particular reflection and wavelength the camera is then set at  $2\theta_B$  to the X-ray beam using the rotary table.

The first crystal is then mounted on the first goniometer and set near the Bragg angle. Again, the optical light source can be used if a surface symmetric reflection is being used with a highly polished crystal. With the detector mounted to look down the axis the angle of the first crystal is adjusted to obtain a maximum count rate. Even if the adjustment of the camera to  $2\theta_B$  is slightly out the wide aperture of the detector should ensure that the reflection is found. This process of finding the reflection can be greatly speeded up by rotating the goniometer with a length of wire. Dental film is then used to determine the position of the diffracted beam with respect to the second axis. If the beam does not pass through the axis the  $2\theta_B$  angle of the camera should be altered to bring it into line and the angle of the first crystal readjusted.

Recently Fewster (1985) has explained a similar method using Kevlar twine to pull the first goniometer. If the twine is then securely fixed the camera can be rotated

without altering the angle of the goniometer with respect to the incident beam. With a narrow slit positioned in front of the detector the camera angle can then easily be adjusted to the optimum position.

The second crystal is then mounted, ensuring that the X-ray beam will intercept the surface. With the crystal set near the appropriate Bragg angle the reflection can be found. A computer searching technique can be used or, for broad reflections, a wire pull technique similar to that used for the first crystal. For the majority of III-V crystal reflections with  $\text{CuK}\alpha_1$  radiation the latter technique can usually be used.

The tilt adjustment of the second crystal is then performed to provide the narrowest possible reflection. A suitable technique based on the change in angular position of the peak as a function of the tilt angle has been described by Fewster (1985).

Once all adjustments have been made the rocking curve can be recorded. As small a beam as possible should be used to reduce the effect of sample curvature and area variations in composition or thickness.

#### 4.3.2 The Twelve Inch Camera

Alignment with a two crystal (+-) arrangement is similar to that described for the six inch camera. Instead of altering the angle of the camera to ensure that the diffracted beam from the first crystal passes through the

second axis the angle of the first crystal alone can be altered. This will change the wavelength diffracted slightly. The angle of the crystals can be set relative to the horizontal X-ray beam with a variable angle set square mounted on the horizontal optical bench. The reflection from the second crystal is easily found with a simple TV imaging detector, consisting of a fluorescent screen mounted on the front of an image intensifier tube (an obsolete Mullard model) with the back screen viewed by a closed circuit TV camera. The peak is best found with a beam roughly the same size as the sample.

When aligning the camera with the black box monochromator, a slightly different technique is required. The angle,  $\theta$ , at which the camera should be set is given by

$$\sin\theta = 2 D \cos\theta_B / L, \quad (4.2)$$

where  $L$  is the axis separation and  $D$  the spacing of the crystals in the monochromator. The easiest alignment process is to initially set the camera horizontal using a precision spirit level. The camera is then rotated downwards from the horizontal by the angle  $\theta - \theta_B$  and the monochromator set horizontal, again using a spirit level. Rotating the camera then back to the required angle above the horizontal puts the monochromator at the required angle. Since the monochromator is not channel cut but consists of two separate crystals, they need to be aligned to allow the X-ray beam through. One of the crystals can be rotated by a

motorised screw or an electromagnet / magnet pair. The correct alignment can then be found by viewing the diffracted X-ray beam with either the TV detector or an ionisation detector. A pointer in the second axis can be used to ensure that the beam passes through this axis. The second crystal can then be mounted and the reflection found using a similar technique to that previously described with a normal (+-) arrangement.

We note that with the SRS the beam divergence is so small that the double crystal arrangement does not need to be adjusted for tilt, as with a conventional source. This greatly increases the speed at which rocking curves can be recorded and helps overcome the delays introduced in finding the reflections by not being able to rotate the crystals with the wire pull technique!



## CHAPTER 5

## SINGLE UNIFORM LAYERS

Rocking curves from single layers would be expected to be the easiest to interpret. It is straightforward to measure the perpendicular and parallel mismatches by measuring the layer and substrate peak separation using symmetric and asymmetric reflections. For a coherent layer/substrate interface, ie with no mismatch dislocations, and a surface symmetric reflection if the peak separation is  $\Delta\theta$  then, from the Bragg equation, we obtain

$$\frac{\Delta d}{d} = \Delta\theta \cot\theta_B \quad (5.1)$$

where  $d$  is the lattice spacing of the substrate and  $\Delta\theta = (\theta_S - \theta_L)$ . The relaxed lattice mismatch is then found using equation (1.34) which gives the composition according to Vegard's Law (see section 1.4). Any angle,  $\Delta\phi$ , between the 001 planes of the layer and substrate can be measured by reversing the X-ray path and recording two rocking curves. From the two peak separations,  $\Delta\theta_1$  and  $\Delta\theta_2$  we find that

$$\frac{\Delta d}{d} = \frac{1}{2}(\Delta\theta_1 + \Delta\theta_2) \cot\theta_B \quad (5.2)$$

$$\Delta\phi = \frac{1}{2}(\Delta\theta_1 - \Delta\theta_2) \quad (5.3)$$

If asymmetric reflections are used an additional peak separation will be introduced due to the difference in the angle between the reflection plane and surface for the layer and substrate. If  $\phi_L$  and  $\phi_S$  are these angles for the layer

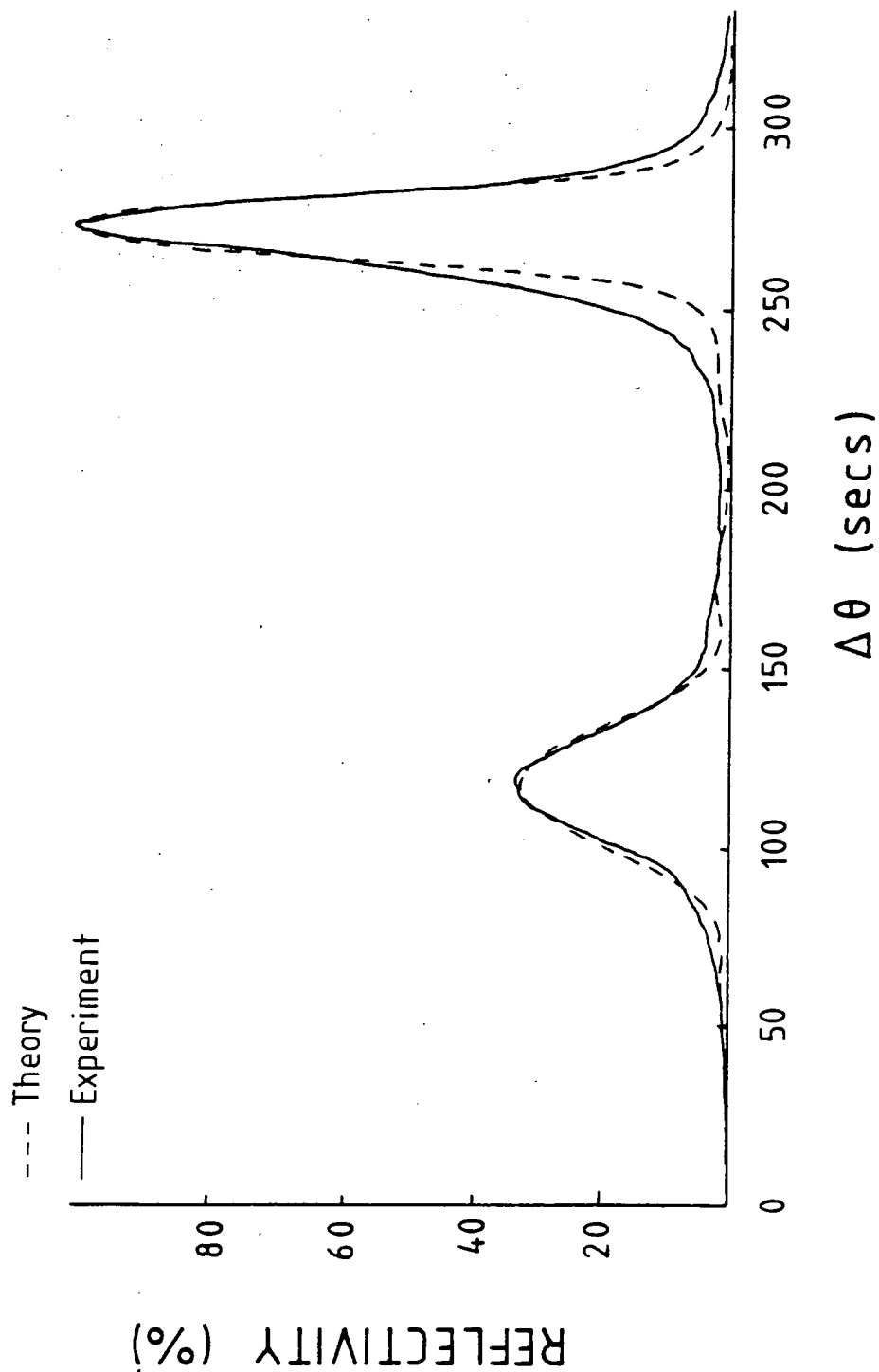


Fig. 5.1 Experimental and computed 004 rocking curves from a 650 ppm mismatched,  $\lambda = 1.3\mu\text{m}$  GaInAsP sample. The solid curve is the experimental curve and the dashed curve the theoretical best fit curve.  $\text{CuK}\alpha_1$  radiation was used and the layer thickness is  $0.45\mu\text{m}$ .

and substrate respectively then when the angle of incidence is  $(\theta - \varphi)$  the peak separation is  $(\theta_S - \theta_L - \varphi_S + \varphi_L)$  and when the angle of incidence is  $(\theta + \varphi)$  it is  $(\theta_S - \theta_L + \varphi_S - \varphi_L)$ .

However, the layer thickness cannot be determined from these measurements. It can be determined by comparing the experimental rocking curve with computed curves for various layer thicknesses, assuming the lattice mismatch already calculated.

### 5.1 Surface symmetric reflections

Fig. 5.1 shows the experimental 004 rocking curve with  $\text{CuK}\alpha_1$  radiation for a sample with a single quaternary layer, with a band gap corresponding to radiation of wavelength  $1.3 \mu\text{m}$ . The substrate is, as usual, 001 InP. The mismatch is determined to be 650 ppm from the separation of the peaks, giving the layer composition as  $\text{Ga}_{0.27}\text{In}_{0.73}\text{As}_{0.61}\text{P}_{0.39}$ . We note that the substrate peak is considerably broader than the theoretical width, indicating that the sample is curved. The amount of broadening provides a measure of the curvature. The calculated curve that best fits this experimental curve is also shown in fig. 5.1, with a layer thickness of  $0.45 \mu\text{m}$ . Agreement between the curves is fairly good, although the tails of the substrate peak are slightly broader than in the calculated curve. The weak Bragg case Pendellosung fringes seen in the computed curve are not visible in the experimental curve. Clearly, the presence of threading dislocations, in the layer, introducing a local lattice curvature, will blurr out this

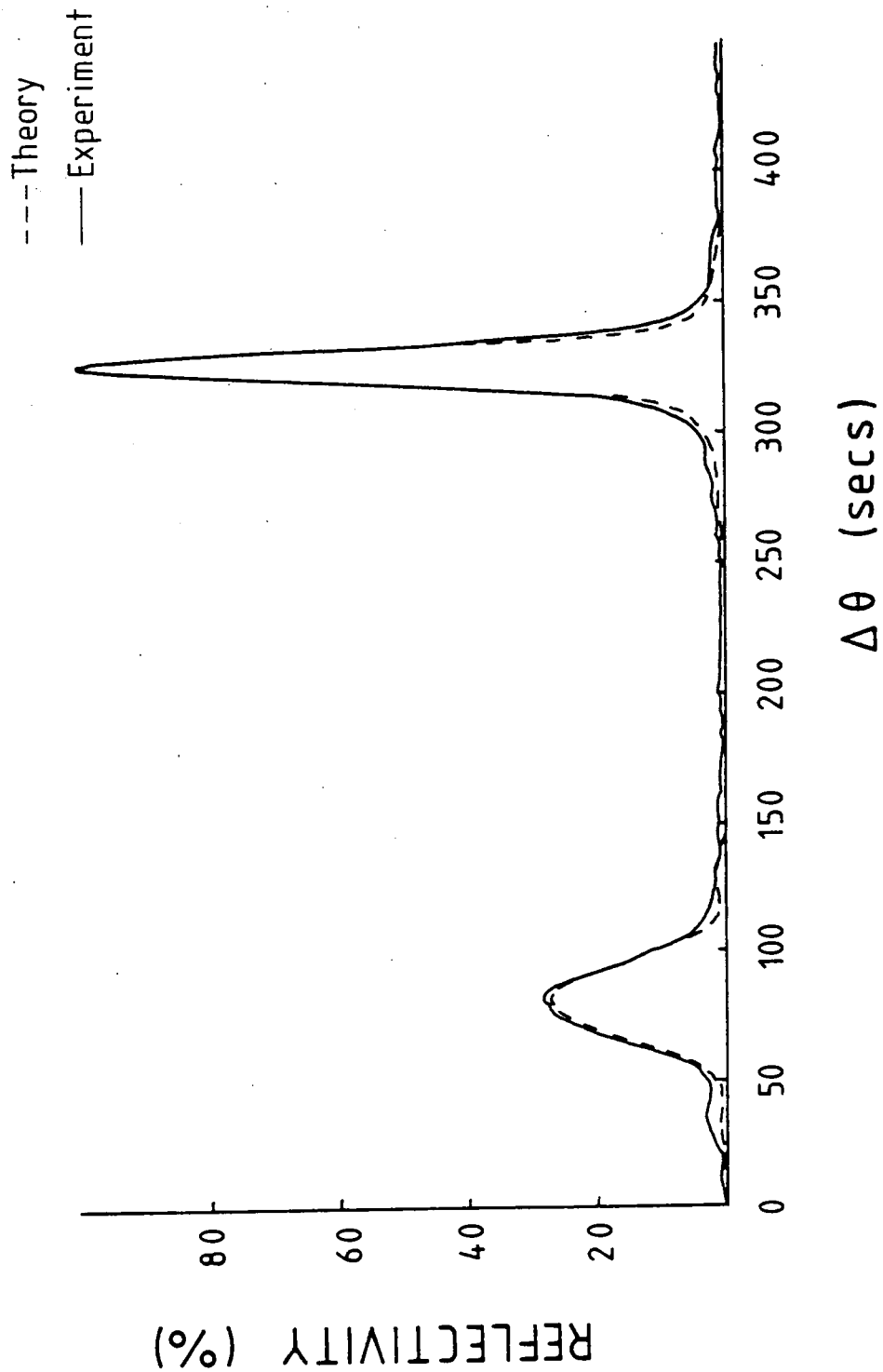


Fig. 5.2 Experimental and theoretical 004 rocking curves from a 960 ppm mismatched GaInAs sample.  $\text{CuK}\alpha_1$  radiation was used and the solid curve is the experimental rocking curve. The layer thickness is  $0.55 \mu\text{m}$ .

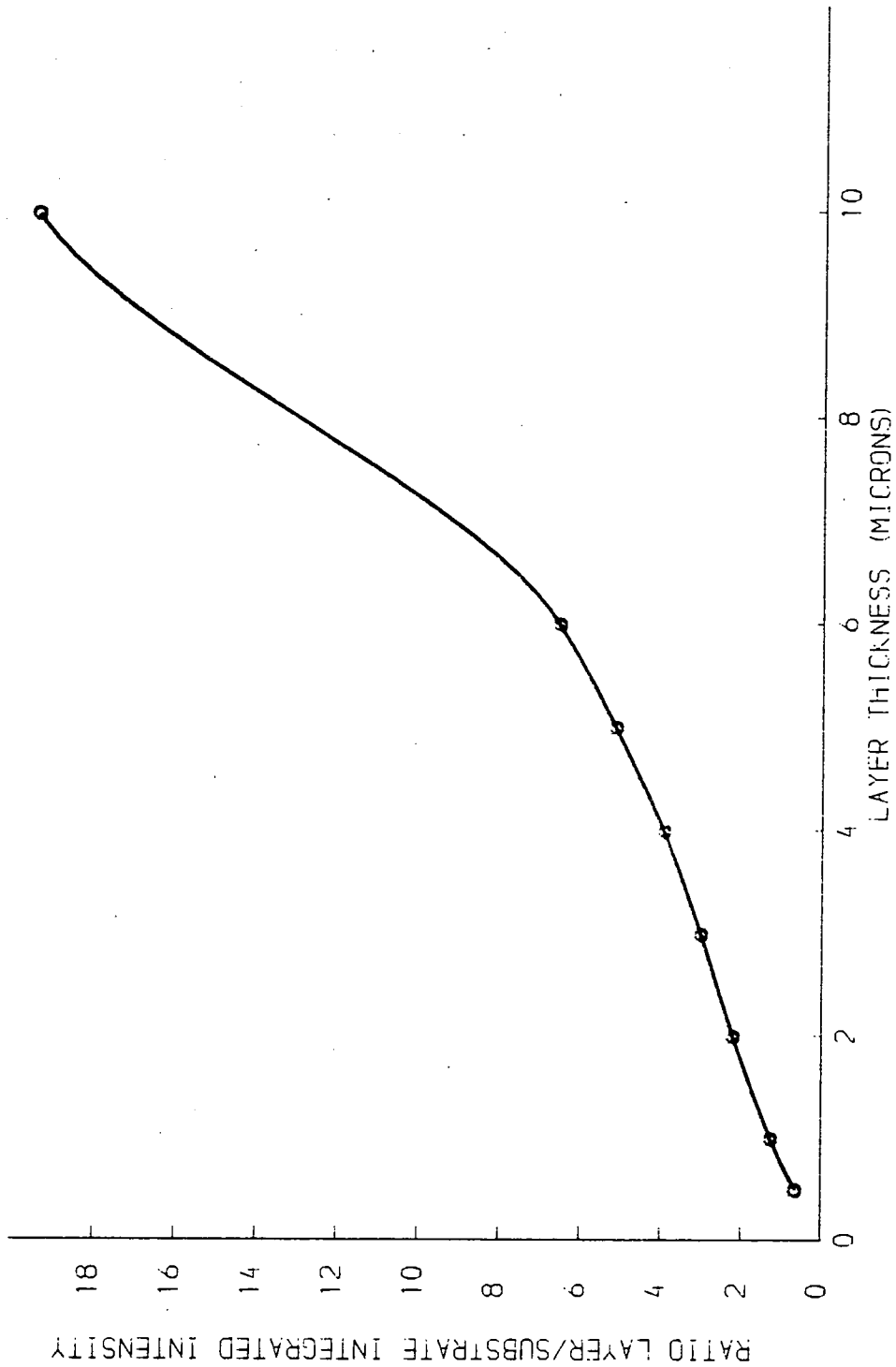


Fig. 5.3 The ratio of integrated intensities from the layer and substrate as a function of layer thickness 004 refl. This curve is for  $\text{CuK}\alpha_1$  radiation and a GaInAs layer of 600 ppm mismatch.

weak structure. Measurement of the rocking curve with the X-ray path reversed showed that there was no tilt angle between the 001 planes of the layer and substrate.

A similar example is shown in fig. 5.2, for another ternary layer. The relaxed lattice mismatch is determined to be 960 ppm, giving  $\text{Ga}_{0.45}\text{In}_{0.55}\text{As}$ , and the computed curve for a 0.55  $\mu\text{m}$  layer thickness is also shown in fig. 5.2. The half width of the substrate peak is nearer the theoretical value than in the previous example. Agreement between the computed and experimental curves is extremely good, being slightly better than the fit in the previous example.

Instead of calculating a number of rocking curves for each sample in order to determine the layer thickness the ratio of integrated intensities of the layer and substrate peaks can be used, provided that the peaks do not overlap. The ratio of peak heights could also be used but these are affected by the sample curvature, as shown in chapter 1. A graph of the ratio of integrated intensities as a function of the layer thickness is shown in fig. 5.3, for the 004 reflection with  $\text{CuK}\alpha_1$  radiation and these values are also given in Table 5.1. These values were calculated for a  $\text{GaInAs}$  ternary layer of 600 ppm mismatch but, due to the very small effect that changing the composition has on the structure factors this curve can be used for any mismatch. Further, since the structure factors for quaternary  $\text{GaInAsP}$  alloys are only slightly different from those of the ternary

GaInAs this curve can also be used for these types of layers without introducing any large errors.

TABLE 5.1

Values of the ratio of integrated intensities of the layer and substrate peaks for a 600 ppm mismatched GaInAs layer as a function of layer thickness.

Layer Thickness ( $\mu\text{m}$ )	Ratio of layer/substrate integrated intensity ( $\pm 0.05$ )
0.5	0.6
1.0	1.3
2.0	2.2
3.0	3.0
4.0	3.9
5.0	5.1
6.0	6.5
7.0	9.4
8.0	13.1
9.0	17.1
10.0	19.4

If the layer is only slightly mismatched from the substrate the peaks will begin to overlap. Their separation can be increased by either increasing the wavelength or narrowing the peaks. Increasing the wavelength will alter the peak separation according to the Bragg equation but will also increase the half width of the peaks. Additionally, due to the increased absorption within the layer the thickness of crystal sampled will be reduced. Alternatively, reducing the wavelength will produce the opposite effect but, due to the reduced Bragg angle, the effect of sample curvature will be increased since the X-ray beam will intercept a larger area of the sample. Fig. 5.4

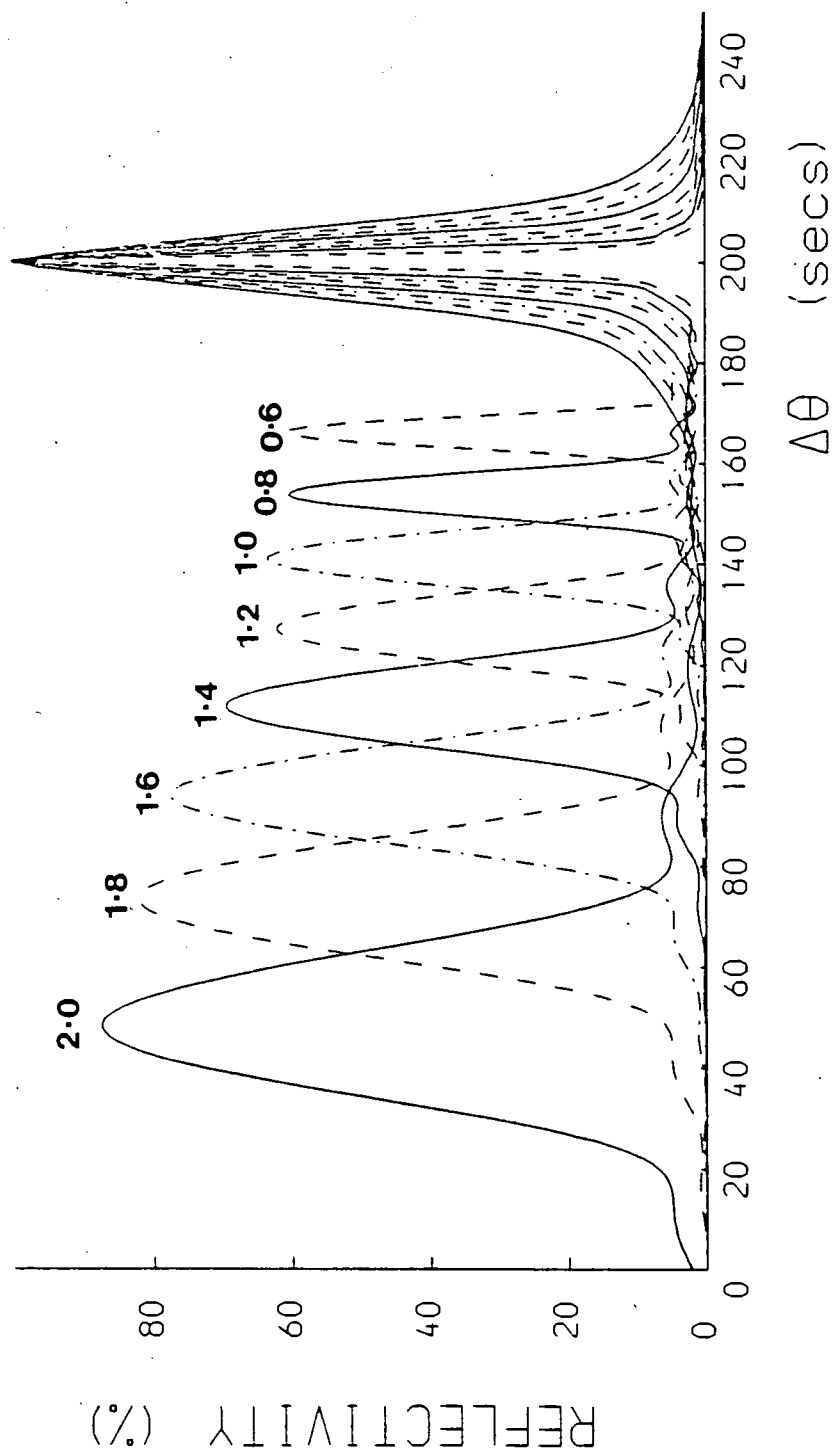
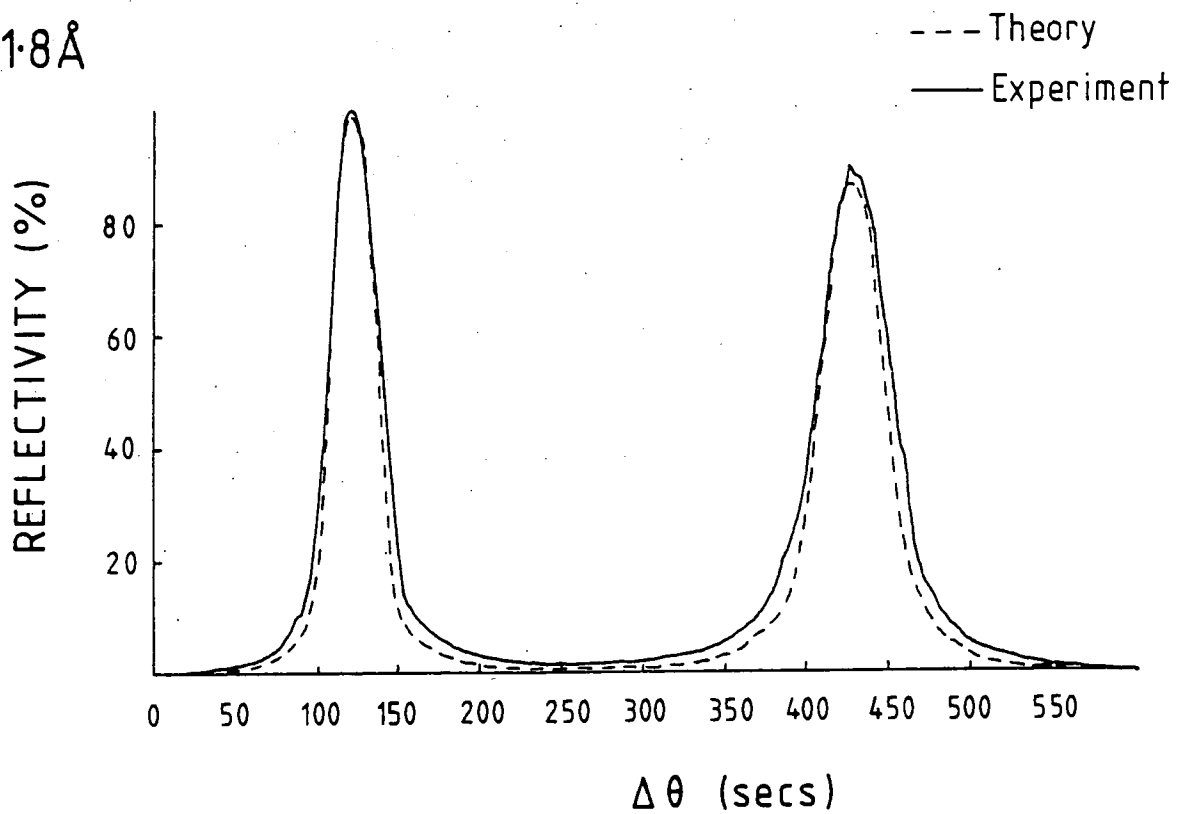


Fig. 5.4 004 Theoretical Rocking curves from a 400 ppm, mismatched, 1 $\mu$ m thick GaInAs layer as a function of wavelength.



1.8 Å



1.5 Å

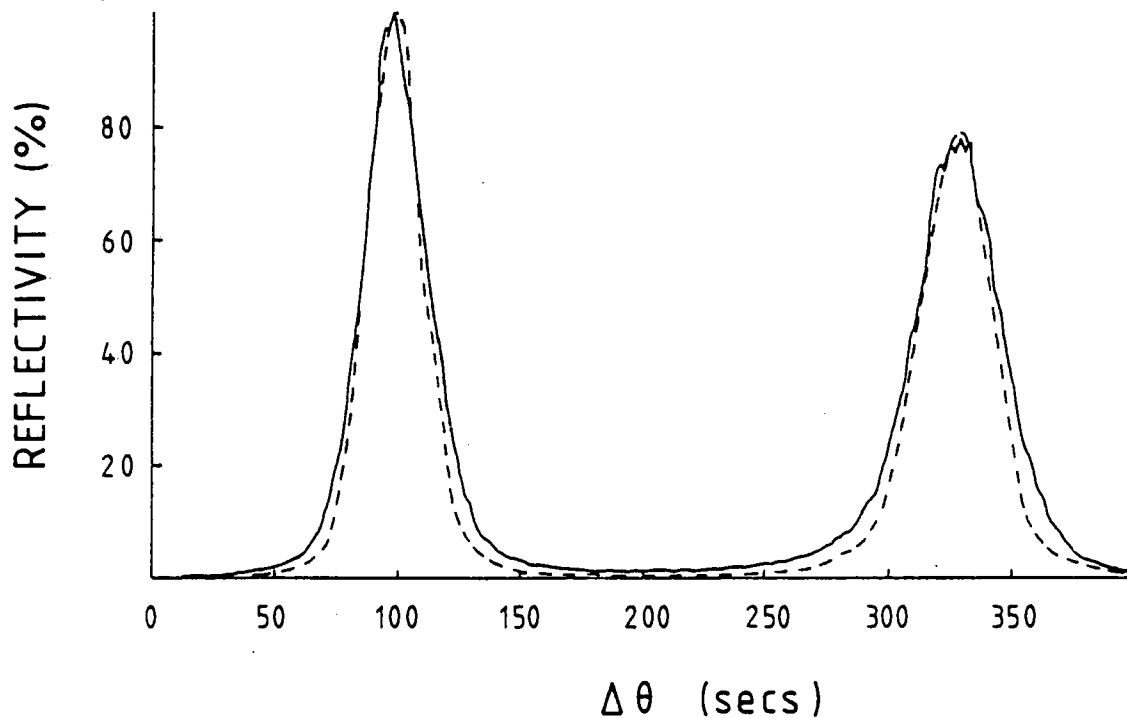
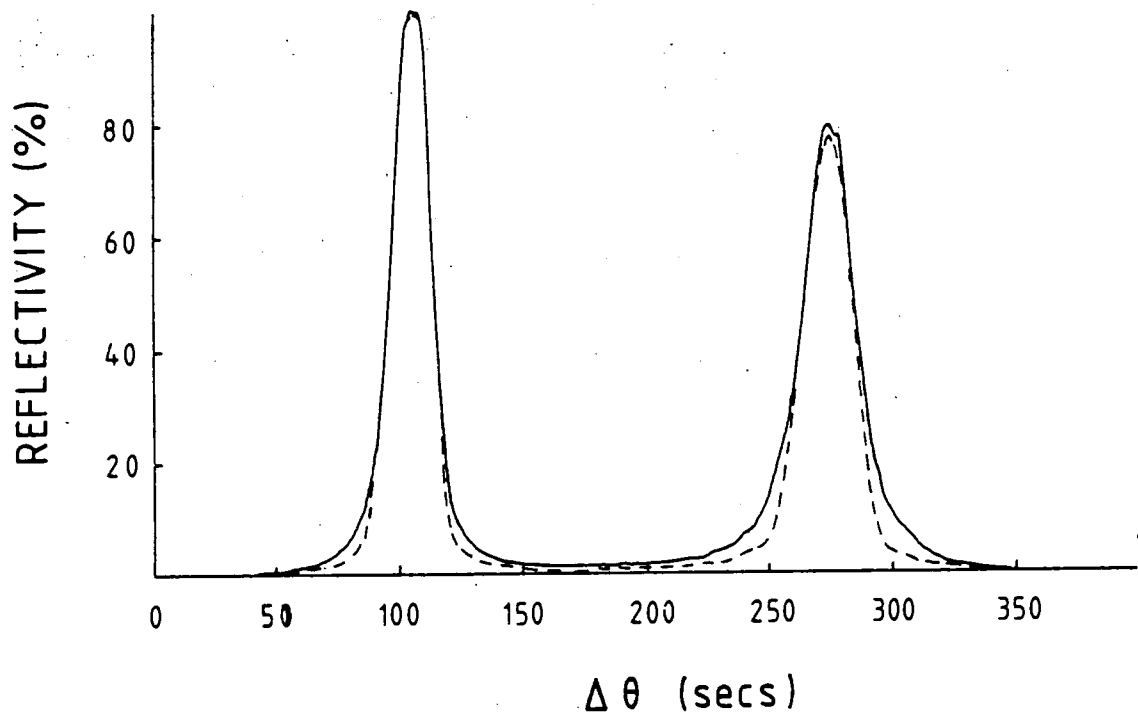
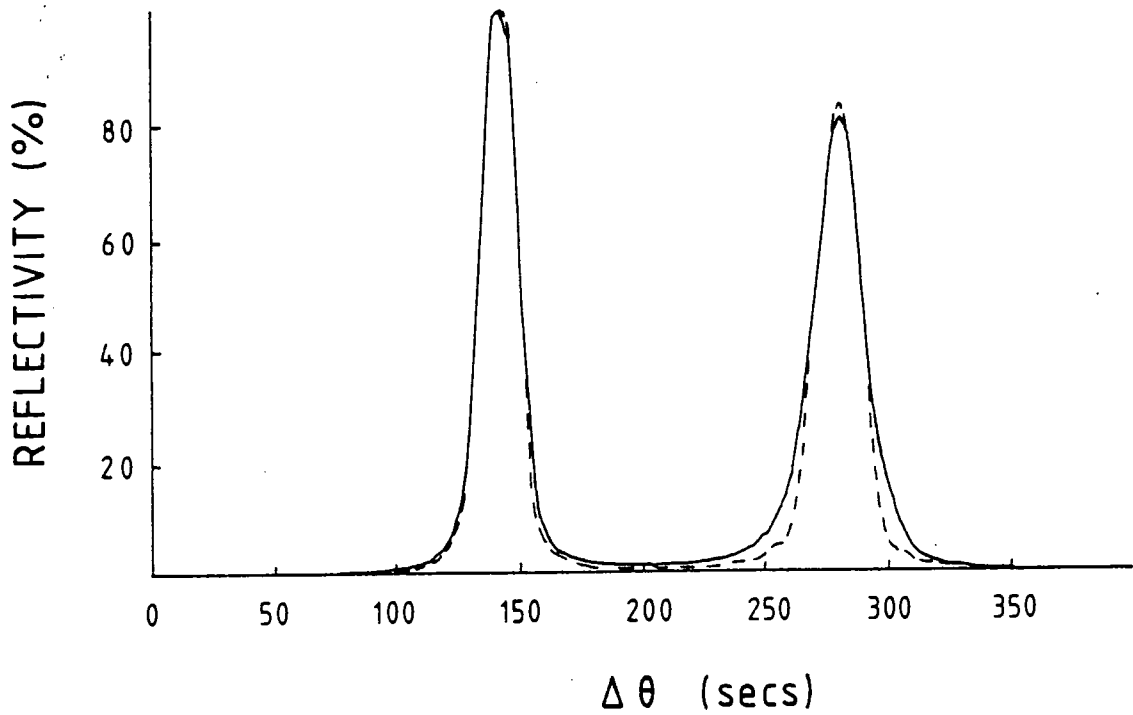


Fig. 5.5 Experimental and calculated 004 rocking curves from a 950 ppm mismatched 0.90  $\mu\text{m}$  thick layer at four wavelengths. The layer material is GaInAsP with  $\lambda = 1.55 \mu\text{m}$ .

1.2 Å



1.0 Å



shows the effect of altering the wavelength on the 004 rocking curve calculated for a 1  $\mu\text{m}$ , 400 ppm mismatch ternary layer.

Since the X-ray parameters used in the calculation change as a function of the wavelength we need to check that the curve calculated as the best fit to the experimental curve at one wavelength still agrees with the experimental curve when the wavelength is altered. This will check that all the variable wavelength parameters, such as the dispersion corrections to the structure factors, are calculated correctly. Fig. 5.5 shows a series of experimental rocking curves for a  $\lambda=1.55 \mu\text{m}$  GaInAsP layer at 1.0, 1.2, 1.5 and 1.8  $\text{\AA}$ . These rocking curves were recorded using the double crystal camera at Daresbury in conjunction with the double reflecting monochromator. The wavelength can then be easily altered without needing to adjust the angle of the camera. From the rocking curve at 1.5  $\text{\AA}$  the mismatch was calculated to be -950 ppm, corresponding to  $\text{Ga}_{0.43}\text{In}_{0.57}\text{As}_{0.89}\text{P}_{0.11}$ , and the best fit computed curve, also shown in fig. 5.5, was found for a 0.8  $\mu\text{m}$  layer thickness. Theoretical curves at the other wavelengths are also shown in fig. 5.5 for comparison with the experimental curves. There is good agreement between these curves at all the wavelengths used, both in the angular separation, peak widths and heights. This confirms that using just one rocking curve at one wavelength gives a layer thickness that is consistent with curves recorded at other wavelengths.

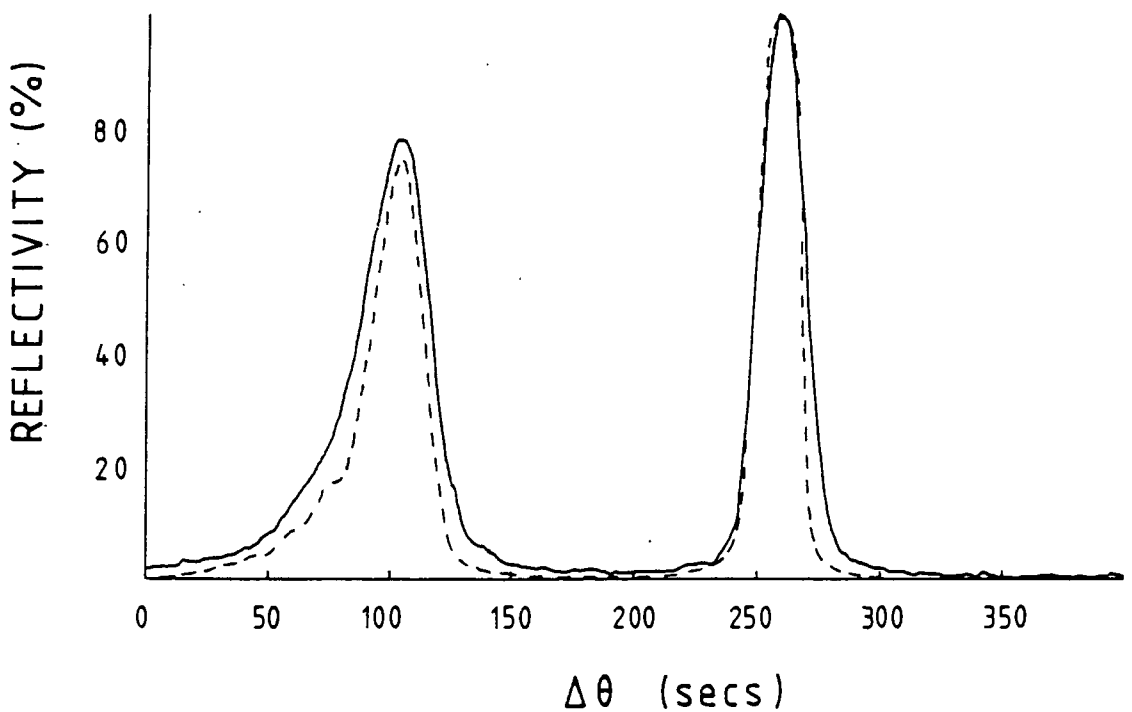
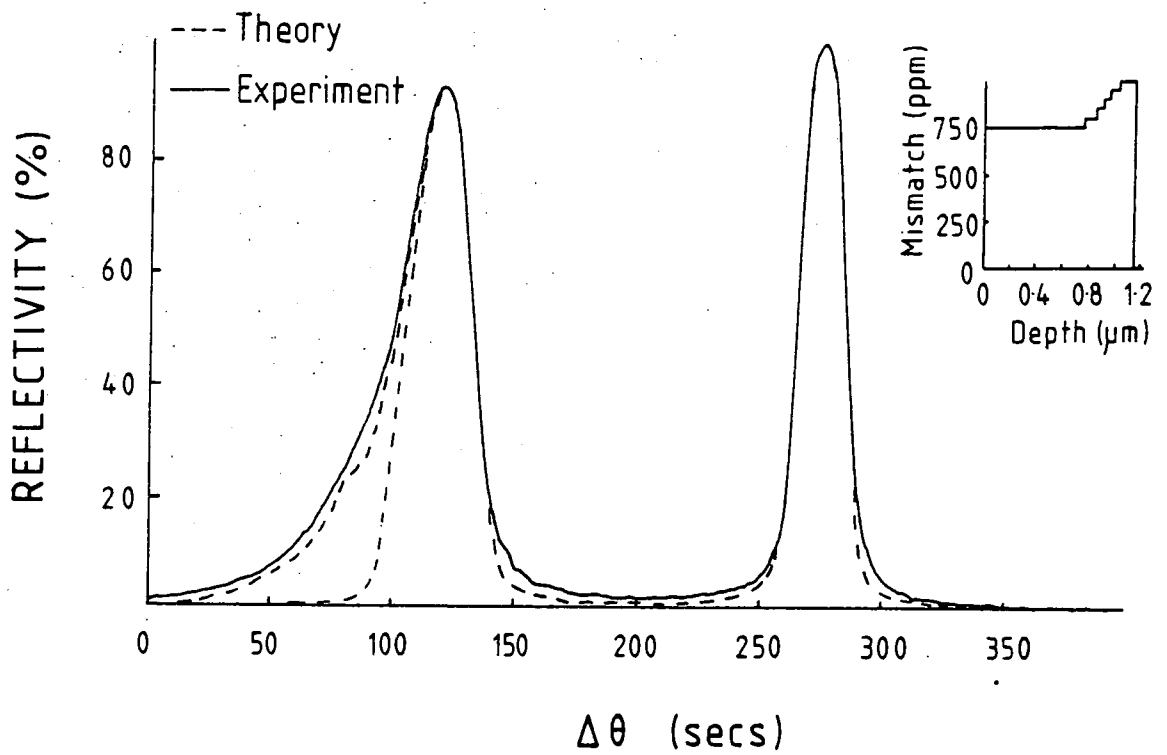


Fig. 5.6 (a) Theoretical and experimental 004 rocking curves from a 750 ppm mismatched, 1.15- $\mu\text{m}$  thick GaInAs layer. Two computed curves are shown, one for a 0.9  $\mu\text{m}$  uniform layer and one from a 1.15  $\mu\text{m}$  thick layer with a region near the interface of larger mismatch, as shown on the inset. The wavelength used was 1.3  $\text{\AA}$  with  $\sigma$  polarisation.

(b) The computed and experimental rocking curves from the same sample at the same wavelength but with the double crystal camera rotated to give  $\pi$  polarisation.

Since only surface symmetric reflections have been used no measure of the interface coherency can be obtained. However, for the majority of samples studied mismatch dislocations could not be observed using Lang topography, hence the parallel mismatch must be zero and the interface coherent. Dislocations are often observed but these are usually threading dislocations existing in both the substrate and layers and are not formed due to layer mismatch. Consequently, the use of a single 004 reflection is a perfectly valid means of measuring the layer composition.

Since with a conventional laboratory generator randomly polarised radiation is produced in the characteristic lines any calculated rocking curves should include the contribution to the rocking curve from the  $\pi$  component as well as from the  $\sigma$  component. This effect is included in the calculation by adding the rocking curves for each polarisation state, according to equation (2.17). The contribution due to the  $\pi$  component can be examined experimentally by using the double crystal camera at the SRS with the diffraction plane rotated through  $90^\circ$  to the horizontal. This setting corresponds to  $\pi$  polarisation for an X-ray beam lying exactly in the plane of the electron orbit.

Fig. 5.6(a) shows the 004 rocking curve at  $1.3 \text{ \AA}$  for a sample with a single GaInAs layer with  $\sigma$  polarisation. The separation of the substrate and layer peaks gives the

mismatch as 750 ppm. The computed curve for a layer thickness of 0.9  $\mu\text{m}$  is also shown in fig. 5.6(a), but does not agree particularly well with the layer peak which is considerably asymmetric with an intense tail on the low angle side. This would suggest that a region of slightly larger lattice parameter was present within the layer and fig. 5.6(a) also shows the computed curve for a layer where a narrow region of larger lattice parameter is included next to the layer/substrate interface, with a total layer thickness of 1.15  $\mu\text{m}$ . The relaxed lattice mismatch as a function of depth is shown in the inset in fig. 5.6(a), corresponding to a range of Indium content from 51.6% at the interface to 52.0% at the surface. It is not unexpected that such a region could exist near to the interface as many similar observations have been reported (see Chapter 2). The agreement between the computed curve and the experimental curve is now considerably improved, with the asymmetric peak being extremely well simulated by the calculated curve.

The double crystal camera was then rotated towards the horizontal,  $\pi$  polarisation position, in 15° steps with the rocking curve being recorded at each stage. Initially, with the black box monochromator the only effect observable was a considerable broadening of the peaks due to the increased dispersion present from the wide X-ray source. The experiment was then repeated with a good quality InP crystal as the first crystal giving an exactly parallel (+--)

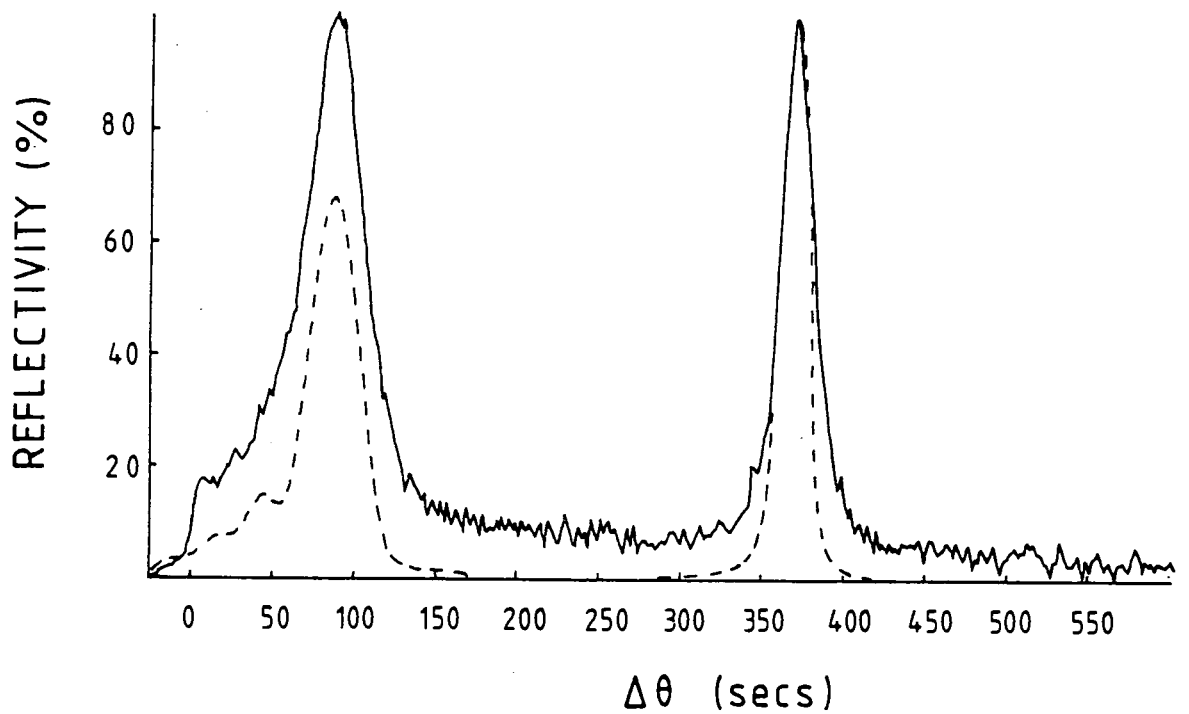
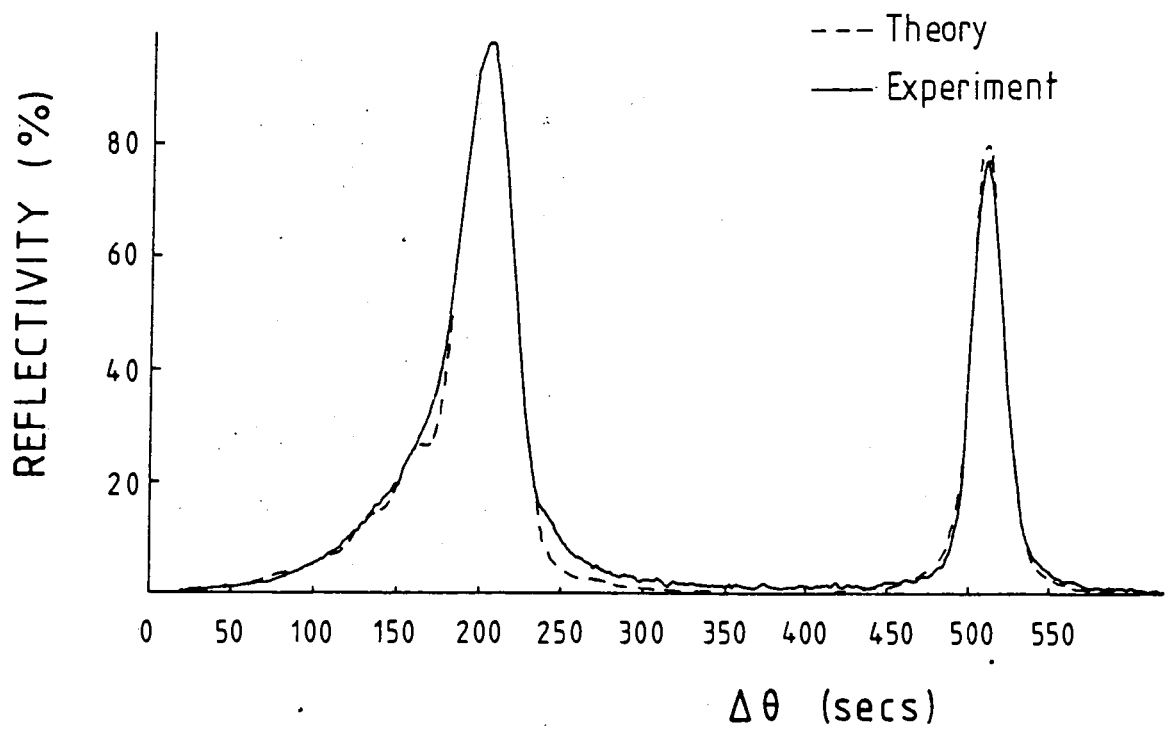


Fig. 5.7 (a) Rocking curves from the same sample used in fig. 5.6 but at 2.0 Å and  $\sigma$  polarisation. The composition used to give the calculated curve is that shown in the inset in fig. 5.6(a).

(b) Computed and experimental curves at the same wavelength but with  $\pi$  polarisation.

arrangement. Although the peaks no longer increased in width little other effects could be observed until complete  $\pi$  polarisation was selected. This rocking curve is shown in fig. 5.6(b). We would expect this result as the diffracted intensity with  $\pi$  polarisation will be smaller than that with  $\sigma$  polarisation thus the  $\sigma$  component will dominate the rocking curve until complete  $\pi$  polarisation is selected. Since the extinction length should be longer with  $\pi$  polarisation the diffracted intensity from the layer would be expected to be smaller than with  $\sigma$  polarisation. Additionally, the half width of the peaks should also be reduced. However, when the effect of sample curvature is included in the calculation of the rocking curve both of these effects are reduced. The experimental rocking curve does show a small reduction in the height of the layer peak, but no change in the peak half widths can be observed. The computed rocking curve, also shown in fig. 5.6(b) does agree fairly well with this experimental curve, although the calculated layer peak is slightly narrower and less intense. Clearly, any part of the X-ray beam lying slightly out of the plane of the electron orbit will not be completely polarised and can provide some  $\sigma$  polarisation contribution to the rocking curve.

This experiment was then repeated at  $2.0 \text{ \AA}$ , giving a Bragg angle of  $43^\circ$ , where the polarisation factor  $C$  is much more significant than at  $1.3 \text{ \AA}$ . The  $\sigma$  polarisation rocking curve is shown in fig. 5.7(a) along with the computed curve



assuming the composition and thickness already determined. Agreement between the curves is again particularly good. We note that the substrate peak is narrower than at  $1.3 \text{ \AA}$  due to the decreased effect of sample curvature at this higher Bragg angle. Fig. 5.7(b) shows the  $\pi$  polarisation rocking curve plus the computed curve. There is rather more discrepancy between these two rocking curves, with the computed curve showing a much less intense layer peak, although the shapes agree fairly well. Due to the very low diffracted intensity the background of the experimental curve is very noisy. Clearly, when the polarisation term is so significant and the diffracted intensity so low any very weak  $\sigma$  polarisation contribution will have a marked effect on the rocking curve. It should be noted that similar experiments, as reported by Bonse, Krasnicki and Teworte (1983), are not straightforward. In their case an additional monochromator crystal was used, with a near  $45^\circ$  Bragg angle, to reduce the amount of the  $\sigma$  component present in the beam.

## 5.2 The Use of Highly Asymmetric Reflections to Study Thin Layers

For very thin layers, less than  $0.5 \text{ \mu m}$ , the diffracted intensity from the layer, using the 004 reflection, becomes very small compared to that from the substrate. Additionally, the half width of the layer peak is greatly increased when low angles of incidence are used. Typically, the extinction distance for the 004 reflection is of the

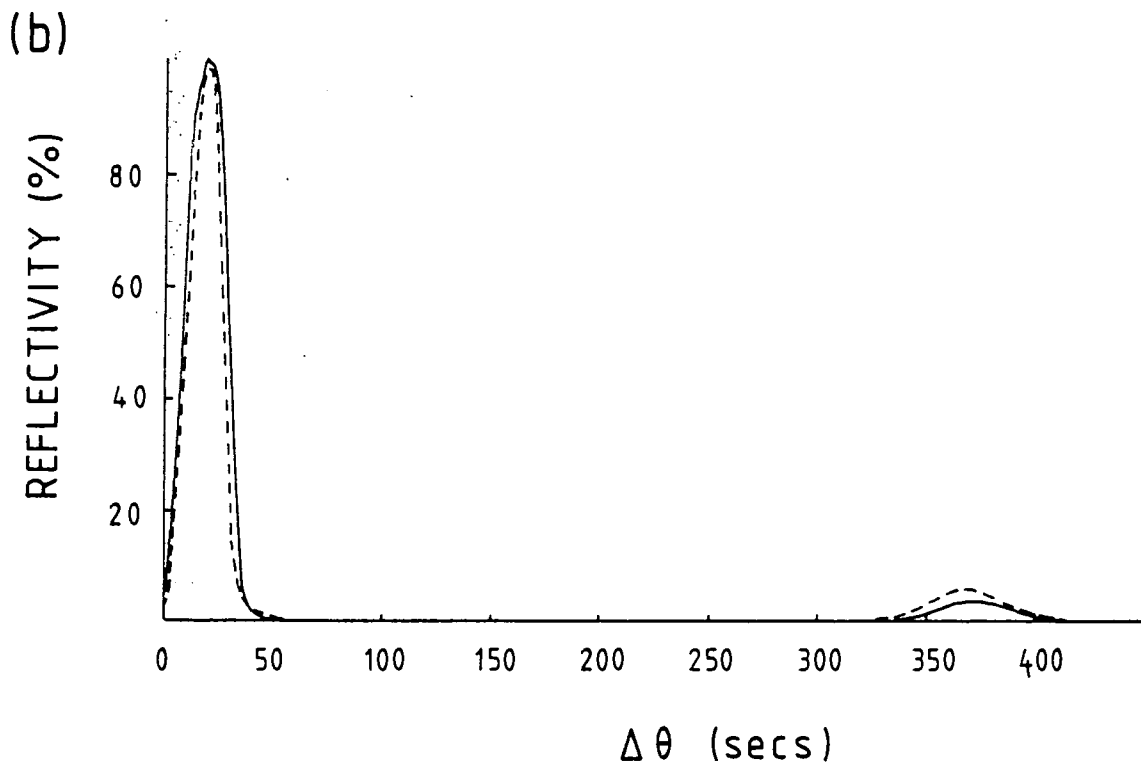
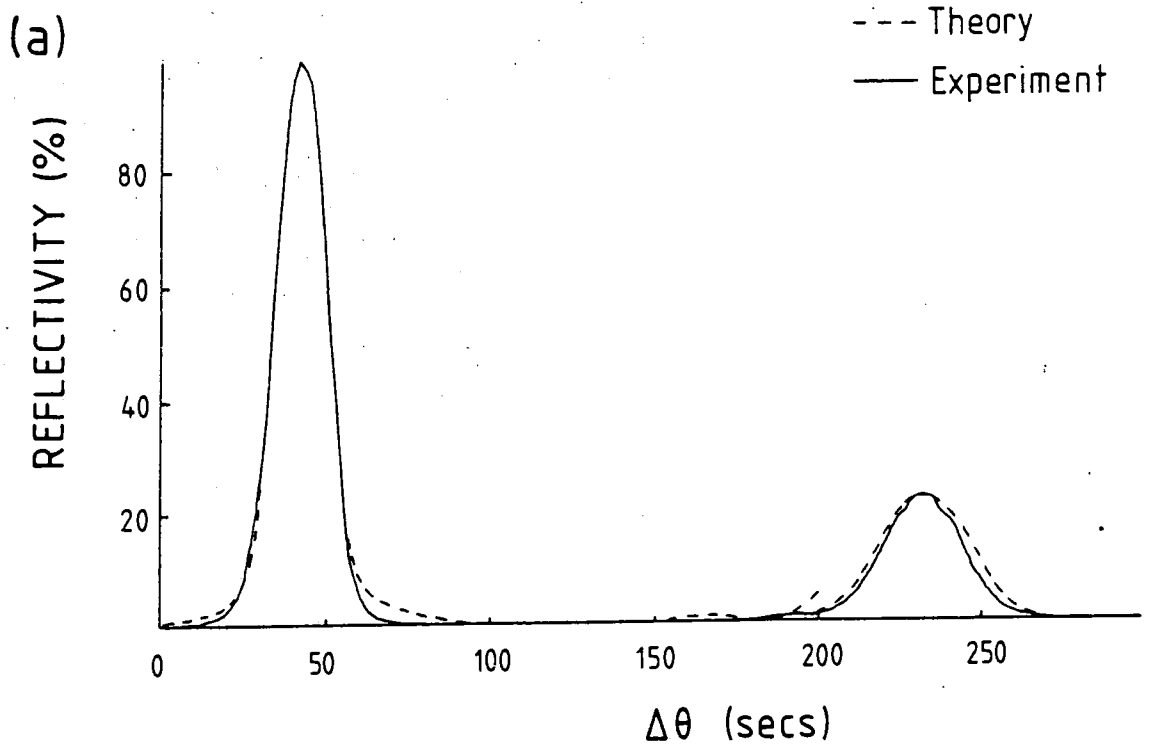


Fig. 5.8 (a) Experimental and computed 004 rocking curves from a  $0.3 \mu\text{m}$ ,  $\lambda = 1.31 \mu\text{m}$ ,  $-780 \text{ ppm}$  mismatched GaInAsP/InP sample. The wavelength is  $1.5 \text{ \AA}$  and  $\sigma$  polarisation from the SRS.

(b) The 115 rocking curves from the same sample and with the same experimental conditions.

order of 10  $\mu\text{m}$ , which is large compared to such layer thicknesses. However, by using a highly asymmetric reflection the extinction distance can be greatly reduced due to the factor  $(\gamma_0|\gamma_h|)^{\frac{1}{2}}$ . Specifically, by reducing the incident or exit angle to below  $5^\circ$  the factor  $\sin(\theta-\phi)$  will ensure that the extinction distance approaches zero. The diffracted intensity from the layer should then be dramatically increased.

A series of rocking curves were recorded for a  $\sim 0.4 \mu\text{m}$ ,  $\lambda=1.31 \mu\text{m}$  GaInAsP layer, grown on an InP substrate, as a function of wavelength for several reflections using the Daresbury double crystal camera. Fig. 5.8(a) shows the 004 rocking curve at 1.5  $\text{\AA}$ , with the double reflecting monochromator as the 'first' crystal. From the peak separation the mismatch is determined as -780 ppm, giving the layer composition as  $\text{Ga}_{0.30}\text{In}_{0.70}\text{As}_{0.62}\text{P}_{0.38}$  and the computed rocking curve for a 0.3  $\mu\text{m}$  thick layer is shown also shown in fig. 5.8(a) for comparison. The two curves again agree extremely well although, as expected, the diffracted intensity from the layer is only approximately 20% of the intensity of the substrate peak.

The 115 rocking curve was also measured at 1.5  $\text{\AA}$  and is shown in fig. 5.8(b). The diffracted intensity from the layer is less than that for the 004 reflection, at approximately 5% of the substrate peak intensity. This is expected since the 115 structure factors are smaller than those for the 004 reflection, giving a larger extinction



distance, and the asymmetry factors are not yet important since  $\theta-\phi$  is still  $25.8^\circ$ . The theoretical curve is also shown in fig. 5.8(b) and again agrees well with the experimental curve. Since the positions of the peaks are in good agreement the parallel mismatch must be negligible. Clearly, there is no advantage in using this reflection over the 004 reflection except when the parallel mismatch is to be determined.

TABLE 5.2

Values of the peak half width and extinction distance for the 224 and 404 reflections as a function of wavelength for an (001) InP crystal.

Wavel. (Å)	224 Reflection		404 Reflection	
	FWHM (secs)	Extin. Len. ( $\mu\text{m}$ )	FWHM (secs)	Extin. Len. ( $\mu\text{m}$ )
2.00	14.96	5.99	19.72	7.09
1.80	14.04	5.30	13.63	6.09
1.60	15.52	4.17	15.95	4.20
1.58	15.94	4.01	16.98	3.88
1.56	16.45	3.84	18.24	3.55
1.54	17.10	3.65	20.09	3.18
1.52	17.90	3.44	22.98	2.73
1.50	18.96	3.21	28.44	2.18
1.48	20.37	2.96	44.41	1.38
1.47	21.70	2.75	93.78	0.65
1.46	22.38	2.66	-	-
1.44	25.46	2.31	-	-
1.42	30.96	1.88	-	-
1.40	44.88	1.28	-	-
1.39	70.03	0.82	-	-

The asymmetry factor becomes especially important for the 224 and 404 reflections, where below  $1.6 \text{ \AA}$  the value of  $\theta-\phi$  is less than  $7^\circ$ . Values of the extinction distance for the 224 and 404 reflections, with a low incidence angle, as a function of wavelength are shown in Table 5.2. Since the

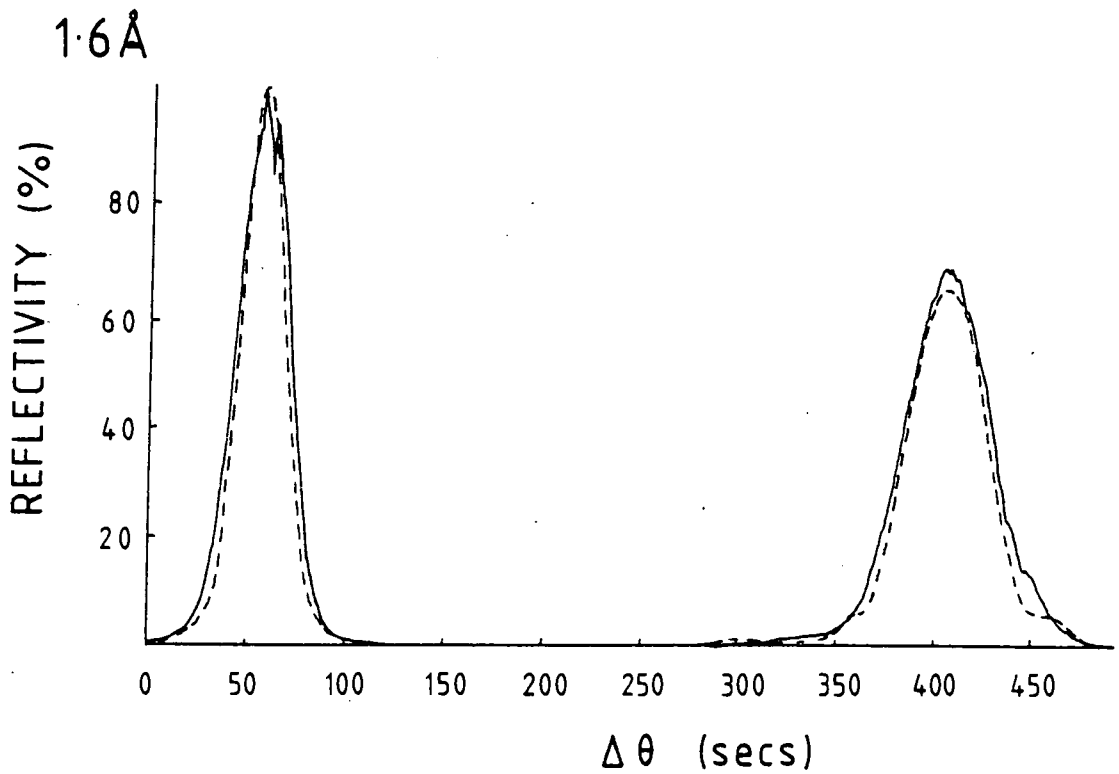
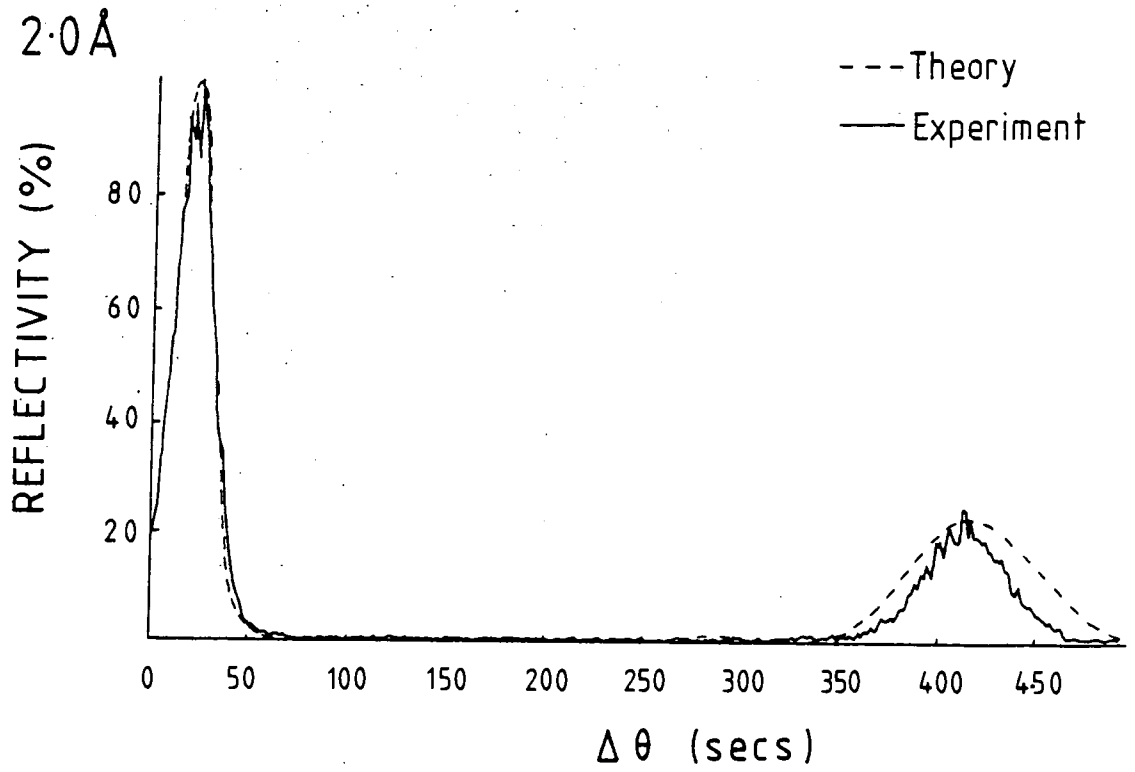
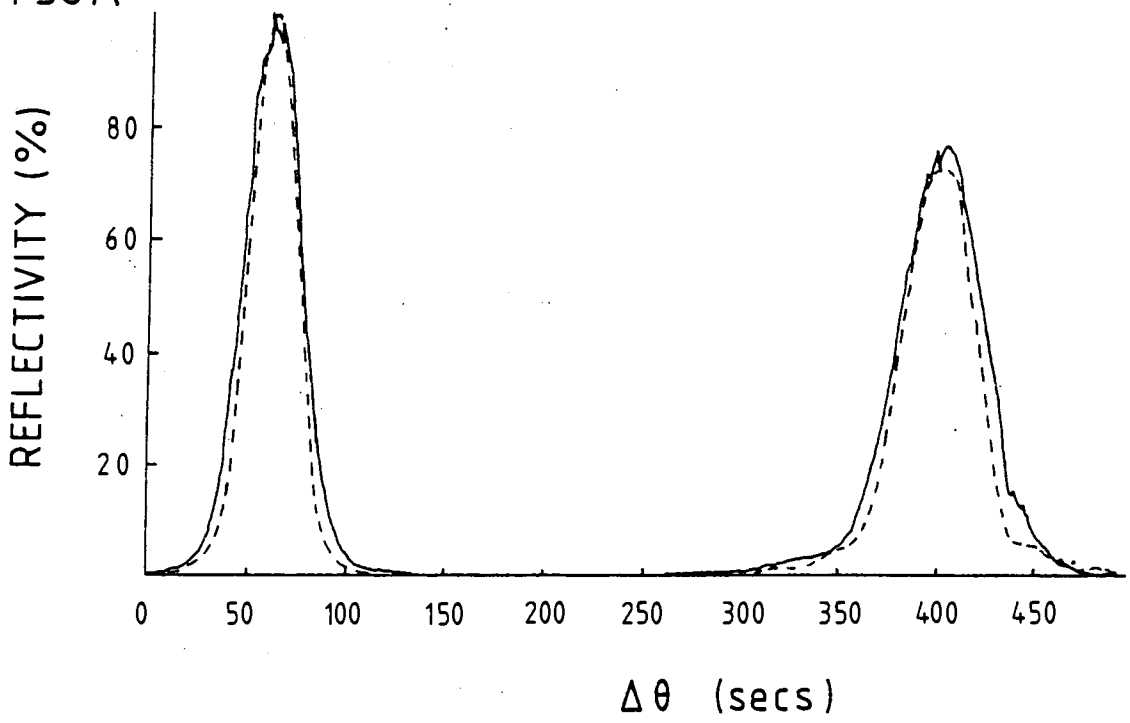
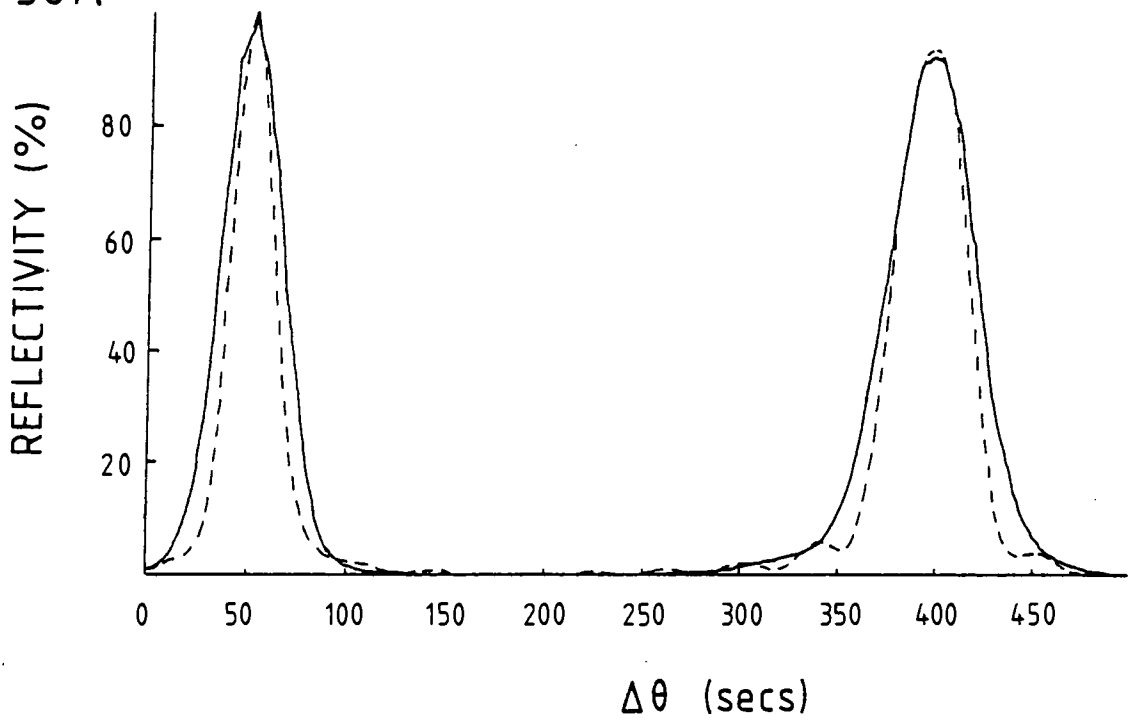


Fig. 5.9 Series of 224 experimental and computed rocking curves from the same sample used in fig. 5.8 at various wavelengths in the range 2.0 Å to 1.40 Å.

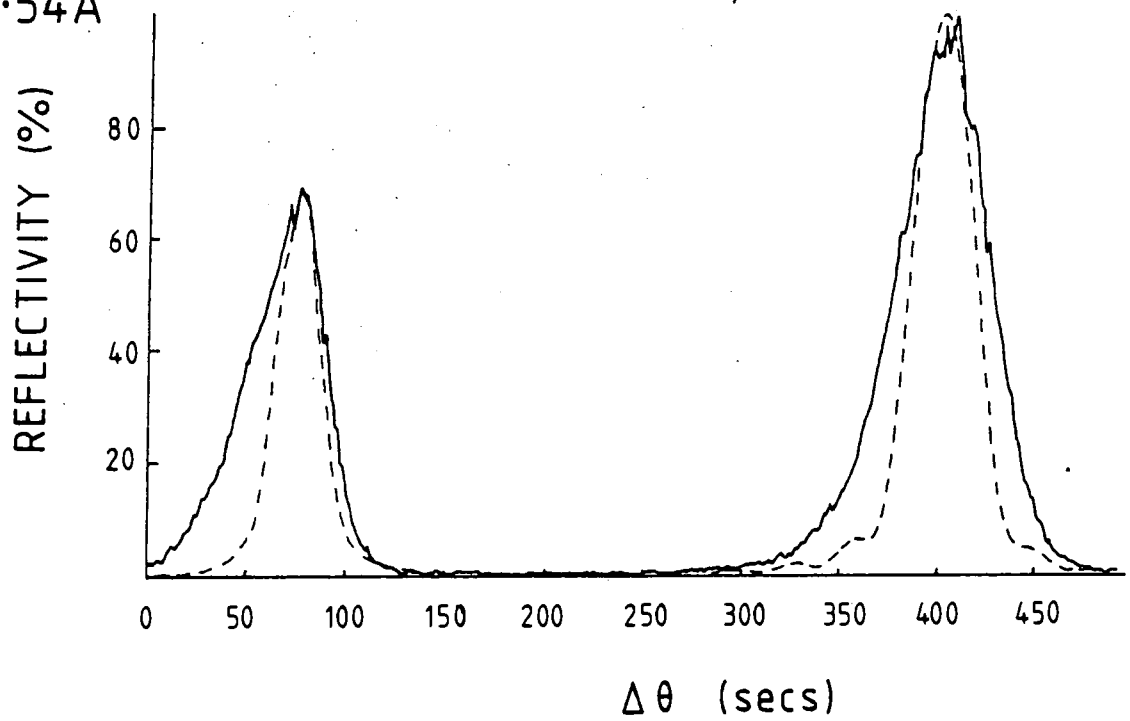
1.58 Å



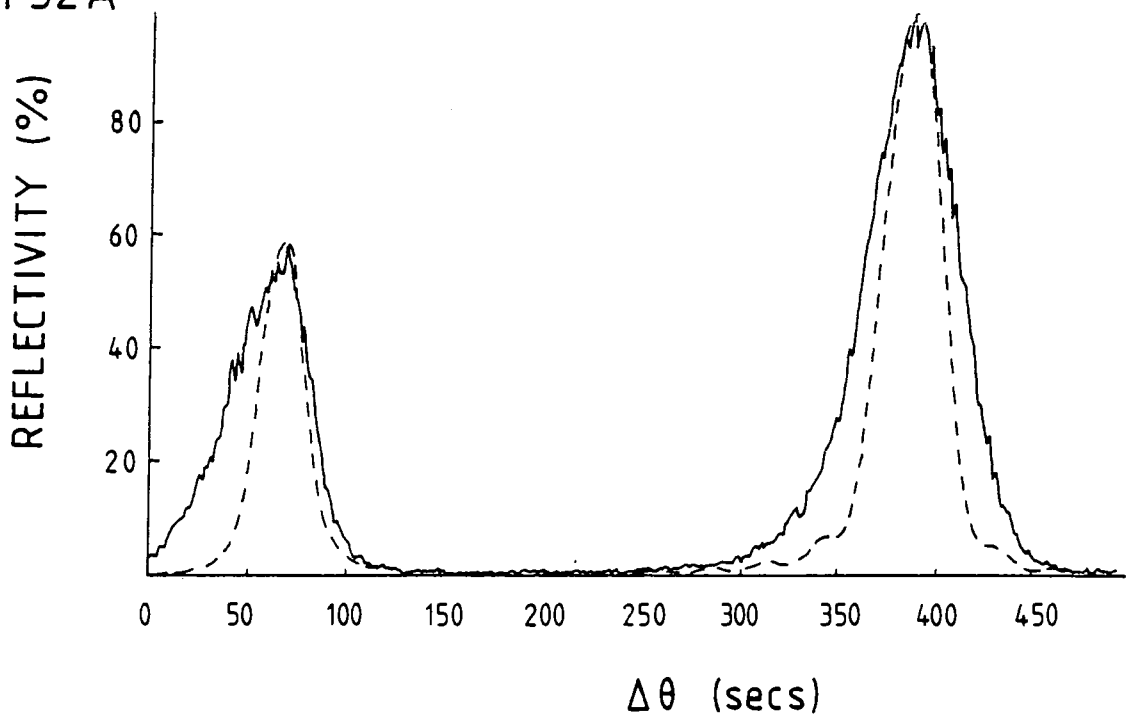
1.56 Å



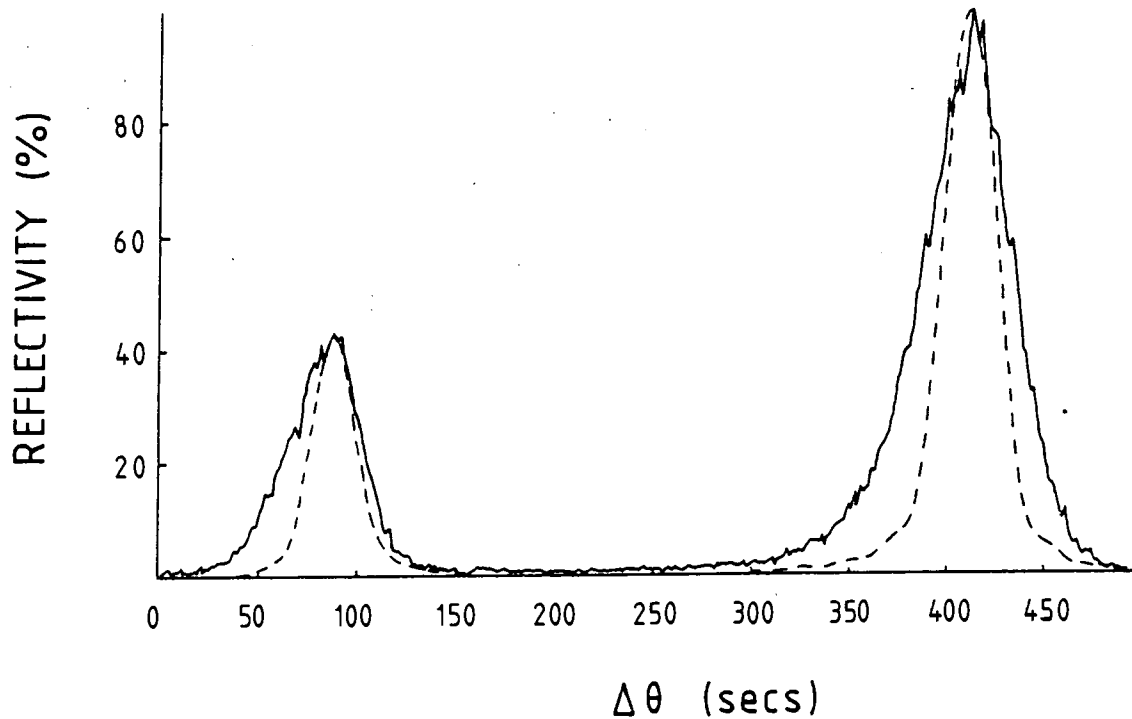
1.54 Å



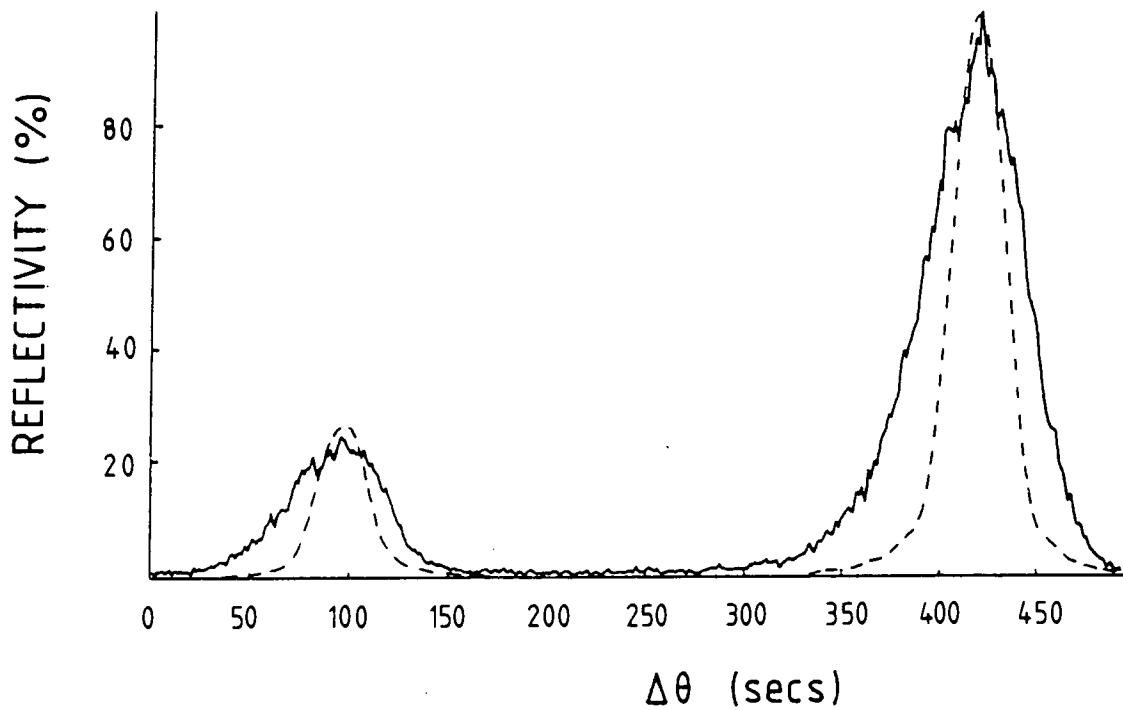
1.52 Å



1.50 Å

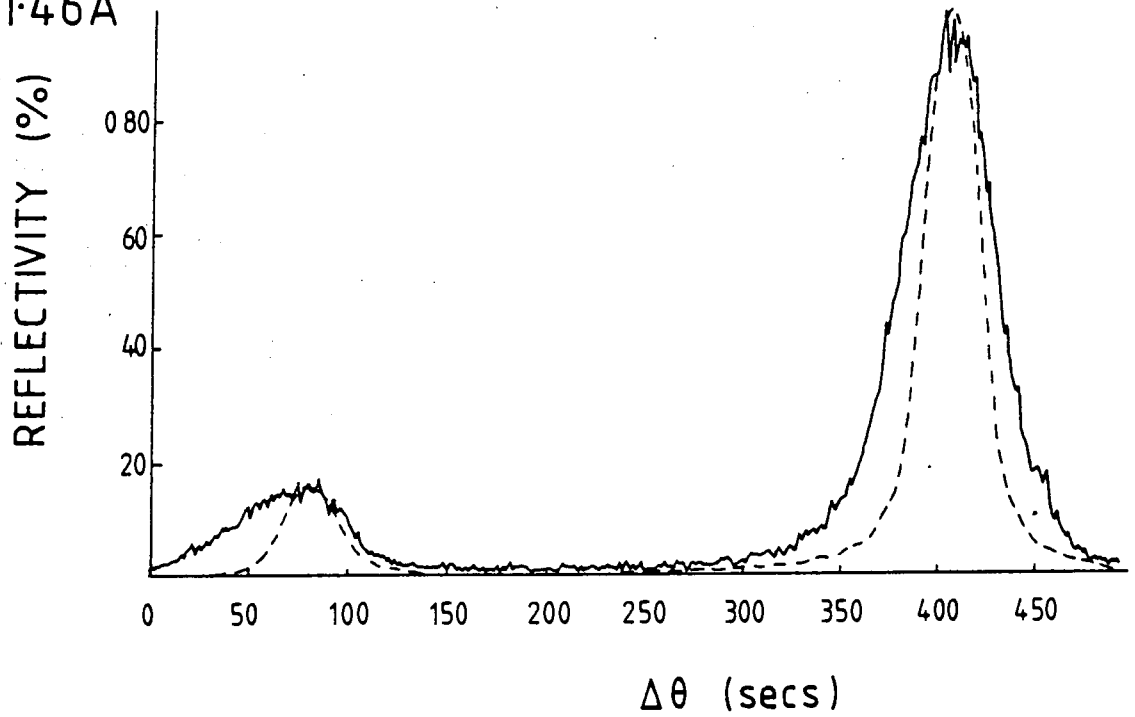


1.48 Å

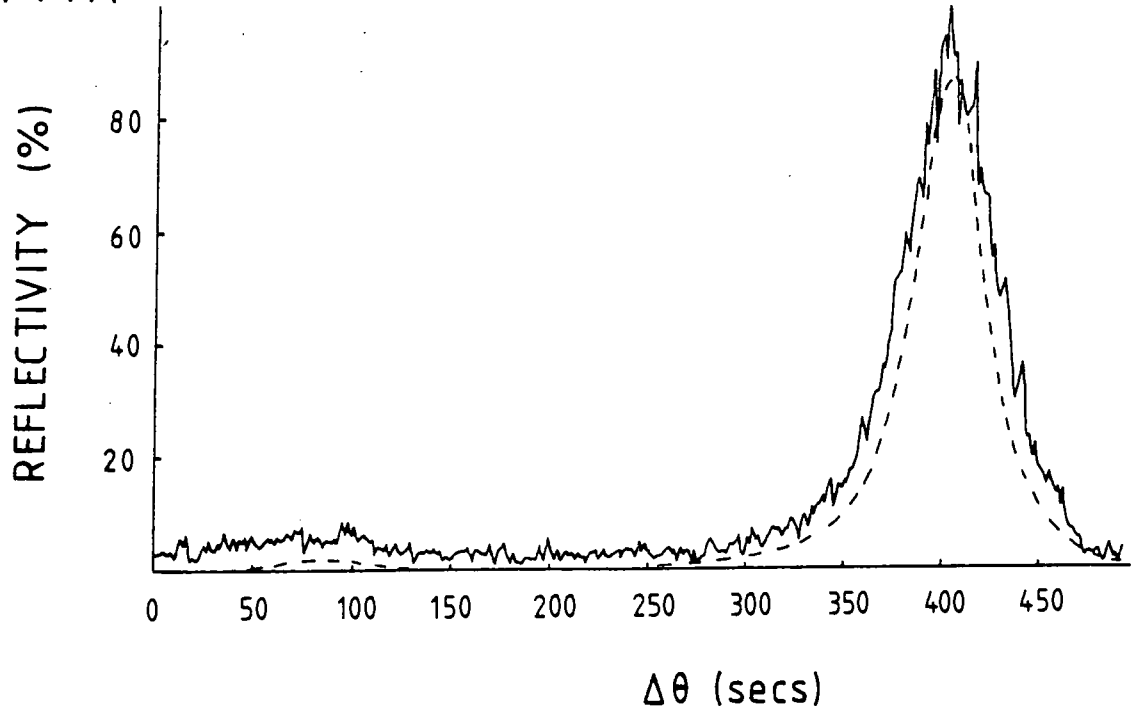




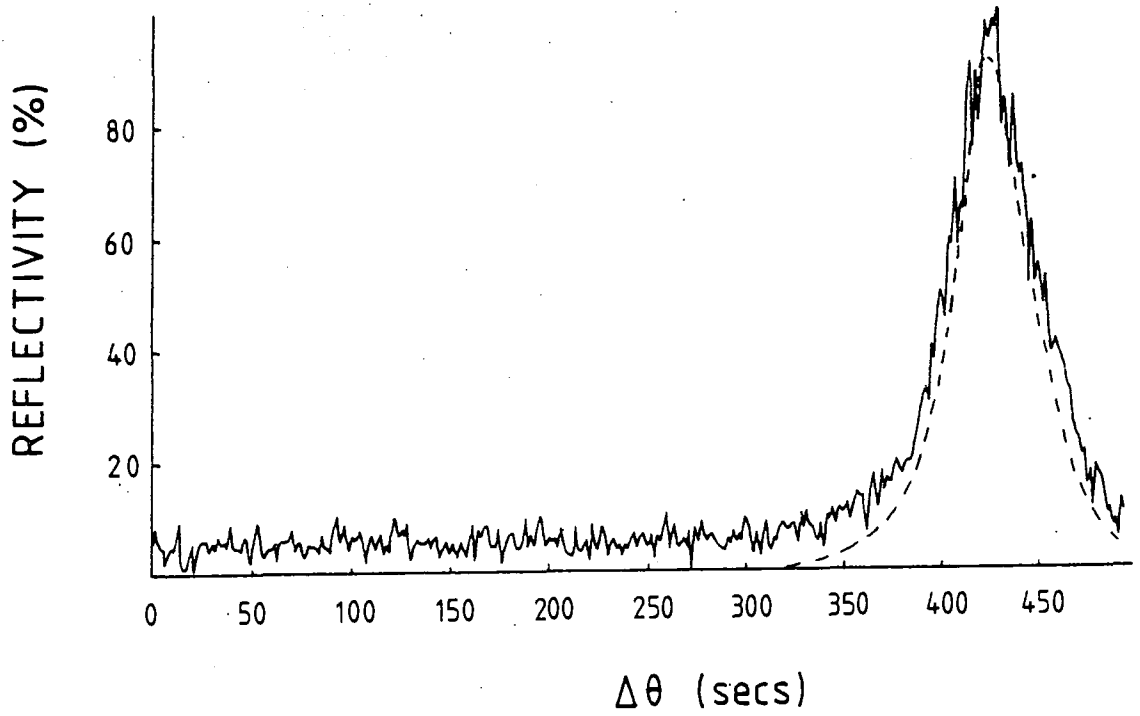
1.46 Å



1.44 Å



1.42 Å



extinction distance decreases so rapidly the peak half width must similarly be affected and values for half widths of the 224 and 404 reflections are also shown in Table 5.2. Fig. 5.9 shows a series of 224 rocking curves recorded at the SRS and using the black-box monochromator. The wavelength is easily altered with this arrangement and over the range 1.6 Å to 1.4 Å the height of the X-ray beam alters very little. A low angle of incidence was used with a 100 μm vertical slit used to limit the area of sample illuminated. Since, even with a very narrow slit, a long length of sample is illuminated due to the low incidence angle an exit slit in front of the detector was used to reduce the area of sample contributing to the rocking curve.

The 1.60 Å rocking curve shows that even at 6.6° incidence angle the diffracted intensity from the layer is already greatly increased over the 004 and 115 reflections. The layer peak is broader than the substrate peak and about 75% of its intensity. Clearly, already there is little doubt as to the usefulness of this reflection for the characterisation of layers with thicknesses less than 0.5 μm. As the wavelength is further reduced, the layer peak rapidly becomes more intense at the expense of the substrate peak. At about 1.54 Å the peaks are almost equally intense with the layer peak again being the broadest. Due to the very low angle of incidence the effect of bulk sample curvature is especially important and further increases the width of the peaks as the wavelength is decreased. At 1.52

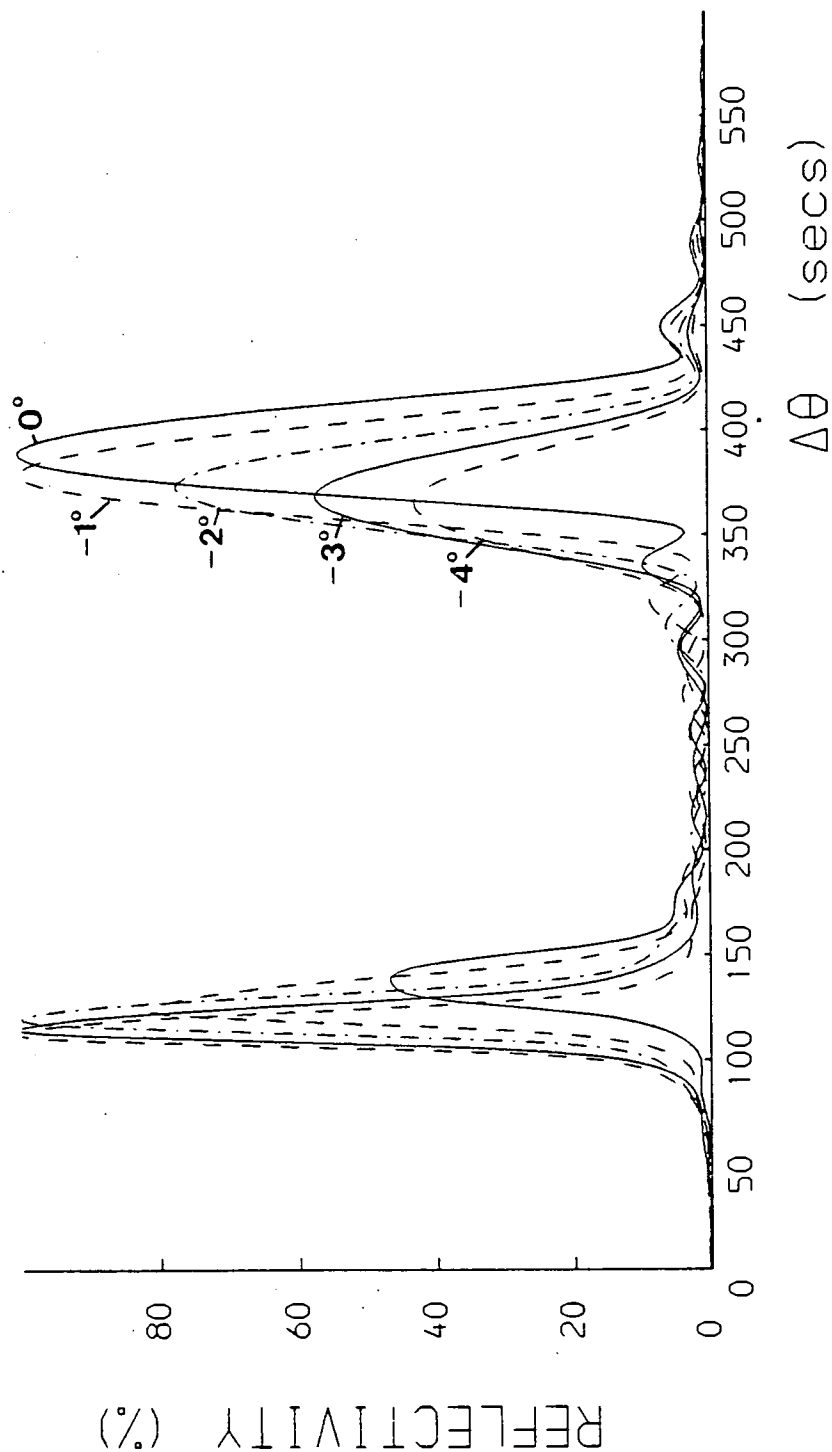


Fig. 5.10 Theoretical 224 reflections for a  $0.2 \mu\text{m}$  thick  $-600$  ppm mismatched GaInAs layer for different values of surface misorientation. Positive angles are taken to decrease the angle between the surface and the x-ray beam for the  $(\theta-\phi)$  angle of incidence case. The wavelength used is  $1.6 \text{ \AA}$  with  $\sigma$  polarisation.

A and below the substrate peak rapidly diminishes and becomes noticeably asymmetric, with a more intense tail on the low angle side. The overall diffracted intensity is also rapidly diminished as the wavelength is further reduced giving rise to considerably more noisy rocking curves. At these low incidence angles the X-ray beam will become increasingly strongly reflected from the crystal surface due to refraction and less intensity will be available in the crystal to be diffracted. From the refractive index of X-rays the critical angle for total external reflection is approximately  $0.5^\circ$ . At  $1.40 \text{ \AA}$ , which corresponds to an incidence angle of only  $0.49^\circ$  only very weak diffraction from the layer can be observed with no intensity detectable from the substrate.

Since the rocking curve is, clearly, so dependent on the value of  $\theta - \phi$  under these conditions it will be particularly sensitive to any surface misorientation. This effect is shown in fig. 5.10 where rocking curves for a  $0.2 \mu\text{m}$ ,  $-600 \text{ ppm}$  mismatched GaInAs layer for  $1.6 \text{ \AA}$  radiation have been calculated including an increasing additional tilt angle. The negative sign indicates that the additional angle increases the incidence angle with respect to the crystal surface. We note how sensitive the layer peak is to this tilt angle, with a  $-4^\circ$  tilt reducing its intensity to less than 50% of its value with no additional tilt. Substrates are often cut upto  $3^\circ$  off orientation in order to improve layer growth. With MBE growth the steps thus

produced on the surface are usually filled up before the layer continues to grow but this may not be the case for LPE grown layers. Consequently, this surface misorientation must be taken into account when computing rocking curves as best fits to the experimental curves. This appeared to be particularly true for this sample as the layer intensities in the calculated curves were considerably greater than those in the experimental curves at the same wavelengths. Although there could easily be an error of  $0.05 \text{ \AA}$  in the wavelength used in the experiment this would not account for these discrepancies and, additionally, the peak separations would not be consistent. However, by including a surface misorientation of  $2^\circ$ , in a direction such as to increase the incidence angle, reasonable fits could be made at the wavelengths expected.

Fig. 5.9 shows such calculated rocking curves for comparison with the experimental curves. Agreement between these curves is reasonable, particularly at the higher wavelengths. At the lower wavelengths used the asymmetry exhibited by the experimental substrate peak is not present in the calculated curve. This is not unexpected as the calculations do not include the effect of the X-ray beam reflected from the surface. Hartwig (1977,1978) has pointed out that for highly asymmetric reflections this reflected beam cannot be neglected and the conventional two beam approximation can no longer be used. He showed that the inclusion of this beam in the calculation of the Bragg

reflection profile does produce asymmetric peaks. Note that artificial symmetry of the rocking curve due to a parallel (+-) arrangement will not be present in rocking curves recorded with the black box monochromator. Additionally, any changes in the layer composition and thickness over the area of the sample will also increasingly affect the rocking curve as the wavelength is reduced, due to the increased area of the sample illuminated. Further, since the rocking curve is also more sensitive to thin regions of the layer any rapid changes in composition near the layer/substrate interface, as reported for LPE grown layers, will also become important.

Although the layer used was not especially thin we have seen that the use of highly asymmetric reflections does lead to a greatly increased layer intensity making characterisation rather more straightforward. The use of reflections where the totally externally reflected beam from the crystal surface cannot be neglected increases the difficulty of calculating rocking curves to best fit the experimental ones and, consequently, hinders the determination of layer thickness. Therefore, 224 reflections at approximately  $1.50 \text{ \AA}$  are more useful. Ample intensity is diffracted by the layer for the peak position to be accurately determined and theoretical curves can easily be computed that agree well with the experimental curve, thus allowing a reasonably accurate determination of layer thickness.

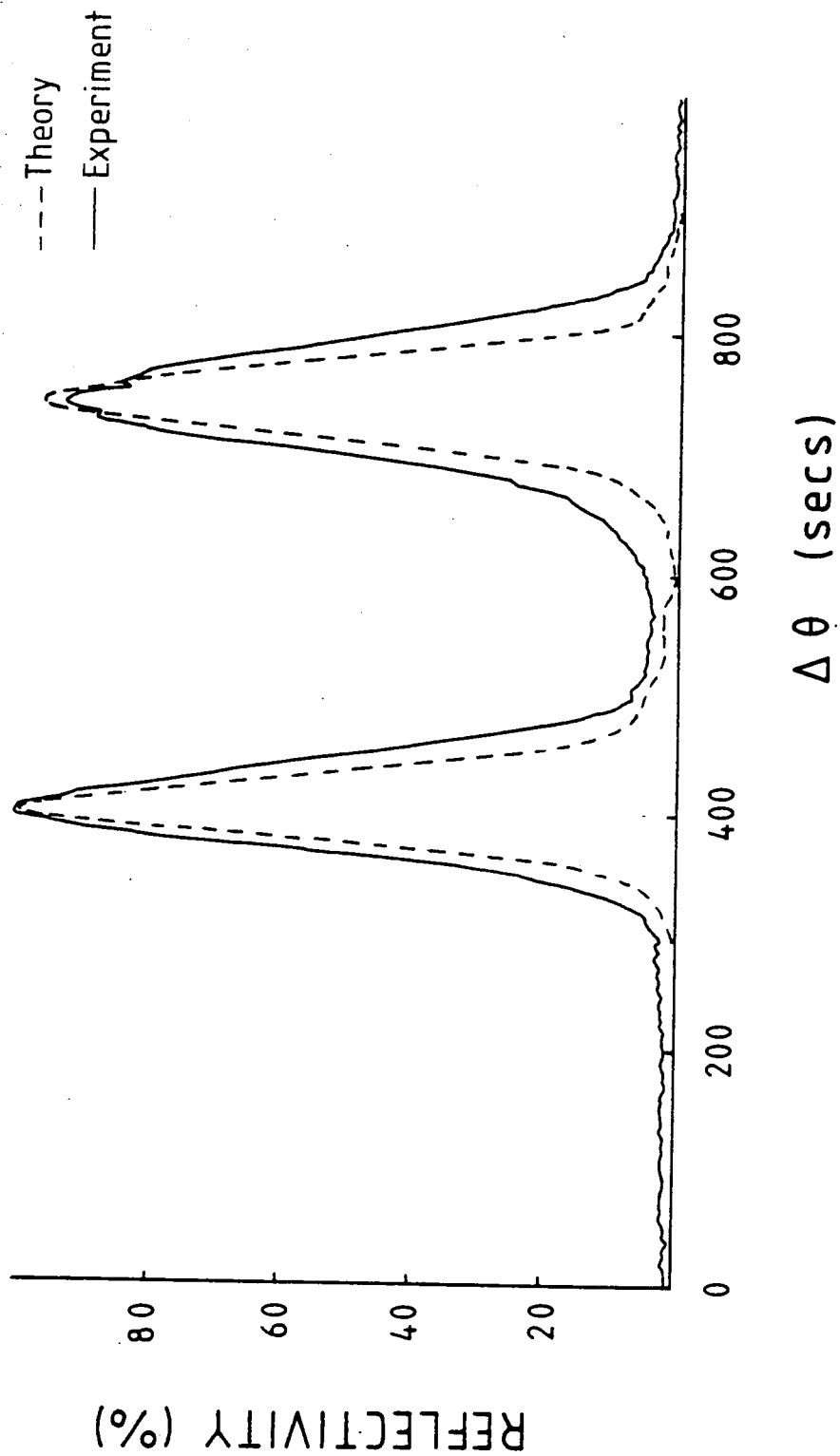


Fig. 5.11 Experimental and computed 404 rocking curves for the same sample used in fig. 5.9 at a wavelength of 1.55 Å.



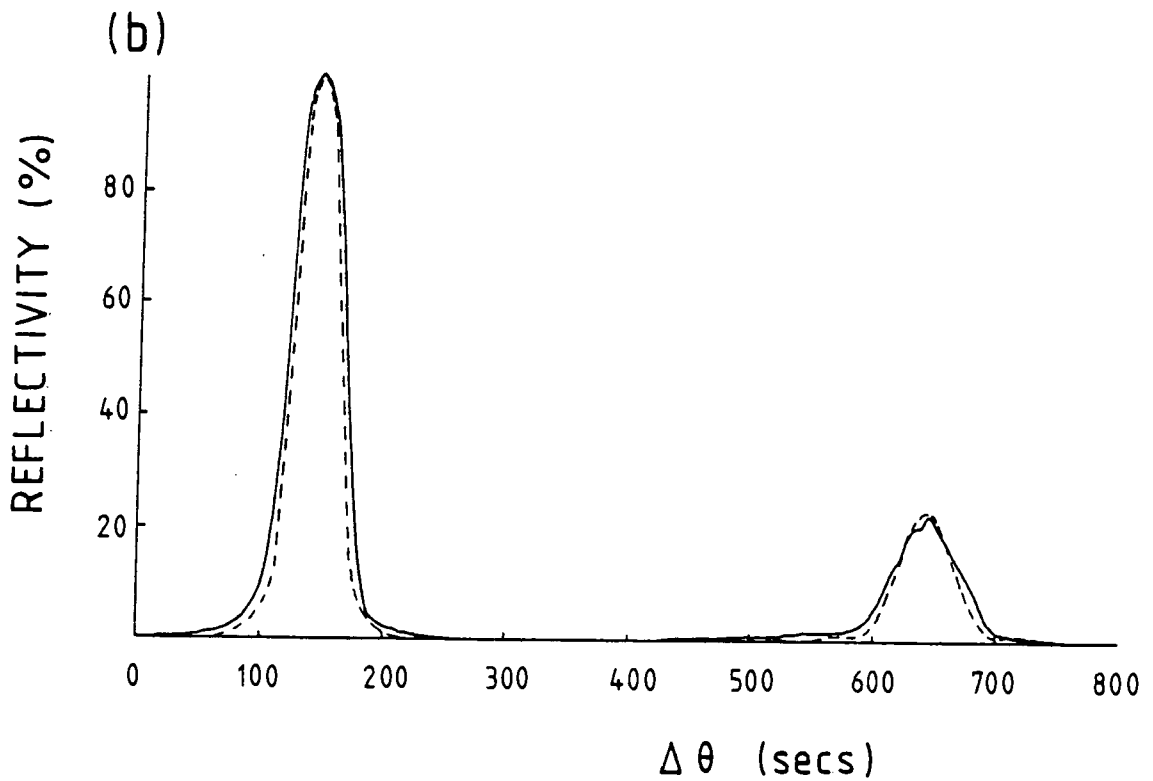
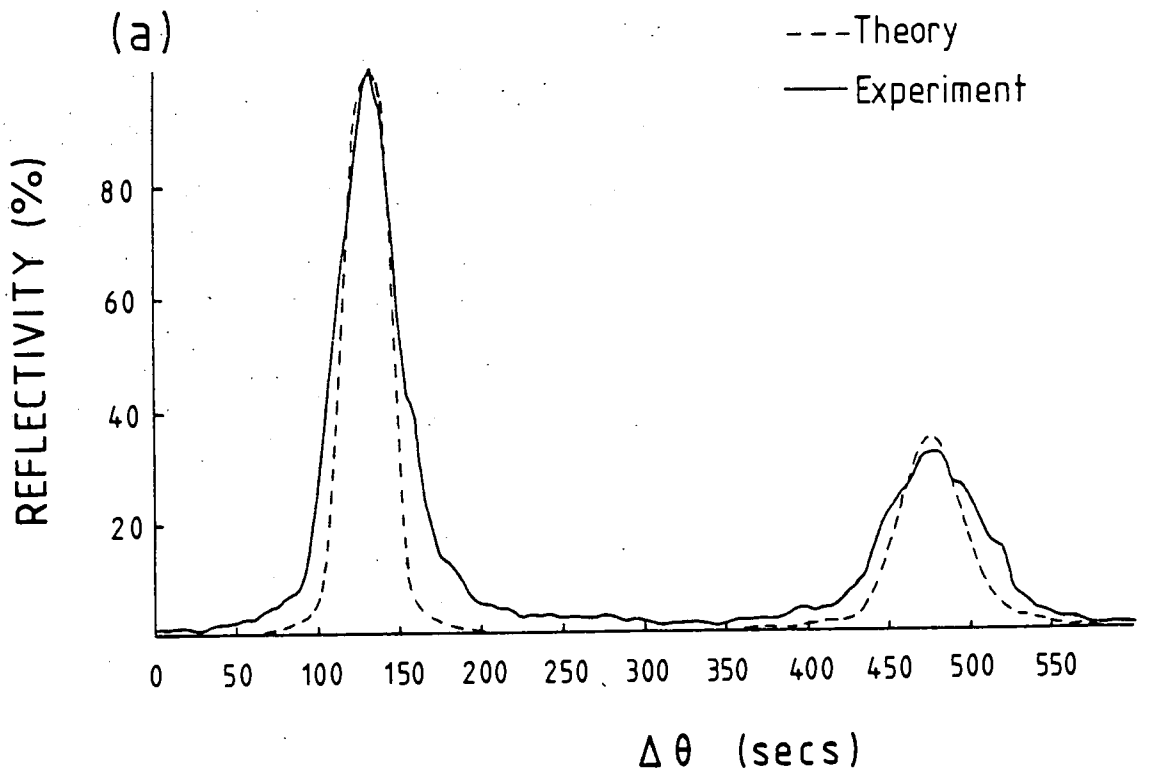


Fig. 5.12 (a) Experimental and theoretical 004 rocking curves from a  $0.45\ \mu\text{m}$  thick,  $\lambda = 10\ \mu\text{m}$ ,  $-1100\ \text{ppm}$  mismatched GaInAsP layer on an InP substrate. The wavelength is  $1.54\ \text{\AA}$ .

(b) The experimental and theoretical 115 rocking curves from the same sample at  $1.5\ \text{\AA}$ .

Fig. 5.9(a) shows the experimental and calculated rocking curves for the same sample at 2.0 Å. Since the asymmetry factor is no longer as important the layer peak is reduced to a similar height to that observed in the 115 and 004 reflections. Consequently, there is no advantage in using this reflection at similar wavelengths over the 004 reflection. If only a non-tunable wavelength source is available, as is a conventional X-ray generator, good results can be obtained with  $\text{CuK}\alpha_1$  radiation.

Similar effects are observed with the 404 reflection at wavelengths in the range 1.45 Å to 1.7 Å. Fig. 5.11 shows the experimental and calculated rocking curves for this reflection with the same sample at 1.55 Å. Again the layer diffracts considerably more intensity than from the 004 and 115 reflections making its position and integrated intensity easily measured. The 404 reflection is slightly weaker than the 224 reflection and consequently has a larger extinction length at the longer wavelengths. The calculated rocking curve again agrees reasonably well with the experimental curve although both experimental peaks are considerably broader than those in the computed curve. A layer thickness of 0.3  $\mu\text{m}$  again gave the best agreement.

Similar results were obtained with another sample with a 0.45  $\mu\text{m}$ ,  $\lambda=1.0 \mu\text{m}$ , GaInAsP layer. The 004 rocking curve at 1.54 Å is shown in fig. 5.12(a) giving the mismatch as -1100 ppm and the calculated rocking curve, assuming a layer thickness of 0.45  $\mu\text{m}$ , is also shown in fig. 5.12(a). The

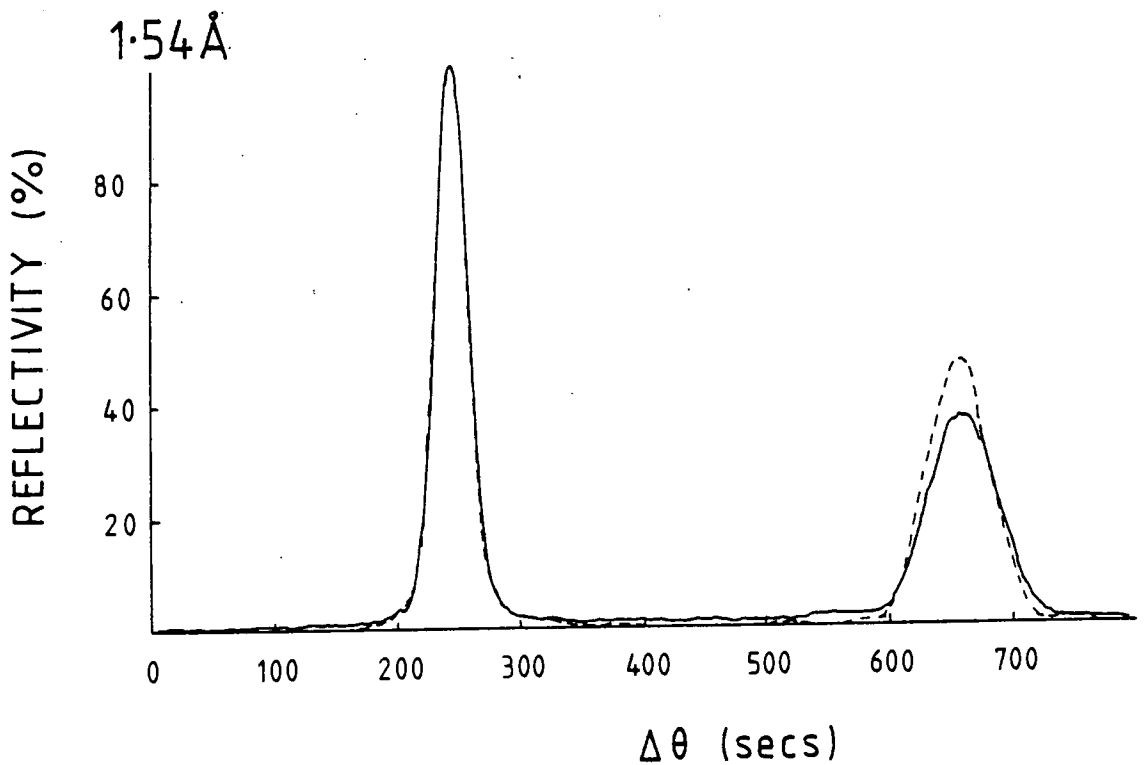
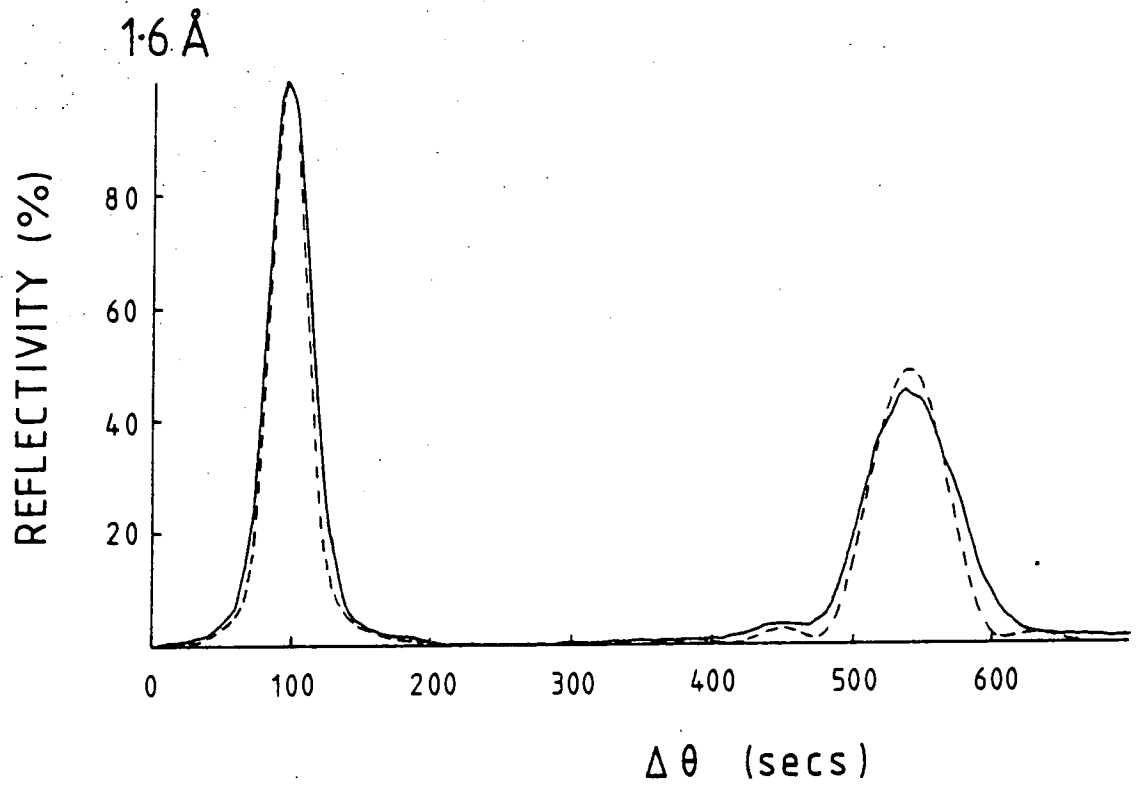
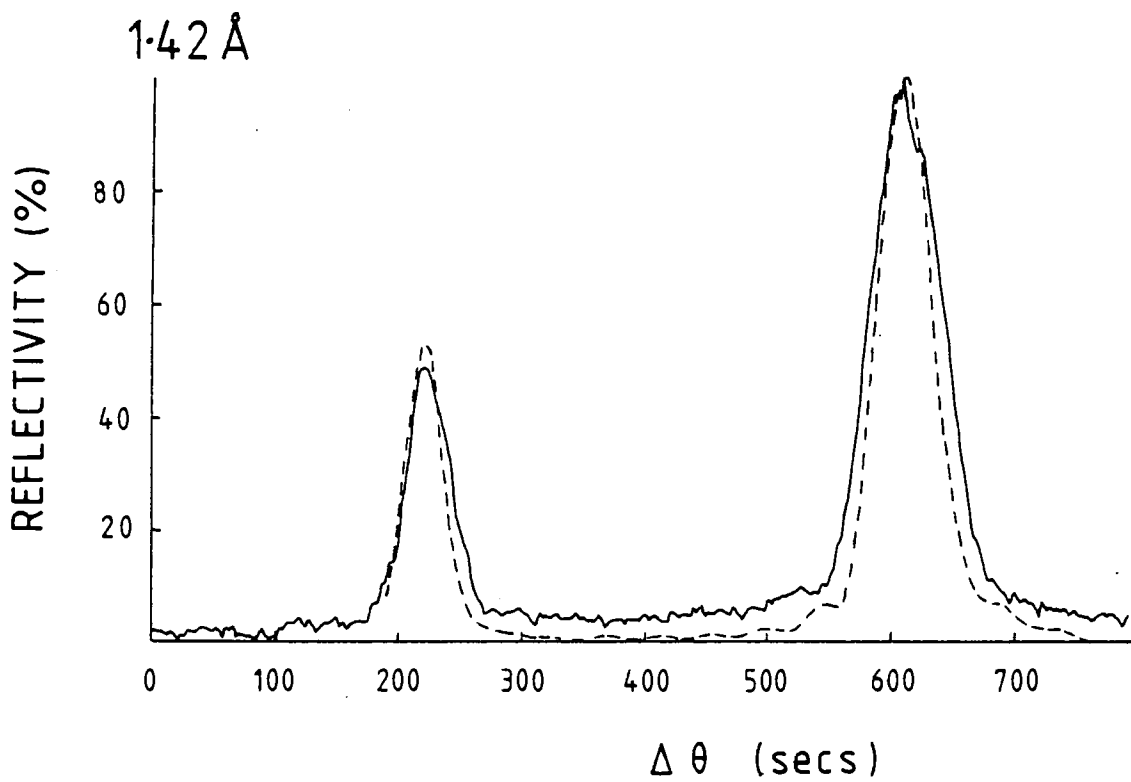
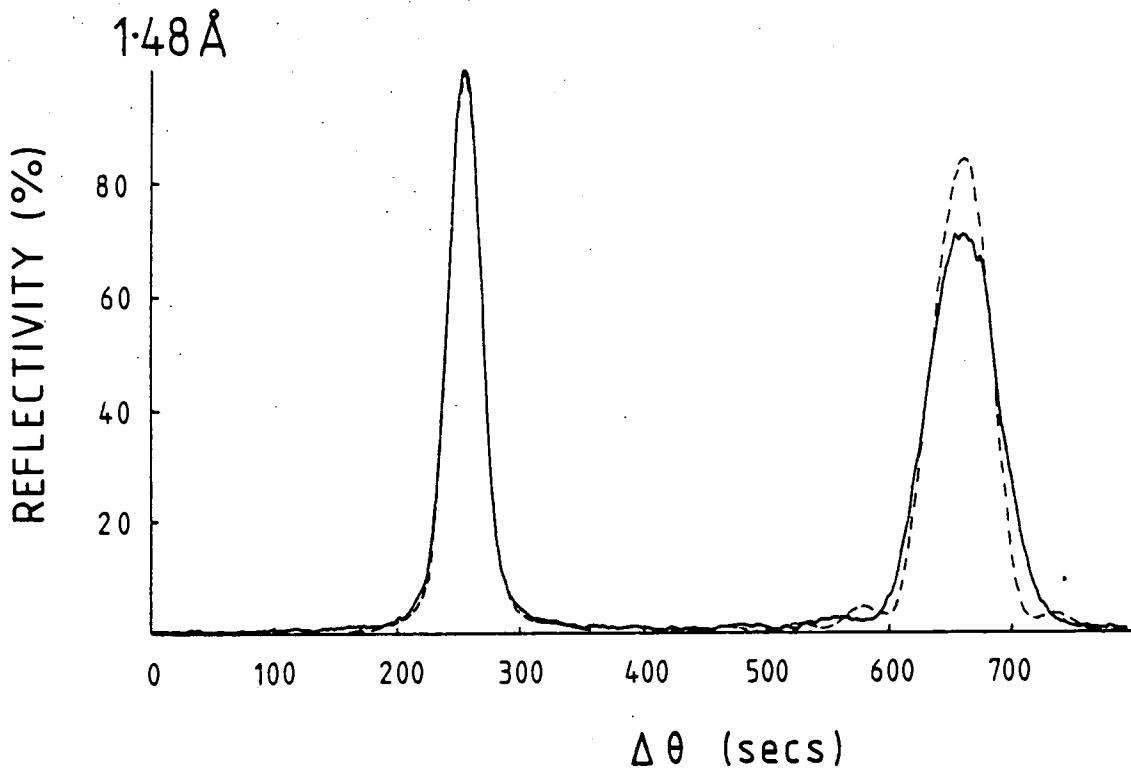


Fig. 5.13 224 experimental and computed rocking curves from the same sample used in fig. 5.12. Wavelengths in the range 1.6Å to 1.42Å. The computed curves are for a layer thickness of 0.2μm.



composition of the layer is determined to be  $\text{Ga}_{0.09}\text{In}_{0.91}\text{As}_{0.15}\text{P}_{0.85}$ . Once again agreement is particularly good with the effect of sample curvature included in the calculation to give equal half widths for the substrate peak. Measurement of the rocking curve with the X-ray path reversed indicated that there was no tilt angle present between the layer and substrate. The 115 reflection was also measured at  $1.5 \text{ \AA}$  and the rocking curve is shown in fig. 5.12(b), again showing only small intensity from the layer. The computed rocking curve is also shown in fig. 5.12(b) and again agrees reasonably well.

Fig. 5.13 shows a number of 224 rocking curves recorded for this sample over the range  $1.6 \text{ \AA}$  to  $1.42 \text{ \AA}$ . The rocking curve behaves in a similar manner that of the previous sample, with the layer peak rapidly becoming more intense than the substrate peak. Good agreement between computed and these experimental curves could only be achieved for a layer thickness of  $0.2 \text{ \mu m}$ , suggesting that a different region of the sample was being illuminated by the X-rays. Since the layer did not extend over the entire region of the substrate it is quite possible that a thinner region near to the edge of the layer was studied. Computed rocking curves for this layer thickness are also shown in each figure for comparison and good agreement is obtained. The asymmetric peaks shown in the experimental curves from the previous sample are not observed in these rocking curves. similar agreements obtained as with the previous sample.

In all of the above examples a low incidence angle was used, giving  $\gamma_0$  less than  $|\gamma_h|$ . A high incidence angle could also be used which would similarly decrease the extinction length, due to the factor  $(\gamma_0 |\gamma_h|)^{\frac{1}{2}}$ , but would decrease the half width of the peaks, due to the factor  $(|\gamma_h|/\gamma_0)^{\frac{1}{2}}$ . At these extremely low exit angles the exit beam would be increasingly totally internally reflected at the crystal surface (Hartwig, 1978). Consequently, the two beam approximation used in the calculation of the rocking curve would again be in error. Hartwig has shown that in this case peaks with an even higher asymmetry are produced.

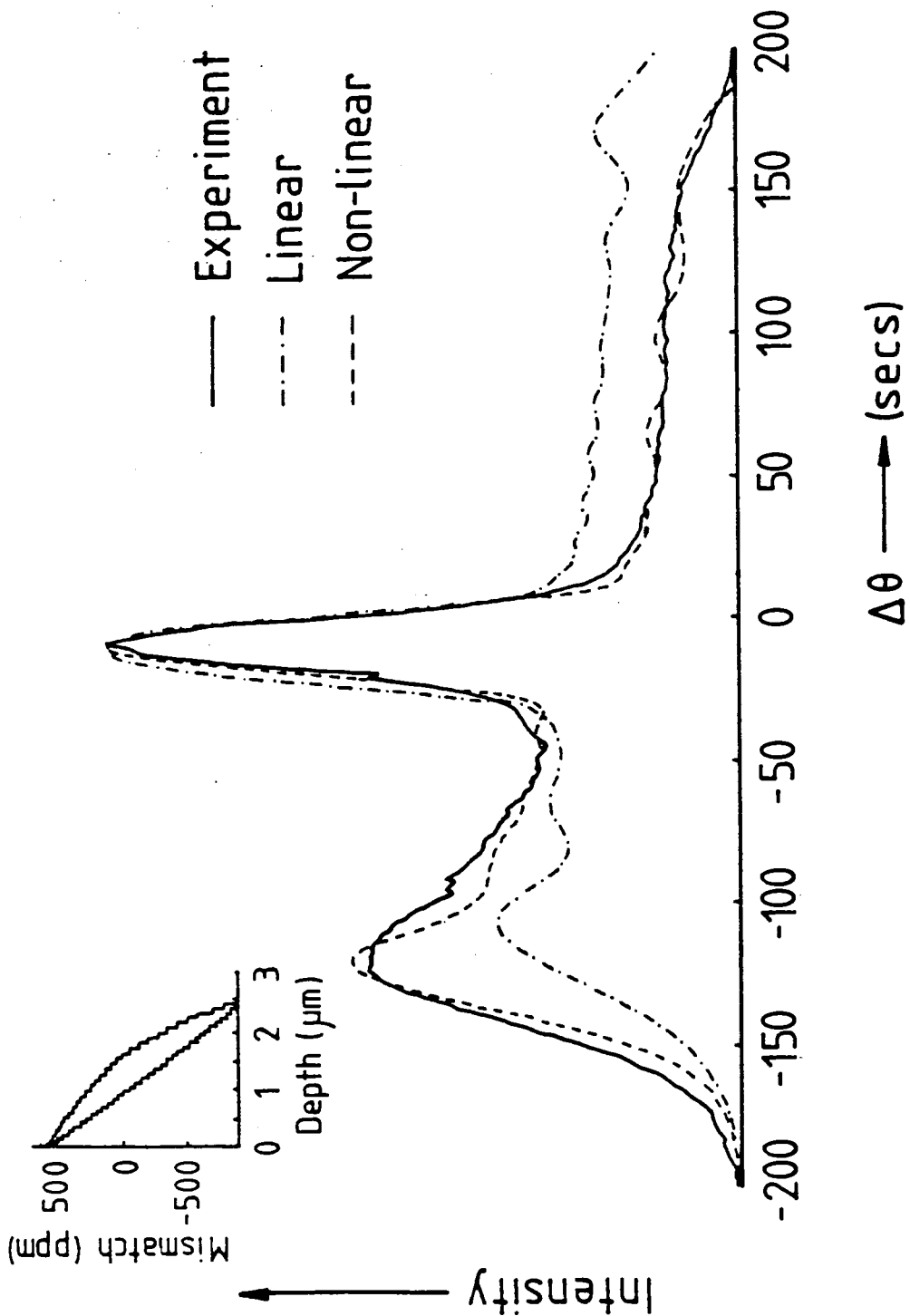


Fig. 6.1 Experimental and computed 004 rocking curves from a 2.3  $\mu\text{m}$  thick GaInAs graded layer grown by VPE on a (001) InP substrate. The computed curves are the best fit curves assuming a linear and non linear composition variation. The composition variations used are shown in the inset.  $\text{CuK}\alpha_1$  radiation was used.

## CHAPTER 6

## SINGLE LAYERS WITH A DEPTH DEPENDENT COMPOSITION

Epitaxial layers in which the composition varies continuously as a function of depth are often referred to as graded layers and are generally grown by the VPE method. For (Ga,In)As ternary layers this composition change can be attributed to a change in the concentration of the two type III species as a function of time (see Chapter 1).

The usual 004 double crystal rocking curves from such structures often appear similar to that shown in fig. 6.1. This rocking curve was recorded with  $\text{CuK}\alpha_1$  radiation from a GaInAs layer grown on a 001 InP substrate by VPE. The narrow central peak visible in the curve is from the substrate while the broad, asymmetric peak extending on either side of substrate peak is from the layer. Since the layer peak extends on both sides of the substrate peak the composition must vary to give lattice parameters both larger and smaller than that of the substrate. The wedge-like shape of the layer peak, having an almost level top with only small undulations, immediately suggests that the lattice parameter decreases continuously with depth since the section of the peak on the low angle side of the substrate peak, corresponding to a larger lattice parameter, has the greatest intensity and, therefore, will be due to the region of the layer nearer to the surface. For VPE grown layers we expect that the composition change should be



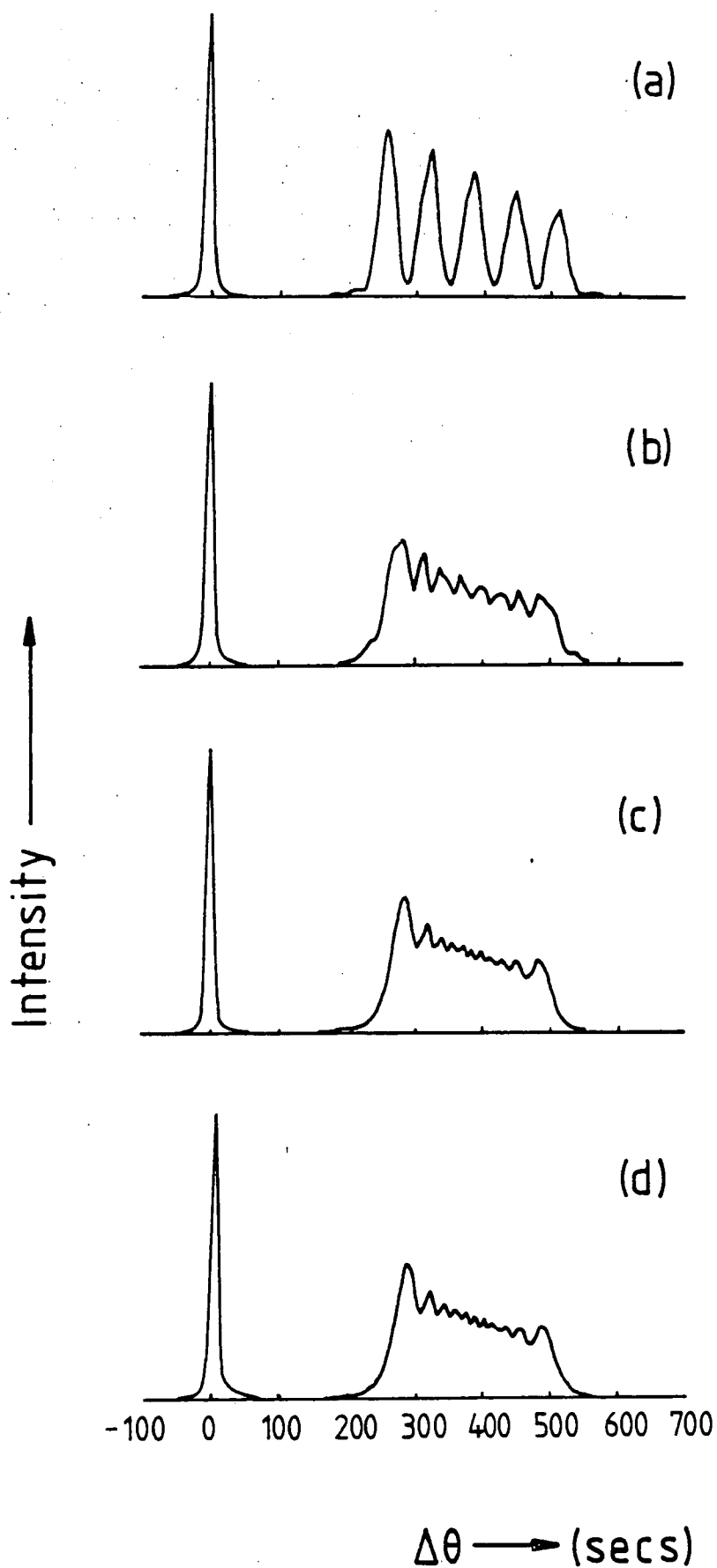


Fig. 6.2 004 computed rocking curves for a  $3\mu\text{m}$  thick GaInAs graded layer with a mismatch range of  $-200$  ppm at the interface and  $-1000$  ppm at the surface, for an increasing number of laminae: (a) 5 laminae, (b) 10 laminae, (c) 20 laminae and (d) 40 laminae.

continuous and monotonic which has been confirmed by X-ray fluorescence microanalysis on bevelled edges (Halliwell, Juler and Norman, 1983). Usually the lattice parameter increases towards the surface due to the layer becoming increasingly indium rich.

In order to calculate the rocking curve from this type of structure the layer must be divided into a number of laminae of constant composition, as already discussed in Chapter 3. It is required to determine into how many laminae the layer should be divided to produce a rocking curve that is a good approximation to one assuming a continuous variation. Clearly, in order to reduce the computation time to a minimum we require the least number that will produce an adequate approximation.

Fig. 6.2 shows a series of rocking curves calculated for an increasing number of laminae. The GaInAs ternary layer is  $3\mu\text{m}$  thick and has a composition range of -2000 ppm at the substrate/layer interface to -1000 ppm at the surface. This corresponds to compositions of  $\text{Ga}_{49.8}\text{In}_{50.2}\text{As}$  at the interface and  $\text{Ga}_{48.4}\text{In}_{51.6}\text{As}$  at the surface. Rocking curves are shown for 5, 10, 20 and 40 laminae assuming a linear variation in composition with depth. For the 5 laminae curve the number of peaks is equal to the number of laminae with the individual peaks well resolved. However, for the 10 laminae curve already the number of peaks, although increased, no longer equals the number of laminae. A wedge-like peak shape has developed with only small

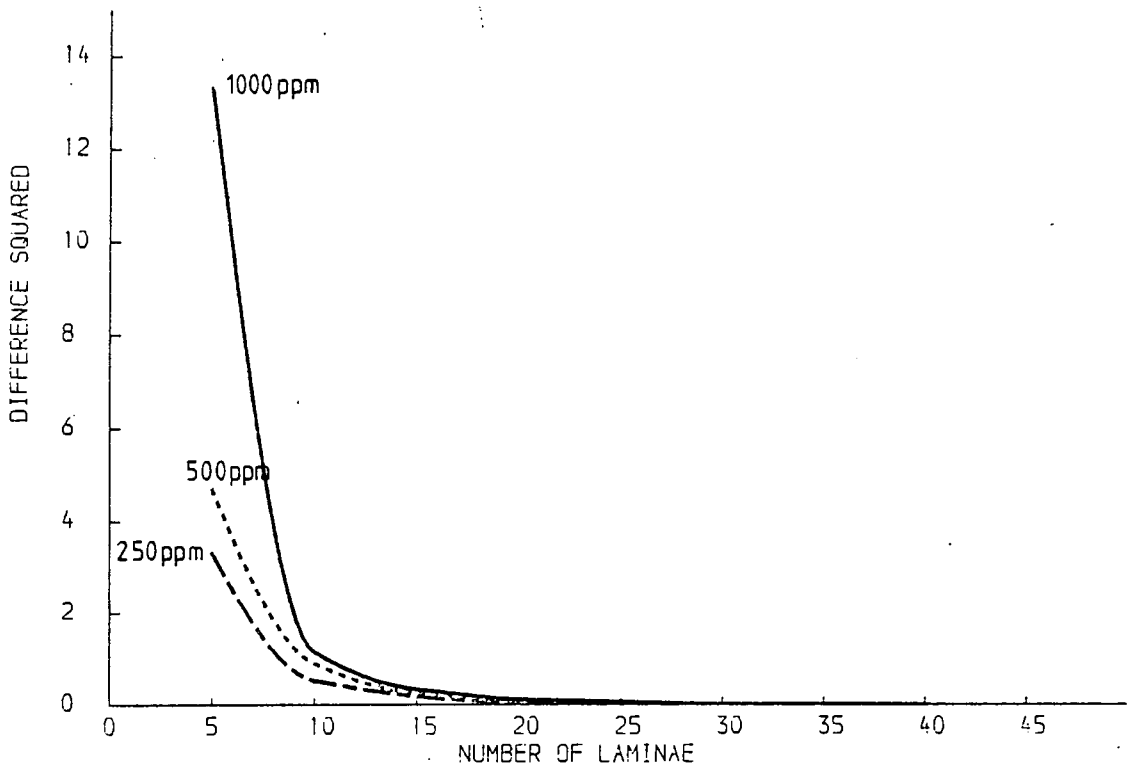
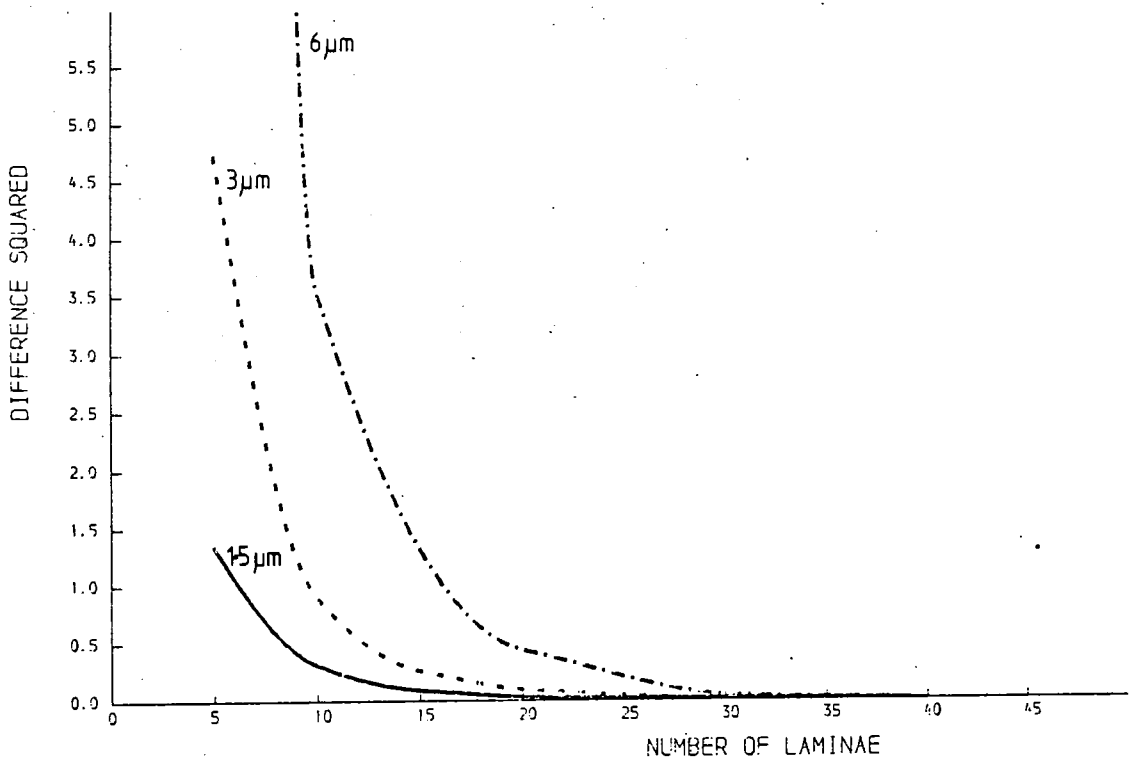


Fig. 6.3 Curves showing the square of the difference between computed rocking curves for an increasing number of laminae and the 40 laminae curve. Curves are shown for a number of mismatch ranges and layer thicknesses.

undulations being visible along the top of the peak. For 20 laminae the peak has fully developed to its final shape and there is no difference between this curve and the one for 40 laminae. This suggests that the peak shape rapidly converges towards that assuming a continuous variation. We note that the number of peaks in the rocking curve cannot be taken as an indication of the number of laminae in the layer.

In order to determine a suitable rule to allow the minimum number of laminae required to give an adequate approximation for a given layer thickness and composition range, curves were calculated for a number of different layer parameters. Assuming that 40 laminae gives a curve that is very close to that required the differences between this curve and those with fewer laminae were calculated. The squares of the difference in intensity at each point in the curve were calculated and are shown in fig. 6.3. Several mismatch ranges and layer thicknesses were used and these curves are also shown in fig. 6.3. From these curves we can deduce that doubling the layer thickness requires double the number of laminae but changing the mismatch range is not as important. As a general rule, for mismatch ranges of the order of 1000 ppm a laminae thickness of 0.1  $\mu\text{m}$  should be perfectly adequate.

Using this approach of calculating rocking curves the curve shown in fig. 6.1 was computed as the best fit to the experimental curve, assuming a linear variation in

composition. The effect of sample curvature has been included so as to equate the half width of the central substrate peak. The composition variation used is shown in the inset in fig. 6.1. Agreement between the calculated and experimental curves is not particularly good, the calculated curve has considerably less intensity on the low angle side of the layer peak, yet has rather more intensity on the high angle side. Fine structure present in the calculated curve is somewhat reduced after including sample curvature but is still more pronounced than in the experimental curve. This discrepancy can be accounted for by the the local lattice deviations introduced by the presence of a large number of threading dislocations ( $\sim 10^7 \text{ m}^{-2}$ ) known to exist within the layer and substrate. The presence of these dislocations was determined by a TEM study at British Telecom Research Laboratories; the absence of any mismatch dislocations was also revealed. Consequently, there must be very little parallel mismatch and the layer/substrate interface can be considered coherent.

Since there is no fundamental reason for the lattice parameter to vary linearly with depth we must be able to calculate the rocking curve for any arbitrary non linear variation. Often the composition will vary rapidly near the interface, ie at the start of growth, when equilibrium conditions have not yet been reached. Using such a variable non linear change in composition the curve shown in fig. 6.1 was calculated. The mismatch variation which gave this best

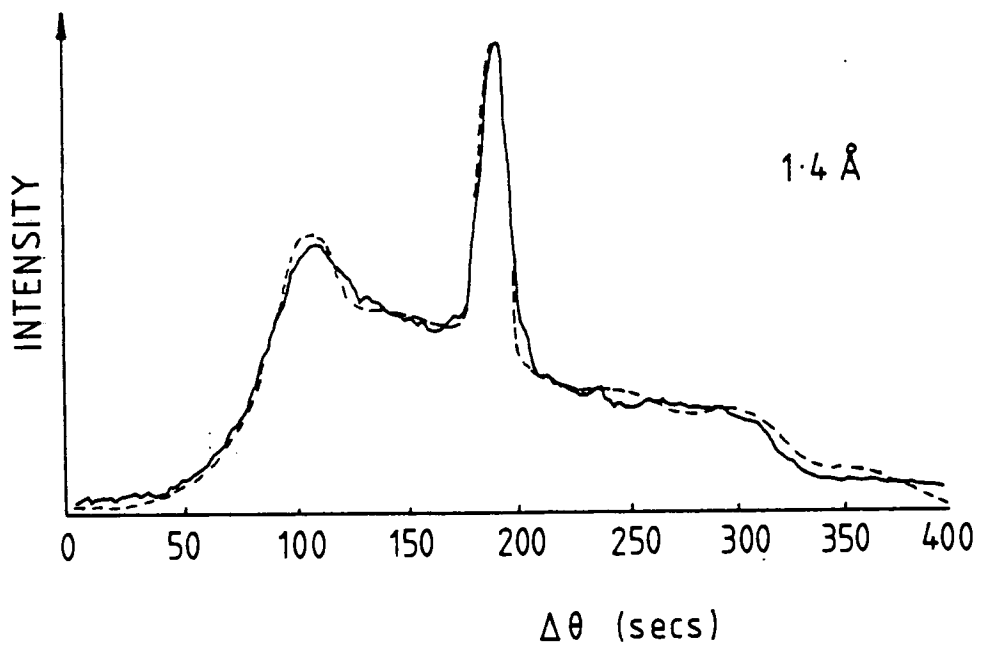
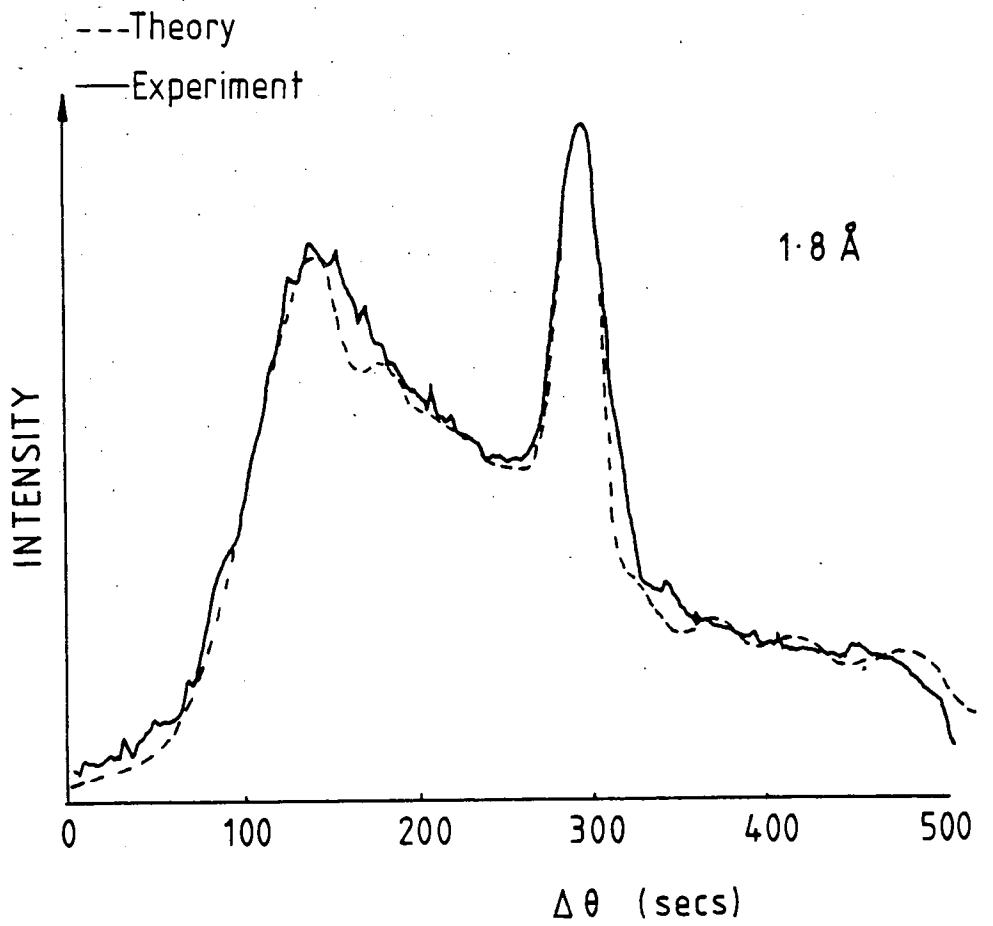
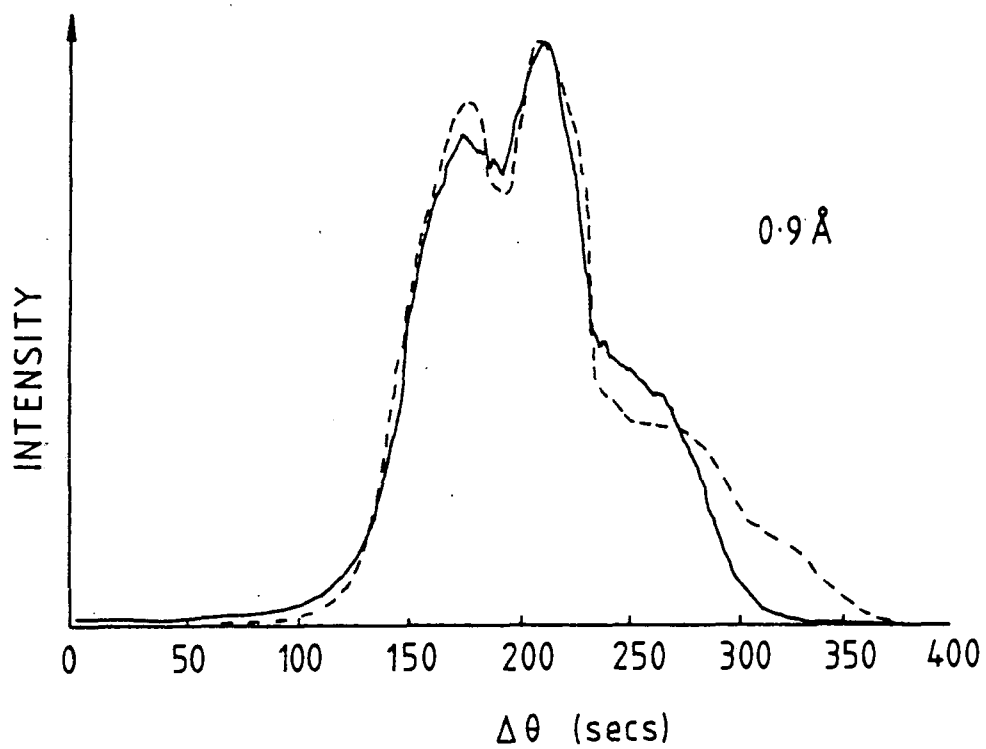
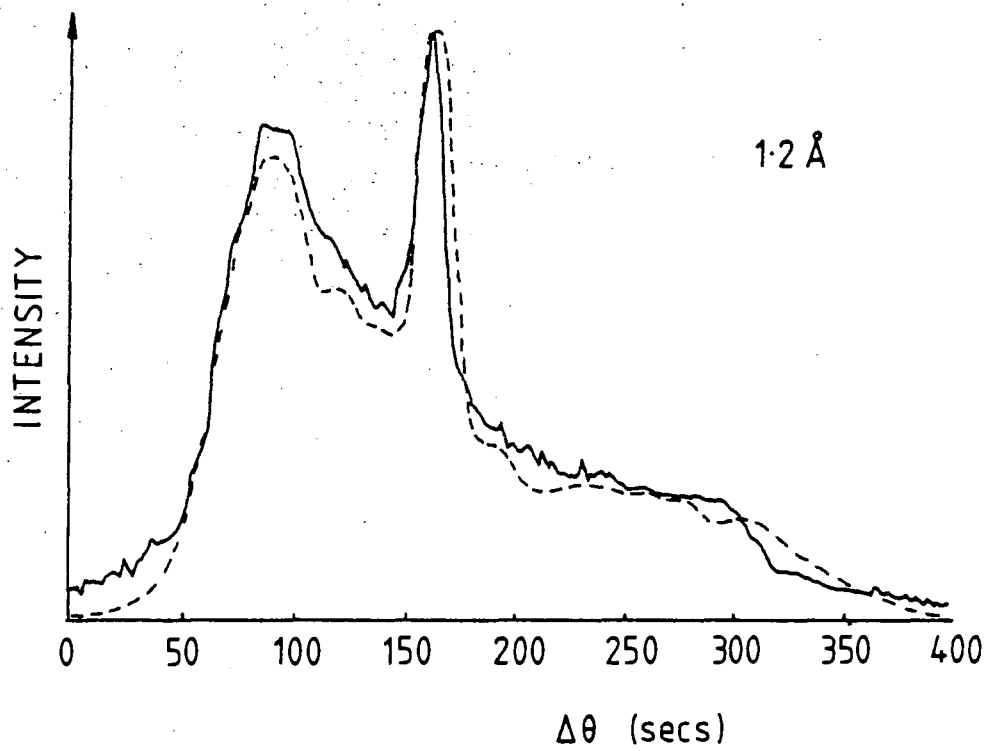


Fig. 6.4 Experimental and computed rocking curves from the sample used in fig. 6.1 at wavelengths of 1.0Å, 1.2Å, 1.6Å and 1.8Å. The non linear variation given in the inset in fig. 6.1 was used for the computed curves.



fit curve is shown in the inset in fig. 6.1, showing that the composition changes more rapidly towards the interface. The agreement between this curve and the experimental curve is extremely good with the only discrepancies occurring on the high angle side of the layer peak. Here rather more fine structure is present in the computed curve. However, the central substrate peak and the low angle side of the layer peak do match very well. The total layer thickness determined is  $2.3 \mu\text{m}$  which agrees well with that expected from the growth conditions.

Since only one reflection at one wavelength has been used to determine the composition variation there must be some doubt as to its uniqueness. In other words, would the variation deduced be different if another set of X-ray optical conditions had been used. Using the double crystal camera at the SRS, the wavelength can easily be altered and the rocking curve recorded as a function of wavelength. If the black-box, double reflecting, monochromator is used the vertical displacement of the beam alters very little making this experiment very straightforward, especially as all the relevant axes, including the detector arm, are motorised. Such rocking curves were recorded over the range  $0.8 \text{ \AA}$  to  $2.0 \text{ \AA}$  at intervals of  $0.2 \text{ \AA}$  and a selection of these are shown in fig. 6.4. As the wavelength is reduced the overall width of the rocking curve decreases, as expected from the differential of the Bragg equation. The half width of the central substrate peak would be expected to decrease with



decreasing wavelength since, for a flat crystal it is directly proportional to the wavelength, but is, instead, observed to increase for the curves below 1 Å. This effect will be due to the increased effect of bulk sample curvature as the Bragg angle is decreased. When finding the reflection with the TV detector the peak can be observed to sweep across the sample due to its curvature and this displacement as a function of the rotation angle can be used to estimate the curvature. Fine detail present in the rocking curves at the longer wavelengths also becomes increasingly blurred out at the shorter wavelengths due to this effect. The ratio of integrated intensity under the layer and substrate peaks changes as a function of both the absorption coefficient and the X-ray path length within the layer, giving a maximum corresponding to the Ga absorption edge. Values of this ratio as a function of wavelength are given in Table 6.1.

Using the composition variation determined from the rocking curve at 1.54 Å computed curves were calculated at each wavelength and are also shown in fig. 6.4. Agreement between these curves and the experimental curves is reasonably good, with better matching obtained at the longer wavelengths. At the shorter wavelengths the same sized X-ray beam will intercept a larger area of the sample making the rocking curve more susceptible to area variations in both thickness and composition. However, for all the wavelengths used better fits could not be obtained by

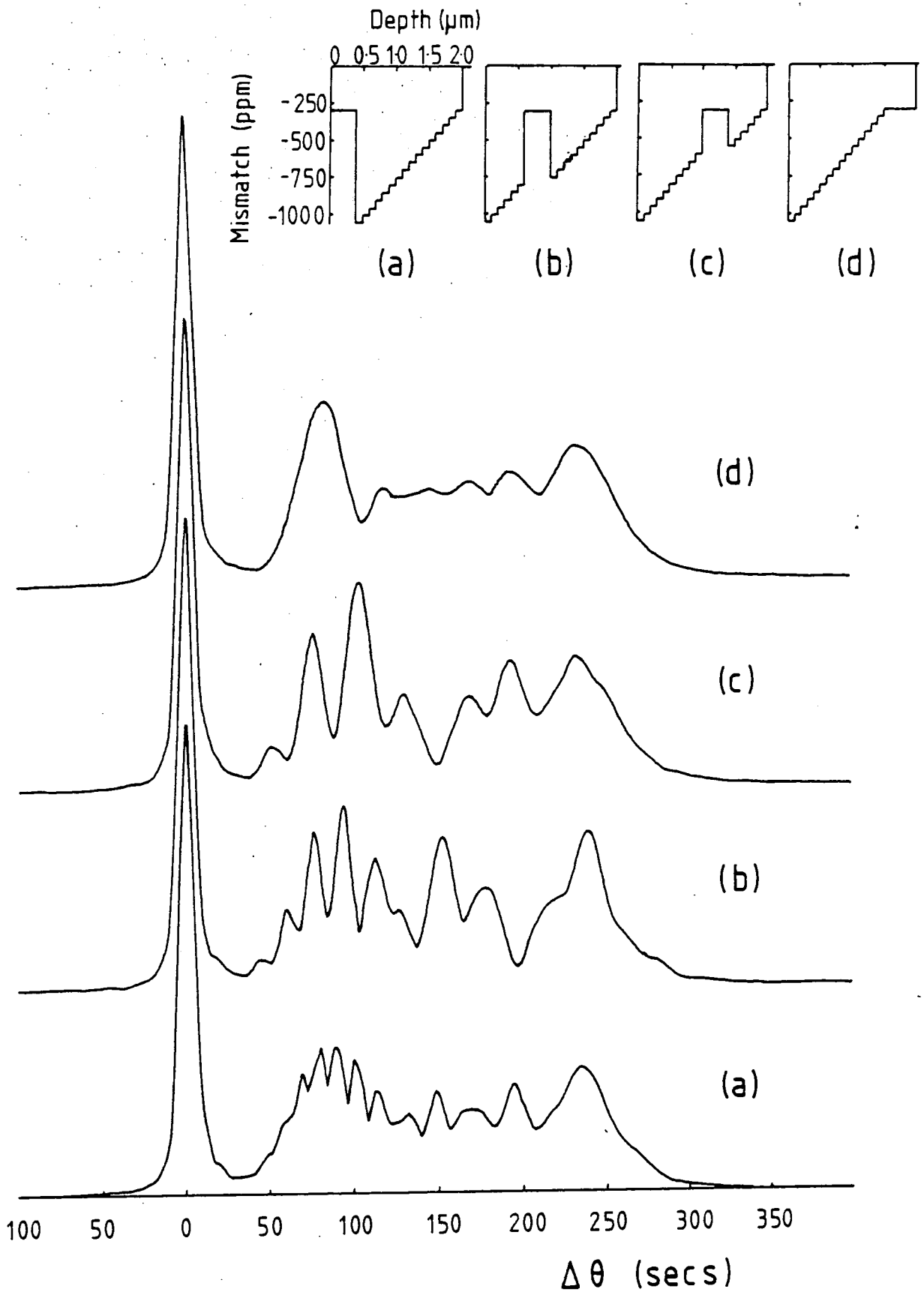


Fig. 6.5 Theoretical 004 rocking curves for a GaInAs graded layer with a  $0.4 \mu\text{m}$  region of  $-300 \text{ ppm}$  mismatch at different depths within the layer. The total layer thickness is  $2.0 \mu\text{m}$  and the composition variations used are shown in the insets. The wavelength used is  $1.5\text{\AA}$ .

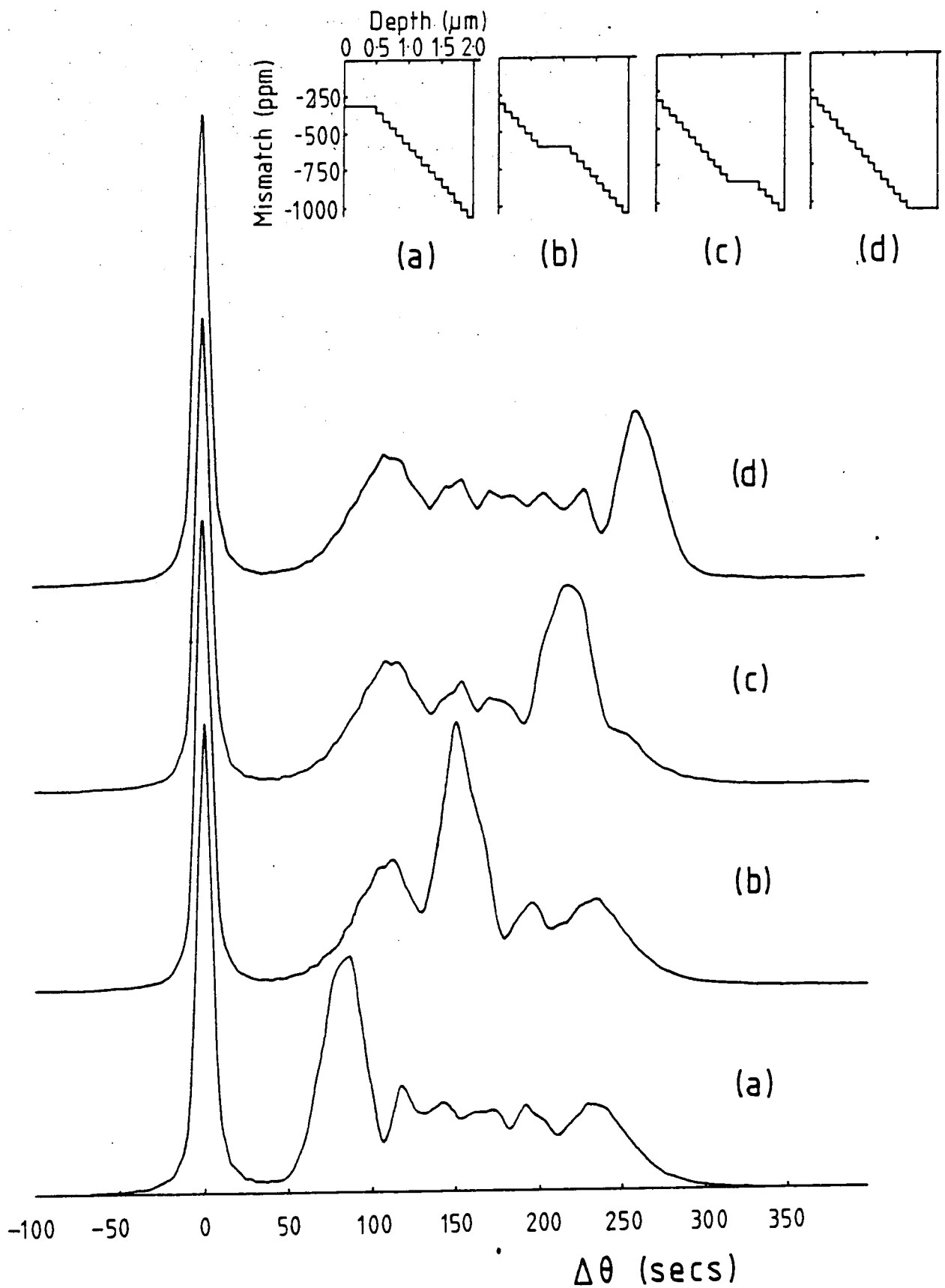


Fig. 6.6 Theoretical 004 rocking curves for a GaInAs graded layers with a  $0.4 \mu\text{m}$  region of constant mismatch at different depths, as shown in the insets. The total layer thickness and overall mismatch range is the same as that in fig. 6.5. The wavelength used is  $1.5\text{\AA}$ .

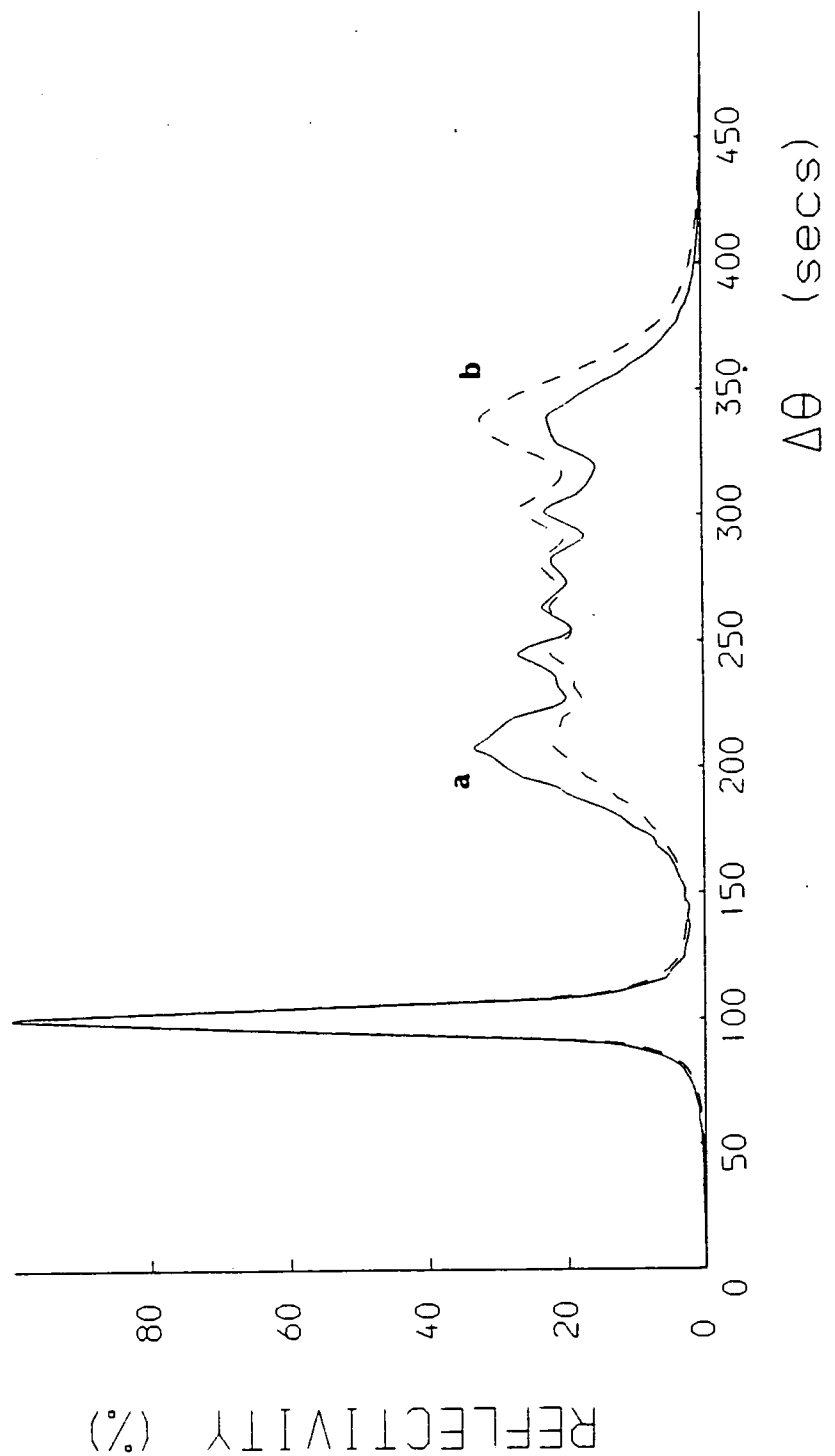


Fig. 6.7 Theoretical 004 rocking curves for a 2.0 μm thick GaInAs graded layer with a mismatch range of -1050 ppm to -300 ppm. The two curves are for the composition variation reversed, i.e. (a) is for -300 ppm at the surface and -1050 ppm at the interface and (b) for -1050 ppm at the surface and -300 ppm at the interface. A linear composition variation is used.

assuming a different composition variation or layer thickness, confirming the use of a single rocking curve to determine these parameters.

TABLE 6.1

Values for the ratio of the areas under the layer and substrate peaks for the experimental curves for a range of wavelengths.

Wavelength (Å) (±0.02)	Ratio of areas under layer and substrate peaks (±0.05)
0.8	1.32
0.9	1.53
1.0	2.50
1.1	3.21
1.2	2.91
1.3	2.21
1.4	1.77
1.5	1.85
1.8	2.36

Polarisation experiments similar to those performed with a single uniform layer were also carried out. Even with a highly perfect InP crystal as the first crystal no effects could be observed that could be ascribed to the polarisation change, although significant modifications were predicted theoretically.

The rocking curve is extremely sensitive to the composition variation used as is demonstrated by the rocking curves shown in figs. 6.5, 6.6 and 6.7. In fig. 6.5 a region of constant composition, 0.4  $\mu\text{m}$  thick and -300 ppm mismatched, has been positioned at different depths in a linearly graded layer in which the mismatch varies from -300 ppm at the interface to -1050 ppm at the surface. As can be

seen, the shape of the rocking curve is extremely sensitive to the position of the constant region, while the wedge shape with a nearly level top is no longer produced. Consequently, it is obvious that a smooth variation in lattice parameter does not exist in the layer. Further, if such a region was known to exist within the layer its position in the layer could be determined. It would be expected that increasing the depth of the constant layer would reduce its effect on the rocking curve just from a consideration of absorption, however, even increasing its thickness to compensate for this effect will not restore the original shape due to the phases of the beams from each laminae also being affected. Fig. 6.6 shows the effect of including a region where the composition remains constant at different depths in a graded layer. The mismatch of the layer varies from -1050 ppm mismatch at the interface and -300 ppm at the surface. Again the layer peak is particularly sensitive to the position of the constant region and the differences when this region is next to the surface or next to the interface are very marked. Further, fig. 6.7 shows the effect on the rocking curve on having the linear grading reversed. The solid curve shows the rocking curve when the mismatch at the interface is -1050 ppm and at the surface is -300 ppm while the broken curve is for -300 ppm at the interface and -1050 ppm at the surface. The curves are completely different in shape and, consequently, from the rocking curves there can be no doubt as to the sign

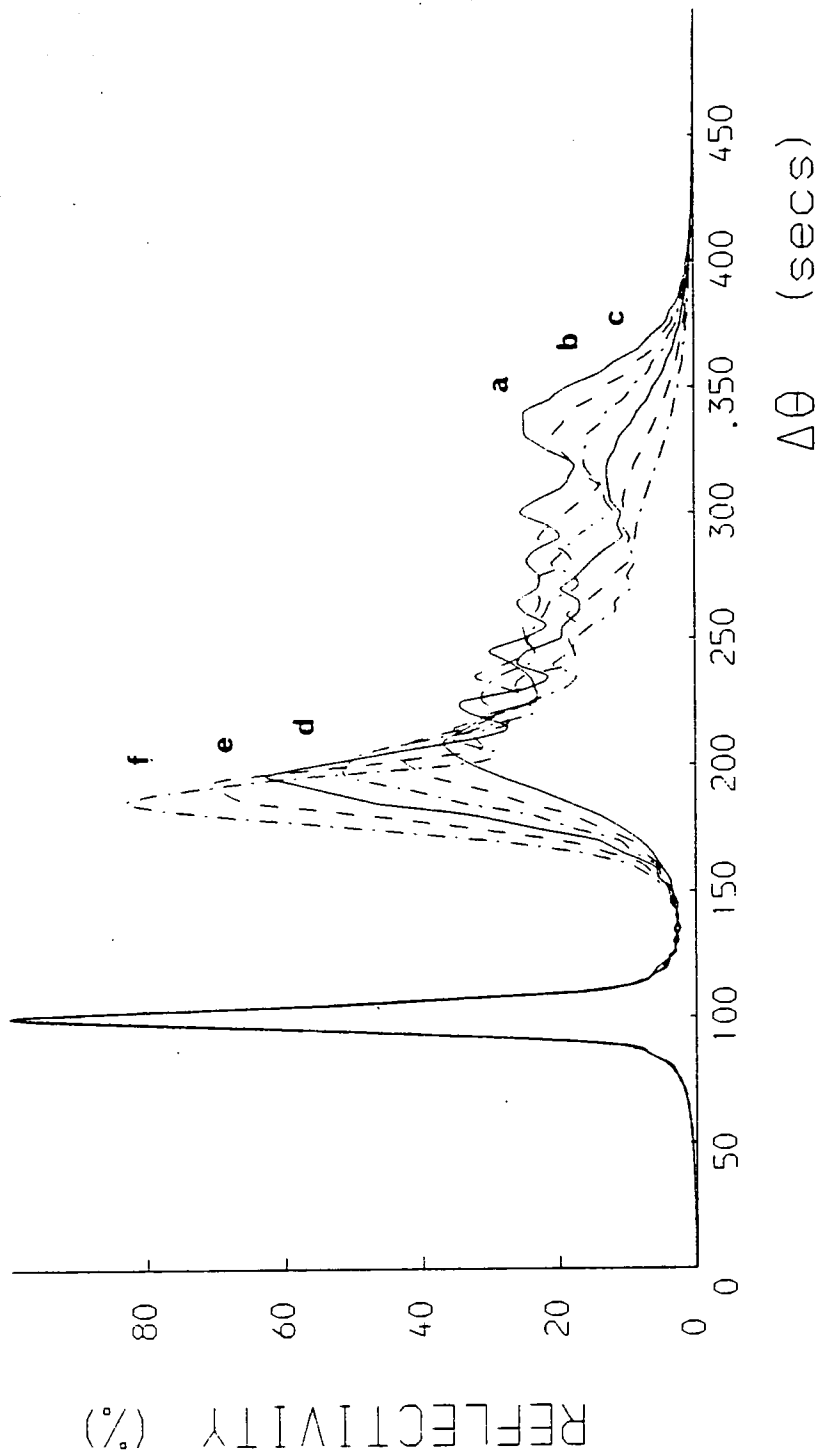


Fig. 6.8 Theoretical rocking curves for the same composition range as in fig. 6.7 with increasing non linearity, giving a greater range of change at the interface. The curves are for (a) linear (b) 20% (c) 40% (d) 60% (e) 80% and (f) 100% non linearity. 100% non linearity corresponds to an elliptical variation which is perpendicular at the intersection with the axes.

of the composition gradient. Some degree of mirror symmetry does exist between the two curves, as might be expected. However, differences do exist between one curve and the mirror image of the other.

Additionally, fig. 6.8 shows the affect of increasing the non linearity of the composition change. The mismatches used are -1050 ppm at the interface and -300 ppm at the surface, for a 2.0  $\mu\text{m}$  layer, and in each consecutive curve the variation is further from linearity. The slope of the top of the wedge-like layer peak is rapidly increased as the rate of change of composition next to the interface is increased and, for the high non linearity curves, the shape approaches that of a single peak with an extended tail on the high angle side. Consequently, if a composition variation can be found that gives a rocking curve that agrees well with the experimental one such a variation can be taken to be a good measure of the actual variation. This same assumption has been extensively used in the characterisation of ion or diffusion implanted layers by rocking curves, as discussed in Chapter 2.

A series of closely related VPE grown GaInAs ternary layers, on (001) InP substrates, have also been studied. In addition to measuring the rocking curves these samples were electrically characterised at British Telecom Research Laboratories. Lang topographs were also recorded to determine the presence of mismatch dislocations that would indicate an incoherent interface.



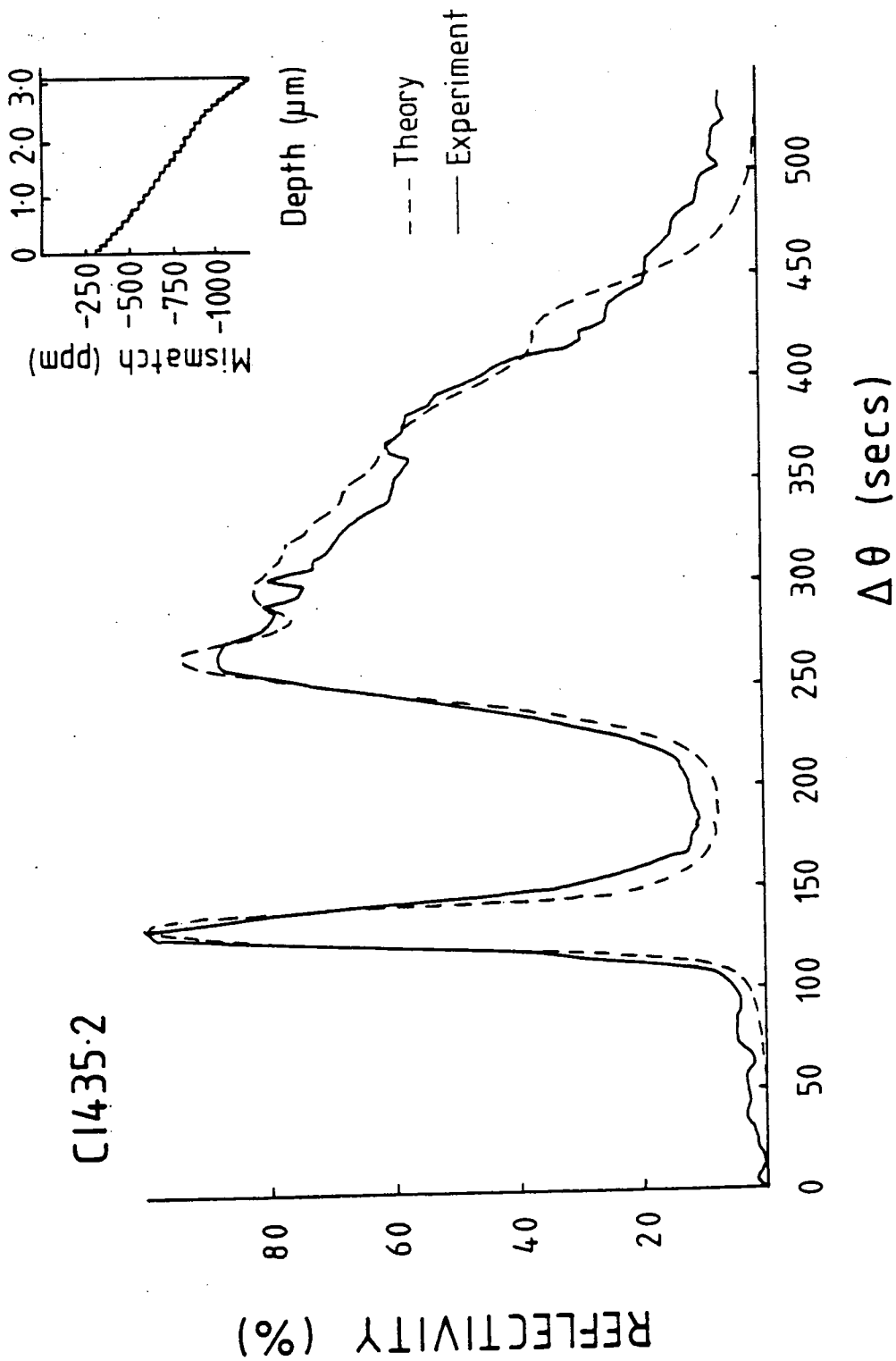
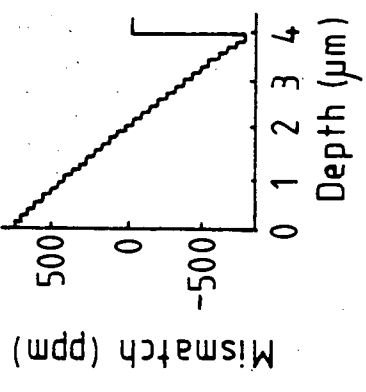
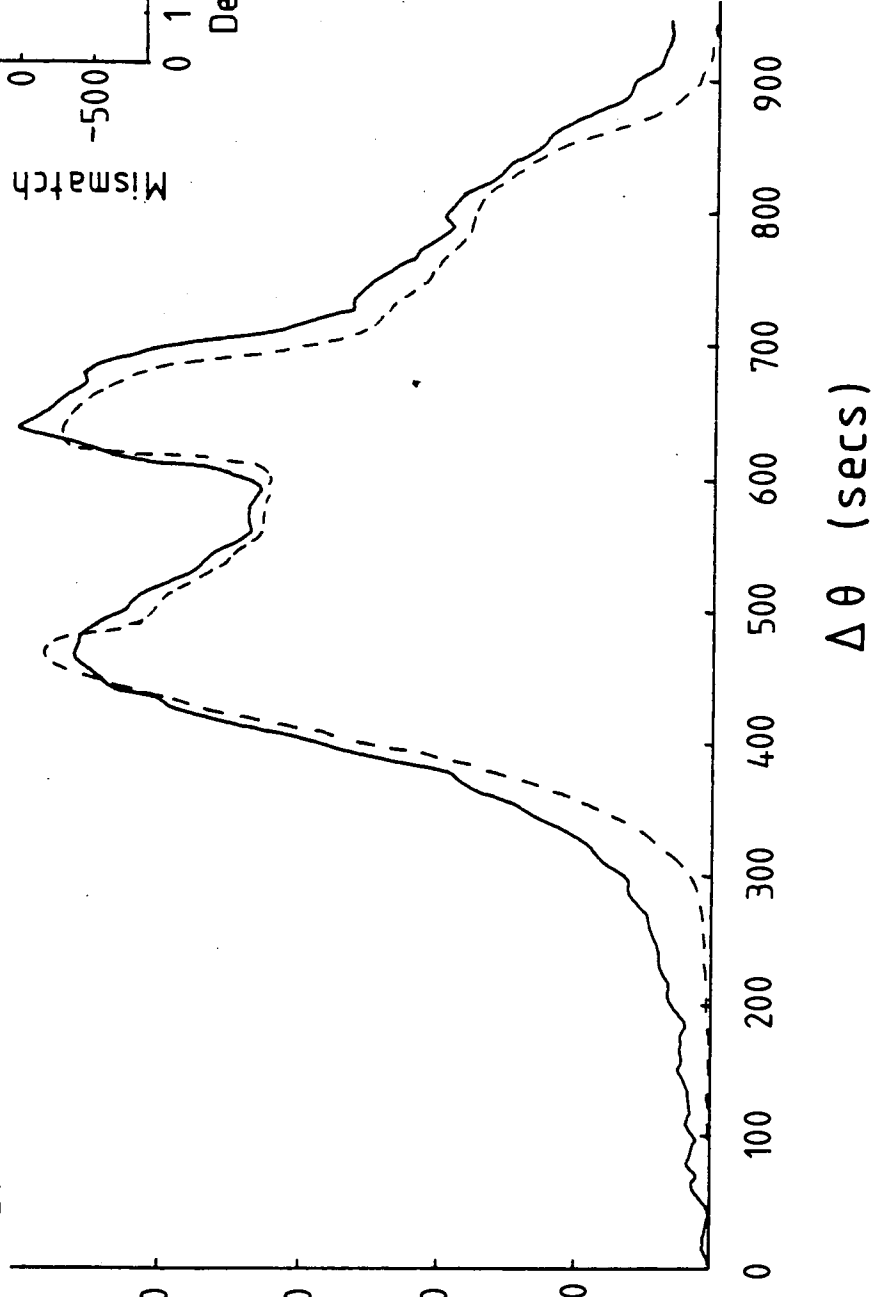
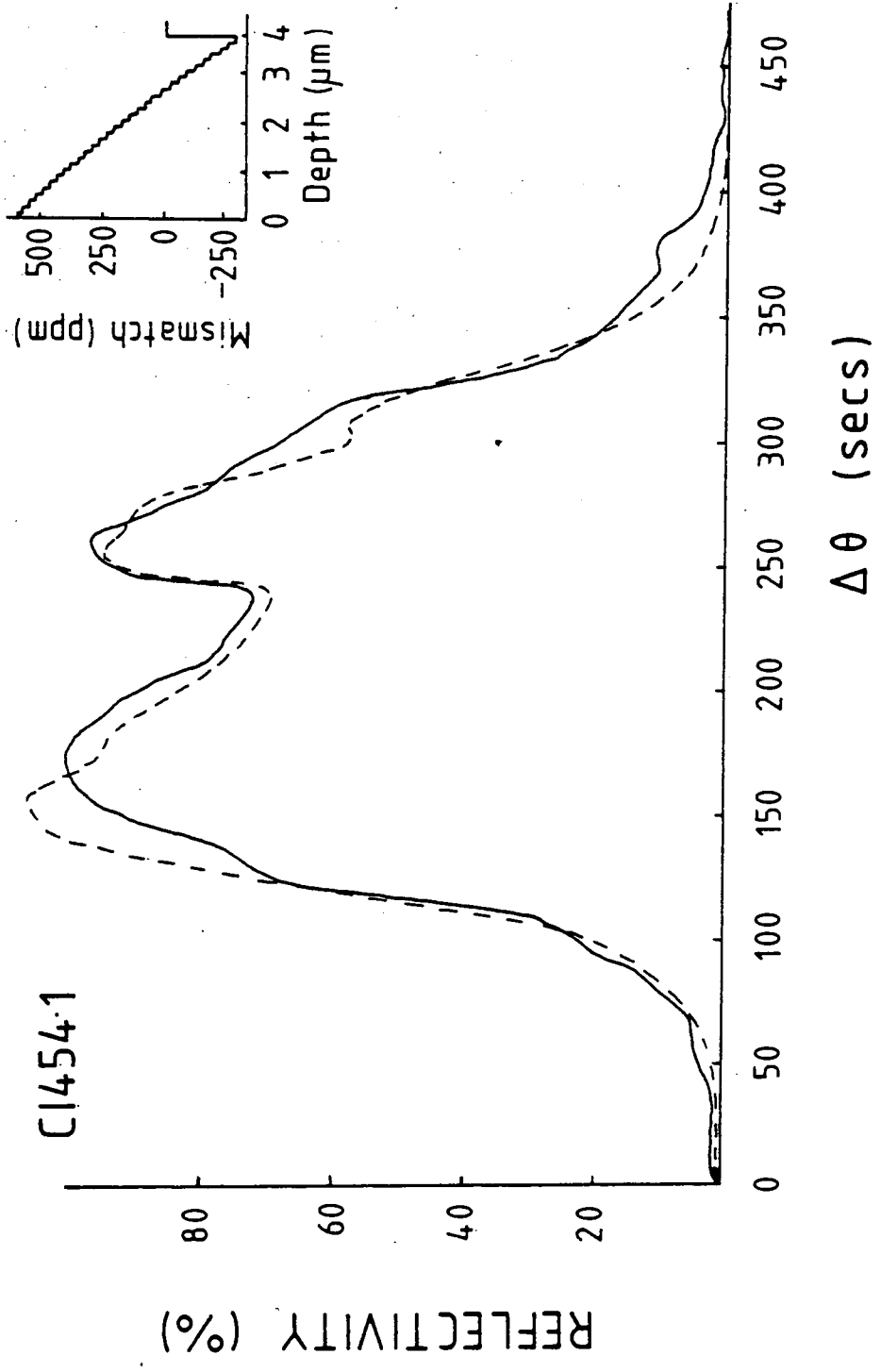


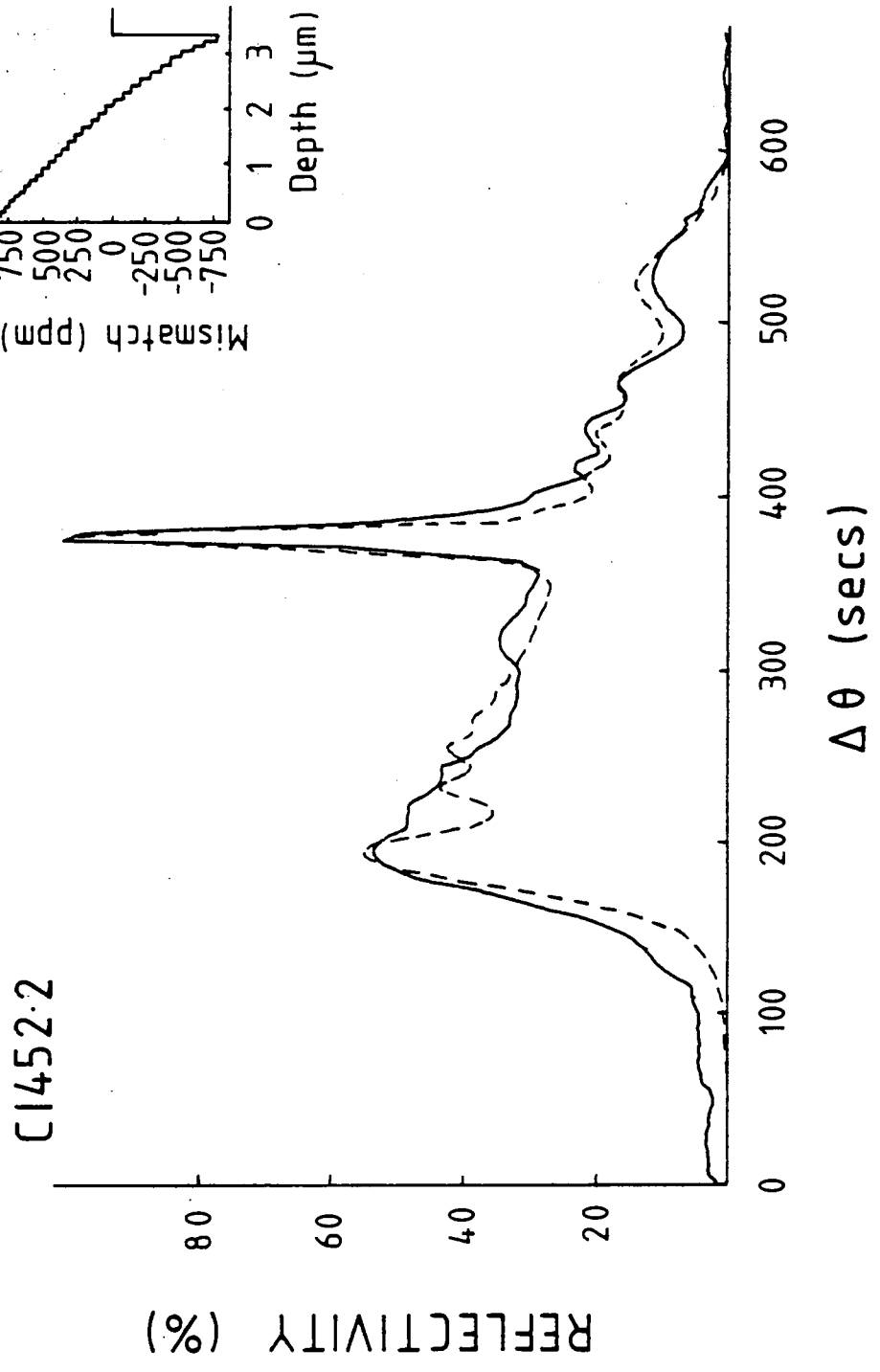
Fig. 6.9 004 experimental and computed rocking curves for a number of GaInAs graded layers, grown by VPE on a (001) InP substrate. The composition variations used to give the computed curves are shown in the insets. All rocking curves were recorded with  $\text{CuK}\alpha_1$  radiation.

C1456.2

REFLECTIVITY (%)

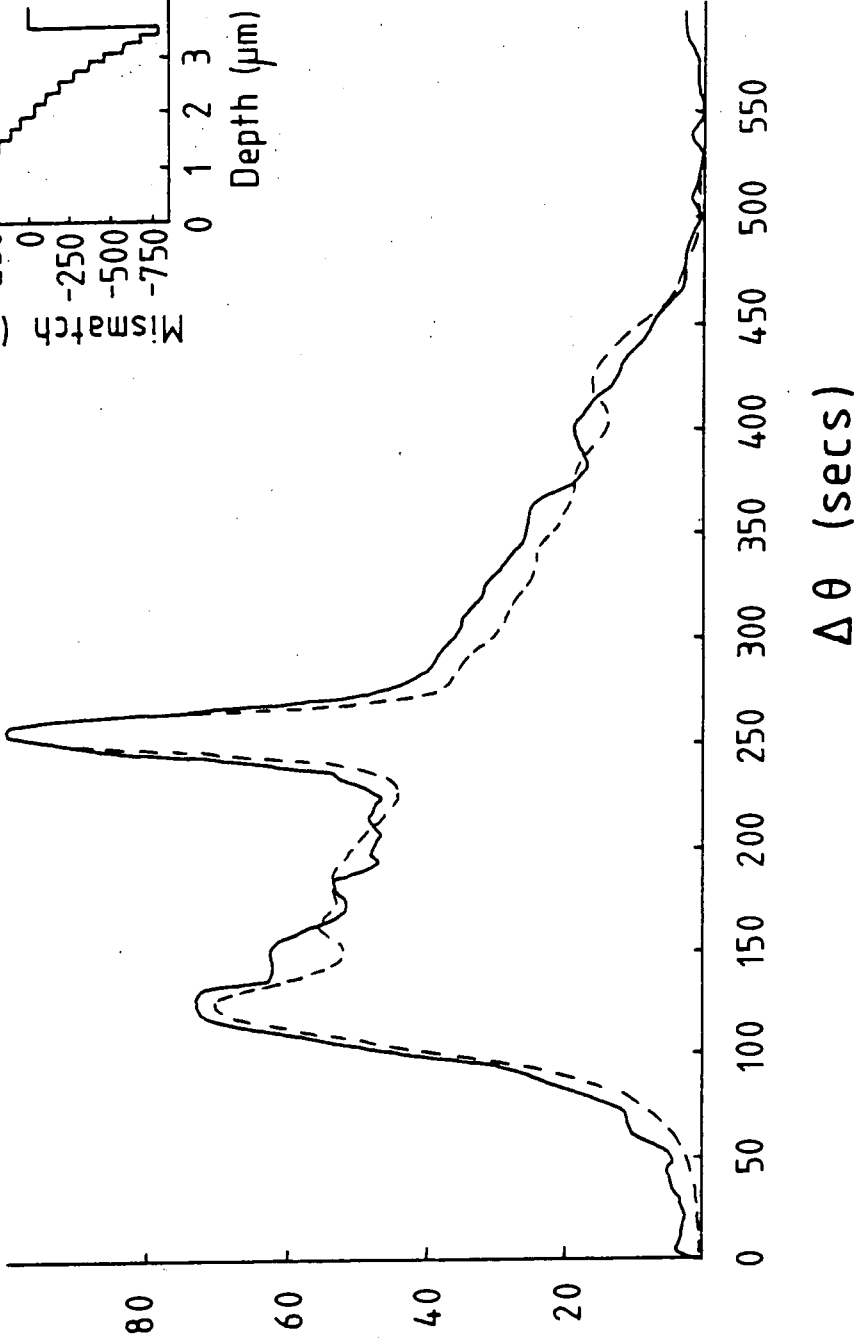






C1454.2

REFLECTIVITY (%)



C1436.2

REFLECTIVITY (%)

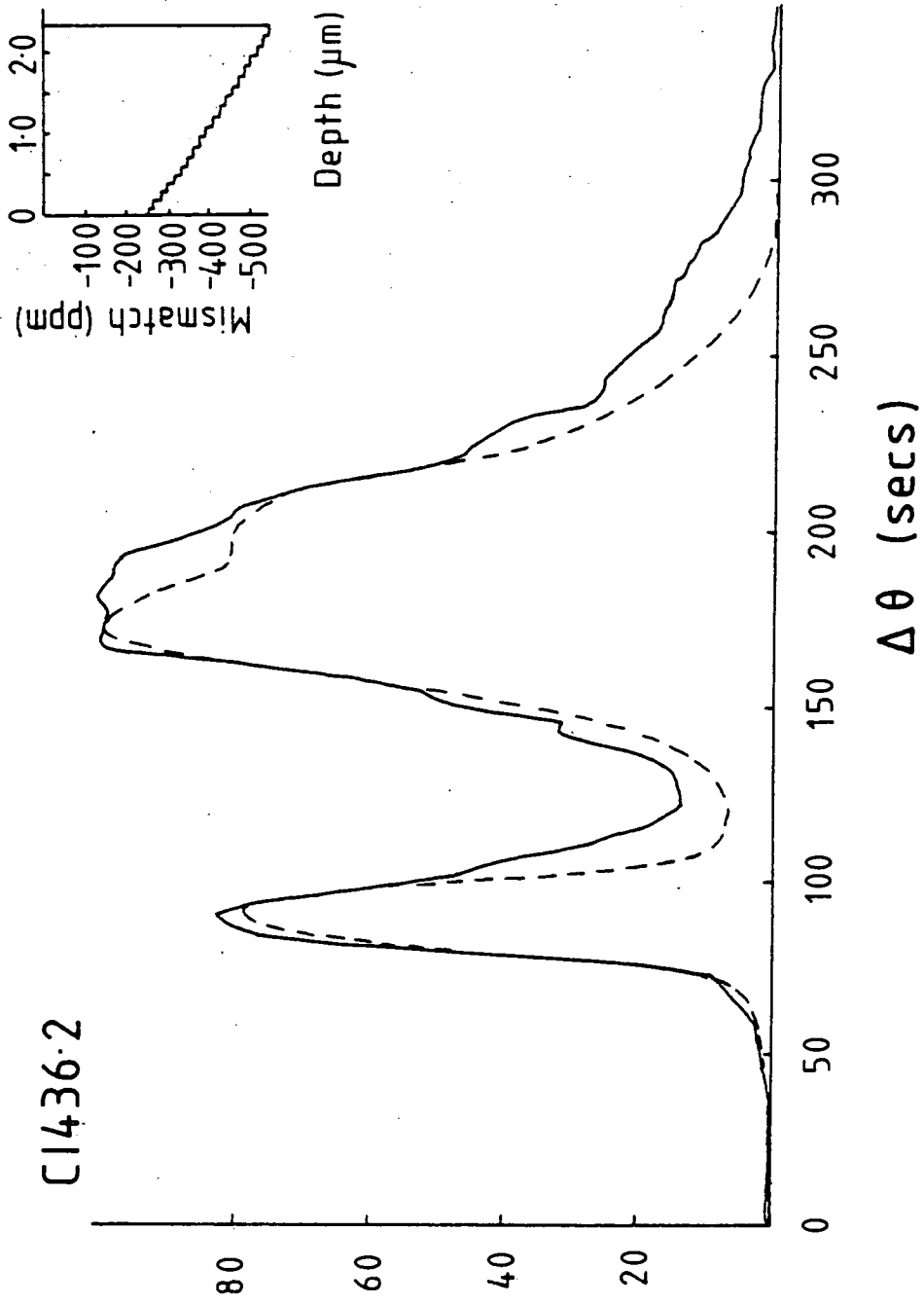


Fig. 6.9 shows the double crystal 004 rocking curves for these samples, recorded with  $\text{CuK}\alpha_1$  radiation and an InP first crystal. There is a very wide variation in the shapes of these rocking curves with two samples in particular giving very broad substrate peaks. All of the curves exhibit a very broad layer peak indicative of a graded layer. Computed rocking curves found to best fit these curves are also shown in fig. 6.9 for comparison, the mismatch variations as a function of depth are shown in the inset in each figure.

The rocking curve from sample CI452.2 shows a narrow, central substrate peak close in half width to the theoretical value. Considerable fine detail is present in the layer peak, although not as much as in the computed curve which does agree reasonably well with the experimental curve. This sample does contain mismatch dislocations which will reduce the overall sample curvature, as shown in Chapter 1, consequently reducing the broadening of the substrate peak and the blurring out of the fine detail. The mismatch variation determined shows some deviation from linearity, with an increased rate of change near to the interface. However, due to the presence of the mismatch dislocations the composition range deduced will not be accurate.

The central substrate peak in the rocking curve from sample CI454.2 is again fairly narrow and only slightly broader than the theoretical value. This sample does not

contain any mismatch dislocations which will reduce the sample curvature. However, since the composition range gives lattice parameters both larger and smaller than that of the substrate the curvature will be reduced as the two regions will produce curvature in the opposite sense. The computed curve does fairly well with the experimental curve, again giving a composition variation that changes more rapidly towards the interface. Fine detail is present in both curves due to the reduced effect of sample curvature.

In the rocking curves from both CI436.2 and CI435.2 the substrate and layer peaks are well separated, with the lattice parameter of the layer always smaller than that of the substrate. The curve from sample CI436.2 is rather unusual in shape, with a flat top on the low angle side followed by a steeply sloping tail on the high angle side. The calculated curve does not agree particularly well with the experimental one, with the flat topped region proving difficult to simulate. Also the extended high angle tail is less intense than in the experimental curve which would suggest that the layer thickness is larger than that determined by matching the heights of the maximum of the layer peak and the substrate peak. The composition variation determined is close to linear. The layer peak from sample CI435.2 is again rather unusually shaped. It is close to a wedge shape but appears to have some extra intensity in the centre and has a steeper slope on the high angle side of this 'bulge'. This would suggest that two different rates



of change of composition are present and the computed curve, which agrees fairly well with the experimental one, does confirm this. The composition variation determined can almost be divided into two regions of linear variation, with a more rapidly varying section next to the interface. This sample contains a large number of threading dislocations hindering the determination of the presence of mismatch dislocations.

Both the rocking curves from samples CI456.2 and CI454.1 show very broadened central substrate peaks and no fine detail is visible in either curve. Sample CI454.1 contains a large number of mismatch dislocations and sample CI456.2 contains so many threading dislocations that the presence of mismatch dislocations could not be determined. Consequently, we would expect fine detail in both curves to be blurred out with the broadened substrate peaks due to a small radius of curvature. Computed curves that agree fairly well with these experimental curves could be found after including this sample curvature, with both requiring a nearly linear composition variation with slightly greater rates of change near to the interface.

A summary of both the X-ray and electrical results is shown in Table 6.2. There does appear to be some correlation between the presence of mismatch dislocations and the dark current. The composition ranges given in the table are those determined from the rocking curves. Generally, the layer thicknesses found from the simulated

rocking curves were found to agree fairly well with those obtained from the electrical measurements. For all the samples composition variations close to linear were found to give computed rocking curves that agree reasonably well with the experimental ones, with many requiring a greater rate of change near to the interface, ie at the start of growth.

These results confirm that the computer simulation of rocking curves, as a best fit to the experimental ones, is an extremely valuable technique for the determination of the composition variation with depth for graded layers. No other technique can match the sensitivity to the composition achieved with this X-ray method. However, due to this high sensitivity and, additionally, sample curvature and defect density, it is not straightforward to achieve good agreement between the computed and experimental rocking curves as there are many parameters to alter.

TABLE 6.2  
SUMMARY OF X-RAY AND ELECTRICAL CHARACTERISATION OF VPE GROWN SAMPLES

SAMPLE	CI435.2	CI454.1	CI454.2	CI436.2	CI452.2	CI456.2
Mismatch Network	?	yes	no	no	yes	?
Electrical Comment <sup>2</sup>	Quite good	Graded from 2 μm	well behaved	pretty good	v. graded from 1 μm	v. poor
Dark Current <sup>2</sup> (mA/cm <sup>2</sup> )	0.1	2.0	0.17	0.06	0.4	>2
Carrier Conc. <sup>2</sup> (10 <sup>16</sup> )	3	1	2	4	2	3-84
Mismatch at surface (ppm)	-300	650	610	-250	850	750
Mismatch at interface (ppm)	-1250	-300	-800	-550	-780	-800
Indium content range (%)	52.7 - 51.3	54.0 - 52.7	54.0 - 51.9	52.7 - 52.3	54.3 - 52.0	54.2 - 51.9
Layer Thickness (X-ray)	3.15	3.8	3.8	2.35	3.4	4.0
Layer Thickness <sup>2</sup> (Elec.)	4.6	~4	~4	2.8	~4	~4

<sup>1</sup> The ? indicates that the presence of mismatch dislocations could not be determined due to the high density of threading dislocations.

<sup>2</sup> These results were provided by British Telecom Research Laboratories.

## CHAPTER 7

### MULTIPLE AND MULTILAYER STRUCTURES

Multiple layer structures, especially multiquantum well structures, are probably one of the most important types of structures for device applications with the majority of devices being developed consisting of more than one layer. Clearly, there is little difference in calculating the complete rocking curve for these structures from calculating the curves for graded layers. Here the layers used in the calculation are the actual physical layers existing in the structure.

Even for a small number of layers great care needs to be taken in the interpretation of the rocking curves. The number of peaks observed will very rarely reflect the number of layers present, with both greater or smaller numbers of peaks than layers possible. This is illustrated by the 004 theoretical curves shown in fig. 7.1, for an increasing number of subdivisions of a GaInAs layer into layers of alternating composition, keeping the total layer thickness and the average mismatch constant. The radiation used is  $\text{CuK}\alpha_1$ , with an InP first crystal. The two layer mismatches used are -500 ppm and -1000 ppm, corresponding to compositions of  $\text{Ga}_{47.6}\text{In}_{52.4}\text{As}$  and  $\text{Ga}_{48.4}\text{In}_{51.6}\text{As}$ . For curve (a), consisting of one pair of such layers each of thickness  $0.5 \mu\text{m}$ , two peaks are formed as expected. In addition, low intensity Bragg case Pendellosung oscillations

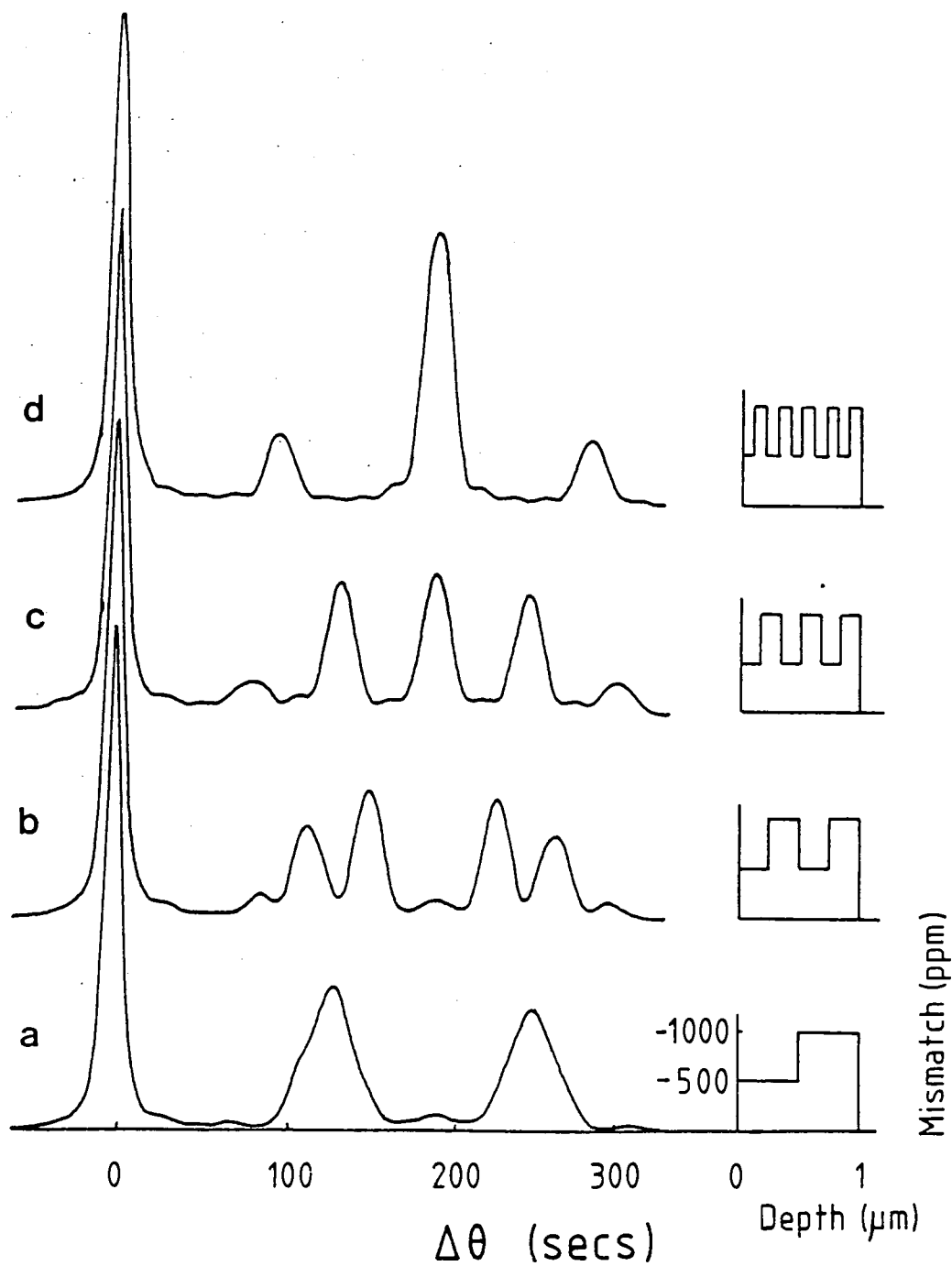


Fig. 7.1 004 theoretical curves with  $\text{CuK}\alpha_1$  radiation for an increasing number of subdivisions of a  $1\ \mu\text{m}$  GaInAs layer into alternating layers of  $-500\ \text{ppm}$  and  $-1000\ \text{ppm}$  mismatch. The curves are for (a) 2 layers, (b) 4 layers, (c) 6 layers and (d) 10 layers. The mismatch variations are shown in the inset.

are visible. For the second curve, (b), for a sample consisting of two such pairs of layers, with individual layer thicknesses of  $0.25 \mu\text{m}$ , there are now four peaks visible in the rocking curve. This is not expected as only two compositions are present in the layer and arises because of the phase differences between the beams from each layer. The angular position of the peaks are different from those in curve (a), the peaks in each pair being on either side of the two peaks in curve (a). This suggests that some degree of destructive interference has occurred at the Bragg angle corresponding to the composition of the two layers. Again weak oscillations are present between and either side of the two pairs of peaks.

As the number of subdivisions is increased to three pairs, as in fig. 7.1(c), the peaks produced are again greatly different from those in the preceding curves. Now three main layer peaks are produced, the central peak in a position exactly midway between the peaks of curve (a). The outer two peaks correspond to the peaks in curve (a), although they are somewhat narrower. Also present in this curve are the beginnings of two satellite peaks either side of the three main peaks.

When the layer has been divided into 5 pairs, as in curve (d), the central peak has developed to be clearly the most intense of all the peaks from the layer. Two satellite peaks on either side of the main peak, equispaced from it, are clearly visible. Their separation is determined by the

thickness of the repeat unit of the pairs of layers within the layer. As the number of divisions are further increased this same pattern of peaks is continued, ie a central peak and satellite peaks. This is the predicted behaviour of a superlattice, as described in Chapter 2. The central peak is referred to as the zeroth order peak and its displacement from the substrate peak gives the average composition of the layer. The two satellite peaks seen in curve (d) are referred to as the +1 and -1 peaks, with positive indices being on the high angle side of the zeroth order peak. Higher order, weaker satellite peaks, again equispaced from the zeroth order peak, will also be produced.

If the superlattice period is considered as a lattice spacing, the peaks correspond to different orders of reflection from this lattice at the wavelength used. Clearly, the satellite peaks will be symmetrically spaced about the zeroth order peak, not from the substrate peak. Therefore, their separation can be used to determine the superlattice period. As more subdivisions are made, more higher order satellite peaks will become visible. The relative intensities of the satellites will depend on the particular structure of the superlattice. Additionally, since superlattices can be constructed of any combination of binary, ternary, quaternary or higher alloys, its average composition will vary not only as a function of the relative thicknesses of the layers but also as a function of the composition of the individual layers. For example, for a

$n_1$ -GaAs/ $n_2$ -AlAs superlattice, where  $n_1$  is the number of monolayers in each layer, the separation of the substrate and zeroth order peaks will depend only on the ratio  $n_1:n_2$ , but for a  $n_1$ -Ga $_{1-x}$ Al $_x$ As/ $n_2$ -GaAs superlattice it will also depend on the value of  $x$ .

Since the individual layers forming the superlattice are usually very thin compared to the extinction distance, the kinematical theory of X-ray diffraction has been extensively used to calculate the satellite intensities, see Chapter 2. However, many of the superlattices have relatively thick buffer layers grown either between the substrate and superlattice or as a cap on top of the superlattice or even in both positions. If this buffer is of a similar composition to that of one of the components of the superlattice the position and/or intensity of the zeroth order peak will be affected. Consequently, an approach based on the dynamical diffraction theory is required and has been used throughout the calculations presented here. For a perfectly periodic superlattice, in which all of the repeat periods are identical, the diffracted intensity calculation can be simplified according to the scheme of Vardanyan, Manoukyan and Petrosyan (1985) and the computational approach is no longer required. However, if imperfect superlattices are to be considered the computational approach must be used.

If the growth of a superlattice is considered, in which the interfaces between the individual layers are perfectly



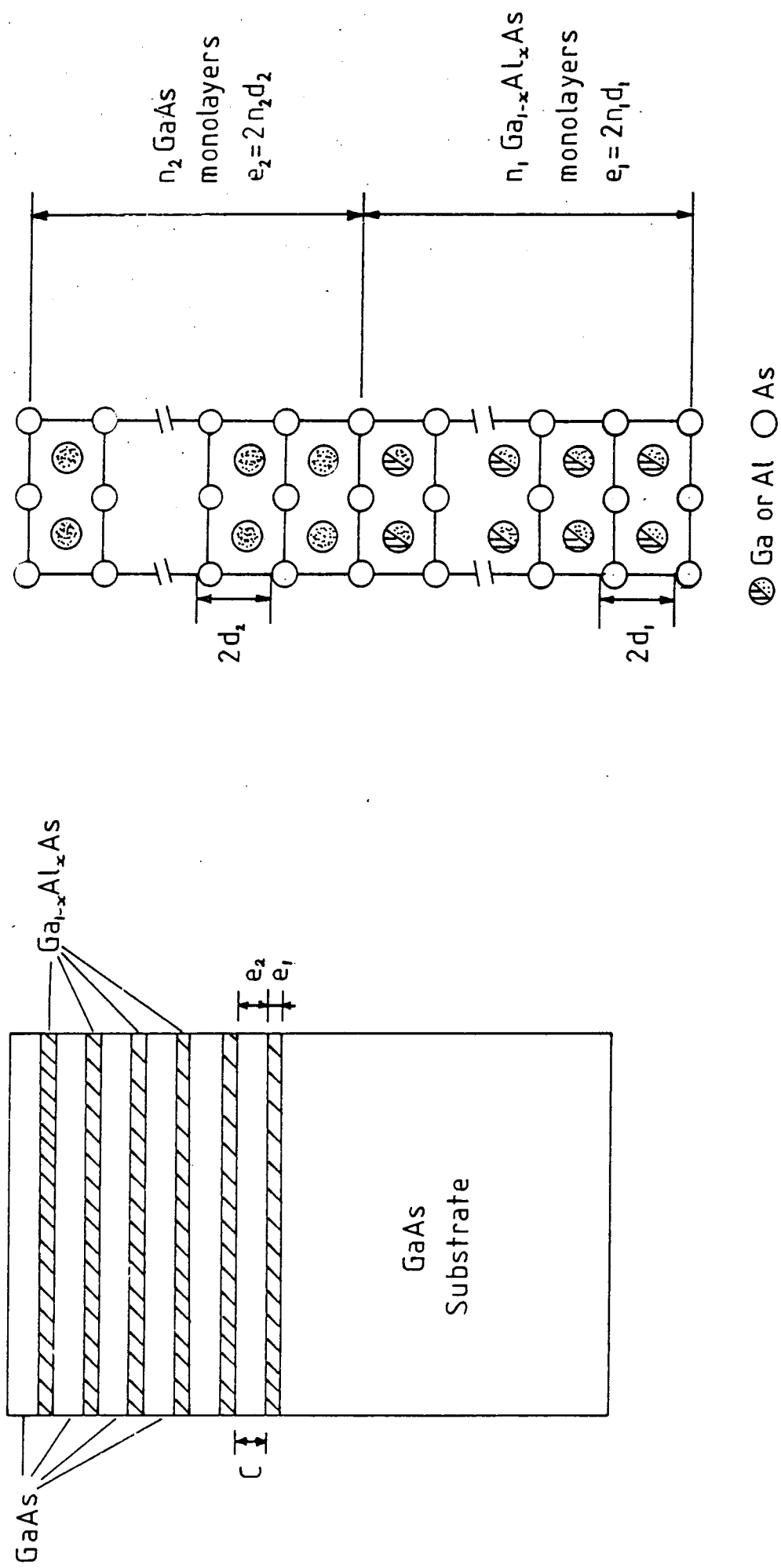


Fig. 7.2 The macroscopic and microscopic construction of a GaAlAs/GaAs superlattice. The individual layers are an integer number of monolayers which is half a unit cell.

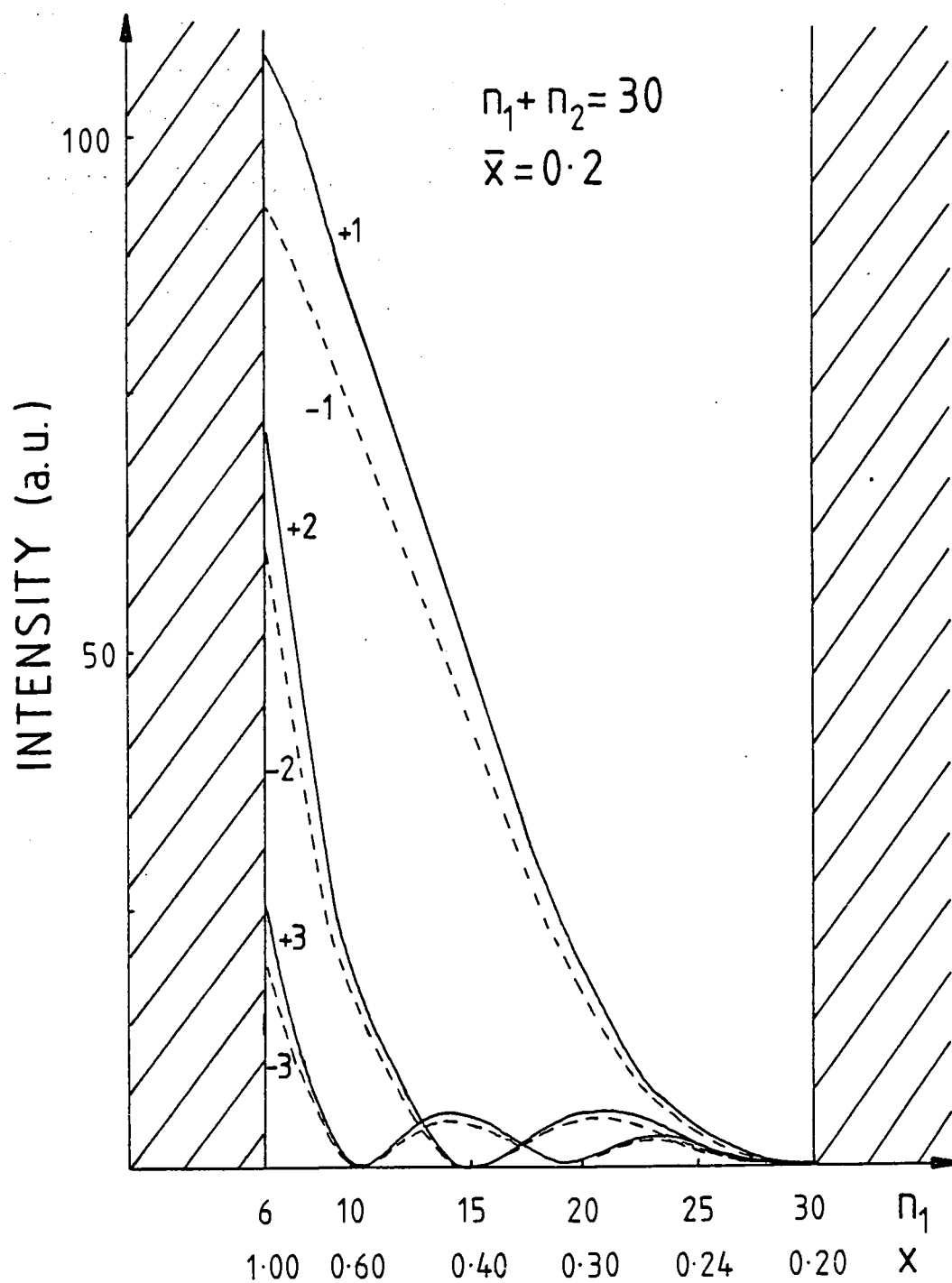


Fig. 7.3 Satellite intensities for the 002 reflection from a  $n_1\text{GaAlAs}/n_2\text{GaAs}$  superlattice as a function  $n_1$  with  $n_1 + n_2$  constant and  $\bar{x}$  constant.

sharp, the structure formed on an atomic scale will be similar to that shown in fig. 7.2. Each layer must be an integer number of monolayers and not necessarily an integer number of unit cells. One monolayer is half a unit cell for a III-V compound. Hence, the individual layers are considered as  $n_1$  monolayers throughout the calculations. In the computer programme the section that allows the automatic entry of multiquantum well layer parameters works in terms of monolayers and calculates the individual layer thicknesses from this number and the lattice parameter, taking into account tetragonal distortion if required.

For a  $n_1$ -Ga<sub>1-x</sub>Al<sub>x</sub>As/ $n_2$ -GaAs superlattice, grown on a (001) GaAs substrate, the satellite intensities as a function of  $n_1$  and  $n_2$ , with  $n_1+n_2$ =constant, are shown in fig. 7.3 for the 002 reflection. From this graph we note that the  $i$ -th order satellite peak has zero intensity when  $i=k(1+n_1/n_2)$ , where  $k$  is an integer. Thus for a superlattice where  $n_1=n_2$  the even ordered satellites will be absent. Also the intensities of different order satellites do not change with the same function of  $n_1:n_2$ , which can be particularly important in the interpretation of rocking curves. Since defects in the periodicity of the superlattice will tend to reduce the intensity of the satellites, particularly the high order ones, the ratio of intensity of just one satellite to the zeroth order peak may give a false indication of the structure of the superlattice. However, by including the ratio of another

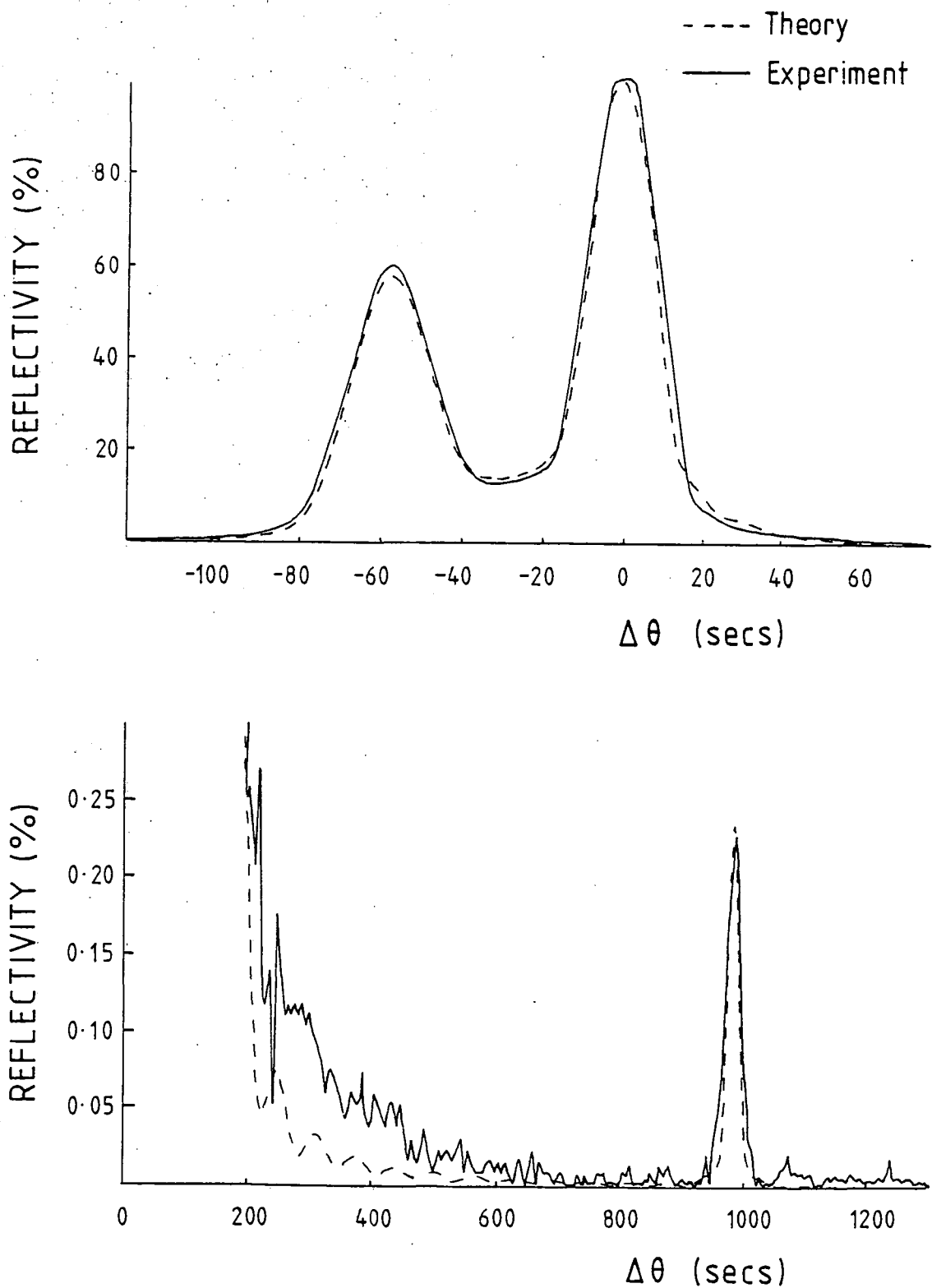


Fig. 7.4 Experimental and theoretical 004 rocking curves from the first  $n_1\text{GaAlAs}/n_2\text{GaAs}$  sample, at 1.54 Å. Curves (a) show the region around the 004 GaAs substrate reflection and curves (b) show the region out to +1200 secs from the substrate reflection and on an expanded vertical scale, revealing the +1 satellite peak. The computed curve is for  $n_1 = 43$ ,  $n_2 = 28$  and  $x = 0.35$ .

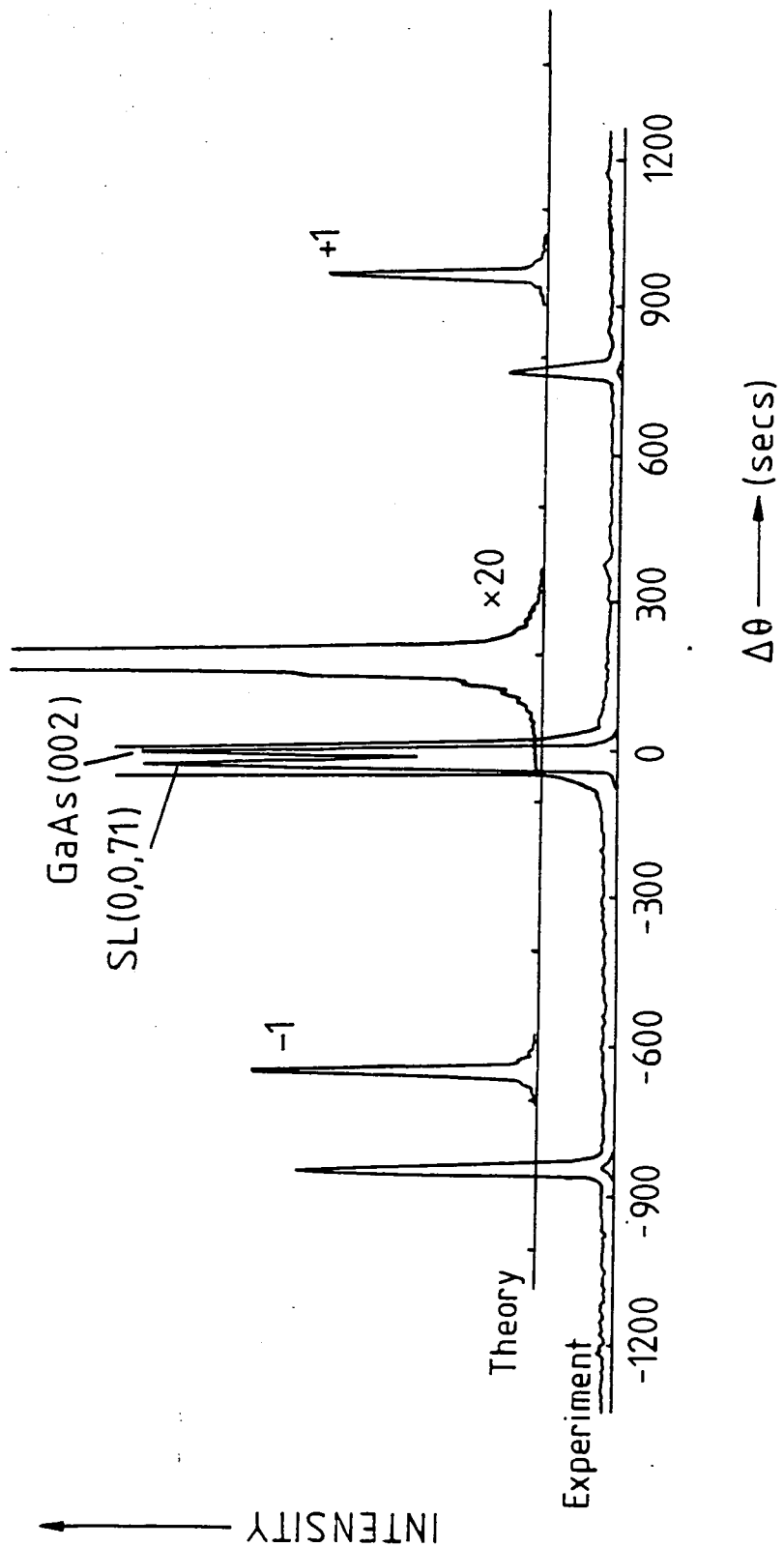


Fig. 7.5 Experimental and computed 002 rocking curves from the same sample used for fig. 7.4. Both the +1 and -1 satellite peaks are easily visible on the vertically expanded scale. The wavelength is 1.5Å.

peak, whose intensity changes as a different function of  $n_1:n_2$ , this error can be reduced.

### 7.1 Experimental Results

Fig. 7.4 shows the 004 rocking curve for a  $\text{Ga}_{1-x}\text{Al}_x\text{As}/\text{GaAs}$  superlattice on a (001) GaAs substrate, grown by MBE. The superlattice consists of 50 repeat units and has a GaAs cap of approximately  $0.3 \mu\text{m}$ . The rocking curve was recorded with  $\text{CuK}\alpha_1$  radiation and an InP first crystal. The zeroth order and substrate peaks are well resolved, but slightly broadened from the theoretical widths due to sample curvature. Only the +1 satellite peak, which is the most intense, could easily be observed and is visible in the expanded region of the curve. No other satellites could be observed near to the 004 GaAs reflection.

Additionally, the 002 rocking curve was recorded at  $1.5 \text{ \AA}$  using the double crystal camera at the SRS and is shown in fig. 7.5. The black-box monochromator was used as the 'first' crystal. Even with the synchrotron source long counting times are needed to provide the extremely good counting statistics required. Consequently, over the recording period the beam intensity decreases due to the decay of the current in the storage ring. Therefore, the incident beam intensity was monitored with an ionisation detector in order that the rocking curve could be compensated for this effect. Because the 002 reflection is a pseudo forbidden reflection for GaAs, being only present

due to the difference in scattering factors of the Ga and As atoms, the presence of Al in the alloy provides a relatively large modulation in the structure factor of the layers. Consequently, the satellite intensities are greater than those near to the 004 reflection and the +1 and -1 satellites are easily visible in the rocking curve.

From the separation of the +1 satellite and the zeroth order peak near the 004 reflection the value of  $L=n_1+n_2$  can be determined. If we label the zeroth order peak as  $2L$  and the +1 peak as  $2L+1$  we have

$$(2L+1)\lambda = 2C\sin\theta_{2L+1} \quad (7.1)$$

and 
$$2L\lambda = 2C\sin\theta_{2L} \quad (7.2)$$

from Bragg's Law, with  $C$  the superlattice period. Thus,

$$\frac{\sin\theta_{2L+1}}{2L+1} = \frac{\sin\theta_{2L}}{2L} \quad (7.3)$$

ie 
$$2L = \frac{\sin\theta_{2L}}{\sin\theta_{2L+1} - \sin\theta_{2L}} \quad (7.4)$$

With the values of  $\theta_{2L}$  and  $\theta_{2L+1}$  determined from the displacement from the substrate peak we find that  $2L=142$ , to the nearest integer value. In fact  $L$  rarely turns out to be an exact integer due to deviations in the periodicity of the superlattice and the nearest value should be taken. With this value of  $2L$  and the absolute position of the zeroth order peak the superlattice period can be determined and is found to be  $C=200.8 \text{ \AA}$ . The zeroth order and +1 peaks can

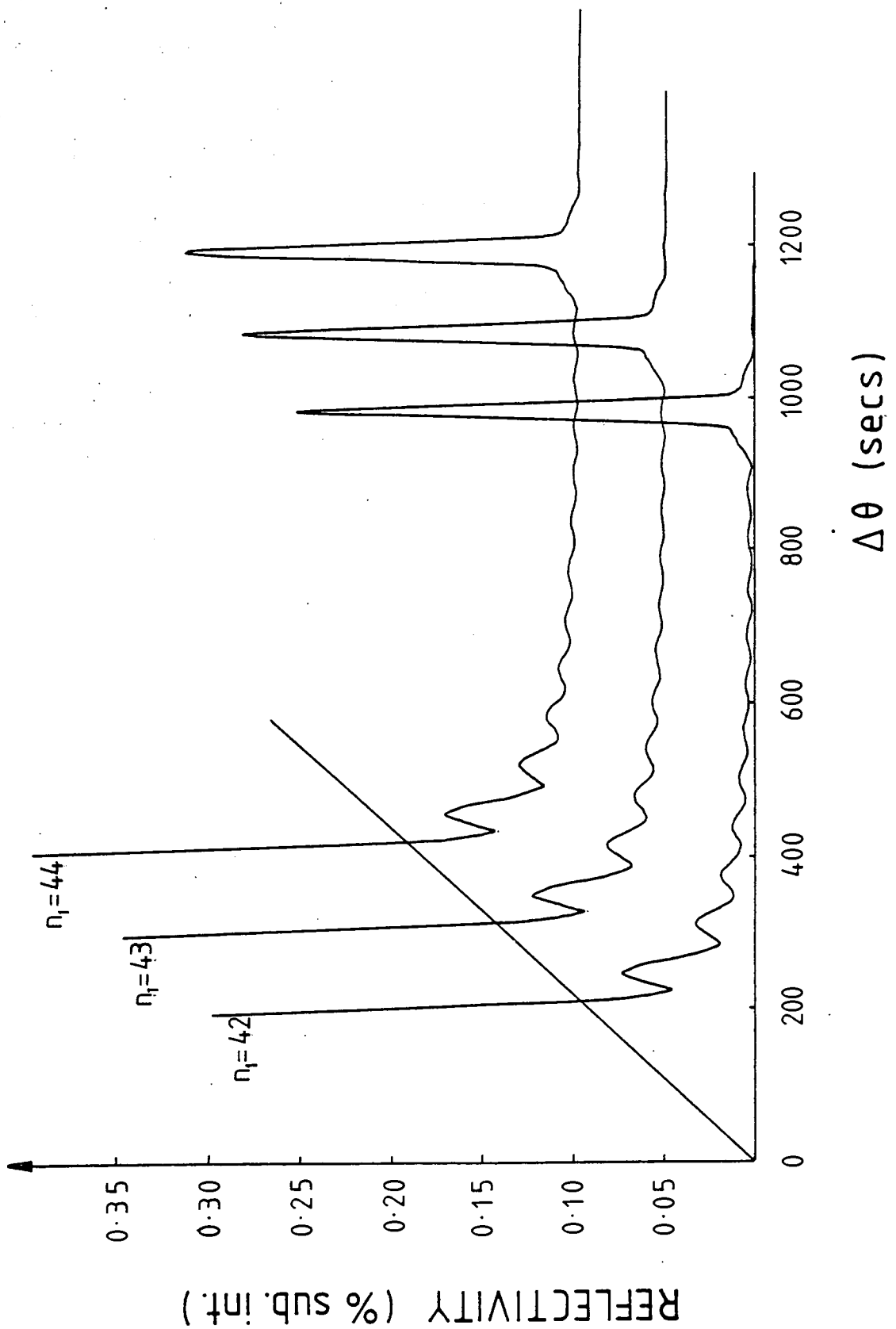


Fig. 7.6 Computed 004 rocking curves for  $\text{CuK}\alpha_1$  radiation for values of  $n_1 = 44, 43$  and  $42$  showing the variation in +1 satellite intensity. The overall parameters are as for the first GaAlAs/GaAs sample.



then be labelled as the (0,0,142) and (0,0,143) reflections from a lattice spacing of 200.8 Å. This value is confirmed from the spacing of the +1 and -1 satellites near to the 002 GaAs reflection. These peaks can be labelled as (0,0,70), (0,0,71) and (0,0,72) for the -1, 0 and +1 respectively.

From the separation of the zeroth order and 004 peaks the average mismatch of the superlattice can be determined. Assuming coherent interfaces this then gives the average composition,  $\bar{x}$ , which is defined as  $\bar{x} = n_1x/(n_1+n_2)$ . The value found, assuming Poisson's ratio for GaAs and GaAlAs are equal, is  $\bar{x}=0.185$  or 213 ppm mismatch.

Rocking curves can then be calculated for this superlattice for varying values of the ratio  $n_1:n_2$  with  $n_1+n_2$  and  $\bar{x}$  constant. A value of the sample curvature was used to give the best fit to the widths of the 004 and zeroth order peaks. The best fit 004 and 002 rocking curves are shown in figs. 7.4 and 7.5 for comparison with the experimental curves. Values of  $n_1$  and  $n_2$  thus determined are  $n_1=43$  and  $n_2=28$ , giving  $x=0.35$ . Fig. 7.6 demonstrates the sensitivity of the +1 satellite intensity to the value of the ratio  $n_1:n_2$  for the 004 reflection. The three curves shown are for the ratios 42:29, 43:28 and 44:27. The satellite intensity of the 42:29 curve is approximately 9% greater than that of the 43:28 curve, while that of the 44:27 curve is approximately 8% weaker. Oscillatory structure on the high angle side of the substrate peak is not changed nor are the shapes of the substrate and zeroth

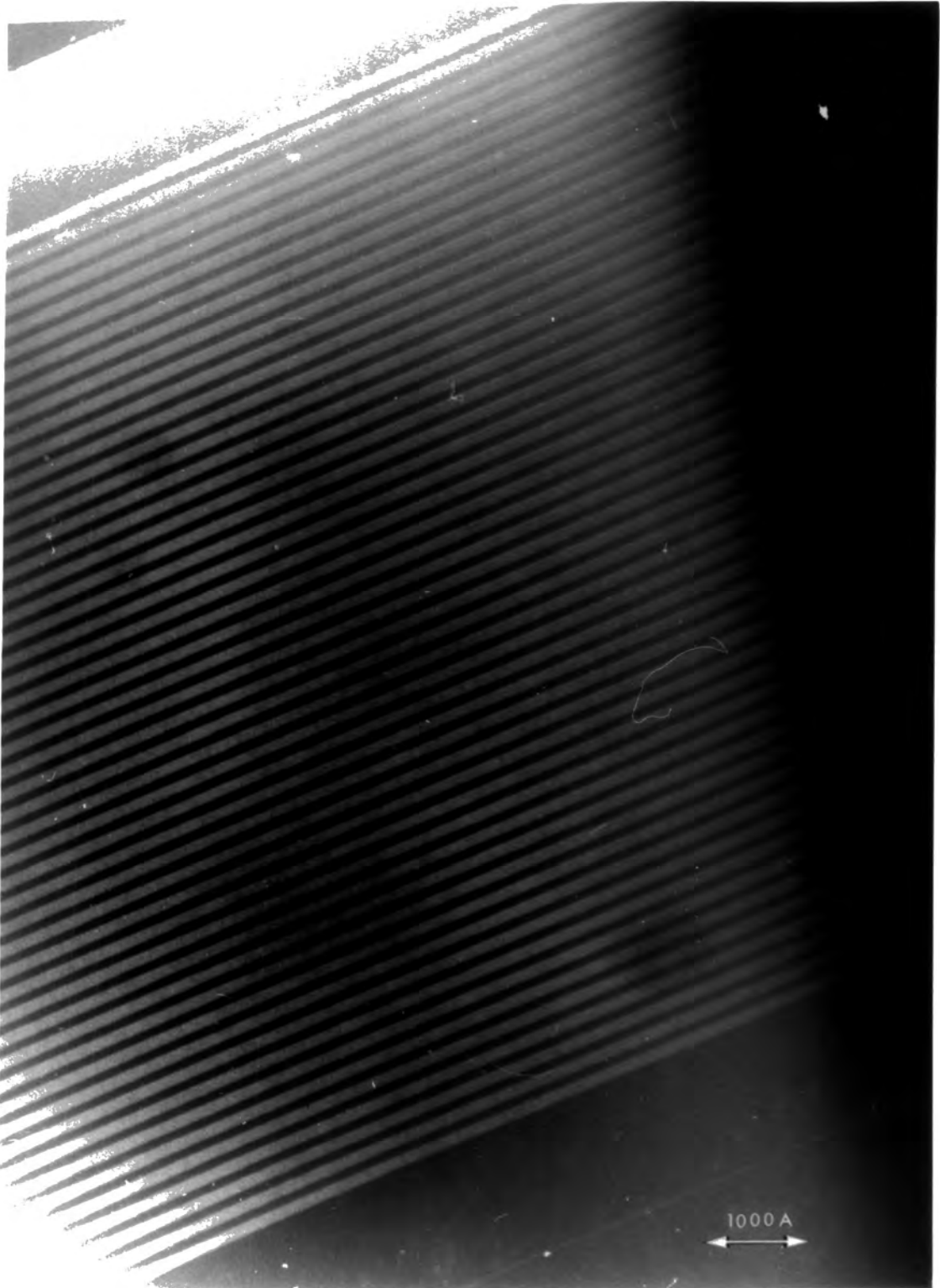


Fig. 7.7 The 002 dark field transmission electron micrograph of the first GaAlAs/GaAs superlattice. The GaAlAs layers are the lighter regions due to the enhanced diffracted intensity.

order peaks. Therefore, this fitting procedure will be unaffected by any superlattice imperfections that reduce the +1 satellite intensity by less than approximately 5%. Imperfections that reduce the intensity by a greater amount would give a larger value of  $n_1$  using this fitting procedure. The intensities of the satellites near the 002 GaAs reflection, particularly the -1 peak, also agree well with those calculated for  $n_1=43$  and  $n_2=28$ . However, the intensity ratio of a higher order satellite, whose intensity varies as a different function of  $n_1:n_2$ , could not be used to improve the fitting procedure since no such peaks could be observed either near the 004 or 002 GaAs reflections. The value of  $x$  deduced agrees well with that expected from the growth conditions. Using this composition the intensity of the -1 satellite was calculated and was found to be much weaker than the +1 satellite, explaining why it could not be observed in the experimental rocking curve.

A transmission electron microscopy study of this sample was also carried out at British Telecom Research Laboratories. Taking a thin section perpendicular to the surface the micrograph shown in fig. 7.7 was obtained. This represents the 002 dark field image, with the GaAs and GaAlAs layers easily distinguished by the enhanced intensity diffracted by the GaAlAs layers. Although the exact magnification could not be accurately determined the values of the relative layer thicknesses agree extremely well with those obtained from the rocking curve. The micrograph is

extremely useful for showing any deviations in the repeat period and for showing the thickness uniformity along the layers.

Some discrepancies do exist between the calculated and experimental rocking curves, particularly in the intensity of the satellite peaks in the region of the 002 GaAs reflection. Further, satellites greater than the first order could not be observed. Both of these facts indicate that the superlattice is not perfect; either the repeat unit varies throughout the superlattice about some mean value or the interfaces are not sharp due to interdiffusion between the GaAlAs and GaAs layers. The effect of these variations on the intensity of the satellite peaks is discussed later.

Another example of a GaAlAs/GaAs superlattice was also studied. This sample consisted of 100 layers of GaAs and 99 layers of GaAlAs with an encapsulating layer of 1  $\mu\text{m}$  of GaAlAs and 200 Å of GaAs, as shown schematically in fig. 7.8.

The diffracted intensity in the region of the 002 GaAs reflection was recorded in a similar manner to that used for the previous sample and is shown in fig. 7.9. Again only the +1 and -1 satellites could be observed, with considerably smaller intensities than those obtained for the previous sample. The intensities of both satellites were approximately one thousandth of the intensity of the zeroth order peak, which could not be completely resolved from the 002 GaAs peak.

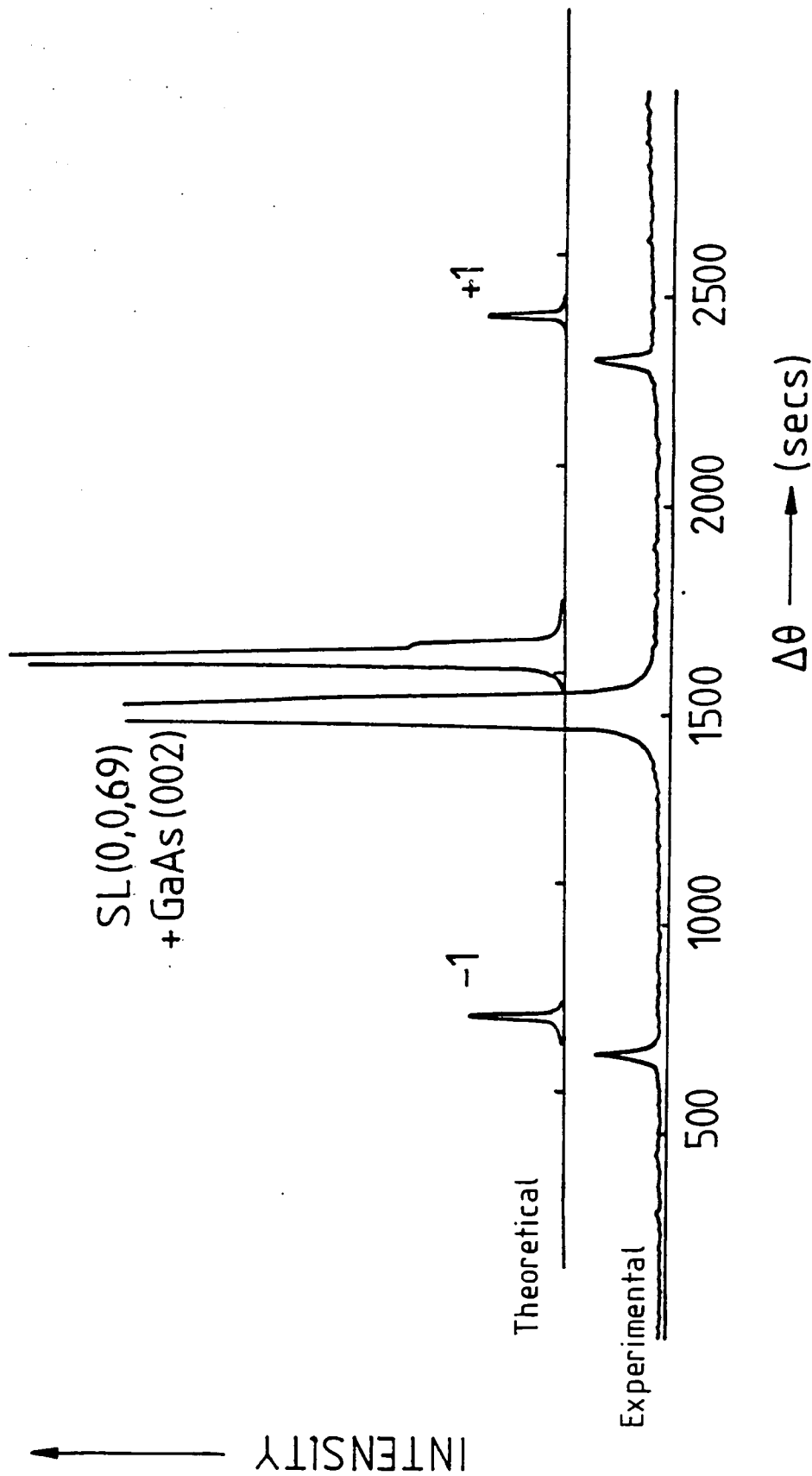


Fig. 7.9 The 002 experimental and computed rocking curves from the second GaAlAs/GaAs superlattice, its construction is shown in fig. 7.8. The vertical scale is expanded to show the +1 and -1 satellite peaks.  $\text{CuK}\alpha_1$  radiation was used. The computed curve as for  $n_1 = 35$ ,  $n_2 = 34$  and  $x = 0.30$ .

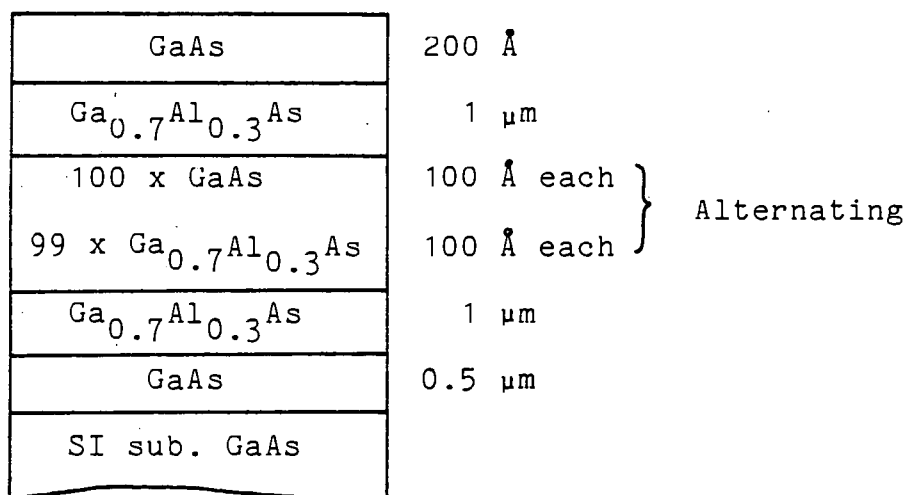


Fig. 7.8 Schematic diagram of the construction of the second GaAlAs/GaAs superlattice.

From the satellite separations the value of  $n_1+n_2$  is found to be 69. Thus, from the position of the zeroth order peak the superlattice period is 195 Å, compared to the 200 Å expected from the growth conditions. The best fit calculated curve is shown in fig. 7.9, for  $n_1=35$  and  $n_2=34$ . Agreement between the satellite positions is very good, although the calculated peaks are slightly more intense and narrower. Since  $n_1 \approx n_2$  we would expect the second order satellite peaks to be particularly weak which explains why they could not be observed. Since the satellite intensities are smaller than those predicted theoretically we again expect there to be some dispersion in the superlattice repeat period.

A similarly designed sample, its construction as shown in fig. 7.10, was also studied. The 002 rocking curve is shown in fig. 7.11, again revealing only satellites up to

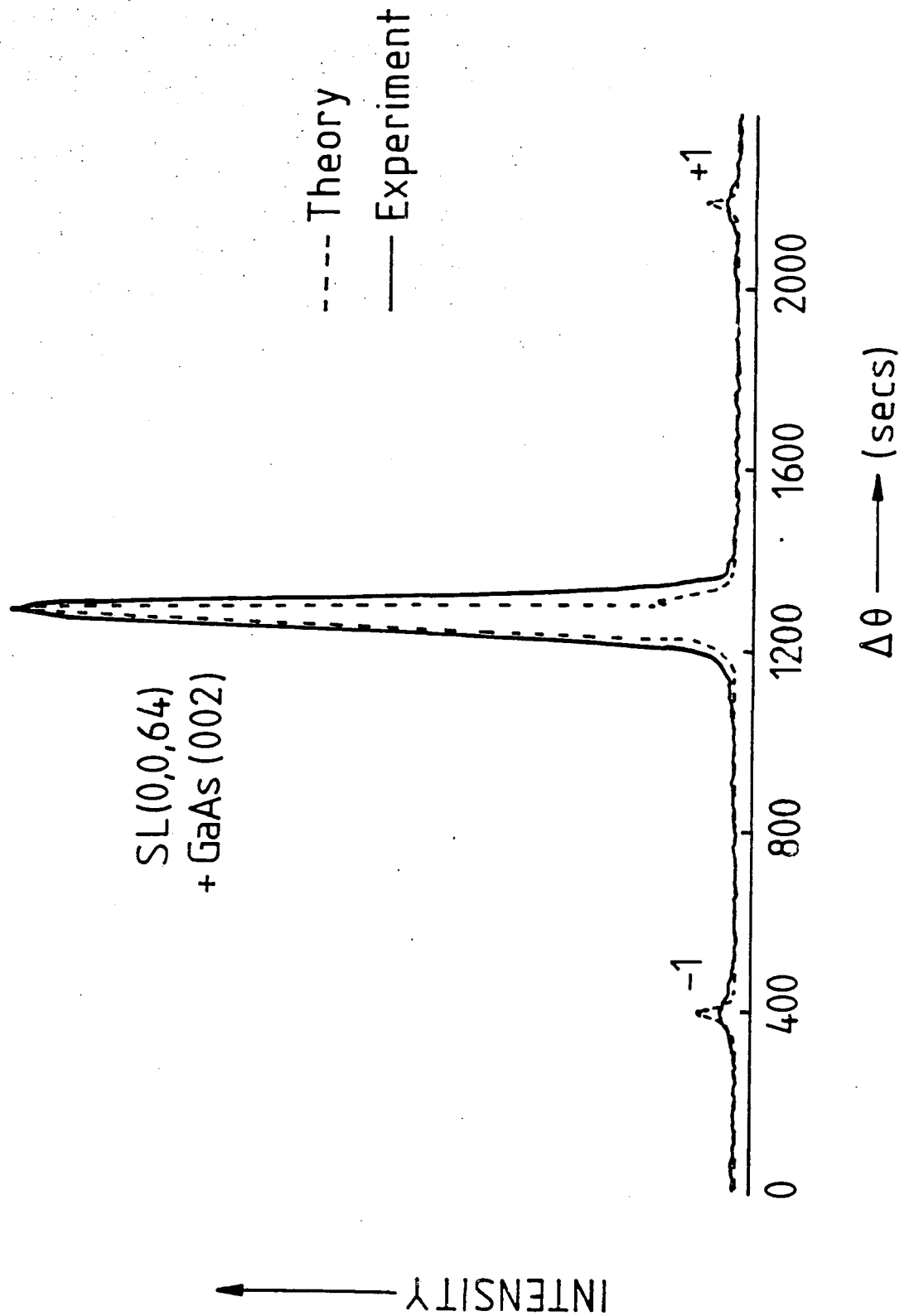


Fig. 7.11 002 experimental and computed rocking curves from the third GaAlAs/GaAs superlattice. The  $\text{CuK}\alpha_1$  radiation was used.

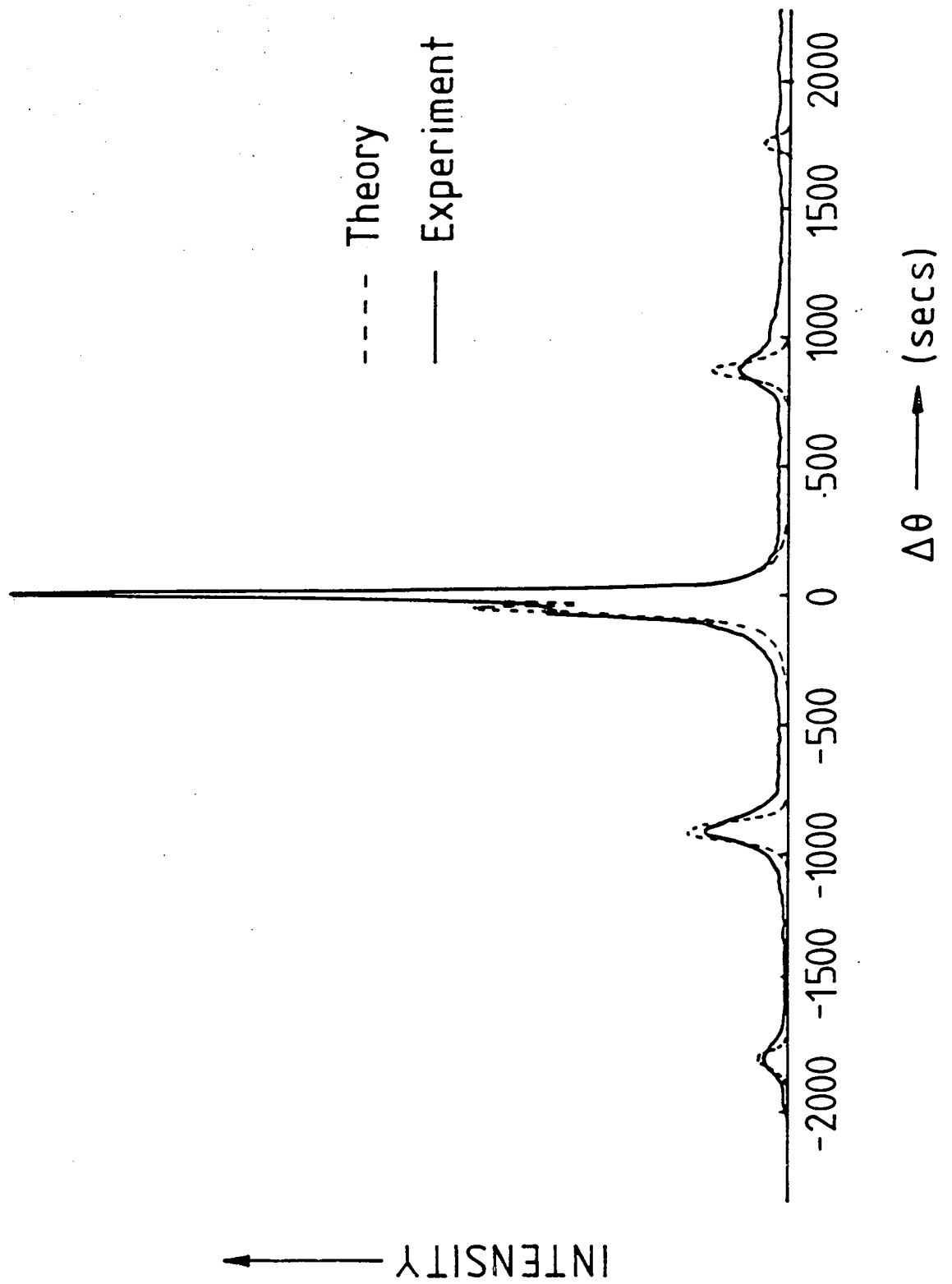


Fig. 7.12 002 experimental and computed rocking curves, with  $\text{CuK}\alpha_1$  radiation, from the GaInAs/InP superlattice. The +1, -1 and -2 satellites are easily visible in the experimental curve. The computed curve is for  $n_1 = 38$ ,  $n_2 = 26$  and  $x = 0.537$ .



the first order. Satellite intensities were similar to those for the previous sample, their spacing giving  $L=n_1+n_2=64$ . From the position of the zeroth order satellite peak, the  $(0,0,64)$  reflection, the superlattice period is found to be  $C=160 \text{ \AA}$ , which agrees reasonably well with the  $175 \text{ \AA}$  expected. The best fit calculated curve for  $n_1=38$ ,  $n_2=26$  is also shown in fig. 7.11. Once again the calculated satellite intensities are slightly smaller than those in the experimental curve.

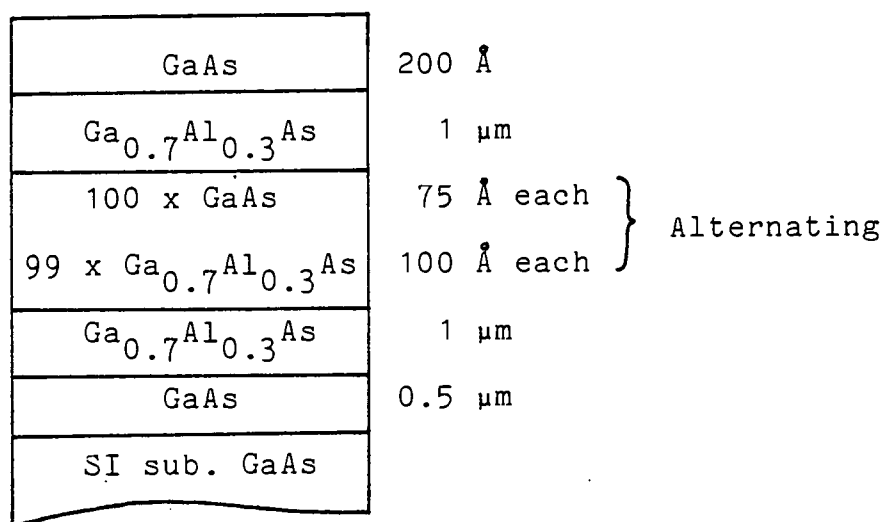


Fig. 7.10 Schematic diagram of the construction of the third GaAlAs/GaAs superlattice sample.

A  $n_1$ -GaInAs/ $n_2$ -InP superlattice, grown by MOCVD on an (001) InP substrate (Moss and Spurdens, 1984), has also been studied. The 002 rocking curve is shown in fig. 7.12, which reveals satellites up to the second order. The -1 and -2 satellites are easily visible, being approximately 10% of the intensity of the zeroth order peak, but only the +1 satellite can be observed on the high angle side of the

zereth order peak. The zeroth order peak is only partially resolved from the 002 InP substrate peak and is on the low angle side. Since for the 002 reflection the difference in structure factor between GaInAs and InP is much greater than that between GaAlAs and GaAs the satellites are much more intense. From the separation of these satellites the value of  $L=n_1+n_2$  is calculated and found to be 64, giving a superlattice period of  $C=188 \text{ \AA}$ . The best fit calculated curve was found for  $n_1=38$ ,  $n_2=26$  and is also shown in fig. 7.12. Here, the ratio of intensities of the -1 and -2 satellites was used to aid the determination of  $n_1:n_2$  and help reduce the errors introduced by superlattice imperfections. From these values and the value of  $\bar{x}$ , determined from the separation of the zeroth order peak and the substrate peak,  $x$  is found to be 0.537.

There are again some discrepancies between the computed and experimental rocking curves, with the experimental satellite peaks being both less intense and broader than the computed ones. Further, the +2 satellite could not be observed in the experimental curve yet is easily visible in the computed curve. These facts again lead to the assumption that the superlattice is imperfect with the most likely deviation being in its repeat period. This is not unexpected for this sample since the control of the growth times for each layer was performed by hand and it is known that perfect timing was not achieved. This was confirmed by a TEM study of the sample and the 002 dark field micrograph

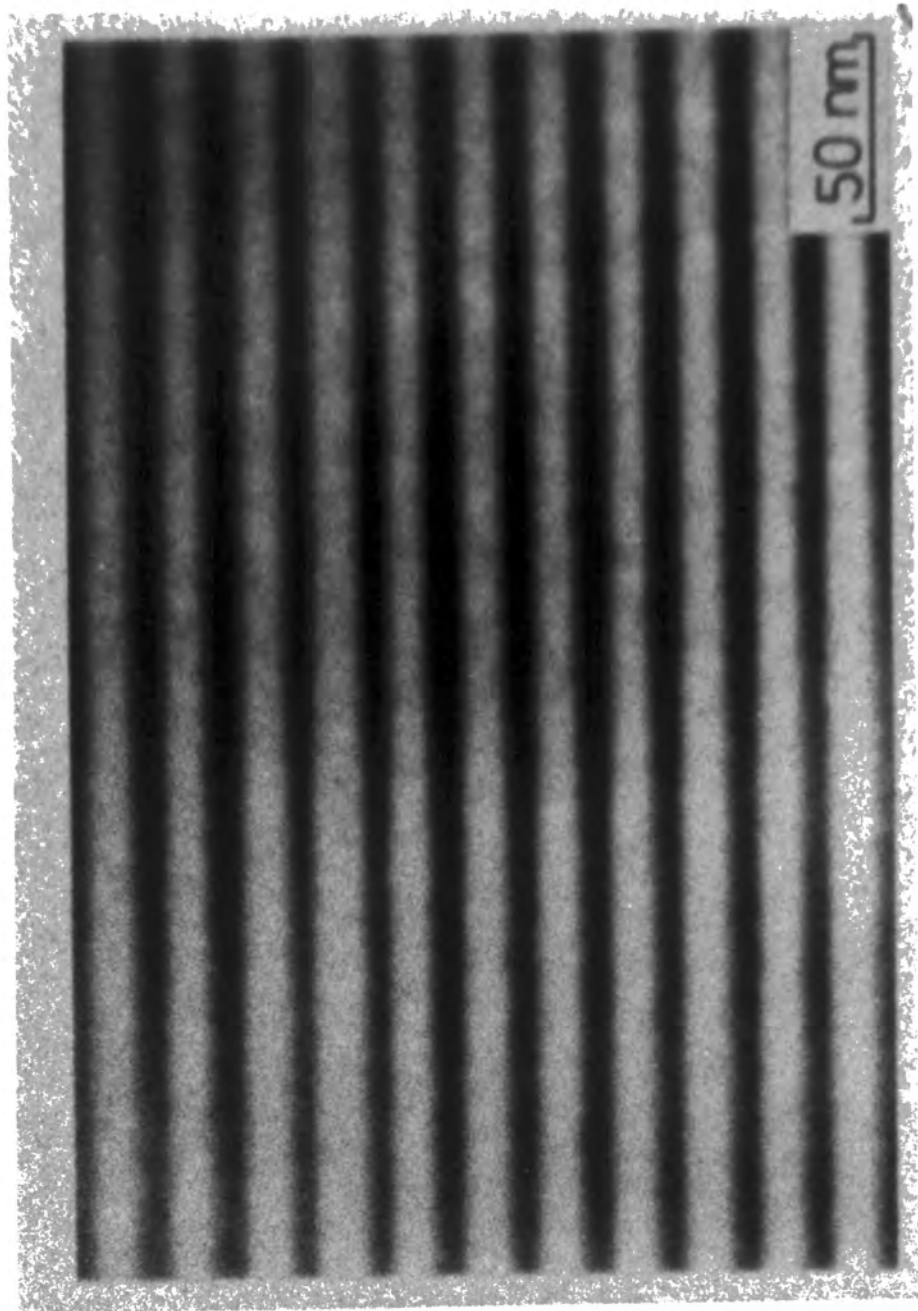


Fig. 7.13 002 transmission electron micrograph of the  $n_1\text{GaInAs}/n_2\text{InP}$  superlattice, revealing the non uniformity in both repeat unit and layer thickness along the layers.

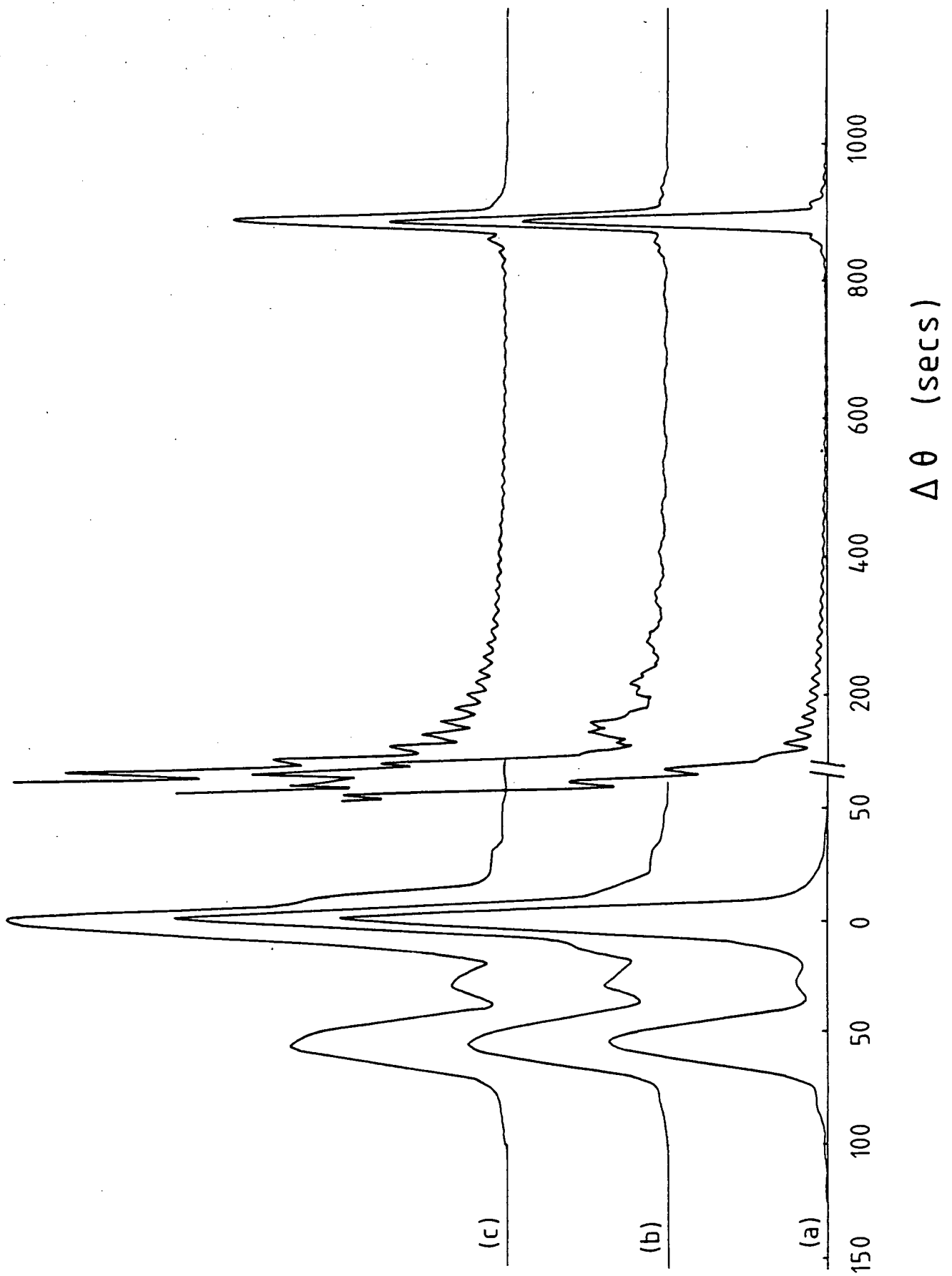


Fig. 7.14 The effect on the 004 computed rocking curve for the first GaAlAs/GaAs superlattice of adding a GaAs capping layer. Curve (a) is for no cap, (b) for 0.3  $\mu\text{m}$  cap and (c) for a 1.0  $\mu\text{m}$  cap. The +1 satellites are shown in the vertically expanded regions.  $\text{CuK}\alpha_1$  radiation is used.

is shown in fig. 7.13. The individual layers are easily distinguishable by the enhanced intensity from the InP layers. There is noticeably a lack of uniformity in thickness along the layers as well as dispersion in the superlattice period.

## 7.2 The Effect of Adding a Capping Layer to the Superlattice

The effect of adding a relatively thick capping layer, of similar composition to one of the components of the superlattice, is demonstrated by the 004 rocking curves shown in fig. 7.14. The radiation is  $\text{CuK}\alpha_1$  and the structure used is that of the first GaAlAs/GaAs sample but the effect of sample curvature has not been included. If the capping layer is sufficiently thick to diffract strongly it is essential that the dynamical theory is used to calculate the overall diffracted intensities and significant changes in the shape of the rocking curve do occur as seen in fig. 7.14. The substrate peak has been considerably affected by the 1  $\mu\text{m}$  cap, being both broadened and with an intense 'bulge' on the high angle side. Additionally, the weak peak between the substrate and zeroth order peak is much more intense than in the curve for the sample without a cap. These main peaks are also similarly affected, although to a somewhat lesser extent, by the addition of a 0.3  $\mu\text{m}$  cap. Also shown in the figures are the expanded regions revealing the +1 satellite peak. Again, for the 1  $\mu\text{m}$  cap

significant modifications are observed with the oscillation on the side of the substrate peak changed as well as the satellite intensity reduced. The position of the satellite peak is not changed with respect to the substrate peak. For the 0.3  $\mu\text{m}$  cap the oscillations are again heavily modified but only an extremely small change in satellite intensity occurs. Since the amplitudes of all of these oscillations on the side of the substrate peak are so small they would not be expected to be observed in any experimental rocking curves. Clearly, if an even thicker cap was to be added the modifications would be greater but these rocking curves show that the presence of a cap that is only about 10% of the extinction distance can make a significant difference to the intensity of the satellite peaks. Further, even the addition of only a 0.3  $\mu\text{m}$  cap does have a significant effect on the shape of the substrate and zeroth order peaks. However, when sample curvature is included in these calculations the effects do become less noticeable.

### **7.3 The Effect of Dispersion in the Superlattice Period and of Interdiffusion between the layers.**

The effect of dispersion in the superlattice period, ie the thickness of the layers forming the repeat unit varies throughout the layer, is discussed first. This effect can easily be modelled by introducing a random deviation in the number of monolayers, about a mean value, for each layer used in the calculation. The size of the random deviation can then be increased and rocking curves calculated. Note

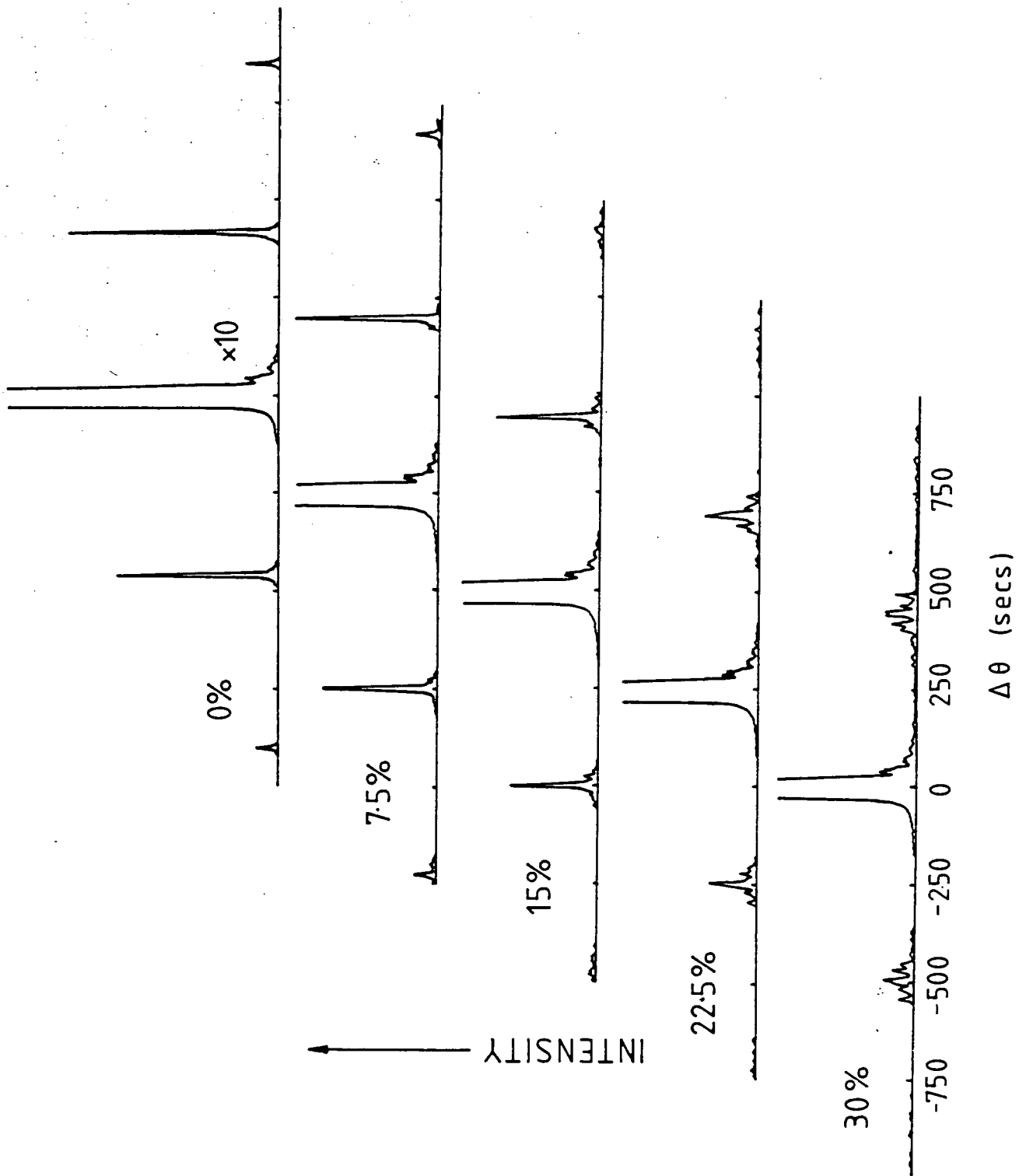


Fig. 7.15 The effect of dispersion in the superlattice period on 002 computed curves for the GaInAs/InP superlattice.  $\text{CuK}\alpha_1$  radiation is used. The individual layer thicknesses vary randomly about the perfect superlattice values within the range (mean - percentage of mean) to (mean + percentage of mean) where the percentage used is as indicated by the curves.

that the satellite intensity formulae developed for perfect superlattices by other workers (see for example Vardanyan, Manoukyan and Petrosyan, 1985) are not well suited to modelling this effect. Fig. 7.15 shows the effect of increasing the size of the random fluctuation in the 002 rocking curve from a GaInAs/InP superlattice with a construction similar to that found for the sample studied experimentally. The amount of random deviation is taken as a percentage of the mean number of monolayers forming each layer. In the curve for zero deviation satellite peaks up to the second order are easily visible with well formed, narrow peaks. However, as the size of the fluctuations are increased the second order peaks rapidly disappear, while the intensity of the first order peaks is less rapidly affected. For the 7.5% fluctuations the second order satellite peaks have already lost their well formed shape and are less intense. The +1 satellites have also lost intensity but still retain a similar shape. The intensity of the satellites is not affected equally on either side of the zeroth order peak which is particularly important and the ratio of intensities of the +1 and -1 satellites does not remain the same; the +1 satellite, which is the most intense, is reduced in intensity more rapidly than is the -1 peak. When the fluctuations are as large as 15% the second order satellites have already reduced to a very spread out peak which would not be visible in any experimental curve. Again the first order satellites have been reduced in



intensity but also have become considerably broadened in the tails. Beyond 15% the first order satellites are further reduced in intensity and broadened and by 30% have only become a very spread out, badly formed peak. This agrees well with the observations of other workers (see for example Kevarec et al, 1984).

Since we have easily observed one second order satellite peak in the experimental curve from the GaInAs/InP superlattice the fluctuations in repeat period must be less than about 10% by comparison with the above computed curves. This agrees well with the measurements taken from the TEM micrograph. Variations in layer thicknesses along the layers would also be expected to have a significant effect on the rocking curve, but this effect is not so easily modelled and would require calculating a number of rocking curves for different layer thicknesses and then adding them.

If interdiffusion has occurred between the layers (for example of Al in a GaAlAs/GaAs superlattice) the interfaces will become less sharp. If a large degree of interdiffusion has occurred the mismatch and composition variations throughout the superlattice will tend towards sinusoidal. Clearly, to model this effect with a computational procedure designed for stepwise variation would require a large number of layers, with the sinusoidal variation modelled by dividing each layer into a number of laminae of constant composition. Consequently, the number of layers required for the computation can easily be up to an order of

magnitude greater than the actual number of layers in the structure, greatly increasing the computation time. Calculations based on a Fourier expansion of the composition variation are perhaps better suited to studying this effect and have been used successfully by a number of workers (see for example Fleming et al, 1980). Kervarec et al (1984) have also calculated the satellite intensities as a function of the interface width by adding a sinusoidal variation to the stepwise variation. This showed that the satellite intensities decrease as the interface width is increased, with the higher order satellites more rapidly affected.

From the TEM results for two of the samples studied the interfaces did appear to be reasonably sharp, which agrees well with the previous observations of Dernier et al (1977) where the GaAl/GaAlAs interfaces were determined to be less than two monolayers wide. The most obvious irregularity in the superlattice was in the repeat period (particularly for the GaInAs/InP sample) and, as shown, this has a very large effect on satellite intensities explaining why those observed were less intense than the computed ones.

## DISCUSSION AND SUGGESTION FOR FUTHER WORK

The computational method developed has been shown to produce rocking curves that agree extremely well with experimental ones for single uniform layers, single layers with depth dependent compositions and multiquantum well structures. Often there are discrepancies between the computed and experimental rocking curve but these can be accounted for by imperfection in the samples. The technique is particularly useful in the determination of the composition variation in graded layers and provides an accurate means of determining layer thicknesses for all types of samples. However, due to the high sensitivity of the rocking curve to composition and the large numbers of parameters that can be altered it can be extremely difficult to fit experimental rocking curves exactly, especially for graded layers. Bulk sample curvature also has a very major affect on the rocking curve and can mask much of the fine detail present in the computed curves neglecting this effect.

It has also been found that the rocking curve from samples with only a few layers of similar composition are not straightforward to interpret. The number of peaks observed in the rocking curve very rarely equal the number of layers. Further problems are encountered if the layer is thin relative to the extinction distance, making the diffracted intensity from the layer only a few percent of that of the substrate peak. Also, if thin layers are

present buried between thicker layers of a similar composition, as in many of the device structures currently being developed, their detection can be extremely difficult. For the thin, single layers the use of highly asymmetric reflections in the low angle of incidence case has been studied. Diffracted intensities from the layer were found to increase dramatically as the angle was reduced to near grazing incidence. However, due to the high sensitivity of the layer peak to the incident angle difficulties arose in the simulation of such rocking curves. This effect could be due to surface misorientation and further experiments are required to ascertain this. For thin layers sandwiched between thicker ones this technique could also be used with angles above those of near grazing incidence so that the top, thick layer does not diffract all of the intensity. When using a synchrotron source the incident angle can be adjusted to tailor the extinction distance to that required and it would be important to assess whether similar techniques could be used with a laboratory source. Since a different first crystal reflection would have to be used in order to prevent either extreme beam compression or expansion a channel cut monochromator would be extremely useful to reduce the effect of the dispersion introduced. The use of a high incidence angle with a grazing exit beam may also be useful for these studies but as yet no experimental results have been obtained to confirm this.

The use of gap fringes may also become extremely useful

for the study of these structures with thin, buried layers, as recently discussed by Tanner and Hill (1985). Here the thin layers produce strong gap fringes in the rocking curve which vary as a function of both their depth and thickness. To date only theoretical curves have been produced and good quality experimental data is required for comparison.

Due to the lack of perfection in the superlattices studied only a small number of satellites were observable even with the 002 forbidden reflection and the extremely good counting statistics afforded by the high intensity of the synchrotron source. The effect of dispersion in the superlattice period has been modelled and found to have a dramatic effect on the satellite intensities. However, the effect of both interdiffusion between the layers and thickness irregularities along the layers remain to be modelled. In order to study the effect of interdiffusion it may well be better to use a different computational approach based on numerically integrating the Takagi-Taupin equations with a continuous composition modulation. If the stepwise approach is used the composition variation would need to be modelled by an extremely large number of laminae, which combined with the large angular ranges required in the calculation will greatly increase the computational time. This may not be a problem with access to a large, powerful computer. However, this approach would have the advantage that the combined effect of both dispersion in the periodicity and interdiffusion could be studied.

Additionally, this technique could also be used to simulate rocking curves from ion implanted superlattices to compare with experimental results similar to those presented by Terauchi et al (1984).

Little use has been made of double crystal topography to study these materials mainly due to the effect of sample curvature. Since any good quality heteroepitaxial layer must produce sample curvature only extremely small regions of the crystal can be imaged in one topograph. Consequently, single crystal topography has been more extensively used to examine the samples for the presence of mismatch dislocations.

Finally, since the need for this technique of rocking curve simulation is becoming more widespread, particularly by the semiconductor manufacturers, ways by which the computation can be become more easily available are required. With the advent of more and more powerful microcomputers, particularly those based around the 68000 series of processors, it may well be feasible to perform the computations on these machines. If this step could be made it is certain that this technique could become more and more important. Further, it ought to be perfectly feasible to automatically analyse rocking curves from single uniform layers provided that well resolved peaks are obtained. The analysis is greatly simplified when the mismatch and areas under each peak are determined. It is unlikely that such a technique could be developed for graded layers due to the

large number of laminae required and the sensitivity of the rocking curve to small variations in the composition profile. Both sample curvature and large dislocation densities would also greatly hinder such an analysis. For multiple layered structures further problems would be encountered due to the additional interference peaks present in the rocking curves. However, even if automated analysis cannot be easily implemented there remains no doubt as to the usefulness of rocking curve simulation to provide a highly sensitive, non-destructive characterisation method.

A P P E N D I X A

## COMPUTER PROGRAMMED FOR THE COMPUTATION OF ROCKING CURVES

This appendix contains complete listings of the computer programme required to calculate and plot rocking curves from III and IV semiconductor crystals with epitaxial layers of any composition. The programmes run on an IBM 4341/I at Durham University.



```
{ PROGRAM TO CALCULATE INPUT PARAMETERS FOR THE CALCULATION
  OF ROCKING CURVES USING THE TAKAGI TAUPIN EQUATIONS. DATA
  IS OUTPUT TO THE FILE 'INPDAT' TO BE USED BY THE PROGRAM
  CRUNCH WHICH CALCULATES THE ROCKING CURVE
```

```
(C) M.J. HILL 1984/5 }
```

```
program INPUT_ROCK(input, output);

const
  PI = 3.1415927;

type
  material = (Im, Ga, As, P, Al, Si);
  mat_data = array [material] of real;
  matset = set of material;
  complex = record
    re, im: real;
  end;
  parameters = record
    napuc: integer;
    coord: array [1 .. 8, 1 .. 3] of real;
  end;
  comstring = array [1 .. 10] of string(25);
  comnumber = array [1 .. 10] of real;
  comset = array [1 .. 10] of set of material;
  matstring = array [material] of string(25);

const
  com_name = comstring('InP', 'GaAs', 'GaInAs', 'GaInAsP',
    'GaAlAs', 'AlAs', 'Si');
  com_param = comnumber(5.8688E-10, 5.6535E-10, 0.0, 0.0, 0.0,
    5.6535E-10, 5.4307E-10);
  com_type = comset([Im, P], [Ga, As], [Im, Ga, As],
    [Im, Ga, As, P], [Ga, As, Al], [As, Al],
    [Si]);
  mat_name = matstring('In', 'Ga', 'As', 'P', 'Al', 'Si');

var
  substrate: string(25);
  first: string(25);
  subcomp: matset;
  firstcomp: matset;
  layer_mat: array [1 .. 200] of matset;
  msource, msink, output_file: text;
  wavelength: real;
  no_layers: integer;
  fh1, fh2, fo: complex;
  ffh1, ffh2, ffo: complex;
  lf1, lf2, lfo: array [1 .. 200] of complex;
  start, finish, alpha_step: real;
  bstart, bfin, beta_step: real;
  stheta, cphi, d_sub: real;
  ftheta, fphi, d_first: real;
  h, k, l: integer;
  ii, jj, kk: integer;
  fh, fk, fl, fii, fj, fkk: integer;
  thick, c: array [1 .. 200] of real;
  data: array [material] of parameters;
  percent: mat_data;
```

```

div_diff: array [material, 1 .. 2, 1 .. 5] of real;
pnts: array [1 .. 5] of real;
query: string(25);
polar: string(25);
first_diff: boolean;
approx: array [material] of record
    a: array [1 .. 4] of real;
    b: array [1 .. 4] of real;
    c: real;
end;
(* procedure to calculate lattice parameter and percentages of *)
(* each element in the composition *)

procedure lattice_param(composition: matset; mismatch: real;
    var d: real);

var
    i: integer;
    eg : real;

procedure initialise;

var
    element: material;

begin
    for element := Im to Si do begin
        percent[element] := 1.0;
    end;
end {initialise};

begin {lattice_param}
    if composition = [Im, Ga, As]
    then begin
        percent[Im] := (5.8688 * mismatch + 0.2153) / 0.405;
        percent[Ga] := 1.0 - percent[Im];
        percent[As] := 1.0;
        d := d_sub * (1.0 + 2.0 * mismatch);
    end
    else
        if composition = [Ga, As, Al]
        then begin
            percent[Al] := 5.6535 * mismatch / 0.0065;
            percent[Ga] := 1.0 - percent[Al];
            percent[As] := 1.0;
            d := d_sub * (1.0 + 2.0 * mismatch);
        end
        else
            if composition = [Im, Ga, As, P]
            then begin
                eg := 1.0E-06;
                eg := 6.6E-34*3.0E8/1.6E-19/eg;
                percent[As] := (0.72 - sqrt(sqr(0.72)-4.0*0.12*
                    (1.35-eg))) / 0.24;
                percent[Ga] := mismatch * 5.8688 - percent[As] *
                    (6.0590 - 5.8688);
                percent[Ga] := percent[Ga] / (percent[As]

```

```

                * 5.6535
                + (1 - percent[As]) * 5.4512
                - percent[As] * 6.0590
                - (1 - percent[As]) * 5.8688);
    percent[Im] := 1.0 - percent[Ga];
    percent[P]  := 1.0 - percent[As];
    d := d_sub * (1.0 + 2.0 * mismatch);
    end
else begin
    for i := 1 to 7 do begin
        if composition = com_type[i]
        then
            d := com_param[i];
        end;
        initialise;
    end;
end {lattice_param};
(* procedure to calculate structure factors for any material *)

procedure structuref(composition: matset; ds: real; ah, ak, al:
                    integer; var ft1, ft2, fto: complex);

var
    element: material;
    f1, f2, f: complex;

(* procedure to obtain the scattering factor from the *)
(* analytical approximation, table is in file ANALAPP.DAT *)

procedure scatt_fact(index: real; element: material;
                    var f: real);

var
    i: integer;

begin
    f := 0.0;
    for i := 1 to 4 do begin
        f := f + approx[element].a[i] *
            exp(- approx[element].b[i] * sqr(index));
    end;
    f := f + approx[element].c;
end {scatt_fact};
(* procedure to calculate absorption and dispersion *)
(* corrections *)

procedure corrections(element: material; var df1, df2: real);

var
    lamda, mult: real;
    fcorr: array [1 .. 2] of real;
    i, j: integer;

begin
    lamda := wavelength * 1.0E10;
    for i := 1 to 2 do begin
        mult := 1.0;
        fcorr[i] := 0.0;
    end;
end;

```

```

    for j := 1 to 5 do begin
      fcorr[i] := fcorr[i] + mult * div_diff[element, i, j];
      mult := mult * (lamda - pnts[j]);
    end;
  end;
  df1 := fcorr[1];
  df2 := fcorr[2];
end {corrections};
(* procedure to calculate structure factors for an element *)
(* corresponding to the h, k, l; -h, -k, -l & 0, 0, 0 *)
(* reflections *)

```

```

procedure sfact(element: material; ds: real;
                var f0, f1, f2: complex);

```

```

var
  index, f: real;
  df1, df2: real;

```

```

procedure eval(hh, kk, ll: integer; var ff: complex);

```

```

var
  temp: complex;
  i: integer;
  position: real;

```

```

begin
  temp.re := 0.0;
  temp.im := 0.0;
  for i := 1 to data[element].napuc do begin
    position := hh * data[element].coord[i, 1] +
               kk * data[element].coord[i, 2] +
               ll * data[element].coord[i, 3];
    temp.re := temp.re + cos(2.0 * PI * position);
    temp.im := temp.im + sin(2.0 * PI * position);
  end;
  ff.re := temp.re * f - temp.im * df2;
  ff.im := temp.re * df2 + temp.im * f;
end {eval};

```

```

begin {sfact}
  index := sqrt(float(sqr(ah) + sqr(ak) + sqr(al))) /
             (ds * 1.0E10 * 2.0);
  scatt_fact(index, element, f);
  corrections(element, df1, df2);
  f := f + df1;
  eval(ah, ak, al, f1);
  eval(- ah, - al, - ak, f2);
  index := 0.0;
  scatt_fact(index, element, f);
  f := f + df1;
  eval(0, 0, 0, f0);
end {sfact};

```

```

begin {structuref}
  ft1.re := 0.0;

```

```

ft1.im := 0.0;
ft2.re := 0.0;
ft2.im := 0.0;
fto.re := 0.0;
fto.im := 0.0;
for element := Im to Si do begin
  if element IN composition
  then begin
    sfact(element, ds, f, f1, f2);
    ft1.re := ft1.re + f1.re * percent[element];
    ft1.im := ft1.im + f1.im * percent[element];
    ft2.re := ft2.re + f2.re * percent[element];
    ft2.im := ft2.im + f2.im * percent[element];
    fto.re := fto.re + f.re * percent[element];
    fto.im := fto.im + f.im * percent[element];
  end;
end;
end {structuref};
(* procedure to check material exists, if it doesn't rc=0, *)
(* else rc=1, code returns the number of elements in      *)
(* the composition *)

```

```

procedure check(inpdat: string(25); var rc, code: integer;
               var composition: matset);

```

```

var
  j: integer;
  elem: material;

```

```

begin
  rc := 1;
  code := 0;
  for j := 1 to 7 do begin
    if inpdat = com_name[j]
    then begin
      composition := com_type[j];
      rc := 0;
    end;
  end;
  if rc = 0
  then begin
    for elem := Im to Si do begin
      if elem IN composition
      then
        code := code + 1;
      end;
    end;
  end {decomp};
(* procedure to read analytic approximation data and *)
(* dispersion and absorption correction data *)

```

```

procedure readparam;

```

```

var
  element: material;
  indata: string(25);
  i, j, m: integer;
(* procedure to convert string input to element type *)

```

```

procedure decode(inpdat: string(25); var element: material);

var
  elem: material;

begin
  for elem := Im to Si do begin
    if inpdat = mat_name[elem]
    then
      element := elem;
    end;
  end {decode};

begin {readparam}
  reset(input, 'file=PHKO:ANALAPP.DAT');
  writeln(msink, 'Reading scattering factor data for',
    ' elements..wait');
  for i := 1 to 5 do begin
    read(input, pnts[i]);
  end;
  read(input, indata);
  repeat
    decode(indata, element);
    for i := 1 to 4 do begin
      read(input, approx[element].a[i], approx[element].b[i]);
    end;
    read(input, approx[element].c);
    for i := 1 to 2 do begin
      for j := 1 to 5 do begin
        read(input, div_diff[element, i, j]);
      end;
    end;
    read(input, data[element].napuc);
    for i := 1 to data[element].napuc do begin
      read(input, data[element].coord[i, 1],
        data[element].coord[i, 2],
        data[element].coord[i, 3]);
    end;
    read(input, indata);
  until indata = 'end';
end {readparam};
(* procedure to list material types available for InP *)
(* substrates *)

```

```

procedure IPchoice(var name: string(25));

begin
  writeln(msink, 'Please choose a layer material from the ',
    ' following types');
  writeln(msink);
  writeln(msink, '      InP');
  writeln(msink, '      GaInAs');
  writeln(msink, '      GaInAsP');
  writeln(msink);
  writeln(msink, 'Layer material ? ');
  readln(msource, name);

```

```

    end {IPchoice};
(* procedure to list material types for GaAs substrates *)

procedure GAchoice(var name: string(25));
begin
  writeln(msink, 'Please choose a layer material from the ',
    'following types');
  writeln(msink);
  writeln(msink, '      GaAs');
  writeln(msink, '      AlAs');
  writeln(msink, '      GaAlAs');
  writeln(msink);
  writeln(msink, 'Layer material ? ');
  readln(msource, name);
end {GAchoice};
(* procedure to calculate layer parameters for a linear *)
(* or graded lattice parameter variation *)

procedure linear(curved : boolean);

var
  total_thick: real;
  curve, xcoord, ycoord, origin, radius : real;
  i, rcode, mcode: integer;
  mism_int, mism_sur: real;
  layer_name: string(25);

begin
  page(msink);
  writeln(msink, 'GRADED LAYER PARAMETER INPUT');
  repeat
    if subcomp = [Im, P]
      then
        IPchoice(layer_name)
      else
        GAchoice(layer_name);
    check(layer_name, rcode, mcode, layer_mat[1]);
    if rcode <> 0
      then
        writeln(msink, 'I don''t know this material - ',
          'please choose again');
    if mcode < 2
      then
        writeln(msink, 'Can''t have linear composition',
          ' variation with binary composition',
          ' - choose again');
    until (rcode = 0) AND (mcode > 2);
  repeat
    writeln(msink, 'Enter mismatch at layer/substrate ',
      'interface (ppm)');
    readln(msource, mism_int);
    writeln(msink, 'Enter mismatch at surface of layer',
      ' (ppm)');
    readln(msource, mism_sur);
    mism_sur := mism_sur * 1.0E-6;
    mism_int := mism_int * 1.0E-6;
    if mism_sur = mism_int

```

```

    then
        writeln(msink, 'No variation possible - choose again');
    until mism_sur <> mism_int;
if curved
    then begin
        writeln(msink, 'Degree of non-linearity (0-100)');
        readln(msource, curve);
    end
    else
        curve := 0.0;
repeat
    writeln(msink, 'How many laminae required');
    readln(msource, no_layers);
    if no_layers <= 0
        then
            writeln(msink, 'Impossible number of laminae - ',
                'try again');
        if no_layers = 1
            then
                writeln(msink, 'Variation with one laminae ?',
                    ' - try again');
            until no_layers > 1;
        writeln(msink, 'Total thickness of epitaxial layer ',
            '(microns)');
        readln(msource, total_thick);
        total_thick := total_thick * 1.0E-6;
        thick[1] := total_thick / float(no_layers);
        if curve > 0.05
            then begin
                curve := (1.0/sqrt(2.0) - 0.5) * curve / 100.0 + 0.5;
                origin := total_thick * (0.5 - sqrt(curve)) /
                    (1.0 - 2.0 * curve);
                radius := 2.0 * sqrt(curve * total_thick - origin);
                for i := 1 to no_layers do begin
                    xcoord := total_thick * (no_layers - i) /
                        (no_layers - 1);
                    ycoord := sqrt(radius - sqrt(xcoord - origin)) + origin;
                    c[i] := ycoord * (mism_sur - mism_int) / total_thick +
                        mism_int;
                    layer_mat[i] := layer_mat[1];
                    thick[i] := thick[1];
                end
            end
            else begin
                xcoord := (mism_sur - mism_int) / float(no_layers - 1);
                c[1] := mism_int;
                for i := 2 to no_layers do begin
                    mism_int := mism_int + xcoord;
                    c[i] := mism_int;
                    layer_mat[i] := layer_mat[1];
                    thick[i] := total_thick / float(no_layers);
                end
            end;
        end {linear};
(* procedure to calculate multi-layer parameters *)

```

```

procedure multilayer;

```

```

    var

```



```

code: array [1 .. 2] of integer;
i, j, no_mono1, no_mono2, rcode: integer;
mism1, mism2: real;
cap: string(10);
layer_names: array [1 .. 2] of string(25);

begin
  page(msink);
  writeln(msink, 'MULTI LAYER SYSTEM CALCULATION');
  writeln(msink);
  writeln(msink, 'For first layer of repeat pair');
  repeat
    if subcomp = [Im, P]
      then
        IPchoice(layer_names[1])
      else
        GAchoice(layer_names[1]);
    check(layer_names[1], rcode, code[1], layer_mat[1]);
    if rcode <> 0
      then
        writeln(msink, 'I don''t know this material - ',
          'please choose again');
    until rcode = 0;
    if (code[1] > 2)
      then begin
        writeln(msink);
        writeln(msink, 'Enter the mismatch for this layer',
          ' (ppm)');
        readln(msource, mism1);
        mism1 := mism1 * 1.0E-6;
        end
      else
        mism1 := 0.0;
    writeln(msink);
    writeln(msink, 'and for the second layer of the repeat',
      ' pair');
    repeat
      repeat
        if subcomp = [Im, P]
          then
            IPchoice(layer_names[2])
          else
            GAchoice(layer_names[2]);
        check(layer_names[2], rcode, code[2], layer_mat[2]);
        if rcode <> 0
          then
            writeln(msink, 'I don''t know this material - ',
              'please choose again');
        until rcode = 0;
        if (code[2] > 2)
          then begin
            writeln(msink);
            writeln(msink, 'Enter the mismatch for this ',
              'material (ppm)');
            readln(msource, mism2);
            mism2 := mism2 * 1.0E-6;
            end
          else
            mism2 := 0.0;
        if (layer_names[1] = layer_names[2]) AND (mism1 = mism2)

```

```

then begin
  writeln(msink, 'You have the same material for both ',
           'layers with the same composition');
  writeln(msink, 'Please choose the second layer again');
end;
until (layer_names[1] <> layer_names[2]) OR
      ((layer_names[1] = layer_names[2]) AND
       (mism1 <> mism2));
writeln(msink, 'Enter the number of monolayers in the',
         ' first layer');
readln(msource, no_mono1);
writeln(msink, 'and the number of monolayers in the second',
         ' layer');
readln(msource, no_mono2);
writeln(msink, 'Enter the total number of repeat units',
         ' required');
writeln(msink, 'ie half the total number of layers');
readln(msource, no_layers);
lattice_param(layer_mat[1], mism1, c[1]);
lattice_param(layer_mat[2], mism2, c[2]);
thick[1] := float(no_mono1) * c[1] / 2.0;
thick[2] := float(no_mono2) * c[2] / 2.0;
writeln(msink, 'Thickness of first layer = ', thick[1]);
writeln(msink, 'Thickness of second layer = ', thick[2]);
writeln(msink);
writeln(msink, 'Total layer thickness = ', (thick[1] +
      thick[2]) * no_layers);
writeln(msink);
writeln(msink, 'Do you require a capping layer (Y/N)');
readln(msource, cap);
if (cap[1] = 'Y') OR (cap[1] = 'y')
  then begin
    i := no_layers * 2 + 1;
    writeln(msink, 'Enter material for capping layer');
    repeat
      if subcomp = [Im,P]
        then IPchoice(layer_names[1])
        else GAchoice(layer_names[1]);
      check(layer_names[1], rcode, code[1], layer_mat[i]);
      if rcode <> 0
        then
          writeln(msink, 'Unknown material - choose again');
          until rcode = 0;
      writeln(msink, 'Enter thickness of capping layer ',
              '(microns)');
      readln(msource, thick[i]);
      thick[i] := thick[i] * 1.0E-6;
      if code[1] > 2
        then begin
          writeln(msink, 'Enter capping layer mismatch (ppm)');
          readln(msource, c[i]);
          c[i] := c[i] * 1.0E-6;
        end
      else
        c[i] := 0.0;
    end;
    writeln(msink, 'OK - calculating multi layer parameters');
    j := 1;
    for i := 1 to no_layers do begin
      thick[j] := thick[1];

```

```

    thick[j + 1] := thick[2];
    c[j] := mism1;
    c[j + 1] := mism2;
    layer_mat[j] := layer_mat[1];
    layer_mat[j + 1] := layer_mat[2];
    j := j + 2;
  end;
  no_layers := no_layers * 2;
  if (cap[1] = 'Y') OR (cap[1] = 'y')
  then
    no_layers := no_layers + 1;
  end {multilayer};
(* procedure to input layer parameters *)

```

```

procedure single_in(num : integer);

```

```

  var
    mism: real;
    rcode, mcode: integer;
    name: string(25);

  begin
    repeat
      readln(msource, name);
      check(name, rcode, mcode, layer_mat[num]);
      if rcode <> 0
      then
        writeln(msink, 'Sorry don''t know this material - ',
              'choose again');

        until rcode = 0;
      if mcode > 2
      then begin
        writeln(msink, 'Enter mismatch (ppm)');
        readln(msource, mism);
        mism := mism * 1.0E-6;
        end
      else
        mism := 0.0;
      writeln(msink, 'Enter thickness of layer (microns)');
      readln(msource, thick[num]);
      thick[num] := thick[num] * 1.0E-6;
      c[num] := mism;
      end {single_in};
(* procedure to input a single layer *)

```

```

procedure single;

```

```

  begin
    page(msink);
    writeln(msink, 'SINGLE LAYER COMPOSITION');
    if subcomp = [Im,P]
    then begin
      writeln(msink);
      writeln(msink, 'Enter the layer material - either ',
            'GaInAs or GaInAsP');

      end
    else begin
      writeln(msink);
    end
  end

```

```

        writeln(msink, 'Enter the layer material - either ',
                'GaAlAs or AlAs');
    end;
    single_in(1);
    no_layers := 1;
    end {single};
(* procedure to input multiple arbitrary layers *)

procedure multiple;

var
    ls : integer;

begin
    page(msink);
    writeln(msink, 'MULTIPLE LAYER INPUT');
    writeln(msink);
    writeln(msink, 'Enter the number of layers required');
    readln(msource, no_layers);
    if subcomp = [Im, P]
    then begin
        writeln(msink, 'Choose the layers from GaInAs, GaInAsP ',
                'or InP only');
        writeln(msink);
        end
    else begin
        writeln(msink, 'Choose the layers from GaAlAs, GaAs or ',
                'AlAs only');
        writeln(msink);
        end;
    for ls := 1 to no_layers do begin
        writeln;
        writeln(msink, 'Enter the layer material for layer ',
                'number ', ls:3);
        single_in(ls);
        end;
    end {multiple};

(* procedure to read layer parameters from a data file *)

procedure read_layer;

var
    filename : string(25);
    infile : text;
    js, ks : integer;

begin
    writeln(msink);
    writeln(msink, 'Enter file name containing layer',
                ' parameters');
    readln(msource, filename);
    filename := 'File=' || filename;
    reset(infile, filename);
    readln(infile, no_layers);
    for js := 1 to no_layers do begin
        readln(infile, thick[js], c[js], filename);
        for ks := 1 to 7 do begin
            if filename = com_name[ks]
            then layer_mat[js] := com_type[ks];
        end;
    end;
end;

```

```

        end;
    end;
    close(infile);
end;

(* procedure to input type of layer variation required and *)
(* call the appropriate routine *)

procedure layerin;

var
    choice: integer;

begin
    repeat
        writeln(msink, 'The following layer types are available');
        writeln(msink);
        writeln(msink, '    Single layer.....1');
        writeln(msink, '    Linear variation.....2');
        writeln(msink, '    Non-linear variation.....3');
        writeln(msink, '    Multilayer structure.....4');
        writeln(msink, '    Other variation.....5');
        writeln(msink, '    Read variation from file.....6');
        writeln(msink);
        writeln(msink, 'Please enter your choice');
        readln(msource, choice);
        until (choice > 0) AND (choice < 7);
        case choice of
            1: single;
            2: linear(false);
            3: linear(true);
            4: multilayer;
            5: multiple;
            6: read_layer;
        end;
    end {layerin};
(* procedure to calculate layer structure factors *)

procedure layer_sfacts;

var
    i: integer;

begin
    page(msink);
    writeln(msink, 'Calculating layer structure factors');
    for i := 1 to no_layers do begin
        lattice_param(layer_mat[i], c[i], c[i]);
        structuref(layer_mat[i], c[i], h, k, l, lfh1[i],
            lfh2[i], lfo[i]);
    end;
end {layer_sfacts};
(* procedure to input substrate parameters etc *)

procedure subin;

var

```

```

rcode, mcode: integer;

begin
  repeat
    writeln(msink, 'Enter material type for substrate of ',
              'the second crystal');
    readln(msource, substrate);
    check(substrate, rcode, mcode, subcomp);
    if rcode <> 0
      then
        writeln(msink, 'Sorry I don''t know of this material');
    if mcode > 2
      then
        writeln(msink, 'You have chosen either a ternary or ',
                  'quaternary for the substrate !');
    if (rcode <> 0) OR (mcode > 2)
      then begin
        writeln(msink, 'Please enter the second crystal ',
                  'substrate again');
        writeln(msink, ' ');
        end;
    until (rcode = 0) AND (mcode < 3);
    writeln(msink, 'Enter h, k, l for reflection');
    readln(msource, h, k, l);
    writeln(msink, 'Enter i, j, k for surface of crystal');
    readln(msource, ii, jj, kk);
    writeln(msink, 'Enter wavelength (A)');
    readln(msource, wavelength);
    wavelength := wavelength * 1.0E-10;
    repeat
      writeln(msink, 'Polarization state : s - sigma; p - pi;',
                'r - random');
      readln(msource, polar);
      until (polar[1] = 's') OR (polar[1] = 'p') OR
            (polar[1] = 'r');
    if polar[1] = 's'
      then
        polar := 'SIGMA'
      else
        if polar[1] = 'p'
          then
            polar := 'PI'
          else
            polar := 'RANDOM';
    writeln(msink, 'Range of angles for reflectivity relative',
              'to Bragg angle (secs)');
    readln(msource, start, finish);
    writeln(msink, 'Angular step between points (secs)');
    readln(msource, alpha_step);
    lattice_param(subcomp, 0, d_sub);
    structuref(subcomp, d_sub, h, k, l, fh1, fh2, fo);
    stheta := wavelength * sqrt(float(sqr(h) + sqr(k) + sqr(l)))
              / (d_sub * 2.0);
    cphi := sqrt(float(sqr(h * ii + k * jj + l * kk)) /
                 float((sqr(h) + sqr(k) + sqr(l)) *
                       (sqr(ii) + sqr(jj) + sqr(kk))));
    end {subin};

  procedure firstin;

```

```

var
  rcode, mcode: integer;

begin
  repeat
    writeln(msink, 'Enter material type for first crystal');
    readln(msource, first);
    check(first, rcode, mcode, firstcomp);
    if rcode <> 0
      then
        writeln(msink, 'Sorry I don''t know of this material');
    if mcode > 2
      then
        writeln(msink, 'You have chosen either a ternary or',
          ' quaternary for the first crystal !');
    if (rcode <> 0) OR (mcode > 2)
      then begin
        writeln(msink, 'Please enter the first crystal again');
        writeln(msink);
        end;
    until (rcode = 0) AND (mcode < 3);
    writeln(msink, 'Enter h, k, l for reflection');
    readln(msource, fh, fk, fl);
    writeln(msink, 'Enter i, j, k for the surface');
    readln(msource, fii, fjj, fkk);
    lattice_param(firstcomp, 0, d_first);
    structuref(firstcomp, d_first, fh, fk, fl, ffh1, ffh2, ffo);
    ftheta := wavelength * sqrt(float(sqr(fh)+sqr(fk)+sqr(fl)))
      / (d_first * 2.0);
    fphi := sqrt(float(sqr(fh*fii + fk*fjj + fl*fkk)) /
      float((sqr(fh)+sqr(fk)+sqr(fl)) *
      (sqr(fii)+sqr(fjj)+sqr(fkk)))));
  end {firstin};

```

(\* procedure to output data to file INPDAT \*)

```

procedure outdat;

```

```

var
  m: integer;
  date, time : alfa;

begin
  rewrite(output, 'File=PHK0:INPDAT');
  writeln(msink);
  writeln(msink, 'Writing data to file INPDAT ....',
    ' please wait');
  datetime(date, time);
  writeln(date);
  writeln(time);
  if NOT(first_diff) then first := substrate;
  writeln(substrate);
  writeln(first);
  if first_diff
    then
      writeln('YES')
    else
      writeln('NO');
  writeln(wavelength);
  writeln(polar);

```

```

writeln(start, finish);
writeln(alpha_step);
writeln(start, finish);
writeln(alpha_step);
writeln(stheta);
writeln(cphi);
writeln(fh1.re, ' ', fh1.im);
writeln(fh2.re, ' ', fh2.im);
writeln(fo.re, ' ', fo.im);
writeln(d_sub);
writeln(no_layers);
writeln(h, k, l);
writeln(ii, jj, kk);
for m := 1 to no_layers do begin
  writeln(c[m]);
  writeln(thick[m]);
  writeln(lfh1[m].re, ' ', lfh1[m].im);
  writeln(lfh2[m].re, ' ', lfh2[m].im);
  writeln(lfo[m].re, ' ', lfo[m].im);
end;
if first_diff
  then begin
    writeln(ftheta);
    writeln(fphi);
    writeln(ffh1.re, ' ', ffh1.im);
    writeln(ffh2.re, ' ', ffh2.im);
    writeln(ffo.re, ' ', ffo.im);
    writeln(d_first);
  end;
end {outdat};

```

(\* procedure to write layer parameters to a file \*)

```
procedure write_layer;
```

```
var
```

```

filename : string(25);
outfile  : text;
js, ks   : integer;

```

```
begin
```

```

writeln(msink);
writeln(msink, 'Enter file name for layer parameters');
readln(msource, filename);
filename := 'File=' || filename;
rewrite(outfile, filename);
writeln(outfile, no_layers);
for js := 1 to no_layers do begin
  for ks := 1 to 7 do begin
    if layer_mat[js] = com_type[ks]
      then filename := com_name[ks];
    end;
  writeln(outfile, thick[js], c[js], filename);
  end;
close(outfile);
end {write_layer};

```

(\* procedure to edit layer parameters \*)

```
procedure edit;
```



```

var
  instring: string(25);
  index, ascii : integer;
  comchar: char;
  number : array [1 .. 3] of real;

procedure command(var ks: integer; stn: string(25);
                  var out: char);

  begin {command}
    repeat
      ks := ks + 1;
      out := stn[ks];
      until (out <> ' ') OR (ks = length(stn));
    end;

procedure substr(var ks: integer; const stn: string(25);
                 var stout : string(25));

  var
    ls : integer;
    out: char;

  begin {substr}
    repeat
      ks := ks + 1;
      out := stn[ks];
      until (out <> ' ') OR (ks = length(stn));
    ls := 1;
    stout := ' ';
    repeat
      stout[ls] := out;
      ls := ls + 1;
      ks := ks + 1;
      if ks <= length(stn) then out := stn[ks];
      until (out = ' ') OR (out = ',') OR (ks > length(stn));
    end {substr};

procedure num_in(n : integer);

  var
    outstring : string(25);
    js : integer;

  begin
    for js := 1 to n do begin
      if index < length(instring)
      then begin
        substr(index, instring, outstring);
        readstr(outstring, number[js]);
      end
      else number[js] := -999;
    end;
  end {num_in};

procedure print(num : integer);

  var
    js : integer;
    name : string(25);

```

```

begin
  name := '          ';
  for js := 1 to 7 do begin
    if layer_mat[num] = com_type[js]
      then name := com_name[js];
    end;
    writeln('          ', num:3, '          ', thick[num]*1.0E6:8:4,
            '          ', c[num]*1.0E6:8:4,
            '          ', name);
  end {print};
end;

procedure print_layers;

var
  js, n1, n2: integer;
  outstring : string(25);

begin
  num_in(2);
  n1 := trunc(number[1]); n2 := trunc(number[2]);
  if n2 > no_layers then n2 := no_layers;
  if n2 = -999 then n2 := n1;
  if (n2 >= n1) AND (n1 <= no_layers)
    then begin
      writeln(' Layer number   thickness (microns)   ',
              ' mismatch (ppm) material');
      writeln;
      for js := n1 to n2 do begin
        print(js);
      end
    end
    else writeln(' layer number range error');
  end;
end;

procedure delete;

var
  n1, js : integer;
  outstring : string(25);

begin
  num_in(1);
  n1 := trunc(number[1]);
  if (n1 > 0) AND (n1 <= no_layers)
    then begin
      for js := n1 to (no_layers - 1) do begin
        thick[js] := thick[js+1];
        c[js] := c[js+1];
        layer_mat[js] := layer_mat[js+1];
      end;
      no_layers := no_layers - 1;
      writeln(' Layer number ', n1:3, ' deleted');
    end
    else writeln(' Layer number out of range');
  end {delete};
end;

procedure insert;

var

```

```

js, n1, rcode, mcode : integer;
mat : matset;
outstring : string(25);

```

```

begin
  num_in(3);
  if index < length(instring)
    then begin
      substr(index, instring, outstring);
      check(outstring, rcode, mcode, mat);
      end;
  n1 := trunc(number[1]);
  if (n1 > 0) AND (number[2] <> -999) AND (number[3] <> -999)
    AND (rcode = 0) AND (n1 <= no_layers)
    then begin
      if (n1 < no_layers) then begin
        for js := no_layers downto (n1+1) do begin
          thick[js+1] := thick[js];
          c[js+1] := c[js];
          layer_mat[js+1] := layer_mat[js];
          end;
        end;
        thick[n1+1] := number[2] * 1.0E-6;
        c[n1+1] := number[3] * 1.0E-6;
        layer_mat[n1+1] := mat;
        no_layers := no_layers + 1;
        print(n1+1);
        end;
    end {insert};

```

```

procedure mismatch;

```

```

var
  n1 : integer;

begin
  num_in(2);
  n1 := trunc(number[1]);
  if (n1 > 0) AND (n1 <= no_layers) AND (number[2] <> -999)
    then begin
      c[n1] := number[2] * 1.0E-6;
      writeln;
      print(n1);
      end
    else
      writeln(' Input command error');
  end {mismatch};

```

```

procedure thickness;

```

```

var
  n1 : integer;

begin
  num_in(2);
  n1 := trunc(number[1]);
  if (n1 > 0) AND (n1 <= no_layers) AND (number[2] <> -999)
    then begin
      thick[n1] := number[2] * 1.0E-6;
      print(n1);
    end;

```

```

        end
      else
        writeln(' Input command error');
      end {thickness};

procedure comp_change;

var
  n1, rcode, mcode : integer;
  outstring : string(25);
  mat : matset;

begin
  num_in(1);
  n1 := trunc(number[1]);
  if index < length(instring)
    then begin
      substr(index, instring, outstring);
      check(outstring, rcode, mcode, mat);
      end;
  if rcode <> 0 then writeln(' Unkown material type - ',
                          'request ignored');
  if (n1 > 0) AND (n1 <= no_layers) AND (rcode = 0)
    then begin
      layer_mat[n1] := mat;
      print(n1);
      end
    else if rcode = 0 then writeln(' Layer number error');
  end {comp_change};

procedure help;

begin
  writeln;
  writeln(' The following commands are available');
  writeln;
  writeln(' P <layer no> <layer no> - Prints layer ',
          'parameters starting');
  writeln('                                at the first layer',
          'no. to the');
  writeln('                                second no. The ',
          'second no. is');
  writeln('                                optional. ');
  writeln;
  writeln(' T <layer no> <number> - Changes thickness of',
          'layer no. to');
  writeln('                                <number>');
  writeln;
  writeln(' M <layer no> <number> - Changes mismatch of',
          'layer no. to');
  writeln('                                <number>');
  writeln;
  writeln(' C <layer no> <material> - Changes material of',
          'layer no. to');
  writeln('                                <material>');
  writeln;
  writeln(' D <layer no> - Deletes data for ',
          'layer no. ');
  writeln;
  writeln(' I <layer no> <number1> <number2> <material> - ',

```

```

        'Inserts layer');
    writeln;
    writeln(' E          -          Exit from editor mode');
    writeln;
    writeln(' Note - all input should be separated by one or',
            ' more spaces');
    writeln;
    end {help};

procedure illegal;

begin
    if (comchar <> 'E') AND (comchar <> 'e')
        then writeln(' command ?');
    end {illegal};

begin {edit}
    reset(input, 'File=*MSOURCE*,Interactive');
    rewrite(output, 'File=*MSINK*, NOCC');
    page;
    writeln(' When prompted enter command - H for help');
    writeln;
    repeat
        writeln('&*');
        readln(instring);
        index := 0;
        command(index, instring, comchar);
        ascii := ord(comchar);
        if (ascii > 192) then ascii := ascii - 64;
        case ascii of
            151 : print_layers;
            163 : thickness;
            148 : mismatch;
            131 : comp_change;
            132 : delete;
            136 : help;
            137 : insert
            otherwise illegal
        end;
        until (comchar = 'E') OR (comchar = 'e');
    end {edit};

(* main program *)

begin {INPUT_ROCK}
    reset(msource, 'File=*MSOURCE*,Interactive');
    rewrite(msink, 'File=*MSINK*');
    page(msink);
    readparam;
    page(msink);
    subin;
    layerin;
    page(msink);
    writeln(msink, 'Do you want to edit the layer parameters ',
            '(Y/N)');
    readln(msource, query);
    if (query[1] = 'Y') OR (query[1] = 'y')
        then edit;
    writeln(msink);
    writeln(msink, 'Do you want to save the layer parameters ',

```

```
        '(Y/N)');  
readln(msource, query);  
if (query[1] = 'Y') OR (query[1] = 'y')  
    then write_layer;  
layer_sfacts;  
writeln(msink, 'Do you want a different first crystal (Y/N)');  
readln(msource, query);  
if (query[1] = 'Y') OR (query[1] = 'y')  
    then begin  
        first_diff := TRUE;  
        firstin;  
    end  
    else  
        first_diff := FALSE;  
outdat;  
writeln(msink);  
end;
```

```

C
C *****
C * THIS PROGRAM DOES THE NUMBER CRUNCHING FOR ROCKING CURVES *
C *   USING THE DATA FROM FILE INPDAT   *
C * WHICH IS GENERATED BY THE PASCAL PROGRAM INPUT.ROCK.P *
C *****
C
REAL ALPHA(2000), FSUB(2000), THETA, PHI, PHIF, PI
REAL CLAYR(200), THICK(200), FLAY(2000), FSIG(2000)
REAL BETA(2000), FPI(2000)
INTEGER H, K, L, II, JJ, KK, PASS
COMPLEX FH1, FH2, FO, ZSUB(2000), FFH1, FFH2, FFO
COMPLEX LFH1(200), LFH2(200), LFO(200)
CHARACTER*10 POLAR, SUBST, FIRST, DIFF
COMMON /AREA1/ ALPHA, ALSTEP, START, FINISH, NOPNTS, WAVE,
1 POLAR, SUBST, FIRST, DIFF
COMMON /AREA2/ FH1, FH2, FO, DSUB, THETA, PHI
COMMON /AREA3/ FFH1, FFH2, FFO, DFIRST, THETF, PHIF
COMMON /AREA4/ BETA, BSTEP, BSTART, BFIN
COMMON /AREA5/ LFH1, LFH2, LFO, CLAYR, THICK, NOLAYS,
1 H, K, L, II, JJ, KK
C
C Read data from file INPDAT
C
C CALL READAT
C
C No of data points in single crystal reflectivity curves
C
C NOPNTS = INT((FINISH - START)/ALSTEP + 1.5)
C PASS = 1
C WRITE (6,10)
10 FORMAT ('&Enter additional tilt angle (degrees) ? ')
C READ (5,*) TILT
C TILT = TILT * 3.142 / 180.
C
C Calculate substrate reflectivity curve
C
C 20 CALL SUBREF(FH1, FH2, FO, DSUB, THETA, PHI, FSUB, ZSUB,
1 TILT)
C
C Calculate layer reflectivity curve
C
C CALL LAYREF(FSUB, ZSUB, FLAY, TILT)
C
C If first crystal <> substrate calculate its reflectivity
C
C IF (DIFF(1:1) .EQ. 'Y') CALL SUBREF(FFH1, FFH2, FFO,
1 DFIRST, THETF, PHIF, FSUB, ZSUB, 0.)
C
C Convolute reflectivity of first and second crystals
C
C IF (PASS .EQ. 1) CALL CONVOL(FSUB, FLAY, FSIG)
C IF (PASS .EQ. 2) CALL CONVOL(FSUB, FLAY, FPI)
C
C If random polarisation redo with pi polarisation
C
C IF ((POLAR(1:1) .NE. 'R') .AND. (PASS .EQ. 1)) GO TO 50
C IF (PASS .EQ. 2) GO TO 30
C POLAR = 'PI'
C PASS = 2

```

GO TO 20

C  
C  
C

Add sigma and pi polarisations if random

30 DO 40 I = 1, NOPNTS  
    FSIG(I) = FSIG(I) + FPI(I)  
40 CONTINUE

C  
C  
C

Write data to output file

50 WRITE (1,\*) NOPNTS  
    WRITE (1,\*) BSTEP  
    WRITE (1,\*) BETA(1)  
    DO 60 I = 1, NOPNTS  
        WRITE (1,\*) FSIG(I)  
60 CONTINUE  
    STOP  
    END

C  
C  
C  
C  
C  
C

\*\*\*\*\*  
\* SUBREF - CALCULATES INFINITE CRYSTAL REFLECTIVITY \*  
\* OVER A RANGE OF ANGLES RELATIVE TO BRAGG ANGLE \*  
\*\*\*\*\*

SUBROUTINE SUBREF(FH1, FH2, FO, DS, THETA, PHI, FSUB,  
1 ZSUB, TILT)  
    REAL ALPHA(2000), FSUB(2000), THETA, PHI, DS, PI  
    COMPLEX ZSUB(2000), FH1, FH2, FO, CHIH1, CHIH2, CHIO  
    COMPLEX CSQRT, CABS, SQ, B, CH1, CH2  
    CHARACTER\*10 POLAR, SUBST, FIRST, DIFF  
    COMMON /AREA1/ ALPHA, ALSTEP, START, FINISH, NOPNTS, WAVE,  
1 POLAR, SUBST, FIRST, DIFF  
    WRITE (6,10)  
10 FORMAT (' CALCULATING SUBSTRATE REFLECTIVITY')  
    PI = 3.1415927  
    CER = 2.817E-15  
    VUC = DS \*\* 3  
    FFACT = -(WAVE\*\*2\*CER) / (VUC\*PI)  
    CHIH1 = FH1 \* FFACT  
    CHIH2 = FH2 \* FFACT  
    CHIO = FO \* FFACT  
    GAMMAO = SIN(THETA - PHI - TILT)  
    GAMMAH = SIN(THETA + PHI + TILT)  
    CHIH1 = CHIH1 / GAMMAH  
    CHIH2 = CHIH2 / GAMMAO  
    ALPHA(1) = START  
    WRITE (6,20) THETA, PHI  
20 FORMAT (' THETA = ', F10.5, ' PHI = ', F10.5, ' RADIANS')  
    DO 40 I = 1, NOPNTS  
        THS = ALPHA(I) \* PI / (3600.0\*180.0)  
        CH1 = CHIH1  
        CH2 = CHIH2  
        IF (POLAR(1:1) .NE. 'P') GO TO 30  
        CH1 = CHIH1 \* COS(2.0\*(THETA + THS))  
        CH2 = CHIH2 \* COS(2.0\*(THETA + THS))  
30 CONTINUE  
    B = (CHIO/GAMMAO + CHIO/GAMMAH + 2.0\*THS\*SIN(2.0\*THETA))/  
1 GAMMAH) / 2.0  
    SQ = CSQRT(B\*\*2 - CH1\*CH2)  
    ZSUB(I) = -(B + SQ\*SIGN(1.,AIMAG(SQ))) / CH2



```

      FSUB(I) = (CABS(ZSUB(I))) ** 2
      ALPHA(I + 1) = ALPHA(I) + ALSTEP
40 CONTINUE
      RETURN
      END
C
C *****
C * LAYREF - CALCULATES LAYER REFLECTIVITIES USING *
C * REFLECTIVITIES FROM SUBSTRATE AS STARTING POINT *
C *****
C
      SUBROUTINE LAYREF(FSUB, ZSUB, FLAY, TILT)
      REAL ALPHA(2000), FSUB(2000), CLAYR(200), THICK(200), PHI
      REAL FLAY(2000), PI
      INTEGER H, K, L, II, JJ, KK
      COMPLEX ZSUB(2000), LFH1(200), LFH2(200), LFO(200)
      COMPLEX FH1, FH2, FO, B, SQ, NUM, DEN, CSQRT, CCOS, CSIN
      COMPLEX CHIH1, CHIH2, CHIO, CH1, CH2, CTN
      CHARACTER*10 POLAR, SUBST, FIRST, DIFF
      COMMON /AREA1/ ALPHA, ALSTEP, START, FINISH, NOPNTS, WAVE,
1      POLAR, SUBST, FIRST, DIFF
      COMMON /AREA2/ FH1, FH2, FO, DSUB, THETA, PHI
      COMMON /AREA5/ LFH1, LFH2, LFO, CLAYR, THICK, NOLAYS,
1      H, K, L, II, JJ, KK
      PI = 3.1415927
      CER = 2.817E-15
      WRITE (6,10)
10 FORMAT (' CALCULATING LAYER REFLECTIVITY')
      AH = FLOAT(H)
      AK = FLOAT(K)
      AL = FLOAT(L)
      AII = FLOAT(II)
      AJJ = FLOAT(JJ)
      AKK = FLOAT(KK)
      DO 50 I = 1, NOLAYS
          VUC = DSUB ** 2 * CLAYR(I)
          FFACT = -(WAVE**2*CER) / (PI*VUC)
          CHIH1 = LFH1(I) * FFACT
          CHIH2 = LFH2(I) * FFACT
          CHIO = LFO(I) * FFACT
          DLAY = SQRT(1/(AH**2/DSUB**2 + AK**2/DSUB**2 +
1          AL**2/CLAYR(I)**2))
          THETL = ARSIN(WAVE/(2.0*DLAY))
          PHIL = (AH*AII/DSUB**2 + AK*AJJ/DSUB**2 +
1          AL*AKK/CLAYR(I)**2) ** 2
          PHIL = PHIL / ((AH**2/DSUB**2 + AK**2/DSUB**2 + AL**2/
1          CLAYR(I)**2)*(AII**2/DSUB**2 + AJJ**2/DSUB**2 + AKK**2/
1          CLAYR(I)**2))
          PHIL = SQRT(PHIL)
          PHIL = ARCOS(PHIL)
          GAMMAO = SIN(THETL - PHIL - TILT)
          GAMMAH = SIN(THETL + PHIL + TILT)
          D = PI / WAVE * SQRT(GAMMAH/GAMMAO)
          CHIH1 = CHIH1 / GAMMAH
          CHIH2 = CHIH2 / GAMMAO
          WRITE (6,20) I, THETL, PHIL
20 FORMAT (' LAYER NO ', I3, ' THETA = ', F10.5, ' PHI = ',
1          F10.5)
          DO 40 J = 1, NOPNTS
              THS = ALPHA(J) * PI / (3600.0*180.) + THETA - THETL +

```

```

1          PHIL - PHI
          CH1 = CHIH1
          CH2 = CHIH2
          IF (POLAR(1:1) .NE. 'P') GO TO 30
          CH1 = CHIH1 * COS(2.0*(THETL + THS))
          CH2 = CHIH2 * COS(2.0*(THETL + THS))
30        CONTINUE
          B = (CHIO/GAMMAH + CHIO/GAMMAO +
1          2.0*THS*SIN(2.0*THETL)/GAMMAH) / 2.0
          SQ = CSQRT(B**2 - CH1*CH2)
          CTN = CSIN(SQ*D*(-THICK(I))) / CCOS(SQ*D*(-THICK(I)))
          NUM = ZSUB(J) * SQ + (0.0,1.0) * (CH1 + ZSUB(J)*B) * CTN
          DEN = SQ - (0.0,1.0) * (B + ZSUB(J)*CH2) * CTN
          ZSUB(J) = NUM / DEN
          FLAY(J) = CABS(ZSUB(J)) ** 2
40        CONTINUE
50        CONTINUE
          RETURN
          END

```

C  
C  
C  
C  
C

```

*****
* CONVOL - CALCULATES CONVOLUTION OF DATA SETS FSUB & FLAY *
*****

```

```

SUBROUTINE CONVOL(FSUB, FLAY, FCON)
REAL FSUB(2000), FLAY(2000), BETA(2000), FCON(2000)
REAL ALPHA(2000), F(2000)
CHARACTER*10 POLAR, SUBST, FIRST, DIFF
COMMON /AREA1/ ALPHA, ALSTEP, START, FINISH, NOPNTS, WAVE,
1 POLAR, SUBST, FIRST, DIFF
COMMON /AREA4/ BETA, BSTEP, BSTART, BFIN
NPNTS = INT((BFIN - BSTART)/BSTEP + 1.5)
WRITE (6,10)
10 FORMAT (' CALCULATING CONVOLUTION')
BETA(1) = BSTART
DO 20 I = 1, NPNTS
CALL MULT(FSUB, FLAY, BETA(I), F, NDP)
FCON(I) = AINTG(ALPHA,F,NDP)
BETA(I + 1) = BETA(I) + BSTEP
20 CONTINUE
RETURN
END

```

C  
C  
C  
C  
C

```

*****
* MULTIPLIES TWO DATA SETS, ONE OFFSET FROM THE OTHER BY BETA *
*****

```

```

SUBROUTINE MULT(FSUB, FLAY, BETA, F, NDP)
REAL FSUB(2000), FLAY(2000), F(2000), ALPHA(2000)
CHARACTER*10 POLAR, SUBST, FIRST, DIFF
COMMON /AREA1/ ALPHA, ALSTEP, START, FINISH, NOPNTS, WAVE,
1 POLAR, SUBST, FIRST, DIFF
NDP = 0
N = NOPNTS - 1
L = 1
IF ((ALPHA(1) + BETA) .GT. ALPHA(NOPNTS)) RETURN
IF ((ALPHA(NOPNTS) + BETA) .LT. ALPHA(1)) RETURN
DO 50 I = 1, NOPNTS
IF ((ALPHA(I) + BETA) .GT. ALPHA(NOPNTS)) GO TO 60
IF ((ALPHA(I) + BETA) .LT. ALPHA(1)) GO TO 40

```

```

DO 20 J = L, N
  H = ALPHA(I) + BETA - ALPHA(J)
  SH = ALPHA(J + 1) - ALPHA(J)
  IF (H .GT. SH) GO TO 10
  G = FLAY(J) * (1 - H/SH) + FLAY(J + 1) * H / SH
  GO TO 30
10  CONTINUE
20  CONTINUE
30  NDP = NDP + 1
    F(NDP) = FSUB(I) * G
    L = J
40  CONTINUE
50  CONTINUE
60  CONTINUE
    RETURN
    END

```

```

C
C *****
C * AINTG - CALCULATES AREA UNDER MULTIPLIED DATA SET F *
C *****
C

```

```

FUNCTION AINTG(ALPHA, F, NDP)
REAL ALPHA(2000), F(2000)
N = NDP - 1
AINTG = 0.0
DO 10 I = 1, N
  H = ALPHA(I + 1) - ALPHA(I)
  AINTG = AINTG + (F(I) + F(I + 1)) * H / 2.0
10 CONTINUE
RETURN
END

```

```

C
C *****
C * READAT - READS DATA FROM FILE INPDAT *
C *****
C

```

```

SUBROUTINE READAT
REAL ALPHA(2000), BETA(2000), FSUB(2000), PHI, PHIF
REAL THICK(200), CLAYR(200)
INTEGER H, K, L, II, JJ, KK
COMPLEX ZSUB(2000), FH1, FH2, FO, FFH1, FFH2, FFO
COMPLEX LFH1(200), LFH2(200), LFO(200)
CHARACTER*10 POLAR, SUBST, FIRST, DIFF, DATE, TIME
COMMON /AREA1/ ALPHA, ALSTEP, START, FINISH, NOPNTS, WAVE,
1 POLAR, SUBST, FIRST, DIFF
COMMON /AREA2/ FH1, FH2, FO, DSUB, THETA, PHI
COMMON /AREA3/ FFH1, FFH2, FFO, DFIRST, THETF, PHIF
COMMON /AREA4/ BETA, BSTEP, BSTART, BFIN
COMMON /AREA5/ LFH1, LFH2, LFO, CLAYR, THICK, NOLAYS,
1 H, K, L, II, JJ, KK

```

```

C
C Read data from file INPDAT
C
CALL FTNCMD('ASSIGN 3=INPDAT;')
READ (3,10) DATE
READ (3,10) TIME
READ (3,10) SUBST
READ (3,10) FIRST
READ (3,10) DIFF
READ (3,*) WAVE

```

```

READ (3,10) POLAR
READ (3,*) START, FINISH
READ (3,*) ALSTEP
READ (3,*) BSTART, BFIN
READ (3,*) BSTEP
10 FORMAT (' ', A10)
WRITE (6,20) TIME, DATE
20 FORMAT (' DATA GENERATED AT ', A10, ' ON ', A10)
WRITE (6,30) FIRST, SUBST
30 FORMAT (' First crystal is ', A10, ' Second crystal is ',
1 A10)
WRITE (6,40) WAVE
40 FORMAT (' Wavelength = ', E12.5)
WRITE (6,50) POLAR
50 FORMAT (' Polarization state is ', A10)
WRITE (1,*) DATE
WRITE (1,*) TIME
WRITE (1,*) SUBST
WRITE (1,*) FIRST
WRITE (1,*) WAVE
WRITE (1,*) POLAR

```

C  
C  
C

Read substrate variables

```

READ (3,*) THETA
READ (3,*) PHI
READ (3,*) FH1
READ (3,*) FH2
READ (3,*) FO
READ (3,*) DSUB
THETA = ARSIN(THETA)
PHI = ARCOS(PHI)
WRITE (1,*) THETA, PHI, DSUB

```

C  
C  
C

Read layer variables

```

READ (3,*) NOLAYS
READ (3,*) H, K, L
READ (3,*) II, JJ, KK
DO 60 I = 1, NOLAYS
  READ (3,*) CLAYR(I)
  READ (3,*) THICK(I)
  READ (3,*) LFH1(I)
  READ (3,*) LFH2(I)
  READ (3,*) LFO(I)
60 CONTINUE
WRITE (1,*) NOLAYS
WRITE (1,*) H, K, L
WRITE (1,*) II, JJ, KK
DO 70 I = 1, NOLAYS
  WRITE (1,*) CLAYR(I), THICK(I)
70 CONTINUE

```

C  
C  
C

Read first crystal variables if necessary

```

IF (DIFF(1:1) .EQ. 'N') GO TO 90
WRITE (6,80)
80 FORMAT (' Reading first crystal parameters')
READ (3,*) THETF
READ (3,*) PHIF

```

```
READ (3,*) FFH1  
READ (3,*) FFH2  
READ (3,*) FFO  
READ (3,*) DFIRST  
THETF = ARSIN(THETF)  
PHIF = ARCOS(PHIF)  
90 CONTINUE  
RETURN  
END
```

```

C *****
C *
C *          PLOTTER
C *
C * This programme plots the reflectivity against angle
C * of incidence from the convoluted data. The effect of
C * curvature can be added by smoothing over a given no.
C * of data points.
C *
C *          THE *GHOST SYSTEM IS USED.
C *****
C
C REAL MAX, MIN, REFS(2000), W(200), M(200), MM, MMIN
C REAL BETA(2000), WOL(200)
C LOGICAL*1 CHOICE(4), EQU
C INTEGER FILE
C INTEGER PNOL, H
C DIMENSION SUBST(3), FIRST(3), POLAR(3), DATE(3), TIME(3)
C
C Define constants used to determine scaling of graph
C
C WRITE (6,10)
C 10 FORMAT (' Please wait ... reading data from disc file')
C FILE = 1
C RMAX = 0.
C RMIN = 1E20
C MAX = 0.
C MIN = 10000.
C MM = 0.
C TOL = 0.
C MMIN = 1000.
C
C Read data from disc file
C
C READ (FILE,20) DATE
C READ (FILE,20) TIME
C 20 FORMAT (3A4)
C WRITE (6,30) TIME, DATE
C 30 FORMAT (' DATA GENERATED AT ', 3A4, ' ON ', 3A4)
C READ (FILE,50) SUBST
C READ (FILE,50) FIRST
C READ (FILE,*) WAVE
C READ (FILE,50) POLAR
C READ (FILE,*) THETA, PHI, DSUB
C READ (FILE,*) NOLAYS
C READ (FILE,*) H, K, L
C READ (FILE,*) II, JJ, KK
C DO 40 I = 1, NOLAYS
C   READ (FILE,*) M(I), W(I)
C   M(I) = (M(I) - DSUB) / DSUB * 1.0E6
C   WOL(I) = W(I) * 1.0E6
C   TOL = TOL + WOL(I)
C   IF (M(I) .GT. MM) MM = M(I)
C   IF (M(I) .LT. MMIN) MMIN = M(I)
C 40 CONTINUE
C 50 FORMAT (3A4)
C READ (FILE,*) NOPNTS
C READ (FILE,*) BSTEP
C READ (FILE,*) BETA(1)
C DO 60 J = 1, NOPNTS
C   READ (FILE,*) REFS(J)
C   IF (BETA(J) .GT. MAX) MAX = BETA(J)

```

```

        IF (BETA(J) .LT. MIN) MIN = BETA(J)
        IF (REFS(J) .GT. RMAX) RMAX = REFS(J)
        IF (REFS(J) .LT. RMIN) RMIN = REFS(J)
        BETA(J + 1) = BETA(J) + BSTEP
60 CONTINUE

```

C  
C  
C

Input of range of data to be plotted

```

        WRITE (6,70) BSTEP
70 FORMAT (' The data has an angular step interval of ', F5.1,
1       ' secs')
        WRITE (6,80)
80 FORMAT (' Enter the change in angle along the incident',
1       ' X-ray beam (secs)')
        READ (5,*) ASMTH
        ISMTH = INT(ASMTH/BSTEP)
        IF (ISMTH .LE. 1) GO TO 110
        RMAX = 0.
        RMIN = 1E20
        NOPNTS = NOPNTS - ISMTH
        DO 100 J = 1, NOPNTS
            REFL = 0.
            DO 90 I = 1, ISMTH
                REFL = REFL + REFS(I + J - 1)
90 CONTINUE
            REFS(J) = REFL
            IF (REFS(J) .GT. RMAX) RMAX = REFS(J)
            IF (REFS(J) .LT. RMIN) RMIN = REFS(J)
100 CONTINUE
110 WRITE (6,120)
120 FORMAT (' Do you require a logarithmic scale (Y/N)')
        READ (5,130) CHOICE
130 FORMAT (4A1)
        IF ( .NOT. (EQUC(CHOICE(1), 'Y'))) GO TO 150
        RMAX = 1E-20
        RMIN = 1E20
        DO 140 I = 1, NOPNTS
            REFS(I) = ALOG10(REFS(I))
            IF (REFS(I) .GT. RMAX) RMAX = REFS(I)
            IF (REFS(I) .LT. RMIN) RMIN = REFS(I)
140 CONTINUE
150 WRITE (6,160)
160 FORMAT (' NORMALIZING DATA')
        DO 170 I = 1, NOPNTS
            REFS(I) = (REFS(I) - RMIN) / (RMAX - RMIN) * 100.
170 CONTINUE
        RMAX = 100.
        RMIN = 0.
        WRITE (6,180)
180 FORMAT (' Range of data to plot is:-')
        WRITE (6,190) MIN, MAX, RMIN, RMAX
190 FORMAT (' Xmin=', F10.4, 2X, 'Xmax=', F9.4, 2X, 'Ymin=',
1       F5.2, 'Ymax=', F10.4)
        WRITE (6,200)
200 FORMAT (' Enter range to be plotted in X direction')
        WRITE (6,210)
210 FORMAT ('&           from ? ')
        READ (5,*) MIN
        WRITE (6,220)
220 FORMAT ('&           to ? ')

```

```

      READ (5,*) MAX
      WRITE (6,230)
230  FORMAT (' Range to be plotted in Y direction')
      WRITE (6,240)
240  FORMAT ('&          to ? ')
      READ (5,*) RMAX

```

```

C
C Plot defined region of data using *GHOST routines

```

```

C
C Information box first

```

```

C

```

```

      CALL PAPER(1)
      CALL BLKPEN
      CALL PSPACE(0.80, 1.0, 0., 0.56)
      CALL CSPACE(0.80, 1.0, 0., 0.56)
      CALL MAP(0., 1., 0., 1.)
      CALL CTRMAG(7)
      CALL BORDER
      CALL PLACE(0, 0)
      CALL CRLNFS(4)
      CALL TYPECS(' DATA GENERATED AT : ', 21)
      CALL TYPECS(TIME, 10)
      CALL CRLNFD
      CALL TYPECS('                ON : ', 21)
      CALL TYPECS(DATE, 10)
      CALL CRLNFS(3)
      CALL TYPECS(' SECOND CRYSTAL : ', 19)
      CALL TYPECS(SUBST, 10)
      CALL CRLNFS(3)
      CALL TYPECS(' FIRST CRYSTAL : ', 17)
      CALL TYPECS(FIRST, 10)
      CALL CRLNFS(3)
      CALL TYPECS(' POLARIZATION : ', 16)
      CALL TYPECS(POLAR, 10)
      CALL CRLNFS(3)
      CALL TYPECS(' WAVELENGTH = ', 14)
      CALL TYPENE(WAVE, 5)
      CALL TYPECS(' M', 2)
      CALL CRLNFS(3)
      CALL TYPECS(' BRAGG ANGLE = ', 16)
      CALL TYPENE(THETA, 5)
      CALL CRLNFS(3)
      CALL TYPECS(' PHI = ', 7)
      CALL TYPENE(PHI, 5)
      CALL CRLNFS(3)
      CALL TYPECS(' REFLECTION = ', 14)
      CALL TYPENI(H, 2)
      CALL TYPENI(K, 2)
      CALL TYPENI(L, 2)
      CALL CRLNFS(3)
      CALL TYPECS(' SURFACE = ', 11)
      CALL TYPENI(II, 2)
      CALL TYPENI(JJ, 2)
      CALL TYPENI(KK, 2)
      CALL CRLNFS(3)
      CALL TYPECS(' LAYER THICKNESS = ', 19)
      CALL TYPENF(TOL, 5)
      CALL CTRSET(4)
      CALL TYPECS(' M', 2)
      CALL CTRSET(1)

```



```

CALL TYPECS('M', 1)
CALL CRLNFS(3)
CALL TYPECS(' NO OF LAYERS : ', 16)
CALL TYPENI(NOLAYS, 3)
IF (ISMTH .LE. 1) GO TO 250
CALL CRLNFS(3)
CALL TYPECS(' CURVATURE ANGLE ', 17)
ASMTH = BSTEP * ISMTH
CALL TYPENF(ASMTH, 5)
CALL TYPECS(' SECS', 5)
250 CONTINUE
C
C Now plot the rocking curve and axes
C
C Labels first
C
CALL PSPACE(.01, .74, 0.08, .5)
CALL CSPACE(.0, 1., .0, 1.)
CALL MAP(0., 1., 0., 1.)
CALL CTRMAG(20)
CALL CTRSET(3)
CALL PLOTCS(0.70, 0.005, 'D', 1)
CALL CTRSET(4)
CALL TYPECS('J', 1)
CALL CTRSET(2)
CALL TYPECS(' (SECS)', 8)
CALL CTRSET(1)
CALL CTRORI(1.0)
CALL PLOTCS(0.02, 0.35, 'REFLECTIVITY (%)', 16)
CALL CTRORI(0.0)
CALL PSPACE(.10, .74, 0.14, 0.5)
CALL CSPACE(.00, .80, 0.00, 0.6)
CALL MAP(MIN, MAX, RMIN, RMAX)
CALL CTRMAG(12)
C
C Draw axes
C
CALL MARK(MAX - MIN, SX)
CALL MARK(RMAX, SY)
CALL AXESSI(SX, SY)
C
C Plot the rocking curve
C
CALL NSCURV(BETA, REFS, 1, NOPNTS)
C
C Draw graph of layer mismatch vs depth
C
CALL PSPACE(0.80, 1.00, 0.00, 0.20)
CALL THICK(1)
CALL BLKPEN
CALL CSPACE(.80, 1.0, .00, 0.2)
CALL MAP(0., 0.2, 0., 0.4)
CALL CTRMAG(6)
CALL PLOTCS(0.05, 0.02, 'DEPTH BELOW SURFACE', 19)
CALL CTRSET(4)
CALL TYPECS(' M', 2)
CALL CTRSET(1)
CALL TYPECS('M', 1)
CALL POSITN(0.01, 0.08)
CALL CTRORI(1.0)

```

```

CALL TYPECS('LATTICE MISMATCH (PPM)', 22)
CALL CTRORI(0.)
IF (MMIN .GT. 0.) MMIN = 0.
CALL PSPACE(.85, .95, .04, .16)
CALL MAP(0., TOL, MMIN, MM)
CALL MARK(TOL*2., SX)
CALL CTRMAG(3)
CALL MARK((MM - MMIN)*2., SY)
CALL AXESSI(SX, SY)
CALL POSITN(0., M(NOLAYS))
WW = WOL(NOLAYS)
PNOL = NOLAYS
IF (NOLAYS .EQ. 1) GO TO 270
NL = NOLAYS - 1
DO 260 L = 1, NL
    CALL JOIN(WW, M(PNOL))
    CALL JOIN(WW, M(PNOL - 1))
    WW = WW + WOL(PNOL - 1)
    PNOL = PNOL - 1
260 CONTINUE
270 CALL JOIN(WW, M(PNOL))
    CALL JOIN(WW, 0.)

```

C

C End plotting

C

```

CALL GREND
STOP
END

```

C

C routine to calculate tick lengths along axes

C

```

SUBROUTINE MARK(RANGE, STEP)
IB = IFIX(ALOG10(RANGE))
A = RANGE / 10.0 ** IB
IF ((A .GE. 1.) .AND. (A .LT. 3.))
1 STEP = 2. * 10. ** (IB - 1)
IF ((A .GE. 3.) .AND. (A .LT. 7.))
1 STEP = 5. * 10. ** (IB - 1)
IF ((A .GE. 7.) .AND. (A .LT. 10.))
1 STEP = 1 * 10. ** IB
RETURN
END

```

C

C routine to provide n crlnfds

C

```

SUBROUTINE CRLNFS(N)
DO 10 I = 1, N
    CALL CRLNFD
10 CONTINUE
RETURN
END

```

## APPENDIX B

## PROGRAMMING THE MINICAM I.C.C. BOARD FOR ASCII SERIAL DATA

The software required to operate the two channel I.C.C. serial interface is described. A full 6502 disassembler and a memory dump utility are also implemented. These follow, in principle, those described in 'Beyond Games: System Software for your 6502 Personal Computer' by Ken Skier. This new software plus the original, slightly modified, 'Minicon' software occupies about 3k of code and therefore requires two of the board's 2k, 2532 type, EPROMS.

The board control software, 'Minicon', occupies the EPROM located at \$F000 to \$FFFF, and also contains the 6502 reset routines. The disassembler and monitor are contained in the EPROM from \$E000 to \$EFFF. Since the monitor uses code located within the other EPROM a jump table is provided at \$F000 onwards to enable these routines to be located even if their absolute location within the other EPROM is altered during development. The jump instructions within this table are guaranteed not to be altered, thus avoiding the need to reprogramme all the EPROMs if code in one is changed. This system is similar to the operating system jump table provided on the BBC microcomputer (OSWRCH, OSBYTE, OSWORD, OSFILE etc).

During RESET the stack is setup and interrupts disabled. The least significant five bits of the address switch on the main board are used to set the GPIB address register in the 68488. Once the two 6850's have been master reset, the word format switch on the serial board is read and the least significant four bits and most significant four bits used to program the second and first 6850's respectively. The clock divide ratio in both chips is set to 16, since the 4702 produces 16 times the standard baud rates. The top three bits of the address switch are then used to determine which mode of operation is required. The location of the required code is copied on to the zero page from the table RESTAB to enable an indirect jump to the code.

If interrupts are enabled by any code the 6502 is vectored to a piece of code that jumps to the location held in \$00,\$01. This location is initially set to the remainder of the interrupt handler in the EPROM \$F000-\$FFFF. However, if the user wishes to provide another interrupt handler the location held in \$00,\$01 can easily be altered.

Routines using the GPIB bus as the host interface set the flags IEEFLG, used to select the input device in the character input routine, and IEEEPR, used to select the output device during character output. Ascii modes also set the flag NEWFLG, which is used by the board control routines to determine whether the existing binary output routines or the new Ascii ones should be used. Additionally, the character output routine uses the flags HOST and PRINTR to determine whether output should go to the host or printer serial ports, and the flag IEEEPR for the GPIB port as output. Note that more than one of the flags HOST, PRINTR

and IEEEPR can be set at once, enabling output to be sent to more than one device simultaneously.

The operating modes supported at present are:

- Monitor - development mode with disassembler and memory dump options. Uses the host serial port or GPIB port.
- Minicon - mode for control of modules, can be used either in binary or ascii. Ascii with host serial port or GPIB port, binary only with GPIB port.
- GPIB to serial - takes data from the GPIB port and transmits it via the host serial port. Hardware handshaking can be used to control the flow of data from the serial port. At present only unidirectional.
- Serial to serial - takes data from the host serial port and transmits it via the printer serial port. No buffering is performed so the printer port should operate at baud rates greater than or equal to the host port baud rate.

### Monitor

This routine is designed to operate with a dumb terminal. Once the routine is entered all variables are initialised by a jump to INIT. The 6850 is set with RTS low, to prevent input from the terminal. The state of the flag IEEFLG is checked to determine whether the GPIB port or the host serial port has been selected. For GPIB operation the flags HOST and PRINTR are cleared and IEEEPR set, while for serial operation HOST is set and PRINTR, IEEEPR cleared. A start up message is then transmitted plus the prompt character, '\*', which is useful to check that communication formats are correctly set. If serial control is selected the RTS line is then set high, allowing input.

Characters are received and stored in the input buffer located at \$0300. If either a backspace or delete is detected action is taken to remove the last character from the buffer, provided that it is not already empty. The character received is echoed back to the terminal unless it was a delete or backspace with an empty buffer, when an ascii bell is echoed. Once a carriage return is received the input routine is exited and the first character checked for a valid command. The commands currently available are selected as below.

Character	Variables	Command
D	Start, End Addresses	Disassemble from start address to end address
M	Start, End Addresses	Dump memory between start address and end address
E	none	Exit to Minicon

P	none	Toggle serial printer flag on and off to provide hardcopy
H	none	Help - displays this information

If a valid character is found the relevant routine is entered otherwise the message '? COMMAND' is transmitted followed by a jump back to the start of this routine. For those commands requiring input of variables, ie D and M, the routine STEASA is entered. Starting from the end of the input buffer each character, corresponding to a hexadecimal digit, is removed and converted to binary. If conversion to binary produces an error because the character was not a valid hexadecimal digit the message 'COMMAND ERROR' is transmitted and the routine terminated with the carry flag set. Once a valid binary value is found it added to the start or end address value as necessary, after multiplying by the required factor of 16 (left shift four times). The two addresses should be separated by a space character. If STEASA is successful in obtaining two valid 16 bit addresses the carry flag is cleared and the routine terminated.

The disassembly and memory dump routines are then entered once valid start and end addresses have been found. Since the table driven disassembler and memory dump are similar to those described in Ken Skier's book they will not be described here. There are, however, some errors present in the tables contained within the book. Output from these routines is performed by the routine PRTCHR, which transmits output according to the previously described flags. The P command can be used to toggle the flag PRINTR on and off to enable hardcopy to be obtained on a serial printer attached to the printer port.

### Minicon

Once entered this routine selects the output devices in a similar manner to the monitor routine. Characters received are placed in the same input buffer but no interpretation of backspace or delete is made. No characters are echoed back to the terminal/microcomputer. This routine is designed, primarily, to operate with a microcomputer where echoing of the input would be unnecessary. Once the currently selected input terminator byte is received the character entry routine is entered and the buffer decoded. Since the number of commands provided by this routine is far greater than those offered by the monitor a rather more sophisticated decoding process is implemented in order to save memory space. Commands are selected by a two letter code and a one number option, eg AD1, thus allowing up to 260 possible commands. The input data, if required, should then follow, separated from the command name by a comma with each number delimited also by a comma (eg. ST1,32,1000,100).

The first character in the buffer is removed from the buffer

and checked to be in the range 'A' to 'Z' by subtracting 65 and testing for the byte to be in the range  $\geq 0$  and  $< 26$ . If the byte is out of this range the message 'BAD COMMAND' is transmitted and the input section reentered. A valid byte is then used as an index to the table of valid second characters CHTAB. This character is compared with the second character in the input buffer and if they do not agree the 'BAD COMMAND' error message is returned as above. The third character is then removed from the buffer and checked for validity by subtracting 48 to give a range of 0 to 9. If it is non valid the error message 'BAD OPTION' is returned. The table JMPTAB contains the addresses minus one of the possible routines and is accessed by the following technique. The valid first character byte is used to obtain an offset number from the table OFFSET which gives the offset of the start of the addresses for a particular command from the start of JMPTAB. The byte obtained from the option number is multiplied by two and added to this offset thus pointing to the high byte of the required address. This value is fetched and pushed onto the stack. The preceding low byte value is then also fetched and pushed onto the stack. An RTS instruction then fetches this address off the stack and sets the program counter to this address plus one which will be the start of the required code.

The majority of the routines accessed in this way then remove the required number of input parameters from the input buffer, converting from ascii decimal to binary, with commas as number delimiters. Conversion from decimal to binary is not so straightforward as from hexadecimal to binary. In order to avoid binary multiplication and increase the speed of the conversion a tabular method is used. The decimal number removed from the buffer is checked for validity, if it is not a '0' to '9' the error 'VARIABLE ERROR' is returned. A valid byte is then used to access tables of 10's, 100's, 1000's, 10000's which contain the binary value of 10,20...90; 100,200...900 etc. The values obtained from these tables are added to the units value to give the binary number. The numbers obtained are stored consequetively from address VA (\$40) which correspond to the original Minicon input values. A jump to the original module handling routines is then made. These routines, slightly modified, are contained in the \$F000 EPROM.

Some of the original Minicon routines have an overlap function, returning data to complete the communication process before actually operating the module, allowing the controlling computer to perform some other tasks while, for example, a stepper motor is driving a large number of steps. This option is implemented in the new software as another option number, with the message 'OK' being returned.

When a routine has finished the software informs the controlling computer by transmitting a message or value read from a module. The value read from the module is converted to ascii before transmission if the flag NEWFLG is set. When NEWFLG is clear the original binary GPIB output routine is used. For modules that are output devices the message 'OK'

is returned, while for input modules that can generate errors, such as an overrange on an A to D module, a meaningful error message is transmitted. Possible error messages are 'OVERRANGE' for an A to D overrange or 'TIMED OUT' for either a faulty or non present A to D or an incomplete handshake on a GPIB (general purpose input board).

If a Minicon routine generates a negative value, such as an A to D, the routine sets the flag NEGFLG, informing the output routine that the value returned is in two's complement. The output routine REPLAN then takes the two's complement of this value before converting to ascii and transmits a minus sign before in front of the ascii coded value. Conversion to ascii is performed by using the well known double babble method. This routine, BINASC, returns with three bytes in the output buffer representing six BCD numbers. The output bytes are then converted to ascii, 4 bits at a time, by adding 48. The flag LEADZ is used to suppress the transmission of leading zeros, but if the output routine ends with LEADZ still clear the value is zero so one zero is transmitted.

In addition to the existing Minicon routines a number of new ones have been added, particularly those enabling use of the extra serial ports. These are detailed along with the other commands available below.

## MINICON COMMAND DESCRIPTIONS

<u>Command</u>	<u>Input</u>	<u>Description</u>
AD1	address	reads A to D number <address>, same as old usr(5).
AD2	add., n1, n2	operates 16 channel autoranging A to D, same as usr(10).
CO1	address, n1	counts for <n1> 100th's second using scalar module number <address>. Same as usr(2).
CO2	address, n1	same as CO1 but overlap option is implemented.
DA1	address, n1	outputs value <n1> to two channel D to A number <address>, same as usr(4) without 512 added to address.
DA2	address, n1	outputs value <n1> to 4 channel D to A number <address>, same as usr(4) with 512 added to address.
GP1	address	inputs 16 bit value from general purpose input board (GPIB), same as usr(8).
MO1	nothing	jumps to the binary version of Minicon for use via the GPIB interface.
MO2	nothing	jumps to the new ascii monitor with the GPIB interface selected as the input and output port.
MO3	nothing	jumps to the ascii version of Minicon with the GPIB interface selected.
MO4	nothing	jumps to the new ascii monitor with the host serial port selected.
MO5	nothing	jumps to the GPIB to host serial port routine.
PR1	string	Outputs the characters in the string via the printer serial port. The carriage return is transmitted plus any other termination byte as selected by PR2 (eg linefeed).
PR2	byte	the character <byte> is used as the terminator byte by PR1.
RD1	nothing	returns value held in output buffer, same as usr(0).
RD2	address	reads counts held in scalar <address>, same as usr(3).
ST1	add., n1, n2	operates the stepper motor board number <add.> for <n1> steps with <n2> x 0.1 millisecs between steps. Same as usr(1)
ST2	add., n1, n2	same as ST1 but overlap option implemented.
ST3	n1, n2, n3	sets speeds for accelerating stepper motor driver ST4. n1 is the start/stop speed (in 0.1 msec), n2 is the top speed (in 0.1 msec) and n3 is the change in speed per step (in 0.1 msec).
ST4	add., n1	drives motor <add.> <n1> number of steps. Speeds set by ST3.



VP1    add., n1, n2   vector plot option using two channel D  
                                  to A board <address>, same as usr(6).  
VP2    add., n1, n2   as VP1 but is the same as usr(7).

#### Parallel to serial conversion

This routine is entered either by the setting of the address switch at reset or by the MO5 command in Minicon. Bytes are taken from the GPIB interface and transmitted via the host serial port completely transparently. No buffering takes place as bytes are only removed from the GPIB interface when the serial port has transmitted the previous byte. Hardwire handshaking can be used to control the flow of data from the serial port, the speed at which data is taken from the GPIB interface will, therefore, also reflect this handshaking. The routine is exited by the receipt of three consecutive escape codes (ascii 27), none of which will be transmitted via the serial port. Single and double escape sequences can, therefore, be sent through the interface for control of Epson printers etc. When the routine exits it returns to the Minicon routine with the GPIB interface selected.

```

;
; MAIN MINICON ROUTINES. OCCUPIES EPROM
; $FOOO TO $FFFF. CONTAINS BOARD CONTROL
; ROUTINES PLUS BINARY AND ASCII USER
; INTERFACES
;

```

```

; M.J. HILL 1985
;

```

```

; SETUP VARIABLES
;

```

```

0006 USRCMD EQU $06 vector for user cmmd.
0010 USRNO EQU $10
0011 SAVX EQU $11
0012 TMPO EQU $12 output bytes
0014 WKSP EQU $14 work space for A to D
001F STATUS EQU $1F third byte of output
0020 VLIST EQU $20 three input variables
0020 VA EQU $20 A%
0022 N EQU $22 N%
0024 T EQU $24 and T%
0026 TEMPT EQU $26 temporary T% location
0028 TVECLO EQU $28
002A TVECHI EQU $2A
002C WKLOC EQU $2C
0030 NEWFLG EQU $30 new ascii version flg
0031 NEGFLG EQU $31 output is negative
0032 BUFFEN EQU $32 buffer end pointer
0034 BPOINT EQU $34 buffer fill pointer
0036 CHAR EQU $36 output char store
0037 HGHBIT EQU $37 highbyte of output
0038 LOWBIT EQU $38 lowbyte of output
0039 CREG EQU $39 command reg of ACIA 1
003A CREG2 EQU $3A command reg of ACIA 2
003B IEEFLG EQU $3B IEEE488 flag
003C IEEEPR EQU $3C IEEE488 as printer
003D PDELM EQU $3D printer delimiter
003E DELIM EQU $3E command delimiter
003F LEADZ EQU $3F leading zero strip
0040 INCNT EQU $40
0041 TPOINT EQU $41 table pointer
0043 SELECT EQU $43
0045 GETPTR EQU $45
0047 PRINTR EQU $47 serial printer flag
0048 HOST EQU $48 serial host flag
0049 RETURN EQU $49 return address loctn
0070 TOP EQU $70 top speed of motor
0072 BOTTOM EQU $72 bottom speed of motor
0074 INC EQU $74 speed increment
0075 FAST EQU $75 top speed flag
0076 SLOW EQU $76 slow down flag
0077 DECL EQU $77 number of steps to
; decelerate
;

```

```

; BOARD ADDRESSES ETC
;

```

```

8000 VIA EQU $8000 via's
8020 IEE EQU $8020 GPIA chip (68488)
801F DATALO EQU VIA+$1F data bus low byte

```

```

8010      DATAHI      EQU VIA+$10      data bus high byte
8025      SRQ          EQU IEE+5        service request byte
8030      ACIA1        EQU $8030        ACIA 1 (host)
8038      ACIA2        EQU $8038        ACIA 2 (printer)
8034      SWITCH       EQU $8034        parity switch
;
; BUFFERS
;
0300      BUFF         EQU $0300        input buffer
0350      OUTBUF       EQU $0350        output buffer
0200      TVHBUF       EQU $0200        work space for vector
0220      TVLBUF       EQU $0220        generator
;
; CONSTANTS
;
000D      NCMD5       EQU $0D          number of commands
0000      APNT         EQU $00
0002      NPNT         EQU $02
0004      TPNT         EQU $04
00FF      ON          EQU $FF
0000      OFF          EQU $0
000D      CR          EQU $0D
000A      LF          EQU $0A
007F      TEX         EQU $7F          defines start of text
00FF      ETX         EQU $FF          and end of text
;
; ENTRY JUMP TABLE IN $E000 EPROM
;
E000      MON          EQU $E000        location of monitor
;
F000      ORG          ORG $F000
;
; JUMP TABLE FOR ROUTINES REQUIRED BY $E000 EPROM
;
F000 4C 4EFC      JMP RESET      these routines are
F003 4C D3F7      JMP PRTCHR     required by code not
F006 4C 20F8      JMP PRINT      contained in this
F009 4C 82F7      JMP HOSTON     Eprom
F00C 4C 87F7      JMP HOSTOF
F00F 4C 8CF7      JMP PRTON
F012 4C 91F7      JMP PRTOFF
F015 4C 96F7      JMP RTSON
F018 4C A0F7      JMP RTSOFF
F01B 4C AAF7      JMP RSRES
F01E 4C 4AF8      JMP PUSHSL
F021 4C 5DF8      JMP POPSL
F024 4C 90F8      JMP GETCHR
F027 4C 28F7      JMP RDOB
F02A 4C 70F8      JMP GETSL
F02D 4C 9BF8      JMP MNSTRT
;
; INITIALISE VIA'S
;
F030 A9 00      INIT          LDA #0
F032 8D 0F80      STA VIA+$0F      address = 0, no oper.
F035 8D 1280      STA VIA+$12      data lines
F038 8D 1380      STA VIA+$13      as inputs
F03B 8D 1B80      STA VIA+$1B      disable special

```

F03E	8D	1C80	STA VIA+\$1C	features
F041	A9	A0	LDA #\$A0	
F043	8D	0280	STA VIA+2	control lines
F046	A9	FF	LDA #\$FF	address byte
F048	8D	0380	STA VIA+3	
F04B	A9	E0	LDA #\$E0	enable timers
F04D	8D	0B80	STA VIA+\$0B	
F050	A9	0A	LDA #\$0A	
F052	8D	0C80	STA VIA+\$0C	strobe operation
F055	A9	7F	LDA #\$7F	
F057	8D	1E80	STA VIA+\$1E	disable interrupts
F05A	8D	0E80	STA VIA+\$0E	
F05D	A9	A0	LDA #\$A0	except timer 2
F05F	8D	0E80	STA VIA+\$0E	
F062	A9	84	LDA #\$84	
F064	8D	0480	STA VIA+4	timers for count
F067	A9	13	LDA #\$13	
F069	8D	0580	STA VIA+5	
F06C	A9	20	LDA #TVLBUF	
F06E	85	28	STA TVECLO	
F070	A9	00	LDA #TVHBUF	
F072	85	2A	STA TVECHI	
F074	A9	02	LDA #TVLBUF/256	
F076	85	29	STA TVECLO+1	
F078	A9	02	LDA #TVHBUF/256	
F07A	85	2B	STA TVECHI+1	
F07C	60		RTS	
			;	
			;	RESTART ROUTINE FOR BOARD CONTROL ROUTINES
			;	
F07D	60		RESTRT RTS	all routines pass
			;	through here on
			;	completion, can be
			;	used to add code
			;	
			;	DUMMY USR(0)
			;	
F07E	20	4EF3	USRO JSR PRIBUF	prints output bytes
F081	4C	7DF0	JMP RESTRT	again
			;	
			;	MOTOR USR(1)
			;	
F084	A5	21	USR1 LDA VA+1	is overlap option on
F086	F0	03	BEQ MT1	
F088	20	2DF3	JSR ZEROUT	send reply if on
F08B	18		MT1 CLC	2's complement number
F08C	A5	22	LDA N	of steps for ease of
F08E	49	FF	EOR #\$FF	counting. Maximum
F090	69	01	ADC #1	steps are therefore
F092	85	22	STA N	32767
F094	A5	23	LDA N+1	
F096	49	FF	EOR #\$FF	
F098	69	00	ADC #0	
F09A	85	23	STA N+1	
F09C	18		CLC	
F09D	A5	24	LDA T	2's complement number
F09F	49	FF	EOR #\$FF	of 100 microsecond
F0A1	69	01	ADC #1	delays per motor step

```

FOA3 85 24          STA T
FOA5 A5 25          LDA T+1
FOA7 49 FF          EOR #$FF
FOA9 69 00          ADC #0
FOAB 85 25          STA T+1
FOAD A5 20          LDA VA          set board address on
FOAF 8D 0F80        STA VIA+$0F        bus
FOB2 A9 62          LDA #$62          set 100 microsecond
FOB4 8D 0680        STA VIA+$06        count on timer 1
FOB7 20 CCFO        MCONT2 JSR STEP          step motor
FOBA E6 22          INC N            increment number of
FOBC D0 F9          BNE MCONT2       steps
FOBE E6 23          INC N+1         and loop until
FOCO D0 F5          BNE MCONT2       non left
FOC2 A5 21          LDA VA+1
FOC4 D0 03          BNE MQ2
FOC6 20 2DF3        JSR ZEROUT       reply that finished
FOC9 4C 7DF0        MQ2   JMP RESTRT

;
; STEP MOTOR AFTER WAITING T LOTS OF 0.1
; MILLISECS
;
FOCC A5 24          STEP  LDA T            copy number of delays
FOCE 85 26          STA TEMPT        into temp location
FODO A5 25          LDA T+1
FOD2 85 27          STA TEMPT+1
FOD4 A9 00          ML1   LDA #0            start timer 1
FOD6 8D 0780        STA VIA+7        and clear timed out
FOD9 AD 0480        LDA VIA+4        flag
FODC A9 40          ML2   LDA #$40         test timed out flag
FODE 2C 0D80        BIT VIA+$0D
FOE1 F0 F9          BEQ ML2           loop until set
FOE3 E6 26          INC TEMPT        increment counter
FOE5 D0 ED          BNE ML1           and loop until
FOE7 E6 27          INC TEMPT+1      zero reached
FOE9 D0 E9          BNE ML1
FOEB AD 0180        LDA VIA+1        strobe to step motor
FOEE 60             RTS            and return

;
; STEPPER MOTOR(3) OR USR(11) - SETS MIN,MAX
; SPEEDS AND ACCLN RATES FOR STEPPER MOTOR(4)
; OR USR(12)
;
FOEF 18             USR11 CLC
FOFO A5 20          LDA VA            2's complement first
FOF2 49 FF          EOR #$FF         var is the start/stop
FOF4 69 01          ADC #1           speed
FOF6 85 72          STA BOTTOM        save it as bottom
FOF8 A5 21          LDA VA+1         speed
FOFA 49 FF          EOR #$FF
FOFC 69 00          ADC #0
FOFE 85 73          STA BOTTOM+1
F100 18             CLC
F101 A5 22          LDA N            2's complement of 2nd
F103 49 FF          EOR #$FF         var is the fast speed
F105 69 01          ADC #1
F107 85 70          STA TOP
F109 A5 23          LDA N+1

```

```

F10B 49 FF      EOR  #$FF
F10D 69 00      ADC  #0
F10F 85 71      STA  TOP+1
F111 18         CLC
F112 A5 24      LDA  T           2's complement of 3rd
F114 49 FF      EOR  #$FF      var is the change in
F116 69 01      ADC  #1         speed per motor step
F118 85 74      STA  INC       ie the accln rate
F11A A5 25      LDA  T+1
F11C 49 FF      EOR  #$FF
F11E 69 00      ADC  #0
F120 85 75      STA  INC+1
F122 20 2DF3    JSR  ZEROUT     reply routine
F125 4C 7DFO    JMP  RESTRT     finished and return
;
; STEPPER MOTOR(4) OR USR(12) - ACCELERATING
; AND DECELERATING STEPPER MOTOR DRIVER
;
F128 A5 72      USR12  LDA  BOTTOM     start off at bottom
F12A 85 24      STA  T           speed
F12C A5 73      LDA  BOTTOM+1
F12E 85 25      STA  T+1
F130 A9 00      LDA  #0
F132 85 75      STA  FAST       clear fast speed flag
F134 85 76      STA  SLOW       and start decelerating
F136 85 77      STA  DECL       zero number of steps
F138 85 78      STA  DECL+1     needed to decelerate
F13A 18         CLC
F13B A5 22      LDA  N           2's complement no. of
F13D 49 FF      EOR  #$FF      steps ie maximum is
F13F 69 00      ADC  #0         32767
F141 85 22      STA  N
F143 A5 23      LDA  N+1
F145 49 FF      EOR  #$FF
F147 69 00      ADC  #0
F149 85 23      STA  N+1
F14B D0 04      BNE  OK         if zero no. of steps
F14D A5 22      LDA  N           exit routine without
F14F F0 28      BEQ  MEXIT      doing anything
F151 A5 20      OK      LDA  VA
F153 8D 0F80    STA  VIA+$OF    set board address
F156 A9 64      LDA  #$64      100 microsec clock
F158 8D 0680    STA  VIA+$06    for execution time
F15B 20 CCFO    MAINLP JSR  STEP       step motor after wait
F15E A5 75      LDA  FAST       reached top speed yet
F160 30 03      BMI  JMP1      yes - don't accel
F162 20 7FF1    JSR  ACCL       no so accelerate
F165 A5 76      JMP1  LDA  SLOW  decelerating yet
F167 F0 03      BEQ  GO         no so continue
F169 20 BDF1    JSR  DECEL     yes so decelerate
F16C E6 22      GO      INC  N
F16E D0 04      BNE  TESTDC   not yet zero so test
;
; if decelerate yet
F170 E6 23      INC  N+1
F172 F0 05      BEQ  MEXIT     zero steps left exit
F174 20 ACF1    TESTDC JSR  TSTDCL    test if decel point
;
; reached yet
F177 90 E2      BCC  MAINLP    continue stepping

```

F179	20	2DF3	MEXIT	JSR ZEROUT	routine has finished
F17C	4C	7DF0		JMP RESTRT	return
			:		
			:		
F17F	18		ACCL	CLC	add accel increment
F180	A5	24		LDA T	to 2's complement of
F182	65	74		ADC INC	delay thus decreasing
F184	85	24		STA T	delay time and
F186	A5	25		LDA T+1	increasing speed
F188	65	75		ADC INC+1	
F18A	85	25		STA T+1	
F18C	B0	0B		BCS PASTF	delay gone past zero
F18E	18			CLC	- use top speed
F18F	C5	71		CMP TOP+1	top speed reached ?
F191	90	12		BCC AEXIT	no continue
F193	A5	24		LDA T	
F195	C5	70		CMP TOP	
F197	90	0C		BCC AEXIT	
F199	A5	70	PASTF	LDA TOP	yes set speed to top
F19B	85	24		STA T	speed
F19D	A5	71		LDA TOP+1	
F19F	85	25		STA T+1	
F1A1	A9	FF		LDA #ON	
F1A3	85	75		STA FAST	
F1A5	E6	77	AEXIT	INC DECL	increment no. of steps
F1A7	D0	02		BNE ACONT	required to decelerate
F1A9	E6	78		INC DECL+1	
F1AB	60		ACONT	RTS	return
			:		
F1AC	18		TSTDCL	CLC	add no. of decel steps
F1AD	A5	22		LDA N	to no. of motor steps
F1AF	65	77		ADC DECL	
F1B1	A5	23		LDA N+1	
F1B3	65	78		ADC DECL+1	
F1B5	90	04		BCC NOTYET	if number passed zero
F1B7	A9	FF		LDA #ON	start decelerating so
F1B9	85	76		STA SLOW	set flag
F1BB	18		NOTYET	CLC	carry cleared before
F1BC	60			RTS	returning
			:		
F1BD	38		DECEL	SEC	
F1BE	A5	24		LDA T	subtract increment
F1C0	E5	74		SBC INC	from step delay thus
F1C2	85	24		STA T	making speed slower
F1C4	A5	25		LDA T+1	
F1C6	E5	75		SBC INC+1	
F1C8	85	25		STA T+1	
F1CA	90	0B		BCS UNDER	
F1CC	18			CLC	compare delay with
F1CD	C5	73		CMP BOTTOM+1	bottom speed
F1CF	B0	0E		BCS DEXIT	if less use bottom
F1D1	A5	24		LDA T	speed
F1D3	C5	72		CMP BOTTOM	
F1D5	B0	08		BCS DEXIT	
F1D7	A5	72	UNDER	LDA BOTTOM	
F1D9	85	24		STA T	
F1DB	A5	73		LDA BOTTOM+1	
F1DD	85	25		STA T+1	

```

F1DF 60          DEXIT   RTS
;
; COUNT USR(2)
;
F1E0 A5 21      USR2     LDA VA+1          check overlap option
F1E2 F0 03              BEQ CT1
F1E4 20 2DF3        JSR ZEROUT
F1E7 A9 A0          CT1     LDA #$A0
F1E9 8D 0E80        STA VIA+$0E
F1EC A9 00              LDA #0
F1EE 8D 0080        STA VIA
F1F1 A5 24              LDA T          set timer 2 to count
F1F3 8D 0880        STA VIA+8        down delay time
F1F6 A5 25              LDA T+1
F1F8 8D 0980        STA VIA+9
F1FB A9 FF              LDA #$FF
F1FD 8D 0080        STA VIA
F200 A9 20              LDA #$20
F202 2C 0D80        CL1     BIT VIA+$0D    check if timer 2 has
F205 F0 FB              BEQ CL1        counted down to zero
;
; READ USR(3)
;
F207 A5 20      USR3     LDA VA          set up board address
F209 8D 0F80        STA VIA+$0F        on address bus
F20C AD 1080        LDA DATAHI        read data bus
F20F 49 FF          EOR #$FF          and invert data bits
F211 85 13          STA TMPO+1
F213 AD 1F80        LDA DATALO        and for low byte
F216 49 FF          EOR #$FF
F218 85 12          STA TMPO          put data in output
F21A A5 21          LDA VA+1          buffer
F21C D0 03          BNE RED1
F21E 20 4EF3        JSR PRTBUF        output data to user
F221 4C 7DF0        RED1    JMP RESTRT        and back to start
;
; D TO A (MK 1)
;
F224 A5 20      USR4     LDA VA          set up VIA's
F226 8D 0F80        STA VIA+$0F
F229 A9 FF          LDA #$FF
F22B 8D 1280        STA VIA+$12
F22E 8D 1380        STA VIA+$13
F231 A9 02          LDA #$02
F233 24 21          BIT VA+1          see if 512 added to
F235 F0 03          BEQ DA1          address - 4 channel
F237 4C F7F2        JMP DAC4          board if yes
F23A A5 23          DA1     LDA N+1          put data on data bus
F23C 8D 1080        STA DATAHI
F23F A5 22          LDA N
F241 8D 1F80        STA DATALO
F244 AD 0180        LDA VIA+1          and latch it (strobe)
F247 20 2DF3        JSR ZEROUT        reply to user
F24A 4C 7DF0        JMP RESTRT
;
; A TO D USR(5)
;
F24D A5 20      USR5     LDA VA          set address

```



F24F	8D	0F80		STA	VIA+\$0F	
F252	A9	00		LDA	#0	
F254	8D	1C80		STA	VIA+\$1C	
F257	AD	1080		LDA	VIA+\$10	clear flag and
F25A	AD	0180		LDA	VIA+1	start conversion
F25D	A9	FF		LDA	#\$FF	2's complement of
F25F	85	26		STA	TEMPT	time out value for
F261	A9	FE		LDA	#\$FE	board error
F263	85	27		STA	TEMPT+1	
F265	A9	08	AD1	LDA	#\$08	test if conversion
F267	2C	1D80		BIT	VIA+\$1D	has begun
F26A	D0	07		BNE	ST1	yes - continue
F26C	20	EOF2		JSR	TOUT	no see if timed out
F26F	90	F4		BCC	AD1	no test bit again
F271	B0	78		BCS	TIMERR	yes - error
F273	A9	40	ST1	LDA	#\$40	
F275	8D	1C80		STA	VIA+\$1C	
F278	8D	1080		STA	VIA+\$10	clear flag
F27B	A9	08		LDA	#\$08	
F27D	2C	1D80	AD2	BIT	VIA+\$1D	conversion complete ?
F280	F0	FB		BEQ	AD2	no - loop
F282	A9	10		LDA	#\$10	
F284	2C	1080		BIT	DATAHI	overrange ?
F287	D0	4B		BNE	OVERR	
F289	A9	20		LDA	#\$20	
F28B	2C	1080		BIT	DATAHI	check sign bit
F28E	D0	1E		BNE	PLUS	clear if positive
F290	A9	FF	NEG	LDA	#ON	set negative flag
F292	85	31		STA	NEGFLG	for output routine
F294	18			CLC		
F295	AD	1F80		LDA	DATALO	2's complement data
F298	49	FF		EOR	#\$FF	before returning
F29A	69	01		ADC	#01	
F29C	48			PHA		
F29D	AD	1080		LDA	DATAHI	
F2A0	29	0F		AND	#\$0F	
F2A2	49	FF		EOR	#\$FF	
F2A4	69	00		ADC	#0	
F2A6	85	13		STA	TMPO+1	
F2A8	68			PLA		
F2A9	85	12		STA	TMPO	data in output buffer
F2AB	18			CLC		
F2AC	90	12		BCC	ZDELY	delay required to
						limit access speed
F2AE	AD	1F80	PLUS	LDA	DATALO	
F2B1	48			PHA		
F2B2	AD	1080		LDA	DATAHI	
F2B5	29	0F		AND	#\$0F	
F2B7	85	13		STA	TMPO+1	
F2B9	68			PLA		
F2BA	85	12		STA	TMPO	data in output buffer
F2BC	A9	00		LDA	#OFF	
F2BE	85	31		STA	NEGFLG	clear negative flag
F2C0	A2	0A	ZDELY	LDX	#\$0A	simple delay loop
F2C2	A0	C8	ZD2	LDY	#\$C8	
F2C4	88		ZD1	DEY		
F2C5	D0	FD		BNE	ZD1	
F2C7	CA			DEX		

```

F2C8 D0 F8          BNE ZD2
F2CA 20 4EF3       JSR PRTBUF      print value to user
F2CD A9 00         LDA #OFF        clear negative flag
F2CF 85 31         STA NEGFLG
F2D1 4C 7DF0       JMP RESTRT      and restart
F2D4 A9 08         OVERR LDA #08        set bit in status
F2D6 05 1F         ORA STATUS      byte
F2D8 85 1F         STA STATUS
F2DA 20 40F7       JSR OVER        output error code
F2DD 4C 7DF0       JMP RESTRT
F2E0 18           TOUT  CLC          increment time out
F2E1 E6 26         INC TEMPT      counter
F2E3 D0 05         BNE T01
F2E5 E6 27         INC TEMPT+1
F2E7 D0 01         BNE T01
F2E9 38           SEC          carry set if timed
F2EA 60           T01  RTS          out
F2EB A9 02         TIMERR LDA #2
F2ED 05 1F         ORA STATUS      set status bit
F2EF 85 1F         STA STATUS
F2F1 20 49F7       JSR TMOUT      output error code
F2F4 4C 7DF0       JMP RESTRT

;
; 4-CHANNEL DAC DRIVER
; USR(4)
;
DAC4
F2F7 A5 22         LDA N          get low data byte
F2F9 8D 1F80       STA DATALO
F2FC A9 00         LDA #0        zero high byte
F2FE 8D 1080       STA DATAHI
F301 AD 0180       LDA VIA+$01  latch lower 4 bits
F304 EE 1080       INC DATAHI  add one to high byte
F307 4E 1F80       LSR DATALO   put top 4 bits of
F30A 4E 1F80       LSR DATALO   low byte into bottom
F30D 4E 1F80       LSR DATALO   4 bits
F310 4E 1F80       LSR DATALO
F313 AD 0180       LDA VIA+$01  and latch it in
F316 EE 1080       INC DATAHI  address for top 4
F319 A5 23         LDA N+1      bits and fetch high
F31B 8D 1F80       STA DATALO   byte of data
F31E AD 0180       LDA VIA+$01  and latch it in
F321 EE 1080       INC DATAHI  and latch start
F324 AD 0180       LDA VIA+$01  conversion
F327 20 2DF3       JSR ZEROOUT  reply to user
F32A 4C 7DF0       JMP RESTRT

;
;
ZEROUT
F32D A5 30         ZEROUT LDA NEWFLG   test if new ascii
F32F F0 03         BEQ IEEEEE   mode - no old routine
F331 4C 3EFB       JMP REPLOK   yes - new routine
F334 A9 20         IEEEEE LDA #$20    set output ready in
F336 8D 2580       STA SRQ     serial poll byte
F339 A9 00         LDA #0     output two null bytes
F33B 20 33F7       JSR WROB   via the GPIB
F33E A9 00         LDA #0
F340 20 33F7       JSR WROB
F343 A5 1F         LDA STATUS  and the status byte
F345 20 33F7       JSR WROB

```

F348	A9	00		LDA #0	serial poll byte to
F34A	8D	2580		STA SRQ	ready for input
F34D	60			RTS	
F34E	A5	30	PRTBUF	LDA NEWFLG	test ascii mode
F350	F0	03		BEQ IEPRT	
F352	4C	DAFB		JMP REPLAN	
F355	A9	20	IEPRT	LDA #\$20	output ready in
F357	8D	2580		STA SRQ	serial poll byte
F35A	A5	12		LDA TMPO	and write out the
F35C	20	33F7		JSR WROB	output buffer
F35F	A5	13		LDA TMPO+1	
F361	20	33F7		JSR WROB	
F364	A5	1F		LDA STATUS	plus the status byte
F366	20	33F7		JSR WROB	
F369	A9	00		LDA #0	
F36B	8D	2580		STA SRQ	clear serial poll
F36E	60			RTS	
;					
F36F	A5	21	USR7	LDA VA+1	
F371	29	FE		AND #\$FE	
F373	4A			LSR A	
F374	85	11		STA SAVX	set up speed
F376	A5	20		LDA VA	
F378	8D	0F80		STA VIA+\$0F	
F37B	A9	FF		LDA #\$FF	
F37D	8D	1280		STA VIA+\$12	
F380	8D	1380		STA VIA+\$13	
F383	A0	02		LDY #NPNT	
F385	20	A8F3		JSR GETV	
F388	A0	07		LDY #7	
F38A	20	B1F3		JSR PUT	X into table
F38D	18			CLC	
F38E	20	E7F4		JSR PLOT	output it
F391	A0	04		LDY #TPNT	
F393	20	A8F3		JSR GETV	
F396	A0	04		LDY #4	
F398	20	B1F3		JSR PUT	Y into table
F39B	38			SEC	
F39C	20	E7F4		JSR PLOT	output it
F39F	20	17F5		JSR DELAY	delay for plotter
;					
F3A2	20	2DF3		JSR ZEROUT	speed
F3A5	4C	7DF0		JMP RESTR	reply to user
;					
F3A8	B9	2000	GETV	LDA VLIST,Y	get variable from
F3AB	AA			TAX	location in VLIST
F3AC	C8			INY	
F3AD	B9	2000		LDA VLIST,Y	
F3B0	60			RTS	
;					
F3B1	91	2A	PUT	STA (TVECHI),Y	put variable in
F3B3	8A			TXA	table TVE
F3B4	91	28		STA (TVECLO),Y	
F3B6	60			RTS	
;					
; VECTOR GENERATOR					
;					
F3B7	A5	21	USR6	LDA VA+1	

F3B9	85	11		STA SAVX	set up speed
F3BB	46	11		LSR SAVX	
F3BD	29	01		AND #01	
F3BF	85	21		STA VA+1	quick reply ?
F3C1	F0	03		BEQ VEC2	
F3C3	20	2DF3		JSR ZEROUT	
F3C6	A5	20	VEC2	LDA VA	set board address
F3C8	8D	0F80		STA VIA+\$0F	
F3CB	A9	FF		LDA #\$FF	
F3CD	8D	1280		STA VIA+\$12	
F3D0	8D	1380		STA VIA+\$13	
F3D3	A0	02		LDY #NPNT	
F3D5	20	A8F3		JSR GETV	
F3D8	A0	08		LDY #8	
F3DA	20	B1F3		JSR PUT	X2 into table
F3DD	A0	04		LDY #TPNT	
F3DF	20	A8F3		JSR GETV	
F3E2	A0	05		LDY #5	
F3E4	20	B1F3		JSR PUT	Y2 into table
F3E7	20	33F4		JSR DELTAX	
F3EA	20	45F4		JSR DELTAY	
F3ED	A0	01		LDY #1	
F3EF	20	70F4		JSR CLEAR	clear accumulator
F3F2	A5	20		LDA VA	
F3F4	A0	07	VLOP	LDY #7	
F3F6	18			CLC	
F3F7	20	E7F4		JSR PLOT	plot X1,Y1
F3FA	A0	04		LDY #4	
F3FC	38			SEC	
F3FD	20	E7F4		JSR PLOT	
F400	A0	08		LDY #8	
F402	20	77F4		JSR SUBTR	
F405	A5	28		LDA TEMPT+2	
F407	F0	20		BEQ RETRN	
F409	A0	01	TESTA	LDY #1	
F40B	20	9EF4		JSR TEST	
F40E	A5	28		LDA TEMPT+2	
F410	10	06		BPL UP	
F412	20	D2F4		JSR LOW	
F415	4C	26F4		JMP BACK	
F418	F0	06	UP	BEQ GOOD	
F41A	20	BDF4		JSR HIGH	
F41D	4C	26F4		JMP BACK	
F420	20	D2F4	GOOD	JSR LOW	
F423	20	BDF4		JSR HIGH	
F426	4C	F4F3	BACK	JMP VLOP	
F429	A5	21	RETRN	LDA VA+1	
F42B	D0	03		BNE VRET	
F42D	20	2DF3		JSR ZEROUT	
F430	4C	7DF0	VRET	JMP RESTRT	
F433	A0	08	DELTAX	LDY #08	
F435	20	77F4		JSR SUBTR	
F438	88			DEY	
F439	20	A9F4		JSR SIGMA	
F43C	A0	02		LDY #2	
F43E	20	5AF4		JSR MOD	
F441	20	10F5		JSR STORE	

```

F444 60          RTS
;
F445 A0 05      DELTAY  LDY #5
F447 20 77F4    JSR SUBTR
F44A 88         DEY
F44B 20 A9F4    JSR SIGMA
F44E A0 00      LDY #0
F450 20 5AF4    JSR MOD
F453 20 5FF4    JSR NEGATE
F456 20 10F5    JSR STORE
F459 60          RTS
;
F45A 18         MOD     CLC
F45B A5 28      LDA TEMPT+2
F45D 10 10      BPL VRET1
F45F A9 FF      NEGATE  LDA #$FF
F461 45 26      EOR TEMPT
F463 69 01      ADC #1
F465 85 26      STA TEMPT
F467 A9 FF      LDA #$FF
F469 45 27      EOR TEMPT+1
F46B 69 00      ADC #0
F46D 85 27      STA TEMPT+1
F46F 60          VRET1  RTS
;
F470 A9 00      CLEAR   LDA #0
F472 91 28      STA (TVECLO),Y
F474 91 2A      STA (TVECHI),Y
F476 60          RTS
;
F477 38         SUBTR   SEC
F478 B1 28      LDA (TVECLO),Y
F47A 88         DEY
F47B F1 28      SBC (TVECLO),Y
F47D 85 26      STA TEMPT
F47F C8         INY
F480 B1 2A      LDA (TVECHI),Y
F482 88         DEY
F483 F1 2A      SBC (TVECHI),Y
F485 85 27      STA TEMPT+1
F487 10 05      TEST2  BPL EUAL
F489 A9 FF      LDA #$FF
F48B 85 28      STA TEMPT+2      sign flag
F48D 60          RTS
;
F48E D0 09      EUAL    BNE POS
F490 A5 26      LDA TEMPT
F492 D0 05      BNE POS
F494 A9 00      LDA #0
F496 85 28      STA TEMPT+2
F498 60          RTS
;
F499 A9 01      POS     LDA #1
F49B 85 28      STA TEMPT+2
F49D 60          RTS
;
F49E B1 28      TEST   LDA (TVECLO),Y
F4A0 85 26      STA TEMPT

```

```

F4A2 B1 2A      LDA (TVECHI),Y
F4A4 85 27      STA TEMPT+1
F4A6 4C 87F4    JMP TEST2

;
F4A9 A5 28      SIGMA LDA TEMPT+2      sign of delta
F4AB 10 05      BPL ZER2
F4AD 91 28      PUTIT STA (TVECLO),Y
F4AF 91 2A      STA (TVECHI),Y
F4B1 60      RTS

;
F4B2 D0 02      ZER2 BNE POSIT
F4B4 F0 F7      BEQ PUTIT
F4B6 91 28      POSIT STA (TVECLO),Y
F4B8 A9 00      LDA #0
F4BA 91 2A      STA (TVECHI),Y
F4BC 60      RTS

;
F4BD A0 07      HIGH LDY #7
F4BF 20 FFF4    JSR ADD
F4C2 A0 07      LDY #7
F4C4 20 10F5    JSR STORE
F4C7 A0 01      LDY #1
F4C9 20 FFF4    JSR ADD
F4CC A0 01      LDY #1
F4CE 20 10F5    JSR STORE
F4D1 60      RTS

;
F4D2 A0 04      LOW LDY #4
F4D4 20 FFF4    JSR ADD
F4D7 A0 04      LDY #4
F4D9 20 10F5    JSR STORE
F4DC A0 02      LDY #2
F4DE 20 FFF4    JSR ADD
F4E1 A0 01      LDY #1
F4E3 20 10F5    JSR STORE
F4E6 60      RTS

;
F4E7 A5 20      PLOT LDA VA          output data in table
F4E9 69 00      ADC #0          to D to A
F4EB 8D 0F80    STA VIA+$OF
F4EE B1 28      LDA (TVECLO),Y
F4F0 8D 1F80    STA DATALO
F4F3 B1 2A      LDA (TVECHI),Y
F4F5 8D 1080    STA DATAHI
F4F8 AD 0180    LDA VIA+1      latch it
F4FB 20 17F5    JSR DELAY      delay for pen speed
F4FE 60      RTS

;
F4FF 18      ADD CLC
F500 B1 28    LDA (TVECLO),Y
F502 88      DEY
F503 71 28    ADC (TVECLO),Y
F505 85 26    STA TEMPT
F507 C8      INY
F508 B1 2A    LDA (TVECHI),Y
F50A 88      DEY
F50B 71 2A    ADC (TVECHI),Y
F50D 85 27    STA TEMPT+1

```

```

F50F 60          RTS
;
F510 A6 26      STORE   LDX TEMPT
F512 A5 27      LDA     TEMPT+1
F514 4C B1F3    JMP     PUT
;
F517 A6 11      DELAY   LDX SAVX
F519 F0 08      BEQ    DRET
F51B A0 64      DL2     LDY  #$64
F51D 88         DL1     DEY
F51E D0 FD      BNE    DL1
F520 CA         DEX
F521 D0 F8      BNE    DL2
F523 60         DRET    RTS
;
; GPIP MODULE DRIVER USR(8)
;
F524 A5 20      USR8    LDA  VA           board address
F526 8D 0F80    STA  VIA+$0F
F529 A9 00      LDA  #0
F52B 8D 0080    STA  VIA           clear flag
F52E A9 FF      LDA  #$FF
F530 8D 0080    STA  VIA
F533 AD 1080    LDA  VIA+$10
F536 A9 40      LDA  #$40
F538 8D 1C80    STA  VIA+$1C      set up handshake
F53B AD 0180    LDA  VIA+1        set DRQ
F53E A9 FF      LDA  #$FF
F540 85 26      STA  TEMPT        set up time out
F542 A9 80      LDA  #$80
F544 85 27      STA  TEMPT+1
F546 A9 08      LDA  #8
F548 2C 1D80    GPL1    BIT  VIA+$1D      wait for reply
F54B D0 08      BNE  GPL2
F54D 20 EOF2    JSR  TOUT
F550 90 F6      BCC  GPL1
F552 4C EBF2    JMP  TIMERR
F555 AD 1080    GPL2    LDA  DATAHI
F558 49 FF      EOR  #$FF
F55A 85 13      STA  TMPO+1
F55C AD 1F80    LDA  DATALO
F55F 49 FF      EOR  #$FF
F561 85 12      STA  TMPO
F563 20 4EF3    JSR  PRIBUF
F566 4C 7DF0    JMP  RESTRT
;
; USR(9) - JUMP TO MONITOR AT $E000
;
F569 AD 00E0    USR9    LDA  $E000
F56C C9 4C      CMP  #$4C      is jump instruction at
;                                     $E000 present
F56E D0 03      BNE  MONERR    no - not there !
F570 4C 00E0    JMP  MON      yes - so jump to it
F573 A5 30      MONERR LDA  NEWFLG   error - monitor chip
F575 D0 06      BNE  MNERR    not installed
F577 20 2DF3    JSR  ZEROUT   old mode so reply
F57A 4C 00F0    JMP  RESET    reset routine
F57D 20 20F8    MNERR JSR  PRINT   print error message

```

```

F580 7F4D4F4E      DB TEX, 'MONITOR EPROM NOT PRESENT', $OD, ETX
F584 49544F52
F588 20455052
F58C 4F4D204E
F590 4F542050
F594 52455345
F598 4E540DFF
F59C 4C 00F0      JMP RESTRT      and reset 6502
      F569      MONITR EQU USR9
;
;  AUTORANGING A TO D DRIVER
;
F59F A5 24      USR10  LDA T
F5A1 FO 03      BEQ S1
F5A3 4C 1BF6      JMP AUTO
F5A6 A9 00      S1    LDA #0
F5A8 85 31      STA NEGFLG
F5AA 20 B0F5      JSR SCONV
F5AD 4C 08F7      JMP RET
;
F5B0 A5 20      SCONV LDA VA
F5B2 8D 0F80      STA VIA+$OF
F5B5 A9 FF      LDA #$FF
F5B7 8D 1280      STA VIA+$12
F5BA 8D 1380      STA VIA+$13
F5BD A5 23      LDA N+1
F5BF 8D 1080      STA DATAHI
F5C2 A5 22      LDA N
F5C4 8D 1F80      STA DATALO
F5C7 AD 0180      LDA VIA+1
F5CA A2 50      LDX #$50
F5CC CA          DECR  DEX
F5CD DO FD      BNE DECR
F5CF A9 00      LDA #0
F5D1 8D 1280      STA VIA+$12
F5D4 8D 1380      STA VIA+$13
F5D7 A9 80      LDA #$80
F5D9 8D 0F80      STA VIA+$OF
F5DC A9 00      LDA #0
F5DE 8D 0F80      STA VIA+$OF
F5E1 A9 00      LDA #0
F5E3 8D 1C80      STA VIA+$1C
F5E6 8D 1080      STA VIA+$10
F5E9 A2 FF      LDX #$FF
F5EB AD 1D80      WCONV LDA VIA+$1D
F5EE 29 08      AND #08
F5F0 DO 12      BNE DONE
F5F2 CA          DEX
F5F3 FO 03      BEQ ATOUT
F5F5 4C EBF5      JMP WCONV
F5F8 A9 FF      ATOUT LDA #$FF
F5FA 85 13      STA TMPO+1
F5FC 85 12      STA TMPO
F5FE 20 4EF3      JSR PRIBUF
F601 4C 7DF0      JMP RESTRT
F604 A9 80      DONE  LDA #$80
F606 8D 0F80      STA VIA+$OF
F609 AD 1080      LDA DATAHI

```



F60C	29	OF		AND	#\$OF
F60E	85	13		STA	TMPO+1
F610	AD	1F80		LDA	DATALO
F613	85	12		STA	TMPO
F615	A9	00		LDA	#0
F617	8D	0F80		STA	VIA+\$OF
F61A	60			RTS	
;					
F61B	20	BOF5	AUTO	JSR	SCONV
F61E	A5	13		LDA	TMPO+1
F620	85	2D		STA	WKLOC+1
F622	A5	12		LDA	TMPO
F624	85	2C		STA	WKLOC
F626	A9	00		LDA	#0
F628	85	2E		STA	WKLOC+2
F62A	A5	22		LDA	N
F62C	29	10		AND	#\$10
F62E	D0	3E		BNE	BIP
F630	A9	00	UNI	LDA	#0
F632	85	31		STA	NEGFLG
F634	A5	2D		LDA	WKLOC+1
F636	F0	10		BEQ	A3
F638	29	08	A1	AND	#\$08
F63A	D0	09		BNE	A2
F63C	E6	2E		INC	WKLOC+2
F63E	06	2D		ASL	WKLOC+1
F640	A5	2D		LDA	WKLOC+1
F642	4C	38F6		JMP	A1
F645	4C	64F6	A2	JMP	A7
F648	A5	2C	A3	LDA	WKLOC
F64A	F0	15		BEQ	A6
F64C	29	08	A4	AND	#\$08
F64E	D0	09		BNE	A5
F650	E6	2E		INC	WKLOC+2
F652	06	2C		ASL	WKLOC
F654	A5	2C		LDA	WKLOC
F656	4C	4CF6		JMP	A4
F659	A2	04	A5	LDX	#\$04
F65B	20	12F7		JSR	INCR
F65E	4C	64F6		JMP	A7
F661	4C	08F7	A6	JMP	RET
F664	A5	2E	A7	LDA	WKLOC+2
F666	85	22		STA	N
F668	20	BOF5		JSR	SCONV
F66B	4C	18F7		JMP	WASL
;					
F66E	A5	2D	BIP	LDA	WKLOC+1
F670	29	08		AND	#\$08
F672	F0	42		BEQ	ANEG
F674	A9	00	APOS	LDA	#0
F676	85	31		STA	NEGFLG
F678	A5	2D		LDA	WKLOC+1
F67A	29	07		AND	#\$07
F67C	F0	10		BEQ	P3
F67E	A5	2D	P1	LDA	WKLOC+1
F680	29	04		AND	#\$04
F682	D0	07		BNE	P2
F684	E6	2E		INC	WKLOC+2

F686	06	2D		ASL	WKLOC+1
F688	4C	7EF6		JMP	P1
F68B	4C	AAF6	P2	JMP	P7
F68E	A5	2C	P3	LDA	WKLOC
F690	F0	15		BEQ	P6
F692	29	80	P4	AND	#\$80
F694	D0	09		BNE	P5
F696	E6	2E		INC	WKLOC+2
F698	06	2C		ASL	WKLOC
F69A	A5	2C		LDA	WKLOC
F69C	4C	92F6		JMP	P4
F69F	A2	03	P5	LDX	#\$03
F6A1	20	12F7		JSR	INCR
F6A4	4C	AAF6		JMP	P7
F6A7	4C	08F7	P6	JMP	RET
F6AA	A5	2E	P7	LDA	WKLOC+2
F6AC	49	10		EOR	#\$10
F6AE	85	22		STA	N
F6B0	20	BOF5		JSR	SCONV
F6B3	4C	18F7		JMP	WASL
;					
F6B6	A9	FF	ANEG	LDA	#\$FF
F6B8	85	31		STA	NEGFLG
F6BA	A5	2D		LDA	WKLOC+1
F6BC	49	07		EOR	#\$07
F6BE	85	2D		STA	WKLOC+1
F6C0	A5	2C		LDA	WKLOC
F6C2	49	FF		EOR	#\$FF
F6C4	85	2C		STA	WKLOC
F6C6	E6	2C		INC	WKLOC
F6C8	D0	02		BNE	NO
F6CA	E6	2D		INC	WKLOC+1
F6CC	A5	2D	NO	LDA	WKLOC+1
F6CE	F0	10		BEQ	N3
F6D0	29	04	N1	AND	#\$04
F6D2	D0	09		BNE	N2
F6D4	E6	2E		INC	WKLOC+2
F6D6	06	2D		ASL	WKLOC+1
F6D8	A5	2D		LDA	WKLOC+1
F6DA	4C	DOF6		JMP	N1
F6DD	4C	FCF6	N2	JMP	N7
F6E0	A5	2C	N3	LDA	WKLOC
F6E2	F0	15		BEQ	N6
F6E4	29	80	N4	AND	#\$80
F6E6	D0	09		BNE	N5
F6E8	E6	2E		INC	WKLOC+2
F6EA	06	2C		ASL	WKLOC
F6EC	A5	2C		LDA	WKLOC
F6EE	4C	E4F6		JMP	N4
F6F1	A2	03	N5	LDX	#\$03
F6F3	20	12F7		JSR	INCR
F6F6	4C	FCF6		JMP	N7
F6F9	4C	08F7	N6	JMP	RET
F6FC	A5	2E	N7	LDA	WKLOC+2
F6FE	49	10		EOR	#\$10
F700	85	22		STA	N
F702	20	BOF5		JSR	SCONV
F705	4C	18F7		JMP	WASL

```

;
F708 20 4EF3   RET      JSR  PRTBUF
F70B A9 00     LDA  #0
F70D 85 31     STA  NEGFLG
F70F 4C 7DF0   JMP  RESTRT

;
F712 E6 2E     INCR     INC  WKLOC+2
F714 CA        DEX
F715 D0 FB     BNE  INCR
F717 60        RTS

;
F718 A2 04     WASL     LDX  #$04
F71A 06 2E     ASL  WKLOC+2
F71C CA        DEX
F71D D0 F9     BNE  WASL
F71F A5 2E     LDA  WKLOC+2
F721 45 13     EOR  TMPO+1
F723 85 13     STA  TMPO+1
F725 4C 08F7   JMP  RET

;
; READ BYTE USING 68488 GPIA CHIP
;
F728 A9 01     RDOB     LDA  #1
F72A 2C 2080   RL1      BIT  IEE
F72D F0 FB     BEQ  RL1
F72F AD 2780   LDA  IEE+7
F732 60        RTS

;
; WRITE OUT BYTE USING GPIA CHIP
;
F733 48        WROB     PHA
F734 A9 40     WR1      LDA  #$40
F736 2C 2080   BIT  IEE
F739 F0 F9     BEQ  WR1
F73B 68        PLA
F73C 8D 2780   STA  IEE+7
F73F 60        RTS

;
; OVERRANGE
;
F740 A5 30     OVER     LDA  NEWFLG      test if ascii mode
F742 F0 02     BEQ  IEQVR      no - binary reply
F744 D0 0D     BNE  RSOVER     yes - send error
F746 4C 2DF3   IEQVR    JMP  ZEROUT     binary reply

;
; TIME OUT
;
F749 A5 30     TMOUT    LDA  NEWFLG      test if ascii mode
F74B F0 03     BEQ  IETIM
F74D D0 14     BNE  RSTIM
F74F 60        RTS
F750 4C 2DF3   IETIM    JMP  ZEROUT     binary reply

;
F753 20 20F8   RSOVER    JSR  PRINT
F756 7F4F5645 DB  TEX, 'OVERRANGE', $OD, ETX
F75A 5252414E
F75E 47450DFF
F762 60        RTS

```

```

;
F763 20 20F8 RSTIM JSR PRINT
F766 7F54494D DB TEX, 'TIMED OUT', $OD, ETX
F76A 4544204F
F76E 55540DFF
F772 60 RTS

;
; VARIABLE INITIALISATION
;
F773 A9 00 VINIT LDA #OFF
F775 85 47 STA PRINTR
F777 85 48 STA HOST
F779 85 36 STA CHAR
F77B 85 3C STA IEEEEPR
F77D A9 0D LDA #$OD
F77F 85 3E STA DELIM
F781 60 RTS

;
; PRINT ROUTINES FOR OUTPUT CONTROL
;
F782 A9 FF HOSTON LDA #ON
F784 85 48 STA HOST
F786 60 RTS
F787 A9 00 HOSTOF LDA #OFF
F789 85 48 STA HOST
F78B 60 RTS
F78C A9 FF PRTON LDA #ON
F78E 85 47 STA PRINTR
F790 60 RTS
F791 A9 00 PRTOFF LDA #OFF
F793 85 47 STA PRINTR
F795 60 RTS
F796 A5 39 RTSON LDA CREG
F798 29 9F AND #$9F
F79A 8D 3080 STA ACIA1
F79D 85 39 STA CREG
F79F 60 RTS
F7A0 A5 39 RTSOFF LDA CREG
F7A2 09 40 ORA #$40
F7A4 8D 3080 STA ACIA1
F7A7 85 39 STA CREG
F7A9 60 RTS
F7AA 18 RSRES CLC
F7AB AD 3480 LDA SWITCH
F7AE 29 70 AND #$70
F7B0 4A LSR A
F7B1 4A LSR A
F7B2 09 43 ORA #$43
F7B4 8D 3080 STA ACIA1
F7B7 29 FD AND #$FD
F7B9 8D 3080 STA ACIA1
F7BC 85 39 STA CREG
F7BE 18 CLC
F7BF AD 3480 LDA SWITCH
F7C2 29 07 AND #$07
F7C4 0A ASL A
F7C5 0A ASL A
F7C6 09 03 ORA #$03

```

read parity select  
switch  
mask bits for ACIA 1  
shift to position  
in command register  
add master reset bit  
put in command reg  
clear reset bit  
store it  
copy to CREG  
same again for ACIA 2  
both have /16 clock  
and RTS set low  
copy of command reg

F7C8	8D	3880		STA ACIA2	kept in RAM as is a
F7CB	29	FD		AND #\$FD	read only register
F7CD	8D	3880		STA ACIA2	in the chip
F7D0	85	3A		STA CREG2	
F7D2	60			RTS	
F7D3	C9	00	PRTCHR	CMP #0	null character ?
F7D5	F0	1D		BEQ PEXIT	yes - exit
F7D7	85	36		STA CHAR	save it
F7D9	A5	48		LDA HOST	host port selected
F7DB	F0	05		BEQ IFPR	no - try printer
F7DD	A5	36		LDA CHAR	yes - get character
F7DF	20	F5F7		JSR SEND1	and transmit it
F7E2	A5	47	IFPR	LDA PRINTR	test printer flag
F7E4	F0	05		BEQ IFIEE	no - try GPIB flag
F7E6	A5	36		LDA CHAR	yes - get character
F7E8	20	02F8		JSR SEND2	and print it
F7EB	A5	3C	IFIEE	LDA IEEPR	GPIB as output ?
F7ED	F0	05		BEQ PEXIT	no - exit
F7EF	A5	36		LDA CHAR	yes - get character
F7F1	20	33F7		JSR WROB	and transmit it
F7F4	60		PEXIT	RTS	
F7F5	AD	3080	SEND1	LDA ACIA1	test transmit enable
F7F8	29	02		AND #2	bit in ACIA
F7FA	F0	F9		BEQ SEND1	not set - wait
F7FC	A5	36		LDA CHAR	is set - put char
F7FE	8D	3180		STA ACIA1+1	in output buffer
F801	60			RTS	
F802	AD	3880	SEND2	LDA ACIA2	same for ACIA 2
F805	29	02		AND #2	
F807	F0	F9		BEQ SEND2	
F809	A5	36		LDA CHAR	
F80B	8D	3980		STA ACIA2+1	
F80E	60			RTS	
F80F	A9	0D	CRLF	LDA #CR	print a carriage
F811	20	D3F7		JSR PRTCHR	return followed
F814	A9	0A		LDA #LF	by a linefeed
F816	20	D3F7		JSR PRTCHR	
F819	60			RTS	
F81A	A9	20	SPACE	LDA #\$20	print a space
F81C	20	D3F7		JSR PRTCHR	
F81F	60			RTS	
F820	68		PRINT	PLA	print message which
F821	AA			TAX	follows the JSR PRINT
F822	68			PLA	instruction
F823	A8			TAY	recover calling
F824	20	4AF8		JSR PUSHSL	address
F827	86	43		STX SELECT	make select=address
F829	84	44		STY SELECT+1	
F82B	20	89F8		JSR INCSL	increment it (TEX)
F82E	20	89F8	NEXTCH	JSR INCSL	increment select
F831	20	70F8		JSR GETSL	get byte pointed to
F834	C9	FF		CMP #ETX	is it ETX ?
F836	F0	06		BEQ ENDIT	yes - exit
F838	20	D3F7		JSR PRTCHR	no - print character
F83B	18			CLC	
F83C	90	F0		BCC NEXTCH	and loop
F83E	A6	43	ENDIT	LDX SELECT	restore select
F840	A4	44		LDY SELECT+1	pointer

F842	20	5DF8		JSR	POPSL	
F845	98			TYA		push address of ETX
F846	48			PHA		onto stack
F847	8A			TXA		
F848	48			PHA		
F849	60			RTS		and return to next
F84A	68		PUSHSL	PLA		pull return address
F84B	85	49		STA	RETURN	and save it
F84D	68			PLA		
F84E	85	4A		STA	RETURN+1	
F850	A5	44		LDA	SELECT+1	push select onto
F852	48			PHA		stack
F853	A5	43		LDA	SELECT	
F855	48			PHA		
F856	A5	4A		LDA	RETURN+1	push return address
F858	48			PHA		back onto the stack
F859	A5	49		LDA	RETURN	
F85B	48			PHA		
F85C	60			RTS		
F85D	68		POPSL	PLA		save return address
F85E	85	49		STA	RETURN	from top of stack
F860	68			PLA		
F861	85	4A		STA	RETURN+1	
F863	68			PLA		
F864	85	43		STA	SELECT	get select from stack
F866	68			PLA		
F867	85	44		STA	SELECT+1	
F869	A5	4A		LDA	RETURN+1	push return back to
F86B	48			PHA		the stack
F86C	A5	49		LDA	RETURN	
F86E	48			PHA		
F86F	60			RTS		
F870	A5	45	GETSL	LDA	GETPTR	fetch byte pointed
F872	48			PHA		to by select
F873	A6	46		LDX	GETPTR+1	
F875	A5	43		LDA	SELECT	
F877	85	45		STA	GETPTR	using GETPTR if
F879	A5	44		LDA	SELECT+1	select is not on
F87B	85	46		STA	GETPTR+1	the zero page
F87D	A0	00		LDY	#0	
F87F	B1	45		LDA	(GETPTR),Y	
F881	A8			TAY		
F882	68			PLA		
F883	85	45		STA	GETPTR	
F885	86	46		STX	GETPTR+1	
F887	98			TYA		
F888	60			RTS		
F889	E6	43	INCSL	INC	SELECT	increment select
F88B	D0	02		BNE	BRANCH	pointer
F88D	E6	44		INC	SELECT+1	
F88F	60		BRANCH	RTS		
F890	AD	3080	GETCHR	LDA	ACIA1	get character from
F893	29	01		AND	#1	host serial port
F895	F0	F9		BEQ	GETCHR	loop until bit set
F897	AD	3180		LDA	ACIA1+1	get character
F89A	60			RTS		

; START OF ASCII MINICON ROUTINES

F89B	20	73F7	MNSTRT	JSR VINIT	initialise variables
F89E	A9	FF		LDA #ON	
F8A0	85	30		STA NEWFLG	minicon routines to return ascii output
F8A2	A5	3B		LDA IEEFLG	
F8A4	F0	0D		BEQ SER3	
F8A6	A9	FF		LDA #ON	
F8A8	85	3C		STA IEEEEPR	
F8AA	20	87F7		JSR HOSTOF	
F8AD	20	91F7		JSR PRTOFF	
F8B0	4C	B9F8		JMP MINCON	
F8B3	20	96F7	SER3	JSR RTSON	RTS high, input OK
F8B6	20	82F7		JSR HOSTON	host port for output
F8B9	20	30F0	MINCON	JSR INIT	initialise VIA's
F8BC	A2	00		LDX #0	buffer counter=0
F8BE	86	32		STX BUFFEN	
F8C0	86	31		STX NEGFLG	clear negative flag
F8C2	A5	3B		LDA IEEFLG	
F8C4	F0	0D		BEQ INLOOP	
F8C6	20	28F7	INLP	JSR RDOB	
F8C9	9D	0003		STA BUFF,X	
F8CC	C5	3E		CMP DELIM	
F8CE	F0	10		BEQ DECODE	
F8D0	E8			INX	
F8D1	D0	F3		BNE INLP	
F8D3	20	90F8	INLOOP	JSR GETCHR	get character
F8D6	9D	0003		STA BUFF,X	store in buffer
F8D9	C5	3E		CMP DELIM	is it the delimiter
F8DB	F0	03		BEQ DECODE	yes - process buffer
F8DD	E8			INX	no - increment pointer
F8DE	D0	F3		BNE INLOOP	and loop
F8E0	86	32	DECODE	STX BUFFEN	save buffer fill pntr
F8E2	A2	00		LDX #0	get first character
F8E4	BD	0003		LDA BUFF,X	
F8E7	38			SEC	prepare to subtract
F8E8	E9	41		SBC #\$41	subtract \$41, 'A'=0
F8EA	90	04		BCC BADCHR	char was less than \$41
F8EC	C9	1B		CMP #27	is character 'Z'
F8EE	90	03		BCC GOODCH	
F8F0	4C	26F9	BADCHR	JMP INERR	input command error
F8F3	A8		GOODCH	TAY	char as index to table of second chars
F8F4	E8			INX	
F8F5	BD	0003		LDA BUFF,X	next char from buffer
F8F8	D9	91FD		CMP CHTAB,Y	agree with 2 nd char
F8FB	D0	F3		BNE BADCHR	no
F8FD	20	3AF9		JSR GETIND	next char as index
F900	B0	11		BCS BADOPT	no. was out of range
F902	0A			ASL A	x2 for low, high byte
F903	18			CLC	
F904	79	ABFD		ADC OFFSET,Y	add offset from table
F907	A8			TAY	use as index to jump
F908	C8			INY	table,high byte first
F909	B9	C5FD		LDA JUMPTB,Y	form indexed jump
F90C	48			PHA	from vectors in
F90D	88			DEY	table JUMPTB
F90E	B9	C5FD		LDA JUMPTB,Y	

```

F911 48          PHA
F912 60          RTS
F913 20 20F8    BADOPT JSR PRINT
F916 7F424144   DB TEX, 'BAD OPTION', CR, ETX
F91A 204F5054
F91E 494F4E0D
F922 FF
F923 4C B9F8    JMP MINCON
F926 20 20F8    INERR JSR PRINT
F929 7F424144   DB TEX, 'BAD COMMAND', CR, ETX
F92D 20434F4D
F931 4D414E44
F935 ODFD
F937 4C B9F8    JMP MINCON
F93A A2 02      GETIND LDX #2
F93C BD 0003    LDA BUFF, X
F93F 38        SEC
F940 E9 30      SBC #$30
F942 90 04      BCC GBAD
F944 C9 06      CMP #06
F946 90 02      BCC GGOOD
F948 38        GBAD SEC
F949 60        RTS
F94A 18        GGOOD CLC
F94B 60        RTS

;
; ASCII MINICON ROUTINES - VARIABLE
; CONVERSION TO OLD FORMAT
;
F94C 20 60FA    STPM1 JSR THREIN      stepper motor no 1
F94F B0 03      BCS J1              get 3 input params
F951 20 84F0    JSR USR1           and jump to usr(1)
F954 4C B9F8    J1 JMP MINCON
F957 20 60FA    STPM2 JSR THREIN      stepper motor no 2
F95A B0 07      BCS J2              as above but set
F95C A9 01      LDA #1             high byte of board
F95E 85 21      STA VA+1          address for quick
F960 20 84F0    JSR USR1           return
F963 4C B9F8    J2 JMP MINCON
F966 20 60FA    STPM3 JSR THREIN      stepper motor no 3
F969 B0 F8      BCS J2              is used to set accln
F96B 20 EFF0    JSR USR11         & decln rates for
F96E 4C B9F8    JMP MINCON        no. 4
F971 20 6FFA    STPM4 JSR TWOIN       stepper motor 4,
F974 B0 ED      BCS J2              only requires board
F976 20 28F1    JSR USR12         address & no. steps
F979 4C B9F8    JMP MINCON
F97C 20 6FFA    CO1 JSR TWOIN       scalar no 1 (counter)
F97F B0 0B      BCS J3             two inputs required
F981 A5 22      LDA N              but second variable
F983 85 24      STA T             needs to be made T%
F985 A5 23      LDA N+1          variable
F987 85 25      STA T+1         usr(2)
F989 20 EOF1    JSR USR2
F98C 4C B9F8    J3 JMP MINCON
F98F 20 6FFA    CO2 JSR TWOIN       scalar no 2
F992 B0 0F      BCS J4             high byte
F994 A5 22      LDA N             of address set

```



F996	85	24		STA	T	
F998	A5	23		LDA	N+1	
F99A	85	25		STA	T+1	
F99C	A9	01		LDA	#1	
F99E	85	21		STA	VA+1	
F9A0	20	EOF1		JSR	USR2	
F9A3	4C	B9F8	J4	JMP	MINCON	
F9A6	20	7DFA	ADC1	JSR	ONEIN	A to D no 1
F9A9	B0	03		BCS	J5	board address reqd
F9AB	20	4DF2		JSR	USR5	usr(5)
F9AE	4C	B9F8	J5	JMP	MINCON	
F9B1	20	60FA	ADC2	JSR	THREIN	A to D no 2
F9B4	B0	03		BCS	J6	multilplexed A to D
F9B6	20	9FF5		JSR	USR10	requires more input
F9B9	4C	B9F8	J6	JMP	MINCON	
F9BC	20	6FFA	DAC1	JSR	TWOIN	D to A no 1
F9BF	B0	03		BCS	J7	two inputs only
F9C1	20	24F2		JSR	USR4	usr(4)
F9C4	4C	B9F8	J7	JMP	MINCON	
F9C7	20	6FFA	DAC2	JSR	TWOIN	D to A no 2
F9CA	B0	07		BCS	J8	address high byte set
F9CC	A9	02		LDA	#2	for 4 channel board
F9CE	85	21		STA	VA+1	
F9D0	20	24F2		JSR	USR4	
F9D3	4C	B9F8	J8	JMP	MINCON	
F9D6	20	7DFA	GP1	JSR	ONEIN	GPI no 1
F9D9	B0	03		BCS	J9	only address required
F9DB	20	24F5		JSR	USR8	usr(8)
F9DE	4C	B9F8	J9	JMP	MINCON	
F9E1	4C	11FD	MO0	JMP	OLDST	old monitor (IEEE)
F9E4	4C	11FD	MO1	JMP	OLDST	old minicon (IEEE)
F9E7	4C	9FFC	MO2	JMP	IEEMON	IEEE ascii monitor
F9EA	4C	A6FC	MO3	JMP	IEECAM	IEEE ascii minicom
F9ED	4C	69F5	MO4	JMP	MONITR	RS232 monitor
F9F0	4C	ADFC	MO5	JMP	IEESER	IEEE to RS232 routine
F9F3	20	60FA	VP1	JSR	THREIN	vector plot no 1
F9F6	B0	03		BCS	J10	
F9F8	20	B7F3		JSR	USR6	usr(6)
F9FB	4C	B9F8	J10	JMP	MINCON	
F9FE	20	60FA	VP2	JSR	THREIN	vector plot no 2
FA01	B0	03		BCS	J11	
FA03	20	6FF3		JSR	USR7	usr(7)
FA06	4C	B9F8	J11	JMP	MINCON	
FA09	20	7EFO	RD1	JSR	USRO	usr(0)
FA0C	4C	B9F8		JMP	MINCON	no inputs
FA0F	20	7DFA	RD2	JSR	ONEIN	usr(3)
FA12	B0	03		BCS	J12	address only required
FA14	20	07F2		JSR	USR3	
FA17	4C	B9F8	J12	JMP	MINCON	
FA1A	20	87F7	PR1	JSR	HOSTOF	output to printer
FA1D	20	8CF7		JSR	PRTON	port only
FA20	A9	00		LDA	#OFF	
FA22	85	3C		STA	IEEEPR	
FA24	A2	03		LDX	#3	
FA26	E8		OUTLP	INX		
FA27	BD	0003		LDA	BUFF,X	char from input buff
FA2A	48			PHA		save it temporarily
FA2B	20	D3F7		JSR	PRTCHR	print it

FA2E 68		PLA		return character
FA2F C9 OD		CMP #13		carriage return ?
FA31 D0 F3		BNE OUTLP		no - continue
FA33 A5 3D		LDA PDELM		printer delimiter
FA35 C9 OD		CMP #13		
FA37 F0 03		BEQ PREX		if CR have printed it
FA39 20 D3F7		JSR PRTCHR		else print current
				printer delimiter
FA3C 20 91F7	PREX	JSR PRTOFF		turn printer off
FA3F A5 3B		LDA IEEFLG		see which port is host
FA41 F0 07		BEQ PSER		serial port - branch
FA43 A9 FF		LDA #ON		IEEE488 port as host
FA45 85 3C		STA IEEEEPR		
FA47 4C 4DFA		JMP PREX2		
FA4A 20 82F7	PSER	JSR HOSTON		serial port 1 as host
FA4D 20 3EFB	PREX2	JSR REPLOK		reply to user
FA50 4C B9F8		JMP MINCON		
FA53 A2 04	PR2	LDX #4		sets printer delimiter
FA55 BD 0003		LDA BUFF,X		to 5th character in
FA58 85 3D		STA PDELM		buffer
FA5A 20 3EFB		JSR REPLOK		
FA5D 4C B9F8		JMP MINCON		
FA60 A9 03	THREIN	LDA #3		buffer empty pointer
FA62 85 34		STA BPOINT		to 4 th character
FA64 85 40		STA INCNT		three inputs required
FA66 20 9CFA		JSR INNVAL		input values
FA69 B0 01		BCS VERROR		carry set gives error
FA6B 60		RTS		
FA6C 4C C5FB	VERROR	JMP VINERR		error in variables
FA6F A9 03	TWOIN	LDA #3		
FA71 85 34		STA BPOINT		
FA73 A9 02		LDA #2		two inputs required
FA75 85 40		STA INCNT		
FA77 20 9CFA		JSR INNVAL		
FA7A B0 F0		BCS VERROR		
FA7C 60		RTS		
FA7D A9 03	ONEIN	LDA #3		one input required
FA7F 85 34		STA BPOINT		
FA81 A9 01		LDA #1		
FA83 85 40		STA INCNT		
FA85 20 9CFA		JSR INNVAL		
FA88 B0 E2		BCS VERROR		
FA8A 60		RTS		
FA8B A6 34	ADVAN	LDX BPOINT		buffer empty pointer
FA8D E8	ADLP	INX		step it on one place
FA8E BD 0003		LDA BUFF,X		get character
FA91 C9 2C		CMP #C',		is it a comma
FA93 F0 04		BEQ ADEND		yes - return
FA95 C9 OD		CMP #13		is it CR
FA97 D0 F4		BNE ADLP		no loop
FA99 86 34	ADEND	STX BPOINT		save empty pointer
FA9B 60		RTS		
FA9C A0 00	INNVAL	LDY #0		loop counter
FA9E 98	ILOOP	TYA		save Y register
FA9F 48		PHA		on stack
FAA0 20 8BFA		JSR ADVAN		empty pointer to ,
FAA3 20 Bafa		JSR ASCBIN		decimal ascii to bin
FAA6 68		PLA		

FAA7 A8		TAY	recover Y register
FAA8 A5 38		LDA LOWBIT	low byte of input
FAAA 99 2000		STA VA,Y	variable list+Y
FAAD A5 37		LDA HGHBIT	high byte
FAAF 99 2100		STA VA+1,Y	in variable list
FAB2 C8		INY	increment Y register
FAB3 C8		INY	twice
FAB4 C6 40		DEC INCNT	decrement counter
FAB6 D0 E6		BNE ILOOP	if non zero loop
FAB8 18		CLC	
FAB9 60		RTS	
FABA A9 00	ASCBIN	LDA #0	initialise low and
FABC 85 38		STA LOWBIT	high bytes
FABE 85 37		STA HGHBIT	
FAC0 A6 34		LDX BPOINT	get empty pointer
FAC2 CA		DEX	to character to left
FAC3 BD 0003		LDA BUFF,X	and fetch it
FAC6 20 2FFB		JSR TSTEND	reached end of number
FAC9 B0 43		BCS EXIT3	
FACB 85 38		STA LOWBIT	-\$30 gives low byte
FACD CA		DEX	get next character
FACE BD 0003		LDA BUFF,X	
FAD1 20 2FFB		JSR TSTEND	test it
FAD4 B0 38		BCS EXIT3	
FAD6 C9 00		CMP #0	
FAD8 F0 0F		BEQ B2	
FADA A8		TAY	index to table
FADB B9 31FE		LDA TABLE1,Y	number equiv in hex
FADE 18		CLC	
FADF 65 38		ADC LOWBIT	add to low byte
FAE1 85 38		STA LOWBIT	
FAE3 A5 37		LDA HGHBIT	add carry to high
FAE5 69 00		ADC #0	byte
FAE7 85 37		STA HGHBIT	
FAE9 A9 3B	B2	LDA #TABLE2	tpointer points to
FAEB 85 41		STA TPOINT	table2
FAED A9 FE		LDA #(TABLE2/256)	
FAEF 85 42		STA TPOINT+1	
FAF1 20 10FB		JSR ADD_IN	add next character
FAF4 B0 18		BCS EXIT3	to low and high bytes
FAF6 A9 4F		LDA #TABLE3	repeat with table3
FAF8 85 41		STA TPOINT	
FAFA A9 FE		LDA #(TABLE3/256)	
FAFC 85 42		STA TPOINT+1	
FAFE 20 10FB		JSR ADD_IN	
FB01 B0 0B		BCS EXIT3	
FB03 A9 63		LDA #TABLE4	and table4
FB05 85 41		STA TPOINT	
FB07 A9 FE		LDA #(TABLE4/256)	
FB09 85 42		STA TPOINT+1	
FB0B 20 10FB		JSR ADD_IN	
FBOE 18	EXIT3	CLC	
FBOF 60		RTS	
FB10 CA	ADD_IN	DEX	move to next left
FB11 BD 0003		LDA BUFF,X	
FB14 20 2FFB		JSR TSTEND	test it
FB17 B0 15		BCS EXIT2	
FB19 C9 00		CMP #0	

```

FB1B FO 10      BEQ EXIT1
FB1D OA        ASL A          mulitply by two
FB1E A8        TAY           use it as index
FB1F B1 41     LDA (TPOINT),Y equiv in hex from
FB21 18        CLC           table
FB22 65 38     ADC LOWBIT    add to low byte
FB24 85 38     STA LOWBIT
FB26 C8        INY           high byte part and
FB27 B1 41     LDA (TPOINT),Y add to high byte
FB29 65 37     ADC HGHBIT
FB2B 85 37     STA HGHBIT
FB2D 18        EXIT1        CLC
FB2E 60        EXIT2        RTS
FB2F C9 2C     TSTEND       CMP #' ',' '      is character a ,
FB31 FO 09     BEQ COMMA    yes - set carry
FB33 C9 20     CMP #$20      is it a space
FB35 FO 05     BEQ COMMA
FB37 38        SEC           prepare to subtract
FB38 E9 30     SBC #$30    subtract $30
FB3A 18        CLC
FB3B 60        RTS
FB3C 38        COMMA       SEC
FB3D 60        RTS

;
; ASCII ROUTINE FOR BOARD ROUTINE COMPLETED
; OK AND ALL QUICK REPLIES
;
FB3E 20 20F8   REPLOK      JSR PRINT      routine completed ok,
FB41 7F4F4BOD DB TEX,'OK',CR,ETX
FB45 FF
FB46 60        RTS

;
; BINARY TO ASCII DECIMAL CONVERSION
;
FB47 A9 00     BINASC      LDA #0          zero output buffer
FB49 8D 5003   STA OUTBUF     double babble method
FB4C 8D 5103   STA OUTBUF+1
FB4F 8D 5203   STA OUTBUF+2
FB52 A2 08     LDX #8
FB54 A9 80     LDA #128
FB56 48        BLOOP       PHA           save acc on stack
FB57 25 37     AND HGHBIT    high bit of high byte
FB59 FO 03     BEQ BNEXT    if clear branch
FB5B 20 84FB   JSR ADD1     else add one to
FB5E 20 A5FB   BNEXT       JSR TIMTWO   output x 2
FB61 68        PLA           return acc
FB62 4A        LSR A       left one place
FB63 CA        DEX          test loop counter
FB64 D0 FO     BNE BLOOP   if non zero loop
FB66 A2 07     LDX #7       now do seven bits of
FB68 A9 80     LDA #128    low byte
FB6A 48        BLOOP2     PHA
FB6B 25 38     AND LOWBIT   AND LOWBIT
FB6D FO 03     BEQ BNEXT2   BEQ BNEXT2
FB6F 20 84FB   JSR ADD1     JSR ADD1
FB72 20 A5FB   BNEXT2     JSR TIMTWO   JSR TIMTWO
FB75 68        PLA
FB76 4A        LSR A

```





```

; INITIALISE VIAS
;
FC53 20 30F0      JSR INIT
FC56 A9 00        LDA #OFF
FC58 85 3B        STA IEEFLG
FC5A 85 30        STA NEWFLG
FC5C A9 0D        LDA #$0D          printer and input
FC5E 85 3D        STA PDELM          delimiters to CR
FC60 85 3E        STA DELIM
FC62 A2 05        LDX #5
FC64 BD 7BFD      RSLP   LDA RESTAB,X   copy reset, IRQ and
FC67 95 00        STA 0,X          NMI vectors to RAM
FC69 CA          DEX
FC6A 10 F8        BPL RSLP
;
; 68488 GPIA RESET
;
FC6C A9 80        LDA #$80
FC6E 8D 2380      STA $8023
FC71 A9 00        LDA #0
FC73 8D 2380      STA $8023
FC76 8D 2080      STA $8020
FC79 8D 2280      STA $8022
FC7C AD 2480      LDA $8024
FC7F 29 1F        AND #$1F
FC81 8D 2480      STA $8024
;
; 6850 ACIAS RESET
;
FC84 20 AAF7      JSR RSRES
;
; DETERMINE START ROUTINE FROM TOP 3 BITS
; OF ADDRESS SWITCH
;
FC87 AD 2480      LDA $8024          top 3 bits of address
FC8A 4A          LSR A              switch as option
FC8B 4A          LSR A              select number
FC8C 4A          LSR A
FC8D 4A          LSR A              have number x 2
FC8E 29 0D        AND #$0E          clear other bits
FC90 A8          TAY
FC91 B9 81FD      LDA STRTAB,Y   low byte of routine
FC94 85 08        STA $08          save it
FC96 C8          INY
FC97 B9 81FD      LDA STRTAB,Y   high byte
FC9A 85 09        STA $09
FC9C 6C 0800      JMP ($0008)      jump to this routine
;
; SOME OF THE POSSIBLE STARTING ROUTINES
;
; GPIB BASED ASCII MONITOR
;
FC9F A9 FF      IEEMON  LDA #ON
FCA1 85 3B      STA IEEFLG
FCA3 4C 69F5      JMP MONITR
;
; GPIB BASED ASCII MINICON
;

```

```

FCA6 A9 FF      IEECAM   LDA #ON
FCA8 85 3B      STA IEEFLG
FCAA 4C 9BF8    JMP MNSTRT
;
; GPIB TO SERIAL ROUTINE
;
FCAD 20 82F7    IEESER   JSR HOSTON   data recieved via
FCB0 A9 FF      LDA #ON      GPIB is transmitted
FCB2 85 3B      STA IEEFLG   to host serial port
FCB4 20 91F7    JSR PRTOFF  until three
FCB7 20 96F7    JSR RTSON   consequetive ESC's
FCBA A9 00      LDA #OFF    are received
FCBC 85 3C      STA IEEPR   character from GPIB
FCBE 20 28F7    IEERPT     JSR RDOB    is character ESC ?
FCC1 C9 1B      CMP #$1B    yes - branch
FCC3 F0 06      BEQ ESCAPE  no - transmit it
FCC5 20 D3F7    JSR PRTCHR  then loop
FCC8 4C BEFC    JMP IEERPT  get next character
FCCB 20 28F7    ESCAPE     JSR RDOB    is it an ESC
FCCE C9 1B      CMP #$1B    no - branch
FCDO D0 0A      BNE ESEXT1  get next character
FCD2 20 28F7    JSR RDOB    is it an ESC
FCD5 C9 1B      CMP #$1B    no branch
FCD7 D0 10      BNE ESEXT2  three ESC's recieved
FCD9 4C 9BF8    JMP MNSTRT  - return to minicon
;
FCDC 48         ESEXT1     PHA        save non ESC char
FCDD A9 1B      LDA #$1B    transmit ESC
FCDF 20 D3F7    JSR PRTCHR
FCE2 68         PLA
FCE3 20 D3F7    JSR PRTCHR  then non ESC char
FCE6 4C BEFC    JMP IEERPT  and back to loop
FCE9 48         ESEXT2     PHA        as above but send
FCEA A9 1B      LDA #$1B    two ESC's before
FCEC 20 D3F7    JSR PRTCHR  character
FCEF A9 1B      LDA #$1B
FCF1 20 D3F7    JSR PRTCHR
FCF4 68         PLA
FCF5 20 D3F7    JSR PRTCHR
FCF8 4C BEFC    JMP IEERPT
;
; HOST SERIAL PORT TO PRINTER SERIAL PORT
;
FCFB 20 87F7    SERSER     JSR HOSTOF
FCFE 20 8CF7    JSR PRTON
FD01 A9 00      LDA #OFF
FD03 85 3C      STA IEEPR
FD05 20 96F7    JSR RTSON
FD08 20 90F8    SERRPT     JSR GETCHR
FD0B 20 D3F7    JSR PRTCHR
FD0E 4C 08FD    JMP SERRPT
;
; ORIGINAL BINARY MINICON USER INTERFACE
;
FD11 20 30F0    OLDST      JSR INIT    initialise VIA's
FD14 A9 10      LDA #$10    set serial poll byte
FD16 8D 2580    STA SRQ
FD19 20 28F7    JSR RDOB    get byte from GPIB

```



```

FD1C 85 10          STA USRNO          save it as the usr
FD1E A2 00          LDX #0            number - then get
FD20 20 28F7       GLP JSR RDOB          six more bytes and
FD23 95 20          STA VLIST,X        save in VLIST
FD25 E8            INX
FD26 E0 06          CPX #6
FD28 D0 F6          BNE GLP
FD2A 20 30FD       JSR BEGIN          choose the routine
FD2D 4C 11FD       JMP OLDST          then start again

;
;
FD30 A9 00         BEGIN LDA #0            set serial poll byte
FD32 8D 2580       STA SRQ
FD35 85 1F         STA STATUS        and status byte

;
; CHOOSE ROUTINE
;
FD37 A5 10         CHOOSE LDA USRNO
FD39 A2 0C         LDX #(NCMDS-1)
FD3B DD 54FD       CHLP1  CMP USR,X        compare first char
FD3E D0 0E         BNE CHLP2        with table USR
FD40 8A           TXA
FD41 0A           ASL A
FD42 AA           TAX
FD43 E8           INX
FD44 BD 61FD       LDA ADDR,X        get address low
FD47 48           PHA            and high bytes
FD48 CA           DEX            put on the stack
FD49 BD 61FD       LDA ADDR,X
FD4C 48           PHA            and jump to it with
FD4D 60           RTS            an RTS instruction
FD4E CA           CHLP2  DEX
FD4F 10 EA        BPL CHLP1        loop until agreement
FD51 6C 0600       JMP (USRCMD)      no agreement - user
;                  supplied routine
;
; TABLE OF FIRST CHARACTERS
;
FD54 00010203     USR      DB 0,1,2,3,4,5,6,7,8,9,10,11,12
FD58 04050607
FD5C 08090A0B
FD60 0C

;
; ADDRESSES OF ROUTINES
;
FD61 7DF0         ADDR      ADDR (USR0-1)
FD63 83F0         ADDR      ADDR (USR1-1)
FD65 DFF1         ADDR      ADDR (USR2-1)
FD67 06F2         ADDR      ADDR (USR3-1)
FD69 23F2         ADDR      ADDR (USR4-1)
FD6B 4CF2         ADDR      ADDR (USR5-1)
FD6D B6F3         ADDR      ADDR (USR6-1)
FD6F 6EF3         ADDR      ADDR (USR7-1)
FD71 23F5         ADDR      ADDR (USR8-1)
FD73 68F5         ADDR      ADDR (USR9-1)
FD75 9EF5         ADDR      ADDR (USR10-1)
FD77 EEF0         ADDR      ADDR (USR11-1)
FD79 27F1         ADDR      ADDR (USR12-1)
;

```

## ; TABLE OF RESET, IRQ AND NMI VECTORS

```

;
FD7B 7DFE  RESTAB  ADDR IRQVEC
FD7D 7EFE  ADDR NMIVC
FD7F 9BF8  ADDR MNSTRT

```

## ; TABLE OF VECTORS FOR START UP IN ASCII

```

;
FD81 11FD  STRTAB  ADDR OLDST
FD83 11FD  ADDR OLDST
FD85 9FFC  ADDR IEEMON
FD87 A6FC  ADDR IEECAM
FD89 69F5  ADDR MONITR
FD8B 9BF8  ADDR MNSTRT
FD8D ADFC  ADDR IEESER
FD8F FBFC  ADDR SERSER

```

; TABLE OF SECOND CHARACTERS FOR ASCII  
; ROUTINES

```

;
FD91 44424F41  CHTAB  DB 'DBOAEFPHIJKLONORQD TTUPWXYZ'
FD95 45465048
FD99 494A4B4C
FD9D 4F4E4F52
FDA1 51445454
FDA5 55505758
FDA9 595A

```

## ; TABLE OF OFFSETS FROM START OF JUMPTB

```

;
FDAB 00000C18  OFFSET  DB 0,0,12,24,0,0,36,0,0,0,0,0,48,0,0,96,0
FDAF 00002400
FDB3 00000000
FDB7 30000060
FDBB 00
FDBC 3C480000  DB 60,72,0,0,84,0,0,0,0
FDC0 54000000
FDC4 00

```

; TABLE OF ADDRESSES OF ASCII MINICON  
; ROUTINES

```

;
FDC5 A5F9  JUMPTB  ADDR (ADC1-1)
FDC7 A5F9  ADDR (ADC1-1)
FDC9 B0F9  ADDR (ADC2-1)
FDCB 0000  ADDR 0
FDCD 0000  ADDR 0
FDCF 0000  ADDR 0
FDD1 7BF9  ADDR (CO1-1)
FDD3 7BF9  ADDR (CO1-1)
FDD5 8EF9  ADDR (CO2-1)
FDD7 0000  ADDR 0
FDD9 0000  ADDR 0
Fddb 0000  ADDR 0
FDDD BBF9  ADDR (DAC1-1)
FDDF BBF9  ADDR (DAC1-1)
FDE1 C6F9  ADDR (DAC2-1)
FDE3 0000  ADDR 0

```

FDE5	0000	ADDR	0
FDE7	0000	ADDR	0
FDE9	D5F9	ADDR	(GP1-1)
FDEB	D5F9	ADDR	(GP1-1)
FDED	D5F9	ADDR	(GP1-1)
FDEF	0000	ADDR	0
FDF1	0000	ADDR	0
FDF3	0000	ADDR	0
FDF5	E0F9	ADDR	(MO0-1)
FDF7	E3F9	ADDR	(MO1-1)
FDF9	E6F9	ADDR	(MO2-1)
FDFB	E9F9	ADDR	(MO3-1)
FDFD	ECF9	ADDR	(MO4-1)
FDFE	EFF9	ADDR	(MO5-1)
FE01	08FA	ADDR	(RD1-1)
FE03	08FA	ADDR	(RD1-1)
FE05	0EFA	ADDR	(RD2-1)
FE07	0000	ADDR	0
FE09	0000	ADDR	0
FE0B	0000	ADDR	0
FE0D	4BF9	ADDR	(STPM1-1)
FE0F	4BF9	ADDR	(STPM1-1)
FE11	56F9	ADDR	(STPM2-1)
FE13	65F9	ADDR	(STPM3-1)
FE15	70F9	ADDR	(STPM4-1)
FE17	0000	ADDR	0
FE19	F2F9	ADDR	(VP1-1)
FE1B	F2F9	ADDR	(VP1-1)
FE1D	FDF9	ADDR	(VP2-1)
FE1F	0000	ADDR	0
FE21	0000	ADDR	0
FE23	0000	ADDR	0
FE25	19FA	ADDR	(PR1-1)
FE27	19FA	ADDR	(PR1-1)
FE29	52FA	ADDR	(PR2-1)
FE2B	0000	ADDR	0
FE2D	0000	ADDR	0
FE2F	0000	ADDR	0

; TABLES OF BINARY EQUIVALENTS OF DECIMAL

FE31	000A141E	TABLE1	DB	0,10,20,30,40,50,60,70,80,90
FE35	28323C46			
FE39	505A			
FE3B	0000	TABLE2	ADDR	0
FE3D	6400		ADDR	100
FE3F	C800		ADDR	200
FE41	2C01		ADDR	300
FE43	9001		ADDR	400
FE45	F401		ADDR	500
FE47	5802		ADDR	600
FE49	BC02		ADDR	700
FE4B	2003		ADDR	800
FE4D	8403		ADDR	900
FE4F	0000	TABLE3	ADDR	0
FE51	E803		ADDR	1000
FE53	D007		ADDR	2000
FE55	B80B		ADDR	3000



```

;
; MONITOR. PROVIDES MEMORY DUMP AND
; DISASSEMBLER VIA GPIB OR RS232 INTERFACES.
; ASCII TRANSMISSION IS USED WITH TERMINAL
; ECHO
;
; M.J. HILL 1985
;
; VARIABLES
;
0043      SELECT      EQU $43      select pointer
0045      GETPTR      EQU $45      zero page pointer
0050      NUMBER      EQU $50      temp number store
0032      BUFFEN      EQU $32      buffer fill pointer
0034      BPOINT      EQU $34      buffer empty pointer
0052      COUNT       EQU $52      counts lines dumped
0054      NUMLIN      EQU $54      number lines to dump
0056      EA          EQU $56      end address
0058      SA          EQU $58      start address
005A      COLUMN      EQU $5A      data cell for dump
0047      PRINTR      EQU $47      printer flag
0048      HOST        EQU $48      output device flag
003B      IEEFLG      EQU $3B      flag for GPIB as host
003C      IEEPR       EQU $3C      GPIB as printer flag
0036      CHAR        EQU $36      char to be output
005C      REPEAT      EQU $5C      loop counter
005D      TEMPX       EQU $5D      temporary X register
0049      RETURN      EQU $49      temp return address
005E      DISLNS      EQU $5E      no. lines disass'ed
005F      LINUM       EQU $5F      no. to disassemble
0060      LETTER      EQU $60      letter from mnem
0061      SUBPTR      EQU $61      pointer to sub'tine
0063      OPBYTES     EQU $63      data cell
0064      OPCHRS      EQU $64      data cell
0065      ADRCOL      EQU $65      start column of field
;
; CONSTANTS
;
00FF      ON          EQU $FF
0000      OFF         EQU $0
000D      CR          EQU $0D
000A      LF          EQU $0A
007F      TEX        EQU $7F
00FF      ETX        EQU $FF
;
; BUFFERS
;
0300      BUFF        EQU $0300    input buffer
0350      OUTBUF      EQU $0350    output buffer
;
; LOCATION OF JUMP INSTRUCTIONS FOR
; ROUTINES IN $F000 EPROM
;
F000      RESET       EQU $F000
F003      PRTCHR      EQU $F003
F006      PRINT       EQU $F006
F009      HOSTON      EQU $F009
F00C      HOSTOF      EQU $F00C

```

FOOF	PRTON	EQU \$FOOF	
F012	PRTOFF	EQU \$F012	
F015	RTSON	EQU \$F015	
F018	RTSOFF	EQU \$F018	
F01B	RSRES	EQU \$F01B	
F01E	PUSHSL	EQU \$F01E	
F021	POPSL	EQU \$F021	
F024	GETCHR	EQU \$F024	
F027	RDOB	EQU \$F027	
F02A	GETSL	EQU \$F02A	
F02D	MINCON	EQU \$F02D	
	:		
E000		ORG X'E000'	
	:		
E000 4C 79E3		JMP START	
	:		
E003 A5 44	PRADR	LDA SELECT+1	print high byte of
E005 20 D7E0		JSR PRTBYT	pointer
E008 A5 43		LDA SELECT	and low byte
E00A 20 D7E0		JSR PRTBYT	
E00D 60		RTS	
E00E 20 2AF0	DUMPSL	JSR GETSL	get byte from pointer
E011 20 D7E0		JSR PRTBYT	and print it
E014 60		RTS	
E015 20 B4E0	PRDUMP	JSR GOTOSA	pointer=start address
E018 20 60E0	HXLOOP	JSR PRLINE	dump one line
E01B 10 FB		BPL HXLOOP	loop if A<&FF
E01D 20 C6E0		JSR CRLF	print cr,lf
E020 60		RTS	
E021 38	SETADS	SEC	
E022 A5 57		LDA EA+1	compare high byte of
E024 C5 59		CMP SA+1	start & end addresses
E026 90 0A		BCC TOLOW	if end start
E028 D0 06		BNE SEXIT	
E02A A5 56		LDA EA	compare low byte of
E02C C5 58		CMP SA	start & end addresses
E02E 90 02		BCC TOLOW	if end start
E030 18	SEXIT	CLC	return carry clear
E031 60		RTS	
E032 38	TOLOW	SEC	return with carry set
E033 60		RTS	
E034 A9 24	PRSA	LDA #C'\$'	print \$
E036 20 03F0		JSR PRTCHR	
E039 A5 59		LDA SA+1	print high byte of
E03B 20 D7E0		JSR PRTBYT	start address
E03E A5 58		LDA SA	and low byte
E040 20 D7E0		JSR PRTBYT	
E043 60		RTS	
E044 A9 24	PREA	LDA #C'\$'	print \$
E046 20 03F0		JSR PRTCHR	
E049 A5 57		LDA EA+1	print high byte of
E04B 20 D7E0		JSR PRTBYT	end address
E04E A5 56		LDA EA	and low byte
E050 20 D7E0		JSR PRTBYT	
E053 60		RTS	
E054 20 34E0	RANGE	JSR PRSA	print start address
E057 A9 2D		LDA #C'-'	hyphen
E059 20 03F0		JSR PRTCHR	

E05C	20	44E0		JSR	PREA	and end address
E05F	60			RTS		
E060	20	C6E0	PRLINE	JSR	CRLF	print cr,lf
E063	A5	43		LDA	SELECT	low byte of pointer
E065	48			PHA		save on stack
E066	29	0F		AND	#\$0F	mask high byte
E068	85	5A		STA	COLUMN	save in col counter
E06A	68			PLA		fetch back from stack
E06B	29	F0		AND	#\$F0	make pointer multiple
E06D	85	43		STA	SELECT	of 16
E06F	20	03E0		JSR	PRADR	print pointer
E072	A2	03		LDX	#\$3	print three spaces
E074	20	EAE0		JSR	SPACES	
E077	A5	5A		LDA	COLUMN	get coulumn counter
E079	F0	0C		BEQ	COLOK	if zero branch
E07B	A2	03	PRLOOP	LDX	#\$3	print three spaces
E07D	20	EAE0		JSR	SPACES	
E080	20	3DE1		JSR	INCSL	increment pointer
E083	C6	5A		DEC	COLUMN	and decrease column
E085	D0	F4		BNE	PRLOOP	if not zero loop
E087	20	0EE0	COLOK	JSR	DUMPSL	byte from pointer
E08A	20	D1E0		JSR	SPACE	print space
E08D	20	9BE0		JSR	NEXTSL	increment pointer
E090	30	08		BMI	EXIT	loop if A<&FF
E092	A5	43	NOTEA	LDA	SELECT	low byte of pointer
E094	29	0F		AND	#\$0F	mask high bits
E096	C9	00		CMP	#0	not dumped 16 bytes
E098	D0	ED		BNE	COLOK	then loop
E09A	60		EXIT	RTS		
E09B	38		NEXTSL	SEC		prepare to subtract
E09C	A5	44		LDA	SELECT+1	high byte of pointer
E09E	C5	57		CMP	EA+1	less than high byte
EOA0	90	09		BCC	SLOK	end address continue
EOA2	D0	0D		BNE	NOINC	if greater then end
EOA4	38			SEC		
EOA5	A5	43		LDA	SELECT	low byte of pointer
EOA7	C5	56		CMP	EA	> end address ?
EOA9	B0	06		BCS	NOINC	
EOAB	20	3DE1	SLOK	JSR	INCSL	increment pointer
EOAE	A9	00		LDA	#0	return with A=0
EOB0	60			RTS		
EOB1	A9	FF	NOINC	LDA	#\$FF	return with A=&FF
EOB3	60			RTS		
EOB4	A5	58	GOTOSA	LDA	SA	pointer equals
EOB6	85	43		STA	SELECT	start address
EOB8	A5	59		LDA	SA+1	
EOBA	85	44		STA	SELECT+1	
EOBC	60			RTS		
EOBD	A5	43	DECSL	LDA	SELECT	decrease pointer
EOBF	D0	02		BNE	BRAN2	low byte
EOC1	C6	44		DEC	SELECT+1	and high byte if
EOC3	C6	43	BRAN2	DEC	SELECT	necessary
EOC5	60			RTS		
EOC6	A9	0D	CRLF	LDA	#CR	print CR
EOC8	20	03F0		JSR	PRTCHR	
EOCB	A9	0A		LDA	#LF	and line feed
EOCD	20	03F0		JSR	PRTCHR	
EOD0	60			RTS		

E0D1	A9	20	SPACE	LDA # \$20	print a space
E0D3	20	03F0		JSR PRTCHR	
E0D6	60			RTS	
E0D7	48		PRTBYT	PHA	save acc
E0D8	4A			LSR A	move top 4 bits to
E0D9	4A			LSR A	lower 4 bits
E0DA	4A			LSR A	
E0DB	4A			LSR A	
E0DC	20	2FE1		JSR ASCII	convert to ascii
E0DF	20	03F0		JSR PRTCHR	and print
EOE2	68			PLA	get back acc
EOE3	20	2FE1		JSR ASCII	and print lower 4
EOE6	20	03F0		JSR PRTCHR	bits in ascii
EOE9	60			RTS	
EOEA	A9	20	SPACES	LDA # \$20	print X number of
EOEC	86	5C	CHARS	STX REPEAT	spaces
EOEE	48		RPLOOP	PHA	
EOEF	A6	5C		LDX REPEAT	
EOF1	F0	09		BEQ RPTEND	
EOF3	C6	5C		DEC REPEAT	
EOF5	20	03F0		JSR PRTCHR	
EOF8	68			PLA	
EOF9	18			CLC	
EOFA	90	F2		BCC RPLOOP	
EOFC	68		RPTEND	PLA	
EOFD	60			RTS	
EOFE	86	5C	CRLFS	STX REPEAT	print X number of
E100	A6	5C	CRLOOP	LDX REPEAT	CR's and LF's
E102	F0	07		BEQ ENDCR	
E104	C6	5C		DEC REPEAT	
E106	20	C6E0		JSR CRLF	
E109	90	F5		BCC CRLOOP	
E10B	60		ENDCR	RTS	
E10C	86	5D	PRMSG	STX TEMPX	save X register
E10E	B5	01		LDA 1,X	save message pointer
E110	48			PHA	
E111	B5	00		LDA 0,X	
E113	48			PHA	
E114	A6	5D	LOOP	LDX TEMPX	X points to message
E116	A1	00		LDA (0,X)	pointer on zero page
E118	C9	FF		CMP #ETX	get character, ETX ?
E11A	F0	0C		BEQ MSGEND	yes - end routine
E11C	F6	00		INC 0,X	no increment pointer
E11E	D0	02		BNE NEXT	
E120	F6	01		INC 1,X	
E122	20	03F0	NEXT	JSR PRTCHR	print character
E125	18			CLC	
E126	90	EC		BCC LOOP	and loop
E128	68		MSGEND	PLA	restore original
E129	95	00		STA 0,X	message pointer
E12B	68			PLA	
E12C	95	01		STA 1,X	
E12E	60			RTS	
E12F	08		ASCII	PHP	save decimal flag
E130	D8			CLD	clear decimal flag
E131	29	0F		AND # \$0F	clear 4 MSB's
E133	C9	0A		CMP # \$0A	is acc > 9
E135	30	02		BMI DECIML	if not must be 0-9



E137	69	06		ADC #6	if so add &#36, A-F
E139	69	30	DECIML	ADC #&#30	add &#30 => ascii
E13B	28			PLP	restore decimal flag
E13C	60			RTS	
E13D	E6	43	INCSL	INC SELECT	increment select
E13F	D0	02		BNE BRANCH	pointer
E141	E6	44		INC SELECT+1	
E143	60		BRANCH	RTS	
E144	A6	32	ADDRES	LDX BUFFEN	X with buffer pointer
E146	A0	02		LDY #2	Y as loop counter
E148	88		ADLOOP	DEY	
E149	CA			DEX	X points to next char
E14A	BD	0003		LDA BUFF,X	to the left in buffer
E14D	20	95E1		JSR BINARY	convert to binary
E150	C9	FF		CMP #&#FF	if acc=&#FF error
E152	F0	20		BEQ ADERR	
E154	99	5000		STA NUMBER,Y	save as low 4 bits
E157	CA			DEX	next character to
E158	BD	0003		LDA BUFF,X	the left
E15B	20	95E1		JSR BINARY	convert to binary
E15E	C9	FF		CMP #&#FF	
E160	F0	12		BEQ ADERR	if error
E162	0A			ASL A	move 4 LSB's to
E163	0A			ASL A	4 MSB's
E164	0A			ASL A	
E165	0A			ASL A	
E166	19	5000		ORA NUMBER,Y	add to 4 LSB's
E169	99	5000		STA NUMBER,Y	and save it
E16C	C0	00		CPY #0	is loop ended
E16E	D0	D8		BNE ADLOOP	no - loop
E170	86	32		STX BUFFEN	update buffer pointer
E172	18			CLC	clear carry and
E173	60			RTS	return
E174	38		ADERR	SEC	set carry and
E175	60			RTS	return
E176	20	44E1	STEASA	JSR ADDRES	4 characters from
E179	B0	18		BCS SERR	buffer to 16 bit no.
E17B	A5	51		LDA NUMBER+1	and make it the end
E17D	85	56		STA EA	address
E17F	A5	50		LDA NUMBER	
E181	85	57		STA EA+1	
E183	C6	32		DEC BUFFEN	jump past space
E185	20	44E1		JSR ADDRES	and repeat for start
E188	B0	09		BCS SERR	address
E18A	A5	51		LDA NUMBER+1	
E18C	85	58		STA SA	
E18E	A5	50		LDA NUMBER	
E190	85	59		STA SA+1	
E192	60			RTS	
E193	38		SERR	SEC	if error set carry
E194	60			RTS	
E195	38		BINARY	SEC	prepare to subtract
E196	E9	30		SBC #&#30	subtract &#30
E198	90	0A		BCC BAD	if char < &#30 bad
E19A	C9	0A		CMP #&#0A	was it &#30 - &#39
E19C	90	08		BCC GOOD	yes - now have binary
E19E	E9	07		SBC #7	subtract 7
E1A0	C9	10		CMP #&#10	was it &#41-&#46

E1A2	90	02		BCC	GOOD	yes - now have binary
E1A4	A9	FF	BAD	LDA	#\$FF	acc with &FF
E1A6	60		GOOD	RTS		
E1A7	20	B4E0	PRDIS	JSR	GOTOSA	select pointer=>start
E1AA	20	C6E0		JSR	CRLF	address, print cr,lf
E1AD	20	B3E1	PRLP	JSR	DSLIN	disassemble one line
E1B0	10	FB		BPL	PRLP	loop until last line
E1B2	60			RTS		done then return
E1B3	20	2AF0	DSLIN	JSR	GETSL	get byte from select
E1B6	48			PHA		save it
E1B7	20	C8E1		JSR	MNEMON	mnemonic for opcode
E1BA	20	D1E0		JSR	SPACE	print space
E1BD	68			PLA		restore opcode
E1BE	20	E1E1		JSR	OPERAN	print operand
E1C1	20	31E2		JSR	FINISH	finish line
E1C4	20	9BE0		JSR	NEXTSL	increment select
E1C7	60			RTS		
E1C8	A2	03	MNEMON	LDX	#3	3 letters to print
E1CA	86	60		STX	LETTER	
E1CC	AA			TAX		use opcode as index
E1CD	BD	FAE5		LDA	MCODES,X	get mnemonic code for
E1D0	AA			TAX		that opcode, as index
E1D1	BD	FAE7	MNLOOP	LDA	MNAMES,X	get letter from table
E1D4	86	5D		STX	TEMPX	save X register
E1D6	20	03F0		JSR	PRTCHR	print it
E1D9	A6	5D		LDX	TEMPX	increment table point
E1DB	E8			INX		
E1DC	C6	60		DEC	LETTER	decrease counter
E1DE	D0	F1		BNE	MNLOOP	if not yet zero loop
E1E0	60			RTS		
E1E1	AA		OPERAN	TAX		lookup addressing mode
E1E2	BD	FAE6		LDA	MODES,X	for the opcode
E1E5	AA			TAX		X indicates addressing
E1E6	20	EAE1		JSR	MODEX	mode, handle it
E1E9	60			RTS		
E1EA	BD	3AE3	MODEX	LDA	SUBS,X	low byte of X pointer
E1ED	85	61		STA	SUBPTR	table of subroutines
E1EF	E8			INX		
E1F0	BD	3AE3		LDA	SUBS,X	high byte
E1F3	85	62		STA	SUBPTR+1	
E1F5	6C	6100		JMP	(SUBPTR)	jump to chosen routine
E1F8	20	3DE1	ONEBYT	JSR	INCSL	advance to byte after
E1FB	20	0EE0		JSR	DUMPSL	opcode and dump it
E1FE	60			RTS		
E1FF	20	3DE1	TWOBYT	JSR	INCSL	get byte after opcode
E202	20	2AF0		JSR	GETSL	
E205	48			PHA		save it on stack
E206	20	3DE1		JSR	INCSL	get high byte
E209	20	0EE0		JSR	DUMPSL	dump it
E20C	68			PLA		recover low byte
E20D	20	D7E0		JSR	PRTBYT	dump it
E210	60			RTS		
E211	A9	28	LPAREN	LDA	#C'('	print left parenthesis
E213	D0	02		BNE	SENDIT	
E215	A9	29	RPAREN	LDA	#C')'	print right
E217	20	03F0	SENDIT	JSR	PRTCHR	parenthesis
E21A	60			RTS		
E21B	A9	2C	XINDEX	LDA	#C','	print comma

E21D	20	03F0		JSR	PRTCHR	
E220	A9	58		LDA	#C'X'	followed by an X
E222	20	03F0		JSR	PRTCHR	
E225	60			RTS		
E226	A9	2C	YINDEX	LDA	#C','	print a comma
E228	20	03F0		JSR	PRTCHR	
E22B	A9	59		LDA	#C'Y'	followed by a Y
E22D	20	03F0		JSR	PRTCHR	
E230	60			RTS		
E231	85	64	FINISH	STA	OPCHRS	save length of the
E233	86	63		STX	OPBYTS	operand in chars and
E235	CA			DEX		in bytes, decrease
E236	30	06		BMI	SELOK	pointer to point to
E238	20	BDE0	LOOP1	JSR	DECSL	opcode
E23B	CA			DEX		
E23C	10	FA		BPL	LOOP1	select => opcode
E23E	08		SELOK	PHP		save decimal flag
E23F	D8			CLD		clear decimal flag
E240	38			SEC		space over to column
E241	A5	65		LDA	ADRCOL	for the address
E243	E9	04		SBC	#4	operand field started
E245	E5	64		SBC	OPCHRS	4 and includes opchrs
E247	28			PLP		restore decimal flag
E248	AA			TAX		print enough spaces
E249	20	EAE0		JSR	SPACES	to reach address col
E24C	20	03E0		JSR	PRADR	print address
E24F	20	D1E0	LOOP2	JSR	SPACE	space once
E252	20	0EE0		JSR	DUMPSL	dump selected byte
E255	20	3DE1		JSR	INCSL	increment pointer
E258	C6	63		DEC	OPBYTS	dumped last byte?
E25A	10	F3		BPL	LOOP2	no - loop
E25C	20	BDE0		JSR	DECSL	select points to last
						byte in operand
E25F	20	C6E0	FINEND	JSR	CRLF	goto a new line
E262	60			RTS		
E263	20	FFE1	ABSLUT	JSR	TWOBYT	print two byte operan
E266	A2	02		LDX	#2	operand has two bytes
E268	A9	04		LDA	#4	and four characters
E26A	60			RTS		
E26B	20	63E2	ABSX	JSR	ABSLUT	
E26E	20	1BE2		JSR	XINDEX	print comma and an X
E271	A2	02		LDX	#2	two bytes
E273	A9	06		LDA	#6	six characters
E275	60			RTS		
E276	20	63E2	ABSY	JSR	ABSLUT	
E279	20	26E2		JSR	YINDEX	print comma and a Y
E27C	A2	02		LDX	#2	two bytes
E27E	A9	06		LDA	#6	six characters
E280	60			RTS		
E281	A9	41	ACC	LDA	#C'A'	print letter A
E283	20	03F0		JSR	PRTCHR	
E286	A2	00		LDX	#0	no bytes
E288	A9	01		LDA	#1	one character
E28A	60			RTS		
E28B	A2	00	IMPLID	LDX	#0	no bytes
E28D	A9	00		LDA	#0	and no characters
E28F	60			RTS		
E290	A9	23	IMMEDT	LDA	#C'#'	print a #

E292	20	03F0		JSR	PRTCHR	
E295	A9	24		LDA	#C'\$'	then a \$ to show hex
E297	20	03F0		JSR	PRTCHR	
E29A	20	F8E1		JSR	ONEBYT	print one byte
E29D	A2	01		LDX	#1	one byte
E29F	A9	04		LDA	#4	and four characters
E2A1	60			RTS		
E2A2	20	11E2	INDRCT	JSR	LPAREN	left parenthesis
E2A5	20	63E2		JSR	ABSLUT	two byte operand
E2A8	20	15E2		JSR	RPAREN	right parenthesis
E2AB	A9	06		LDA	#6	six characters
E2AD	A2	02		LDX	#2	and two bytes
E2AF	60			RTS		
E2B0	20	11E2	INDX	JSR	LPAREN	
E2B3	20	07E3		JSR	ZEROX	print zero page
						address, comma and X
E2B6	20	15E2		JSR	RPAREN	right parenthesis
E2B9	A2	01		LDX	#1	one byte
E2BB	A9	08		LDA	#8	eight characters
E2BD	60			RTS		
E2BE	20	11E2	INDY	JSR	LPAREN	
E2C1	20	FAE2		JSR	ZEROPG	
E2C4	20	15E2		JSR	RPAREN	
E2C7	20	26E2		JSR	YINDEX	
E2CA	A2	01		LDX	#1	
E2CC	A9	08		LDA	#8	
E2CE	60			RTS		
E2CF	20	3DE1	RELATV	JSR	INCSL	select next byte
E2D2	20	1EFO		JSR	PUSHSL	save select pointer
E2D5	20	2AF0		JSR	GETSL	get operand byte
E2D8	48			PHA		save it on stack
E2D9	20	3DE1		JSR	INCSL	increment pointer
E2DC	68			PLA		restore operand byte
E2DD	C9	00		CMP	#0	is it plus or minus
E2DF	10	02		BPL	FORWRD	plus forward branch
E2E1	C6	44		DEC	SELECT+1	branching backwards
						is like branching
						forwards from one
						page lower
E2E3	08		FORWRD	PHP		save callers flags
E2E4	D8			CLD		binary arithmetic
E2E5	18			CLC		prepare to add
E2E6	65	43		ADC	SELECT	add operand
E2E8	90	02		BCC	RELEND	
E2EA	E6	44		INC	SELECT+1	
E2EC	85	43	RELEND	STA	SELECT	select => branch
E2EE	28			PLP		restore decimal flag
E2EF	20	03E0		JSR	PRADR	print address
E2F2	20	21F0		JSR	POPSL	restore select
E2F5	A2	01		LDX	#1	one byte
E2F7	A9	04		LDA	#4	and four characters
E2F9	60			RTS		
E2FA	A9	00	ZEROPG	LDA	#0	print two ascii '0's
E2FC	20	D7E0		JSR	PRTBYT	
E2FF	20	F8E1		JSR	ONEBYT	print 1 byte operand
E302	A2	01		LDX	#1	one byte
E304	A9	04		LDA	#4	and four characters
E306	60			RTS		

E307	20	FAE2	ZEROX	JSR ZEROPG	zero page address
E30A	20	1BE2		JSR XINDEX	comma and an X
E30D	A2	01		LDX #1	one byte
E30F	A9	06		LDA #6	and six characters
E311	60			RTS	
E312	20	FAE2	ZEROY	JSR ZEROPG	
E315	20	26E2		JSR YINDEX	
E318	A9	01		LDA #1	
E31A	A9	06		LDA #6	
E31C	60			RTS	
E31D	68		TXMODE	PLA	pop return address to
E31E	68			PLA	operan
E31F	68			PLA	and return address to
E320	68			PLA	dsline
E321	20	9BE0		JSR NEXTSL	advance past TEX
E324	30	0D		BMI TXEXIT	return if reached end
E326	20	2AFO		JSR GETSL	get character
E329	C9	FF		CMP #ETX	is it ETX
E32B	F0	06		BEQ TXEXIT	yes - exit
E32D	20	03FO		JSR PRTCHR	print character
E330	18			CLC	loop next character
E331	90	EE		BCC TXMODE+4	
E333	20	C6E0	TXEXIT	JSR CRLF	print cr,lf
E336	20	9BE0		JSR NEXTSL	advance next opcode
E339	60			RTS	
E33A	8BE2		SUBS	ADDR IMPLID	mode zero is invalid
E33C	81E2			ADDR ACC	
E33E	90E2			ADDR IMMEDT	
E340	FAE2			ADDR ZEROPG	
E342	07E3			ADDR ZEROX	
E344	12E3			ADDR ZEROY	
E346	63E2			ADDR ABSLUT	
E348	6BE2			ADDR ABSX	
E34A	76E2			ADDR ABSY	
E34C	8BE2			ADDR IMPLID	
E34E	CFE2			ADDR RELATV	
E350	BOE2			ADDR INDX	
E352	BEE2			ADDR INDY	
E354	A2E2			ADDR INDRCT	
E356	1DE3			ADDR TXMODE	

```

;
; USER INTERFACE SECTION
;

```

E358	A9	00	INIT	LDA #0	initialise variables
E35A	85	52		STA COUNT	
E35C	85	5A		STA COLUMN	
E35E	85	36		STA CHAR	
E360	85	5C		STA REPEAT	
E362	85	5D		STA TEMPX	
E364	85	49		STA RETURN	
E366	85	4A		STA RETURN+1	
E368	85	5F		STA LINUM	
E36A	85	60		STA LETTER	
E36C	A9	04		LDA #4	
E36E	85	54		STA NUMLIN	
E370	A9	05		LDA #5	
E372	85	5E		STA DISLNS	
E374	A9	10		LDA #16	

E376	85	65		STA	ADRCOL	
E378	60			RTS		
E379	20	58E3	START	JSR	INIT	initialise variables
E37C	20	1BF0		JSR	RSRES	reset 6850
E37F	20	18F0		JSR	RTSOFF	RTS low
E382	A5	3B		LDA	IEEFLG	RS232 or IEEE488 ?
E384	F0	0D		BEQ	SERIAL	
E386	A9	FF		LDA	#ON	
E388	85	3C		STA	IEEEPR	IEEE as output
E38A	20	0CFO		JSR	HOSTOF	
E38D	20	12F0		JSR	PRTOFF	
E390	4C	9DE3		JMP	START2	
E393	20	09F0	SERIAL	JSR	HOSTON	use host for output
E396	20	12F0		JSR	PRTOFF	
E399	A9	00		LDA	#OFF	
E39B	85	3C		STA	IEEEPR	
E39D	20	C6E0	START2	JSR	CRLF	print a couple of
E3A0	20	C6E0		JSR	CRLF	cr's and lf's
E3A3	20	06F0		JSR	PRINT	print title
E3A6	7F			DB	TEX	
E3A7	23232320			DB	'### I.C.C. RS232/IEEE MONITOR	
E3AB	492E432E				VS 1.0 ###'	
E3AF	432E2052					
E3B3	53323332					
E3B7	2F494545					
E3BB	45204D4F					
E3BF	4E49544F					
E3C3	52205653					
E3C7	20312E30					
E3CB	20232323					
E3CF	0DOA			DB	CR,LF	
E3D1	28632920			DB	'(c) M.J.HILL 1984/5'	
E3D5	4D2E4A2E					
E3D9	48494C4C					
E3DD	20313938					
E3E1	342F35					
E3E4	ODOAFF			DB	CR,LF,ETX	
E3E7	20	C6E0		JSR	CRLF	
E3EA	20	06F0	VISMON	JSR	PRINT	print prompt
E3ED	7F0DOA2A			DB	TEX,CR,LF,'*',ETX	
E3F1	FF					
E3F2	A5	3B		LDA	IEEFLG	
E3F4	F0	1A		BEQ	SER2	IEEE or RS232 input
E3F6	A2	00		LDX	#0	
E3F8	20	27F0	NXTIN	JSR	RDOB	get byte from GPIB
E3FB	9D	0003		STA	BUFF,X	
E3FE	C9	08		CMP	#8	
E400	F0	2B		BEQ	DELETE	
E402	C9	7F		CMP	#\$7F	
E404	F0	27		BEQ	DELETE	
E406	20	40E4		JSR	ECHO	
E409	C9	0D		CMP	#13	
E40B	F0	39		BEQ	PROCES	
E40D	E8			INX		
E40E	D0	E8		BNE	NXTIN	
E410	20	15F0	SER2	JSR	RTSON	RTS high
E413	A2	00		LDX	#0	
E415	20	24F0	NEXTIN	JSR	GETCHR	characters from 6850

E418	9D	0003		STA	BUFF,X	and place in buffer
E41B	C9	08		CMP	#8	handle delete and
E41D	F0	0E		BEQ	DELETE	backspace alike
E41F	C9	7F		CMP	#\$7F	
E421	F0	0A		BEQ	DELETE	
E423	20	40E4		JSR	ECHO	echo to terminal
E426	C9	0D		CMP	#13	stop when CR received
E428	F0	1C		BEQ	PROCES	
E42A	E8			INX		
E42B	D0	E8		BNE	NEXTIN	
E42D	E0	00	DELETE	CPX	#0	buffer pointer back
E42F	D0	08		BNE	NONZ	one but not past zero
E431	A9	07		LDA	#7	
E433	20	40E4		JSR	ECHO	
E436	18			CLC		
E437	90	DC		BCC	NEXTIN	
E439	CA		NONZ	DEX		
E43A	20	40E4		JSR	ECHO	
E43D	18			CLC		
E43E	90	D5		BCC	NEXTIN	
E440	48		ECHO	PHA		
E441	20	03F0		JSR	PRTCHR	
E444	68			PLA		
E445	60			RTS		
E446	86	32	PROCES	STX	BUFFEN	save buffer pointer
E448	A2	00		LDX	#0	
E44A	BD	0003		LDA	BUFF,X	get first character
E44D	C9	0D		CMP	#13	if CR back to monitor
E44F	F0	99		BEQ	VISMON	
E451	C9	44		CMP	#C'D'	if D then disassemble
E453	D0	0B		BNE	VB1	if not test another
E455	20	76E1		JSR	STEASA	decode addresses
E458	B0	4F		BCS	ERROR	carry set if error
E45A	20	A7E1		JSR	PRDIS	jump to disas
E45D	4C	EAE3		JMP	VISMON	finished
E460	C9	45	VB1	CMP	#C'E'	if E then exit to
E462	D0	03		BNE	VB2	minicon routines
E464	4C	2DF0		JMP	MINCON	
E467	C9	4D	VB2	CMP	#C'M'	if M then dump
E469	D0	0B		BNE	VB3	
E46B	20	76E1		JSR	STEASA	
E46E	B0	39		BCS	ERROR	
E470	20	15E0		JSR	PRDUMP	
E473	4C	EAE3		JMP	VISMON	
E476	C9	50	VB3	CMP	#C'P'	if P then toggle
E478	D0	10		BNE	VB4	printer on or off
E47A	A5	47		LDA	PRINTR	
E47C	F0	06		BEQ	PON	off so put on
E47E	20	12F0		JSR	PRTOFF	on so put off
E481	4C	EAE3		JMP	VISMON	
E484	20	OFF0	PON	JSR	PRTON	
E487	4C	EAE3		JMP	VISMON	
E48A	C9	48	VB4	CMP	#C'H'	
E48C	D0	06		BNE	VB5	
E48E	20	C4E4		JSR	MENU	
E491	4C	EAE3		JMP	VISMON	
E494	20	06F0	VB5	JSR	PRINT	unrecognised command
E497	7F0DOA			DB	TEX,CR,LF	

```

E49A 3F20434F          DB '? COMMAND'
E49E 4D4D414E
E4A2 44
E4A3 ODOAFF           DB CR,LF,ETX
E4A6 4C EAE3          JMP VISION            back to monitor
E4A9 18                ERROR CLC                command error
E4AA 20 06FO
E4AD 7FODOA
E4B0 434F4D4D
E4B4 414E4420
E4B8 4552524F
E4BC 52
E4BD FF
E4BE 20 C6E0
E4C1 4C EAE3          MENU JMP VISION
E4C4 20 06FO          JSR PRINT
E4C7 7FODOA           DB TEX,CR,LF
E4CA 4D4F4E49         DB 'MONITOR COMMANDS : ',CR,LF,LF
E4CE 544F5220
E4D2 434F4D4D
E4D6 414E4453
E4DA 203A0DOA
E4DE OA
E4DF 4D203C73         DB 'M <start address> <end address>'
E4E3 74617274         Dumps memory between'
E4E7 20616464
E4EB 72657373
E4EF 3E203C65
E4F3 6E642061
E4F7 64647265
E4FB 73733E20
E4FF 20204475
E503 6D707320
E507 6D656D6F
E50B 72792062
E50F 65747765
E513 656E
E515 20616464         DB ' addresses given (in hex)',CR,LF
E519 72657373
E51D 65732067
E521 6976656E
E525 2028696E
E529 20686578
E52D 290DOA
E530 44203C73         DB 'D <start address> <end address>'
E534 74617274         Disassembles memory '
E538 20616464
E53C 72657373
E540 3E203C65
E544 6E642061
E548 64647265
E54C 73733E20
E550 20204469
E554 73617373
E558 656D626C
E55C 6573206D
E560 656D6F72
E564 7920

```



E566 62657477  
 E56A 65656E20  
 E56E 67697665  
 E572 6E206164  
 E576 64726573  
 E57A 7365730D  
 E57E 0A  
 E57F 50202020  
 E583 20202020  
 E587 20202020  
 E58B 20202020  
 E58F 20202020  
 E593 20202020  
 E597 20202020  
 E59B 20202020  
 E59F 2020546F  
 E5A3 67676C65  
 E5A7 73207072  
 E5AB 696E7465  
 E5AF 7220706F  
 E5B3 7274  
 E5B5 206F6E20  
 E5B9 6F72206F  
 E5BD 66660D0A  
 E5C1 45202020  
 E5C5 20202020  
 E5C9 20202020  
 E5CD 20202020  
 E5D1 20202020  
 E5D5 20202020  
 E5D9 20202020  
 E5DD 20202020  
 E5E1 20204578  
 E5E5 69747320  
 E5E9 746F206D  
 E5ED 696E6963  
 E5F1 6F6E  
 E5F3 0D0A0AFF  
 E5F7 4C EAE3

DB 'between given addresses', CR, LF

DB 'P  
 Toggles printer port'

DB 'on or off', CR, LF

DB 'E  
 Exits to minicon'

DB CR, LF, LF, ETX  
 JMP VISMON

back to monitor

TABLES FOR DISASSEMBLER

E5FA 226A0101  
 E5FE 016A0A01  
 E602 706A  
 E604 0A01016A  
 E608 0A011F6A  
 E60C 0101  
 E60E 016A0A01  
 E612 2B6A0101  
 E616 01640A  
 E619 01580701  
 E61D 01160779  
 E621 0176  
 E623 07790116  
 E627 07790119  
 E62B 0701  
 E62D 01010779

MCODES

DB \$22, \$6A, \$01, \$01, \$01, \$6A, \$0A,  
 \$01, \$70, \$6A  
 DB \$0A, \$01, \$01, \$6A, \$0A, \$01, \$1F,  
 \$6A, \$01, \$01  
 DB \$01, \$6A, \$0A, \$01, \$2B, \$6A, \$01,  
 \$01, \$01, \$64, \$0A  
 DB \$01, \$58, \$07, \$01, \$01, \$16, \$07,  
 \$79, \$01, \$76  
 DB \$07, \$79, \$01, \$16, \$07, \$79, \$01,  
 \$19, \$07, \$01  
 DB \$01, \$01, \$07, \$79, \$01, \$88, \$07,

E631	01880701		\$01, \$01
E635	01		
E636	01077901	DB	\$01, \$07, \$79, \$01, \$7F, \$49, \$01,
E63A	7F490101		\$01, \$01, \$49
E63E	0149		
E640	64016D49	DB	\$64, \$01, \$6D, \$49, \$64, \$01, \$55,
E644	64015549		\$49, \$64, \$01
E648	6401		
E64A	25490101	DB	\$25, \$49, \$01, \$01, \$01, \$49, \$64,
E64E	01496401		\$01, \$31, \$49
E652	3149		
E654	01010149	DB	\$01, \$01, \$01, \$49, \$64, \$01, \$82,
E658	64018204		\$04, \$01, \$01
E65C	0101		
E65E	01047C01	DB	\$01, \$04, \$7C, \$01, \$73, \$04, \$7C,
E662	73047C01		\$01, \$55, \$04
E666	5504		
E668	7C012804	DB	\$7C, \$01, \$28, \$04, \$01, \$01, \$01,
E66C	01010104		\$04, \$7C, \$01
E670	7C01		
E672	8E040101	DB	\$8E, \$04, \$01, \$01, \$01, \$04, \$7C,
E676	01047CAC		\$AC, \$01, \$91
E67A	0191		
E67C	01019791	DB	\$01, \$01, \$97, \$91, \$94, \$01, \$46,
E680	94014601		\$01, \$A3, \$01
E684	A301		
E686	97919401	DB	\$97, \$91, \$94, \$01, \$0D, \$91, \$01,
E68A	0D910101		\$01, \$97, \$91
E68E	9791		
E690	9401A991	DB	\$94, \$01, \$A9, \$91, \$A6, \$01, \$01,
E694	A6010191		\$91, \$01, \$01
E698	0101		
E69A	615B5E01	DB	\$61, \$5B, \$5E, \$01, \$61, \$5B, \$5E,
E69E	615B5E01		\$01, \$9D, \$5B
E6A2	9D5B		
E6A4	9A01615B	DB	\$9A, \$01, \$61, \$5B, \$5E, \$01, \$10,
E6A8	5E01105B		\$5B, \$01, \$01
E6AC	0101		
E6AE	615B5E01	DB	\$61, \$5B, \$5E, \$01, \$34, \$5B, \$9E,
E6B2	345B9E01		\$01, \$61, \$5B
E6B6	615B		
E6B8	5E013D37	DB	\$5E, \$01, \$3D, \$37, \$01, \$01, \$3D,
E6BC	01013D37		\$37, \$40, \$01
E6C0	4001		
E6C2	52374301	DB	\$52, \$37, \$43, \$01, \$3D, \$37, \$40,
E6C6	3D374001		\$01, \$1C, \$37
E6CA	1C37		
E6CC	01010137	DB	\$01, \$01, \$01, \$37, \$40, \$01, \$2E,
E6D0	40012E37		\$37, \$01, \$01
E6D4	0101		
E6D6	01374001	DB	\$01, \$37, \$40, \$01, \$3A, \$85, \$01,
E6DA	3A850101		\$01, \$3A, \$85
E6DE	3A85		
E6E0	4C014F85	DB	\$4C, \$01, \$4F, \$85, \$67, \$01, \$3A,
E6E4	67013A85		\$85, \$4C, \$01
E6E8	4C01		
E6EA	13850101	DB	\$13, \$85, \$01, \$01, \$01, \$85, \$4C,
E6EE	01854C01		\$01, \$8B, \$85

E6F2	8B85		
E6F4	01010185		DB \$01,\$01,\$01,\$85,\$4C,\$01
E6F8	4C01		
E6FA	12160000	MODES	DB 18,22,00,00,00,06,06,00,18,04,02
E6FE	00060600		
E702	120402		
E705	00000C0C		DB 00,00,12,12,00,20,24,00,00,00
E709	00141800		
E70D	0000		
E70F	0E0E0012		DB 14,14,00,18,16,00,00,00,22,22
E713	10000000		
E717	1616		
E719	000C1600		DB 00,12,22,00,00,06,06,06,00,18
E71D	00060606		
E721	0012		
E723	0402000C		DB 04,02,00,12,12,12,00,20,24,00
E727	0C0C0014		
E72B	1800		
E72D	00000808		DB 00,00,08,08,00,18,16,00,00,00
E731	00121000		
E735	0000		
E737	0E0E0012		DB 14,14,00,18,22,00,00,00,06,06
E73B	16000000		
E73F	0606		
E741	00120402		DB 00,18,04,02,00,12,12,12,00,20
E745	000C0C0C		
E749	0014		
E74B	18000000		DB 24,00,00,00,08,08,00,18,16,00
E74F	08080012		
E753	1000		
E755	00000E0E		DB 00,00,14,14,00,18,22,00,00,00
E759	00121600		
E75D	0000		
E75F	06060012		DB 06,06,00,18,04,02,00,26,12,12
E763	0402001A		
E767	0C0C		
E769	00141800		DB 00,20,24,00,00,00,08,08,00,18
E76D	00000808		
E771	0012		
E773	10000000		DB 16,00,00,00,14,14,28,00,22,00
E777	0E0E1C00		
E77B	1600		
E77D	00060606		DB 00,06,06,06,00,18,00,18,00,12,12
E781	00120012		
E785	000C0C		
E788	0C001418		DB 12,00,20,24,00,00,08,08,10,00
E78C	00000808		
E790	0A00		
E792	12101200		DB 18,16,18,00,00,14,00,00,04,22
E796	000E0000		
E79A	0416		
E79C	04000606		DB 04,00,06,06,06,00,18,04,18,00
E7A0	06001204		
E7A4	1200		
E7A6	0C0C0C00		DB 12,12,12,00,20,24,00,00,08,08
E7AA	14180000		
E7AE	0808		
E7B0	0A001410		DB 10,00,20,16,18,00,14,14,16,00

E7B4	12000E0E	
E7B8	1000	
E7BA	04160000	DB 04,22,00,00,06,06,06,00,18,04
E7BE	06060600	
E7C2	1204	
E7C4	12000C0C	DB 18,00,12,12,12,00,20,24,00,00
E7C8	0C001418	
E7CC	0000	
E7CE	00080800	DB 00,08,08,00,18,16,00,00,00,14
E7D2	12100000	
E7D6	000E	
E7D8	0E000416	DB 14,00,04,22,00,00,06,06,06,00
E7DC	00000606	
E7E0	0600	
E7E2	12041200	DB 18,04,18,00,12,12,12,00,20,24
E7E6	0C0C0C00	
E7EA	1418	
E7EC	00000008	DB 00,00,00,08,08,00,12,16,00,00
E7F0	08000C10	
E7F4	0000	
E7F6	000E0E00	DB 00,14,14,00
E7FA	7F	MNAMES DB TEX
E7FB	42414441	DB 'BAD', 'ADC', 'AND', 'ASL', 'BCC',
E7FF	4443414E	'BCS', 'BEQ'
E803	4441534C	
E807	42434342	
E80B	43534245	
E80F	51	
E810	42495442	DB 'BIT', 'BMI', 'BNE', 'BPL', 'BRK',
E814	4D49424E	'BVC', 'BVS'
E818	4542504C	
E81C	42524B42	
E820	56434256	
E824	53	
E825	434C4343	DB 'CLC', 'CLD', 'CLI', 'CLV', 'CMP',
E829	4C44434C	'CPX', 'CPY'
E82D	49434C56	
E831	434D5043	
E835	50584350	
E839	59	
E83A	44454344	DB 'DEC', 'DEX', 'DEY', 'EOR', 'INC',
E83E	45584445	'INX', 'INY'
E842	59454F52	
E846	494E4349	
E84A	4E58494E	
E84E	59	
E84F	4A4D504A	DB 'JMP', 'JSR', 'LDA', 'LDX', 'LDY',
E853	53524C44	'LSR', 'NOP'
E857	414C4458	
E85B	4C44594C	
E85F	53524E4F	
E863	50	
E864	4F524150	DB 'ORA', 'PHA', 'PHP', 'PLA', 'PLP',
E868	48415048	'ROL', 'ROR'
E86C	50504C41	
E870	504C5052	
E874	4F4C524F	
E878	52	

E879	52544952	DB	'RTI', 'RTS', 'SBC', 'SEC', 'SED',
E87D	54535342		'SEI', 'STA'
E881	43534543		
E885	53454453		
E889	45495354		
E88D	41		
E88E	53545853	DB	'STX', 'STY', 'TAX', 'TAY', 'TSX',
E892	54595441		'TXA', 'TXS'
E896	58544159		
E89A	54535854		
E89E	58415458		
E8A2	53		
E8A3	54594154	DB	'TYA', 'TEX'
E8A7	4558		
E8A9	FF	DB	ETX
0000			END

## DOUBLE CRYSTAL CONTROL PROGRAMS FOR THE BBC MICROCOMPUTER

INTRODUCTION

The double crystal control programs are all written in standard BBC Basic and employ no machine code, thus making them easily altered. Since the programs are designed to run in the high resolution mode (Mode 0) only a small amount of RAM is available for program use (about 10K). The control system is, therefore, segmented into a number of small programs which are individually run as required by a menu program. This makes it necessary to keep the 'system' disc permanently in one drive, with data being stored on a second drive. A considerable amount of code is, therefore, common to all of the programs, particularly the device handling routines. In order to exchange data between programs use is made of the resident integer variables A% to Z%, which keep their values all the time the machine is powered. Data from the rocking curve measuring routine is stored in a temporary file on the system disc for access from the replotting routines. In order to permanently save this data on the second drive the SAVE routine should be used.

The individual programs required to form the complete system are described below with the common sections of code described afterwards. The programs required are:

START	-	initialisation routines
MENU	-	main menu routine which executes programs below
COUNT	-	counts the photomultiplier pulses
SCAN	-	repeatedly steps an axis and counts the PM pulses
STEP	-	moves an axis
PLOT	-	steps an axis through given range recording PM counts
TILT	-	tilts a goniometer by specified angle
REPLOT	-	reads disc data and plots it on the screen
HPLOT	-	reads disc data and plots it on hardcopy device
AUTO	-	automatically optimises the sample tilt
TABLE	-	moves the XY scanning table
PEAK	-	monitors the counts and drives the axis to remain on peak
UTILIT	-	utilities package, calculates Bragg angles etc
EPSPLOT	-	reads disc data and plots it on an Epson printer
SAVE	-	makes a permanent copy of the temporary data file
HELP	-	help package, instructions on the use of each routine
CALIB	-	resets the positions of the axes etc as held in memory
FIND	-	moves an axis and counts PM pulses until peak is found

## DESCRIPTION OF PROGRAMS

### Start

This program is run by the autoboot file \$.!BOOT. The display is partitioned so that the positions of the axes, the time and date, the users name and the count rate can be continuously displayed. The time and date plus the positions of the two tilt micrometers are entered by the user. The positions of the axes are stored in the variables S%, T%, U% and V% for the two axes and goniometers and K% and L% for the position of the XY table. These values are converted to the appropriate units by the variables step(1) to step(6). The communication protocol to the minicam interface is set to 4800 baud, 8 data bits and no parity. The MENU program is loaded and run when finished.

Procedures used are PROCupdate, PROCTime and PROCTitle.

### Menu

The main system menu is displayed on the screen and the user requested to input a two letter code corresponding to each option. While the program idles, waiting for keys to be pressed, the time is updated in the display at the top of the screen using the procedure PROCTime. Once a valid two letter code is entered the corresponding program is loaded and run. This program also contains the code for altering the sample description file maintained on the system disc which is added to a data file during permanent saving, although this code is not a procedure due to the restraints of the error handling mechanism it is described in the procedures section for clarity.

Procedures used are PROCdirectory, PROCTime and PROCTitle.

### Count

The scalar module defined by the variable scalar1% is used to count the PM pulses for a given number of 100th's of a second. The counts are then displayed on the screen and in the partitioned section. This process is repeated indefinitely until a key is pressed. The user is then able to repeat this operation or return to the menu.

Procedures used are PROCTitle, PROCcommand, PROCTime and FNminicam.

### Scan

Once the user enters the required axis to be scanned its previous direction of motion is displayed according to whether the relevant bit is set in the variable E%. The angle step and counting time are then entered and the routine performs the step and count operation the required number of times. After each step the counts are displayed and the position of the axis held in memory updated and displayed in the partitioned section of the screen. The

step-count repeat operation can be stopped prematurely by pressing any key. Once finished the routine can be rerun or return to the menu.

Procedures used are PROCtitle, PROCcommand, FNmotor, PROCstep\_scan, PROCstep\_count, PROCprint, PROCprint, PROCtime and FNminicam.

### Step

Similar to SCAN but only drives an axis by a given angle after which it updates the positions held in memory.

Procedures used are PROCtitle, PROCcommand, PROCupdate, FNmotor, PROCstep\_scan, PROCtime, PROCprint and FNminicam.

### Plot

The chosen axis is repeatedly stepped and the PM pulses counted for a given number of times. The counts are displayed graphically while they are being collected with automatic scaling to display from the minimum count to the maximum count. If a new count is collected that is either greater than the previous maximum or smaller than the previous minimum the graph is erased and redrawn with a new scale. The repeated step\_count operation can be stopped early by pressing any key, the graph is the redrawn with a new x-axis. The temporary data file is emptied and then filled with the counts collected and the angular step length. Once completed the axis is driven back to the starting point. Again the routine can be repeated or the user returned to the menu.

Procedures used are PROCaxes, FNminicam, PROCplot, PROCpoint, PROCerase, PROCredraw, PROCsave, PROCtitle, PROCcommand and PROCtime.

### Replot

The filename containing the data is requested and if return is entered it is defaulted to the temporary file. If no drive number is given a default of 2 is added to the file name. The file is opened and if unsuccessful the error is trapped and the user requested for a new file name if the previously entered one does not exist or the name was too long. Data is read to determine the range of angles and counts and the user asked for which range to be plotted. Data is then read again from the disc to avoid entering it into memory and plotted on the screen. Again the routine can be repeated or the user returned to the manu.

Procedures used are PROCplot, PROCaxes, PROCpaper, PROCpspace, PROCmspace, PROCmove, PROCpoint, PROCdraw\_rel, PROCnotch, PROClabel\_x, PROClabel\_y, PROCmark, PROCplots, PROCtitle, PROCtime and PROCcommand.



Hplot

This routine is identical to the REPLOT routine but plots the graph on the hardcopy device attached to the printer port of the minicam interface. Devices catered for are the PIXY3 and HP7470A plotters. If the data is read from a permanent file the data consisting of the sample name, date, time and generator conditions is also read and added to the plot.

Procedures used are PROCplot, PROCaxes, PROCpaper, PROCpspace, PROCmspace, PROCmove, PROCpoint, PROCdraw\_rel, PROCnotch, PROClabel\_x, PROClabel\_y, PROCmark, PROCplots, PROCtitle, PROCtime, PROCminicam and PROCcommand.

Epsplot

Again this routine is identical to the REPLOT routine and plots the disc data on the screen. Once the data has been plotted on the screen the screen is dumped onto an Epson compatible printer. A standard screen dump routine is used.

Calib

Allows positions of the axes, tilt goniometers and scanning table to be altered. If return is pressed when a new position is requested the value is unaltered. If a position is altered the new value is displayed in the partitioned screen and the appropriate resident integer variable updated.

Procedure used is PROCtitle.

Find

Similar in operation to the scan routine but instead of performing a given number of repeat step-counts it continues to step-count until either a count equal to a given limit is recorded or a given maximum angular scan range is exceeded. If a count greater than the limit is encountered the count is repeated to check that it was not due to spurious noise, if it is less than the limit the scan is recommenced. If the maximum scan range is reached and a scan in both directions from the start position was requested the axis is driven back to the start and step-counted in the opposite direction. The counts measured and the position of the axis are updated after each step-count. The routine can again be stopped before either of the stop conditions are encountered by pressing any key.

Procedures used are FNmotor, PROCstep\_scan, PROCstep\_count, PROCtitle, PROCcommand, PROCprint, FNminicam, PROCupdate and PROCtime.

Tilt

Once a goniometer is chosen the previous direction is

displayed according to the state of the relevant bit in the variable G%. The goniometer is tilted by driving the micrometer a given number of millimetres. If the given number would take the micrometer past either of its limits it is driven only to this limit and the user warned.

Procedures used are FNmotor, PROCstep\_scan, PROctitle, PROCcommand, FNminicam, PROCprint and PROCtime.

### Save

This routine reads the data stored in the temporary file and stores it in the given file. If temporary file cannot be opened the error is trapped and the user returned to the main menu. The sample description file is also read and the data added to the given file allowing a record of the x-ray, generator and sample conditions to be kept. The current date and time are also added to the file. If the file cannot be opened the error is trapped and the user prompted for another name. However, an existing file will be overwritten as the filing system does not detect this as an error.

Procedures used are PROctitle and PROCcommand.

### Peak

This routine will keep the axis positioned either on top or on the flanks of a peak and is suitable for recording topographs over a long time period. The axis should be positioned as required before the routine is used. The count rate is measured at this position and the standard error calculated. The count rate is then measured every 5 seconds and if it lies outside the error bar the axis is moved until the count rate lies within the error bar. If the count rate drops to below the background rate the routine stops and reports an error. Axis positions are updated as required on the screen so that the drift can be measured.

Procedures used are FNmotor, PROctitle, PROCcommand, FNminicam, PROCprint, PROCflank, PROctop, PROCincrease, PROCdecrease, PROCdelay, PROCintensity.

### Auto

This routine only drives the second axis. The axis is scanned with steps and counting time as specified by the user until the peak is found. The criterion for finding a peak is that the count should be twice the background count. Once the peak is found the axis is stepped until background is again reached. The peak is then scanned to find the maximum count. The goniometer is then tilted by the user supplied number of millimetres and the process of finding the peak maximum repeated. This process is repeated so that the peak height is measured with the tilt on either side of the starting position. The optimum setting is determined and the axis and goniometer moved to this position. The whole process is then repeated with the tilt step length halved. During the process of finding the peak the axis is scanned

in one direction up to a maximum range specified by the user and then scanned in the other direction. If no peak can be found the routine stops and informs the user.

Procedures used are FNmotor, PROctitle, PROCcommand, FNminicam, PROCprint, PROctilt\_opt, PROctilt, PROCmove, PROCfind, PROCupdate and PROCtime.

### Help

The help menu is displayed and the user requested for a two letter code corresponding to each of the choices. If a valid choice is made the data file on the system disc containing the relevant help text is opened and the data displayed on the screen as it is read. Pressing any key once this is done returns the user to the help menu. The option QUIT returns the user to the main system menu.

Procedures used are PROctitle, PROCcommand and PROCdisplay.

### Utilit

The utilities menu is displayed and a two letter code requested. If a valid choice is entered the relevant program is loaded from disc and run. This routine is, therefore, similar in operation to MENU but provides access to some of the less often used routines. Routines available at present are:

- Bragg - calculates the Bragg angle for a given reflection, wavelength and lattice parameter.
- Refl - calculates the single crystal reflectivity curve for a given material and structure factors assuming the crystal to be infinitely thick.
- Spdata - produces a text file of rocking curve data as stored in another disc file. Is useful for data transfer to another computer.

### Table

The XY scanning table is moved to the user requested position. The distance required to drive the micrometers is calculated by subtracting the requested position from the present position as held in memory. It is therefore important that the position in memory is correct. The position is maintained in millimetres in the partitioned screen.

Procedures used are PROCupdate, PROctitle, PROCcommand, PROCtime, FNminicam and PROCprint.

## COMMON PROCEDURES

### PROCdirectory

The drive number is requested and if it lies between 0 and 3

the disc operating system command \*CAT <Drive number> is called using the OSCLI (Operating System Command Line Interpreter) vector at &FFF7. Pressing any key exits the procedure.

PROCupdate no parameters

The screen window corresponding to the partitioned region at the top of the screen is set using the VDU 28 command and inverse video selected. The number output format is set to 10 figures and 5 decimal places with the @% variable. The resident integer variables corresponding to the positions of the axes, goniometers and XY table are multiplied by their scaling factors held in step(1 .. 6) and printed in the relevant positions.

PROctime no parameters

The number of seconds, minutes and hours are calculated from the TIME variable and printed in standard format in the partitioned region of the screen. Leading zeros are used if the values are less than 10. Note that  $TIME = ((hours*60 + minutes)*60 + seconds)*100$ .

PROctitle (xcoord, ycoord, string)

Sets current screen to the partitioned region and selects inverse video then prints the string at the position xcoord, ycoord. Xcoord and ycoord are in text units. Screen is reset to main area minus top partition and bottom line.

PROCcommand (string)

Sets current screen to the bottom line only of the display. Selects inverse video and clears the screen. String is then printed centred on this line. Screen is then reset to main area minus the top partition and bottom line.

FNminicam (string, address, time, number) returns integer

Calls the procedure PROctime to update the time display. Sets print output to the RS423 serial port and prints the following:

string;address;time;number;carriage\_return

Print output is then set to dummy, ie no output, and input is selected as the serial port. One string is then input and the input is selected as the keyboard. The value of the string is then returned.

FNmotor (string) returns one integer

If the string is "I" the relevant bit in the variable E% is set (bit 0 is axis 1 and bit 1 is axis 2) otherwise the bit is cleared. According to which axis is selected (held in the variable M%) a stepper motor number is selected from the variables held in AX%(1..4). Allowance is made in the

selection for the fact that driving the motor on both axes in the same direction drives the axes in opposite senses of theta. The variable P% is set to the number of motor steps (MO%) with the sign according to whether increasing or decreasing theta. P% can then be used to update the position counters S%,T%,U% and V%.

PROCstep\_scan no parameters

FNmotor is called to get the address of the stepper motor. The position of the first count value to be printed is set in the variables X% and Y%. PROCcommand is called to display the 'Press any key to stop' message. A tight loop is then executed in which PROCstep\_count is called to step the axis and count the PM pulses and the count returned printed at the position X%,Y% on the main screen. X% and Y% are increased to the next position, if the bottom of the screen is reached two linefeeds are printed and Y% kept at this line number. The number of step-counts is counted and the loop stops if this count equals the number selected by the user or if a key has been pressed. The procedure then terminates.

PROCstep\_count (address, number, time)

The minicam controlled stepper motor with address <address> is moved <number> of steps with speed given by speed%. The position of the axis is then updated and displayed on the screen by calling the procedure PROCprint. The minicam scalar is then used to count for <time> 100th's of a second and the count returned displayed on the screen by calling the procedure PROCTitle. The variable R% is returned containing the count.

PROCprint (xcoord, ycoord, number)

Similar in operation to PROCTitle but the value of <number> number is printed at the position xcoord, ycoord in the partitioned screen.

PROCaxes no parameters

Routine to draw axes on the currently selected output device. Since this routine is independent of the output device being used it can be used for either the screen or hardcopy devices. The x and y ranges are determined from the maximum and minimum coordinates of the plotter space currently being used. Once the range is calculated the tick spacing is determined by the procedure PROCmark. The axes are then drawn using the procedures PROCdraw\_re1 and PROCnotch which respectively draw a line relative to the present cursor position and draw a tick. The axes are then labelled using the procedures PROClabell\_x and PROClabell\_y.

PROCpspace (xmin, xmax, ymin, ymax)

This routine sets the scaling factors required to produce output on the plotter device. The plotting space is defined

assuming the total area runs from 0,0 to 1,1. The users coordinates should then be mapped onto this area by calling PROCmspace. The variables xscale% and yscale% are the actual ranges of numbers possible for the graphic device.

PROCmspace (xmin, xmax, ymin, ymax)

This routine scales the plotter space being used, as defined by calling PROCpspace, to the user units. Consequent calls to draw lines etc can then be called with variables in the user units - the scaling factors produced by this procedure are then used to convert the user units into the device units.

PROCmove (xcoord, ycoord)

Routine to move the cursor or pen to the coordinates xcoord, ycoord. Xcoord and ycoord are in user units and are converted to the device coordinates using the scaling factors determined by a previous call to PROCpspace and PROCmspace. This routine is device dependent, the particular device command for moving the cursor/pen is used.

PROCpoint (xcoord, ycoord)

PROCmove is called to move the cursor/pen to the position xcoord, ycoord and a dot is then made. This routine is device dependent, the command to produce a dot depends on the device.

PROCdraw\_rel (xinc, yinc)

This routine calls the device's relative drawing command after scaling the variables xinc and yinc.

PROCnotch (switch)

If switch is 1 a tick in the y direction is drawn and if switch is 2 a tick in the x direction is drawn. This routine is device dependent, the device's relative drawing command is used.

PROClabel\_x (xcoord)

The cursor/pen is moved to the xcoord position along the x axis and the value of xcoord is written below the position. The device's printing commands are used so it is not device independent.

PROClabel\_y (ycoord)

Similar to the above routine but writes the value of ycoord to the left of the position.

PROCmark (range)

According to the magnitude of range a suitable value of tick spacing is chosen and returned in the variable SX (which is

in user units). Logarithms to the base ten are used to convert range into a variable in the range  $\geq 1$  and  $< 10$ .

PROCplotcs (xcoord, ycoord, string)

PROCmove is called to move the cursor/pen to the position xcoord, ycoord and the string is then printed using the device's printing command. It is, therefore, device dependent.

PROCdraw (xcoord, ycoord)

Draws a line from the present position to the position xcoord, ycoord after scaling to the device units. Calls the device's absolute drawing routine so it is device dependent.

PROCpen (pen)

Selects the plotter pen by calling the device's pen select command for choosing pen number <pen>.

PROCminicam (string)

This is very similar to the function FNminicam but only the string is printed followed by a carriage return. It is used by the hardcopy plotting routines to pass the string to the minicam interface which then passes the string to the device via the serial printer port. This enables the plotters to be used without unplugging the minicam from the BBC and also converts to the plotter's baud rate and word format.

PROCflank no parameters

Routine that adjusts the position of an axis to keep on the flank of a peak. The count rate at the starting position is determined by calling FNintensity which counts the PM pulses for 5 seconds. The standard error is then determined and if the count rate strays more than three standard errors from the start position PROCincrease or PROCdecrease are called to move the motor. If the count rate is in the required range a five second delay is used to prevent needless hunting.

PROCTop no parameters

Similar to PROCflank but adjusts the axis so as to remain on the top of a peak. A slightly tighter adjustment loop is used as the direction required to move to refind the peak is not known, for PROCflank it is known which direction will increase or decrease the count rate depending on which side of the peak is being used.

PROCincrease no parameters

Moves the stepper motor determined by calling FNmotor a given number of steps with speed given by speed%. Display and resident variables are updated as required.

PROCdecrease no parameters

Similar to PROCincrease but moves the motor in the opposite direction.

PROCfind no parameters

The present position of the second axis is saved as now%. The stepper motor address is determined for increasing theta by calling FNmotor and the command 'looking for peak' displayed on the bottom line of the display. PROCstep\_count is then called repeatedly until a count greater than twice the background is found or the maximum scan range reached. If the maximum scan range is reached the motor is driven back to the start position and step scanned in the opposite direction. If a peak is not found the variable fault is set to true and the routine exited. If a peak is found stepping is continued in the decreasing theta direction until background is found again. The peak is then scanned in the increasing theta direction until a maximum is found. The maximum count and the axis position of the maximum are returned in the variables maximum% and maxpos% respectively.

PROCsave no parameters

The temporary data file on the system disc (D.RTEMP) is deleted by calling the disc operating system's delete file function. This is called by setting up a file descriptor block in memory containing the file name. X% and Y% are then set to the low and high bytes of a memory address that contains the address of the file descriptor block. A% is set to 6 and the disc operating system called via the vector OSFILE at &FFDD. The temporary data file is then opened and the data consisting of the number of counts, the angular step between the counts, and the counts is then stored in the file. This process prevents the 'Can't extend' error which occurs if an existing file is opened for output and more data stored in it than when it was first created.

Sample descriptor file updating

This routine updates the sample descriptor file maintained on the system disc. It is not a procedure since it needs to trap the 'file doesn't exist' error when it is first run and no file exists. The file is opened and the contents displayed on the screen so that they can be altered. Once the user has finished updating the descriptions entering return to the command prompt writes the data back to the disc file. Data that is maintained consists of seven strings; the experimental site, the sample name, the generator voltage, the generator current, the first crystal, the wavelength and the reflection being used.



## DATA FORMAT USED FOR THE STORAGE OF ROCKING CURVES

Rocking curve data is stored in disc files in the following format:

1. Number of counts in the file (integer).
2. Angular step between each count in arc seconds (real).
3. The actual counts stored sequentially as integers.
4. The date (string).
5. The time (integer).
6. Experimental site name (string).
7. Sample name (string).
8. Generator voltage (string).
9. Generator current (string).
10. First crystal (string).
11. Wavelength (string).
12. Reflection (string).

Since BBC Basic stores numbers and strings in internal format these files cannot be typed or transferred to another computer without first converting to a text file. This operation is easily performed using the SPOOL DATA option available in the utilities package.

```

10 REM -----
20 REM ----- THIS IS THE STARTING PROGRAM -----
30 REM -----
40 :
50 MODE0
60 DIM step(6): step(1)=0.1776: step(2)=0.121: step(3)=1.0/(96.0*50):
  step(4)=1.0/(96.0*50)
70 step(5)=1.0/96.0: step(6)=1.0/96.0
80 PROCinit
90 PRINT'' This is the new double crystal control program - welcome''
100 INPUT'' Please enter your name "name$
110 PROCtitle(12,1,name$)
120 PRINTTAB(0,7); : INPUT" and your group "group$
130 PROCtitle(12,2,group$)
140 PRINTTAB(0,9); : INPUT" and the date (dd/mm/yy) "date$
150 PROCtitle(12,3,date$)
160 PRINTTAB(0,11); : INPUT" and the time ho,mi,se "ho%,mi%,se%
170 TIME=((ho%*60+mi%)*60+se%)*100
180 PROCtime
190 PRINTTAB(0,13); : INPUT" Enter the micrometer reading for the 1st
  goniometer "a
200 U%=a/step(3)
210 PROCupdate
220 PRINTTAB(0,15); : INPUT" and the reading for the 2nd goniometer "a
230 V%=a/step(4)
240 PROCupdate
250 PRINTTAB(0,17); : INPUT" Enter the generator H.T. (kV) "kV
260 PROCtitle(64,4,STR$(kV))
270 PRINTTAB(0,19); : INPUT" and the generator current (mA) "mA
280 PROCtitle(64,5,STR$(mA))
290 CHAIN"P.MENU"
300 :
310 REM init procedure - produces table of axes etc
320 :
330 DEFPROCinit
340 VDU28,0,6,79,0: REM text window at top of screen
350 COLOUR0: COLOUR129: CLS
360 PRINT TAB(3,1); "USER"; TAB(3,2); "GROUP"; TAB(3,3); "DATE";
  TAB(3,4); "TIME"; TAB(3,5); "OPTION";
370 PRINT TAB(25,1); "Axis 1"; TAB(25,2); "Axis 2"; TAB(25,3); "Gon 1";
  TAB(25,4); "Gon 2"; TAB(25,5); "Slit 1"
380 PRINT TAB(44,1)"Scan-Table (mm)"; TAB(44,2)"X"; TAB(44,3)"Y";
390 PRINT TAB(61,1); "Scint."; TAB(61,2); "Ionis."; TAB(61,4); "kV";
  TAB(61,5); "mA";
400 PROCupdate
410 VDU28,0,31,79,7: COLOUR1: COLOUR128: CLS
420 *FX8,6
430 *FX7,6
440 ENDPROC
450 :
460 DEFPROCupdate
470 VDU28,0,6,79,0: COLOUR0: COLOUR129
480 @%=&2050A
490 PRINTTAB(34,1); S%*step(1)/3600; TAB(34,2); T%*step(2)/3600;
  TAB(34,3); U%*step(3); TAB(34,4); V%*step(4)
500 PRINT TAB(47,2); K%*step(5); TAB(47,3); L%*step(6);
510 @%=10
520 VDU28,0,31,79,7: COLOUR1: COLOUR128
530 ENDPROC
540 :

```

```

550 DEFPROCtitle(X%,Y%,string$)
560 VDU28,0,6,79,0: COLOUR0: COLOUR129: PRINTTAB(X%,Y%); string$;
570 VDU28,0,31,79,7: COLOUR1: COLOUR128
580 ENDPROC
590 :
600 DEFPROCtime
610 se%=(TIME DIV 100) MOD 60
620 mi%=(TIME DIV 6000)MOD 60
630 ho%=(TIME DIV 360000)MOD 24
640 VDU28,0,6,79,0: COLOUR0: COLOUR129
650 PRINTTAB(12,4); : IF ho%<10 PRINT"0"; ho%; ELSE PRINT; ho%;
660 IF mi%<10 PRINT":0"; mi%; ELSE PRINT":"; mi%; -
670 IF se%<10 PRINT":0"; se%; ELSE PRINT":"; se%;
680 VDU28,0,31,79,7: COLOUR1: COLOUR128
690 ENDPROC

```

```

10 REM -----
20 REM ----- This program prints the menu, asks for input -----
30 REM ----- then chains the relevant program. -----
40 REM -----
50 DIM C 20
60 PROCtitle(12,5,"MENU")
70 CLS
80 X%=20
90 PRINT
100 PRINTTAB(X%); "Calibrate axis positions.....CA"
110 PRINTTAB(X%); "Count.....CO"
120 PRINTTAB(X%); "Scan axis and count.....SC"
130 PRINTTAB(X%); "Step axis without count.....SS"
140 PRINTTAB(X%); "Tilt goniometer.....TI"
150 PRINTTAB(X%); "Find peak.....FI"
160 PRINTTAB(X%); "Plot rocking curve and collect data..PL"
170 PRINTTAB(X%); "Replot data from disc.....RP"
180 PRINTTAB(X%); "Epson printer plot of disc data.....EP"
190 PRINTTAB(X%); "Automatic tilt optimise.....AU"
200 PRINTTAB(X%); "Peak hold.....PK"
210 PRINTTAB(X%); "Move scanning table.....MT"
220 PRINTTAB(X%); "Disc directory of data.....DI"
230 PRINTTAB(X%); "Save temporary data file.....SA"
240 PRINTTAB(X%); "Update your data header file.....UP"
250 PRINTTAB(X%); "Run the utilities package.....UT"
260 PRINTTAB(X%); "Help.....HE"
270 PRINT
280 PRINTTAB(0,20); "
290 COLOUR0: COLOUR129: PRINTTAB(0,20); "Enter command >> ";
300 COLOUR1: COLOUR128
310 choice$=""
320 REPEAT
330 AS=INKEY$(50)
340 PROCtime
350 IF AS<>" " choice$=choice$+AS: PRINTTAB(18,20); choice$;
355 IF ASC(AS)=127 AND LEN(choice$)=1 choice$="" ELSE IF ASC(AS)=127
choice$=LEFT$(choice$,LEN(choice$)-2)
360 UNTIL LEN(choice$)=3
370 choice$=LEFT$(choice$,2)
380 IF choice$="CA" CHAIN"P.CALIB"
390 IF choice$="CO" CHAIN"P.COUNT"
400 IF choice$="SC" CHAIN"P.SCAN"
410 IF choice$="SS" CHAIN"P.STEP"

```

```

420 IF choice$="TI" CHAIN"P.TILT"
430 IF choice$="FI" CHAIN"P.FIND"
440 IF choice$="PL" CHAIN"P.PLOT"
450 IF choice$="RP" CHAIN"P.REPLOT"
460 IF choice$="MT" CHAIN"P.TABLE"
470 IF choice$="HP" CHAIN"P.HPLOT"
480 IF choice$="AU" CHAIN"P.AUTO"
490 IF choice$="PK" CHAIN"P.PEAK"
500 IF choice$="EP" CHAIN"P.EPSPLOT"
510 IF choice$="DI" PROCdirectory: GOTO10
520 IF choice$="UP" GOTO780
530 IF choice$="SA" CHAIN"P.SAVE"
540 IF choice$="UT" CHAIN"P.UTILIT"
550 IF choice$="HE" CHAIN"P.HELP"
560 VDU7: GOTO280
570 :
580 DEFPROCtitle(X%,Y%,string$)
590 VDU28,0,6,79,0: COLOUR0: COLOUR129: PRINTTAB(X%,Y%); string$;
600 FOR I%=1TO(10-LEN(string$)): VDU32: NEXT
610 VDU28,0,31,79,7: COLOUR1: COLOUR128
620 ENDPROC
630 :
640 DEFPROCdirectory
650 PROCtitle(12,5,"DIRECT.")
660 CLS
670 INPUT"" Which drive's directory do you require "drive%
680 PRINT""
690 IF drive%<0 AND drive%>3 CLS: PRINT"" Illegal drive number - try
again": GOTO670
700 CLS
710 A$="CAT"+STR$(drive%): $C=A$: X%=C MOD 256: Y%=C DIV 256: CALL &FFF7
720 VDU28,0,31,79,31: COLOUR0: COLOUR129: CLS: A$="Press any key for
menu"
730 PRINTTAB(INT(40-LEN(A$)/2)); A$;
740 VDU28,0,31,79,7: COLOUR1: COLOUR128
750 A%=GET
760 ENDPROC
770 :
780 PROCtitle(12,5,"UPDATE")
790 CLS
800 PRINT"" Reading your header file from disc"
810 ON ERROR GOTO 1220
820 X%=OPENIN("D.HEADER")
830 INPUT#X%,place$
840 INPUT#X%,sname$
850 INPUT#X%,volt$
860 INPUT#X%,current$
870 INPUT#X%,first_crystal$
880 INPUT#X%,wave$
890 INPUT#X%,refl$
900 CLOSE#X%
910 CLS
920 PRINTTAB(2,2); " Your current header file contains the following
information"
930 PRINTTAB(5,4)"1. Experiment running at
"; TAB(30,4); place$
940 PRINTTAB(5,6); "2. Sample name "; TAB(20,6);
sname$
950 PRINTTAB(5,8); "3. Generator voltage "; TAB(26,8); volt$
960 PRINTTAB(5,10); "4. Generator current "; TAB(26,10);

```

```

current$
970 PRINTTAB(5,12); "5. First crystal                                "; TAB(22,12);
first_crystal$
980 PRINTTAB(5,14); "6. Wavelength                                "; TAB(19,14);
wave$
990 PRINTTAB(5,16); "7.. Reflection being used                                ";
TAB(31,16); refl$
1000 PRINTTAB(1,20); "
1010 COLOUR0: COLOUR129: PRINTTAB(1,18); " Enter choice to update or <CR>
for menu "
1020 COLOUR1: COLOUR128: choice=GET
1030 IF choice=13 GOTO 1120
1040 IF choice=&31 INPUT' " Enter experimental site "place$: GOTO920
1050 IF choice=&32 INPUT' " Enter sample name "sname$: GOTO920
1060 IF choice=&33 INPUT' " Enter generator voltage "volt$: GOTO920
1070 IF choice=&34 INPUT' " Enter generator current "current$: GOTO920
1080 IF choice=&35 INPUT' " Enter first crystal "first_crystal$: GOTO920
1090 IF choice=&36 INPUT' " Enter wavelength "wave$: GOTO920
1100 IF choice=&37 INPUT' " Enter reflection being used "refl$: GOTO920
1110 VDU7: GOTO920
1120 X%=OPENOUT("D.HEADER")
1130 PRINT#X%,place$
1140 PRINT#X%,sname$
1150 PRINT#X%,volt$
1160 PRINT#X%,current$
1170 PRINT#X%,first_crystal$
1180 PRINT#X%,wave$
1190 PRINT#X%,refl$
1200 CLOSE#X%
1210 GOTO1250
1220 IF ERR=222 CLS: PRINTTAB(5,2); "You have no header file as yet"
1230 place$="": sname$="": volt$="": current$="": first_crystal$="":
wave$="": refl$=""
1240 IF ERR=222 GOTO 930 ELSE REPORT: END
1250 GOTO10
1260 :
1270 DEFPROCtime
1280 se%=(TIME DIV 100)MOD 60: mi%=(TIME DIV 6000)MOD 60: ho%=(TIME DIV
360000)MOD 24
1290 VDU28,0,6,79,0: COLOUR0: COLOUR129: PRINTTAB(12,4);
1300 IF ho%<10 PRINT"0"; ho%; ELSE PRINT; ho%;
1310 IF mi%<10 PRINT":0"; mi%; ELSE PRINT":": mi%;
1320 IF se%<10 PRINT":0"; se%; ELSE PRINT":": se%;
1330 VDU28,0,30,79,7: COLOUR1: COLOUR128
1340 ENDPROC

10 REM -----
20 REM ----- COUNTING ROUTINE -----
30 REM -----
40 :
50 scaler1%=56: scaler2%=55
60 PROCtitle(12,5,"COUNT")
70 CLS: INPUT' " Enter counting time, in 100th's secs "TT%
80 PROCcommand("Press any key to stop")
90 X%=5: Y%=5
100 REPEAT
110 R%=FNminicam("CO1",scaler1%,TT%,0) + 256*256*FNminicam("RD2",
scaler2%,0,0)
120 R$=STR$(R%): PROCtitle(68,1,R$)

```

```

130 PRINT TAB(X%,Y%); R%;
140 X%=X%+15: IF X%=80 X%=5: Y%=Y%+1
150 IF (Y%=23 AND X%=5) VDU10,10: Y%=22
160 UNTIL INKEY(0)<>-1
170 PROCcommand("Press <CR> for repeat, any other key for menu")
180 A=GET
190 IF A=13 PROCcommand(" "): GOTO 70
200 CHAIN"P.MENU"
210 :
220 DEFPROCtitle(X%,Y%,string$)
230 VDU28,0,6,79,0: COLOUR0: COLOUR129: PRINTTAB(X%,Y%); " ";
240 PRINTTAB(X%,Y%); string$;
250 VDU28,0,30,79,7
260 COLOUR1: COLOUR128
270 ENDPROC
280 :
290 DEFPROCcommand(string$)
300 VDU28,0,31,79,31: COLOUR0: COLOUR129: CLS
310 PRINTTAB(INT(40-LEN(string$)/2)); string$;
320 VDU28,0,30,79,7: COLOUR1: COLOUR128
330 ENDPROC
340 :
350 DEFFNminicam(usr$,AD%,NN%,TT%)
360 PROCtime
370 *FX3,7
380 PRINTusr$; ", "; AD%; ", "; NN%; ", "; TT%; CHR$(13);
390 *FX3,6
400 *FX2,1
410 INPUT""return$
420 *FX2,2
430 *FX3,0
440 =VAL(return$)
450 :
460 DEFPROCtime
470 se%=(TIME DIV 100)MOD 60: mi%=(TIME DIV 6000)MOD 60: ho%=(TIME DIV
360000)MOD 24
480 VDU28,0,6,79,0: COLOUR0: COLOUR129: PRINTTAB(12,4);
490 IF ho%<10 PRINT"0"; ho%; ELSE PRINT; ho%;
500 IF mi%<10 PRINT":0"; mi%; ELSE PRINT": "; mi%;
510 IF se%<10 PRINT":0"; se%; ELSE PRINT": "; se%;
520 VDU28,0,30,79,7: COLOUR1: COLOUR128
530 ENDPROC

```

```

10 REM -----
20 REM ----- STEP SCAN ROUTINE; SCANS AXIS AND COUNTS -----
30 REM -----
40 DIM AX%(8)
50 AX%(1)=34: AX%(2)=35: AX%(3)=36: AX%(4)=37
60 AX%(5)=33: AX%(6)=32: AX%(7)=33: AX%(8)=32
70 scaler1%=56: scaler2%=55: speed%=20
80 DIM step(2)
90 step(1)=0.1776: step(2)=0.121
100 PROCtitle(12,5,"SCAN-COUNT")
110 CLS
120 INPUT"" Which axis to scan (1 or 2) "M%"
130 IF M%<>1 AND M%<>2 THEN 110
140 F%=(E%ANDM%)
150 IF F% increasing=TRUE ELSE increasing=FALSE
160 PRINT"" Previous motion was ";

```

```

170 IF increasing PRINT"increasing"; ELSE PRINT "decreasing";
180 PRINT" theta"
190 INPUT" Counting time, in 100th's secs "TT%
200 INPUT" Step length per cycle (secs) "step_length
210 MO%=INT(step_length/step(M%))
220 INPUT" Number of cycles "NU%
230 INPUT" Increasing or decreasing theta (I/D) "inc$
240 PROCstep_scan
250 PROCcommand("Press <CR> for repeat, any other key for menu")
260 A=GET: IF A=13 PROCcommand(" "): GOTO 100
270 CHAIN"P.MENU"
280 :
290 DEFFNmotor(dir$)
300 IFdir$="I" E%=(E% OR M%) ELSE E%=(E% AND(&FF EOR M%))
310 IF dir$="I" THEN F%=1 ELSE F%=0
320 IF M%=1 THEN stepper%=AX%(M%+1-F%)
330 IF M%=2 THEN stepper%=AX%(M%+1+F%)
340 I%=0: IF dir$="I" P%=MO% ELSE P%=-MO%
350 =stepper%
360 :
370 DEFPROCstep_scan
380 IF NU%=0 ENDPROC
390 stepper%=FNmotor(inc$)
400 X%=5: Y%=15
410 PROCcommand("Press any key to stop")
420 REPEAT
430 I%=I%+1
440 PROCstep_count(stepper%,MO%,TT%)
450 PRINTTAB(X%,Y%); R%;
460 X%=X%+15: IFX%=80 X%=5: Y%=Y%+1
470 IF (Y%=23 AND X%=5) VDU10,10: Y%=22
480 Z%=INKEY(0)
490 UNTIL I%=NU% OR Z%<>-1
500 ENDPROC
510 :
520 DEFPROCtitle(X%,Y%,string$)
530 VDU28,0,6,79,0: COLOUR0: COLOUR129: PRINTTAB(X%,Y%); " ";
540 PRINTTAB(X%,Y%); string$;
550 VDU28,0,30,79,7
560 COLOUR1: COLOUR128
570 ENDPROC
580 :
590 DEFPROCcommand(string$)
600 VDU28,0,31,79,31: COLOUR0: COLOUR129: CLS
610 PRINTTAB(INT(40-LEN(string$)/2)); string$;
620 VDU28,0,30,79,7: COLOUR1: COLOUR128
630 ENDPROC
640 :
650 DEFPROCstep_count(stepper%,MO%,TT%)
660 A%=FNminicam("ST1",stepper%,MO%,speed%)
670 @%=&2050A
680 IF M%=1 S%=S%+P%: R=S%*step(1)/3600: PROCprint(34,1,R)
690 IF M%=2 T%=T%+P%: R=T%*step(2)/3600: PROCprint(34,2,R)
700 @%=10
710 R%=FNminicam("CO1",scaler1%,TT%,0)+256*256*FNminicam("RD2",
scaler2%,0,0)
720 R$=STR$(R%): PROCTitle(68,1,R$)
730 ENDPROC
740 :
750 DEFFNminicam(usr$,AD%,NN%,TT%)

```

```

760 PROCtime
770 *FX2,2
780 *FX3,7
790 PRINTusr$; ",,"; AD%; ",,"; NN%; ",,"; TT%; CHR$(13);
800 *FX3,6
810 *FX2,1
820 INPUT"reply$
830 *FX2,2
840 *FX3,0
850 =VAL(reply$)
860 :
870 DEFPROCprint(X%,Y%,R)
880 VDU28,0,6,79,0: COLOUR0: COLOUR129: PRINTTAB(X%,Y%); "
890 PRINTTAB(X%,Y%); R;
900 VDU28,0,30,79,7
910 COLOUR1: COLOUR128
920 ENDPROC
930 :
940 DEFPROCtime
950 se%=(TIME DIV 100)MOD 60: mi%=(TIME DIV 6000)MOD 60: ho%=(TIME DIV
360000)MOD 24
960 VDU28,0,6,79,0: COLOUR0: COLOUR129: PRINTTAB(12,4);
970 IF ho%<10 PRINT"0"; ho%; ELSE PRINT; ho%;
980 IF mi%<10 PRINT":0"; mi%; ELSE PRINT":"; mi%;
990 IF se%<10 PRINT":0"; se%; ELSE PRINT":"; se%;
1000 VDU28,0,30,79,7: COLOUR1: COLOUR128
1010 ENDPROC

```

```

10 REM -----
20 REM ----- STEP ROUTINE; SCANS AXIS ONLY -----
30 REM -----
40 DIM AX%(8)
50 AX%(1)=34: AX%(2)=35: AX%(3)=36: AX%(4)=37
60 AX%(5)=33: AX%(6)=32: AX%(7)=33: AX%(8)=32
70 scaler1%=56: scaler2%=55: speed%=20
80 DIM step(2)
90 step(1)=0.1776: step(2)=0.121
100 PROCtitle(12,5,"SCAN-AXIS")
110 CLS
120 INPUT"" Which axis to scan (1 or 2) "M%"
130 IF M%<>1 AND M%<>2 THEN 110
140 F%=(E%ANDM%)
150 IF F% increasing=TRUE ELSE increasing=FALSE
160 PRINT"" Previous motion was ";
170 IF increasing PRINT"increasing"; ELSE PRINT "decreasing";
180 PRINT" theta"
190 INPUT"" Scan length required (secs) "step_length
200 MO%=INT(step_length/step(M%))
210 INPUT"" Increasing or decreasing theta (I/D) "inc$
220 PRINT"" Driving axis number "; M%
230 PROCstep_scan
240 VDU7
250 PROCcommand("Press <CR> for repeat, any other key for menu")
260 A=GET: IF A=13 PROCcommand(" "): GOTO 100
270 CHAIN"P.MENU"
280 :
290 DEFFNmotor(dir$)
300 IFdir$="I" E%=(E% OR M%) ELSE E%=(E% AND(&FF EOR M%))
310 IF dir$="I" THEN F%=1 ELSE F%=0

```



```

320 IF M%=1 THEN stepper%=AX%(M%+1-F%)
330 IF M%=2 THEN stepper%=AX%(M%+1+F%)
340 I%=0: IF dir$="I" P%=MO% ELSE P%=-MO%
350 =stepper%
360 :
370 DEFPROCstep_scan
380 stepper%=FNmotor(inc$)
390 IF MO%>&7FFF A=FNminicam("ST1",stepper%,&7FFF,speed%): MO%=MO%-&7FFF:
GOTO390
400 PROCupdate
410 A=FNminicam("ST1",stepper%,MO%,speed%)
420 PROCupdate
430 ENDPROC
440 :
450 DEFPROCtitle(X%,Y%,string$)
460 VDU28,0,6,79,0: COLOUR0: COLOUR129: PRINTTAB(X%,Y%); " ";
470 PRINTTAB(X%,Y%); string$;
480 VDU28,0,30,79,7
490 COLOUR1: COLOUR128
500 ENDPROC
510 :
520 DEFPROCcommand(string$)
530 VDU28,0,31,79,31: COLOUR0: COLOUR129: CLS
540 PRINTTAB(INT(40-LEN(string$)/2)); string$;
550 VDU28,0,30,79,7: COLOUR1: COLOUR128
560 ENDPROC
570 :
580 DEFPROCupdate
590 @%=&2050A
600 IF M%=1 S%=S%+P%: R=S%*step(1)/3600: PROCprint(34,1,R)
610 IF M%=2 T%=T%+P%: R=T%*step(2)/3600: PROCprint(34,2,R)
620 @%=10
630 ENDPROC
640 :
650 DEFFNminicam(usr$,AD%,NN%,TT%)
660 PROCtime
670 *FX2,2
680 *FX3,7
690 PRINTusr$; ", "; AD%; ", "; NN%; ", "; TT%; CHR$(13);
700 *FX3,6
710 *FX2,1
720 INPUT""reply$
730 *FX2,2
740 *FX3,0
750 =VAL(reply$)
760 :
770 DEFPROCprint(X%,Y%,R)
780 VDU28,0,6,79,0: COLOUR0: COLOUR129: PRINTTAB(X%,Y%); " "
790 PRINTTAB(X%,Y%); R;
800 VDU28,0,30,79,7
810 COLOUR1: COLOUR128
820 ENDPROC
830 :
840 DEFPROCtime
850 se%=(TIME DIV 100)MOD 60: mi%=(TIME DIV 6000)MOD 60: ho%=(TIME DIV
360000)MOD 24
860 VDU28,0,6,79,0: COLOUR0: COLOUR129: PRINTTAB(12,4);
870 IF ho%<10 PRINT"0"; ho%; ELSE PRINT; ho%;
880 IF mi%<10 PRINT":0"; mi%; ELSE PRINT": "; mi%;
890 IF se%<10 PRINT":0"; se%; ELSE PRINT": "; se%;

```

```
900 VDU28,0,30,79,7: COLOUR1: COLOUR128
910 ENDPROC
```

```
1 REM -----
2 REM ---- PLOT; COLLECTS DATA AND DISPLAYS IN REAL TIME ----
3 REM -----
10 DIM AX%(4),step(2),CO%(400),C% 20: scaler1%=56: scaler2%=55:
    speed%=50
20 AX%(1)=34: AX%(2)=35: AX%(3)=36: AX%(4)=37
30 step(1)=0.1776: step(2)=0.121
40 max%=&7FFFFFFF: min%=0: min_count%=&7FFFFFFF: max_count%=0.
50 xorig%=100: yorig%=100
60 PROCtitle(12,5,"PLOT")
70 CLS
80 INPUT"" Which axis to scan "M%
```

```

90 PRINT" Recording data can only be performed with increasing theta"
100 INPUT" Counting time, in 100th's secs "TT%
110 INPUT" Step length per cycle (secs) "step_length
120 MO%=step_length/step(M%)
130 INPUT" Number of data points required "NU%
140 xstep=(1200-xorig%)/NU%: ystep=(700-yorig%)/(max%-min%)
150 CLS
160 PROCsetup
170 PROCaxes: VDU5: MOVE100,85: PRINT"0": MOVE1100,85: PRINT
    NU%*MO%*step(M%)
180 MOVE0,725: PRINT""; max%: MOVE0,yorig%: PRINT""; min%: VDU4
190 PROCcommand("Press any key to stop")
200 PROCplot
210 PROCerase: xstep=(1200-xorig%)/I%: PROCredraw
220 PROCsave
230 VDU7
240 PROCcommand("Press <CR> to repeat, any other key for menu")
250 REPEAT: A=INKEY(50): PROCtime: UNTIL A<>-1
260 IF A=13 PROCcommand(" "): RUN
270 CHAIN"P.MENU"
280 DEFPROCtitle(X%,Y%,string$)
290 VDU28,0,6,79,0: COLOUR0: COLOUR129: PRINTTAB(X%,Y%); "
300 PRINTTAB(X%,Y%); string$;
310 VDU28,0,30,79,7: COLOUR1: COLOUR128
320 ENDPROC
330 DEFPROCcommand(string$)
340 VDU28,0,31,79,31: COLOUR0: COLOUR129: CLS
350 PRINTTAB(INT(40-LEN(string$)/2)); string$;
360 VDU28,0,30,79,7: COLOUR1: COLOUR128
370 ENDPROC
380 DEFPROCprint(X%,Y%,R)
390 VDU28,0,6,79,0: COLOUR0: COLOUR129: PRINTTAB(X%,Y%); "
400 PRINTTAB(X%,Y%); R;
410 VDU28,0,30,79,7: COLOUR1: COLOUR128
420 ENDPROC
430 DEFPROCaxes
440 MOVExorig%,yorig%: DRAW1200,yorig%: MOVExorig%,yorig%: DRAW
    xorig%,675
450 FOR I%=1 TO 9: J%=(1200-xorig%)*I%/10: MOVE J%+xorig%,yorig%
460     DRAW J%+xorig%,yorig%+10: NEXT
470 FOR I%=1TO9: J%=(700-yorig%)*I%/10: MOVExorig%,J%+yorig%
480     DRAW xorig%+10,J%+yorig%: NEXT
490 MOVE600,80: VDU5: PRINT"Seconds": VDU4
500 ENDPROC
510 :
520 DEFFNminicam(usr$,AD%,NN%,TT%)
530 PROCtime
540 *FX3,7
550 PRINTusr$; ", "; AD%; ", "; NN%; ", "; TT%; CHR$(13);
560 *FX3,6
570 *FX2,1
580 INPUT""reply$
590 *FX2,2
600 *FX3,0
610 =VAL(reply$)
620 :
630 DEFPROCplot
640 IF M%=1 stepper%=AX%(1) ELSE stepper%=AX%(4)
650 MOVExorig%,yorig%
660 I%=0

```

```

670 REPEAT
680   I% = I% + 1: A = FNminicam("ST1", stepper%, MO%, speed%)
690   @% = &2050A
700   IF M% = 1 S% = S% + MO%: R = S% * step(1) / 3600: PROCprint(34, 1, R)
710   IF M% = 2 T% = T% + MO%: R = T% * step(2) / 3600: PROCprint(34, 2, R)
720   @% = 10
730   R% = FNminicam("CO1", scaler1%, TT%, 0) + 256 * 256 * FNminicam("RD2",
       scaler2%, 0, 0)
740   CO%(I%) = R%
750   IF R% > max_count% max_count% = R%
760   IF R% < min_count% min_count% = R%
770   PROCtitle(68, 1, STR$(R%))
780   PROCpoint(I%, R%)
790   UNTIL I% = NU% OR INKEY(0) <> -1
800   PROCcommand("Stopped...rewinding axis to start position")
810   IF M% = 1 stepper% = AX%(2) ELSE stepper% = AX%(3)
820   A = FNminicam("ST1", stepper%, MO% * I%, speed%)
830   @% = &2050A
840   IF M% = 1 S% = S% - MO% * I%: R = S% * step(1) / 3600: PROCprint(34, 1, R)
850   IF M% = 2 T% = T% - MO% * I%: R = T% * step(2) / 3600: PROCprint(34, 2, R)
860   @% = 10
870 ENDPROC
880 :
890 DEFPROCpoint(I%, R%)
900 PLOT69, I% * xstep + xorig%, (R% - min%) * ystep + yorig%
910 IF I% < 5 ENDPROC
920 IF I% = 5 PROCerase: ystep = (700 - yorig%) / (max_count% - min_count%):
       max% = max_count%: min% = min_count%: PROCredraw: ENDPROC
930 IF max_count% <= max% AND min_count% >= min% ENDPROC
940 PROCerase: ystep = (700 - yorig%) / (max_count% - min_count%):
       max% = max_count%: min% = min_count%: PROCredraw
950 ENDPROC
960 DEFPROCsetup
970 VDU24, 0; 0; 1279; 740;
980 ENDPROC
990 DEFPROCerase
1000 FOR J% = 1 TO I%: PLOT70, J% * xstep + xorig%, (CO%(J%) - min%) * ystep + yorig%:
       NEXT
1010 MOVE0, yorig%: VDU5: PRINT" "; : FORK% = 1 TO 6: VDU127: NEXT: VDU4
1020 MOVE0, 725: VDU5: PRINT" "; : FORK% = 1 TO 15: VDU127: NEXT:
       VDU4
1030 ENDPROC
1040 DEFPROCredraw
1050 MOVE0, yorig%: VDU5: PRINT""; min_count%: MOVE0, 725: PRINT"";
       max_count%: VDU4
1060 FOR J% = 1 TO I%: PLOT69, J% * xstep + xorig%, (CO%(J%) - min%) * ystep + yorig%:
       NEXT
1070 ENDPROC
1080 DEFPROCsave
1090 $C% = "D.RTEMP": ?(C% + 19) = C% MOD 256: ?(C% + 20) = C% DIV 256: X% = (C% + 19)
       MOD 256: Y% = (C% + 19) DIV 256: A% = 6: CALL &FFDD
1100 X% = OPENOUT("D.RTEMP")
1110 PRINT#X%, I%: PRINT#X%, step(M%) * MO%: FOR J% = 1 TO I%: PRINT#X%, CO%(J%):
       NEXT
1120 CLOSE#X%
1130 ENDPROC
1140 DEFPROCtime
1150 O% = (TIME DIV 100) MOD 60: P% = (TIME DIV 6000) MOD 60: Q% = (TIME DIV
       360000) MOD 24
1160 VDU28, 0, 6, 79, 0: COLOUR0: COLOUR129: PRINTTAB(12, 4);

```

```

1170 IF Q%<10 PRINT"0"; Q%; ELSE PRINT; Q%;
1180 IF P%<10 PRINT":0"; P%; ELSE PRINT":"; P%;
1190 IF O%<10 PRINT":0"; O%; ELSE PRINT":"; O%;
1200 VDU28,0,30,79,7: COLOUR1: COLOUR128
1210 ENDPROC

```

```

10 REM -----
20 REM --- FIND ROUTINE - SCANS AXIS AND COUNTS UNTIL PEAK FOUND ---
30 REM -----
40 DIM AX%(8)
50 AX%(1)=34: AX%(2)=35: AX%(3)=36: AX%(4)=37
60 AX%(5)=33: AX%(6)=32: AX%(7)=33: AX%(8)=32
70 scaler1%=56: scaler2%=55: speed%=50
80 DIM step(2): step(1)=0.1776: step(2)=0.121
90 PROCtitle(12,5,"FIND PEAK")
100 CLS
110 INPUT"" Which axis to scan (1 or 2) "M%"
120 IF M%<>1 AND M%<>2 THEN 100
130 F%=(E%ANDM%)
140 IF F% increasing=TRUE ELSE increasing=FALSE
150 PRINT"" Previous motion was ";
160 IF increasing PRINT"increasing"; ELSE PRINT "decreasing";
170 PRINT" theta"
180 INPUT"" Counting time, in 100th's secs "TT%"
190 INPUT"" Step length per cycle (secs) "step_length"
200 MO%=INT(step_length/step(M%))
210 INPUT"" Counts required to assume peak found "LT%"
220 INPUT"" Increasing or decreasing theta (I/D) or both (B) "inc$"
230 both=FALSE: rewind=FALSE
240 IF inc$="B" both=TRUE: INPUT"" Which direction first (I/D) "inc$"
250 INPUT"" Maximum scan range (degrees) "max_scan"
260 max_scan=max_scan*3600/step(M%)
270 PROCstep_scan
280 IF end_scan THEN 310
290 IF both AND inc$="I" inc$="D": rewind=TRUE: PROCstep_scan: GOTO 310
300 IF both AND inc$="D" inc$="I": rewind=TRUE: PROCstep_scan
310 PROCcommand("Press <CR> for repeat, any other key for menu")
320 A=GET: IF A=13 PROCcommand(" "): GOTO 90
330 CHAIN"P.MENU"
340 :
350 DEFFNmotor(dir$)
360 IFdir$="I" E%=(E% OR M%) ELSE E%=(E% AND(&FF EOR M%))
370 IF M%=2 THEN IF dir$="I" F%=1 ELSE F%=0
380 IF M%=1 THEN stepper%=AX%(M%+1-F%)
390 IF M%=2 THEN stepper%=AX%(M%+1+F%)
400 I%=0: IF dir$="I" P%=MO% ELSE P%=-MO%
410 =stepper%
420 :
430 DEFPROCstep_scan
440 stepper%=FNmotor(inc$)
450 IFrewind THEN A%=FNminicam("ST1",stepper%,MO%*JJ%,speed%):
PROCupdate(M%,P%*JJ%)
460 X%=5: Y%=20
470 PROCcommand("Press any key to stop")
480 I%=0
490 REPEAT
500 I%=I%+1
510 CO%=FNstep_count(stepper%,MO%,TT%)
520 PRINTTAB(X%,Y%); CO%;

```

```

530 X%=X%+15: IFX%=80 X%=5: Y%=Y%+1
540 IF (Y%=23 AND X%=5) VDU10,10: Y%=22
550 Z%=INKEY(0)
560 UNTIL CO%>=LT% OR Z%<>-1 OR I%*MO%>=max_scan
570 IF CO%>=LT% THEN CO%=FNminicam("CO1",scaler1%,TT%,0) +
256*256*FNminicam("RD2",scaler2%,0,0): IF CO%<LT% THEN 490
580 IF I%*MO%>=max_scan THEN end_scan=FALSE ELSE end_scan=TRUE
590 JJ%=I%
610 ENDPROC
620 :
630 DEFPROCtitle(X%,Y%,string$)
640 VDU28,0,6,79,0: COLOUR0: COLOUR129: PRINTTAB(X%,Y%); " ";
650 PRINTTAB(X%,Y%); string$;
660 VDU28,0,30,79,7
670 COLOUR1: COLOUR128
680 ENDPROC
690 :
700 DEFPROCcommand(string$)
710 VDU28,0,31,79,31: COLOUR0: COLOUR129: CLS
720 PRINTTAB(INT(40-LEN(string$)/2)); string$;
730 VDU28,0,30,79,7: COLOUR1: COLOUR128
740 ENDPROC
750 :
760 DEFFNstep_count(stepper%,MO%,TT%)
770 A%=FNminicam("ST1",stepper%,MO%,speed%)
780 PROCupdate(M%,P%)
790 R%=FNminicam("CO1",scaler1%,TT%,0)+256*256*FNminicam("RD2",
scaler2%,0,0)
800 R$=STR$(R%): PROCtitle(55,1,R$)
810 =R%
820 :
830 DEFFNminicam(usr$,AD%,NN%,TT%)
840 *FX3,7
850 PRINTusr$; ", "; AD%; ", "; NN%; ", "; TT%; CHR$(13);
860 *FX3,6
870 *FX2,1
880 INPUT" "reply$
890 *FX2,2
900 *FX3,0
910 =VAL(reply$)
920 :
930 DEFPROCupdate(M%,P%)
940 @%=&2050A
950 IF M%=1 S%=S%+P%: R=S%*step(1)/3600: PROCprint(34,1,R)
960 IF M%=2 T%=T%+P%: R=T%*step(2)/3600: PROCprint(34,2,R)
970 @%=10
980 ENDPROC
990 :
1000 DEFPROCprint(X%,Y%,R)
1010 VDU28,0,6,79,0: COLOUR0: COLOUR129: PRINTTAB(X%,Y%); " ";
1020 PRINTTAB(X%,Y%); R;
1030 VDU28,0,30,79,7: COLOUR1: COLOUR128
1040 ENDPROC

10 REM -----
20 REM ----- GONIOMETER TILT ROUTINE -----
30 REM -----
40 DIM AX%(8)
50 AX%(1)=34: AX%(2)=35: AX%(3)=36: AX%(4)=37

```

```

60 AX%(5)=33: AX%(6)=32: AX%(7)=33: AX%(8)=32
70 scaler1%=56: scaler2%=55: speed%=100
80 DIM step(2): step(1)=1.0/(96.0*50): step(2)=1.0/(96.0*50)
90 PROCtitle(12,5,"TILT")
100 CLS
110 INPUT'' Which goniometer to tilt (1 or 2) "M%"
120 IF M%<>1 AND M%<>2 THEN 100
130 F%=(G%ANDM%)
140 IF F% increasing=TRUE ELSE increasing=FALSE
150 PRINT'' Previous motion was ";
160 IF increasing PRINT"compressing"; ELSE PRINT "expanding";
170 PRINT" spring"
180 INPUT'' Distance to drive micrometer (mm) "step_length
190 MO%=step_length/step(M%)
200 INPUT'' Compressing or expanding spring (C/E) "inc$
210 PROCstep_scan
220 VDU7: PROCcommand("Press <CR> for repeat, any other key for menu")
230 A=GET: IF A=13 PROCcommand(" "): GOTO 100
240 CHAIN"P.MENU"
250 :
260 DEFFNmotor(dir$)
270 IFdir$="C" G%=(G% OR M%) ELSE G%=(G% AND(&FF EOR M%))
280 IF dir$="C" F%=1 ELSE F%=0
290 IF M%=1 THEN stepper%=AX%(M%+4+F%)
300 IF M%=2 THEN stepper%=AX%(M%+5+F%)
310 I%=0: IF dir$="C" P%=MO% ELSE P%=-MO%
320 =stepper%
330 :
340 DEFPROCstep_scan
350 stepper%=FNmotor(inc$)
360 IF (V%+P%)<0 OR (V%+P%)>(25/step(M%)) PRINT'' Limit will be passed
by this scan - driving to limit"
370 IF (V%+P%)<0 MO%=V%
380 IF (V%+P%)>(25/step(M%)) MO%=25/step(M%)-V%
390 stepper%=FNmotor(inc$)
400 PRINT'' OK - tilting goniometer "; M%; ", "; MO%; " steps"
410 IF MO%>&FFFF A%=FNminicam("ST1",stepper%,&7FFF,speed%): MO%=MO%-
&7FFF: GOTO410
420 A=FNminicam("ST1",stepper%,MO%,speed%)
430 @%=&2050A
440 IF M%=1 U%=U%+P%: R=U%*step(1): PROCprint(34,3,R)
450 IF M%=2 V%=V%+P%: R=V%*step(2): PROCprint(34,4,R)
460 @%=10
470 ENDPROC
480 :
490 DEFPROCtitle(X%,Y%,string$)
500 VDU28,0,6,79,0: COLOUR0: COLOUR129: PRINTTAB(X%,Y%); " ";
510 PRINTTAB(X%,Y%); string$;
520 VDU28,0,30,79,7
530 COLOUR1: COLOUR128
540 ENDPROC
550 :
560 DEFPROCcommand(string$)
570 VDU28,0,31,79,31: COLOUR0: COLOUR129: CLS
580 PRINTTAB(INT(40-LEN(string$)/2)); string$;
590 VDU28,0,30,79,7: COLOUR1: COLOUR128
600 ENDPROC
610 :
620 DEFFNminicam(usr$,AD%,NN%,TT%)
630 PROCtime

```

```

640 *FX2,2
650 *FX3,7
660 PRINTusr$; ",,"; AD%; ",,"; NN%; ",,"; TT%; CHR$(13);
670 *FX3,6
680 *FX2,1
690 INPUT""reply$
700 *FX2,2
710 *FX3,0
720 =VAL(reply$)
730 :
740 DEFPROCprint(X%,Y%,R)
750 VDU28,0,6,79,0: COLOUR0: COLOUR129: PRINTTAB(X%,Y%); " ";
760 PRINTTAB(X%,Y%); R;
770 VDU28,0,30,79,7
780 COLOUR1: COLOUR128
790 ENDPROC
800 :
810 DEFPROCtime
820 se%=(TIME DIV 100)MOD 60: mi%=(TIME DIV 6000)MOD 60: ho%=(TIME DIV
360000)MOD 24
830 VDU28,0,6,79,0: COLOUR0: COLOUR129: PRINTTAB(12,4);
840 IF ho%<10 PRINT"0"; ho%; ELSE PRINT; ho%;
850 IF mi%<10 PRINT":0"; mi%; ELSE PRINT":"; mi%;
860 IF se%<10 PRINT":0"; se%; ELSE PRINT":"; se%;
870 VDU28,0,30,79,7: COLOUR1: COLOUR128
880 ENDPROC

```

```

10 REM -----
20 REM ----- REPLOT ROUTINE - PLOTS DATA FROM DISC FILE -----
30 REM -----
40 DIM PS(4),MS(4),map(4)
50 PROCtitle(12,5,"REPLOT")
60 max_count%=0: min_count%=&7FFFFFFF
70 CLS
80 PRINT"" When prompted you can enter the name of a data file":
PRINT" or press RETURN to plot the last recorded curve"
90 INPUT" Enter the data file to be plotted "file$
100 IF file$="" file$=":0.D.RTEMP"
110 IF INSTR(file$,".")=0 file$=":2.D."+file$
120 DER%=0
130 ON ERROR GOTO 380
140 X%=OPENIN(file$)
150 IF DER%<>0 AND ERR=214 INPUT" File does not exist - choose another"
file$: DER%=0: GOTO100
160 IF DER%<>0 AND ERR=204 INPUT" File name too long - choose another"
file$: DER%=0: GOTO 100
170 INPUT#X%,NU%
180 IF DER%<>0 AND ERR=222 INPUT" File does not exist - choose another"
file$: CLOSE#X%: DER%=0: GOTO100
190 INPUT#X%,step
200 FOR J%=1 TO NU%
210 INPUT#X%,A%
220 IF A%>max_count% THEN max_count%=A%
230 IF A%<min_count% THEN min_count%=A%
240 NEXT
250 CLOSE#X%
260 IF max_count%=0 THEN max_count%=100
270 CLS: PRINT" X-range of data is 0 to "; step*NU%; " secs"
280 INPUT" Enter X-range to be plotted "xmin,xmax

```



```

290 PRINT'' Y-range of data is "; min_count%; " to "; max_count%; "
    counts"
300 INPUT'' Enter range to be plotted "min_count%,max_count%
310 CLS
320 PROCplot
330 PROCcommand("Press <CR> for repeat, any other key for menu")
340 *FX21,0
350 REPEAT: A=INKEY(50): PROCtime: UNTIL A<>-1
360 IF A=13 PROCcommand(" "): GOTO 60
370 CHAIN"P.MENU"
380 DER%=DER%+1
390 IF ERR=204 OR ERR=199 THEN 150
400 IF ERR=222 THEN 180 ELSE REPORT: END
410 DEFPROCplot
420 PROCpaper
430 PROCpspace(0,1,0.05,1): PROCmspace(0,1,0,1)
440 A$="EXPERIMENTAL ROCKING CURVE ": PROCplotcs(0.2,0.96,A$)
450 PROCplotcs(0.6,0.96,file$)
460 A$="RELATIVE BRAGG ANGLE (secs)": PROCplotcs(0.5,0.03,A$)
470 PROCpspace(0.1,0.9,0.15,0.92):
    PROCmspace(xmin,xmax,min_count%,max_count%)
480 PROCaxes
490 PROCmove(map(1),map(3))
500 X%=OPENIN(file$): INPUT#X%,NU%: INPUT#X%,step
510 FOR J%=1 TO NU%
520     INPUT#X%,A%
530     IF J%*step<xmin THEN 580
540     IF J%*step>xmax THEN 600
550     IF A%>max_count% THEN 580
560     IF A%<min_count% THEN 580
570     PROCpoint(J%*step,A%)
580     NEXT
590 CLOSE#X%
600 ENDPROC
610 DEFPROCpaper
620 xscale%=1279: yscale%=800
630 VDU24,0; 0; 1279; 800;
640 CLG
650 ENDPROC
660 DEFPROCpspace(PS(1),PS(2),PS(3),PS(4))
670 ZX%=xscale%*PS(1): ZY%=yscale%*PS(3)
680 VX%=xscale%*PS(2)-ZX%: VY%=yscale%*PS(4)-ZY%
690 ENDPROC
700 DEFPROCmspace(MS(1),MS(2),MS(3),MS(4))
710 map(1)=MS(1): map(2)=MS(2): map(3)=MS(3): map(4)=MS(4)
720 IF map(1)<0 AND map(2)>0 THEN xorig=0 ELSE xorig=map(1)
730 IF map(3)<0 AND map(4)>0 THEN yorig=0 ELSE yorig=map(3)
740 ENDPROC
750 DEFPROCmove(x,y)
760 A%=(x-map(1))*VX%/(map(2)-map(1))+ZX%
770 B%=(y-map(3))*VY%/(map(4)-map(3))+ZY%
780 PLOT4,A%,B%
790 ENDPROC
800 DEFPROCpoint(x,y)
810 PROCmove(x,y)
820 PLOT65,0,0
830 ENDPROC
840 DEFPROCaxes
850 xrange=map(2)-map(1): yrange=map(4)-map(3)
860 PROCmark(xrange)

```

```

870 PROCmove(map(1),yorig): PROCnotch(1)
880 step%=xrange/SX
890 FOR J%=1 TO step%
900   PROCdraw_rel(SX,0)
910   PROCnotch(1)
920   NEXT
930 PROCdraw(map(2),yorig)
940 FOR J%=step% TO 0 STEP -1
950   x=J%*SX+map(1)
960   PROClabel_x(x)
970   NEXT
980 PROCmark(yrange)
990 PROCmove(xorig,map(3)): PROCnotch(2)
1000 step%=yrange/SX
1010 FOR J%=1 TO step%
1020   PROCdraw_rel(0,SX)
1030   PROCnotch(2)
1040   NEXT
1050 PROCdraw(xorig,map(4))
1060 FOR J%=step% TO 0 STEP -1
1070   x=J%*SX+map(3)
1080   PROClabel_y(x)
1090   NEXT
1100 ENDPROC
1110 DEFPROCdraw_rel(x,y)
1120 A%=x*VX%/(map(2)-map(1))
1130 B%=y*VY%/(map(4)-map(3))
1140 PLOT1,A%,B%
1150 DEFPROCnotch(C%)
1160 IF C%=1 THEN PLOT1,0,10: PLOT1,0,-10
1170 IFC%=2 THEN PLOT1,10,0: PLOT1,-10,0
1180 ENDPROC
1190 DEFPROClabel_x(x)
1200 A%=(x-map(1))*VX%/(map(2)-map(1))+ZX%-8*LEN(STR$(x))
1210 B%=(yorig-map(3))*VY%/(map(4)-map(3))+ZY%-22
1220 PLOT4,A%,B%: VDU5: PRINTSTR$(x): VDU4
1230 ENDPROC
1240 DEFPROClabel_y(x)
1250 A%=(xorig-map(1))*VX%/(map(2)-map(1))+ZX%-16*LEN(STR$(x))-20
1260 B%=(x-map(3))*VY%/(map(4)-map(3))+ZY%
1270 PLOT4,A%,B%: VDU5: PRINTSTR$(x): VDU4
1280 ENDPROC
1290 DEFPROCmark(range)
1300 B%=LOG(range)
1310 A=range/10.^B%
1320 IF A>=1 AND A<3 THEN SX=2*10^(B%-1)
1330 IF A>=3 AND A<7 THEN SX=5*10^(B%-1)
1340 IF A>=7 AND A<10 THEN SX=1*10^B%
1350 ENDPROC
1360 DEFPROCplotcs(x,y,A$)
1370 PROCmove(x,y): VDU5: PRINTA$: VDU4: ENDPROC
1380 DEFPROCtitle(X%,Y%,string$)
1390 VDU28,0,6,79,0: COLOUR0: COLOUR129: PRINTTAB(X%,Y%); "
1400 PRINTTAB(X%,Y%); string$;
1410 VDU28,0,30,79,7: COLOUR1: COLOUR128
1420 ENDPROC
1430 DEFPROCcommand(string$)
1440 VDU28,0,31,79,31: COLOUR0: COLOUR129: CLS
1450 PRINTTAB(40-INT(LEN(string$)/2)); string$;
1460 VDU28,0,30,79,7: COLOUR1: COLOUR128

```

```

1470 ENDPROC
1480 DEFPROCdraw(x,y)
1490 A%=(x-map(1))*VX%/(map(2)-map(1))+ZX%: B%=(y-map(3))*VY%/(map(4)-
map(3))+ZY%
1500 PLOT5,A%,B%: ENDPROC
1510 :
1520 DEFPROCtime
1530 se%=(TIME DIV 100)MOD 60: mi%=(TIME DIV 6000)MOD 60: ho%=(TIME DIV
360000)MOD 24
1540 VDU28,0,6,79,0: COLOUR0: COLOUR129: PRINTTAB(12,4);
1550 IF ho%<10 PRINT"0"; ho%; ELSE PRINT; ho%;
1560 IF mi%<10 PRINT":0"; mi%; ELSE PRINT":"; mi%;
1570 IF se%<10 PRINT":0"; se%; ELSE PRINT":"; se%;
1580 VDU28,0,30,79,7: COLOUR1: COLOUR128
1590 ENDPROC

```

```

10 REM:-----
20 REM:-----  HARDCOPY PLOT ROUTINE- PLOTS DATA FROM DISC  -----
30 REM:-----
40 DIM PS(4),MS(4),map(4)
50 PROCtitle(12,5,"HARDCOPY")
60 max_count%=0: min_count%=&7FFFFFFF
70 CLS
80 PRINT'" When prompted you can enter the name of a data file":
PRINT" or press RETURN to plot the last recorded curve"
90 INPUT'" Enter the data file to be plotted "file$
100 IF file$="" file$=":0.D.RTEMP"
110 IF INSTR(file$,".")=0 file$=":2.D."+file$
120 DER%=0
130 ON ERROR GOTO 370
140 X%=OPENIN(file$)
150 IF DER%<>0 AND ERR=214 INPUT'" File does not exist - choose another"
file$: DER%=0: GOTO100
160 IF DER%<>0 AND ERR=204 INPUT'" File name too long - choose another"
file$: DER%=0: GOTO 100
170 INPUT#X%,NU%
180 IF DER%<>0 AND ERR=222 INPUT'" File does not exist - choose another"
file$: CLOSE#X%: DER%=0: GOTO100
190 INPUT#X%,step
200 FOR J%=1 TO NU%
210 INPUT#X%,A%
220 IF A%>max_count% THEN max_count%=A%
230 IF A%<min_count% THEN min_count%=A%
240 NEXT
250 CLOSE#X%
260 IF max_count%=0 THEN max_count%=100
270 CLS: PRINT'" X-range of data is 0 to "; step*NU%; " secs"
280 INPUT'" Enter X-range to be plotted "xmin,xmax
290 PRINT'" Y-range of data is "; min_count%; " to "; max_count%; "
counts"
300 INPUT'" Enter range to be plotted "min_count%,max_count%
310 PRINT'" "; : COLOUR0: COLOUR129: PRINT"Plotting data from
disc file "; file$: COLOUR1: COLOUR128
320 PROCplot
330 PROCcommand("Press <CR> for repeat, any other key for menu")
340 *FX21,0
350 A=GET: IF A=13 PROCcommand(" "): GOTO 60
360 CHAIN"P.MENU"
370 DER%=DER%+1

```

```

380 IF ERR=204 OR ERR=199 THEN 150
390 IF ERR=222 THEN 180 ELSE REPORT: END
400 DEFPROCplot
410 PROCpaper: PROCpen(1)
420 PROCpspace(0,1,0,1): PROCmspace(0,1,0,1)
430 PROCctrmag(6): PROCplotcs(0.1,0.92,"EXPERIMENTAL ROCKING CURVE ")
440 PROCplotcs(0.7,0.92,file$)
450 PROCctrmag(4): PROCplotcs(0.5,0.03,"RELATIVE BRAGG ANGLE (secs)")
460 PROCctrori(1): PROCplotcs(0.025,0.3,"COUNTS (unit time)"):
  PROCctrori(0)
470 PROCpspace(0.1,0.9,0.1,0.9):
  PROCmspace(xmin,xmax,min_count%,max_count%)
480 PROCaxes
490 PROCmove(map(1),map(3))
500 X%=OPENIN(file$): INPUT#X%,NU%: INPUT#X%,step
510 FOR J%=1 TO NU%
520   INPUT#X%,CO%
530   IF J%*step<xmin THEN 580
540   IF J%*step>xmax THEN 590
550   IF CO%>max_count% THEN 580
560   IF CO%<min_count% THEN 580
570   PROCdraw((J%-1)*step,CO%): PROCdraw(J%*step,CO%)
580   NEXT
590 PROCpen(0)
600 ENDPROC
610 DEFPROCpaper
620 xscale%=2400: yscale%=1800
630 PROCminicam("PR2,"+CHR$(10))
640 ENDPROC
650 DEFPROCpspace(PS(1),PS(2),PS(3),PS(4))
660 ZX%=xscale%*PS(1): ZY%=yscale%*PS(3)
670 VX%=xscale%*PS(2)-ZX%: VY%=yscale%*PS(4)-ZY%
680 ENDPROC
690 DEFPROCmspace(MS(1),MS(2),MS(3),MS(4))
700 map(1)=MS(1): map(2)=MS(2): map(3)=MS(3): map(4)=MS(4)
710 IF map(1)<0 AND map(2)>0 THEN xorig=0 ELSE xorig=map(1)
720 IF map(3)<0 AND map(4)>0 THEN yorig=0 ELSE yorig=map(3)
730 ENDPROC
740 DEFPROCmove(x,y)
750 A%=(x-map(1))*VX%/(map(2)-map(1))+ZX%
760 B%=(y-map(3))*VY%/(map(4)-map(3))+ZY%
770 PROCminicam("PR1,"+"M"+STR$(A%)+", "+STR$(B%))
780 ENDPROC
790 DEFPROCaxes
800 xrange=map(2)-map(1): yrange=map(4)-map(3)
810 PROCmark(xrange)
820 PROCmove(map(1),yorig): PROCnotch(1)
830 step%=xrange/SX
840 FOR J%=1 TO step%
850   PROCdraw_rel(SX,0)
860   PROCnotch(1)
870   NEXT
880 PROCdraw(map(2),yorig)
890 FOR J%=step% TO 0 STEP -1
900   x=J%*SX+map(1)
910   PROClabel_x(x)
920   NEXT
930 PROCmark(yrange)
940 PROCmove(xorig,map(3)): PROCnotch(2)
950 step%=yrange/SX

```

```

960 FOR J%=1 TO step%
970   PROCdraw_rel(0, SX)
980   PROCnotch(2)
990   NEXT
1000 PROCdraw(xorig, map(4))
1010 FOR J%=step% TO 0 STEP-1
1020   x=J%*SX+map(3)
1030   PROClabel_y(x)
1040   NEXT
1050 ENDPROC
1060 DEFPROCdraw_rel(x, y)
1070 A%=x*VX%/(map(2)-map(1))
1080 B%=y*VY%/(map(4)-map(3))
1090 PROCminicam("PR1, "+"I"+STR$(A%)+", "+STR$(B%))
1100 DEFPROCnotch(C%)
1110 IF C%=1 THEN PROCminicam("PR1, I0, 25, 0, -25")
1120 IFC%=2 THEN PROCminicam("PR1, I25, 0, -25, 0")
1130 ENDPROC
1140 DEFPROClabel_x(x)
1150 A%=(x-map(1))*VX%/(map(2)-map(1))+ZX%-8*LEN(STR$(x))
1160 B%=(yorig-map(3))*VY%/(map(4)-map(3))+ZY%-65
1170 PROCminicam("PR1, "+"M"+STR$(A%)+", "+STR$(B%))
1180 PROCminicam("PR1, "+"P"+STR$(x))
1190 ENDPROC
1200 DEFPROClabel_y(x)
1210 A%=(xorig-map(1))*VX%/(map(2)-map(1))+ZX%-16*LEN(STR$(x))-100
1220 B%=(x-map(3))*VY%/(map(4)-map(3))+ZY%
1230 PROCminicam("PR1, "+"M"+STR$(A%)+", "+STR$(B%))
1240 PROCminicam("PR1, "+"P"+STR$(x))
1250 ENDPROC
1260 DEFPROCmark(range)
1270 B%=LOG(range)
1280 A=range/10.^B%
1290 IF A>=1 AND A<3 THEN SX=2*10^(B%-1)
1300 IF A>=3 AND A<7 THEN SX=5*10^(B%-1)
1310 IF A>=7 AND A<10 THEN SX=1*10^B%
1320 ENDPROC
1330 DEFPROCplots(x, y, CS)
1340 PROCmove(x, y): CS="PR1, "+"P"+CS: PROCminicam(CS)
1350 DEFPROCtitle(X%, Y%, string$)
1360 VDU28, 0, 6, 79, 0: COLOUR0: COLOUR129: PRINTTAB(X%, Y%); " ";
1370 PRINTTAB(X%, Y%); string$;
1380 VDU28, 0, 30, 79, 7: COLOUR1: COLOUR128
1390 ENDPROC
1400 DEFPROCcommand(string$)
1410 VDU28, 0, 31, 79, 31: COLOUR0: COLOUR129: CLS
1420 PRINTTAB(40-INT(LEN(string$)/2)); string$;
1430 VDU28, 0, 30, 79, 7: COLOUR1: COLOUR128
1440 ENDPROC
1450 DEFPROCdraw(x, y)
1460 A%=(x-map(1))*VX%/(map(2)-map(1))+ZX%: B%=(y-map(3))*VY%/(map(4)-
map(3))+ZY%
1470 A$="PR1, "+"D"+STR$(A%)+", "+STR$(B%): PROCminicam(A$)
1480 ENDPROC
1490 DEFPROCpen(C%)
1500 A$="PR1, "+"J"+STR$(C%): PROCminicam(A$)
1510 ENDPROC
1520 DEFPROCctrmag(C%)
1530 ctrsize%=C%+1: A$="PR1, "+"S"+STR$(C%): PROCminicam(A$)
1540 ENDPROC

```

```

1550 DEFPROCctrori(C%)
1560 A$="PR1,"+"Q"+STR$(C%): PROCminicam(A$): ENDPROC
1570 DEFPROCminicam(A$)
1580 *FX3,7
1590 *FX2,2
1600 PRINTA$; CHR$(13);
1610 *FX3,6
1620 *FX2,1
1630 INPUT" "A$
1640 *FX2,2
1650 *FX3,0
1660 ENDPROC

```

```

10 REM -----
20 REM -----  AUTOMATIC TILT OPTIMISE ROUTINE  -----
30 REM -----
40 DIM AX%(8)
50 AX%(1)=34: AX%(2)=35: AX%(3)=36: AX%(4)=37
60 AX%(5)=33: AX%(6)=32: AX%(7)=33: AX%(8)=32
70 scaler1%=56: scaler2%=55: speed%=20: gspeed%=100
80 DIM step(4),max%(9),position%(9)
90 step(1)=0.1776: step(2)=0.121: step(3)=1.0/(96.0*50):
   step(4)=1.0/(96.0*50)
100 here%=T%: tilt_here%=V%
110 PROCtitle(12,5,"AUTO TILT")
120 CLS
130 PRINT'"'  Second axis only is driven by this routine"
140 M%=2
150 F%=(E%ANDM%)
160 IF F% increasing=TRUE ELSE increasing=FALSE
170 PRINT'"  Previous motion of this axis was ";
180 IF increasing PRINT"increasing"; ELSE PRINT "decreasing";
190 PRINT" theta"
200 INPUT'"  Counting time for peak scanning, in 100th's secs "TT%
210 INPUT'"  Step length for peak scanning (secs) "step_length
220 MO%=INT(step_length/step(M%))
230 INPUT'"  Maximum range to be scanned when looking for peaks (secs) "
   range
240 limit%=range/step(M%)
250 INPUT'"  Tilt step length for tilt optimisation "tilt_step
260 INPUT'"  Enter the background count rate (counts/sec) "background
270 tstep%=tilt_step/step(M%+2)
280 FOR C%=1 TO 3
290   PROCtilt_opt
300   tstep%=tstep%/2
310   NEXT C%
320 PROCcommand("Press <CR> for repeat, any other key for menu")
330 A=GET: IF A=13 PROCcommand(" "): GOTO 110
340 CHAIN"P.MENU"
350 :
360 DEFFNmotor(dir$)
370 IFdir$="I" E%=(E% OR M%) ELSE E%=(E% AND(&FF EOR M%))
380 IF dir$="I" THEN F%=1 ELSE F%=0
390 IF M%=1 THEN stepper%=AX%(M%+1-F%)
400 IF M%=2 THEN stepper%=AX%(M%+1+F%)
410 I%=0: IF dir$="I" P%=MO% ELSE P%=-MO%
420 =stepper%
430 :
440 DEFPROCtitle(X%,Y%,string$)

```

```

450 VDU28,0,6,79,0: COLOUR0: COLOUR129: PRINTTAB(X%,Y%); "
460 PRINTTAB(X%,Y%); string$;
470 VDU28,0,30,79,7
480 COLOUR1: COLOUR128
490 ENDPROC
500 :
510 DEFPROCcommand(string$)
520 VDU28,0,31,79,31: COLOUR0: COLOUR129: CLS
530 PRINTTAB(INT(40-LEN(string$)/2)); string$;
540 VDU28,0,30,79,7: COLOUR1: COLOUR128
550 ENDPROC
560 :
570 DEFPROCstep_count(stepper%,MO%,TT%)
580 A%=FNminicam("ST1",stepper%,MO%,speed%)
590 @%=&2050A
600 IF M%=1 S%=S%+P%: R=S%*step(1)/3600: PROCprint(34,1,R)
610 IF M%=2 T%=T%+P%: R=T%*step(2)/3600: PROCprint(34,2,R)
620 @%=10
630 R%=FNminicam("CO1",scaler1%,TT%,0)+256*256*FNminicam("RD2",
scaler2%,0,0)
640 R$=STR$(R%): PROCtitle(68,1,R$)
650 ENDPROC
660 :
670 DEFFNminicam(usr$,AD%,NN%,TT%)
680 *FX2,2
690 *FX3,7
700 PRINTusr$; ",,"; AD%; ",,"; NN%; ",,"; TT%; CHR$(13);
710 *FX3,6
720 *FX2,1
730 INPUT""reply$
740 *FX2,2
750 *FX3,0
760 =VAL(reply$)
770 :
780 DEFPROCprint(X%,Y%,R)
790 VDU28,0,6,79,0: COLOUR0: COLOUR129: PRINTTAB(X%,Y%); "
800 PRINTTAB(X%,Y%); R;
810 VDU28,0,30,79,7
820 COLOUR1: COLOUR128
830 ENDPROC
840 :
850 DEFPROCtilt_opt
860 CLS: PRINTTAB(8); "Tilt (mm)"; TAB(18); "Maximum count"; TAB(28);
"Axis position of max"
870 FOR I%=1 TO 5
880 PROCfind
890 PRINT'TAB(10); V%*step(4); TAB(20); maximum%; TAB(30);
maxpos%*step(2)/3600
900 max%(I%)=maximum%; position%(I%)=maxpos%
910 IF I%<>5 PROCTilt("I",tstep%)
920 NEXT
930 PROCTilt("D",5*tstep%)
940 IF (T%-here%)>0 PROCmove("D",T%-here%) ELSE PROCmove("I",here%-T%)
950 FOR I%=6 TO 9
960 PROCfind
970 max%(I%)=maximum%; position%(I%)=maxpos%
980 PRINT'TAB(10); V%*step(4); TAB(20); maximum%; TAB(30);
maxpos%*step(2)/3600
990 IF I%<>9 PROCTilt("D",tstep%)
1000 NEXT

```

```

1010 maximum%=0: FOR I%=1 TO 9: IF max%(I%)>maximum% maximum%=max%(I%):
    J%=position%(I%): Z%=I%: NEXT
1020 IF Z%<=5 PROCtilt("I", (Z%+3)*tstep%) ELSE PROCtilt("I", (9-Z%)*tstep%)
1030 IF (T%-J%)>0 PROCmove("D", T%-J%) ELSE PROCmove("I", J%-T%)
1040 ENDPROC
1050 :
1060 DEFPROCtilt(dir$, step%)
1070 IF dir$="I" stepper%=AX%(9): P%=step% ELSE stepper%=AX%(8): P%=-step%
1080 IF step%>&7FFF A%=FNminicam("ST1", stepper%, &7FFF, gspeed%):
    step%=step%-&7FFF:GOTO 1080
1090 A%=FNminicam("ST1", stepper%, step%, gspeed%)
1100 @%=&2050A: V%=V%+P%: R=V%*step(4): PROCprint(34, 4, R)
1110 @%=10
1120 ENDPROC
1130 :
1140 DEFPROCmove(dir$, step%)
1150 stepper%=FNmotor(dir$)
1160 IF step%>&7FFF A%=FNminicam("ST1", stepper%, &7FFF, speed%):
    step%=step%-&7FFF:GOTO 1160
1170 A%=FNminicam("ST1", stepper%, step%, speed%)
1180 ENDPROC
1190 :
1200 DEFPROCfind
1210 now%=T%
1220 stepper%=FNmotor("I")
1230 step_count
1240 REPEAT
1250   PROCstep_count(stepper%, MO%, 100)
1260   UNTIL (R%>(2*background)) OR (T%>=now%+limit%)
1270 IF R%>(2*background) THEN stepper%=FNmotor("D"):GOTO 1350
1280 PROCmove("D", T%-now%)
1290 stepper%=FNmotor("D")
1300 REPEAT
1310   PROCstep_count(stepper%, MO%, 100)
1320   UNTIL (R%>(2*background)) OR (T%<=now%-limit%)
1330 IF R%>(2*background) THEN 1350
1340 fault=TRUE: ENDPROC
1350 REPEAT: PROCstep_count(stepper%, MO%, 100): UNTIL R%<(1.5*background):
    maximum%=0: stepper%=FNmotor("I")
1360 REPEAT
1370   PROCstep_count(stepper%, MO%, 100): IF R%>maximum% maximum%=R%:
    maxpos%=T%
1380   UNTIL R%<(1.5*background) AND maximum%>(1.5*background)
1390 ENDPROC

```

```

10 REM -----
20 REM ----- MOVE SCANNING TABLE -----
30 REM -----
40 DIM AX%(12)
50 AX%(1)=34: AX%(2)=35: AX%(3)=36: AX%(4)=37
60 AX%(5)=33: AX%(6)=32: AX%(7)=33: AX%(8)=32
70 AX%(9)=32: AX%(10)=33: AX%(11)=34: AX%(12)=35
80 speed%=50
90 DIM step(2)
100 step(1)=1.0/96.0: step(2)=1.0/96.0
110 PROCtitle(12, 5, "SCAN TABLE")
120 CLS
130 PRINT''' The present position of the scanning table is"
140 PRINT''' X = "; K%*step(1); " nm"

```



```

150 PRINT"          Y = "; L%*step(2); " mm"
160 INPUT"" Enter the X coord and Y coord of desired position (mm) "
    new_x,new_y
170 PRINT"" OK - moving to desired position"
180 PROCmove
190 PROCcommand("Press <CR> for repeat, any other key for menu")
200 A=GET: IF A=13 PROCcommand(" "): GOTO 120
210 CHAIN"P.MENU"
220 :
230 DEFPROCmove
240 steps%=(new_x/step(1)-K%)
250 IF steps%>=0 THEN A%=FNminicam("ST1",AX%(9),steps%,speed%) ELSE
    A%=FNminicam("ST1",AX%(10),-steps%,speed%)
260 PROCupdate(1,steps%)
270 steps%=(new_y/step(2)-L%)
280 IF steps%>=0 THEN A%=FNminicam("ST1",AX%(11),steps%,speed%) ELSE
    A%=FNminicam("ST1",AX%(12),-steps%,speed%)
290 PROCupdate(2,steps%)
300 ENDPROC
310 :
320 DEFPROCupdate(motor%,steps%)
330 @%=&2050A
340 IF motor%=1 K%=K%+steps%: R=K%*step(1): PROCprint(47,2,R)
350 IF motor%=2 L%=L%+steps%: R=L%*step(2): PROCprint(47,3,R)
360 @%=10
370 ENDPROC
380 :
390 DEFPROCtitle(X%,Y%,string$)
400 VDU28,0,6,79,0: COLOUR0: COLOUR129: PRINTTAB(X%,Y%); "          ";
410 PRINTTAB(X%,Y%); string$;
420 VDU28,0,30,79,7
430 COLOUR1: COLOUR128
440 ENDPROC
450 :
460 DEFPROCcommand(string$)
470 VDU28,0,31,79,31: COLOUR0: COLOUR129: CLS
480 PRINTTAB(INT(40-LEN(string$)/2)); string$;
490 VDU28,0,30,79,7: COLOUR1: COLOUR128
500 ENDPROC
510 :
520 DEFFNminicam(usr$,AD%,NN%,TT%)
530 PROCtime
540 *FX2,2
550 *FX3,7
560 PRINTusr$; ", "; AD%; ", "; NN%; ", "; TT%; CHR$(13);
570 *FX3,6
580 *FX2,1
590 INPUT""reply$
600 *FX2,2
610 *FX3,0
620 =VAL(reply$)
630 :
640 DEFPROCprint(X%,Y%,R)
650 VDU28,0,6,79,0: COLOUR0: COLOUR129: PRINTTAB(X%,Y%); "          ";
660 PRINTTAB(X%,Y%); R;
670 VDU28,0,30,79,7: COLOUR1: COLOUR128
680 ENDPROC
690 :
700 DEFPROCtime
710 se%=(TIME DIV 100)MOD 60: mi%=(TIME DIV 6000)MOD 60: ho%=(TIME DIV

```

```

360000)MOD 24
720 VDU28,0,6,79,0: COLOUR0: COLOUR129: PRINTTAB(12,4);
730 IF ho%<10 PRINT"0"; ho%; ELSE PRINT; ho%;
740 IF mi%<10 PRINT":0"; mi%; ELSE PRINT":"; mi%;
750 IF se%<10 PRINT":0"; se%; ELSE PRINT":"; se%;
760 VDU28,0,30,79,7: COLOUR1: COLOUR128
770 ENDPROC

10 REM -----
20 REM ----- PEAK HOLD ROUTINE - FOR TOPOGRAPHS -----
30 REM -----
40 DIM AX%(8)
50 AX%(1)=34: AX%(2)=35: AX%(3)=36: AX%(4)=37
60 AX%(5)=33: AX%(6)=32: AX%(7)=33: AX%(8)=32
70 scaler1%=56: scaler2%=55: speed%=20
80 DIM step(2)
90 step(1)=0.1776: step(2)=0.121
100 decr$="": incr$="": fault=FALSE: end=FALSE
110 PROCtitle(12,5,"PEAK HOLD")
120 CLS
130 PRINT"" Only the second axis is driven by this routine"
140 M%=2
150 F%=(E%ANDM%)
160 IF F% increasing=TRUE ELSE increasing=FALSE
170 PRINT"" The last motion of this axis was ";
180 IF increasing PRINT"increasing"; ELSE PRINT "decreasing";
190 PRINT" theta"
200 PRINT"" Are you positioned at"
210 PRINT"" 1. Top of peak"
220 PRINT "" 2. High angle side"
230 PRINT "" 3. Low angle side"
240 INPUT"" Enter which one (1,2 or 3) "position%"
250 INPUT"" Step size required for adjustments (secs) "step_length
260 MO%=INT(step_length/step(M%))
270 INPUT"" Enter the background count rate (counts/sec) "background
280 CLS: PRINT"" Holding peak position": PROCcommand("Press any key
to stop")
290 IF position%=1 PROCTop ELSE PROCflank
300 IF fault=TRUE CLS: PRINT"" Count rate is less than background -
check generator"
310 PROCcommand("Press <CR> for repeat, any other key for menu")
320 A=GET: IF A=13 PROCcommand(" "): GOTO 110
330 CHAIN"P.MENU"
340 :
350 DEFFNmotor(dir$)
360 IFdir$="I" E%=(E% OR M%) ELSE E%=(E% AND(&FF EOR M%))
370 IF dir$="I" THEN F%=1 ELSE F%=0
380 IF M%=1 THEN stepper%=AX%(M%+1-F%)
390 IF M%=2 THEN stepper%=AX%(M%+1+F%)
400 I%=0: IF dir$="I" P%=MO% ELSE P%=-MO%
410 =stepper%
420 :
430 :
440 DEFPROCtitle(X%,Y%,string$)
450 VDU28,0,6,79,0: COLOUR0: COLOUR129: PRINTTAB(X%,Y%); " ";
460 PRINTTAB(X%,Y%); string$;
470 VDU28,0,30,79,7
480 COLOUR1: COLOUR128
490 ENDPROC

```

```

500 :
510 DEFPROCcommand(string$)
520 VDU28,0,31,79,31: COLOUR0: COLOUR129: CLS
530 PRINTTAB(INT(40-LEN(string$)/2)); string$;
540 VDU28,0,30,79,7: COLOUR1: COLOUR128
550 ENDPROC
560 :
570 DEFFNminicam(usr$,AD%,NN%,TT%)
580 *FX2,2
590 *FX3,7
600 PRINTusr$; ", "; AD%; ", "; NN%; ", "; TT%; CHR$(13);
610 *FX3,6
620 *FX2,1
630 INPUT" "reply$
640 *FX2,2
650 *FX3,0
660 =VAL(reply$)
670 :
680 DEFPROCprint(X%,Y%,R)
690 VDU28,0,6,79,0: COLOUR0: COLOUR129: PRINTTAB(X%,Y%); "
700 PRINTTAB(X%,Y%); R;
710 VDU28,0,30,79,7
720 COLOUR1: COLOUR128
730 ENDPROC
740 :
750 DEFPROCflank
760 rate=FNminicam("CO1",scalar1%,500,0)+256*256*FNminicam("RD2",
scalar2%,0,0)
770 error=SQR(rate)*3/5: rate=rate/5
780 if position%=2 decr$="I": incr$="D" ELSE decr$="D": incr$="I"
790 IF end=TRUE ENDPROC ELSE count=FNintensity
800 IF count<(background-SQR(background)) fault=TRUE: ENDPROC
810 IF (count<(rate+error)) AND (count>(rate-error)) PROCdelay(500): GOTO
790
820 IF count<(rate-error) PROCincrease: GOTO790
830 IF count>(rate+error) PROCdecrease: GOTO790
840 ENDPROC
850 :
860 DEFPROCincrease
870 stepper%=FNmotor(incr$)
880 A%=FNminicam("ST1",stepper%,MO%,speed%)
890 @%=&2050A
900 IF M%=1 S%=S%+P%: R=S%*step(1)/3600: PROCprint(34,1,R)
910 IF M%=2 T%=T%+P%: R=T%*step(2)/3600: PROCprint(34,2,R)
920 @%=10
930 ENDPROC
940 :
950 DEFPROCdecrease
960 stepper%=FNmotor(decr$)
970 A%=FNminicam("ST1",stepper%,MO%,speed%)
980 @%=&2050A
990 IF M%=1 S%=S%+P%: R=S%*step(1)/3600: PROCprint(34,1,R)
1000 IF M%=2 T%=T%+P%: R=T%*step(2)/3600: PROCprint(34,2,R)
1010 @%=10
1020 ENDPROC
1030 :
1040 PROCdelay(time%)
1050 A=INKEY(time%)
1060 IF A<>-1 end=TRUE
1070 ENDPROC

```

```

1080 :
1090 DEFPROCtop
1100 rate=FNminicam("CO1",scalar1%,500,0)+256*256*FNminicam("RD2",
    scalar2%,0,0)
1110 error=SQR(rate)*3/5: rate=rate/5
1120 decr$="D": incr$="I"
1130 IF end=TRUE ENDPROC ELSE count=FNintensity
1140 IF count<(background-SQR(background)) fault=TRUE: ENDPROC
1150 IF (count<(rate+error)) AND (count>(rate-error)) PROCdelay(500):
    GOTO1130
1160 last_count=count: PROCdecrease: count=FNintensity: IF
    count<last_count GOTO 1180
1170 IF count>(rate-error) GOTO 1130 ELSE GOTO 1160
1180 last_count=count: PROCincrease: count=FNintensity: IF
    count<last_count GOTO 1160
1190 IF count>(rate-error) GOTO 1130 ELSE GOTO 1180
1200 :
1210 DEFFNintensity
1220 A%=FNminicam("CO1",scalar1%,500,0)+256*256*FNminicam("RD2",
    scalar2%,0,0)
1230 =A%/5

10 REM -----
20 REM ----- UTILITIES PROGRAM -----
30 REM -----
40 :
50 PROCtitle(12,5,"UTILITIES"): CLS: PROCcommand(" ")
60 PROCmenu
70 PRINTTAB(0,19); " "; : COLOUR0: COLOUR129: PRINT"Enter
    utilities subject >> "; : COLOUR1: COLOUR128: PRINT" ";
80 INPUT""choice$
90 IF LEN(choice$)>2 VDU7: GOTO70
100 IF choice$="BR" CHAIN"P.BRAGG"
110 IF choice$="RE" CHAIN"P.REFL"
120 IF choice$="SP" CHAIN"P.SPDATA"
130 IF choice$="QU" CHAIN"P.MENU"
140 VDU7: GOTO70
150 :
160 DEFPROCtitle(X%,Y%,string$)
170 VDU28,0,6,79,0: COLOUR0: COLOUR129: PRINTTAB(X%,Y%); " ";
180 PRINTTAB(X%,Y%); string$;
190 VDU28,0,30,79,7: COLOUR1: COLOUR128
200 ENDPROC
210 :
220 DEFPROCcommand(string$)
230 VDU28,0,31,79,31: COLOUR0: COLOUR129: CLS
240 PRINTTAB(INT(40-LEN(string$)/2)); string$;
250 VDU28,0,30,79,7: COLOUR1: COLOUR128
260 ENDPROC
270 DEFPROCmenu
280 PRINT'
290 PRINT'" BRagg angle - calculate Bragg angle for a material"
300 PRINT'" Reflectivity - calculates single crystal reflectivity
    curve"
310 PRINT'" SPool data - spools a data file to an ascii file"
320 PRINT'" QUIT - leave help, return to main menu"
330 PRINT'" Select choice by keying in the two letters in capitals shown
    above"
340 ENDPROC

```

```

10 REM -----
20 REM ----- SAVE ROUTINE - COPIES TEMPORARY FILE -----
30 REM -----
40 :
50 DIM CO%(600)
60 PROCtitle(12,5,"SAVE DATA"): CLS
70 PRINT'"'"' When prompted enter the file name for data storage,'"':
PRINT" if no drive number is given drive 2 is assumed"
80 INPUT'"'"' Enter file name "file$
90 IF INSTR(file$,".")=0 file$="D."+file$
100 IF INSTR(file$,":")=0 file$=":2."+file$
110 PRINT'"'"' Reading data from file :0.D.RTEMP, writing data to file '"':
file$
120 ON ERROR GOTO 510
130 DER%=0
140 X%=OPENIN(" :0.D.RTEMP")
150 INPUT#X%,NU%
160 IF DER%<>0 AND ERR=222 PRINT'"'"' There is no temporary data file -
press any key for menu": A=GET: CLOSE#X%: CHAIN"P.MENU"
170 INPUT#X%,step
180 FOR I%=1 TO NU%: INPUT#X%,CO%(I%): NEXT
190 CLOSE#X%
200 DER%=0
210 X%=OPENIN(" :0.D.HEADER")
220 INPUT#X%,place$
230 IF DER%<>0 AND ERR=222 PRINT'"'"' There is no header file - press key
for menu and use UPDATE": A=GET: CLOSE#X%: CHAIN"P.MENU"
240 INPUT#X%,sname$
250 INPUT#X%,volt$
260 INPUT#X%,current$
270 INPUT#X%,first_crystal$
280 INPUT#X%,wave$
290 INPUT#X%,refl$
300 CLOSE#X%
310 DER%=0
320 X%=OPENOUT(file$)
330 IF DER%<>0 AND ERR=204 PRINT'"'"' Chosen file name too long - choose
another '"': INPUTfile$: GOTO 90
340 PRINT#X%,NU%
350 PRINT#X%,step
360 FOR I%=1 TO NU%
370 PRINT#X%,CO%(I%)
380 NEXT
390 PRINT#X%,place$
400 PRINT#X%,sname$
410 PRINT#X%,volt$
420 PRINT#X%,current$
430 PRINT#X%,first_crystal$
440 PRINT#X%,wave$
450 PRINT#X%,refl$
460 CLOSE#X%
470 :
480 PROCcommand("Press <CR> for repeat, any other key for menu")
490 A=GET: IF A=13 PROCcommand(""): CLS: GOTO70
500 CHAIN"P.MENU"
510 REM ERROR TRAP FOR ILLEGAL DISC ACCESS
520 DER%=DER%+1
530 IF ERR=214 PRINT'"'"' File does not exist"

```

```

540 IF ERR=204 PRINT'' File name too long"
550 IF ERR=222 PRINT'' File does not exist"
560 IF ERR<>214 AND ERR<>204 AND ERR<>222 REPORT: END
570 IF ERL<=190 GOTO 160
580 IF ERL>190 AND ERL<=300 GOTO 230
590 IF ERL>300 GOTO 330
600 :
610 DEFPROCtitle(X%,Y%,string$)
620 VDU28,0,6,79,0: COLOUR0: COLOUR129: PRINTTAB(X%,Y%); " ";
630 PRINTTAB(X%,Y%); string$;
640 VDU28,0,30,79,7: COLOUR1: COLOUR128
650 ENDPROC
660 :
670 DEFPROCcommand(string$)
680 VDU28,0,31,79,31: COLOUR0: COLOUR129: CLS
690 PRINTTAB(INT(40-LEN(string$)/2)); string$;
700 VDU28,0,30,79,7: COLOUR1: COLOUR128
710 ENDPROC

10 REM -----
20 REM ----- HELP PROGRAM -----
30 REM -----
40 :
50 PROCtitle(12,5,"HELP"): CLS: PROCcommand(" ")
60 PROCmenu
70 PRINTTAB(0,19); " "; : COLOUR0: COLOUR129: PRINT"Enter
  help subject >> "; : COLOUR1: COLOUR128: PRINT" ";
80 INPUT""choice$
90 IF LEN(choice$)>2 VDU7: GOTO70
100 IF choice$="IN" PROCintro: CLS: GOTO60
110 IF choice$="MM" PROCmove: CLS: GOTO60
120 IF choice$="PL" PROCplot: CLS: GOTO60
130 IF choice$="DA" PROCsave: CLS: GOTO60
140 IF choice$="TR" PROCtransfer: CLS: GOTO60
150 IF choice$="QU" CHAIN"P.MENU"
160 VDU7: GOTO70
170 :
180 DEFPROCtitle(X%,Y%,string$)
190 VDU28,0,6,79,0: COLOUR0: COLOUR129: PRINTTAB(X%,Y%); " ";
200 PRINTTAB(X%,Y%); string$;
210 VDU28,0,30,79,7: COLOUR1: COLOUR128
220 ENDPROC
230 :
240 DEFPROCcommand(string$)
250 VDU28,0,31,79,31: COLOUR0: COLOUR129: CLS
260 PRINTTAB(INT(40-LEN(string$)/2)); string$;
270 VDU28,0,30,79,7: COLOUR1: COLOUR128
280 ENDPROC
290 DEFPROCmenu
300 PRINT'
310 PRINT'' INtro - gives a brief introduction to the use of these
  programs"
320 PRINT'' Moving Motors - info on driving the axes and updating of
  poistions"
330 PRINT'' PPlotting - how to record a rocking curve and obtain hard
  copy etc"
340 PRINT'' Data storage - how to save data and its format on disc"
350 PRINT'' Transfer - how to transfer data to a remote host etc"
360 PRINT'' Quit - leave help, return to main menu"

```

```

370 PRINT'' "Select choice by keying in the two letters in capitals shown
      above"
380 ENDPROC
390 :
400 DEFPROCintro
410 CLS: PRINT'
420 X%=OPENIN("T.INTRO")
430 PROCdisplay
440 ENDPROC
450 :
460 DEFPROCmove
470 CLS: PRINT'
480 X%=OPENIN("T.MOTORS")
490 PROCdisplay
500 ENDPROC
510 :
520 DEFPROCdisplay
530 REPEAT: A%=BGET#X%: VDUA%: IF A%=13: VDU10
540 UNTIL EOF#X%
550 CLOSE#X%
560 PROCcommand("Press any key for menu")
570 A=GET
580 PROCcommand(" ")
590 ENDPROC
600 :
610 DEFPROCplot
620 CLS
630 X%=OPENIN("T.PLOTS")
640 PROCdisplay
650 ENDPROC
660 :
670 DEFPROCsave
680 CLS: PRINT'
690 X%=OPENIN("T.SAVE")
700 PROCdisplay
710 ENDPROC
720 :
730 DEFPROCtransfer
740 CLS: PRINT'
750 X%=OPENIN("T.TRANS")
760 PROCdisplay
770 ENDPROC

10 REM -----
20 REM -----  RESET POSITIONS ROUTINE  -----
30 REM -----
40 :
50 DIM step(6): step(1)=0.1776: step(2)=0.121: step(3)=1.0/(96.0*50):
      step(4)=1.0/(96.0*50): step(5)=1.0/96.0: step(6)=1.0/96.0
60 PROCtitle(12,5,"RESET")
70 CLS
80 PRINT'' " The current positions of the axes are as shown above"
90 PRINT'' " When prompted enter the new position or <CR> to leave
      unaltered"
100 INPUT'' " Enter the position of axis 1 (deg) "val$
110 IF val$<>" S%=VAL(val$)*3600/step(1): PROCtitle(34,1,val$)
120 PRINTTAB(0,6)""
130 INPUT'' " Enter the position of axis 2 (deg) "val$
140 IF val$<>" T%=VAL(val$)*3600/step(2): PROCtitle(34,2,val$)

```

```
150 PRINTTAB(0,8)""
160 INPUT' " Enter the position of goniometer 1 (mm) "val$
170 IF val$<>" U%=VAL(val$)/step(3): PROCtitle(34,3,val$)
180 PRINTTAB(0,10)""
190 INPUT' " Enter the position of goniometer 2 (mm) "val$
200 IF val$<>" V%=VAL(val$)/step(4): PROCtitle(34,4,val$)
210 PRINTTAB(0,12)""
220 INPUT' " Enter the position of X-table micrometer (mm) "val$
230 IF val$<>" K%=VAL(val$)/step(5): PROCtitle(47,2,val$)
240 PRINTTAB(0,14)""
250 INPUT' " Enter the position of Y-table micrometer (mm) "val$
260 IF val$<>" L%=VAL(val$)/step(6): PROCtitle(47,3,val$)
270 CHAIN"P.MENU"
280 :
290 DEFPROCtitle(X%,Y%,string$)
300 VDU28,0,6,79,0: COLOUR0: COLOUR129: PRINTTAB(X%,Y%); "
310 PRINTTAB(X%,Y%); string$;
320 VDU28,0,30,79,7
330 COLOUR1: COLOUR128
340 ENDPROC
```





## REFERENCES

- AINSLIE, B.J., DAY, C.R., FRANCE, P.W., BEALES, K.J. and NEWNS, G.R. (1979) *Electron. Lett.* **15**, 411-413.
- ALLISON, S.K. and WILLIAMS, J.H. (1930) *Phys. Rev.* **35**, 1476-1490.
- ALLISON, S.K. (1932) *Phys. Rev.* **41**, 1-20.
- BARTELS, W.J. and NIJMAN, W. (1978) *J. Cryst. Growth*, **44**, 518-525.
- BARTELS, W.J. (1983) *J. Vac. Sci. Technol. B* **1(2)**, 338-345.
- BATTERMAN, B.W. and COLE, H.C. (1964) *Rev. Mod. Phys.* **36**, 3, 681-717.
- BIEFILED, R.M., OSBOURN, G.C., GOURLEY, P.L. and FRITZ, I.J. (1983) *J. Electron. Mater.* **12** 903-908.
- BOHM, H. (1975) *Acta Cryst.* **A31**, 622-628.
- BONSE, U., KRASNICKI, S. and TEWORTE, R. (1983) *Nucl. Instrum. Methods*, **208**, 711-712.
- BONSE, U., OLTHOFF-MUNTER, K. and RUMPF, A. (1983) *J. Appl. Cryst.* **16**, 524-531.
- BOWEN, D.K. and DAVIES, S.T. (1983) *Nucl. Instrum. Methods*, **208**, 725-729.
- BURGEAT, J. and COLELLA, R. (1969) *J. Appl. Phys.* **40**, 3505-3509.
- BURGEAT, J., QUILLEC, M., PRIMOT, J., LeROUX, G. and LAUNOIS, H. (1981) *Appl. Phys. Lett.* **38(7)**, 711-712.
- CHANG, L.L., ESAKI, L., HOWARD, W.E. and LUDEKE, R. (1973) *J. Vac. Sci. Technol.*, **10**, 11-17.
- CHANG, L.L., SEGMULLER, A. and ESAKI, L. (1976) *Appl. Phys. Lett.*, **28(1)**, 39-41.
- CHANG, L.I. and KOMA, A. (1976) *Appl. Phys. Lett.* **29**, 138-140.
- CHANG, S.L., PATEL, N.B., NANNICHI, Y. and DePRINCE, F.C. (1979) *J. Appl. Phys.*, **50**, 2975-2976.
- CHANG, L.L. (1980) *Handbook Of Semiconductors*, edited by S.P. Keller (Amsterdam: North Holland).

- CHANG, S.L. (1980) Appl. Phys. Lett. 37, 819-821.
- CHATERJEE, A.K., FAKTOR, M.M., LYONS, M.H. and MOSS, R.H. (1982), J. Cryst. Growth, 56, 591-604.
- CHO, A.Y. and ARTHUR, J.R. (1975) Prog. Solid State Chem., 10, 157-160.
- CHU, S.N.G., MACRANDER, A.T., STREGE, K.E. and JOHNSTON Jr., W.D. (1985) J. Appl. Phys. 57(2), 249-257.
- COMPTON, A.H. (1931) Rev. Sci. Instrum., 2, 365-371.
- COMPTON, A.H. and ALLISON, S.K. (1935) X-Rays In Theory And Experiment, New York: Van Norstrand.
- DANIEL, V. and LIPSON, H. (1943) Proc. Roy. Soc. London Ser A, 181, 378.
- DANIEL, V. and LIPSON, H. (1944) Proc. Roy. Soc. London Ser A, 182, 378.
- DAVIDENKOV, N.N. (1961) Sov. Phys. Solid State 2, 2595-2598.
- DEHLINGER, U. (1927) Z. Kristallogr., 65, 615-631.
- DINGLE, R., GOSSARD, A.C. and WEIGMANN, W. (1975) Phys. Rev. Lett., 34, 21, 1327-1330.
- DINGLE, R. (1975) Advances In Solid State Physics Vol XV, edited by H.J. Quesser (Braunschweig: Pergamon-Vieweg).
- DINGLE, R. (1977) J. Vac. Sci. Technol. 14, 1006-1011.
- DINGLE, R., STORMER, H.L., GOSSARD, A.C. and WEIGMANN, W. (1978) Appl. Phys. Lett., 33, 665-667.
- DOHLER, G.H. (1972) Phys. Stat. Sol., (b) 52, 79-92.
- DOHLER, G.H. (1972) Phys. Stat. Sol., (b) 52, 533-545.
- DOHLER, G.H., KUNZEL, H., OLEGO, D., PLOOG, K., RUDEN, P., STOLTZ, H.J. and ABSTREITER, G. (1981) Phys. Rev. Lett., 47, 864-867.
- DuMOND, J.W.M. (1937) Phys. Rev. 52, 872-883.
- DuMOND, J.W.M. and MARLOW, D. (1937) Rev. Sci. Instrum. 8, 112-121.
- EBERT, G., Von KLITZING, K., PROBST, C. and PLOOG, K. (1982) Solid State Commun. 44, 95-98.
- ENTIN, I.R. (1978) Phys. Stat. Sol. (b) 90, 575-584.

- ESAKI, L. and TSU, R. (1970) IBM Jnl. Res. Dev. 14, 61-65.
- ESAKI, L. CHANG, L.L. and TSU, R. (1971) Proceedings Of 12th International Conference on Low Temperature Physics, pp 531-553. Edited by Eizo Kanda, Tokyo:Keigaku.
- ESAKI, L. and CHANG, L.L. (1974) Phys. Rev. Lett. 33, 495-498.
- FEWSTER, P.F. (1985) J. Appl. Cryst. (In Press).
- FLEMING, R.M., McWHAN, D.B., GOSSARD, A.C., WEIGMANN, W. and LOGAN, R.A. (1980) J. Appl. Phys. 51(1), 357-363.
- FONTAINE, D.De, (1966) Local Atomic Arrangements Studied By X-Ray Diffraction. Metallurgical Society Conferences Vol 36.
- FOXON, C.T. and JOYCE, B.A. (1981) Current Topics In Materials Science Vol. 7, Edited by E. Kaldis (Amsterdam: North Holland).
- FUKUHARA, A. and TAKANO, Y. (1977) Acta Cryst. A33, 137-142.
- FUKUHARA, A. and TAKANO, Y. (1977) J. Appl. Cryst. 10, 387-391.
- GOETZ, K.-H., BIMBERG, D., JURGENSEN, H., SELDERS, J., SOLOMONOV, A.V., GLINSKII, G.F. and RAZEGHI, M. (1983) J. Appl. Phys. 54(6) 4543-4552.
- GOURLEY, P.L. and BIELIELD, R.M. (1984) Appl. Phys. Lett. 45(7), 749-751.
- HALLIWELL, M.A.G., LYONS, M.H., TANNER, B.K. and ILCZYSZYN, P. (1983) J. Cryst. Growth, 65, 672-678.
- HALLIWELL, M.A.G., JULER, J. and NORMAN, A.G. (1983) Microscopy of Semiconductor Materials, Oxford, 1983, Inst. Phys. Conf. Ser. No.67 (Inst. Phys., London-Bristol, 1983), p.365.
- HARGREAVES, M.E. (1951) Acta Cryst. 4, 301-309.
- HART, M. (1980) Characterization Of Crystal Growth Defects By X-Ray Methods, edited by B.K. Tanner and D.K. Bowen (New York: Plenum) pp 421-432.
- HARTWIG, J. (1977) Phys. Stat. Sol. (a) 42, 495-500.
- HARTWIG, J. (1978) Exper. Technik. Physik 26, 5, 447-456.
- HORNSTRA, J. and BARTELS, W.J. (1978) J. Cryst. Growth, 44, 513-517.

- HSEIH, J.J., FINN, M.C. and ROSSI, J.A. (1977) Gallium Arsenide and Related Compounds (St Louis, 1976), Inst. Phys. Conf. Ser. No.33b, pp 37-44.
- ISHERWOOD, B.J., BROWN, B.R. and HALLIWELL, M.A.G. (1981) J. Cryst. Growth, 44, 449-460.
- INTERNATIONAL TABLES FOR X-RAY CRYSTALLOGRAPHY (1974) Vol. IV, Birmingham: Kynoch Press (Present Distributor D. Reidal: Dordrecht).
- JAGER, H. (1965) Z. Angew. Phys. 20, 73-79.
- JAGER, H. (1966) Z. Angew. Phys. 21, 543-548.
- JAMES, R.W. (1948) The Optical Principles Of The Diffraction Of X-Rays: The Crystalline State Vol. II. edited by L. Bragg (London: Bell).
- JESSER, W.A. and KUHLMAN-WILSDORF, D. (1967) Phys. Stat. Sol. 19, 95-105.
- JUNG, H., DOHLER, G.H., KUNZEL, H., PLOOG, K., RUDDEN, P. and STOLTZ, H.J. (1982) Solid State Commun. 43, 291-294.
- JUNG, H., DOHLER, G.H., GOBEL, E.O. and PLOOG, K. (1983) Appl. Phys. Lett. 43,
- KAWAMURA, Y. and OKAMOTO, H. (1979) J. Appl. Phys. 50(6), 4457-4458.
- KERVAREC, J., BAUDET, M., CUALET, J., AUVRAY, P. EMERY, J.Y. and REGRENY, A. (1984) J. Appl. Cryst. 17, 196-205.
- KISHINO, S., OGIRIMA, M. and KUHRATA, K. (1972) J. Electrochem. Soc. 119(5), 617-622.
- KLITZING, K.Von, OBLOH, H., EBERT, G., KNECHT, J. and PLOOG, K. (1981) Natn. Bur. Stand. Spec. Publ. No. 617, 382.
- KLAR, B. and RUSTICHELLI, F. (1973) Il Nuovo Cimento 13B(2), 249-269.
- KOCHENDORFER, A. (1939) Z. Kristallogr. 101, 149-155.
- KOMENOU, K., HIRAI, I., ASAMA, K. and SAKAI, M. (1978) J. Appl. Phys. 49(12), 5846-5822.
- KUNZEL, H., DOHLER, G.H., RUDEN, P. and PLOOG, K. (1982) Appl. Phys. Lett. 41, 852-854.
- LARSON, B.C. and BARHORST, J.F. (1980) J. Appl. Phys. 51(6), 3181-3185.

- LAUE, M.Von, (1931) Z. Physik 72, 472-477.
- LAUE, M.Von, (1960) Rontgenstrahl Interferenzen, Akademische (Frankfurt: Verlag).
- LUDOWISE, M.J., DIETZE, W.T., LEWIS, C.R., HOLONYAK Jr., N., HESS, K., CAMRAS, M.D. and NIXON, M.A. (1983) Appl. Phys. Lett. 42, 257-259.
- MAAN, J.C., ENGLERT, Th., UIHLEIN, Ch., KUNZEL, H., PLOOG, K. and FISCHER, A. (1983) J. Vac. Sci. Technol. B1, 289.
- MACRANDER, A.T., CHU, S.N.G., STREGE, K.E., BLOEMEKE, A.F. and JOHNSTON Jr., W.D. (1984) Appl. Phys. Lett. 44, 615-617.
- MATSUI, J., ONABE, K., KAMEJIMA, T. and HIYASHI, I. (1979) J. Electrochem. Soc. 126, 664-667.
- MATSUI, J., WATANBE, H. and SEKI, Y. (1979) J. Cryst. Growth 46, 563-568.
- MATTHEWS, J.W. and BLAKESLEE, A.E. (1977) J. Vac. Sci. Technol. 14, 989.
- MERIAM ABDUL GANI, S. (1982) PhD Thesis, University of Durham.
- MEYER, K.E., FLETCHER, G.P., SINHA, S.K. and SCHULLER, I.K. (1981) J. Appl. Phys. 52(11), 6608-6610.
- MOSS, R.H. and SPURDENS, P.C. (1984) Electronics Lett. 20, 978-979.
- MOTOROLA MCU/MPU APPLICATIONS MANUAL VOL. 2 (1985), (Motorola).
- MOTOROLA MCU/MPU INTERFACE COMPONENTS (1984), (Motorola).
- NAHORY, R.E., POLLACK, M.A., JOHNSTON Jr., W.D. and BARNES, R.L. (1978) Appl. Phys. Lett. 33, 659-662.
- NEWMAN, D. (1982) New Electronics, May 18.
- OE, K., SHINODA, Y. and SUGIYAMA, K. (1978) Appl. Phys. Lett. 33(11), 962-964.
- OLSEN, G.H. and ETTEBERG, M. (1977) J. Appl. Phys. 48, 2543-2547.
- OSBOURN, G.C. (1982) J. Appl. Phys. 53(3), 1586-1589.

- OSBOURN, G.C., BIEFIELD, R.M. and GOURLEY, P.L. (1982) Appl. Phys. Lett. 41(2), 172-174.
- PETROFF, P.M. (1977) J. Vac. Sci. Technol. 14, 973-981.
- PETROFF, P.M., GOSSARD, A.C., WEIGMANN, W. and SAVAGE, A. (1978) J. Cryst. Growth, 44, 5-13.
- PINSKER, Z.G. (1978) Dynamical Scattering Of X-Rays In Crystals (Berlin: Springer-Verlag).
- PLOOG, K. (1980) Crystals: Growth Properties and Applications Vol. 3, edited by H.C. Freyhardt (Berlin, Heidelberg: Springer-Verlag).
- PLOOG, K. (1981) A Rev. Mat. Sci. 11, 171-179.
- PLOOG, K. (1982) A Rev. Mat. Sci. 12, 123-132.
- PLOOG, K. and DOHLER, G.H. (1983) Advances In Physics, 32(3), 285-359.
- REZEK, E.A., VOJAK, B.A., CHIN, R. and HOLONYAK Jr., N. (1980) Appl. Phys. Lett. 36, 744-746.
- ROZGONYI, G.A. and CIESIELKA, T.J. (1973) Rev. Sci. Instrum. 44(8), 1053-1057.
- SAI-HALASZ, G.A., TSU, R. and ESAKI, L. (1977) Appl. Phys. Lett. 30, 651-653.
- SAI-HALASZ, G.A., ESAKI, L. and HARRISON, W.A. (1978) Phys. Rev. B 18, 2812-2818.
- SAKAKI, H., CHANG, L.L., LUDEKE, R., CHANG, C.A., SAI-HALASZ, G.A. and ESAKI, L. (1977) Appl. Phys. Lett. 31, 211-213.
- SAUL, R.H. (1969) J. Appl. Phys. 46(8), 3273-3279.
- SCHWARZSCHILD, M.M. (1928) Phys. Rev. 32, 162-171.
- SEGMULLER, A. (1973) Thin Solid Films 18, 287-294.
- SEGMULLER, A. and BLAKESLEE, A.E. (1973) J. Appl. Cryst. 6, 19-25.
- SEGMULLER, A., KRISHNA, P. and ESAKI, L. (1977) J. Appl. Cryst. 10, 1-6.
- SKIER, K. (1981) Beyond Games: System Software For Your 6502 Personal Computer (BYTE, McGraw-Hill: Peterborough, New Hampshire).

- SPERIOSU, V.S., GLASS, H.L. and KOBAYASHI, T. (1979) Appl. Phys. Lett. 34(9), 539-542.
- SPERIOSU, V.S. (1981) J. Appl. Phys. 52(10), 6094-6103.
- SPERIOSU, V.S., PAINE, B.M., NICOLET, M.A. and GLASS, H. (1982) Appl. Phys. Lett. 40(7), 604-606.
- SPERIOSU, V.S. and WILTS, C.H. (1983) J. Appl. Phys. 54(6), 3025-3343.
- SPERIOSU, V.S. and VREELAND Jr., T. (1984) J. Appl. Phys. 56(6), 1591-1600.
- SPERIOSU, V.S., NICOLET, M.-A., PICRAUX, S.T. and BIEFIELD, R.M. (1984) Appl. Phys. Lett. 45(3), 223-225.
- SPERIOSU, V.S., NICOLET, M.-A., TANDON, J.L. and YEH, Y.C.M. (1985) J. Appl. Phys. 57(4), 1377-1379.
- STRINGFELLOW, G.B. (1972) J. Appl. Phys. 43, 3455-3460.
- TAKAGI, S. (1962) Acta Cryst. 15, 1311-1312.
- TAKAGI, S. (1969) J. Phys. Soc. Jpn. 26, 1239-1254.
- TAKEUCHI, T., OHATA, N., SUGITA, Y. and FUKUHARA, A. (1983) J. Appl. Phys. 54(2), 715-720.
- TANNER, B.K., BARNETT, S.J. and HILL, M.J. (1985) Microscopy of Semiconductor Materials, Oxford 1985. (In Press).
- TANNER, B.K. and HILL, M.J. (1985) Proc. Denver Conf. Applications of X-ray Analysis, Denver, Colorado. To be published in: Advances in X-ray Analysis Vol. 29 (1986).
- TASHIMA, M.M., COOK, L.W. and STILLMAN, G.E. (1981) J. Cryst. Growth 54, 132-137.
- TAUPIN, D. (1964) Bull. Soc. Franc. Miner. Cryst. 88, 469-511.
- TERAUCHI, H., SEKIMOTO, S., SANO, N., KATO, H. and NAKAYAMA, M. (1984) Appl. Phys. Lett. 44(10), 971-973.
- TIMOSHENKO, S. (1925) J. Opt. Soc. 11, 233-248.
- TSUI, D.C., STORMER, H.L. and GOSSARD, A.C. (1982) Phys. Rev. B 25, 1405-1407.
- TSUI, D.C., STORMER, H.L. and GOSSARD, A.C. (1982) Phys. Rev. Lett. 48, 1559-1561.

- VARDANYAN, D.M. and MANOUKYAN, H.M. (1982) Phys. Stat. Sol.  
(a) **69**, 475-482.
- VARDANYAN, D.M., MANOUKYAN, H.M. and PETROSYAN, H.M. (1985)  
Acta Cryst. **A41**, 212-217.
- VARDANYAN, D.M., MANOUKYAN, H.M. and PETROSYAN, H.M. (1985)  
Acta Cryst. **A41**, 218-222.
- VILMS, J. and KERPS, D. (1982) J. Appl. Phys. **53**, 1536-1537.
- VOGLI, O., CALHOUN, B.A., ROSIER, L.L., and SLONCZEWSKI,  
J.C. (1974) AIP Conf. Proc. **24**, 617-623.
- YOSHIMURA, J. (1984) J. Appl. Cryst. **17**, 426-434.
- ZACHARIASEN, W.H. (1945) Theory of X-ray Diffraction in  
Crystals (New York: John Wiley).
- ZELLER, C.H., VINTER, B., ABSTREITER, G. and PLOOK, K.  
(1982) Phys. Rev. **B26**, 2124-2132.

